DE GRUYTER

CARBON ALLOTROPES

NANOSTRUCTURED ANTI-CORROSIVE MATERIALS

Edited by Jeenat Aslam, Chandrabhan Verma, Dakeshwar Kumar Verma, Ruby Aslam

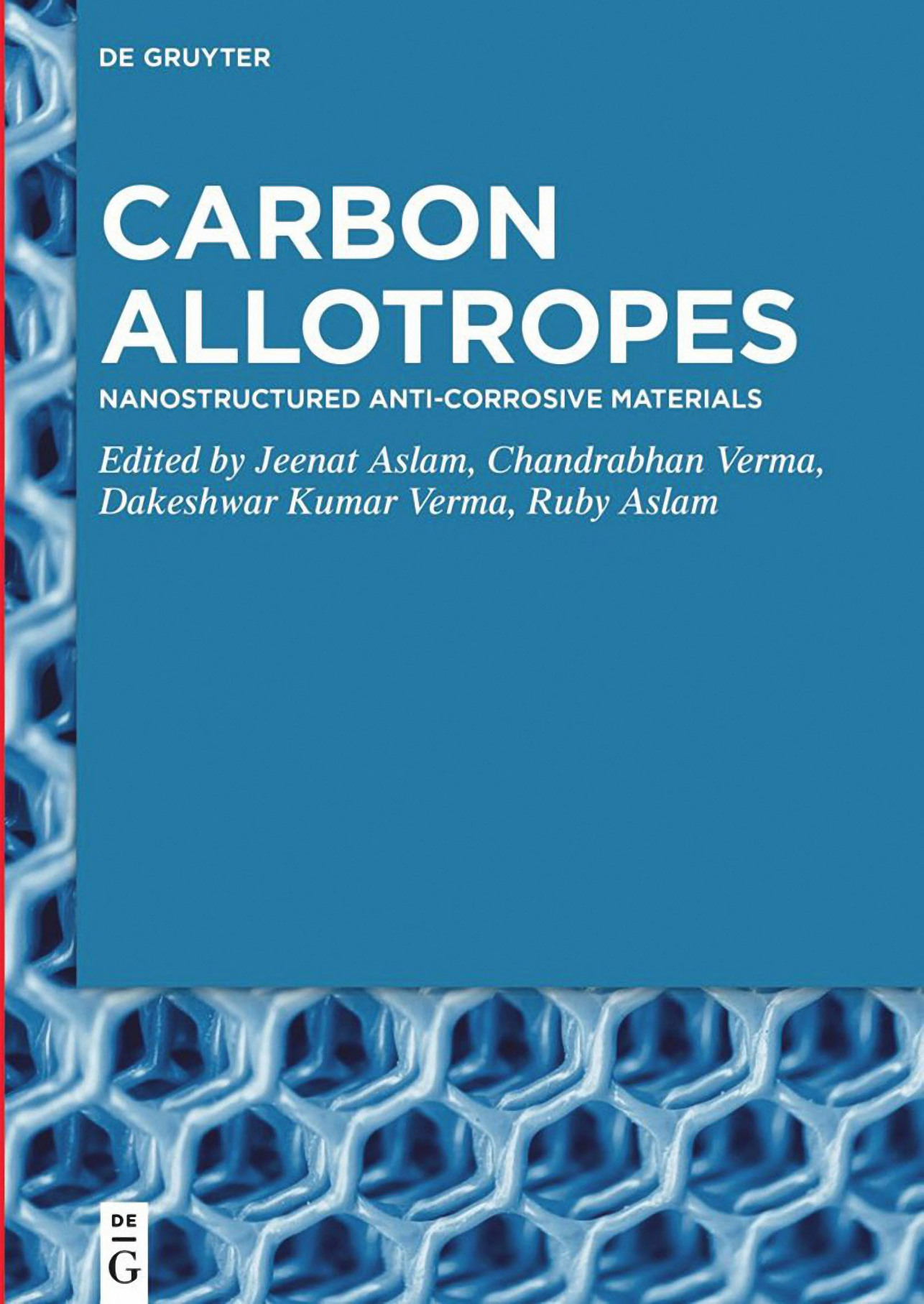

Jeenat Aslam, Chandrabhan Verma, Dakeshwar Kumar Verma and Ruby Aslam (Eds.)
Carbon Allotropes

Also of Interest

Carbon-Based Smart Materials
Constantinos A. Charitidis, Elias P. Koumoulos and Dimitrios A. Dragatogiannis (Eds.), 2020
ISBN 978-3-11-047774-0, e-ISBN 978-3-11-047913-3

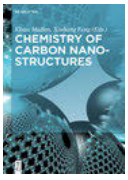

Chemistry of Carbon Nanostructures
Klaus Muellen and Xinliang Feng, 2017
ISBN 978-3-11-028450-8, e-ISBN 978-3-11-028464-5

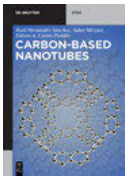

Carbon-Based Nanotubes
Raúl Hernández Sánchez, Saber Mirzaei and Edison Arley Castro Portillo, 2022
ISBN 978-1-5015-1931-4, e-ISBN 978-1-5015-1934-5

Carbon Allotropes

Nanostructured Anti-Corrosive Materials

Edited by
Jeenat Aslam, Chandrabhan Verma,
Dakeshwar Kumar Verma and Ruby Aslam

DE GRUYTER

Editors
Jeenat Aslam
Department of Chemistry
College of Science
Taibah University, Yanbu-30799
Al-Madina
Saudi Arabia
Email: drjeenataslam@outlook.com

Dakeshwar Kumar Verma
Department of Chemistry
Govt. Digvijay Autonomous
Postgraduate College
Chhattisgarh 491441
India
Email: dakeshwarverma@gmail.com

Chandrabhan Verma
Interdisciplinary Research Center for Advanced Materials
King Fahd University of Petroleum and Minerals
Dharan 31261
Saudi Arabia
Email: Chandraverma.rs.apc@itbhu.ac.in

Ruby Aslam
Department of Applied Chemistry
Faculty of Engineering and Technology
Aligarh Muslim University
Aligarh 202002
India
Email: drrubyaslam@gmail.com

ISBN 978-3-11-078280-6
e-ISBN (PDF) 978-3-11-078282-0
e-ISBN (EPUB) 978-3-11-078286-8

Library of Congress Control Number: 2022938811

Bibliographic information published by the Deutsche Nationalbibliothek
The Deutsche Nationalbibliothek lists this publication in the Deutsche Nationalbibliografie; detailed bibliographic data are available on the internet at http://dnb.dnb.de.

Cover image: Gettyimages/coffeekai
Typesetting: Integra Software Services Pvt. Ltd.
Printing and binding: CPI books GmbH, Leck

www.degruyter.com

About the editors

Jeenat Aslam Department of Chemistry, College of Science,
Taibah University, Yanbu-30799,
Al-Madina, Saudi Arabia
drjeenataslam@outlook.com

Jeenat Aslam, Ph.D., is currently working as an Assistant Professor at the Department of Chemistry, College of Science, Taibah University, Yanbu, Al-Madina, Saudi Arabia. Her research mainly focuses on the materials and corrosion, nanotechnology, and surface chemistry. Dr. Jeenat has published several research and review articles in peer-reviewed international journals of ACS, Wiley, Elsevier, Springer, Taylor & Francis, Benthum Science, etc. She has edited 2 books and has contributed 20 book chapters.

Chandrabhan Verma
Interdisciplinary Research Center for Advanced Materials,
King Fahd University of Petroleum and Minerals,
Dhahran, 31261, Saudi Arabia
Chandraverma.rs.apc@itbhu.ac.in

Chandrabhan Verma, works at the Interdisciplinary Center for Research in Advanced Materials King Fahd University of Petroleum and Minerals (KFUPM), Saudi Arabia. He obtained his PhD in Material Science/ Chemistry at the Indian Institute of Technology (Banaras Hindu University) Varanasi, India. He is a member of American Chemical Society (ACS) and serves as reviewer and editorial board member for various internationally recognized of ACS, RSC, Elsevier, Wiley, and Springer platform. Dr. Verma is Associate Editor-in-Chief of journal *Organic Chemistry Plus*. He is the author of several research and review articles published at ACS, Elsevier, RSC, Wiley, Springer etc. platforms. He has total citation of more than 6,987 with H-index of 46 and i-10 index of 116. Dr. Verma has edited eight books for the ACS, Elsevier, RSC, and Wiley. He received several awards for his academic achievements.

https://doi.org/10.1515/9783110782820-202

Dakeshwar Kumar Verma
Department of Chemistry,
Govt. Digvijay Autonomous Postgraduate College,
Rajnandgaon, Chhattisgarh, INDIA 491441
dakeshwarverma@gmail.com

Dakeshwar Kumar Verma, Ph.D., is an Assistant Professor of Chemistry at the Govt. Digvijay Autonomous Postgraduate College, Rajnandgaon, Chhattisgarh, India. His research mainly focuses on the preparation and designing of organic compounds for various applications and green chemistry. Dr. Verma is the author of more than 50 research papers, review articles, and book chapters in peer-reviewed international journals of ACS, RSC, Wiley, Elsevier, Springer, Taylor & Francis, etc. He has also worked as an editor/co-editor/author on various books published by Elsevier, Wiley Science, and De Gruyter. He has total citation of more than 730 with H-index of 13 and i-10 index of 17. Recently, two full-time Ph.D. research scholars are working under his guidance. Dr. Verma received Council of Scientific and Industrial Research Junior Research Fellowship award in 2013. He also availed MHRD National fellowship during his Ph.D. in 2013.

Dr. Ruby Aslam
Department of Applied Chemistry,
Aligarh Muslim University, Aligarh, India.
drrubyaslam@gmail.com

Ruby Aslam, PhD., is a Research Associate in the Department of Applied Chemistry, Aligarh Muslim University, Uttar Pradesh, India. She graduated with an M.Sc. in Chemistry at Aligarh Muslim University and presented her M.Phil. dissertation and Ph.D. thesis in Applied Chemistry at Aligarh Muslim University. She has published widely on corrosion inhibition and corrosion protective coatings.

Preface

Corrosion is a high-cost and potentially hazardous issue in numerous industries. The potential use of diverse carbon nanoallotropes in corrosion protection, prevention, and control is a subject of rising attention. The corrosion, protection, and control using carbon nanoallotropes is a precious reference tool for researchers and engineers employed with nanostructure materials in various industries such as automotive, aerospace, petroleum, oil and gas, and chemical engineering, along with academics learning the exclusive protection and control offered via carbon nanoallotropes against corrosion. The nanostructure materials-based protective approaches can suggest numerous advantages over their traditional complements; for example, protection for primary phase, improved corrosion control, and higher corrosion resistance (due to high surface area and high degree of hydrophobicity). However, inorganic, organic, and mixed material inhibitors were used for a long period to combat corrosion. The usage of carbon nanoallotropes as inhibitors has expanded its importance because of its improved corrosion efficiency owing to the enlarged surface-to-volume ratio. The carbon nanoallotropes are good corrosion inhibitor because it has numerous advantages; for example, low cost, low toxicity, easy production, and high protection efficiency. Nanostructures and nanostructure materials can assist as outstanding carriers for corrosion inhibitors. The nanostructure materials advantages are controlled and activated release of corrosion inhibitors to protect corrosion.

This book will summarize existing research and technology on nanostructure materials as corrosion inhibitors, obstacles in exploiting these materials, and then outline future research prospects. The book is divided into three parts, and each part contains numerous chapters. Part 1 "investigates the overview of carbon allotropes and corrosion" and covers topics in Chapters 1 to 5 are properties, applications, synthesis, and characterization of carbon allotropes, basics, economic adverse effects and mitigation of corrosion, challenges and opportunities of carbon allotropes for anticorrosive applications, and mechanism of corrosion prevention and control. Part 2, "recent advancements of carbon allotropes as nanostructured corrosion inhibitors," studies the topics in Chapters 6 to 12 are graphene and graphene oxide, chemically modified graphene and graphene oxides, polymer composites of graphene and graphene oxides, carbon nanotubes (CNTs) their composites, chemically modified CNTs, carbon quantum dots (CQDs), carbon nanorods (CNRs) and their composites as nanostructured corrosion inhibitors, and recent advances in carbon allotropes nanostructured as anticorrosive coatings. Part 3, "carbon allotropes as nanostructured corrosion inhibitors: industrialization, economics, and commercialization," covers the topics in Chapters 13 to 15 are carbon allotropes nanostructured as ideal substitutes for industrial corrosion inhibitors and recent advancements and future proponents of carbon allotropes-based materials as ideal substitutes for industrially

https://doi.org/10.1515/9783110782820-203

useful self-healing coatings, economics, and commercialization of carbon allotropes nanostructured corrosion inhibitors.

This book is intended for a very wide-ranging audience working in the fields of advanced materials science, chemistry, chemical engineering and technology, etc. It will be an invaluable reference source for the libraries in universities and industrial institutions, government and independent institutes, individual research groups, and scientists. Overall, this book is written for scholars in academia and industry, working corrosion engineers, and students of materials science and applied and engineering chemistry. The editors and contributors are renowned researchers, scientists, and true professionals from academia and industry. On behalf of De Gruyter, we are very thankful to the contributors of all chapters for their amazing and passionate efforts in the making of this book. Our special thanks are dedicated to Dr. Christene Smith (Acquisitions Editor), Mrs. Stella Müller (Content Editor), and the Editorial Team at De Gruyter for their devoted support and help during this project. In the end, all gratitude goes to De Gruyter for publishing the book.

Editors
Jeenat Aslam
Chandrabhan Verma
Dakeshwar Kumar Verma
and Ruby Aslam

Contents

Bhawana Jain*, Reena Rawat, Daniel Amoako Darko

Chapter 1
Carbon allotropes: properties and applications – state of the art

Abstract: For ages, carbon has been used in technology and in human existence, both as a single entity and in many forms. Since prehistoric times, carbon-based substances such as graphite, charcoal, and carbon black have been employed as writing and drawing materials. Conjugated carbon nanomaterials, including carbon nanotubes, fullerenes, activated carbon, and graphite, have been used as energy sources over the past two and a half decades due to their unique properties. Because of their amazing chemical, mechanical, electrical, and thermal capabilities, carbon nanostructures have lately found usage in a range of sectors, including drug administration, electronics, composite materials, sensors, field emission devices, and energy storage and conversion. Carbon nanoparticles (when employed as energy materials) are thought to be an adequate and promising way to mitigate the hazard. Subsequently, these materials' astounding properties, as well as the best possibilities for greener and harmless to the ecosystem combination strategies and modern-scale creation of carbon nanostructured materials are irrefutably significant and can consequently be viewed as a point of convergence of numerous researchers and specialists in the twenty-first century. This book chapter tries to summarize recent advances in their synthesis, properties, and applications as described in the literature.

Keywords: carbon nanomaterials, carbon allotropes, fullerenes, properties, applications

1.1 Introduction

Carbon is a unique and important element on our planet; it is the sixth most frequent element in the universe, the fourth most common element in the solar system, and the 17th most abundant element in the Earth's crust [1]. Carbon has been estimated to have a relative abundance of 180–270 parts per million [2]. Amazingly, after oxygen it is a most prevalent mineral found in the human body [3], accounting

*Corresponding author: **Bhawana Jain,** Siddhachalam Laboratory, Raipur 493221, Chhattisgarh, India
Reena Rawat, Department of Chemistry, Echelon Institute of Technology, Faridabad 121101, Haryana, India
Daniel Amoako Darko, Institute for Environment and Sanitation Studies, University of Ghana, Legon

https://doi.org/10.1515/9783110782820-001

for roughly 18% of a person's body weight. One of the most striking attributes of carbon is its capacity to generate an extensive variety of metastable phases in close proximity to ambient conditions, as well as their large fields of kinetic balance. Although there is a scarcity of elemental carbon on the planet's surface, accounting for only 0.2% of the planet's total mass [4], its role is critical because it has the ability to make bond with different light materials and also by itself. As a result, carbon's ability to catenate prepared the door for the expansion of chemistry and biology, allowing for the emergence of life's marvels [3]. Different low-dimensional allotropes of carbon are identified as carbon nanostructures, such as activated carbon (AC), carbon nanotubes (CNTs), graphite, and the C_{60} family of buckyballs, polyaromatic molecules [5–8], and graphene [9–11] that arise like the shining stars in the fields of materials science, nanoscience, engineering, and technology. Recently nanotechnology has gathered a lot of studies because it can be used to create new materials with unique features. Nanostructures are appropriate for the vast variety of implementation due to many aspects such as superior directionality, high surface area, and flexibility [12–17]. As a result, considering the essential role that these materials have played in many new advanced technologies, they have piqued the interest of researchers from a variety of fields. This feature offers up a slew of new chemical possibilities for nanomaterial design, such as the formation of functional nanoparticle arrays for catalytic applications [8, 18, 19], for the delivery of drug-specific isolation of chemicals [11, 18, 20–23], melting of phase change materials in building prototype [24–29], and the formation of mesoporous monolithic structures as low potassium dielectric materials [10, 30, 31], and so on. The carbon distribution on and in the Earth is depicted in Fig. 1.1, which can be described as follows:

1) The carbon content of the Earth's crust is 2,700 parts per million.
2) Oceanic crusts contain 200 parts per million of carbon.
3) There are 400 parts per million of carbon in our atmosphere.
4) The carbon content of the hydrosphere is 30 ppm.

All biological life on this planet is made from carbon allotropes. Carbon is found in all living species, including humans, animals, and plants. After oxygen, carbon is the second most commonly found element in the human body as per mass [32].

Many novel carbon allotropes have been discovered since Kroto et al. [34] identified fullerene in 1985. CNTs, which were discovered in 1991 by Iijima [35], and graphene, which is a single sheet of carbon atoms arranged in a honeycomb lattice and was discovered in 2004 by Novoselov et al. [36], are two among them. In 2010, they were honored by the Nobel Prize in Physics [36], demonstrating the relevance of carbon nanomaterials.

The mechanical and physical properties of a range of carbon allotropes, comprising seven two-dimensional (2D) and eight three-dimensional (3D) materials, have been compared in this research. The previously reported comparative findings are presented in Tabs. 1.2 and 1.3 will be useful for future research into the properties of

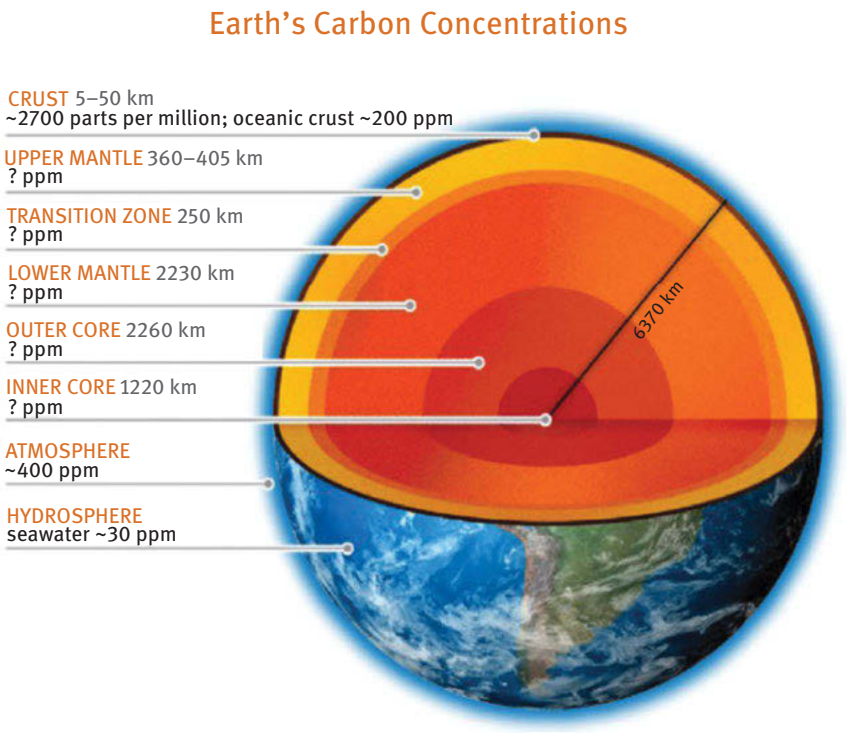

Fig. 1.1: Carbon content in and on the Earth [33].

these carbon allotropes. By studying the relationship between the structural topology of these carbon allotropes, we propose a systematic technique to synthesize these carbon allotropes by altering the carbon atoms or C–C bonds in the two mother structures, graphene and diamond. This theoretical research could aid in the systematic finding of novel carbon allotropes.

In this book chapter, we are going to present the current research in these fields, but we will also include few fresh and fascinating applications. We will concentrate on the characteristics of carbon nanomaterials and how they can be manufactured and modified for definite applications.

1.2 Classifications of carbon allotropes

1.2.1 Carbon nanotubes

In the family of nanocarbon, CNTs are very well-known materials. Multiwalled CNTs (MWCNTs) and single-walled CNTs (SWCNTs) were identified by Iijima in 1991

and 1993, respectively [35, 37]. Because of their exceptional electrical, mechanical, and structural properties, these species have sparked a lot of interest since then. SWCNTs are formed by single layer of sp^2-hybridized carbon atoms which are wrapped in a form of seamless cylinder which has length and diameter in nanoscale and micrometer range. On the other side, MWCNTs are made up of several concentric CNTs which has 3.4 interlayer spacing [38]. In comparison to any nanomaterial, CNTs have one of the greatest length-to-diameter aspect ratios, often reaching 10,000, and therefore, it is considered as the most anisotropic nanomaterials yet created. Because of the strong sp^2 connections between the individual carbon atoms, CNTs are one of the strongest and stiffest fibers mechanically.

Due to their surface characteristics, CNTs are difficult to disperse in liquid like organic or polar solvents. Even while the O_2-carrying moieties on the two ends of CNTs are normally hydrophilic, the large amount of surface area of CNTs which is made of the wall is hydrophobic [39, 40]. As a result of the strong van der Waals contact, CNTs are frequently held together in bundles. Dispersion and modification of hydrophobic CNTs during the functionalization of CNTs onto optical fibers is typically a severe difficulty [41]. Because CNTs gather easily in aqueous or polar solvents, they are commonly dispersed in nonpolar organic solvents like dimethylformamide, or by modifying them with polymers or surfactants. The dispersity obstacle in aqueous solution might be regarded as an indirect advantage since optical fibers functionalized with CNTs scattered in organic solvents allow the solvent to be readily removed by evaporation [42].

Carbon nanotubes have a physical structure that includes the atomic arrangement of carbon atoms (chirality), length, and diameter, which has a significant impact on their electrical properties (Fig. 1.2). SWCNT chirality relates to the angle at which a graphene sheet is rolled up, as well as the alignment of the orbitals. The atomic structure of CNTs can be expressed as a chiral vector: $\vec{c_h} = n\vec{a_1} + m\vec{a_2}$, where n and m are the number of steps along with the honeycomb lattice's zigzag carbon bonds, and $\vec{a_1}$ and $\vec{a_2}$ are the unit vectors. CNTs are divided into three categories: armchair, zigzag, and chiral tubes. Armchair tubes feature equal n and m values, as well as a 30° chiral angle. Zigzag tubes, on the other hand, have $m = 0$ and a chiral angle of 0°, whereas chiral tubes can have any value. The chirality of CNTs is crucial in determining their conductivity. Conducting CNTs are arranged in an achiral and armchair pattern (n, n). Alternatively, chiral (n, m) and achiral zigzag (n, 0) CNTs are semiconductors unless the $(n-m)/3$ yields a whole integer. The bandgap shrinks as the diameter of CNTs grows, potentially leading to a zero-bandgap semiconductor [41].

Aside from chirality, catalytic particles and dopants [43, 44], as well as functionalization of the side walls [45, 46], can affect the characteristics of CNTs. CNTs have been integrated into sensors with numerous sorts of sensing modalities due to their physical and electrical features, demonstrating exceptional adaptive and sensory capabilities.

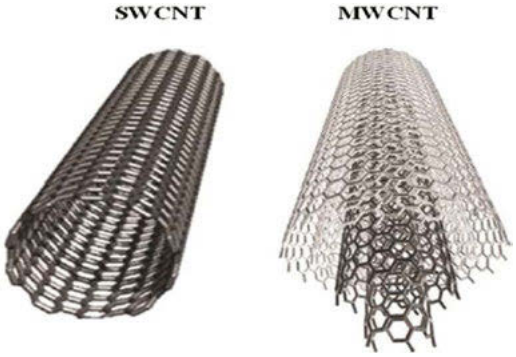

Fig. 1.2: Difference between single-walled carbon nanotubes (SWCNTs) and multiwalled CNTs (MWCNTs) [33].

1.2.2 Graphene

Graphene is made up of covalently bonded 2D monolayer carbon atoms structured in a hexagonal network. Until graphene was practically proven by Novoselov et al., it was thought as a hypothetical structure [36], whose groundbreaking discovery led them to win the Nobel Prize in 2010. Novoselov et al. [35] used a scotch tape peeling approach to isolate single-layer graphene from highly oriented pyrolytic graphite. Due to graphene's many unique properties, a very rapid and vast growth seen in research is used in optoelectronics [47], energy storage [48], energy conversion [49], and biological applications [50, 51] since then. Because each carbon atom is a surface atom, the surface-to-volume ratio is exceptionally high in graphene [52]. Due to its strong sensitivity property to external stimuli, it is a high-demanding choice in the field of sensing applications. Because of the delocalized electrons on its surface, the physical characteristics of graphene may be twisted and tweaked to allow specialized interactions with certain molecules [53].

In sensing applications, graphene's electrical characteristics are also essential. Particularly, the electrical conductivity of graphene will change, once molecules are incorporated on its surface because the molecules may act as electron donors or receivers, affecting the carrier concentration [54, 55]. Furthermore, because graphene is extremely conductive and has low Johnson noise, a tiny change in carrier concentration can cause a significant effect on electrical conductivity. Graphene also has a surface-enhanced Raman scattering property, which allows for the detection of trace-level target molecules by magnifying the distinctive Raman signals [56, 57]. At infrared and THz frequencies, graphene exhibits adjustable surface plasmons, making it a potential alternative to noble metals like gold and silver [58, 59]. The electronic band structure of graphene is determined by a combination of linear dispersion relations and vanishing density of states at the Fermi level in its neutral state [60, 61]. Graphene

exhibits metallic optical response when the Fermi energy moves farther from the point of neutrality, which indicates the presence of plasmons. Long duration, extensive spatial confinement, and field augmentation, as well as tunability via electrostatic grating are all advantages of graphene plasmons, according to many researchers [62].

Aside from its electronic properties, graphene has unique optical features that make it a popular material for sensing applications. Despite being a zero-bandgap material in its pristine condition, graphene oxide (GO) containing heterogeneous functional moieties emit significantly from the UV to near-infrared range [63]. The intense emission is considered to be caused by an electrical transition between the pure sp^2 carbon domain and the functional moieties positioned at the edges of the GO sheets [64]. The fluorescence emission of GO can be enhanced or quenched depending on the presence and concentration of target molecules [65]. GO is frequently used as a functionalized active material on an optical fiber. In many cases, the optical fiber was employed to transmit the excitation signal as well as to collect and transfer the fluorescence emission to the photodetector. As a result, especially for microstructure optical fibers, it is critical to have a system that can relate maximal fluorescence emission intensity back to the fiber [66].

1.2.3 Carbon dots

Fluorescent carbon dots (CDs) were discovered accidently during a normal gel electrophoresis purification of SWCNTs manufactured by an arc-discharge process [67]. Fluorescent carbon nanoparticles, subsequently known as CDs, are identified and isolated from carbon soot as a by-product of the arc-discharge process. CDs, also known as carbon quantum dots or carbon nanodots, are another form of carbonaceous material. CDs and graphene quantum dots (GQDs) are often used interchangeably. There are several physical distinctions between CDs and GQDs, though. GQDs are graphene monolayers that have been fractured into nanosized bits and have the bulk of their carbon atoms hybridized with sp^2 [68]. CDs, on the other hand, are quasi-spherical carbon nanoparticles with a diameter of less than 10 nm [69–71]. Amorphous or crystalline cores with sp^2-hybridized carbon arrangement are common in CDs. CDs have also been reported as having a diamond-like sp^3 carbon structure in several researches [72]. CDs generally have surface moieties incorporated during the production process. Depending on the precursors used, several different types of surface functional groups, such as C = O, C–O, C–OH, and C = C, can appear on the surface of CDs. For example, to create fluorescent CDs, Dong et al. [72] employed citric acid, branched polyethyleneimine (BPEI), and low-temperature heating. The final product was discovered to be covered in BPEI, which is high in amino acids. These functional groups are useful in sensing applications because they may form particular coordination bonds with certain molecules, causing changes in optical properties. CD precursors

can inject several kinds of dopant ions into the disks, changing the optical and sensing capabilities of the disks [73, 74]. Shan et al. [75] employed boron-doped CDs manufactured via a one-pot solvothermal synthesis using boron tribromide as the boron source and hydroquinone as the carbon precursor to sensitively detect hydrogen peroxide and glucose. Post-functionalizing CD with certain chelating groups or biomolecules is another technique to provide them sensitive and precise targeting capabilities [75]. In several CD-based sensing systems, changes in fluorescence emission intensity may be ascribed to three important mechanisms: the inner filter effect, photoinduced electron transfer, and Forster resonance energy transfer [76].

CDs have a unique fluorescence property that is frequently used in sensor applications, and their emissions can be excitation-dependent or excitation-independent [77–79]. With a progressive rise in excitation wavelength, the fluorescence emission wavelength of excitation-dependent CDs may be adjusted from 400 to 750 nm [80]. Environmental parameters such as solvent types [81], pH [82], temperature [83], and CD concentration [84] can also affect the fluorescence intensity of CDs. CDs, interestingly, emit up-conversion fluorescence, which is extremely useful for in vivo biological applications [71, 79, 85, 86]. Although the origin of the fluorescence property is still under debate, the quantum confinement effect, different surface functional groups, and the presence of fluorophore species on the CD's surface are all typical causes [76].

1.2.4 Nanodiamonds

Diamond's remarkable qualities, including high thermal conductivity and extraordinary hardness, have long been known. However, Soviet scientists only found nanoscaled diamonds, also known as nanodiamonds (NDs), in the 1960s [87]. The NDs were detected in the soot after the detonation of an oxygen-deficient TNT (trinitrotoluene)/hexogen composition in an inert environment with no further carbon input [88]. NDs remained a largely unknown condition until the late 1980s [89]. NDs have a diamond-like morphology and are made up of just sp^3 carbon atoms, unlike CNTs, graphene, and CDs, which are made up of sp^2 graphitic carbon. NDs are 2–20 nm in size, which is smaller than bulk diamond and diamond-abrasive particles but bigger than organic diamond molecules [63]. NDs tend to clump together, and even commercial NDs can include large ND clusters that defy ultrasonic treatment [90]. As a result, numerous ways for de-aggregating NDs have been devised. Osawa et al. [91] devised two ways for dissolving ND aggregates in nonaqueous media. Stirred media milling with zirconia microbeads is the first method, which can decrease ND diameters from 200 to 4–5 nm in 100 min. Although this method may break up large aggregates, it wears down the beads, blades, and containers, exposing the ND solution to zirconia contamination. To eliminate the zirconia nanoparticles, more treatment with strong acids is required. The second method

involves the use of zirconia beads and high-powered ultrasonication. When compared to the first technique, this bead-assisted sonic disintegration method may reduce aggregate size to a similar dimension without the need for posttreatment. Dry milling is another cost-effective and simple method for reducing the size of ND aggregates from micrometer to nanoscale ranges without introducing any contaminating species [92]. Pentecost employed water-soluble compounds such as sodium chloride and sucrose during the milling process, which may be removed by washing NDs with water. Although the yield of single-digit NDs is exceedingly low, ultracentrifugation is another contaminant-free method for sorting NDs into different sizes depending on mass and dimension [93].

The presence of the fluorescent defect center, also known as the nitrogen-vacancy (N-V) center, is the property that distinguishes NDs from other carbon allotropes. N-V focuses have been significant for detecting applications in light of the fact that their photoluminescence (PL) is exceptionally impervious to photobleaching with an undeniable zero-phonon line even at encompassing temperature, the electron turns trio nature of the electronic ground state, and the reliance of PL emanation force on the strength of twist projection on the evenness hub of the N-V focus [94]. The N-V center, as depicted in Fig. 1.3, is a fault in the crystal structure of NDs. One of the two neighboring carbon atoms is replaced by a nitrogen atom in the crystalline lattice of NDs, while the other is a vacancy with no replacement atom. Two unpaired nitrogen electrons create the spin triplet ground and excited states ms = 0, ± 1, respectively. These states may be optically initiated, manipulated, and determined at room temperature. After being optically stimulated, the N-V centers can transition between the ground and electrically excited states. The N-V centers can relax to their ground state through both radial and nonradial routes. The radiative transition can provide a wide PL spectrum with a zero-phonon line at 637 nm in practice, which can be exploited for accurate sensing measurement [96, 97]. The intersystem crossover (ISC) to the singlet levels below the excited triplet state, on the other hand, is a nonradiative approach [95].

A resonant microwave frequency can be used as an excitation source to stimulate the population to the ms = ± 1 spin level. As a result of ISC, nonradiative decay can occur, and a reduction in PL emission can be recorded. Under an unknown magnetic field, the N-V center will cause a split between the ms = ± 1 spin sublevel for magnetometry. The electron spin resonance transition between sublevels may be used to calculate the magnetic field's intensity and direction. In summary, Tab. 1.1 compares the features of several carbon allotropes.

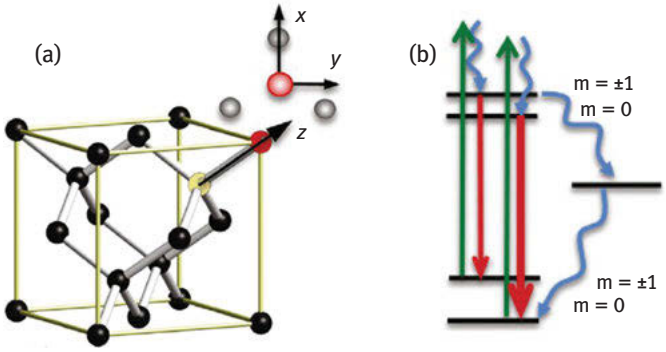

Fig. 1.3: (a) N-V center in NDs. N and C are colored in red and black, respectively, while vacancy is represented by yellow. The *x*- and *y*-axes are shown on top of the *z*-axis. (b) The electronic states of NDs at room temperature. There are two orthogonal transition dipole moments in the excited spin-triplet state due to the double degeneracy of the molecular orbitals. Green and red arrows represent spin-preserving PL and optical excitation, respectively [94]. Copyright © 2017, Elsevier.

1.2.5 Activated carbon

AC is classified as amorphous carbon due to its nature, properties, and forms. It is regarded to be the most well-known and well-established one of all renewable carbons. A carbon that has been chemically changed to form a tiny porous structure is known as AC. AC generates materials that are good at adsorbing a range of chemical species because of its surface functionality. It is noted for having a high-surface-area-to-volume ratio, making it an effective adsorbent material [96, 97]. As a result, it is frequently used as an adsorbent in cholesterol reduction, internal gas reduction, poisoning, flatulence reduction, and other applications [98, 99]. Historically, AC was primarily utilized for cleansing air and water supply in the previous century, and demand for its expansion significantly. Carbon fibers were invented in the 1950s, paving the door for a new lightweight and extraordinarily strong material.

Traditionally, AC has been manufactured from biomass precursors such as lignocellulosic materials (palm kernel shells, olive bagasse, oil palm trunks, oil palm empty fruit bunches, olive cake, date palm seeds, wood, coconut shells, rice husk, and so on) [97–103], various types of coal, or other types of carbon [24]. The starting raw material is frequently annealed in a reducing environment to form a carbonaceous surface during the manufacturing process. To improve the material's surface even more, the process is followed by activation of chemical oxidation or heat treatment. It is vital to keep in mind that not all ACs are created the same way or have the same physicochemical characteristics. A carbon material with a wide set of surface qualities can come from a variety of starting materials, various activation procedures, and operating settings, among other things. These characteristics are assumed to be

connected to the pore size distribution of the activated surface and the types of functional groups present in the pores [101, 102, 104–109]. According to a data from the worldwide AC industry, in the global market, the price of AC increased rapidly between 2007 and 2012. Similarly, in 2013, there was a significant increase. The worldwide AC market was anticipated to be valued 2.23 billion USD in 2013 due to severe regulatory limitations on mercury removal in power plants, and the industry was expected to grow at a compound annual rate of 5% through 2018.

Tab. 1.1: The characteristics of carbon allotropes are compared.

Carbon allotropes	Properties
Carbon nanotubes	– Electronic properties are based on chirality, length, and diameter of CNTs – Requires functionalization to minimize hydrophobicity – Tends to aggregate, owing to strong van der Waals contact – Electronic processes are dependent on chirality, length, and diameter of CNTs
Graphene	– Excellent surface-to-volume ratio – Can be used for different sensing modalities based on their electronic, surface-enhanced Raman scattering, and fluorescence features – Conductivity of graphene can be altered by the attachment of analyte
Carbon dots	– Have controllable fluorescence – Can be excitation dependent or independent – Have many surface moieties – Doping and cross-linking can increase sensing capabilities – Flexibility in choosing the starting precursors
Nanodiamonds	– The nitrogen-vacancy center influences the fluorescence – Photobleaching susceptibility – Fluorescence is susceptible to magnetic field variations
Activated carbon	– Nonhazardous carbon-bearing substance with a highly porous and a large interior surface area – Stable structure at high temperatures in the absence of air – Physically bind components using the van der Waals force or the London dispersion force

1.3 Properties

A diversity of features of several selected carbon nanoparticles were provided in Tab. 1.2. The intrinsic strength of carbon nanostructures (particularly graphene), which has been proven to outperform any other material [113], is 200 times stronger than steel but flexible, which has piqued the scientific community's interest. Furthermore, when pure, it is nearly 97% transparent [110], extremely stable, and chemically inert materials with a large surface area that can be expanded by around 20% [111]. This, together with a plethora of other qualitative features, made graphene a "very promising competitor" for a range of applications, including energy storage. The graphene family includes GO, reduced GO (rGO), GQDs, and other related materials. The GO has been modified by a number of scientists throughout the years after its discovery in 1859, including Staudenmaier [112], Hummers [113], and Offeman [113] in 1898, 1898, and 1958, respectively.

When completely oxidized, the modified GO possesses turbostratic random ordering with sixfold symmetry of stacking and an interlayer spacing of 0.625 nm. It was possible to intercalate H_2O molecules between layers with interlayer spacing varying from 6.4 to 11.3 nm because of GO's strong water affinity [114, 115].

Due to its affinity for water, GO is well suited for electrical applications because thin films of it may be evenly formed on the substrate surface. As a result, GO is thought to be one of the most appropriate precursors for commercial manufacture of modified graphene-like structures with well-situated mechanical, transport, electrical, and optoelectronic capabilities [116].

Tab. 1.2: A comparison of characteristics of graphite and diamond, both well-known allotropes of carbon.

Properties	Graphene	Diamond
The structure and system of crystals	Hexagonal, with noticeable lamellar veins and earthen masses	Isometric; cubes and octahedrons
Specific gravity	2.2	3.5
Density (g/cm^3)	2.267	3.52
Pigment/ presence	Brown	Pale yellows, browns, and earth tones, as well as white, blue, black, crimson, greenish, colorless, and sparkling
Stiffness (Mohs)/ field indicator	1–2; luster, density, and streak are soft, greasy, soapy, and oily	10; extremely hard
Shine	From shiny to filthy	Clumpy to adamantine

Tab. 1.2 (continued)

Properties	Graphene	Diamond
Cleavage	Perfect in one direction	Perfect octahedrons in four directions
Transparency	Virtually transparent to light	In rough crystals, the crystals are clear to translucent
Fracture properties	Crumbly	Conchoidal
Electrical and heat conductivity (E&H)	Highly conductive towards both E & H	Poor electrical conductor; good thermal conductor
Burning in the air	900 °C	900 °C

1.4 Synthesis methods of carbon allotropes

Carbon allotropes are created by reorganizing carbon atoms from carbon precursors such as graphite, organic gases, green organic compounds, or volatile organic compounds using various synthetic techniques. The preparation procedures for CNTs, CDs, graphene, and NDs will be thoroughly addressed and reviewed in this section.

1.4.1 Carbon nanotubes

The arc-discharge method, chemical vapor deposition (CVD), and laser ablation methods are the three basic approaches for producing CNTs. Arc discharge is performed in a vacuum chamber with two carbon electrodes as the predecessor. To speed up carbon deposition and create MWCNTs with near-perfect shape, the chamber is filled with inert gas. The creation of SWCNTs requires a similar set of conditions but with the addition of catalysts including Ni, Fe, Co, Pt, and Rh. Laser ablation, on the other hand, uses a strong laser pulse and a catalyst to hit a carbon target in a furnace filled with inert air. The carbon precursor will be vaporized, and a graphene film will form on the substrate as a result of the laser beam bombardment. Despite the ability to create high-quality CNTs, both procedures necessitate high preparation temperatures of around 3,000–4,000 °C to evaporate the carbon atoms from the carbon precursor. The CVD process, on the other hand, may be utilized to make CNTs at a significantly lower temperature.

1.4.2 Graphene

Graphene is often prepared by mechanical exfoliation, which involves a repetitive peeling procedure with Scotch tape to produce tiny graphene flakes. The energy needed to exfoliate graphite into single-layer graphene is offset by the solvent–graphene interaction, which governs the exfoliation mechanism. Nevertheless, this liquid exfoliation approach suffers from the incapability to control the number of graphene layers, flaws, as well as difficulties to remove the leftover solvents, which can have an unfavorable effect when utilized as a sensing material on OFS-Optical fiber sensor. The reduction of GO is another chemical method for obtaining graphene. The key disadvantage of this method is that the reduction procedure is unable to entirely reduce the GO. This technique also produces flaws that cannot be removed by annealing and is usually of worse grade than pure graphene. Reduced graphene oxide is a term used to describe the end product.

1.4.3 Carbon dots

The top-down and bottom-up approaches are the two most common approaches for creating CDs. Optical, chemical, and thermal methods can be used to carry out these synthesis approaches. A laser is often used to ablate a carbon target in water or solvents in the optical synthesis process. Prior to the creation of CDs, the carbon precursor typically goes through numerous processes such as dehydration, polymerization, and carbonization. To induce the carbonization process, the carbon precursor is subjected to direct heat treatment at a high temperature. However, this pyrolysis technique looks to be less favorable because it is time-consuming, with heating times ranging from a few hours to several days. As a result, microwave-assisted synthesis emerges as a convenient option because it is quick, consistent, and can be done in a home microwave oven.

1.4.4 Nanodiamonds

Detonating an explosive carbon precursor such as TNT or hexogen (1,3,5-triazinane) is a common way to make NDs. The detonation process takes place in a sealed chamber with either an inert gas or a water coolant, often known as the “dry” or “wet” synthesis. The carbon soot contains a mixture of NDs with a diameter of 4–5 nm, various carbon allotropes, and impurities after the detonation process. The weight concentration of NDs in carbon soot can be as high as 75%, while the yield of NDs is roughly 4–10% of the explosive precursor’s weight. Pressures and temperatures were discovered to have a substantial influence on the development of NDs in a study. Although the temperature and pressure at the Jouguet point are insufficient

to make liquid bulk carbon, they can produce nanosized liquid carbon. For nanocarbon, the area of liquid carbon is shifted to a lower temperature, while the area of stability of NDs is shifted to a greater pressure.

As a result, it is assumed that NDs are created by homogeneous nucleation in supersaturated carbon vapor, followed by liquid carbon condensation and crystallization. The NDs tend to clump and are not dispersible in organic solvents or water, which is a major disadvantage of this approach. To make matters worse, ND aggregates are frequently covered with a layer of graphitic material, which makes ND dispersion much more difficult. Mechanical milling or ultrasonication can be used to break down the ND aggregates.

To attain particle dimension in the nanoscale range, the NDs were homogeneously nucleated by dissociating ethanol vapor and promptly quenched with a reaction time of less than 1 ms. The non-diamond phase is eliminated with the help of hydrogen gas, while the diamond phase is maintained and stabilized, resulting in a high-purity NDs. The average size of NDs produced is 3 nm, which is consistent with theoretical calculations. The production methods for each form of carbon allotrope are summarized in Tab. 1.3.

Tab. 1.3: Comparison of synthesis approaches for carbon allotropes.

Types of carbon allotropes	Synthesis methods	Advantages	Disadvantages
Carbonnanotubes	Arc discharge	– Can provide high-quality CNTs – Simple apparatus – High reproducibility	– High synthesis temperature – Contaminated with impurities
	Chemical vapor deposition	– Lower synthesis temperature – Uses hydrocarbon gas as the precursors – Different types of CNTs can be prepared by varying the precursors	– Contaminated with impurities – Requires many optimization processes from the catalyst preparation to the CVD reaction
	Laser ablation	– Higher yield and greater purity than arc-discharge method	– High synthesis temperature – Contaminated with impurities

Tab. 1.3 (continued)

Types of carbon allotropes	Synthesis methods	Advantages	Disadvantages
Graphene	Mechanical exfoliation	– Simple procedure – High-quality graphene	– Low yield
	Liquid exfoliation	– Large-scale production	– Difficult to control the number of layers and defects – Difficult to remove residual solvents
	Chemical treatment	– Large-scale production	– Requires harsh chemicals – Long duration
Carbon dots	Optical	– Simple experimental setup – Can tune the dimension of CDs by adjusting experiment parameters	– Low yield
	Chemical	– High yield – Large-scale production – Inexpensive apparatus	– Requires harsh chemicals – Environmentally unfriendly
	Thermal	– Rapid process – Can be prepared using simple apparatus such as domestic microwave oven – Can be carried out without harsh chemicals	– Uneven heating – Large-size distribution
Nanodiamonds	Detonation	– Can be prepared from precursors such as old munitions	– Requires purification – High synthesis temperature
	Pulsed laser	– Can be carried out in water – Environmentally friendly procedure	– Resultant product contains impurities

1.5 Applications

Material science and nanotechnology have witnessed enormous progress in recent years in virtually all industrial sectors. This is due to a number of important advantages that traditional manufacturing cannot offer. Mass customization, geometrical intricacy, and so forth are examples of these. Medical [117], defense components, aerospace, home and energy-related uses [29], car, and other applications are shown in Tab. 1.4. Carbon nanoparticle application in the global energy scene has gained a lot of attention in the current years.

Tab. 1.4: Carbon nanoparticles used in a variety of applications, each with its own set of features.

	Characteristics	Applications
Why carbon nanomaterials?	High current density, high electron mobility, high thermal conductivity, metallic/semiconductive properties, highly opaque and permittivity properties	Transparent thin films, for instance, have been used in electronics, transistors, LSI wiring, etc.
	Nonscale configurations, high surface area, ion absorption, catalysis support	Capacitors, fuel cells, and lithium-ion batteries are examples of energy storage applications
	Lightweight, nanostructures, metallic/semiconductive properties, slim and strong, high thermal conductivity, high electrical conductivity, nanostructures, high physical strength	Nanotechnology applications such as automotive, defense, aerospace
	High-affinity binding, strong absorption, high surface area	Biotechnology applications such as biosensors, cell cultivating, drug delivery systems, etc.

1.5.1 Electrochemical energy storage (nanoenergy) application

When we examine the global energy future thoroughly, we can see that the scientific community has given the energy concerns of the twenty-first century a lot of attention. The problem occurred as a result of the rapidly depleting fossil fuel supplies. It is well understood that fossil fuels are neither ecologically friendly, sustainable, nor renewable energy sources [118]. Electrochemical devices for electric power applications, such as supercapacitors, fuel cells, and other energy storage technologies, are widely known, and the process is achieved by electrolysis. The chemical process that produces electrical energy utilizing fuel cells is regarded safe and environmentally friendly because it produces no toxic gases (usually greenhouse gases) that are generally thought to be harmful to the atmosphere [5, 49, 119, 120]. Despite all of these benefits, it is perplexing that fuel cells can only be employed properly with electrocatalyst. The electrocatalyst speeds up oxygen reduction processes in the cell in general [121]. Due to its superior electrocatalytic activity when compared to other catalysts, most commonly used catalyst for the purpose is platinum. The catalyst, on the other hand, is both costly and unreliable. As a result, researchers felt it was vital to come up with new approaches to improve their performance while lowering production costs. As a result, frontline carbon-based materials like graphene and its derivatives are being explored as platinum substitutes. Carbon-based compounds have the advantage of being less expensive than metal catalysts such as platinum. New hybrid

nanoplatelets with remarkable catalytic properties in alkaline settings were developed, utilizing GQDs generated and self-assembled on graphene by a hydrothermal method, outperforming commercial Pt/C [122]. As a result, the clear prospect of creating carbon-based nanomaterials from renewable sources may be able to supply the energy needs of the twenty-first century, perhaps replacing fossil fuel sources. CNTs [123–125], graphene, AC, and other materials have been used to improve the standard and recharge time of supercapacitor–battery hybrids, supercapacitors, and lithium batteries. When porous GO was examined, it was found to have ultra-high capacitances of 283 F/g and 234 F/cm^3. Capacitance of 1,100 F/cm^3 was reached by mixing graphene with manganese dioxide (MnO_2). It is fascinating to think that these materials may be used to store massive amounts of power generated by more efficient solar panels more effectively. Similarly, electric vehicle range, recharge time, and dependability will be improved, and they will become substantially less expensive [126].

1.5.2 Biomedical application

Due to its ultrahigh surface area (2,630 m^2/g) [120] and sp^2-hybridized carbon area, graphene (an exceptionally resourceful carbon nanomaterial) has been used as an efficient drug transporter to load vast numbers of drug molecules on both sides of the single atom layer sheet. Dai et al. [127] were the first to think of a medication delivery application. These researchers discovered that physisorption via stacking can be used to load anticancer medicines such as SN38. It is worth noting that graphene and other graphene-related and derived materials have recently received a lot of attention in the field of biomedicine, and they have a promising future ahead of them. In the realm of biosensing technology, carbon nanomaterials (e.g., graphene-based materials) have been used to construct a variety of biosensors based on different sensing modalities, such as optical and electrochemical signaling [128]. The electrochemical technique has been described as one of the most effective methods for detecting biomolecules [129]. This was due to its ease of use, outstanding sensitivity, low cost, and quick reaction. Graphene is presently being employed as an electrode material to increase biomolecule detection due to its enticing electrochemical properties. For example, graphene has demonstrated outstanding electrocatalytic activity toward H_2O_2; this 2D carbon crystal may now be used as an electrode material for oxidase-based biosensors. Detecting glucose levels in the patient's body is obviously critical for the diagnosis of diabetes. As a result, glucose oxidase could be used as a mediator or detecting element in electrochemical detection of glucose in the blood [130]. In one remarkable work, Dan Du et al. developed a sensitive cancer biomarker immunosensor based on a dual-signal amplification approach involving graphene sheets and multienzyme-functionalized carbon nanospheres. In comparison to an immunosensor without graphene modification or carbon nanosphere labeling, the immunosensor was shown to have a sevenfold increase in detection signal [135]. As a result, this

amplification approach might be particularly useful for evaluating tumor biomarkers in the clinic and developing point-of-care diagnostics.

1.5.3 Nanoelectronics

Nanoelectronics is the application of nanotechnology in the realm of electronic systems. Nanoelectronics is a vast subject that includes, among other things, electrical devices, mechanical devices, biodevices, and chemical devices [131–133]. In order to produce more efficient electronic systems, nanotechnology is used to construct new components by combining them with electronic components [131–133]. Displays, radios, new optoelectronic devices, quantum computers, computers, memory storage, and other nanoelectronic devices are all examples of nanoelectronic devices. GR has been used in the realm of nanoelectronics because of its extraordinarily high conductive qualities [133, 134]. It boasts a zero bandgap, a large surface area, rapid electron mobility, and many other important characteristics that contribute to its uniqueness [134]. Every modern micro-chip is produced in today's world of ever-evolving technology. Nanotechnology is the answer to these production problems [134]. Nanotechnology has contributed significantly to transistor chips, interconnects, and integrated circuits (IC). According to the recent research, GR can be used in "interconnects in all computer chips" [131, 133–136]. Interconnects are the electrical channels that link transistors and other circuit components [131, 135, 136].

Graphene, a wonderful and wonder material, has several applications in a number of sectors. Because of its excellent operating abilities, low cost, and simplicity of supply, it has found applications in sectors such as nanoelectronics, bioenergy, nanobiotechnology, nanosensors, and nanocatalysis [53, 131, 137–141]. Since the discovery of graphene, several major corporations such as IBM, Samsung, Apple, and Lockheed Martin have used graphene and its derivatives to develop next-generation electronic devices [53, 137–141]. China has filed almost 2,200 patents on GR, according to Cambridge IP, a British patent firm. The United States came in second with over 1,700 patents, followed by South Korea with approximately 1,200 patents [137, 141]. GR, although a lot of progress, still has a long way to go before it can be commercialized. Figure 1.4 [131] detailed some of GR's contributions to many fields. In the following sections, we will go through some of the most cutting-edge graphene applications in science and technology [131, 137].

Interconnects act as an umbilical cord, linking the elements of the IC to the outside environment [136, 139–141]. The copper metal used as interconnects earlier had a multitude of defects that could only be corrected by GR. Copper interconnects are also smaller in compact computer chips; however, this increases copper resistance and hence decreases conductivity [131, 133–136, 142, 143]. GR has smooth electron transmission even at room temperature and lower because of its unique band structure, leading to low resistance and high conductivity [134]. The use of GR can help

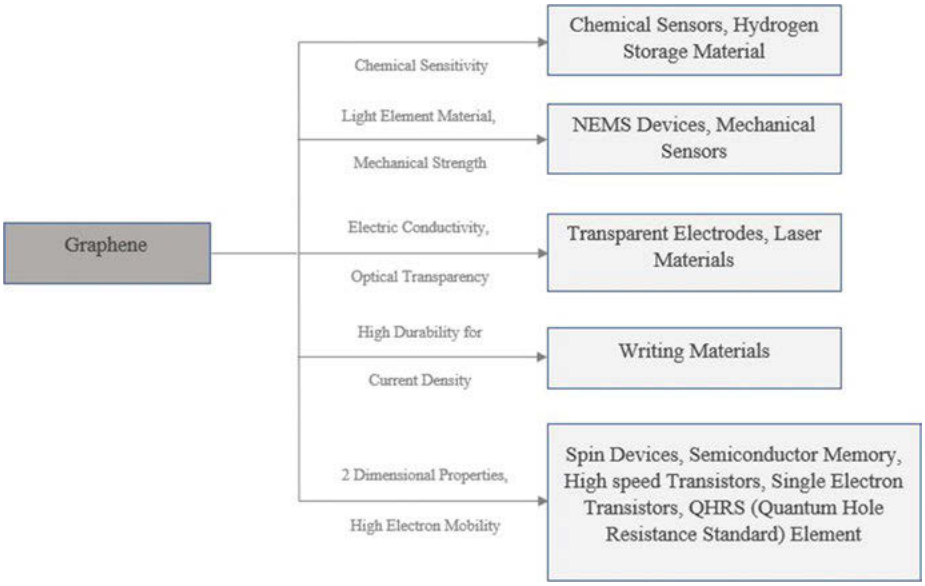

Fig. 1.4: The chart shows a wide range of application of GR in various fields of science and technology.

silicon-based IC technology to last longer [134, 143]. Apart from improved resistivity in GR, interconnects also have improved electron transport, thermal and mechanical strength, and capacitance. Transistors are another widely used application of GR. A transistor is a semiconductor device used in a wide range of electronic devices. Electronic signals and equipment are switched and amplified using it [143, 144]. The transistor revolutionized IC technology, opening the way for smaller calculators, more affordable radios, and computers, among other advancements. This is why the transistor is included in IEEE's list of electronic milestones. The preparation of field-effect transistors (FET) has received a lot of attention. Semiconductor factories are relatively expensive due to the complexity of IC manufacturer. A recent achievement in digital logics is the creation of smaller silicon metal–oxide–semiconductor FETs. For high-speed applications, FETs require short gates and fast carriers in the channel (Fig. 1.5) [144, 145]. According to the scaling theory, FETs with a thin barrier and a tiny gate-controlled region should be protected from short-channel effects down to very short gate lengths [143–145]. Perhaps, the most tempting characteristic of GR for transistor applications is the ability to have channels that are just one atomic layer thick [145].

Changing the cooking mix has increased the chances of the "wonder material" GR achieving its promise in electronics [134]. Optoelectronic devices such as touch screens, monitors, solar cells, and LEDs require materials with low sheet resistance and high transparency [150–152]. New fields of research are currently focusing on the usage of GR in display screens. The rising cost of indium tin oxide (ITO), which

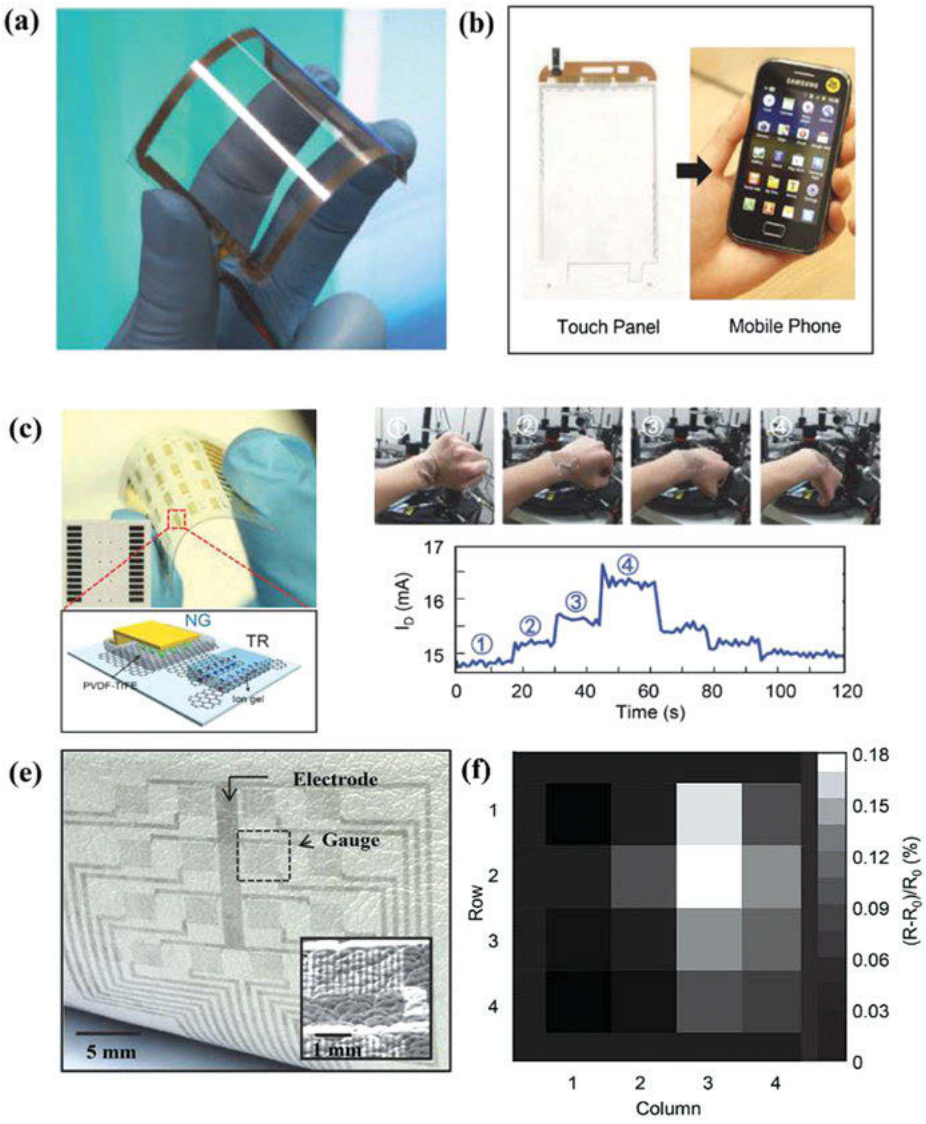

Fig. 1.5: (a, b) Graphene-based resistive-type touch panel (a) and capacitive-type touch panel (b) that is integrated into a smart phone. (a) Reproduced with permission [146], Copyright 2010, Nature Publishing Group. (b) Reproduced with permission [147], Copyright 2014, American Chemical Society. (c) Optical image and schematic illustration of active matrix strain sensors consisting of graphene and PVDF connected by an ion gel. (d) An example of motion monitoring and the corresponding current change in the time domain. Reproduced with permission [148], Copyright 2015, Wiley-VCH. (e) Optical image and SEM image (inset) of the graphene-based conformal strain sensor arrays. (f) Relative resistance change of the graphene strain sensor array when a pressure of 9 kPa is applied. Reproduced with permission [149], Copyright 2014, American Chemical Society.

is used in displays, has pushed GR into the limelight as a potential substitute [131, 132]. ITO has a number of drawbacks, including the fact that it is scarce and fragile, posing a danger of breaking, and being environment-sensitive. GR, on the other side, is extremely robust, translucent, and has a lower resistance [144, 145]. In modern technologies, using GR in photovoltaic devices (devices that convert light into electricity; see Fig. 1.6) has also been a difficulty. Photovoltaic technology is now based on silicon cells, which have a 25% efficiency. In solar cells, GR can serve as a transparent voltage window, a photoactive material, a charge transport channel, and a catalyst, among other things.

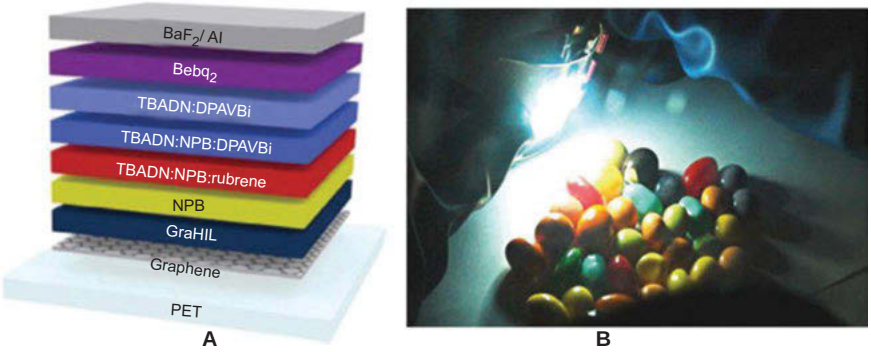

Fig. 1.6: (A) Structure of OLED and (B) highly flexible OLED lighting device with a graphene anode on a 5 cm × 5 cm PET substrate (© Nature Publishing Group. Reproduced with permission from T. H. Han et al. [153]; permission to reuse must be obtained from the rights holder).

Organic light-emitting diodes (OLEDs) feature electroluminescent layers between charge injecting electrodes, at least one of which is transparent [46, 153, 154]. Digital displays such as television screens, computer monitors, and mobile phones use OLEDs [154–157]. ITO can be used as a transparent electrode with a 4.4–4.5 eV work function. However, due to ITO's numerous drawbacks, it is swiftly superseded by GR, which has a similar work function of 4.5 eV [153, 158]. Many changes were made to GR in order to improve the work function and provide better outcomes. Tae-Woo Lee and colleagues at Korea's Pohang University of Science and Technology found a way for increasing the work function of GR layers to around 6 eV [158]. The scientists also claimed that by doping with chemicals like HNO_3 and $AuCl_3$, the sheet resistance might be reduced to 30 V/sq [132, 159, 160]. GR absorbs wavelengths ranging from ultraviolet to terahertz (THz). As a result, GR could be highly beneficial in photodetectors. Photodetectors are sensors that detect light or electromagnetic radiation. Photodetectors based on GR can work over a wider range of wavelengths. Solid-state technology devices are used to detect or sense light [132, 159, 160]:

- carrier production in a semiconducting layer by absorption of an incoming photon;
- if available, carrier transportation and application; and
- photogenerated carriers are extracted as a junction or device current.

1.5.4 Carbon allotropes in corrosion inhibition

The ionic resistance of polymer coatings is increased by corrosion protection mechanisms, which may be explored in the case of GO and/or functionalized carbon nanofillers with negative charges on their surface. The negative charges on the surface of carbon-based nanofillers prevent Cl^- and OH^- anions from permeating into the coatings. As a result, the number of Cl^- anions at the coating–metal contact falls. Furthermore, OH^- anions formed in the cathodic reactions at the coating–metal contact do not permeate into the coating, preventing delamination. Furthermore, carbon-based nanomaterials are classified as conductive (CB, graphene, and CNT), semiconductive (CDs), or insulating (GO) nanofillers. Electrically conductive carbon-based nanoparticles can be employed in conductive polymer coatings to boost electrical conductivity while also improving the barrier performance of the conductive polymer matrix. Furthermore, these conductive nanomaterials might be used in coatings with cathodic protection mechanisms, such as zinc-rich epoxy coatings, to enable electrical contact between zinc particles while reducing zinc particle loading and enhancing barrier protection against corrosive agent diffusion.

1.6 Future prospects

1.6.1 Searching for more carbon allotropes

1.6.1.1 Theoretical design of more carbon allotropes

We learned how to construct new carbon allotropes by changing the elemental structures (carbon atoms or C–C bonds) in the two most fundamental carbon materials – graphene and diamond – by comparing the structural topology of current carbon allotropes in the above. Allotropes produced from graphene (diamond) are always in a 2D (3D) configuration because the derivative structure inherits the dimensionality of the mother structure. With the use of first-principles calculations, new carbon allotropes can be anticipated in a systematic fashion along this path. By recursively employing this design technique, it is feasible to create more complicated structures. The twin-graphene, for example, can be thought of as the covalent bonding of two graphene single layers. Repetition of this twin process will result in

a new structure with a finite thickness four times that of graphene. As a result, the theoretical designing method can result in an infinite number of carbon-based allotropes.

1.6.1.2 More experimental studies needed

New allotropes are sometimes discovered experimentally and subsequently theoretically evaluated, as was the case with the discovery of C60 buckyball. The exact atomic structure of a freshly discovered allotrope was still a difficulty for theoreticalists few decades ago. However, with the rapid advancement of observation tools, theoreticalists can now investigate the structure of new materials on an atomic level, making it easier for them to determine the real configuration of the new allotrope when it is synthesized in the lab. Theoreticalists, on the other hand, are now able to create novel carbon allotropes in a systematic manner, owing to advances in computational speed and the rapid growth of the first-principles calculation technique. Theoretically, many carbon allotropes with novel hypothetical configurations have been predicted. The experimental verification of these projected carbon allotropes is a major difficulty because the experiment's output frequently contains a large number of distinct allotropes. The T-carbon, for example, was originally predicted theoretically in 2011 and confirmed empirically in 2017. More experiments are needed to confirm these new carbon allotropes' theoretical predictions.

1.7 Conclusions

To summarize, this analysis has demonstrated how carbon nanomaterials have piqued the interest of scientists from several domains, including materials science, chemistry, and engineering, and condensed matter physics, as well as from both industry and academia. Thus, in recent years, the development of new carbon nanomaterials such as graphene, CNTs, and other carbon nanomaterials has undoubtedly aided the science of nanotechnology; their unique properties have proven invaluable in a variety of technologies such as electronics, optics, and energy storage. All of this has been made possible by the material's distinctiveness, which is closely linked to their extraordinary qualities and their nanoscale structure, which is unrivaled by any other known substance that aids them. Furthermore, structural illustrations of some 0D, 1D, 2D, and 3D carbon nanomaterials with sp^2 and sp^3 hybridization allotropes occurring in various crystallographic forms revealed that carbon nanomaterials/allotropes encompass or represent a group of materials with a variety of structure, morphology, and properties, but with one major common element, carbon, as the main building block of their structures. Carbon's chemical flexibility (especially its ability

to catenate) is what allows it to transition from sp^2 to sp^3 hybridization and interact with other atoms. This backs up the belief that carbon is one of the most beautiful elements on the periodic table, as well as one of the most crucial on our planet. It is also worth mentioning that the synthesis of carbon nanostructures from biomass resources has progressed significantly. Exploring the maximum potentials for greener and more ecologically friendly synthesis procedures and industrial-scale production of these materials, on the other hand, is unquestionably required and may thus be considered as the focus point of many scientists and engineers in the twenty-first century. As a result, this will aid in the reduction of the world's most dreaded energy and environmental challenges, particularly in developing countries.

Websites

https://www.ncbi.nlm.nih.gov/pmc/articles/PMC5848992/
https://www.nature.com/articles/nmat2885
https://www.bbc.co.uk/bitesize/guides/zjfkw6f/revision/4
https://www.britannica.com/science/carbon-chemical-element/Structure-of-carbon-allotropesallotropes

References

[1] Zhang, Y.; Yin, Q.-Z. Carbon and other light element contents in the earth's core based on first-principles molecular dynamics. Proc. Natl. Acad. Sci. U.S.A. 2012, 109(48), 19579–19583, doi:10.1073/pnas.1203826109.
[2] Allègre, C.J.; Poirier, J.-P.; Humler, E.; Hofmann, A.W. The chemical composition of the Earth. Earth Planet. Sci. Lett. 1995, 134(3), 515–526, doi:10.1016/0012-821X(95)00123-T.
[3] Pace, N.R. The universal nature of biochemistry. PNAS. 2001, 98(3), 805–808, doi:10.1073/pnas.98.3.805.
[4] Marty, B.; Alexander, C.M.O.; Raymond, S.N. Primordial Origins of Earth's Carbon. Rev. Mineral. Geochem. 2013, 75(1), 149–181, doi:10.2138/rmg.2013.75.6.
[5] Titirici, -M.-M. et al. Sustainable carbon materials. Chem. Soc. Rev. 2014, 44(1), 250–290, doi:10.1039/C4CS00232F.
[6] Marcio Loos. https://scholar.google.com.br/citations?user=3pcn0qAAAAAJ&hl=pt-BR (accessed Dec. 24, 2021).
[7] Deng, J.; You, Y.; Sahajwalla, V.; Joshi, R.K. Transforming waste into carbon-based nanomaterials. Carbon. 2016, C(96), 105–115, doi:10.1016/j.carbon.2015.09.033.
[8] The role of carbon materials in heterogeneous catalysis – ScienceOpen. https://www.scienceopen.com/document?vid=5ed33b82-2a35-4cbc-9836-af7ddbcc2057 (accessed Dec. 24, 2021).
[9] Allen, M.J.; Tung, V.C.; Kaner, R.B. Honeycomb carbon: A review of graphene. Chem. Rev. 2010, 110(1), 132–145, doi:10.1021/cr900070d.
[10] The rise of graphene | Nature Materials. https://www.nature.com/articles/nmat1849 (accessed Dec. 24, 2021).

[11] Novoselov, K.S.; Fal'ko, V.I.; Colombo, L.; Gellert, P.R.; Schwab, M.G.; Kim, K. A roadmap for graphene. Nature. 2012, 490(7419), 192–200, doi:10.1038/nature11458.
[12] Stankovich, S. et al. Synthesis of graphene-based nanosheets via chemical reduction of exfoliated graphite oxide. Carbon. 2007, 45(7), 1558–1565, doi:10.1016/j.carbon.2007.02.034.
[13] Zhu, Y. etal. Carbon-based supercapacitors produced by activation of graphene. Science. 2011, 332(6037), 1537–1541, doi:10.1126/science.1200770.
[14] Gadipelli, S.; Guo, Z.X. Graphene-based materials: Synthesis and gas sorption, storage and separation. Prog. Mater. Sci. 2015, 69, 1–60, doi:10.1016/j.pmatsci.2014.10.004.
[15] 2D materials. Graphene, related two-dimensional crystals, and hybrid systems for energy conversion and storage – PubMed. https://pubmed.ncbi.nlm.nih.gov/25554791/ (accessed Dec. 24, 2021).
[16] Sun, M.-J.; Cao, X.; Cao, Z. Si(C≡C)4-based single-crystalline semiconductor: Diamond-like superlight and superflexible wide-bandgap material for the UV photoconductive device. ACS Appl. Mater. Interfaces. 2016, 8(26), 16551–16554, doi:10.1021/acsami.6b05502.
[17] Chen, Y. etal. Reduced graphene oxide films with ultrahigh conductivity as li-ion battery current collectors. Nano Lett. 2016, 16(6), 3616–3623, doi:10.1021/acs.nanolett.6b00743.
[18] Georgakilas, V. et al. Noncovalent functionalization of graphene and graphene oxide for energy materials, biosensing, catalytic, and biomedical applications. Chem. Rev. 2016, 116(9), 5464–5519, doi:10.1021/acs.chemrev.5b00620.
[19] Peng, W.; Liu, S.; Sun, H.; Yao, Y.; Zhi, L.; Wang, S. Synthesis of porous reduced graphene oxide as metal-free carbon for adsorption and catalytic oxidation of organics in water. J. Mater. Chem. A. 2013, 1(19), 5854–5859, doi:10.1039/C3TA10592J.
[20] Liu, J.; Cui, L.; Losic, D. Graphene and graphene oxide as new nanocarriers for drug delivery applications. Acta Biomater. 2013, 9(12), 9243–9257, doi:10.1016/j.actbio.2013.08.016.
[21] Sharma, D.; Kanchi, S.; Sabela, M.I.; Bisetty, K. Insight into the biosensing of graphene oxide: Present and future prospects. Arabian J. Chem. 2016, 9(2), 238–261, doi:10.1016/j.arabjc.2015.07.015.
[22] Usman, M.S.; Hussein, M.Z.; Fakurazi, S.; Ahmad Saad, F.F. Gadolinium-based layered double hydroxide and graphene oxide nano-carriers for magnetic resonance imaging and drug delivery. Chem Cent J. 2017, 11(1), 47, doi:10.1186/s13065-017-0275-3.
[23] Gurunathan, S.; Han, J.W.; Kim, E.S.; Park, J.H.; Kim, J.-H. Reduction of graphene oxide by resveratrol: a novel and simple biological method for the synthesis of an effective anticancer nanotherapeutic molecule. Int. J. Nanomedicine. 2015, 10, 2951–2969, doi:10.2147/IJN.S79879.
[24] Khadiran, T.; Hussein, M.Z.; Zainal, Z.; Rusli, R. Activated carbon derived from peat soil as a framework for the preparation of shape-stabilized phase change material. Energy. 2015, 82(C), 468–478.
[25] Zhang, Y.; Zhou, G.; Lin, K.; Zhang, Q.; Di, H. Application of latent heat thermal energy storage in buildings: State-of-the-art and outlook. Build. Environ. 2007, 42, 2197–2209, doi:10.1016/j.buildenv.2006.07.023.
[26] Baetens, R.; Jelle, B.P.; Gustavsen, A. Phase change materials for building applications: A state-of-the-art review. Energy Build. 2010, 42(9), 1361–1368, doi:10.1016/j.enbuild.2010.03.026.
[27] Kalnæs, S.E.; Jelle, B.P. Phase change materials and products for building applications: a state-of-the-art review and future research opportunities. Energy Build. 2015, doi:10.1016/J.ENBUILD.2015.02.023.
[28] Pielichowska, K.; Pielichowski, K. Phase change materials for thermal energy storage. Prog. Mater. Sci. 2014, 65, 67–123, doi:10.1016/j.pmatsci.2014.03.005.

[29] Application of Nano-technologies in the Energy Sector – Hessen – there's no way around us. https://www.readkong.com/page/application-of-nano-technologies-in-the-energy-sector-2557046 (accessed Dec. 24, 2021).
[30] Wu, Y. et al. High-frequency, scaled graphene transistors on diamond-like carbon. Nature. 2011, 472(7341), 74–78, doi:10.1038/nature09979.
[31] Deng, J.; Li, M.; Wang, Y. Biomass-derived carbon: synthesis and applications in energy storage and conversion. Green Chem. 2016, 18(18), 4824–4854, doi:10.1039/C6GC01172A.
[32] Chang, R. Chang chemistry, 9th Edition, McGraw Hill Higher Education, USA, 2007.
[33] C60: Buckminsterfullerene | Nature. https://www.nature.com/articles/318162a0 (accessed Dec. 24, 2021).
[34] Iijima, S. Helical microtubules of graphitic carbon. Nature. 1991, 354(6348), 56–58, doi:10.1038/354056a0.
[35] Novoselov, K.S. et al. Electric field effect in atomically thin carbon films. Science. 2004, 306 (5696), 666–669, doi:10.1126/science.1102896.
[36] Functionalization of Single-Walled Carbon Nanotubes – Hirsch – 2002 – Angewandte Chemie International Edition – Wiley Online Library. https://onlinelibrary.wiley.com/doi/abs/10.1002/1521-3773%2820020603%2941%3A11%3C1853%3A%3AAID-ANIE1853%3E3.0.CO%3B2-N (accessed Dec. 24, 2021).
[37] Jain, R.; Pandey, A.; Pandeya, S.S. Mechanism of dissolution of delayed release formulation of diclofenac sodium. 9.
[38] Bahr, J.L.; Yang, J.; Kosynkin, D.V.; Bronikowski, M.J.; Smalley, R.E.; Tour, J.M. Functionalization of carbon nanotubes by electrochemical reduction of aryl diazonium salts: a bucky paper electrode. J. Am. Chem. Soc. 2001, 123(27), 6536–6542, doi:10.1021/ja010462s.
[39] Agnihotri, S.; Mota, J.P.B.; Rostam-Abadi, M.; Rood, M.J. Structural characterization of single-walled carbon nanotube bundles by experiment and molecular simulation. Langmuir. 2005, 21(3), 896–904, doi:10.1021/la047662c.
[40] Gao, S.; Zhuang, R.-C.; Zhang, J.; Liu, J.-W.; Mäder, E. Glass Fibers with Carbon Nanotube Networks as Multifunctional Sensors. Adv. Funct. Mater. 2010, 20(12), 1885–1893, doi:10.1002/adfm.201000283.
[41] Jain R, D.M.;. Method validation for stability indicating method of related substance in active pharmaceutical ingredients dabigatran etexilate mesylate by reverse phase chromatography. J. Chromatogr. Sep. Tech. 2014, 06(02), doi:10.4172/2157-7064.1000263.
[42] Niyogi, S. et al. Chemistry of single-walled carbon nanotubes. Acc. Chem. Res. 2002, 35(12), 1105–1113, doi:10.1021/ar010155r.
[43] Conductivity enhancement in single-walled carbon nanotube bundles doped with K and Br | Nature. https://www.nature.com/articles/40822 (accessed Dec. 24, 2021).
[44] Claye, A.S.; Fischer, J.E.; Huffman, C.B.; Rinzler, A.G.; Smalley, R.E. Solid-State Electrochemistry of the Li Single Wall Carbon Nanotube System. J. Electrochem. Soc. 2000, 147(8), 2845, doi:10.1149/1.1393615.
[45] Ma, J.; Jin, W.; Ho, H.L.; Dai, J.Y. High-sensitivity fiber-tip pressure sensor with graphene diaphragm. Opt. Lett. OL. 2012, 37(13), 2493–2495, doi:10.1364/OL.37.002493.
[46] Kamaras, K.; Itkis, M.E.; Hu, H.; Zhao, B.; Haddon, R.C. Covalent bond formation to a carbon nanotube metal. Science. 2003, 301(5639), 1501, doi:10.1126/science.1088083.
[47] J. R; J. R. A systemic review: Structural mechanism of SARS-CoV-2A promising preventive cure by phytochemicals. doi:10.23937/2378-3672/1410051.
[48] Pumera, M. Graphene-based nanomaterials for energy storage. Energy Environ. Sci. 2011, 4 (3), 668–674, doi:10.1039/C0EE00295J.

[49] Bonaccorso, F. et al. 2D materials. Graphene, related two-dimensional crystals, and hybrid systems for energy conversion and storage. Science. 2015, 347(6217), 1246501, doi:10.1126/science.1246501.
[50] Shen, H.; Zhang, L.; Liu, M.; Zhang, Z. Biomedical applications of graphene. Theranostics. 2012, 2(3), 283–294, doi:10.7150/thno.3642.
[51] Yang, C. et al. Biodegradable polymer-coated multifunctional graphene quantum dots for light-triggered synergetic therapy of pancreatic cancer. ACS Appl. Mater. Interfaces. 2019, 11(3), 2768–2781, doi:10.1021/acsami.8b16168.
[52] Carbon Nanomaterials for Biological Imaging and Nanomedicinal Therapy | Chemical Reviews. https://pubs.acs.org/doi/10.1021/acs.chemrev.5b00008 (accessed Dec. 25, 2021).
[53] Liu, J.; Liu, Z.; Barrow, C.J.; Yang, W. Molecularly engineered graphene surfaces for sensing applications: A review. Anal. Chim. Acta. 2015, 859, 1–19, doi:10.1016/j.aca.2014.07.031.
[54] Huang, Y.; Dong, X.; Shi, Y.; Li, C.M.; Li, L.-J.; Chen, P. Nanoelectronic biosensors based on CVD grown graphene. Nanoscale. 2010, 2(8), 1485–1488, doi:10.1039/C0NR00142B.
[55] Kwak, Y.H. et al. Flexible glucose sensor using CVD-grown graphene-based field effect transistor. Biosens. Bioelectron. 2012, 37(1), 82–87, doi:10.1016/j.bios.2012.04.042.
[56] Ling, X. et al. Can graphene be used as a substrate for Raman enhancement? Nano. Lett. 2010, 10(2), 553–561, doi:10.1021/nl903414x.
[57] Zhou, H. et al. Thickness-dependent morphologies of gold on N-layer graphenes. J. Am. Chem. Soc. 2010, 132(3), 944–946, doi:10.1021/ja909228n.
[58] Ju, L. et al. Graphene plasmonics for tunable terahertz metamaterials. Nat. Nanotechnol. 2011, 6(10), 630–634, doi:10.1038/nnano.2011.146.
[59] Fei, Z. et al. Infrared nanoscopy of dirac plasmons at the graphene–SiO2 interface. Nano. Lett. 2011, 11(11), 4701–4705, doi:10.1021/nl202362d.
[60] Wallace, P.R. The band theory of graphite. Phys. Rev. 1947, 71(9), 622–634, doi:10.1103/PhysRev.71.622.
[61] Castro Neto, A.H.; Guinea, F.; Peres, N.M.R.; Novoselov, K.S.; Geim, A.K. The electronic properties of graphene. Rev. Mod. Phys. 2009, 81(1), 109–162, doi:10.1103/RevModPhys.81.109.
[62] Marini, A.; Silveiro, I.; García de Abajo, F.J. Molecular Sensing with Tunable Graphene Plasmons. ACS Photonics. 2015, 2(7), 876–882, doi:10.1021/acsphotonics.5b00067.
[63] Alwahib, A.A.; Alhasan, S.F.; Yaacob, M.; Lim, H.-N.; Mahdi, M.A. Surface plasmon resonance sensor based on D-shaped optical fiber using fiberbench rotating wave plate for sensing pb ions. Optik. 2020, doi:10.1016/j.ijleo.2019.163724.
[64] Shang, J.; Ma, L.; Li, J.; Ai, W.; Yu, T.; Gurzadyan, G.G. The Origin of Fluorescence from Graphene Oxide. Sci. Rep. 2012, 2, 792, doi:10.1038/srep00792.
[65] Hernaez, M.; Zamarreño, C.R.; Melendi-Espina, S.; Bird, L.R.; Mayes, A.G.; Arregui, F.J. Optical fibre sensors using graphene-based materials: A review. Sensors (Basel). 2017, 17(1), 155, doi:10.3390/s17010155.
[66] Ruan, Y.; Ding, L.; Duan, J.; Ebendorff-Heidepriem, H.; Monro, T.M. Integration of conductive reduced graphene oxide into microstructured optical fibres for optoelectronics applications. Sci. Rep. 2016, 6(1), 21682, doi:10.1038/srep21682.
[67] Xu, X. et al. Electrophoretic analysis and purification of fluorescent single-walled carbon nanotube fragments. J. Am. Chem. Soc. 2004, 126(40), 12736–12737, doi:10.1021/ja040082h.
[68] Ponomarenko, L.A. et al. Chaotic Dirac billiard in graphene quantum dots. Science. 2008, 320(5874), 356–358, doi:10.1126/science.1154663.
[69] Jiang, J.; He, Y.; Li, S.; Cui, H. Amino acids as the source for producing carbon nanodots: microwave assisted one-step synthesis, intrinsic photoluminescence property and intense

chemiluminescence enhancement. Chem. Commun. 2012, 48(77), 9634–9636, doi:10.1039/C2CC34612E.
[70] Hsu, P.-C.; Chang, H.-T. Synthesis of high-quality carbon nanodots from hydrophilic compounds: role of functional groups. Chem. Commun. 2012, 48(33), 3984–3986, doi:10.1039/C2CC30188A.
[71] Salinas-Castillo, A. et al. Carbon dots for copper detection with down and upconversion fluorescent properties as excitation sources. Chem. Commun. 2013, 49(11), 1103–1105, doi:10.1039/C2CC36450F.
[72] Hu, S.-L.; Niu, K.-Y.; Sun, J.; Yang, J.; Zhao, N.-Q.; Du, X.-W. One-step synthesis of fluorescent carbon nanoparticles by laser irradiation. J. Mater. Chem. 2009, 19(4), 484–488, doi:10.1039/B812943F.
[73] Sun, D.; Ban, R.; Zhang, P.-H.; Wu, G.-H.; Zhang, J.-R.; Zhu, -J.-J. Hair fiber as a precursor for synthesizing of sulfur- and nitrogen-co-doped carbon dots with tunable luminescence properties. Carbon. 2013, 64, 424–434, doi:10.1016/j.carbon.2013.07.095.
[74] Xu, Q. et al. Preparation of highly photoluminescent sulfur-doped carbon dots for Fe(III) detection. J. Mater. Chem. A. 2014, 3(2), 542–546, doi:10.1039/C4TA05483K.
[75] Jiang, G.; Jiang, T.; Li, X.; Wei, Z.; Du, X.; Wang, X. Boronic acid functionalized N-doped carbon quantum dots as fluorescent probe for selective and sensitive glucose determination. Mater. Res. Express. 2014, 1(2), 025708, doi:10.1088/2053-1591/1/2/025708.
[76] Chan, K.K.; Yap, S.H.K.; Yong, K.-T. Biogreen Synthesis of Carbon Dots for Biotechnology and Nanomedicine Applications. Nano-Micro Lett. 2018, 10(4), 72, doi:10.1007/s40820-018-0223-3.
[77] Pan, L., et al. Truly Fluorescent Excitation-Dependent Carbon Dots and Their Applications in Multicolor Cellular Imaging and Multidimensional Sensing. Adv. Mater. Weinheim. 2015, 27 (47), 7782–7787, doi:10.1002/adma.201503821.
[78] Li, X.; Zhang, S.; Kulinich, S.A.; Liu, Y.; Zeng, H. Engineering surface states of carbon dots to achieve controllable luminescence for solid-luminescent composites and sensitive Be2+ detection. Sci. Rep. 2014, 4(1), 4976, doi:10.1038/srep04976.
[79] Chien, Y.-H.; Chan, K.K.; Anderson, T.; Kong, K.V.; Ng, B.K.; Yong, K.-T. Advanced Near-Infrared Light-Responsive Nanomaterials as Therapeutic Platforms for Cancer Therapy. Adv. Therap. 2019, 2(3), 1800090, doi:10.1002/adtp.201800090.
[80] Sun, Y.-P., et al. Quantum-sized carbon dots for bright and colorful photoluminescence. J. Am. Chem. Soc. 2006, 128(24), 7756–7757, doi:10.1021/ja062677d.
[81] Wang, H. et al. Excitation wavelength independent visible color emission of carbon dots. Nanoscale. 2017, 9(5), 1909–1915, doi:10.1039/C6NR09200D.
[82] Wang, C.; Xu, Z.; Cheng, H.; Lin, H.; Humphrey, M.G.; Zhang, C. A hydrothermal route to water-stable luminescent carbon dots as nanosensors for pH and temperature. Carbon. 2015, 82, 87–95, doi:10.1016/j.carbon.2014.10.035.
[83] Temperature-Dependent Fluorescence in Carbon Dots | The Journal of Physical Chemistry C. https://pubs.acs.org/doi/abs/10.1021/jp307308z (accessed Dec. 25, 2021).
[84] Meng, X.; Chang, Q.; Xue, C.; Yang, J.; Hu, S. Full-colour carbon dots: from energy-efficient synthesis to concentration-dependent photoluminescence properties. Chem. Commun. 2017, 53(21), 3074–3077, doi:10.1039/C7CC00461C.
[85] Jia, X.; Li, J.; Wang, E. One-pot green synthesis of optically pH-sensitive carbon dots with upconversion luminescence. Nanoscale. 2012, 4(18), 5572–5575, doi:10.1039/C2NR31319G.
[86] PRIME PubMed | Nanocarbons for Biology and Medicine: Sensing, Imaging, and Drug Delivery. https://www.unboundmedicine.com/medline/citation/31287663/Nanocarbons_for_Biology_and_Medicine:_Sensing_Imaging_and_Drug_Delivery_ (accessed Dec. 25, 2021).

[87] Zhang, Y.; Rhee, K.Y.; Hui, D.; Park, S.-J. A critical review of nanodiamond based nanocomposites: Synthesis, properties and applications. Compos. Part B Eng. 2018, 143, 19–27, doi:10.1016/j.compositesb.2018.01.028.
[88] Shenderova, O.A.; Zhirnov, V.V.; Brenner, D.W. Carbon Nanostructures. Crit. Rev. Solid State Mater. Sci. 2002, 27(3–4), 227–356, doi:10.1080/10408430208500497.
[89] Greiner, N.R.; Phillips, D.S.; Johnson, J.D.; Volk, F. Diamonds in detonation soot. Nature. 1988, 333(6172), 440–442, doi:10.1038/333440a0.
[90] Mochalin, V.N.; Neitzel, I.; Etzold, B.J.M.; Peterson, A.; Palmese, G.; Gogotsi, Y. Covalent incorporation of aminated nanodiamond into an epoxy polymer network. ACS Nano. 2011, 5 (9), 7494–7502, doi:10.1021/nn2024539.
[91] Liang, Y.; Ozawa, M.; Krueger, A. A General Procedure to Functionalize Agglomerating Nanoparticles Demonstrated on Nanodiamond. ACS Nano. 2009, 3(8), 2288–2296, doi:10.1021/nn900339s.
[92] Pentecost, A.; Gour, S.; Mochalin, V.; Knoke, I.; Gogotsi, Y. Deaggregation of nanodiamond powders using salt- and sugar-assisted milling. ACS Appl. Mater. Interfaces. 2010, 2(11), 3289–3294, doi:10.1021/am100720n.
[93] Morita, Y. et al. A Facile and Scalable Process for Size-Controllable Separation of Nanodiamond Particles as Small as 4 nm. Small. 2008, 4(12), 2154–2157, doi:10.1002/smll.200800944.
[94] Plakhotnik, T. Diamonds for quantum nano sensing. Curr. Opin. Solid State Mater. Sci. 2017, 1(21), 25–34, doi:10.1016/j.cossms.2016.08.001.
[95] Aman, H.; Plakhotnik, T. Accuracy in the measurement of magnetic fields using nitrogen-vacancy centers in nanodiamonds. J. Opt. Soc. Am. B JOSAB. 2016, 33(3), B19–B27, doi:10.1364/JOSAB.33.000B19.
[96] Wu, F.-C.; Tseng, R.-L. Preparation of highly porous carbon from fir wood by KOH etching and CO2 gasification for adsorption of dyes and phenols from water. J. Colloid Interface Sci. 2006, 294(1), 21–30, doi:10.1016/j.jcis.2005.06.084.
[97] Mahmoudi, K.; Hamdi, N.; Srasra, E. Preparation and characterization of activated carbon from date pits by chemical activation with zinc chloride for methyl orange adsorption. 2014, 12.
[98] Pereira, R.G. et al. Preparation of activated carbons from cocoa shells and siriguela seeds using H3PO4 and ZnCL2 as activating agents for BSA and α-lactalbumin adsorption. Fuel Process. Technol. 2014, 126, 476–486.
[99] Teo, E.Y.L. et al. High surface area activated carbon from rice husk as a high performance supercapacitor electrode. Electrochim. Acta. 2016, C(192), 110–119, doi:10.1016/j.electacta.2016.01.140.
[100] Abdel-Ghani, N.T.; El-Chaghaby, G.A.; ElGammal, M.H.; Rawash, E.-S.A. Optimizing the preparation conditions of activated carbons from olive cake using KOH activation. New Carbon Mater. 2016, 31(5), 492–500, doi:10.1016/S1872-5805(16)60027-6.
[101] Yahya, M.A.; Al-Qodah, Z.; Ngah, C.W.Z. Agricultural bio-waste materials as potential sustainable precursors used for activated carbon production: A review. Renewable Sustainable Energy Rev. 2015, 46, 218–235, doi:10.1016/j.rser.2015.02.051.
[102] Rafatullah, M.; Ahmad, T.; Ghazali, A.; Sulaiman, O.; Danish, M.; Hashim, R. Oil Palm Biomass as a Precursor of Activated Carbons: A Review. Crit. Rev. Environ. Sci. Technol. 2013, 43(11), 1117–1161, doi:10.1080/10934529.2011.627039.
[103] Preparation and characterization of activated carbon from oil palm empty fruit bunch wastes using zinc chloride | JurnalTeknologi. https://journals.utm.my/jurnalteknologi/article/view/4876 (accessed Dec. 25, 2021).

[104] Yang, T.; Lua, A.C. Textural and chemical properties of zinc chloride activated carbons prepared from pistachio-nut shells. Mater. Chem. Phys. 2006, 100(2), 438–444, doi:10.1016/j.matchemphys.2006.01.039.
[105] Gao et al. Optimization of high surface area activated carbon production from Enteromorpha prolifra with low-dose activating agent. Fuel Process. Technol. 2015, 132, 180–187.
[106] Benaddi, H.; Legras, D.; Rouzaud, J.; Béguin, F. Influence of the atmosphere in the chemical activation of wood by phosphoric acid. Carbon. 1998, doi:10.1016/S0008-6223(98)80123–1.
[107] Herawan, S.G.; Hadi, M.S.; Ayob, M.R.; Putra, A. Characterization of activated carbons from oil-palm shell by CO2 activation with no holding carbonization temperature. Sci. World J. 2013, 2013, 624865, doi:10.1155/2013/624865.
[108] Molina-Sabio, M.; Rodríguez-Reinoso, F. Role of chemical activation in the development of carbon porosity. Colloids Surf. A: Physicochem Eng Aspects. 2004, doi:10.1016/J.COLSURFA.2004.04.007.
[109] Dolas, H.; Sahin, O.; Saka, C.; Demir, H. New method on producing high surface area activated carbon: The effect of salt on the surface area and the pore size distribution of activated carbon prepared from pistachio shell. Chem. Eng. J. 2011, Accessed: Dec. 252021. [Online]. Available, doi:https://doi.org/10.1016/j.cej.2010.10.061.
[110] Blake, P. et al. Making graphene visible. Appl. Phys. Lett. 2007, 91(6), 063124, doi:10.1063/1.2768624.
[111] Li, N.; Huang, X.; Zhang, H.; Li, Y.; Wang, C. Transparent and Self-Supporting Graphene Films with Wrinkled- Graphene-Wall-Assembled Opening Polyhedron Building Blocks for High Performance Flexible/Transparent Supercapacitors. ACS Appl. Mater. Interfaces. 2017, 9(11), 9763–9771, doi:10.1021/acsami.7b00487.
[112] Staudenmaier, L.;. VerfahrenzurDarstellung der Graphitsäure. Ber. Dtsch. Chem. Ges. 1898, 31(2), 1481–1487, doi:10.1002/cber.18980310237.
[113] Preparation of Graphitic Oxide | Journal of the American Chemical Society. https://pubs.acs.org/doi/10.1021/ja01539a017 (accessed Dec. 26, 2021).
[114] Graphene Oxide: Fundamentals and Applications | Wiley. Wiley.com. https://www.wiley.com/en-us/Graphene+Oxide%3A+Fundamentals+and+Applications-p-9781119069409 (accessed Dec. 25, 2021).
[115] Chua, C.K.; Pumera, M. Chemical reduction of graphene oxide: a synthetic chemistry viewpoint. Chem. Soc. Rev. 2013, 43(1), 291–312, doi:10.1039/C3CS60303B.
[116] Zhu, Y. et al. Graphene and graphene oxide: synthesis, properties, and applications. Adv. Mater. Weinheim. 2010, 22(35), 3906–3924, doi:10.1002/adma.201001068.
[117] Pinheiro, A.V.; Han, D.; Shih, W.M.; Yan, H. Challenges and opportunities for structural DNA nanotechnology. Nat. Nanotechnol. 2011, 6(12), 763–772, doi:10.1038/nnano.2011.187.
[118] Lackner, K. Comparative Impacts of Fossil Fuels and Alternative Energy Sources. Carbon Capture Sequestration Storage Issues Environ. Sci. Technol. 2010, 29, doi:10.1039/9781847559715-00001.
[119] Kalyani, P.; Anitha, A. Biomass carbon & its prospects in electrochemical energy systems. Int. J. Hydrogen Energy. 2013, 38(10), 4034–4045, doi:10.1016/j.ijhydene.2013.01.048.
[120] Candelaria, S.L. et al. Nanostructured carbon for energy storage and conversion. Nano. Energy. 2012, 1(2), 195–220, doi:10.1016/j.nanoen.2011.11.006.
[121] Adzic, R. Platinum Monolayer Electrocatalysts for Oxygen Reduction Reaction. 29.
[122] Vinoth, R. et al. Synergistically Enhanced Electrocatalytic Performance of an N-Doped Graphene Quantum Dot-Decorated 3D MoS2–Graphene Nanohybrid for Oxygen Reduction Reaction. ACS Omega. 2016, 1(5), 971–980, doi:10.1021/acsomega.6b00275.

[123] Nitrogen plasma functionalization of carbon nanotubes for supercapacitor applications. springerprofessional.de. https://www.springerprofessional.de/en/nitrogen-plasma-functionalization-of-carbon-nanotubes-for-superc/3520540 (accessed Dec. 25, 2021).
[124] (PDF) Novel felt pseudocapacitor based on carbon nanotube/metal oxides. https://www.researchgate.net/publication/280498446_Novel_felt_pseudocapacitor_based_on_carbon_nanotubemetal_oxides (accessed Dec. 25, 2021).
[125] Abbas, S.M.; Hussain, S.; Ali, S.; Ahmad, N.; Ali, N.; Abbas, S. Structure and electrochemical performance of ZnO/CNT composite as anode material for lithium-ion batteries. J. Mater. Sci. 2013, doi:10.1007/s10853-013-7336-3.
[126] Ambrosi, A.; Chua, C.K.; Bonanni, A.; Pumera, M. Electrochemistry of graphene and related materials. Chem. Rev. 2014, 114(14), 7150–7188, doi:10.1021/cr500023c.
[127] Liu, Z.; Robinson, J.T.; Sun, X.; Dai, H. PEGylated nanographene oxide for delivery of water-insoluble cancer drugs. J. Am. Chem. Soc. 2008, 130(33), 10876–10877, doi:10.1021/ja803688x.
[128] Liu, Y.; Dong, X.; Chen, P. Biological and chemical sensors based on graphene materials. Chem. Soc. Rev. 2012, 41(6), 2283–2307, doi:10.1039/C1CS15270J.
[129] Sensitive Electrochemical Detection of Enzymatically-generated Thiocholine at Carbon Nanotube Modified Glassy Carbon Electrode | PNNL. https://www.pnnl.gov/publications/sensitive-electrochemical-detection-enzymatically-generated-thiocholine-carbon (accessed Dec. 25, 2021).
[130] Kang, X.; Wang, J.; Wu, H.; Aksay, I.A.; Liu, J.; Lin, Y. Glucose oxidase-graphene-chitosan modified electrode for direct electrochemistry and glucose sensing. Biosens. Bioelectron. 2009, 25(4), 901–905, doi:10.1016/j.bios.2009.09.004.
[131] Wu, J. et al. Organic Light-Emitting Diodes on Solution-Processed Graphene Transparent Electrodes. ACS Nano. 2010, 4(1), 43–48, doi:10.1021/nn900728d.
[132] Kumar, A.; Zhou, C. The race to replace tin-doped indium oxide: Which material will win? ACS Nano. 2010, 4(1), 11–14, doi:10.1021/nn901903b.
[133] Cao, Y.; Treacy, G.M.; Smith, P.; Heeger, A.J. Solution-cast films of polyaniline: Optical-quality transparent electrodes. Appl. Phys. Lett. 1992, 60(22), 2711–2713, doi:10.1063/1.106852.
[134] Graphene transistors in high-performance demonstration. BBC News, Jul. 18, 2012. Accessed: Dec. 25, 2021. [Online]. Available: https://www.bbc.com/news/science-environment–18868848
[135] Nair, R.R. et al. Fine structure constant defines visual transparency of graphene. Science. 2008, 320(5881), 1308, doi:10.1126/science.1156965.
[136] Graphene Mode-Locked Ultrafast Laser | ACS Nano. https://pubs.acs.org/doi/10.1021/nn901703e (accessed Dec. 25, 2021).
[137] Tiwari, S.K.; Huczko, A.; Oraon, R.; Adhikari, A.D.; Nayak, G.C. Facile electrochemical synthesis of few layered graphene from discharged battery electrode and its application for energy storage. Arabian J. Chem. Art. no. 4, 2015, Accessed: Dec. 262021, 10(4), [Online]. Available, https://cyberleninka.org/article/n/1172052.
[138] Clean and highly ordered graphene synthesized in the gas phase – Chemical Communications (RSC Publishing). https://pubs.rsc.org/en/content/articlelanding/2009/cc/b911395a (accessed Dec. 26, 2021).
[139] Stolyarova, E. et al. High-resolution scanning tunneling microscopy imaging of mesoscopic graphene sheets on an insulating surface. Proc. National Acad. Sci. 2007, 104(22), 9209–9212, doi:10.1073/pnas.0703337104.

[140] Graphene application as a counter electrode material for dye-sensitized solar cell. https://www.infona.pl/resource/bwmeta1.element.elsevier-c851ee56-985d-391b-bcc0-6d93a697ab31 (accessed Dec. 26, 2021).
[141] Liang, M.; Luo, B.; Zhi, L. Application of graphene and graphene-based materials in clean energy-related devices. Int. J. Energy Res. 2009, 33(13), 1161–1170, doi:10.1002/er.1598.
[142] Castillejo, M.; Ossi, P.; Zhigilei, L. Lasers in materials science. Spring. Ser. Mater. Sci. 2014, doi:10.1007/978-3-319-02898-9.
[143] Wang, X.; Zhi, L.; Müllen, K. Transparent, Conductive Graphene Electrodes for Dye-Sensitized Solar Cells. Nano. Lett. 2008, 8(1), 323–327, doi:10.1021/nl072838r.
[144] Stretchable active-matrix organic light-emitting diode display using printable elastic conductors – PubMed. https://pubmed.ncbi.nlm.nih.gov/19430465/ (accessed Dec. 25, 2021).
[145] Blake, P. et al. Graphene-ased liquid crystal device. Nano Lett. 2008, 8(6), 1704–1708, doi:10.1021/nl080649i.
[146] Mechanical properties of suspended graphene sheets: Journal of Vacuum Science & Technology B: Microelectronics and Nanometer Structures Processing, Measurement, and Phenomena: Vol 25, No 6. https://avs.scitation.org/doi/abs/10.1116/1.2789446 (accessed Dec. 26, 2021).
[147] Lee, C.; Wei, X.; Kysar, J.W.; Hone, J. Measurement of the elastic properties and intrinsic strength of monolayer graphene. Science. 2008, 321(5887), 385–388, doi:10.1126/science.1157996.
[148] A Chemical Route to Graphene for Device Applications | Nano Letters. https://pubs.acs.org/doi/10.1021/nl0717715 (accessed Dec. 26, 2021).
[149] Han, T.H. et al. Extremely efficient flexible organic light-emitting diodes with modified graphene anode. Nat Photonics. 2012, 6(2), 105–110, doi:10.1038/nphoton.2011.318.
[150] Liu, M. et al. A graphene-based broadband optical modulator. Nature. 2011, 474(7349), 64–67, doi:10.1038/nature10067.
[151] Multilayered graphene used as anode of organic light emitting devices: Applied Physics Letters: Vol 96, No 13. https://aip.scitation.org/doi/abs/10.1063/1.3373855 (accessed Dec. 25, 2021).
[152] Graphene photonics and optoelectronics | Nature Photonics. https://www.nature.com/articles/nphoton.2010.186 (accessed Dec. 25, 2021).
[153] Mueller, T.; Xia, F.; Avouris, P. Graphene photodetectors for high-speed optical communications. Nature Photon. 2010, 4(5), 297–301, doi:10.1038/nphoton.2010.40.
[154] Mohanty, N. et al. Nanotomy-based production of transferable and dispersible graphene nanostructures of controlled shape and size. Nat. Commun. 2012, 3(1), 844, doi:10.1038/ncomms1834.
[155] Kwon, W. et al. Electroluminescence from graphene quantum dots prepared by amidative cutting of tattered graphite. Nano Lett. 2014, 14(3), 1306–1311, doi:10.1021/nl404281h.
[156] Kruis, F.E.; Fissan, H.; Peled, A. Synthesis of nanoparticles in the gas phase for electronic, optical and magnetic applications – a review. J. Aerosol. Sci. 1998, 29(5–6), 511–535, doi:10.1016/S0021-8502(97)10032-5.

Alimorad Rashidi*, Maryam Sirati Gohari, Seyed Ali Rezaei

Chapter 2
Carbon allotropes: synthesis and characterization

Abstract: Carbon can be formed in various zero-dimensional, one-dimensional, two-dimensional, and three-dimensional structures, besides its magnificent mechanical, chemical, thermal, and electrical properties, which can be used in different industries. Carbon nanomaterials, such as carbon nanotubes, graphene and its derivatives, carbon nanofibers, and carbon quantum dots are considered as important carbon nano-allotropes since they are applicable in many industries, especially in corrosion protection. Optimized production methods to synthesize such materials on a large scale with high quality are one of the most important concerns. Characterization of carbon allotropes is also important since the different properties of such materials can be evaluated.

Keywords: carbon allotropes, graphene derivatives, carbon nanotubes, synthesis, characterization

2.1 Introduction

Due to the ability to form various structures with outstanding chemical, mechanical, electrical, and thermal features, carbon is considered as one of the most fascinating materials. Carbon nanomaterials have recently found application in many areas, such as electronics, sensors, energy storage, composite materials, and drug delivery. Carbon nanotubes (CNTs), graphene and its derivatives, carbon nanofibers (CNFs), and carbon quantum dots (CQDs) are considered as important carbon nano-allotropes since they are applicable in many industries, especially in corrosion protection. Developing new efficient methods and improving existing ones to prepare high-quality carbon allotropes on a large scale are obtaining increasing attention [1, 2]. In this chapter, the

*Corresponding author: **Alimorad Rashidi,** Nanotechnology Research Center, Research Institute of Petroleum Industry (RIPI), Tehran, Iran, e-mail: rashidiam@ripi.ir
Maryam Sirati Gohari, Research Department of Ceramic, Materials and Energy Research Center, Alborz, Iran; e-mails: m.sirati@merc.ac.ir
Seyed Ali Rezaei, Research Department of Ceramic, Materials and Energy Research Center, Alborz, Iran, e-mail: sa.rezaei@merc.ac.ir

https://doi.org/10.1515/9783110782820-002

synthesis methods related to some of the well-known carbon nanomaterials that can be used to improve corrosion protection and their characterization methods are provided.

2.2 Synthesis of carbon nanotubes (CNT)

Mainly, there are three well-known approaches, including laser ablation, electric arc discharge, and chemical vapor deposition (CVD), for the synthesis of CNTs, but many new approaches have been reported to produce such materials with better properties in a cheaper way. Similar experimental parameters such as carbon sources and catalysts have been used in these new techniques. Based on the parameters related to the synthesis method, some of them are suitable for single-walled CNTs (SWCNTs), such as laser ablation and template/bottom-up [3], while others are related to the production of multiwalled CNTs (MWCNTs) such as electrolysis [4], hydrothermal [5], and CVD.

2.2.1 Electric arc discharge

In this method, a chamber filled with inert gas (helium) containing two graphite electrodes (with diameters 6–12 mm) and metal catalysts is used. The graphite rods are placed near each other with a millimeter-scaled gap and connected to a power supply. When the positive electrode comes closer to the negative one, DC current (100 amps) generated by a connected source is passed through electrodes to create an arc, and by getting the chamber under pressure, the temperature can be raised up to 4,000 K, which can lead to carbon vaporization and formation of a plasma (Fig. 2.1). By choosing suitable catalyst precursors, different kinds of CNTs deposit on the negative electrode. Mainly, SWCNTs are prepared by this method with the presence of suitable catalyst precursors, including nickel (Ni), cobalt (Co), gadolinium (Gd), palladium (Pd), iron (Fe), platinum (Pt), silver (Ag), or mixtures of Ni, Co, and Fe with different elements such as Co–ruthenium (Ru), Co–Pt, Fe–Ni, Ni–yttrium (Y), Co–Ni, Ni–copper (Cu), Co–Cu, Ni–titanium (Ti), Fe–nobelium (No), and Ni–Y. In order to synthesize MWNTs, the presence of catalyst precursors is not necessary and they can be prepared through this process by controlling the inert gas pressure only. Controlling arc current and inert gas pressure are known as two essential parameters. Through this technique, CNTs (d = 2–30 nm, L = up to 1 mm) with fewer structural flaws can be prepared compared to other methods due to the high-temperature condition (>1,700 °C). The electric arc discharge method is capable of creating a considerable number of nanotubes. However, since the metallic catalyst is used, the impurity of the final product is inevitable, so purification of produced CNTs is necessary [1, 2, 6–8].

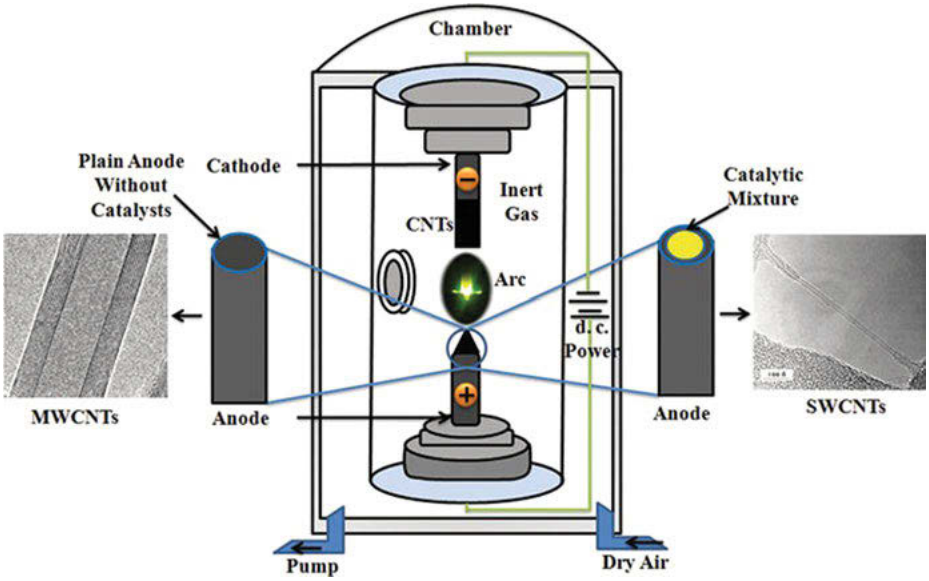

Fig. 2.1: Schematic illustration of electric arc discharge method for synthesizing different types of CNTs (reprinted from ref. [9], open-access article).

2.2.2 Laser ablation

This technique's mechanisms and principles are similar to the electric arc discharge method, except that a high-power pulsed laser provides the energy for vaporizing carbon from a graphitic target in an inert atmosphere (usually argon or helium) with constant pressure (Fig. 2.2). CO_2 or Nd:YAG laser is mostly employed to ablate the pure graphite target, which usually contains cobalt or nickel as the metal catalyst. This method is applicable for synthesizing SWCNTs and MWCNTs with a large amount and fewer defects compared to electric arc discharge. High-purity and high-quality CNTs ($d = 5–20$ nm, $L =$ up to several microns), especially SWCNTs (using high-intensity UV laser), can be synthesized through this technique but, generally, the properties of final products depend on several parameters which should be controlled. These parameters can be divided into two groups: the parameters related to laser, such as wavelength, energy fluence, and type of laser and its power, and the other parameters such as the ones related to the inert gas (flow and type), catalyst precursors, chamber's pressure, temperature, the gap between substrate and target, and chemical composition and structure properties of carbon target. It has been proposed that CNTs are produced by direct ablation or carbon particle suspension in the reaction zone [6, 10, 11].

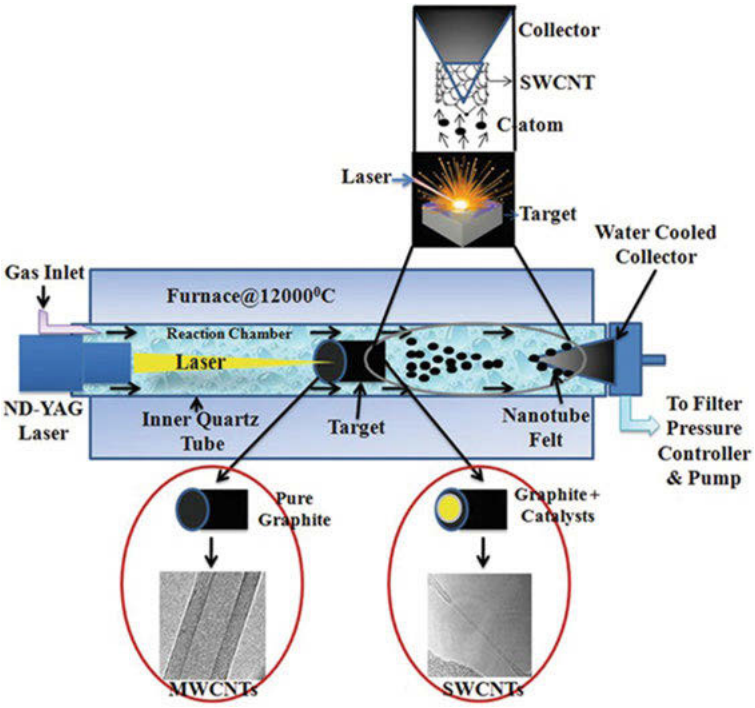

Fig. 2.2: Schematic illustration of laser ablation approach for different types of CNT production (reprinted from ref. [9], open-access article).

2.2.3 Chemical vapor deposition (CVD)

It was mentioned that the methods indicated above have some drawbacks such as being high-temperature processes, high impurity in final products, and more importantly, they are not acceptable for mass production. The CVD approach can provide a well-controlled reaction and produce a considerable amount of CNTs with perfect structure at a reasonable price via a simple mechanism using cheap carbon feedstock and catalysts. In this method, decomposition of hydrocarbon occurs by applying temperature in the presence of a catalyst so that such an approach is also called catalytic CVD (CCVD) or thermal CVD (TCVD). CVD obtains increasing attention due to many reasons, including being low-temperature process, large-scale production with high aspect ratio, perfect crystallization, and high purity, broad carbon source (gas, liquid, and solid). A two-phase reaction was proposed for synthesizing CNTs through CVD, including catalyst precipitation or deposition on support (substrate) and using different induced systems to shape CNTs (Fig. 2.3). In this method, a substrate is placed in the midsection of the tube in an oven or a furnace where the temperature is uniform and optimum and heated up to 650–900 °C with a controlled

gas pressure blown into the reaction chamber through a gas inlet. Two different sorts of gases are usually used, including hydrocarbon for carbon source (acetylene (C_2H_2), methane (CH_4), or ethylene (C_2H_4)) and working gas (argon (Ar), hydrogen (H_2), or nitrogen (N_2)). Catalyst is usually placed on the substrate to bring the decomposition reaction of hydrocarbons and provides smaller gaseous carbon which is precipitated on catalyst, and the structure of CNTs is shaped. It is possible to produce catalyst-free CNTs or use gas, liquid, or solid ones. In order to use liquid carbon sources such as benzene (C_6H_6) and toluene (C_7H_8), a flask containing the selected source is heated up to vaporize the liquid carbon source and directed into the reaction chamber through a gas inlet. For using solid carbon sources, such as ferrocene ($C_{10}H_{10}Fe$) and camphor ($C_{10}H_{16}O$), it is possible to place them into the reaction chamber in low-temperature zones in order to be converted into the gas phase and pass at high-temperature region. Many types of CVD have been introduced so far, and among them, plasma-enhanced CVD (PECVD) (a low-temperature process and suitable for synthesizing CNTs with vertically freestanding structures) and TCVD (an economical setting with more surface area and capability of using different substrate coatings) are frequently employed.

Table 2.1 presents all currently employed kinds of CVD methods in order to prepare different types of CNTs, including SWCNTs and DWCNTs, which are considered as few-walled CNTs (FWCNTs) and MWCNTs [1, 2, 6, 12, 13].

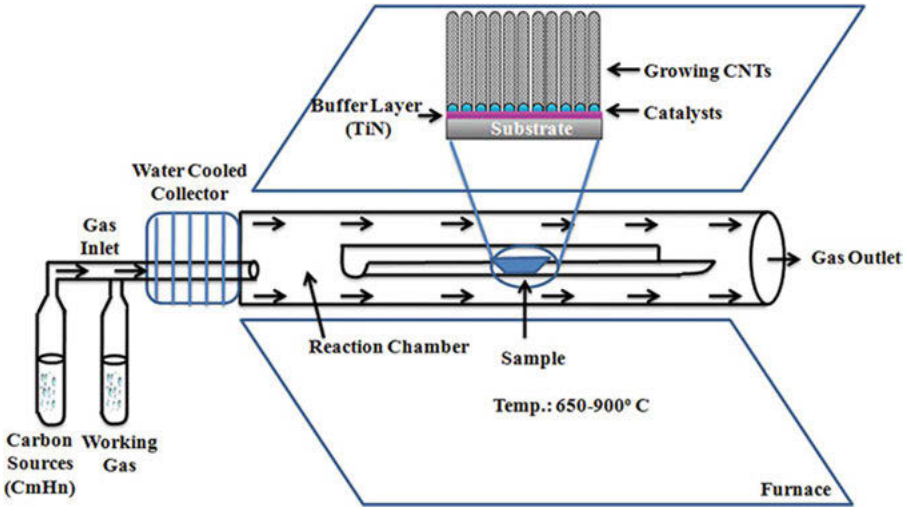

Fig. 2.3: Schematic illustration of CVD approach for CNT production (reprinted with permission from ref. [6]).

Tab. 2.1: Different types of CVD method for CNT production.

Technique	Abbreviation	Effective for	Ref.	Technique	Abbreviation	Effective for	Ref.
Plasma-enhanced CVD	PECVD	FWCNTs MWCNTs	[14]	Metal-organic CVD	MOCVD	MWCNTs	[15]
Microwave plasma-enhanced CVD	MPECVD	FWCNTs MWCNTs	[16]	Microwave CVD	MWCVD	FWCNTs	[17]
Extreme plasma flux CVD	EPFCVD	MWCNTs	[18]	Hot filament CVD	HFCVD	MWCNTs	[19]
Plasma-enhanced hot filament CVD	PEHFCVD	MWCNTs	[20]	Water-assisted CVD	WACVD	FWCNTs MWCNTs	[21]
Antenna-type remote plasma CVD	ARPCVD	FWCNTs	[22]	Biological CVD	BCVD	FWCNTs MWCNTs	[23]
Remote plasma CVD	RPCVD	FWCNTs	[24]	Sulfur-assisted CVD	SACVD	FWCNTs	[25]
Radio frequency plasma-enhanced CVD	RFPECVD	FWCNTs MWCNTs	[26]	Oxygen-assisted floating catalyst CVD	OAFCCVD	FWCNTs	[27]
Oxygen-assisted plasma-enhanced CVD	OAPECVD	FWCNTs	[28]	Sulfur-assisted floating catalyst CVD	SAFCCVD	FWCNTs	[29]
Temperature CVD	TCVD	FWCNTs MWCNTs	[30]	Aerosol-assisted catalytic CVD	AACCVD	MWCNTs	[31]
Temperature gradient CVD	TGCVD	FWCNTs	[32]	Solid CVD	SCVD	MWCNTs	[33]
Hot filament thermal CVD	HFTCVD	MWCNTs	[34]	Liquid gas catalytic CVD	LGCCVD	–	[35]
Low ambient temperature CVD	LATCVD	FWCNTs MWCNTs	[36]	Graphite antenna CVD	GACVD	MWCNTs	[37]
Injection-assisted CVD	IACVD	MWCNTs	[38]	Laser-assisted CVD	LACVD	–	[39]
Radio frequency-catalytic CVD	RFCCVD	MWCNTs	[40]	Alumina aerogel CVD	AACVD	FWCNTs	[41]
Alcohol catalytic CVD	ACCVD	FWCNTs	[42]	Aerogel-supported CVD	ASCVD	FWCNTs MWCNTs	[43]

Tab. 2.1 (continued)

Technique	Abbreviation	Effective for	Ref.	Technique	Abbreviation	Effective for	Ref.
Co–Mo catalysis	CoMoCat	FWCNTs	[12, 44]	High-pressure Co	HiPco	FWCNTs	[45]
Vapor phase growth method	VPGM	MWCNTs	[46]				

2.3 Graphene (G) synthesis

There are two different paths, including top-down and bottom-up methods, in the production of graphene. In top-down approaches, such as mechanical exfoliation, liquid-phase exfoliation, and unzipping of CNTs, conversion of materials with bulk size (graphitic sources) to small compounds occur. On the other hand, bottom-up methods such as CVD, laser synthesis, and epitaxial growth are defined as the production of graphene from carbon sources (liquids or gasses).

2.3.1 Mechanical exfoliation

This method is considered as the first reported approaches to separate graphene sheets from a high-quality graphitic piece using adhesive tape, which can peel off this two-dimensional material due to poor interlayer bonding forces in the structure of graphite [47, 48]. Repeating this process makes it possible to obtain thinner graphene and turn a few layers of graphene into monolayer graphene. Highly ordered pyrolytic graphite [49], natural graphite [50], and monocrystal graphite [51] have been used to prepare graphene sheets by this method. This approach can be divided into two categories, including shear force and normal force (applying force direction orthogonal to the sheets) (Fig. 2.4b). In order to peel off the graphite layer, different techniques such as using an ultra-sharp single-crystal diamond wedge [52] and using a three-roll mill machine [53] have been employed. Recently, fluid dynamic and ball milling have been considered as two well-known shear force-based approaches (Fig. 2.4a, b). Ball milling has been employed to facilitate the exfoliation of graphite and separate graphene sheets as well as the functionalization of such carbon-based material and composite production by mixing graphene and other materials [54]. Several parameters such as the initial size of precursor, type of grinding media, speed, and time can determine the quality of the final product [55]. Generally, exfoliation of graphite by mechanical approaches to prepare graphene sheets is time-consuming and it is not an efficient method. More importantly, the control of the thickness or

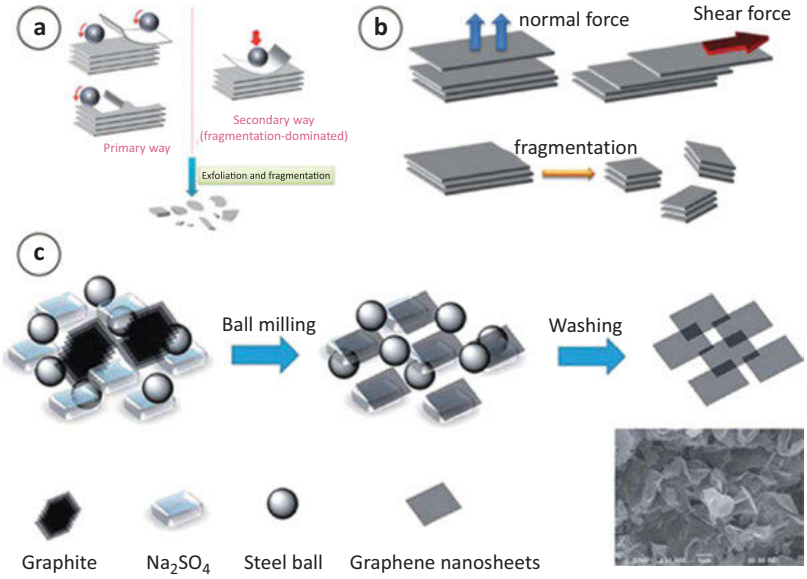

Fig. 2.4: Schematic illustration of mechanical exfoliation through ball milling (a) and salt-assisted ball milling methods. Shear force and normal force mechanical routes for graphite exfoliation (c) (reprinted with permission from ref. [53]).

number of graphene sheets is not possible and it does not have the capability to produce such a material on a large scale.

2.3.2 Electrochemical (liquid-phase) exfoliation

This technique is known as a promising one for synthesizing graphene with high quality through which the graphene sheets are separated by the insertion of metal atoms or molecules that are larger than the space between the layers in graphite structure to weaken the van der Waals forces [56–58] (Fig. 2.5). By sonication of graphite in different liquid chemicals and optimization of the related parameter such as power and time, the interlayer forces are weakened so that graphene with different sizes and numbers of layers (few layers or monolayer) can be obtained [59–61]. The choice of proper liquid solvent is the most important step in this method since it can directly affect the process yield as well as the stability of the G suspension. In order to exfoliate the graphite efficiently through this method, several parameters should be considered, including the surface tension of chosen solvent, the ability to overcome the van der Waals force between G sheets in graphite structure, and the ability to stabilize the G sheet distribution in suspension. In addition, since water is known as an effective medium for graphite exfoliation, the surface energy of water should be

decreased by adding aqueous medium of other chemical species for better efficiency [62, 63]. Various organic solvents have been employed for liquid-phase exfoliation method, including benzyl benzoate, *N*,*N*-dimethylacetamide, 1,3-dimethyl-2-imidazolidinone, benzylamine, dimethyl sulfoxide, cyclohexanone, *y*-butyrolactone, tetramethylurea, dimethyl formamide, and *n*-methyl-2-pyrrolidone [64].

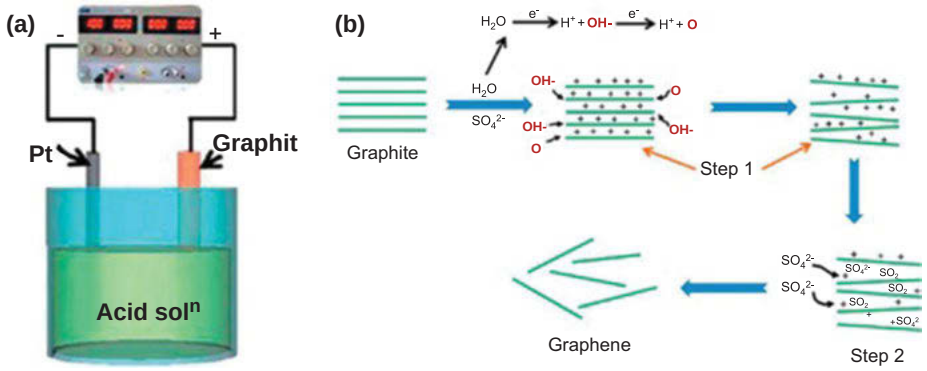

Fig. 2.5: Schematic illustration of setup for graphite exfoliation (a) and recommended mechanism (b) via electrochemical approach (reprinted with permission from ref. [65]).

2.3.3 Unzipping of CNTs

This method is considered as an effective technique for preparing graphene nanoribbons (GNRs), which can be carried out in different ways. Using oxidizing agents, such as potassium permanganate ($KMnO_4$), sulfuric acid (H_2SO_4) is one of the methods in which CNTs are treated with such compounds for oxidation at 55–70 °C to fully and semi-unzip CNTs (Fig. 2.6). The final product can be soluble in various solvents such as ethanol (C_2H_5OH) and water [66]. The electrochemical process for unzipping CNTs to synthesize GNRs is another method in which CNTs are used as working electrodes, and an anode potential is applied versus a reference electrode. Long GNRs with few defects and smooth edges can be prepared through this method [67]. Other methods such as exfoliation of CNTs by insertion, applying electron beam to CNTs, using metal nanoparticles for longitudinal cutting of CNTs, and laser-induced unzipping of CNTs have been employed to produce high-quality G with high yield [68–70].

2.3.4 Chemical vapor deposition (CVD)

Although the cost of this method is not comparable with liquid phase and mechanical exfoliation, it obtains increasing attention since, through this method, it is

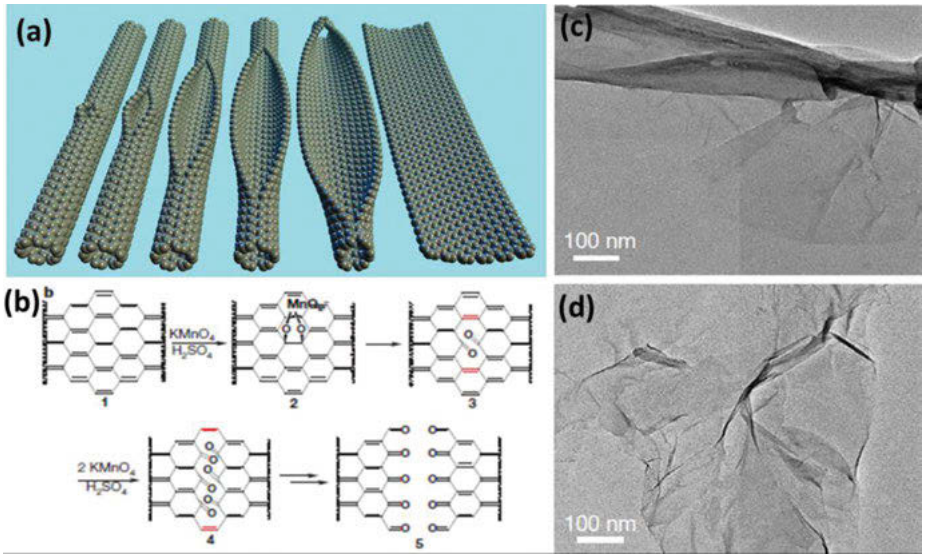

Fig. 2.6: Schematic illustration of unzipping process of CNTs (a) and recommended mechanism (b) to prepare G. TEM images of semi- (c) and fully unzipped CNTs (d) (reprinted with permission from ref. [66]).

possible to synthesize large-area graphene sheets with high quality applicable in electronic industries [71, 72] (Fig. 2.7). One of the most important advantages of this approach is the flexibility in the selection of carbon precursors, which can be solids (polymers, camphor ($C_{10}H_{16}O$), sucrose ($C_{12}H_{22}O_{11}$)), liquids (turpentine oil ($C_{10}H_{16}$), benzene (C_6H_6), ethanol (C_2H_5OH), and hexane (C_6H_{14}),), or gases (ethylene (C_2H_4), acetylene (C_2H_2), and methane (CH_4)) [73]. There are several suitable supports (substrate), including nickel (Ni), cobalt (Co), copper (Cu), platinum (Pt), gold (Au), ruthenium (Ru), iridium (Ir), palladium (Pd), rhodium (Rh), germanium (Ge), and rhenium (Re) to prepare G sheets via the CVD method [74–77]. Based on the substrate used for the CVD method, the synthesis mechanism can have different stages, but generally, decomposition, adsorption, dissolution, dehydrogenation, diffusion, nucleation, segregation, and precipitation can be mentioned as the main steps for graphene growth [78, 79]. In order to synthesize few to multilayers of graphene, Ni is employed since, at high temperatures, carbon has a high solubility in such material [80]. In contrast, Cu is used extensively to prepare graphene, especially single-layer structure, due to low solubility of such material which can properly control the formation of graphene layers [81]. There are a variety of techniques which can be used for graphene growth through CVD, including remote PECVD, low-pressure CVD, microwave plasma CVD, radio frequency PECVD, ultra-high vacuum CVD, microwave-assisted surface wave plasma CVD, PECVD, inductively coupled plasma CVD, surface wave plasma CVD [82, 83].

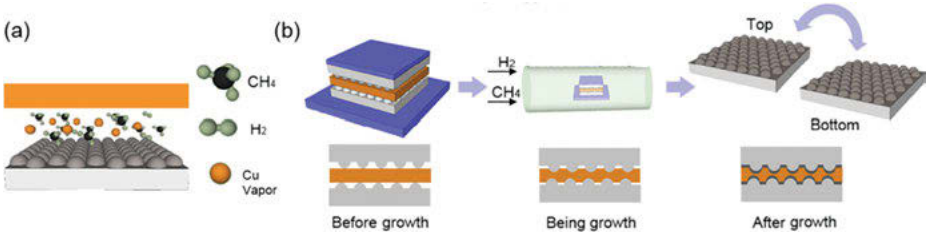

Fig. 2.7: Schematic illustration of the growth of G on 3D structures (a) and the preparation processes of 3D G on patterned sapphire substrates (b) (reprinted with permission from ref. [84]).

2.3.5 Epitaxial growth

This is an alternative approach in which epitaxial graphenegrowth is provided, and silicon carbide (SiC) can be used as substrate and carbon feedstock simultaneously. In this process, thermal decomposition of SiC occurred in an ultra-high vacuum at high temperatures to prevent contamination so that silicon atoms sublimate and leave behind carbon atoms (provide a carbon-rich surface), which form large-scale few-layer graphene. Epitaxial graphene growth on SiC is obtaining increasing attention since it can be applicable to high-end electronics (Fig. 2.8). One of the biggest challenges is that the thickness of the resulting graphene is nonuniform, which can directly affect the electronic features. Sublimation rate is considered as the most critical parameter for mass production of high-quality G through this approach [85–87].

2.3.6 Laser synthesis

This method is obtaining increasing attention since, in addition to preventing extra high-temperature heating, which is common in TCVD, there is no need for following treatments or solvents so that it has a short processing time [89–92]. Laser synthesis can provide simple patterning and deliver concentrated energy in order to prepare graphene from carbon sources with desirable quality. There are various parameters such as the rate of scanning and pulse width and power of laser to control the quality of structure and the number of graphene sheets [93]. Several laser-assisted approaches have been reported for the production of G from different carbon feedstock, such as laser exfoliation, unzipping of CNTs via laser-induced, laser-pulsed/ablation laser deposition, laser-induced CVD (LCVD) (Fig. 2.9), and laser-induced epitaxial growth [94–97]. Regardless of the atmosphere (gas or vacuum), LCVD provides concentrated heating with a fast heating rate which can increase the temperature of catalyst/substrate rapidly and decompose the carbon source so that deposition and patterning of graphene structure at desirable temperature can be achieved [98, 99].

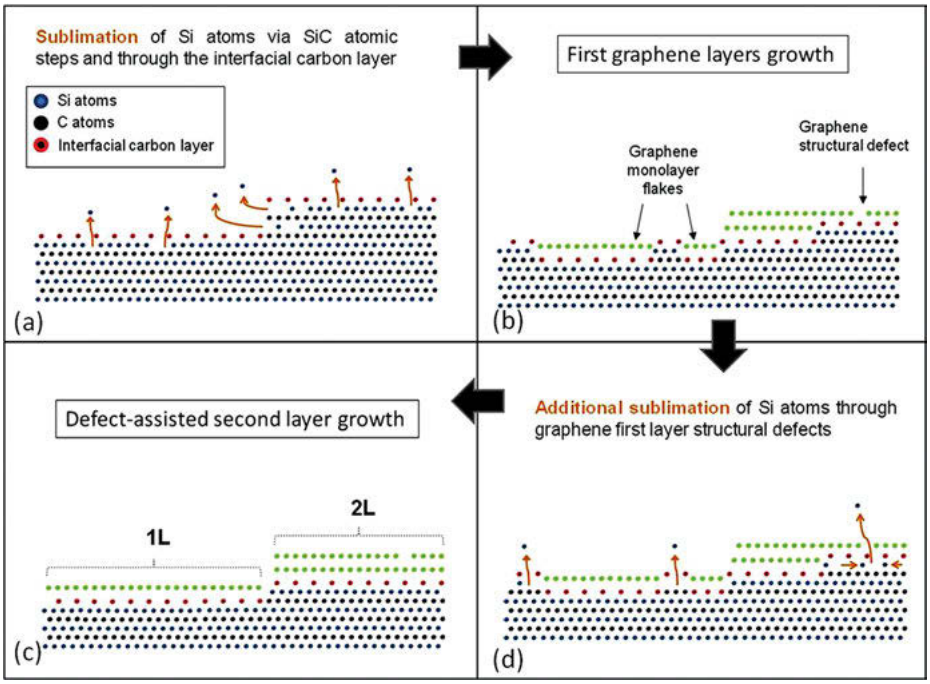

Fig. 2.8: Schematic illustration of synthesis mechanism for G on SiC (reprinted with permission from ref. [88]).

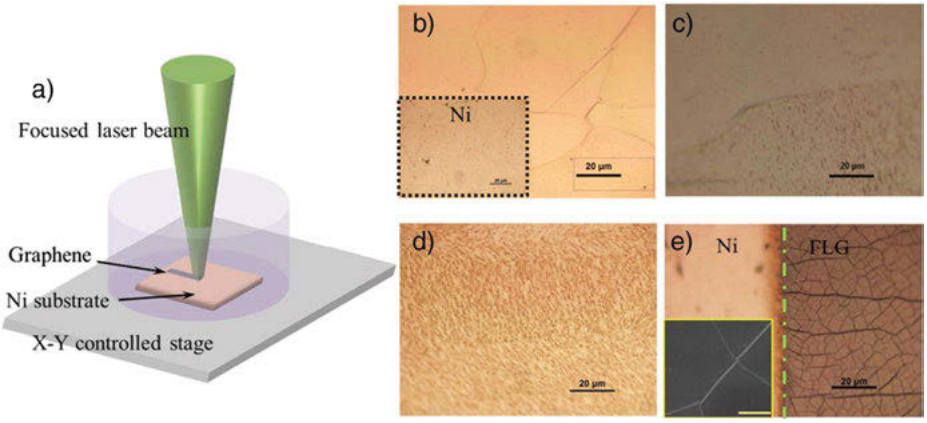

Fig. 2.9: Schematic illustration of the G synthesis via LCVD method (a). Optical micrographs of the Ni surface after the LCVD with different scanning speeds: 3 mm/s (b), 2.5 mm/s (c), 2 mm/s (d), and 1.3 mm/s (e) (reprinted with permission from ref. [98]).

When the laser spot moves forward, the regional temperature of the substrate can decrease suddenly, affecting the carbon solubility so that the formation of graphene sheets occurs on the catalyst surface due to the reduction of solubility by the cooling process [100].

2.4 Graphene oxide (GO)

GO is synthesized by the reaction of oxidizing agent with graphite powder through which the interlayer spacing of the structure is usually increased. Due to the oxidation of G for GO preparation, the final products show a proper dispersion in different media. There are four main methods in order to produce GO (Fig. 2.10), including Brodie, Staudenmaier, Hofmann, and Hummers, in which graphite powder reacted with acids, followed by the intercalation of alkali metal compounds into the graphitic structure to break layers.

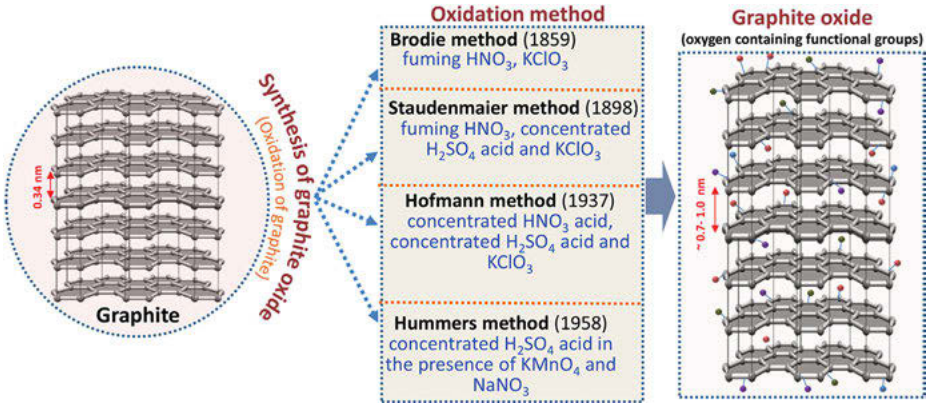

Fig. 2.10: Different methods of graphite oxide synthesis from graphite (reprinted with permission from ref. [101]).

2.4.1 Brodie's method

As one of the first attempts, GO was synthesized via graphite powder reaction with potassium chlorate ($KClO_3$) employed as a strong oxidizing agent and the presence of fuming nitric acid (HNO_3) in order to prepare a compound containing C, H, and oxygen, which was proposed as $C_{11}H_4O_5$ (Brodie's GO (BR-GO)). The final product was found dispersible in basic water while it was not soluble in acidic environments; hence, it was decided to name this material "graphic acid." A heat treatment was employed in order to change the composition, which resulted in a loss of

carbonic oxide (CO) and carbonic acid (H_2CO_3), although this time-consuming method had a variety of flaws, such as releasing toxic gasses [102]. There are several reports related to synthesis of GO via this method [103–105].

2.4.2 Staudenmaier's method

This method is also known as a chlorine route with some modifications to the Brodie method such as controlling the potassium chlorate addition and using sulfuric acid (H_2SO_4) as an extra additive (Staudenmaier's GO (ST-GO)). The modification led to simplify the graphitic oxidation process with the similar product (BR-GO). Following this process, chlorine dioxide (ClO_2) should be eradicated using inert gasses which is mentioned as a dangerous process. The main purpose of adding H_2SO_4 to $KClO_3$–fuming HNO_3 was to increase the acidity of environment in order to decrease the time of reaction. However, to prevent the explosion, potassium chlorate was gradually added in several aliquots (over a week) which can be a time-consuming process [106]. This approach or modified one has been employed for preparation of GO [107, 108].

2.4.3 Hofmann's method

Hofmann employed $KClO_3$ and non-fuming HNO_3 and H_2SO_4 to synthesize Hofmann's GO (HO-GO), and based on the results the concentration of HNO_3 can directly affect the oxidation degree of GO. The results proved that as HNO_3 concentration decreased, the oxidation level of GO is higher [109, 110]. Other researchers have prepared GO through this method [111, 112].

2.4.4 Hummers' method

This method is known as the most effective fast conventional one in order to produce GO in which sodium nitrate ($NaNO_3$) and graphite powder are mixed in concentrated H_2SO_4 and by using an ice bath temperature reaches to zero (0 °C) followed by the addition of potassium permanganate ($KMnO_4$). The diluted suspension needs to be treated with hydrogen peroxide (H_2O_2) for the reduction of manganese dioxide (MnO_2) and residual permanganate, followed by filtering and washing in order to eradicate the soluble salt of mellitic acid (Hummers' GO (HU-GO)) [113]. Compared to other approaches, this one is considered a safe approach due to the prevention of explosive ClO_2 generation. However, it was mentioned that this one is not considered an environment-friendly one due to evolving NOx. There are other types of Hummers' methods with some modifications, including two-step, nitrate-free, low-temperature, and co-oxidant [114–117].

2.5 Reduced graphene oxide (rGO)

The chemical and physical features of reduced GO (rGO) are similar to G, although rGO has obtained increasing attention in electronics, optics, and energy storage because of its high electrical conductivity. Deoxygenation of GO can be carried out through several methods in which functional species are eradicated, leading to changing the structure of GO.

2.5.1 Chemical reduction

In this method, the attached functional groups, which contain oxygen, are removed from the surface of GO leading to improve electrical conductivity. There are a variety of chemicals which can be used as reducing agents, including hydrazine (N_2H_4) [118–120] and hydrazine hydrate ($N_2H_4{\cdot}H_2O$) [121, 122]. Sodium borohydride ($NaBH_4$) was employed for reduction of GO, which completely removed the oxygen-containing groups, resulting in lower resistance compared to N_2H_4-rGO [123], and concentrated sulfuric acid (H_2SO_4) was used for dehydration [124] (Fig. 2.11). Hydroiodic acid (HI) is known as an effective agent in order for reduction of GO at low temperatures through which reduced films with higher electrical conductivity and more shrinkage in thickness than N_2H_4 and $NaBH_4$-rGO can be achieved [125]. Ascorbic acid (vitamin C) is known as a green reducing agent, which can be efficient for GO reduction [126].

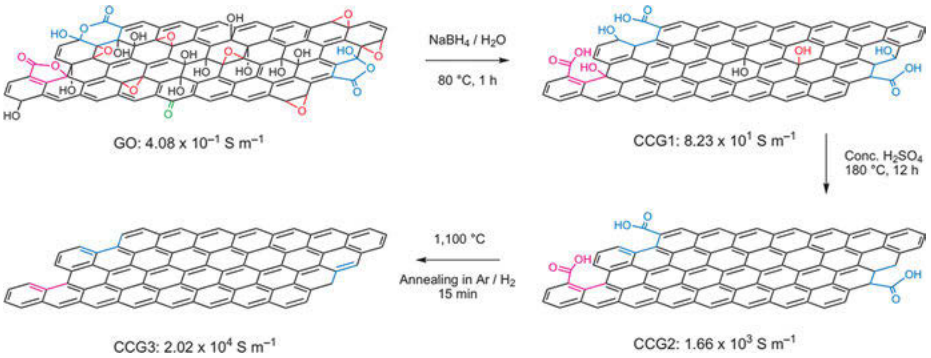

Fig. 2.11: Schematic illustration of the GO chemical reduction by sulfuric acid and sodium borohydride (reprinted with permission from ref. [124]).

2.5.2 Thermal reduction

Applying a fast heating rate to eradicate the oxygen-containing groups on the edges and the surface of GO is known as an efficient method to prepare rGO with high

electrical conductivity [127, 128]. Through this approach, CO/CO_2 gases are generated, which can cause an increase in interlayer spacing and weaken the van der Waals forces and lead to the exfoliation of GO into fewer layers and smaller sizes [129, 130]. The diffusion rate of gasses increases by decomposition of hydroxyl sites so that high pressure is generated, facilitating the exfoliation process. It was calculated that by rising the temperature from 200 to 1,000 °C, the pressure between the sheets in the graphitic structure increases from 40 to 130 MPa, which is more than the calculated pressure for the exfoliation process (2.5 MPa) [131]. This method can also be carried out in low temperatures (260 °C) and high-pressure processes using an autoclave in a suitable atmosphere (N_2) [132]. Mainly Ar, H_2, or N_2 or a mixture of them is used as reducing atmosphere [119, 133] (Fig. 2.12).

2.5.3 Microwave reduction

In comparison with conventional heating methods, microwave heating has some important advantages, including heating propagation (heating moves from core to surface), and based on the wave absorption features of materials, it is possible to apply selective heating, which is more effective, especially for solid materials though which uniform and efficient heating process can be done. Microwave irradiation is considered as an effective and fast approach for exfoliation of graphite and reducing GO since these carbonous structures contain π electrons which can be efficiently transformed into heat energy [135, 136] (Fig. 2.13). Utilizing microwave in order to apply uniform heating with fast heating rates can deoxygenize GO via expansion in interlayer spacing resulting from molecular vibration and produce rGO [137, 138]. It was suggested that mild annealing at low temperatures (300 °C) is necessary to improve the efficiency of exfoliation and reduction [139]. CO_2 and CO were reported as the main gaseous products in microwave reduction of GO [140].

2.5.4 Laser reduction

Photoreduction (photothermal reduction, GO conversion to rGO) by different kinds of lasers such as CO_2 [142], Nd:YAG [143], diode-pumped solid state [144], fiber-rod amplified femtosecond [145], and picosecond [146] is considered as an effective method to deoxygenize GO [147–149]. This kind of reduction is entirely carried out in solid state without using any harsh chemical or solvent and high-temperature process. Laser irradiation is known as a single-step process, which can shorten the time of conversion considerably, and due to the high quality of the final product, it is applicable for different purposes [142, 143, 145, 150]. The main parameters to control the reduction degree in this approach are the speed of scanning, pulse repetition frequency, and laser fluence, besides the number of exposure cycles [150] (Fig. 2.14).

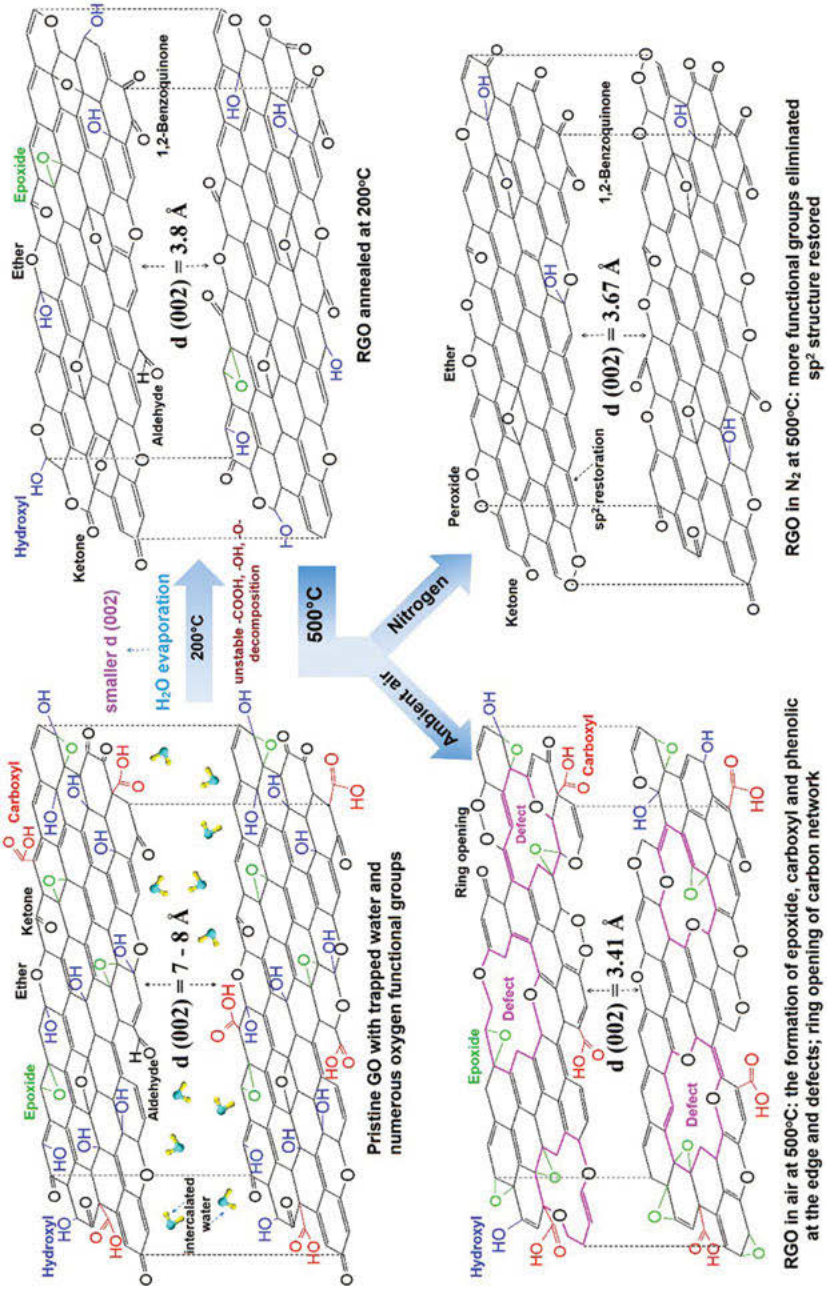

Fig. 2.12: Schematic illustration of GO thermal reduction in ambient air and nitrogen atmosphere (black: non-adsorptive species; colored: potential adsorption sites) (reprinted with permission from ref. [134]).

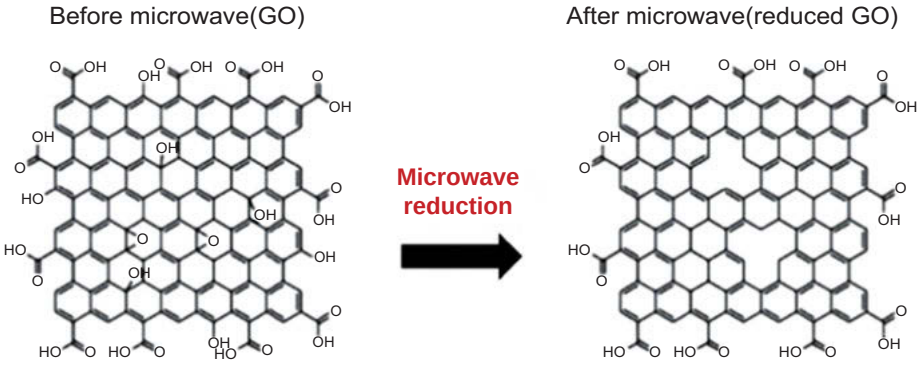

Fig. 2.13: Schematic illustration of GO reduction mechanism via microwave (reprinted with permission from ref. [141]).

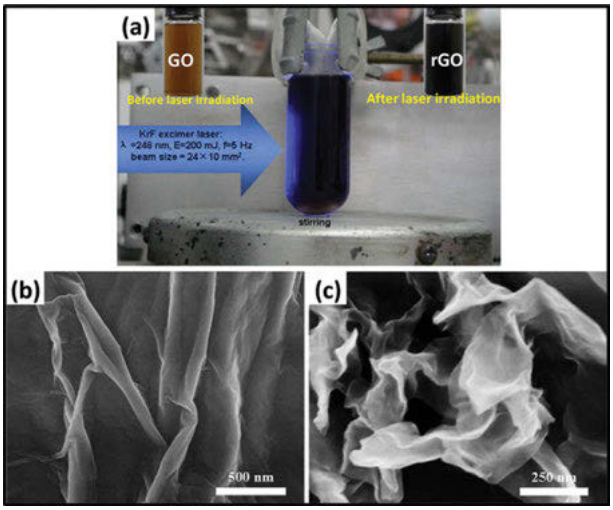

Fig. 2.14: Pulsed laser reduction setup (a), SEM images of GO (b), and rGO reduced by pulsed laser irradiation (c) (reprinted with permission from ref. [151]).

2.6 Other carbon allotropes

CQDs and CNFs are two carbon nanomaterials that are widely used in different industries. Some of the well-known formation methods of these carbon allotropes and their advantages and disadvantages are summarized in Tab. 2.2.

Tab. 2.2: Different types of CQDs and CNF synthesis methods.

Material	Method	Advantages	Disadvantages	Ref.
CQDs	Arc discharge	Oxygen-rich CQDs, accessible	Costly, high-energy method, hard to purify, harsh conditions, low quantum yield, nonuniform particle size distribution	[152]
	Laser ablation	Effortlessness, effective, ability to synthesis with different particle size and morphology, excellent water solubility	Complex process, costly, low quantum yield	[153]
	Plasma reactor	Oxygen-rich CQDs, good water solubility, uniform particle size distribution	Complex process, costly	[154]
	Ultrasound synthesis	Excellent physicochemical stability, nontoxic	High temperature, high pressure, high energy	[155]
	Chemical exfoliationand combustion	Good dispersibility in water, high purity, high stability	Nonuniform particle size distribution	[156]
	Electrochemical	Uniform particle size distribution, high crystallinity high purity, high quantum yield	Complex process	[157]
	Microwave synthesis	Control on particle's size, less time-consuming, uniform particle size distribution	High energy, costly	[158]
	Hydrothermal	Ability to control the solubility of the final product (water-soluble and insoluble), cost-effective, high quantum yield, nontoxic	Less productivity	[159]
	Thermal pyrolysis	Scalable, nontoxic, cost-effective	Nonuniform particle size distribution	[160]
	MOF template-assisted	Ability to synthesize different shapes with control on size and morphology	Time-consuming, less productive, limited quantum yield, template needs to be removed	[161]

Tab. 2.2 (continued)

Material	Method	Advantages	Disadvantages	Ref.
CNFs	Electrospinning	Effective, ability to synthesize porous, long, and continuous CNFs, easy operation, industrial method, effective	Low conductivity, post treating, and carbonization is needed, require high voltage	[162]
	CVD	High conductivity, high quality, high efficiency, high aspect ratio	Costly, high energy, many factors should be considered, especially utilizing catalyst	[163]
	Templated synthesis	Ability to synthesize tubular, porous, and core–shell CNFs, controllable and simple process	Costly, limitation in types of templates, template needs to be eradicated	[164]
	Hydrothermal synthesis	Ability to synthesize porous CNFs, CNFs with wide applications, high yield	Costly, high energy, hard to control the reaction	[165]
	Catalytic hydrogenation	Ability to synthesize porous CNFs, high yield	Costly, high energy	[166]

2.7 Characterization of carbon allotropes

There are a variety of characterization techniques used for carbon allotropes, including (high-resolution) transmission electron microscopy ((HR)TEM), (field emission) scanning electron microscopy ((FE)SEM), atomic force microscopy (AFM), X-ray diffraction (XRD), Raman spectroscopy (RS), Fourier-transform infrared spectroscopy (FTIR), ultraviolet–visible spectroscopy (UV–Vis), X-ray photoelectron spectroscopy (XPS), thermogravimetric analysis (TGA), and Brunauer–Emmett–Teller (BET). Usage of the mentioned methods are summarized in Tab. 2.3.

Tab. 2.3: Characterization techniques for carbon allotropes.

Methods	Used for	Note
(FE)SEM	Morphological analysis, measurement (thickness, diameter, and length), and state of aggregation	
(HR)TEM	Morphological analysis, studying the number of layers and interlayer spacing, and atomic resolution images	

Tab. 2.3 (continued)

Methods	Used for	Note
AFM	2D and 3D images of carbon nanomaterial surfaces	GO: to determine the number of layers, their thickness, thickness of monolayered sample of GO = 0.8–1.2 nm
XRD	Phase analysis, determination of particle size, phase purity, and crystal structure	CNTs: (002) → $2\theta \approx 24°$, (100) → $2\theta \approx 43$ GO: (002) → $2\theta \approx 10.0–12.0°$ rGO: (002) → $2\theta \approx 24°$, (100) → $2\theta \approx 43°$ CQDs: (002) → $2\theta \approx 24°$
RS	Studying bonding information and analyzing purity	Graphitic band (G band) = 1,500–1,600 cm^{-1} Defect or disorder band (D band) = 1,300–1,350 cm^{-1}
FTIR	Analyzing purity and determination of functional groups on the surface of allotropes	O–H stretching vibrations ≈ 3,340 cm^{-1} C = O carboxylic and/or carbonyl stretching vibrations ≈ 1,730–1,622 cm^{-1} C–O stretching vibrations ≈ 1,226–1,044 cm^{-1} C–O–C stretching vibrations ≈ 1,375 cm^{-1} C–OH stretching vibrations ≈ 1,190–1,382 cm^{-1} C–H stretching vibrations ≈ 2,854 cm^{-1}
UV–Vis NIRS	Determination of dispersion efficiency, diameter, and length distribution	GO: main absorption peak ≈ 230 nm, second absorption peak ≈ 300 nm
XPS	Determination of composition of materials and studying functional groups	
TGA	Determination of purity, presence of by-products, quality control, and oxidation resistance	GO: to determine exfoliation temperature
BET	Determination of specific surface areas, pore size distribution, and porosities	

2.8 Challenges, opportunities, and future

The prominent role of carbon nanomaterials in all fields of science and technology is undeniable so that the investigation of optimized nanomaterial synthesis has obtained increasing attention. For developing new production methods or optimizing the existence ones for synthesizing carbon nanomaterials, some concerns should be taken into account for the future, including the quality, cost, and ability to mass

production, which can provide their usage in different applications such as corrosion protection coatings. Due to the high cost, the usage of carbon allotropes is limited, which can be addressed by developing methods with reasonable prices or studying cheap carbon feedstock such as different waste materials. Characterization of such materials can determine the properties of these nano-allotropes and the effect of production methods on their features, such as morphology, particle size, and surface area. There are some concerns about the poisonous production methods of carbon allotropes which should be addressed in parallel to provide researchers with a situation in which they can enhance and optimize the properties of carbon nanomaterials applicable in different industries.

References

[1] Rathinavel, S.; Priyadharshini, K.; Panda, D. A review on carbon nanotube: An overview of synthesis, properties, functionalization, characterization, and the application. Mater. Sci. Eng. B Solid-State Mater. Adv. Technol. 2021, 268, 115095, doi:https://doi.org/10.1016/j.mseb.2021.115095.

[2] Shoukat, R.; Khan, M.I. Carbon nanotubes: A review on properties, synthesis methods and applications in micro and nanotechnology. Microsyst. Technol. 2021, 27, 4183–4192, doi:https://doi.org/10.1007/s00542-021-05211-6.

[3] Wang, H.; Moore, J.J. Low temperature growth mechanisms of vertically aligned carbon nanofibers and nanotubes by radio frequency-plasma enhanced chemical vapor deposition. Carbon N. Y. 2012, 50, 1235–1242, doi:https://doi.org/10.1016/j.carbon.2011.10.041.

[4] Schwandt, C.; Dimitrov, A.T.; Fray, D.J. The preparation of nano-structured carbon materials by electrolysis of molten lithium chloride at graphite electrodes. J. Electroanal. Chem. 2010, 647, 150–158, doi:https://doi.org/10.1016/j.jelechem.2010.06.008.

[5] Manafi, S.; Rahaei, M.B.; Elli, Y.; Joughehdoust, S. High-yield synthesis of multi-walled carbon nanotube by hydrothermal method. Can. J. Chem. Eng. 2010, 88, 283–286, doi:https://doi.org/10.1002/cjce.20275.

[6] Das, R.; Das Tuhi, S., Carbon Nanotubes Synthesis, n.d.

[7] Arora, N.; Sharma, N.N. Sustained arc temperature: Better marker for phase transformation of carbon black to multiwalled carbon nanotubes in arc discharge method. Mater. Res. Express. 2016, 3, 1–9, doi:https://doi.org/10.1088/2053-1591/3/10/105030.

[8] Roch, A.; Jost, O.; Schultrich, B.; Beyer, E. High-yield synthesis of single-walled carbon nanotubes with a pulsed arc-discharge technique. Phys. Status Solidi Basic Res. 2007, 244, 3907–3910, doi:https://doi.org/10.1002/pssb.200776135.

[9] Das, R.; Shahnavaz, Z.; Ali, M.E.; Islam, M.M.; Abd Hamid, S.B. Can we optimize arc discharge and laser ablation for well-controlled carbon nanotube synthesis?. Nanoscale Res. Lett. 2016, 11, doi:https://doi.org/10.1186/s11671-016-1730-0.

[10] Ismail, I.; Hashim, M.; Yahya, N. Magnetic characterization of web-like carbon nanotubes catalyzed by Fe 2O3 via pulsed Laser Ablation Deposition (PLAD) technique. Int. J. Nanosci. 2011, 10, 403–412, doi:https://doi.org/10.1142/S0219581X11008149.

[11] Yuge, R.; Toyama, K.; Ichihashi, T.; Ohkawa, T.; Aoki, Y.; Manako, T. Characterization and field emission properties of multi-walled carbon nanotubes with fine crystallinity prepared

by CO 2 laser ablation. Appl. Surf. Sci. 2012, 258, 6958–6962, doi:https://doi.org/10.1016/j.apsusc.2012.03.143.

[12] Rashidi, A.M.; Akbarnejad, M.M.; Khodadadi, A.A.; Mortazavi, Y.; Ahmadpourd, A. Single-wall carbon nanotubes synthesized using organic additives to Co–Mo catalysts supported on nanoporous MgO. Nanotechnology. 2007, 18, 315605, doi:https://doi.org/10.1088/0957-4484/18/31/315605.

[13] Rashidi, A.M.; Nouralishahi, A.; Khodadadi, A.A.; Mortazavi, Y.; Karimi, A.; Kashefi, K. Modification of single wall carbon nanotubes (SWNT) for hydrogen storage. Int. J. Hydrogen Energy. 2010, 35, 9489–9495, doi:https://doi.org/10.1016/j.ijhydene.2010.03.038.

[14] Kim, J.B.; Kong, S.J.; Lee, S.Y.; Kim, J.H.; Lee, H.R.; Kim, C.D.; Min, B.K. Characteristics of nitrogen-doped carbon nanotubes synthesized by using PECVD and thermal CVD. J. Korean Phys. Soc. 2012, 60, 1124–1128, doi:https://doi.org/10.3938/jkps.60.1124.

[15] Marangoni, R.; Serp, P.; Feurer, R.; Kihn, Y.; Kalck, P.; Vahlas, C. Carbon nanotubes produced by substrate free metalorganic chemical vapor deposition of iron catalysts and ethylene. Carbon N. Y. 2001, 39, 443–449, doi:https://doi.org/10.1016/S0008-6223(00)00149-4.

[16] Lee, J.H.; Hong, B.; Park, Y.S. The electrical and structural properties of carbon nanotubes grown by microwave plasma-enhanced chemical vapor deposition method for organic thin film transistor. Thin Solid Films. 2013, 546, 77–80, doi:https://doi.org/10.1016/j.tsf.2013.05.025.

[17] Teng, I.J.; Hsu, H.L.; Jian, S.R.; Wang, L.C.; Chen, K.L.; Kuo, C.T.; Pan, F.M.; Wang, W.H.; Juang, J.Y. Temperature-dependent electrical and photo-sensing properties of horizontally-oriented carbon nanotube networks synthesized by sandwich-growth microwave plasma chemical vapor deposition. Thin Solid Films. 2013, 529, 190–194, doi:https://doi.org/10.1016/j.tsf.2012.09.019.

[18] Bystrov, K.; Van De Sanden, M.C.M.; Arnas, C.; Marot, L.; Mathys, D.; Liu, F.; Xu, L.K.; Li, X.B.; Shalpegin, A.V.; De Temmerman, G. Spontaneous synthesis of carbon nanowalls, nanotubes and nanotips using high flux density plasmas. Carbon N. Y. 2014, 68, 695–707, doi:https://doi.org/10.1016/j.carbon.2013.11.051.

[19] Breza, J.; Pastorková, K.; Kadlečíková, M.; Jesenák, K.; Čaplovičová, M.; Kolmačka, M.; Lazišťan, F. Synthesis of nanocomposites based on nanotubes and silicates. Appl. Surf. Sci. 2012, 258, 2540–2543, doi:https://doi.org/10.1016/j.apsusc.2011.10.089.

[20] Wang, B.B.; Zheng, K.; Shao, R.W. Comparative study on catalyst-free formation and electron field emission of carbon nanotips and nanotubes grown by chemical vapor deposition. Appl. Surf. Sci. 2013, 273, 268–272, doi:https://doi.org/10.1016/j.apsusc.2013.02.030.

[21] Somanathan, T.; Dijon, J.; Fournier, A.; Okuno, H. Effective supergrowth of vertical aligned carbon nanotubes at low temperature and pressure. J. Nanosci. Nanotechnol. 2014, 14, 2520–2526, doi:https://doi.org/10.1166/jnn.2014.8504.

[22] Ohashi, T.; Kato, R.; Ochiai, T.; Tokune, T.; Kawarada, H. High quality single-walled carbon nanotube synthesis using remote plasma CVD. Diam. Relat. Mater. 2012, 24, 184–187, doi:https://doi.org/10.1016/j.diamond.2012.01.014.

[23] Kim, H.J.; Oh, E.; Lee, J.; Lee, K.H. Synthesis of single-walled carbon nanotubes using hemoglobin-based iron catalyst. Carbon N. Y. 2012, 50, 722–726, doi:https://doi.org/10.1016/j.carbon.2011.09.038.

[24] Wei, L.; Bai, S.; Peng, W.; Yuan, Y.; Si, R.; Goh, K.; Jiang, R.; Chen, Y. Narrow-chirality distributed single-walled carbon nanotube synthesis by remote plasma enhanced ethanol deposition on cobalt incorporated MCM-41 catalyst. Carbon N. Y. 2014, 66, 134–143, doi:https://doi.org/10.1016/j.carbon.2013.08.051.

[25] Zhang, Y.L.; Hou, P.X.; Liu, C.; Cheng, H.M. De-bundling of single-wall carbon nanotubes induced by an electric field during arc discharge synthesis. Carbon N. Y. 2014, 74, 370–373, doi:https://doi.org/10.1016/j.carbon.2014.03.020.
[26] Ramakrishnan, S.; Jelmy, E.J.; Dhakshnamoorthy, M.; Rangarajan, M.; Kothurkar, N. Synthesis of carbon nanotubes from ethanol using RF-CCVD and Fe-Mo catalyst. Synth. React. Inorganic Met. Nano-Metal Chem. 2014, 44, 873–876, doi:https://doi.org/10.1080/15533174.2013.796977.
[27] Yu, B.; Liu, C.; Hou, P.X.; Tian, Y.; Li, S.; Liu, B.; Li, F.; Kauppinen, E.I.; Cheng, H.M. Bulk synthesis of large diameter semiconducting single-walled carbon nanotubes by oxygen-assisted floating catalyst chemical vapor deposition. J. Am. Chem. Soc. 2011, 133, 5232–5235, doi:https://doi.org/10.1021/ja2008278.
[28] Lee, D.H.; Lee, W.J.; Kim, S.O. Vertical single-walled carbon nanotube arrays via block copolymer lithography. Chem. Mater. 2009, 21, 1368–1374, doi:https://doi.org/10.1021/cm8034533.
[29] Paukner, C.; Koziol, K.K.K. Ultra-pure single wall carbon nanotube fibres continuously spun without promoter. Sci. Rep. 2014, 4, 1–7, doi:https://doi.org/10.1038/srep03903.
[30] Shahzad, M.I.; Giorcelli, M.; Perrone, D.; Virga, A.; Shahzad, N.; Jagdale, P.; Cocuzza, M.; Tagliaferro, A. Growth of vertically aligned multiwall carbon nanotube columns. J. Phys. Conf. Ser. 2013, 439, doi:https://doi.org/10.1088/1742-6596/439/1/012008.
[31] Castro, C.; Pinault, M.; Porterat, D.; Reynaud, C.; Mayne-L'Hermite, M. The role of hydrogen in the aerosol-assisted chemical vapor deposition process in producing thin and densely packed vertically aligned carbon nanotubes. Carbon N. Y. 2013, 61, 585–594, doi:https://doi.org/10.1016/j.carbon.2013.05.040.
[32] Youn, S.K.; Frouzakis, C.E.; Gopi, B.P.; Robertson, J.; Teo, K.B.K.; Park, H.G. Temperature gradient chemical vapor deposition of vertically aligned carbon nanotubes. Carbon N. Y. 2013, 54, 343–352, doi:https://doi.org/10.1016/j.carbon.2012.11.046.
[33] Kucukayan, G.; Ovali, R.; Ilday, S.; Baykal, B.; Yurdakul, H.; Turan, S.; Gulseren, O.; Bengu, E. An experimental and theoretical examination of the effect of sulfur on the pyrolytically grown carbon nanotubes from sucrose-based solid state precursors. Carbon N. Y. 2011, 49, 508–517, doi:https://doi.org/10.1016/j.carbon.2010.09.050.
[34] Asli, N.A.; Shamsudin, M.S.; Falina, A.N.; Azmina, M.S.; Suriani, A.B.; Rusop, M.; Abdullah, S. Field electron emission properties of vertically aligned carbon nanotubes deposited on a nanostructured porous silicon template: The hidden role of the hydrocarbon/catalyst ratio. Microelectron. Eng. 2013, 108, 86–92, doi:https://doi.org/10.1016/j.mee.2013.02.095.
[35] Buang, N.A.; Ismail, F.; Othman, M.Z. Synthesis of carbon nanotube heterojunctions from the decomposition of ethanol. Fullerenes Nanotub. Carbon Nanostruct. 2014, 22, 307–315, doi:https://doi.org/10.1080/1536383X.2012.684178.
[36] Dittmer, S.; Nerushev, O.A.; Campbell, E.E.B. Low ambient temperature CVD growth of carbon nanotubes. Appl. Phys. A Mater. Sci. Process. 2006, 84, 243–246, doi:https://doi.org/10.1007/s00339-006-3614-0.
[37] Yokoyama, D.; Iwasaki, T.; Ishimaru, K.; Sato, S.; Nihei, M.; Awano, Y.; Kawarada, H. Low-temperature synthesis of multiwalled carbon nanotubes by graphite antenna CVD in a hydrogen-free atmosphere. Carbon N. Y. 2010, 48, 825–831, doi:https://doi.org/10.1016/j.carbon.2009.10.035.
[38] Yu, D.; Xue, Y.; Dai, L. Vertically aligned carbon nanotube arrays co-doped with phosphorus and nitrogen as efficient metal-free electrocatalysts for oxygen reduction. J. Phys. Chem. Lett. 2012, 3, 2863–2870, doi:https://doi.org/10.1021/jz3011833.

[39] Li, Y.; Ruan, W.; Wang, Z. Localized synthesis of carbon nanotube films on suspended microstructures by laser-assisted chemical vapor deposition. IEEE Trans. Nanotechnol. 2013, 12, 352–360, doi:https://doi.org/10.1109/TNANO.2013.2248091.
[40] Xu, Y.; Dervishi, E.; Biris, A.R.; Biris, A.S. Chirality-enriched semiconducting carbon nanotubes synthesized on high surface area MgO-supported catalyst. Mater. Lett. 2011, 65, 1878–1881, doi:https://doi.org/10.1016/j.matlet.2011.03.040.
[41] Hanifeh Toubestani, D.; Ghoranneviss, M.; Mahmoodi, A.; Rahbar Zareh, M. CVD growth of carbon nanotubes and nanofibers: Big length and constant diameter. Macromol. Symp. 2010, 287, 143–147, doi:https://doi.org/10.1002/masy.201050120.
[42] Maruyama, S.; Kojima, R.; Miyauchi, Y.; Chiashi, S.; Kohno, M. Low-temperature synthesis of high-purity single-walled carbon nanotubes from alcohol. Chem. Phys. Lett. 2002, 360, 229–234, doi:https://doi.org/10.1016/S0009-2614(02)00838-2.
[43] Morales, N.J.; Goyanes, S.; Chiliotte, C.; Bekeris, V.; Candal, R.J.; Rubiolo, G.H. One-step chemical vapor deposition synthesis of magnetic CNT-hercynite (FeAl2O4) hybrids with good aqueous colloidal stability. Carbon N. Y. 2013, 61, 515–524, doi:https://doi.org/10.1016/j.carbon.2013.04.106.
[44] Lolli, G.; Zhang, L.; Balzano, L.; Sakulchaicharoen, N.; Tan, Y.; Resasco, D.E. Tailoring (n,m) structure of single-walled carbon nanotubes by modifying reaction conditions and the nature of the support of CoMo catalysts. J. Phys. Chem. B. 2006, 110, 2108–2115, doi:https://doi.org/10.1021/jp056095e.
[45] Bronikowski, M.J.; Willis, P.A.; Colbert, D.T.; Smith, K.A.; Smalley, R.E. Gas-phase production of carbon single-walled nanotubes from carbon monoxide via the HiPco process: A parametric study. J. Vac. Sci. Technol. A Vacuum Surf Film. 2001, 19, 1800–1805, doi:https://doi.org/10.1116/1.1380721.
[46] Lyu, S.C.; Kim, H.W.; Kim, S.J.; Park, J.W.; Lee, C.J. Synthesis and crystallinity of carbon nanotubes produced by a vapor-phase growth method. Appl. Phys. A Mater. Sci. Process. 2004, 79, 697–700, doi:https://doi.org/10.1007/s00339-003-2252-z.
[47] Novoselov, K.S.; Geim, A.K.; Morozov, S.V.; Jiang, D.; Zhang, Y.; Dubonos, S.V.; Grigorieva, I.V.; Firsov, A.A. Electric field in atomically thin carbon films. Science. 2004, 80-. 306, 666–669, doi:https://doi.org/10.1126/science.1102896.
[48] Novoselov, K.S.; Jiang, D.; Schedin, F.; Booth, T.J.; Khotkevich, V.V.; Morozov, S.V.; Geim, A.K. Two-dimensional atomic crystals. Proc. Natl. Acad. Sci. U. S. A. 2005, 102, 10451–10453, doi:https://doi.org/10.1073/pnas.0502848102.
[49] Bernhardt, T.M.; Kaiser, B.; Rademann, K. Formation of superperiodic patterns on highly oriented pyrolytic graphite by manipulation of nanosized graphite sheets with the STM tip. Surf. Sci. 1998, 408, 86–94, doi:https://doi.org/10.1016/S0039-6028(98)00152-6.
[50] Hiura, H.; Ebbesen, T.W.; Fujita, J.; Tanigaki, K.; Takada, T. Role of sp3 defect structures in graphite and carbon nanotubes. Nature. 1994, 367, 148–151, doi:https://doi.org/10.1038/367148a0.
[51] Lu, X.; Yu, M.; Huang, H.; Ruoff, R.S. Tailoring graphite with the goal of achieving single sheets. Nanotechnology. 1999, 10, 269–272, doi:https://doi.org/10.1088/0957-4484/10/3/308.
[52] Jayasena, B.; Subbiah, S. A novel mechanical cleavage method for synthesizing few-layer graphenes, Nanoscale Res. Letter. 2011, 6, 1–7, doi:https://doi.org/10.1186/1556-276X-6-95.
[53] Yi, M.; Shen, Z. A review on mechanical exfoliation for the scalable production of graphene. J. Mater. Chem. A. 2015, 3, 11700–11715, doi:https://doi.org/10.1039/c5ta00252d.
[54] Fan, X.; Chang, D.W.; Chen, X.; Baek, J.B.; Dai, L. Functionalized graphene nanoplatelets from ball milling for energy applications. Curr. Opin. Chem. Eng. 2016, 11, 52–58, doi:https://doi.org/10.1016/j.coche.2016.01.003.

[55] Zhuang, S.; Nunna, B.B.; Boscoboinik, J.A.; Lee, E.S. Nitrogen-doped graphene catalysts: High energy wet ball milling synthesis and characterizations of functional groups and particle size variation with time and speed. Int. J. Energy Res. 2017, 41, 2535–2554, doi: https://doi.org/10.1002/er.3821.
[56] Amiri, A.; Naraghi, M.; Ahmadi, G.; Soleymaniha, M.; Shanbedi, M. A review on liquid-phase exfoliation for scalable production of pure graphene, wrinkled, crumpled and functionalized graphene and challenges. Flat Chem. 2018, 8, 40–71, doi:https://doi.org/10.1016/j.flatc.2018.03.004.
[57] Jiang, F.; Yu, Y.; Feng, A.; Song, L. Effects of ammonia on graphene preparation via microwave assisted intercalation exfoliation method. Ceram. Int. 2018, 44, 12763–12766, doi:https://doi.org/10.1016/j.ceramint.2018.04.081.
[58] Ma, H.; Shen, Z.; Yi, M.; Ben, S.; Liang, S.; Liu, L.; Zhang, Y.; Zhang, X.; Ma, S. Direct exfoliation of graphite in water with addition of ammonia solution. J. Colloid Interface Sci. 2017, 503, 68–75, doi:https://doi.org/10.1016/j.jcis.2017.04.070.
[59] Baig, Z.; Mamat, O.; Mustapha, M.; Mumtaz, A.; Munir, K.S.; Sarfraz, M. Investigation of tip sonication effects on structural quality of graphene nanoplatelets (GNPs) for superior solvent dispersion. Ultrason. Sonochem. 2018, 45, 133–149, doi:https://doi.org/10.1016/j.ultsonch.2018.03.007.
[60] Asgar, H.; Deen, K.M.; Riaz, U.; Rahman, Z.U.; Shah, U.H.; Haider, W. Synthesis of graphene via ultra-sonic exfoliation of graphite oxide and its electrochemical characterization. Mater. Chem. Phys. 2018, 206, 7–11, doi:https://doi.org/10.1016/j.matchemphys.2017.11.062.
[61] Bakhshandeh, R.; Shafiekhani, A. Ultrasonic waves and temperature effects on graphene structure fabricated by electrochemical exfoliation method. Mater. Chem. Phys. 2018, 212, 95–102, doi:https://doi.org/10.1016/j.matchemphys.2018.03.004.
[62] Hernandez, Y.; Nicolosi, V.; Lotya, M.; Blighe, F.M.; Sun, Z.; De, S.; McGovern, I.T.; Holland, B.; Byrne, M.; Gun'ko, Y.K.; Boland, J.J.; Niraj, P.; Duesberg, G.; Krishnamurthy, S.; Goodhue, R.; Hutchison, J.; Scardaci, V.; Ferrari, A.C.; Coleman, J.N. High-yield production of graphene by liquid-phase exfoliation of graphite. Nat. Nanotechnol. 2008, 3, 563–568, doi:https://doi.org/10.1038/nnano.2008.215.
[63] Narayan, R.; Kim, S.O. Surfactant mediated liquid phase exfoliation of graphene. Nano Converg. 2015, 2, doi:https://doi.org/10.1186/s40580-015-0050-x.
[64] Guardia, L.; Fernández-Merino, M.J.; Paredes, J.I.; Solís-Fernández, P.; Villar-Rodil, S.; Martínez-Alonso, A.; Tascón, J.M.D. High-throughput production of pristine graphene in an aqueous dispersion assisted by non-ionic surfactants. Carbon N. Y. 2011, 49, 1653–1662, doi:https://doi.org/10.1016/j.carbon.2010.12.049.
[65] Parvez, K.; Li, R.; Puniredd, S.R.; Hernandez, Y.; Hinkel, F.; Wang, S.; Feng, X.; Müllen, K. Electrochemically exfoliated graphene as solution-processable, highly conductive electrodes for organic electronics. ACS Nano. 2013, 7, 3598–3606, doi:https://doi.org/10.1021/nn400576v.
[66] Kosynkin, D.V.; Higginbotham, A.L.; Sinitskii, A.; Lomeda, J.R.; Dimiev, A.; Price, B.K.; Tour, J.M. Longitudinal unzipping of carbon nanotubes to form graphene nanoribbons. Nature. 2009, 458, 872–876, doi:https://doi.org/10.1038/nature07872.
[67] Shinde, D.B.; Debgupta, J.; Kushwaha, A.; Aslam, M.; Pillai, V.K. Electrochemical unzipping of multi-walled carbon nanotubes for facile synthesis of high-quality graphene nanoribbons. J. Am. Chem. Soc. 2011, 133, 4168–4171, doi:https://doi.org/10.1021/ja1101739.
[68] Elias, A.L.; Botello-Méndez, A.R.; Meneses-Rodríguez, D.; González, V.J.; Ramírez-González, D.; Ci, L.; Muñoz-Sandoval, E.; Ajayan, P.M.; Terrones, H.; Terrones, M. Longitudinal cutting of pure and doped carbon nanotubes to form graphitic nanoribbons using metal clusters as nanoscalpels. Nano Lett. 2010, 10, 366–372, doi:https://doi.org/10.1021/nl901631z.

[69] Terrones, M.;. Sharpening the chemical scissors to unzip carbon nanotubes: Crystalline graphene nanoribbons. ACS Nano. 2010, 4, 1775–1781, doi:https://doi.org/10.1021/nn1006607.
[70] Kim, K.; Sussman, A.; Zettl, A. Graphene nanoribbons obtained by electrically unwrapping carbon nanotubes. ACS Nano. 2010, 4, 1362–1366, doi:https://doi.org/10.1021/nn901782g.
[71] Zhong, Y.; Zhen, Z.; Zhu, H. Graphene: Fundamental research and potential applications. Flat Chem. 2017, 4, 20–32, doi:https://doi.org/10.1016/j.flatc.2017.06.008.
[72] Ambrosi, A.; Chua, C.K.; Latiff, N.M.; Loo, A.H.; Wong, C.H.A.; Eng, A.Y.S.; Bonanni, A.; Pumera, M. Graphene and its electrochemistry-an update. Chem. Soc. Rev. 2016, 45, 2458–2493, doi:https://doi.org/10.1039/c6cs00136j.
[73] Han, T.H.; Kim, H.; Kwon, S.J.; Lee, T.W. Graphene-based flexible electronic devices. Mater. Sci. Eng. R Rep. 2017, 118, 1–43, doi:https://doi.org/10.1016/j.mser.2017.05.001.
[74] Kairi, M.I.; Zuhan, M.K.N.M.; Khavarian, M.; Vigolo, B.; Bakar, S.A.; Mohamed, A.R. Co-synthesis of large-area graphene and syngas via CVD method from greenhouse gases. Mater. Lett. 2018, 227, 132–135, doi:https://doi.org/10.1016/j.matlet.2018.05.031.
[75] Di Gaspare, L.; Scaparro, A.M.; Fanfoni, M.; Fazi, L.; Sgarlata, A.; Notargiacomo, A.; Miseikis, V.; Coletti, C.; De Seta, M. Early stage of CVD graphene synthesis on Ge(001) substrate. Carbon N. Y. 2018s, 134, 183–188, doi:https://doi.org/10.1016/j.carbon.2018.03.092.
[76] Ge, X.; Zhang, Y.; Chen, L.; Zheng, Y.; Chen, Z.; Liang, Y.; Hu, S.; Li, J.; Sui, Y.; Yu, G.; Jin, Z.; Liu, X. Mechanism of SiOx particles formation during CVD graphene growth on Cu substrates. Carbon N. Y. 2018, 139, 989–998, doi:https://doi.org/10.1016/j.carbon.2018.08.007.
[77] Bayev, V.G.; Fedotova, J.A.; Kasiuk, J.V.; Vorobyova, S.A.; Sohor, A.A.; Komissarov, I.V.; Kovalchuk, N.G.; Prischepa, S.L.; Kargin, N.I.; Andrulevičius, M.; Przewoznik, J.; Kapusta, C.; Ivashkevich, O.A.; Tyutyunnikov, S.I.; Kolobylina, N.N.; Guryeva, P.V. CVD graphene sheets electrochemically decorated with "core-shell" Co/CoO nanoparticles. Appl. Surf. Sci. 2018, 440, 1252–1260, doi:https://doi.org/10.1016/j.apsusc.2018.01.245.
[78] Chen, X.; Zhang, L.; Chen, S. Large area CVD growth of graphene. Synth. Met. 2015, 210, 95–108, doi:https://doi.org/10.1016/j.synthmet.2015.07.005.
[79] Yu, J.; Li, J.; Zhang, W.; Chang, H. Synthesis of high quality two-dimensional materials via chemical vapor deposition. Chem. Sci. 2015, 6, 6705–6716, doi:https://doi.org/10.1039/c5sc01941a.
[80] Li, X.; Cai, W.; Colombo, L.; Ruoff, R.S. Evolution of graphene growth on Ni and Cu by carbon isotope labeling. Nano Lett. 2009, 9, 4268–4272, doi:https://doi.org/10.1021/nl902515k.
[81] López, G.A.; Mittemeijer, E.J. The solubility of C in solid Cu. Scr. Mater. 2004, 51, 1–5, doi:https://doi.org/10.1016/j.scriptamat.2004.03.028.
[82] Woehrl, N.; Ochedowski, O.; Gottlieb, S.; Shibasaki, K.; Schulz, S. Plasma-enhanced chemical vapor deposition of graphene on copper substrates. AIP Adv. 2014, 4, 0–9, doi:https://doi.org/10.1063/1.4873157.
[83] Bo, Z.; Yang, Y.; Chen, J.; Yu, K.; Yan, J.; Cen, K. Plasma-enhanced chemical vapor deposition synthesis of vertically oriented graphene nanosheets. Nanoscale. 2013, 5, 5180–5204, doi:https://doi.org/10.1039/c3nr33449j.
[84] Shin, J.H.; Kim, S.H.; Kwon, S.S.; Il Park, W. Direct CVD growth of graphene on three-dimensionally-shaped dielectric substrates. Carbon N. Y. 2018, 129, 785–789, doi:https://doi.org/10.1016/j.carbon.2017.12.097.
[85] Kruskopf, M.; Pierz, K.; Pakdehi, D.M.; Wundrack, S.; Stosch, R.; Bakin, A.; Schumacher, H.W. A morphology study on the epitaxial growth of graphene and its buffer layer. Thin Solid Films. 2018, 659, 7–15, doi:https://doi.org/10.1016/j.tsf.2018.05.025.
[86] Kim, K.S.; Park, G.H.; Fukidome, H.; Takashi, S.; Takushi, I.; Fumio, K.; Iwao, M.; Suemitsu, M. A table-top formation of bilayer quasi-free-standing epitaxial-graphene on SiC

(0001) by microwave annealing in air. Carbon N. Y. 2018, 130, 792–798, doi:https://doi.org/10.1016/j.carbon.2018.01.074.
[87] Le Quang, T.; Huder, L.; Lipp Bregolin, F.; Artaud, A.; Okuno, H.; Mollard, N.; Pouget, S.; Lapertot, G.; Jansen, A.G.M.; Lefloch, F.; Driessen, E.F.C.; Chapelier, C.; Renard, V.T. Epitaxial electrical contact to graphene on SiC. Carbon N. Y. 2017, 121, 48–55, doi:https://doi.org/10.1016/j.carbon.2017.05.048.
[88] Ouerghi, A.; Ridene, M.; Mathieu, C.; Gogneau, N.; Belkhou, R. From nanographene to monolayer graphene on 6H-SiC(0001) substrate. Appl. Phys. Lett. 2013, 102, doi:https://doi.org/10.1063/1.4812516.
[89] Park, J.B.; Xiong, W.; Gao, Y.; Qian, M.; Xie, Z.Q.; Mitchell, M.; Zhou, Y.S.; Han, G.H.; Jiang, L.; Lu, Y.F. Fast growth of graphene patterns by laser direct writing. Appl. Phys. Lett. 2011, 98, 16–19, doi:https://doi.org/10.1063/1.3569720.
[90] Park, J.B.; Xiong, W.; Xie, Z.Q.; Gao, Y.; Qian, M.; Mitchell, M.; Mahjouri-Samani, M.; Zhou, Y.S.; Jiang, L.; Lu, Y.F. Transparent interconnections formed by rapid single-step fabrication of graphene patterns. Appl. Phys. Lett. 2011, 99, 25–28, doi:https://doi.org/10.1063/1.3622660.
[91] Ye, R.; James, D.K.; Tour, J.M. Laser-induced graphene: From discovery to translation. Adv. Mater. 2019, 31, 1–15, doi:https://doi.org/10.1002/adma.201803621.
[92] Mi, J.; Lackey, W.J. SiC line deposition using laser CVD. J. Mater. Process. Technol. 2009, 209, 3818–3829, doi:https://doi.org/10.1016/j.jmatprotec.2008.08.041.
[93] Palneedi, H.; Park, J.H.; Maurya, D.; Peddigari, M.; Hwang, G.T.; Annapureddy, V.; Kim, J.W.; Choi, J.J.; Hahn, B.D.; Priya, S.; Lee, K.J.; Ryu, J. Laser irradiation of metal oxide films and nanostructures: Applications and advances. Adv. Mater. 2018, 30, 1–38, doi:https://doi.org/10.1002/adma.201705148.
[94] Zhao, Y.; Han, Q.; Cheng, Z.; Jiang, L.; Qu, L. Integrated graphene systems by laser irradiation for advanced devices. Nano Today. 2017, 12, 14–30, doi:https://doi.org/10.1016/j.nantod.2016.12.010.
[95] Kumar, R.; Singh, R.K.; Singh, D.P.; Joanni, E.; Yadav, R.M.; Moshkalev, S.A. Laser-assisted synthesis, reduction and micro-patterning of graphene: Recent progress and applications. Coord. Chem. Rev. 2017, 342, 34–79, doi:https://doi.org/10.1016/j.ccr.2017.03.021.
[96] Tseng, S.F.;. Picosecond laser micropatterning of graphene films for rapid heating chips. Appl. Surf. Sci. 2018, 450, 380–386, doi:https://doi.org/10.1016/j.apsusc.2018.04.212.
[97] Kasischke, M.; Subaşı, E.; Bock, C.; Pham, D.V.; Gurevich, E.L.; Kunze, U.; Ostendorf, A. Femtosecond laser patterning of graphene electrodes for thin-film transistors. Appl. Surf. Sci. 2019, 478, 299–303, doi:https://doi.org/10.1016/j.apsusc.2019.01.198.
[98] Jiang, J.; Lin, Z.; Ye, X.; Zhong, M.; Huang, T.; Zhu, H. Graphene synthesis by laser-assisted chemical vapor deposition on Ni plate and the effect of process parameters on uniform graphene growth. Thin Solid Films. 2014, 556, 206–210, doi:https://doi.org/10.1016/j.tsf.2014.01.078.
[99] Tu, R.; Liang, Y.; Zhang, C.; Li, J.; Zhang, S.; Yang, M.; Li, Q.; Goto, T.; Zhang, L.; Shi, J.; Li, H.; Ohmori, H.; Kosinova, M.; Basu, B. Fast synthesis of high-quality large-area graphene by laser CVD. Appl. Surf. Sci. 2018, 445, 204–210, doi:https://doi.org/10.1016/j.apsusc.2018.03.184.
[100] Liu, N.; Fu, L.; Dai, B.; Yan, K.; Liu, X.; Zhao, R.; Zhang, Y.; Liu, Z. Universal segregation growth approach to wafer-size graphene from non-noble metals. Nano Lett. 2011, 11, 297–303, doi:https://doi.org/10.1021/nl103962a.
[101] Kumar, R.; Sahoo, S.; Joanni, E.; Singh, R.K.; Tan, W.K.; Kar, K.K.; Matsuda, A. Recent progress in the synthesis of graphene and derived materials for next generation electrodes

of high performance lithium ion batteries. Prog. Energy Combust. Sci. 2019, 75, 100786, doi: https://doi.org/10.1016/j.pecs.2019.100786.
[102] Brodie, B.C.;. On the atomic weight of graphite. Philos. Trans. R. Soc. B Biol. Sci. 1983, 303, 1–62, http://rstb.royalsocietypublishing.org/cgi/doi/10.1098/rstb.1983.0080.
[103] Dreyer, D.R.; Park, S.; Bielawski, C.W.; Ruoff, R.S. The chemistry of graphene oxide. Chem. Soc. Rev. 2010, 39, 228–240, doi:https://doi.org/10.1039/B917103G.
[104] Ferrari, A.C.; Bonaccorso, F.; Fal'ko, V.; Novoselov, K.S.; Roche, S.; Bøggild, P.; Borini, S.; Koppens, F.H.L.; Palermo, V.; Pugno, N.; Garrido, J.A.; Sordan, R.; Bianco, A.; Ballerini, L.; Prato, M.; Lidorikis, E.; Kivioja, J.; Marinelli, C.; Ryhänen, T.; Morpurgo, A.; Coleman, J.N.; Nicolosi, V.; Colombo, L.; Fert, A.; Garcia-Hernandez, M.; Bachtold, A.; Schneider, G.F.; Guinea, F.; Dekker, C.; Barbone, M.; Sun, Z.; Galiotis, C.; Grigorenko, A.N.; Konstantatos, G.; Kis, A.; Katsnelson, M.; Vandersypen, L.; Loiseau, A.; Morandi, V.; Neumaier, D.; Treossi, E.; Pellegrini, V.; Polini, M.; Tredicucci, A.; Williams, G.M.; Hee Hong, B.; Ahn, J.H.; Min Kim, J.; Zirath, H.; Van Wees, B.J.; Van Der Zant, H.; Occhipinti, L.; Di Matteo, A.; Kinloch, I.A.; Seyller, T.; Quesnel, E.; Feng, X.; Teo, K.; Rupesinghe, N.; Hakonen, P.; Neil, S.R.T.; Tannock, Q.; Löfwander, T.; Kinaret, J. Science and technology roadmap for graphene, related two-dimensional crystals, and hybrid systems. Nanoscale. 2015, 7, 4598–4810, doi:https://doi.org/10.1039/c4nr01600a.
[105] Kuila, T.; Mishra, A.K.; Khanra, P.; Kim, N.H.; Lee, J.H. Recent advances in the efficient reduction of graphene oxide and its application as energy storage electrode materials. Nanoscale. 2013, 5, 52–71, doi:https://doi.org/10.1039/C2NR32703A.
[106] Staudenmaier, L.;. Method for the preparation of the graphite acid. Eur. J. Inorg. Chem. 1898, 31, 1481–1487.
[107] Sali, S.; Mackey, H.R.; Abdala, A.A. Effect of graphene oxide synthesis method on properties and performance of polysulfone-graphene oxide mixed matrix membranes. Nanomaterials. 2019, 9, doi:https://doi.org/10.3390/nano9050769.
[108] Singh, R.K.; Kumar, R.; Singh, D.P. Graphene oxide: Strategies for synthesis, reduction and frontier applications. RSC Adv. 2016, 6, 64993–65011, doi:https://doi.org/10.1039/C6RA07626B.
[109] Hofmann, U.; Holst, R. Über die Säurenatur und die Methylierung von Graphitoxyd. Berichte Der Dtsch. Chem. 1939, Gesellschaft (A B Ser 72, 754–771, doi:https://doi.org/10.1002/cber.19390720417.
[110] Hofmann, U.; König, E. Untersuchungen über Graphitoxyd. Zeitschrift Für Anorg. Und Allg. Chemie. 1937, 234, 311–336, doi:https://doi.org/10.1002/zaac.19372340405.
[111] Jiříčková, A.; Jankovský, O.; Sofer, Z.; Sedmidubský, D. Synthesis and applications of graphene oxide. Materials (Basel). 2022, 15, doi:https://doi.org/10.3390/ma15030920.
[112] Adetayo, A.; Runsewe, D. Synthesis and fabrication of graphene and graphene oxide: A review. Open J. Compos. Mater. 2019, 09, 207–229, doi:https://doi.org/10.4236/ojcm.2019.92012.
[113] Hummers, W.S.; Offeman, R.E. Preparation of graphitic oxide. J. Am. Chem. Soc. 1958, 80, 1339–1339, doi:https://doi.org/10.1021/ja01539a017.
[114] Kovtyukhova, N.I.; Ollivier, P.J.; Martin, B.R.; Mallouk, T.E.; Buzaneva, E.V.; Gorchinskiy, A.D. Layer-by-layer assembly of ultrathin composite films from micron-sized graphite oxide sheets and polycations. Chem. Mater. 1999, 11, 771–778, doi:https://doi.org/10.1021/cm981085u.
[115] Eigler, S.;. Graphite sulphate – A precursor to graphene. Chem. Commun. 2015, 51, 3162–3165, doi:https://doi.org/10.1039/c4cc09381j.

[116] Yu, H.; Zhang, B.; Bulin, C.; Li, R.; Xing, R. High-efficient synthesis of graphene oxide based on improved Hummers method. Sci. Rep. 2016, 6, 1–7, doi:https://doi.org/10.1038/srep36143.
[117] Eigler, S.; Enzelberger-Heim, M.; Grimm, S.; Hofmann, P.; Kroener, W.; Geworski, A.; Dotzer, C.; Röckert, M.; Xiao, J.; Papp, C.; Lytken, O.; Steinrück, H.P.; Müller, P.; Hirsch, A. Wet chemical synthesis of graphene. Adv. Mater. 2013, 25, 3583–3587, doi:https://doi.org/10.1002/adma.201300155.
[118] Yin, Z.; Wu, S.; Zhou, X.; Huang, X.; Zhang, Q.; Boey, F.; Zhang, H. Electrochemical deposition of ZnO nanorods on transparent reduced graphene oxide electrodes for hybrid solar cells. Small. 2010, 6, 307–312, doi:https://doi.org/10.1002/smll.200901968.
[119] Mattevi, C.; Eda, G.; Agnoli, S.; Miller, S.; Mkhoyan, K.A.; Celik, O.; Mastrogiovanni, D.; Granozzi, G.; Carfunkel, E.; Chhowalla, M. Evolution of electrical, chemical, and structural properties of transparent and conducting chemically derived graphene thin films. Adv. Funct. Mater. 2009, 19, 2577–2583, doi:https://doi.org/10.1002/adfm.200900166.
[120] He, Q.; Sudibya, H.G.; Yin, Z.; Wu, S.; Li, H.; Boey, F.; Huang, W.; Chen, P.; Zhang, H. Centimeter-long and large-scale micropatterns of reduced graphene oxide films: Fabrication and sensing applications. ACS Nano. 2010, 4, 3201–3208, doi:https://doi.org/10.1021/nn100780v.
[121] Stankovich, S.; Piner, R.D.; Chen, X.; Wu, N.; Nguyen, S.T.; Ruoff, R.S. Stable aqueous dispersions of graphitic nanoplatelets via the reduction of exfoliated graphite oxide in the presence of poly(sodium 4-styrenesulfonate). J. Mater. Chem. 2006, 16, 155–158, doi:https://doi.org/10.1039/b512799h.
[122] Stankovich, S.; Dikin, D.A.; Piner, R.D.; Kohlhaas, K.A.; Kleinhammes, A.; Jia, Y.; Wu, Y.; Nguyen, S.B.T.; Ruoff, R.S. Synthesis of graphene-based nanosheets via chemical reduction of exfoliated graphite oxide. Carbon N. Y. 2007, 45, 1558–1565, doi:https://doi.org/10.1016/j.carbon.2007.02.034.
[123] Shin, H.J.; Kim, K.K.; Benayad, A.; Yoon, S.M.; Park, H.K.; Jung, I.S.; Jin, M.H.; Jeong, H.K.; Kim, J.M.; Choi, J.Y.; Lee, Y.H. Efficient reduction of graphite oxide by sodium borohydride and its effect on electrical conductance. Adv. Funct. Mater. 2009, 19, 1987–1992, doi:https://doi.org/10.1002/adfm.200900167.
[124] Gao, W.; Alemany, L.B.; Ci, L.; Ajayan, P.M. New insights into the structure and reduction of graphite oxide. Nat. Chem. 2009, 1, 403–408, doi:https://doi.org/10.1038/nchem.281.
[125] Pei, S.; Zhao, J.; Du, J.; Ren, W.; Cheng, H.M. Direct reduction of graphene oxide films into highly conductive and flexible graphene films by hydrohalic acids. Carbon N. Y. 2010, 48, 4466–4474, doi:https://doi.org/10.1016/j.carbon.2010.08.006.
[126] Fernández-Merino, M.J.; Guardia, L.; Paredes, J.I.; Villar-Rodil, S.; Solís-Fernández, P.; Martínez-Alonso, A.; Tascón, J.M.D. Vitamin C is an ideal substitute for hydrazine in the reduction of graphene oxide suspensions. J. Phys. Chem. C. 2010, 114, 6426–6432, doi:https://doi.org/10.1021/jp100603h.
[127] da Silva, A.F.; Christmann, A.M.; Costa, T.M.H.; Muniz, A.R.; Balzaretti, N.M. Thermal annealing of graphite oxide under high pressure: An experimental and computational study. Carbon N. Y. 2018, 139, 1035–1047, doi:https://doi.org/10.1016/j.carbon.2018.08.006.
[128] Zhang, X.; Han, S.; Xiao, P.; Fan, C.; Zhang, W. Thermal reduction of graphene oxide mixed with hard carbon and their high performance as lithium ion battery anode. Carbon N. Y. 2016, 100, 600–607, doi:https://doi.org/10.1016/j.carbon.2016.01.033.
[129] Eigler, S.; Dotzer, C.; Hirsch, A.; Enzelberger, M.; Müller, P. Formation and decomposition of CO2 intercalated graphene oxide. Chem. Mater. 2012, 24, 1276–1282, doi:https://doi.org/10.1021/cm203223z.

[130] Bagri, A.; Mattevi, C.; Acik, M.; Chabal, Y.J.; Chhowalla, M.; Shenoy, V.B. Structural evolution during the reduction of chemically derived graphene oxide. Nat. Chem. 2010, 2, 581–587, doi:https://doi.org/10.1038/nchem.686.
[131] McAllister, M.J.; Li, J.; Adamson, D.H.; Schniepp, H.C.; Abdala, A.A.; Liu, J.; Herrera-Alonso, M.; Milius, D.L.; Car, R.; Prud'homme, R.K.; Aksay, I.A. Single sheet functionalized graphene by oxidation and thermal expansion of graphite. Chem. Mater. 2007, 19, 4396–4404, doi: https://doi.org/10.1021/cm0630800.
[132] Shang, Y.; Li, T.; Li, H.; Dang, A.; Zhang, L.; Yin, Y.; Xiong, C.; Zhao, T. Preparation and characterization of graphene derived from low-temperature and pressure promoted thermal reduction. Compos. Part B Eng. 2016, 99, 106–111, doi:https://doi.org/10.1016/j.compositesb.2016.06.030.
[133] Yang, D.; Velamakanni, A.; Bozoklu, G.; Park, S.; Stoller, M.; Piner, R.D.; Stankovich, S.; Jung, I.; Field, D.A.; Ventrice, C.A.; Ruoff, R.S. Chemical analysis of graphene oxide films after heat and chemical treatments by X-ray photoelectron and Micro-Raman spectroscopy. Carbon N. Y. 2009, 47, 145–152, doi:https://doi.org/10.1016/j.carbon.2008.09.045.
[134] Le, G.T.T.; Manyam, J.; Opaprakasit, P.; Chanlek, N.; Grisdanurak, N.; Sreearunothai, P. Divergent mechanisms for thermal reduction of graphene oxide and their highly different ion affinities. Diam. Relat. Mater. 2018, 89, 246–256, doi:https://doi.org/10.1016/j.diamond.2018.09.006.
[135] Tryba, B.; Morawski, A.W.; Inagaki, M. Preparation of exfoliated graphite by microwave irradiation. Carbon N. Y. 2005, 43, 2417–2419, doi:https://doi.org/10.1016/j.carbon.2005.04.017.
[136] Falcao, E.H.L.; Blair, R.G.; Mack, J.J.; Viculis, L.M.; Kwon, C.W.; Bendikov, M.; Kaner, R.B.; Dunn, B.S.; Wudl, F. Microwave exfoliation of a graphite intercalation compound. Carbon N. Y. 2007, 45, 1367–1369, doi:https://doi.org/10.1016/j.carbon.2007.01.018.
[137] Han, H.J.; Chen, Y.N.; Wang, Z.J. Effect of microwave irradiation on reduction of graphene oxide films. RSC Adv. 2015, 5, 92940–92946, doi:https://doi.org/10.1039/c5ra19268d.
[138] Zhu, Y.; Murali, S.; Stoller, M.D.; Ganesh, K.J.; Cai, W.; Ferreira, P.J.; Pirkle, A.; Wallace, R.M.; Cychosz, K.A.; Thommes, M.; Su, D.; Stach, E.A.; Ruoff, R.S. Carbon-based supercapacitors produced by activation of graphene. Science. 2011, 80-. 332, 1537–1541, doi:https://doi.org/10.1126/science.1200770.
[139] Voiry, D.; Yang, J.; Kupferberg, J.; Fullon, R.; Lee, C.; Jeong, H.Y.; Shin, H.S.; Chhowalla, M. High-quality graphene via microwave reduction of solution-exfoliated graphene oxide. Science. 2016, 80-. 353, 1413–1416, doi:https://doi.org/10.1126/science.aah3398.
[140] Shulga, Y.M.; Baskakov, S.A.; Knerelman, E.I.; Davidova, G.I.; Badamshina, E.R.; Shulga, N.Y.; Skryleva, E.A.; Agapov, A.L.; Voylov, D.N.; Sokolov, A.P.; Martynenko, V.M. Carbon nanomaterial produced by microwave exfoliation of graphite oxide: New insights. RSC Adv. 2014, 4, 587–592, doi:https://doi.org/10.1039/c3ra43612h.
[141] Kim, N.; Xin, G.; Cho, S.M.; Pang, C.; Chae, H. Microwave-reduced graphene oxide for efficient and stable hole extraction layers of polymer solar cells. Curr. Appl. Phys. 2015, 15, 953–957, doi:https://doi.org/10.1016/j.cap.2015.05.011.
[142] Bhattacharjya, D.; Kim, C.-H.; Kim, J.-H.; You, I.-K.; In, J.B.; Lee, S.-M. Fast and controllable reduction of graphene oxide by low-cost CO2 laser for supercapacitor application. Appl. Surf. Sci. 2018, 462, 353–361, doi:https://doi.org/10.1016/j.apsusc.2018.08.089.
[143] Papazoglou, S.; Tsouti, V.; Chatzandroulis, S.; Zergioti, I. Direct laser printing of graphene oxide for resistive chemosensors, Opt. Laser Technol. 2016, 82, 163–169, doi:https://doi.org/10.1016/j.optlastec.2016.03.009.

[144] Fatt Teoh, H.; Tao, Y.; Soon Tok, E.; Wei Ho, G.; Haur Sow, C. Direct laser-enabled graphene oxide-Reduced graphene oxide layered structures with micropatterning. J. Appl. Phys. 2012, 112, doi:https://doi.org/10.1063/1.4752752.
[145] Kasischke, M.; Maragkaki, S.; Volz, S.; Ostendorf, A.; Gurevich, E.L. Simultaneous nanopatterning and reduction of graphene oxide by femtosecond laser pulses. Appl. Surf. Sci. 2018, 445, 197–203, doi:https://doi.org/10.1016/j.apsusc.2018.03.086.
[146] Trusovas, R.; Ratautas, K.; Račiukaitis, G.; Barkauskas, J.; Stankevičiene, I.; Niaura, G.; Mažeikiene, R. Reduction of graphite oxide to graphene with laser irradiation. Carbon N. Y. 2013, 52, 574–582, doi:https://doi.org/10.1016/j.carbon.2012.10.017.
[147] Antonelou, A.; Sygellou, L.; Vrettos, K.; Georgakilas, V.; Yannopoulos, S.N. Efficient defect healing and ultralow sheet resistance of laser-assisted reduced graphene oxide at ambient conditions. Carbon N. Y. 2018, 139, 492–499, doi:https://doi.org/10.1016/j.carbon.2018.07.012.
[148] Lazauskas, A.; Marcinauskas, L.; Andrulevicius, M. Photothermal reduction of thick graphene oxide multilayer films via direct laser writing: Morphology, structural and chemical properties. Superlattices Microstruct. 2018, 122, 36–45, doi:https://doi.org/10.1016/j.spmi.2018.08.024.
[149] Torrisi, L.; Silipigni, L.; Cutroneo, M. Radiation effects of IR laser on graphene oxide irradiated in vacuum and in air. Vacuum. 2018, 153, 122–131, doi:https://doi.org/10.1016/j.vacuum.2018.04.010.
[150] Yang, C.R.; Tseng, S.F.; Chen, Y.T. Laser-induced reduction of graphene oxide powders by high pulsed ultraviolet laser irradiations. Appl. Surf. Sci. 2018, 444, 578–583, doi:https://doi.org/10.1016/j.apsusc.2018.03.090.
[151] Huang, L.; Liu, Y.; Ji, L.C.; Xie, Y.Q.; Wang, T.; Shi, W.Z. Pulsed laser assisted reduction of graphene oxide. Carbon N. Y. 2011, 49, 2431–2436, doi:https://doi.org/10.1016/j.carbon.2011.01.067.
[152] Dey, S.; Govindaraj, A.; Biswas, K.; Rao, C.N.R. Luminescence properties of boron and nitrogen doped graphene quantum dots prepared from arc-discharge-generated doped graphene samples. Chem. Phys. Lett. 2014, 595–596, 203–208, doi:https://doi.org/10.1016/j.cplett.2014.02.012.
[153] Li, B.; Jiang, L.; Li, X.; Ran, P.; Zuo, P.; Wang, A.; Qu, L.; Zhao, Y.; Cheng, Z.; Lu, Y. Preparation of monolayer MoS2 quantum dots using temporally shaped femtosecond laser ablation of bulk MoS2 targets in water. Sci. Rep. 2017, 7, 1–12, doi:https://doi.org/10.1038/s41598-017-10632-3.
[154] Lim, S.Y.; Shen, W.; Gao, Z. Carbon quantum dots and their applications. Chem. Soc. Rev. 2015, 44, 362–381, doi:https://doi.org/10.1039/c4cs00269e.
[155] Kumar, R.; Kumar, V.B.; Gedanken, A. Sonochemical synthesis of carbon dots, mechanism, effect of parameters, and catalytic, energy, biomedical and tissue engineering applications, Ultrason. Sonochem. 2020, 64, 105009, doi:https://doi.org/10.1016/j.ultsonch.2020.105009.
[156] Wang, J.; Sahu, S.; Sonkar, S.K.; Tackett II, K.N.; Sun, K.W.; Liu, Y.; Maimaiti, H.; Anilkumar, P.; Sun, Y.-P. Versatility with carbon dots – From overcooked BBQ to brightly fluorescent agents and photocatalysts. RSC Adv. 2013, 3, 15604, doi:https://doi.org/10.1039/c3ra42302f.
[157] Liu, M.; Xu, Y.; Niu, F.; Gooding, J.J.; Liu, J. Carbon quantum dots directly generated from electrochemical oxidation of graphite electrodes in alkaline alcohols and the applications for specific ferric ion detection and cell imaging. Analyst. 2016, 141, 2657–2664, doi:https://doi.org/10.1039/c5an02231b.

[158] Wang, X.; Feng, Y.; Dong, P.; Huang, J.; Mini, A. Review on carbon quantum dots: Preparation, properties, and electrocatalytic application. Front. Chem. 2019, 7, 1–9, doi:https://doi.org/10.3389/fchem.2019.00671.
[159] Wang, W.; Ni, Y.; Xu, Z. One-step uniformly hybrid carbon quantum dots with high-reactive TiO2 for photocatalytic application. J. Alloys Compd. 2015, 622, 303–308, doi:https://doi.org/10.1016/j.jallcom.2014.10.076.
[160] Wang, F.; Pang, S.; Wang, L.; Li, Q.; Kreiter, M.; Liu, C.Y. One-step synthesis of highly luminescent carbon dots in noncoordinating solvents. Chem. Mater. 2010, 22, 4528–4530, doi:https://doi.org/10.1021/cm101350u.
[161] Xu, H.; Zhou, S.; Xiao, L.; Wang, H.; Li, S.; Yuan, Q. Fabrication of a nitrogen-doped graphene quantum dot from MOF-derived porous carbon and its application for highly selective fluorescence detection of Fe3+. J. Mater. Chem. C. 2015, 3, 291–297, doi:https://doi.org/10.1039/c4tc01991a.
[162] Abdalla, I.; Elhassan, A.; Yu, J.; Li, Z.; Ding, B. A hybrid comprised of porous carbon nanofibers and rGO for efficient electromagnetic wave absorption. Carbon N. Y. 2019, doi:https://doi.org/10.1016/j.carbon.2019.11.004.
[163] Cheng, X.; Zhang, Q.; Wang, H.; Tian, G.; Huang, J.; Peng, H.; Zhao, M.; Wei, F. Nitrogen-doped herringbone carbon nanofibers with large lattice spacings and abundant edges: Catalytic growth and their applications in lithium ion batteries and oxygen reduction reactions. Catal. Today. 2015, 249, 244–251, doi:https://doi.org/10.1016/j.cattod.2014.10.047.
[164] Xing, Y.; Wang, Y.; Zhou, C.; Zhang, S.; Fang, B. Simple synthesis of mesoporous carbon nanofibers with hierarchical nanostructure for ultrahigh lithium storage. ACS Appl. Mater. Interfaces. 2014, 6, 2561–2567, doi:https://doi.org/10.1021/am404988b.
[165] Chu, H.; Lin, X.; Li, M.; Liang, L.; Zhou, J.; Shang, R.; Luo, X. Rapid synthesis of carbon materials by microwave-assisted hydrothermal method at low temperature and its adsorption properties for uranium (VI). J. Radioanal. Nucl. Chem. 2019, 321, 629–646, doi:https://doi.org/10.1007/s10967-019-06613-7.
[166] Chen, C.S.; Lin, J.H.; You, J.H.; Yang, K.H. Effects of potassium on Ni–K/Al 2 O 3 catalysts in the synthesis of carbon nanofibers by catalytic hydrogenation of CO 2. J. Phys. Chem. A. 2010, 114, 3773–3781, doi:https://doi.org/10.1021/jp904434e.

Sourav Kr. Saha*, Namhyun Kang*

Chapter 3
Corrosion: basics, economic adverse effects, and its mitigation

Abstract: Corrosion is a natural phenomenon. As all the natural processes have the tendency to attain lowest energy state, iron or steel also combines with other chemical elements in order to return to their lowest energy state. To return to lowest energy state, iron or steel always combines with oxygen and water present in the environment and forms hydrated iron oxide (rust), which has similar composition to the iron ore. The major reason for concerning about the corrosion is economy, safety, and conservation. Due to corrosion, huge amount of economic loss as well as causalities occur worldwide. According to the report, the annual cost of corrosion in the United States was US $276 billion which is equivalent to 3.1% of the US gross domestic product. Therefore, it is very essential to minimize the corrosion to save considerable expenses in equipment, structure, and materials. This chapter provides a brief overview about corrosion and its adverse effects related to the economy and safety. Additionally, proper methods to mitigate corrosion were also discussed in detail.

Keywords: Corrosion, Effect of corrosion, Corrosion cost, Corrosion inhibition

3.1 Introduction

"Corrosion" means rust, and it is the universal object of hatred. Rust is more specifically reserved for the corrosion of irons. Although almost all metals and their alloys face corrosion-related problems, corrosion is an undesirable phenomenon which can be defined as the "destruction or deterioration of a material due to its reactions with the environment." The three major reasons for concerning about the corrosion are economics, safety, and conservation. In any developed country, economy and safety are directly related to corrosion. Corrosion of metals creates negative impact on the overall growth of the economy and may also cause tragic accident resulting in human injury or even loss of life [1–5]. In 2002, the United States Federal Highway Administration (FHWA) published a report associated with the metallic corrosion in a wide range of industries [6]. The results suggest that the total annual cost of corrosion in the USA was US $276 billion which is equivalent to 3.1% of the US

*Corresponding author: Sourav Kr. Saha, Namhyun Kang, Department of Materials Science and Engineering, Pusan National University, Busan 46241, Republic of Korea,
e-mails: sksaha@pusan.ac.kr; nhkang@pusan.ac.kr

https://doi.org/10.1515/9783110782820-003

gross domestic product (GDP). An article recently published in the *Times of India* reported that India loses wealth of approximately Rs 2 lakh crores per year due to corrosion [7]. The survey conducted by the Corrosion Science Society of Korea suggested that corrosion-related cost is around 2.9% of the Korean GDP (2005) [8]. In view of this, suitable understanding of corrosion phenomenon and its mitigation is very crucial.

Due to corrosion chemical changes occur. To understand corrosion reaction properly understanding of electrochemistry is very much important. Corrosion is also related to the structure and composition of the metal; therefore, fundamentals of physical metallurgy are also important. There are some suitable methods by which corrosion can be minimized. The most useful methods among them are: (a) materials can be selected in such a manner that it does not corrode in the actual environment, (b) suitable design that will avoid corrosion, (c) cathodic and anodic protection, (d) application of coatings, and (e) use of inhibitors. In this chapter, it has been focused to discuss the basics of corrosion, its adverse effects, and the proper implementation of the methods by which corrosion can be minimized.

3.2 Basic of corrosion

Corrosion is mainly defined as the environmental degradation of materials, and it is a complex process that entirely depends on the environment where the material is exposed. Apart from the environment, corrosion also depends on the composition of materials, crystal structure of the metals, and in which circumstances metals are used. Corrosion is mainly controlled by the kinetic and thermodynamic factors. In order to control or minimize the rate of corrosion, proper understanding of kinetic and thermodynamic fundamentals of corrosion is important.

The corrosion process can be explained by chemical or electrochemical reactions where the metal dissolves away from the anodic sites (oxidation), and the corresponding reduction reaction occurs at the cathode in the presence of an electrolyte [9]. Dissolution of metal (M), which is an anodic reaction, is represented by the half-cell reaction:

$$\mathrm{M} \rightarrow \mathrm{M}^{n+} + n\mathrm{e}^{-} \tag{3.1}$$

The electrons liberated by the anodic reaction are consumed by the cathodic reaction to precede the corrosion phenomenon. In aqueous corrosion, two predominating cathodic reactions are oxygen reduction and hydrogen evolution. The half-cell reactions for the cathodic reactions are represented as follows:

$$O_2 + 4e^- + 4H^+ \rightarrow 2H_2O \quad \text{(in acidic solution)} \tag{3.2}$$

$$O_2 + 4e^- + 2H_2O \rightarrow 4OH^- \quad \text{(in basic solution)} \tag{3.3}$$

$$2H^+ + 2e^- \rightarrow H_2 \quad \text{(in acidic solution)} \tag{3.4}$$

$$2H_2O + 2e^- \rightarrow H_2 + 2OH^- \quad \text{(in basic solution)} \tag{3.5}$$

Oxygen reduction can only occur in the aerated solution and hydrogen evolution can occur in both deaerated and aerated solutions.

In the basic solutions, the overall corrosion process with oxygen reduction in the cathodic sites can be represented as follows:

$$2M \rightarrow 2M^{2+} + 4e^-$$

$$O_2 + 4e^- + 2H_2O \rightarrow 4OH^-$$

$$\text{————————————————————}$$

$$2M + O_2 + 2H_2O \rightarrow 2M^{2+} + 4OH^-$$

In acidic solutions, the overall corrosion reaction can be represented as follows:

$$M \rightarrow M^{2+} + 2e^-$$

$$2H^+ + 2e^- \rightarrow H_2$$

$$\text{————————————————————}$$

$$M + 2H^+ \rightarrow M^{2+} + H_2$$

herein, hydrogen is evolved during the cathodic reaction.

It is also important to remember that although metallic dissolution is taking place through the anodic reaction, cathodic reaction is also equally important. Whatever the electrons are liberated from the anodic reaction is consumed by the cathodic process. As there is no charge accumulated at the corroding metal surfaces, it can be said that the two partial reactions, that is, oxidation and reduction, proceed simultaneously (Fig. 3.1).

3.3 Factors affecting corrosion

Corrosion inhibition is a global issue which concerns the nations due to its adverse impact on major industrial plants, automobile body panels, and many more. Worldwide, all industries face problems due to corrosion. One of the largest expenditures which concern industries is the maintenance of metallic materials from the adverse

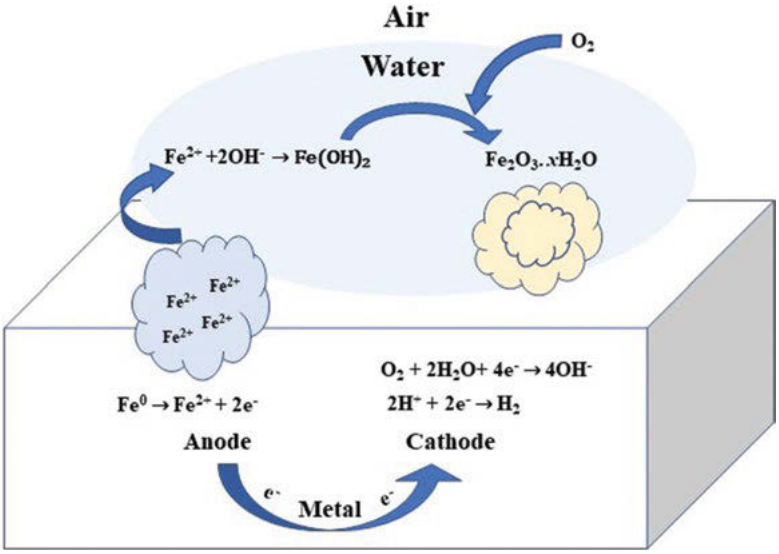

Fig. 3.1: Illustration of electrochemical corrosion of metal (here iron).

corrosive attack. The corrosion of metals is significantly affected by several factors. It mainly depends on the materials' properties as well as environments where metal is exposed. Figure 3.2 represents the major factors predominantly responsible for corrosion [10].

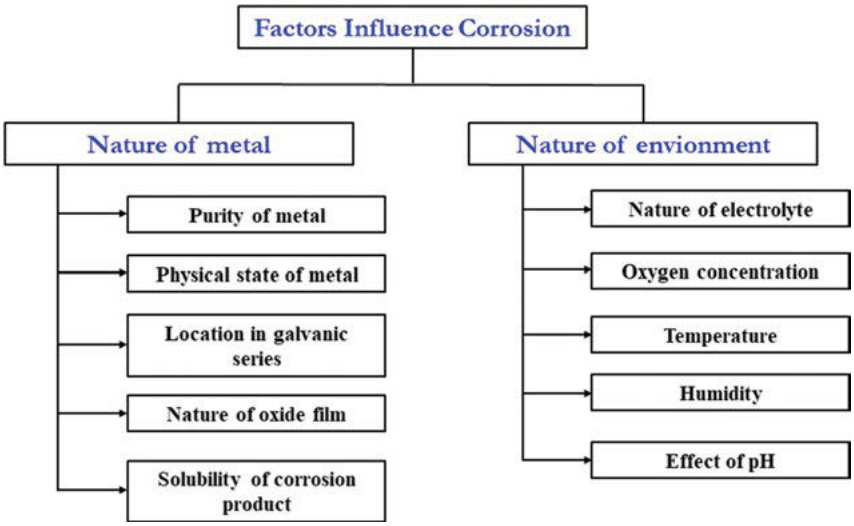

Fig. 3.2: Schematic flowchart representing the factors influencing corrosion.

All factors responsible for corrosion, illustrated in Fig. 3.2, are explained briefly in the following sections.

3.3.1 Nature of the metal

3.3.1.1 Purity of the metal

Impurity in the metal promoted heterogeneity and thereby the galvanic cell is built up with different anodic and cathodic regions in the metal. The extent of corrosion increases by increasing the impurity of metals.

3.3.1.2 Physical state of the metal

The rate of corrosion is influenced by the physical state of the metal. Smaller grain size containing alloy possesses high solubility and hence greater will be its corrosion. In addition to it, the area of the metal possessed stress to be anodic and corrosion takes place at these sites.

3.3.1.3 Location in galvanic series

The location of the metal in the galvanic series is also related to the extent of corrosion. The higher active metal endures more corrosion.

3.3.1.4 Nature of the surface film

In the aerated atmosphere all metals are covered by the thin surface film of metal oxide. The ratio of the volume of metal oxide to the metal is called specific volume ratio. Those metals that have greater specific volume ratio possess lesser corrosion rate.

3.3.1.5 Solubility of corrosion product

Solubility of the corrosion product is related to the extent of corrosion. If the corrosion product is soluble in the corroding medium, then the corrosion occurs at the faster rate. On the other hand, if the corrosion product is insoluble in the corroding medium or interacts with the corroding medium to form another insoluble product, then the corrosion product acts as a barrier and thereby reduces further corrosion.

3.4 Nature of environment

3.4.1 Nature of electrolyte

The rate of corrosion depends on the behavior of the electrolyte. If the metal situated in an electrolyte comprises silicate ions, then generate insoluble silicates that inhibit corrosion. But if the metal is in contact with chloride ions, then the protective layer is destroyed by the attack of chloride ions and the surface is subjected to extensive corrosion. If the conductance of the electrolyte is high enough, then the corrosion current is effectively conducted and thereby the extent of corrosion is enhanced.

3.4.2 Oxygen concentration

Oxygen plays a major role in corrosion phenomena. It is established that oxygen is reduced in the cathodic reaction. In that respective if the concentration of oxygen is increased, the cathodic reaction is more feasible and thereby the corrosion rate is increased.

3.4.3 Temperature

The degree of chemical reactivity as well as the diffusion rate is enhanced with increasing temperature. In this respect, corrosion rate is generally enhanced with increasing temperature.

3.4.4 Humidity

Metal corrodes at a much higher rate under humid conditions. This happens because moisture behaves as an electrolyte for establishing a corrosion cell. Longer the metallic components are exposed to humid air, the faster they will generally corrode.

3.4.5 Effect of pH

Corrosion rate increases with decreasing the pH of the solution.

3.5 Forms of metallic corrosion

Corrosion of metallic materials can be described in many forms. Fontana et al. suggest that there are mainly eight forms of corrosion, which are general (or uniform) corrosion, pitting corrosion, galvanic corrosion, intergranular corrosion, crevice corrosion, hydrogen damage, stress corrosion cracking (SCC), and erosion corrosion [11]. Apart from this some other forms of corrosion are biological corrosion, hydrogen damage, and filiform corrosion. In this chapter, some major forms of corrosion will be highlighted.

3.5.1 Uniform corrosion

The most common and simplest form of metal corrosion is the uniform corrosion. It is characterized as the homogeneous attack on the exposed metal surfaces by the corrosive environment. It is generally thought that metal loss occurs through a chemical attack or dissolution of the metallic component into metallic ions. In the high temperature, uniform corrosion of metal occurs due to combining with other species of corrosive media such as oxygen to produce oxides.

3.5.2 Galvanic corrosion

This form of corrosion is generally referred to as dissimilar metal corrosion. Galvanic corrosion can be observed when copper piping is connected to the carbon steel piping. The coupling of the copper to the carbon steel causes corrosion on the carbon steel. When two dissimilar materials are electrically connected and immersed in an electrolyte, an electric potential exists. The existence of the potential difference provides a stronger driving force for the dissolution of the less noble (more electrically negative) material. In this process, the tendency to dissolve more novel metal is also reduced.

3.5.3 Pitting corrosion

Pitting corrosion is a kind of localized corrosion, in which small volume of metals are removed from certain areas of surfaces as a form of pits. This type of corrosion is one of the most destructive as well as insidious form, and it can cause components to fail. In order to form pits, long imitation period is required and usually grows in the gravitational direction. The initiation of the pits is also responsible for the breakdown of protective film on the metal surface. Pits may also support in

fatigue failure, brittle failure, environment-assisted cracking *like* SCC, and corrosion fatigue by providing sites of stress concentration.

3.5.4 Crevice corrosion

Crevice corrosion is a kind of localized corrosion that takes part within/near to narrow gaps or openings formed by metal-to-metal or metal-to-nonmetal conjunctions. This type of corrosion mainly occurs if there are local differences in oxygen concentrations, gaskets, lap joints, associated deposits on a metal surface, or small amounts of liquid when stagnant in the crevices under a bolt or a round rivet head. This particular type of corrosion can take place on any metal and in any corrosive medium, although metals, particularly aluminum, and stainless steels (where oxide film is generally formed on the surface of these metals) are prone to crevice corrosion, especially in chloride-containing corrosive environments.

3.5.5 Erosion corrosion

Erosion corrosion associated with the mechanically assisted corrosion, which also includes cavitation damage, fatigue, and fretting corrosion. The erosion corrosion usually occurs when the gaseous or aqueous aggressive fluid flowing over the metallic components and increased mechanical wear on the surfaces. All metals which are exposed in the flowing fluids are subject to face erosion corrosion. Erosion corrosion is most commonly observed in the piping and heat exchanger systems. Erosion corrosion is mainly affected by the temperature, turbulence, velocity, prevailing cavitation, impingement, and the presence of suspended solid conditions. Low-strength metals such as copper and aluminum are very much susceptible to erosion corrosion, whereas all grades of stainless steels are resistant to erosion corrosion.

3.5.6 Stress corrosion cracking

SCC is usually caused by the simultaneous presence of specific corrosive medium and the tensile stress. SCC mainly occurs at the point of stress. In SCC, metal surfaces look as if it is free from corrosion although fine cracks developed throughout the surfaces at the points of stress, which can have serious consequences. Based on the corrosive medium and alloy composition, SCC can be classified as intergranular or transgranular. The rate of SCC depends on the temperature, stress levels, and concentration of the corrosive medium. All type of metals is susceptible toward SCC.

3.5.7 Hydrogen damage

Hydrogen damage is the general term used for the description of mechanical damage of metals created in the presence or interaction with hydrogen. Hydrogen damage is mainly classified into four categories: hydrogen blistering, decarburization, hydrogen embrittlement, and hydrogen attack. Hydrogen blistering occurs due to the penetration of hydrogen inside the metal. Removal of carbon from the steel or decarburization happens due to the moist hydrogen at high temperature. Decarburization usually lowers the tensile property of the steel. Hydrogen embrittlement also happens due to the diffusion of hydrogen inside the metals and thereby lowers down the most important property of the metals such as tensile strength, elongation, and ductility. Hydrogen attack refers to the interaction between the metallic components and hydrogen at high temperature.

Hydrogen blistering and hydrogen embrittlement are the most dangerous as well as concerning among the four types of hydrogen damage listed above and may occur during picking, exposure to petroleum, welding process, and in chemical process stream. As mechanical damage is produced by these two effects, catastrophic failure may occur if it is not prevented.

3.6 Economic adverse effects of corrosion

The effect of corrosion shades our daily life by both direct and indirect ways. Corrosion is a universal enemy and it is inevitable. Corrosion can be easily recognized in our home on the automobile body panels, furniture, metal tools, grills, and so on. In order to prevent such items from corrosion, one of the significant preventative measures usually used is the painting. Corrosion is more concerning in the perspective of economics and safety. The corrosion of steel reinforcing bars in concrete can be easily noticed. It causes the failure of the building, parking structure, bridge, highway overbridge, and collapse of the electrical towers, thereby resulting in significant amount of economic losses and increased casualties. Corrosion, which resulted in the major industrial plants such as electrical power plant, oil industry, and chemical processing plant, is perhaps more dangerous and major concern. There are many direct and indirect consequences of corrosion. Economic consequence is the major cause of the following issues [12, 13]:

- Corroded equipment replacement
- Shutdown of equipment due to corrosion failure
- Protection cost such as the use of coating, inhibitors, and cathodic protection
- Product contamination
- Loss of efficiency of the equipment: as, for example, corrosion products decrease the heat transfer rate in heat exchangers

- Slowdown of production
- Use of more expensive corrosion-resistant materials
- Research and development

Some other consequences are social and can cause the following issues:
- Health; for example, the product which is escaping from the corroded equipment can also create pollution.
- Safety: for example, failure of the metallic equipment/components can cause explosion, release of toxic product, fire, and so on. Collapse of the construction also increases casualties.
- Depletion of natural resources, including metals and fuels, is used to manufacture them.

3.6.1 Corrosion-related accidents

Disaster is an accident that can lead to tremendous destruction to the environment: equipment's, plant's, and people's life. Corrosion is a kind of disaster which not only destroys the metallic structures of the equipment but also increases the possibility of causalities in other way around. Herein, some huge disasters due to corrosion have been summarized and presented in Tab. 3.1 [12].

Tab. 3.1: List of some accident which are directly and/or indirectly related to corrosion.

Year	Place	Name of accidents	Reason
1967	Ohio, USA	Silver Bridge collapse	Silver Bridge collapsed due to the overweight, resulting in the death of 46 people. For this collapse, corrosion fatigue and stress corrosion cracking were responsible.
1984	Bhopal, India	Bhopal accident	From a storage tank, methyl isocyanate (MIC) gas is leaked due to corroded pipelines and valves. The surrounding area was exposed to toxic gas *like* MIC and other life-threatening chemicals. In this accident, over 3,000 people were killed and 500,000 people were injured.
1985	Uster, Switzerland	Swimming pool roof collapse	Due to stress corrosion cracking, the concrete roof supported by stainless steel was collapsed, where 12 people were killed.

Tab. 3.1 (continued)

Year	Place	Name of accidents	Reason
1988	Island of Maui, Hawaii	The Aloha incident	Due to multiple corrosion fatigue damage, a 19-year-old Boeing 737 lost its significant portion of the upper fuselage in operating flight. It was reported that one flight attendant lost her life.
1992	Guadalajara, Mexico	Guadalajara sewer explosion	This accident was caused due to the galvanic corrosion of pipelines. In this explosion, 215 people were killed and 1,500 people were injured. In addition to it, this accident damaged 1,600 buildings.
1999	Brittany, France	Sinking of the Erika	The tanker was broken due to corrosion, releasing thousand tons of oil into the sea which kill marine life and polluting shores around Brittany, France.
2000	New Mexico, USA	Carlsbad pipeline explosion	El Paso Natural Gas Company (EPNG) operates a few tens (~30-inch) of diameter pipelines for the transportation of natural gases. It was found that the pipeline system suffered from massive damage due to internal corrosion. In this tragic incidence, 12 people were killed.
2017	Ohio, USA	Ohio State Fair accident	A pendulum-type thrill ride failed during operation due to the rust. In this accident, one person was dead and several others were injured.

3.6.2 Corrosion-related costs

Corrosion is one of the major problems throughout the world. In industries, corrosion of equipment and other metallic components always deserves to be a considerable issue. The oil sector expensed lot of money to mitigate corrosion. Corrosion creates severe failure in the blades of motors/turbines, boiler tanks, harmful/aggressive chemical containers, pressure basins, automotive routing devices and so on. Huge amount of money is lost in order to replace the corroded parts or due to its maintenance.

In the USA (2002), FHWA published a report associated with the metallic corrosion in a wide range of industries [6]. The results published in this study suggest that the total annual cost of corrosion in the USA was US $276 billion which is equivalent to 3.1% of the US GDP. In Japan, the study carried out by the Japan Society of Corrosion Engineering and the Japan Association of Corrosion Control estimated that the total cost of corrosion was equivalent to 1.88% of the 1997 gross national product (GNP) (1.73% of GDP) [14]. In 1982, the Commonwealth Department of Science and Technology conducted a study for annual cost of corrosion in

Australia. The report suggested that the annual cost of corrosion was AUD2 billion at 1982 prices to the Australian economy, which is approximately equivalent to 1.5% of Australia's GNP in that year [15]. In 1992, Kuwait also carried out corrosion-related cost, which suggests that the total cost of corrosion is around US $1 billion (at 1987 price of dollars), which is closely equivalent to 5.2% of Kuwait's 1987 GDP [16]. In 2003, Saudi Aramco (national oil company in Saudi Arabia) performed a study to derive the corrosion-related cost toward the focusing of areas that had the largest economic impact on corporate performance, that is; plant, engineering, and research investment [17]. According to this report, corrosion-related cost in the company's existing operations was ~US $900 million per year. They also concluded that approximately 25% or US $225 million can be avoidable by modifying/improving of corrosion technology and management. The recent study (in 2011–2012) accomplished by R. Bhaskaran et al. suggest that the direct cost of corrosion in India was US $26.1 billion or 2.4% of India's GDP. The indirect cost of corrosion was evaluated to be US $39.8 billion or 3.6% of India's GDP [18]. In 2015, Chinese Academy of Engineering carried out the national cost of corrosion and costs associated with the industries in China. The study summarized that the cost of corrosion was ~2127.8 billion RMB (~310 billion USD) or 3.34% of the GDP of China [19]. According to the report published in 2013 suggests that the current global cost of corrosion was estimated to be US $2.5 trillion, equivalent to 3.4% of the global GDP (2013) [20, 21]. It was estimated that by using proper corrosion control, it is possible to save 15% and 35% of the corrosion cost. Several industries realize that lack of corrosion management increases the corrosion cost in terms of accidents, forced shutdowns of plants, product contamination, and through proper corrosion management, it is possible to save the significant amount of cost.

3.7 Corrosion prevention

It is quite impossible to stop corrosion completely. However, it is possible to minimize or control the corrosion by various methods. In order to prevent corrosion, the main aim is the reduction of the effects of conditions that are responsible for corrosion. There are many methods for corrosion minimization, and the most widely accepted methods among them are [22]:

(i) materials can be selected in such a fashion that it does not corrode in the actual environment;
(ii) suitable design that will avoid corrosion;
(iii) cathodic and anodic protection;
(iv) application of coatings; and
(v) change of environment.

Among all the aforesaid methods, the selection of the proper method depends on the economic consideration, safety, environmental issues, appearance and so on. In the first method, it has been highlighted that materials have been chosen in such a way that it does not corrode in the actual environment. It suggests that according to the environment condition, materials should be selected. The second method is the suitable design that will be helpful toward corrosion inhibition. In this particular method, all the individual components, the interaction between them, and their effect to the other structures and the existing surroundings have been taken care of. Cathodic protection is another method by which corrosion can be minimized. In this method, the protected metal (the metal which needs to be protected from corrosion) acts as a cathode and another sacrificial metal which is not that much expensive and corrodes more easily than that of the protected metal acts as an anode in the electrochemical cell. In this method, the sacrificial metal corrodes instead of the protected metal. Whereas in the anodic protection, the protected metal acts as anode of the electrochemical cell, and the electrode potential of which is maintained in the zone where the metal is passive. Apart from the aforementioned techniques, coating is the widely used technique which is most commonly used to inhibit the metallic materials from the adverse effect. Herein, coating acts as a barrier for the adsorption and penetration of corrosive species such as oxygen, moisture, and ionic ingredients toward the metal surfaces. Modification of the environment is another method which is also useful for corrosion mitigation. In this particular method, change of environment by the following ways reduces the corrosion rate of metals: decreasing (or increasing) the flow velocity, decreasing (or increasing) the temperature, decreasing (or increasing) the aggressive species or oxygen content, and addition of corrosion inhibitor in the aggressive media. In general, corrosion rates are reduced by reducing the content of oxygen, aggressive species, temperature, and flow rates. Uses of corrosion inhibitors in the aggressive media also reduce the rate of corrosion. In this method, organic/inorganic molecules that have the potential to absorb on the metallic surfaces are used. The adsorbed inhibitor molecules formed a protective layer on the metallic surfaces and protect it from corrosion.

In this chapter, detailed discussion of metallic corrosion inhibition using protective coating and corrosion inhibitors has been emphasized. Corrosion inhibition using application of the protective coating has been addressed in detail followed by the use of proper inhibitors.

3.7.1 Corrosion control by the use of applied coatings

To inhibit the degradation of metallic materials, the application of coating materials is one of the best methods. Intensive efforts are in progress to develop the promising coating materials which are able to inhibit corrosion in the structural and industrial equipment. Coating acts as a barrier to inhibit the penetration of corrosion species

such as moisture, oxygen, and ionic ingredients toward the metallic surfaces. Depending on the requirements, coating may be single layer or multilayer. Generally, multilayer coating is comprised of the pretreated surface, primer, intermediate coat, and topcoat. Pretreated surface and primer coat enhance the adhesion of coating. Addition of anticorrosion materials into the intermediate coat enhances the corrosion inhibition property as well as durability of the coating. Aesthetics value is generally provided by the topcoat layer. The final coat also added environmental resistance to the coating.

3.7.2 Components of coating

To obtain good-quality coating, it is needed to understood how to formulate the coating. Three major components, such as binders (or resins), vehicle (or fluid carrier, i.e., solvent), and pigments are the pillar of the coating. Apart from these, cosolvents and additives are also used to obtain desired properties. The nature of the components used in the coating formulation decided adhesion, durability, glossiness, resistance against corrosive ingredients, impact resistance, hardness, and so on. Thus, it can be said that proper planning and selection of individual components for coating formulation is very much important. In the following sections, various components of coating formulations have been discussed.

3.7.2.1 Binder or resin

The dense solid film formed on the substrate after its application is called binder. The binder generally provides cohesive and adherent film on the substrate surface. Intrinsic molecular property, molecular size, and complexity of the binder determine the compactness of the coating film. It is observed that those binders that have high molecular size adsorbed easily on the substrate surfaces upon evaporation of the solvents. On the contrary, small size binders react with the substrate surface atoms and form chemical bond. In general, according to the chemical reactivity, binders are classified. The most important categories of binders are oxygen-reactive binders, heat conversion binders, inorganic binders, lacquers, coreactive binders, condensation binders, coalescent binders and so on. Several polymers are generally used as binders.

3.7.2.2 Pigment

In the coating formulation, another major component is pigment. It is useful to enhance the glossiness of the coatings, inhibit metallic corrosion, color the coatings, and so on. Corrosion-inhibitive pigments also increase the anticorrosive property of

the applied coatings. Pigment should be selected in such a way that it has minimum solubility so that it prevents from leaching out of the coating layers. Water-soluble pigments are not useful as water or diffuse moisture may dissolve the pigment and cause blister formations. Another factor is the pH of the pigment. High pH-containing pigment has adverse effect on the curing of the acid-catalyzed systems, whereas very low pH-containing pigments have lethal effect on stability of waterborne coatings. Thus, there is a need to use pigment with optimum pH concentration for the stability of the coating. Literature suggests that a wide range of organic, inorganic, and ion-exchange-type compounds are used as pigments in coating formulation.

3.7.2.3 Solvent

Solvents provide one of the major roles in the coating formulation. It dissolves major components in the coating *like* binders and pigments, thereafter, applied on the substrate. Solvent evaporates after successful application of the coating and allows to form a thin layer on the substrate surfaces. Household paints are mainly water-based paints. Solvent-based paint mainly uses aromatic hydrocarbons (like ethylbenzene, toluene, mixed xylenes, benzene, and high-flash aromatic naphtha) and aliphatic hydrocarbons (such as heptanes, mineral spirits, kerosene, and hexanes).

3.7.2.4 Thinner

Thinners are used as a cosolvent to decrease the viscosity of the paint. Thinners are also used to reduce the use of expensive solvents. Sometimes it is called as diluent. Commonly used thinners are acetone, benzene, mineral spirits, *n*-butyl acetate, turpentine, butan-1-ol, 2-butoxyethanol, xylene, toluene, naphtha, methyl ethyl ketone, and so on. In water-based paints, thinners are useful for emulsion and dispersion of coating materials in water.

3.7.2.5 Additive

Other than the three major components (binders, solvents, and pigments), another component used in paint formulation is the additive. Various properties of the coatings such as appearance after coating applications, thickness, ease of cleaning, durability of coating, re-coating ability, hydrophobic or hydrophilic properties, and leveling influence the additives. These properties highly depend on the structure and chemical composition of additives. As per the uses, additives can be categorized as follows: thickening agents, surface-active agents, surface modifiers, leveling agent and coalescing agents, catalytically active additives, and special effect additives.

Till now, detailed description of coating materials formulation has been discussed. In the next section, corrosion inhibition using inhibitors has been emphasized.

3.8 Corrosion control by the use of inhibitors

In the petroleum industry, corrosion is a well-known phenomenon and it creates maximum damage on the oil field equipment. Corrosion effect on the oil field equipment can be reduced or controlled by the use of chemical substances to the corrodent. The chemical substances added to the corrodent are known as corrosion inhibitors. Added inhibitors reduce the rate of corrosion (either anodic oxidation, cathodic reduction, or both). The advantage of using corrosion inhibitors is that it can be applied without modifying or disrupting any processes. Corrosion inhibitors are used in chemical manufacturing, petroleum refineries, water treatment, and product additive industry. Inhibitors can be classified based on the inhibition mechanism (cathodic, anodic, or both), application (pickling, acid cleaning, descaling, etc.), or their chemical nature (inorganic and organic). Based on the chemical nature, inhibitors are generally classified (Fig. 3.3). Inorganic inhibitors have anodic or cathodic action, whereas organic inhibitors have both the action.

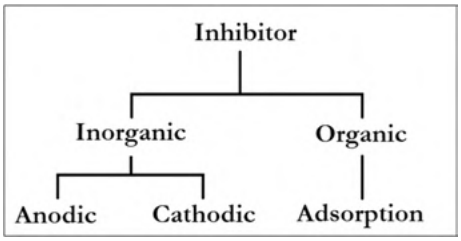

Fig. 3.3: Classification of corrosion inhibitor molecules.

Molybdates, chromates, phosphates, nitrites, and nitrates are examples of the anodic-type inhibitors, whereas antimony, bismuth, and arsenic are examples of cathodic-type inhibitors. Organic compounds such as Schiff base, imidazole, thiazole, quinoline, and thiourea are used as organic corrosion inhibitors (Tab. 3.2) [23]. Organic inhibitors generally adsorb on the metallic surfaces by the heteroatoms (N, O, S, etc.), aromatic rings, π-electrons, and so on present in the inhibitors and form a protective layer over the surfaces. Protective layer acts as a barrier film which blocks anodic and cathodic active sites of the metal substrates. Film-forming organic compounds may exhibit anodic, cathodic, or mixed properties.

Tab. 3.2: Chemical structures of different types of organic inhibitors.

Imidazoline based	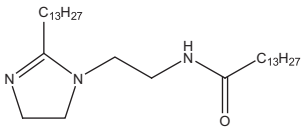 *N*-(2-(4,5-Dihydro-2-tridecylimidazol-1-yl)ethyl) tetradecanamide	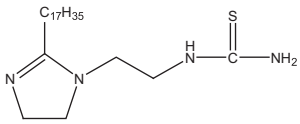 1-(2-(2-Heptadecyl-4,5-dihydroimidazol-1-yl) ethyl)thiourea
Triazole based	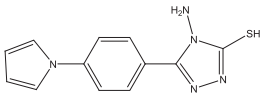 1-Amino-2-mercapto-5-(4-(pyrrol-1-yl)phenyl)-1,3,5-triazole	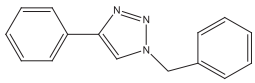 1-Benzyl-4-phenyl-1H-1,2,3-triazole
Pyridine based	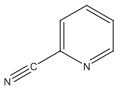 2-Pyridinecarbonitrile	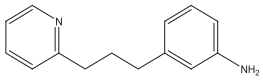 3-(3-(pyridin-2-yl)propyl)benzenamine
Quinoline based	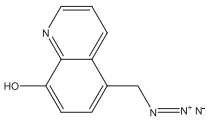 5-(Azidomethyl)quinolin-8-ol	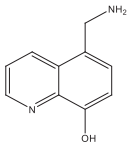 5-(Aminomethyl)quinolin-8-ol 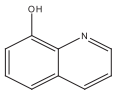 8-Hydroxyquinoline
Thiourea based	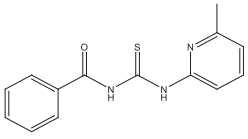 *N*-(6-Methylpyridin-2-ylcarbamothioyl)benzamide	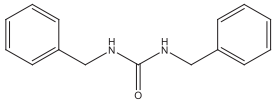 1,3-Dibenzylurea
Ionic liquids	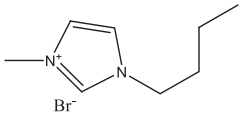 1-Hexadecyl-3-methylimidazoliumbromide	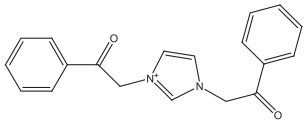 1-Vinyl-3-butylimidazolium bromide

Tab. 3.2 (continued)

Benzimidazole based	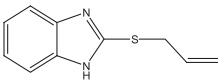 2-(Allylthio)-1H-benzo[d] imidazole	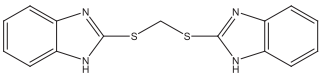 Bis(1H-benzo[d]imidazol-2-ylthio)methane	
Schiff base	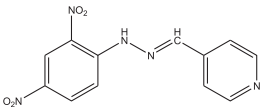 (*E*)-1-(2,4-Dinitrophenyl)-2-((pyridin-4-yl)methylene) hydrazine	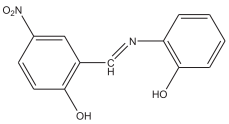 (*E*)-2-(2-Hydroxy-5-nitrobenzylideneamino) phenol	
Pyrazine based	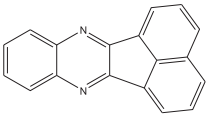 Acenaphtho[1,2-b]quinoxaline	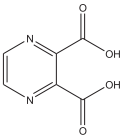 Pyrazine-2,3-dicarboxylic acid	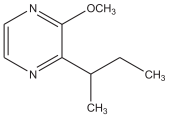 2-Sec-butyl-3-methoxypyrazine
Pyrimidine based	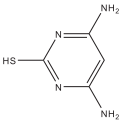 4,6-Diamino-2-pyrimidinethiol	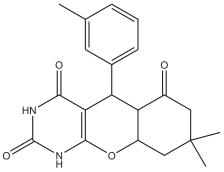 5,5a,7,8,9,9a-Hexahydro-8,8-dimethyl-5-m-tolyl-1Hchromeno[2,3-d] pyrimidine-2,4,6(3H)-trione	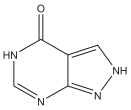 2H-Pyrazolo[3,4-d]pyrimidin-4 (5H)-one

Corrosion inhibitors adsorbed on the metallic surfaces by physical adsorption and/or chemical adsorption thereby formed a thin film which reduces the rate of corrosion. Herein, these two adsorption phenomena are elaborately discussed.

3.8.1 Physical adsorption

In physical adsorption, inhibitor molecules adsorb on the metallic surfaces by an electrostatic interaction. The charge on the metallic specimen is developed due to the formation of electric field at the outer Helmholtz plane of the electrical double layer, whereas charge on the inhibitors is due to the ions or dipoles. The difference between

corrosion potential (E_{corr}) and its zero-charge potential ($E_q = 0$) determine the charge on the metallic surfaces [24]. If ($E_{corr} - E_q$) is less than zero, the metal surface is negatively charged, similarly when ($E_{corr} - E_q$) is greater than zero, the metal surface is positively charged. The inhibitor molecule adsorbs as per the charge on the metallic surfaces. When the metallic surface is comprised of positive charge, anionic species such as Cl^- and SO_4^{2-} ions present in the solution first adsorb at the metal/solution interface. Therefore, charge on the surface of the metal toward the solution side changes from positive to negative. On the other hand, when inhibitors are placed in the acidic solution, some of the inhibitors gets protonated and adsorbs electrostatically on the metallic surfaces over the primarily adsorbed negatively charged ions. When the metal surface is negatively charged, the positively charged inhibitor molecule directly adsorbs on the metallic surfaces.

3.8.2 Chemical adsorption

Chemical adsorption is the coordinate bond formation between the charge transfer or share between the inhibitor molecule and metallic surface atom. In comparison to the physical adsorption, it takes place more slowly and requires higher activation energy. Additionally, chemical adsorption also depends on the temperature and it is more feasible at elevated temperature. Chemical adsorption is generally irreversible in nature, and the formation of chemical bond mainly depends on the type of inhibitors and metals. In chemical adsorption, electron transfer occurs from the highest occupied molecular orbital (HOMO) of the inhibitor to the vacant d-orbital of metal, whereas electrons coming from the valence bond of the metal also accommodate to the lowest unoccupied molecular orbital (LUMO) of the inhibitors. Therefore, those inhibitors that have higher energy of HOMO and lower energy of LUMO easily adsorb on the metallic surfaces. In this way, surface-adsorbed inhibitor molecules act as a protective barrier film for minimizing corrosive attack from the corrosive environments.

3.9 Summary

This chapter briefly discussed the basic concept of corrosion, its economic adverse effect, and the methods of corrosion mitigation. In order to inhibit corrosion, it is mandate to have a proper knowledge of the basic principles of electrochemistry, kinetic as well as thermodynamic fundamentals of corrosion, and several other factors that are described in this chapter. In addition to it, fundamentals of physical metallurgy are also important as corrosion is related to the microstructure and chemical composition of the metal. This chapter also highlighted economic adverse effect of corrosion and the proper methods useful for corrosion inhibition. The choice of corrosion prevention

methods should be selected according to the economic consideration, safety, and environmental issues. One of the most widely used corrosion preventive measures in the industrial field is the coating and corrosion inhibitor. Eco-friendly coating materials and corrosion inhibitors have been effectively used in the industrial field for corrosion inhibition of metallic materials from a wide range of adverse environments. These two inhibition techniques remain an active area of research for both the academic and industrial scientists.

References

[1] https://www.g2mtlabs.com/cost-of-corrosion/.
[2] https://economictimes.indiatimes.com/news/economy/finance/india-loses-rs-2-trillion-annually-to-corrosion-of-infrastructure-government/articleshow/48792499.cms.
[3] https://www.academia.edu/2233096/Case_study_on_some_of_the_major_corrosion_catastrophes_in_the_history.
[4] https://timesofindia.indiatimes.com/india/14-killed-15-injured-in-gas-pipeline-blast-in-Andhra-Pradesh/articleshow/37299930.cms.
[5] https://en.wikipedia.org/wiki/1992_Guadalajara_explosions.
[6] Koch, G.; Brongers, M.; Thompson, N.; Virmani, P.; Payer, J. Corrosion cost and preventive strategies in the United States, FHWA-RD-01-156, March 2002.
[7] Tanwer, S.; Shukla, S.K. Recent advances in the applicability of drugs as corrosion inhibitor on metal surface: A review. Curr. Res. Green Sustainable Chem. 2022, *5*, 100227.
[8] Kim, Y.S.; Lim, H.K.; Kim, J.J.; Hwang, W.S.; Park, Y.S. Corrosion cost and corrosion map of Korea. Corros. Sci. Tech. 2011, 10, 52–59.
[9] Schweitzer, P.A. Fundamentals of corrosion: Mechanisms, causes, and preventative methods, CRC Press, Taylor and Francis Group, 2010.
[10] Roberge, P. R. Corrosion engineering: Principles and practice, McGraw-Hill Companies, New York, 2008.
[11] Fontana, M.G. Corrosion engineering, McGraw-Hill, New York, 1987.
[12] Mazumder, M.A.J. Global impact of corrosion: Occurrence, cost and mitigation. Glob. J. Eng. Sci. 2020, 5, 1–5.
[13] Davis, J. R. Corrosion: Understanding the Basics, ASM International, Materials Park, Ohio, USA, 2000.
[14] Survey of corrosion cost in Japan, Committee on Cost of Corrosion in Japan, Japan Society of Corrosion Engineering and Japan Association of Corrosion Control, 1997.
[15] Cherry, B.W.; Skerry, B.S. Corrosion in Australia: The report of the Australian National Centre for corrosion prevention and control feasibility study, 1983.
[16] Al-Kharafi, F.; Al-Hashem, A.; Martrouk, F. Economic Effects of Metallic Corrosion in the State of Kuwait, Final Report No. 4761, KISR Publications, December 1995.
[17] Tems, R.; Al Zahrani, A.M. Cost of corrosion in oil production and refining. Saudi Aramco J. Technol. 2006.
[18] Bhaskaran, R.; Bhalla, L.; Rahman, A.; Juneja, S.; Sonik, U.; Kaur, S.; Kaur, J.; Rengaswamy, N.S. An analysis of the updated cost of corrosion in India. Mater. Perform. 2015, 53, 56–65.
[19] Hou, B.; Li, X.; Ma, X.; Du, C.; Zhang, D.; Zheng, M.; Xu, W.; Lu, D.; Ma, F. The cost of corrosion in China. Npj. Mater. Degrad. 2017, 1, 4.

[20] Koch, G.; Varney, J.; Thompson, N.; Moghissi, O.; Gould, M.; Payer, J. International measures of prevention, application, and economics of corrosion technologies study, NACE International, 15835 Park Ten Place, Houston, TX 77084, 2016.
[21] El-Sherik, A.M. Trends in oil and gas corrosion research and technologies, Elsevier, Woodhead Publishing, UK, 2017.
[22] Bardal, E. Corrosion and protection, Springer, London, 2004.
[23] Saha, S.K.; Banerjee, P. Inhibition of metallic corrosion by N, O, S donor Schiff base molecules, Apple Academic Press, Taylor & Francis, USA, 2018, 145–194.
[24] Deng, S.; Li, X.; Fu, H. Two pyrazine derivatives as inhibitors of the cold rolled steel corrosion in hydrochloric acid solution. Corros. Sci. 2011, 53, 822–828.

Maryam Sirati Gohari, Seyed Ali Rezaei, Alimorad Rashidi*

Chapter 4
Carbon allotropes for anticorrosive applications, challenges, and opportunities

Abstract: One of the best strategies to control surface corrosion is using protective coatings. A set of protective coatings created from different materials, such as organic, have been studied for their use as a barrier in controlling surface degradation. However, defects and porosities usually occur inside organic coatings during the applying processes or hardening stage, which can negatively affect the corrosion protection performance of such layers. Incorporating fillers can effectively enhance the barrier properties and corrosion resistance. Carbon-based nanofillers have achieved increasing attention due to their magnificent properties to address the mentioned issues and improve the durability and impermeability of aggressive species.

Keywords: carbon allotropes, anticorrosive coating, nanocomposite coating, carbon nanotubes, graphene

4.1 Introduction

Corrosion is an undesirable progressive chemical reaction that cannot be completely controlled in a wide variety of environments. Different approaches are only focused on slowing down the reaction rate and developing effective corrosion protection mechanisms. Using protective coatings is one of the best techniques to control surface corrosion. A set of protective coatings created from different materials, such as organic, have been studied as a barrier to control metal surface degradation by restricting the corrosive species penetration [1]. The conventional coatings for corrosion protection, usually made from heavy metals including chromium (Cr), zinc (Zn), phosphate (p), and copper-based alloys, are poisonous and harmful to the environment [2–4]. As a result, there have been many studies to find proper and effective

*Corresponding author: **Alimorad Rashidi**, Nanotechnology Research Center, Research Institute of Petroleum Industry (RIPI), Tehran, Iran, e-mail: rashidiam@ripi.ir
Maryam Sirati Gohari, Research Department of Ceramic, Materials and Energy Research Center, Alborz, Iran, e-mails: m.sirati@merc.ac.ir
Seyed Ali Rezaei, Research Department of Ceramic, Materials and Energy Research Center, Alborz, Iran, e-mail: sa.rezaei@merc.ac.ir

https://doi.org/10.1515/9783110782820-004

alternatives with less harmful consequences on the ecosystem. Nowadays, using organic coatings is known as a cost-effective method through which significant physical protection properties from the diffusion of corrosive ions can be provided. However, defects, cavities, and free volumes usually occur inside organic coatings during the applying or curing processes, generating microscopic pathways and making them permeable to corrosive species. A variety of strategies have been proposed to improve the anticorrosive features of such coatings. Incorporating different fillers has been investigated as an impressive strategy to improve corrosion resistance. Carbon-based nanofillers (Fig. 4.1) have obtained significant research interest to provide proper anticorrosion performance for nanocoatings, due to their magnificent properties [5]. This chapter presents challenges, such as uncontrolled distribution and limited solubility, in different matrixes and different kinds of mechanisms for corrosion inhibitor systems through some well-known carbon-based materials, as well as an outlook towards the future of carbon allotropes for anticorrosive application.

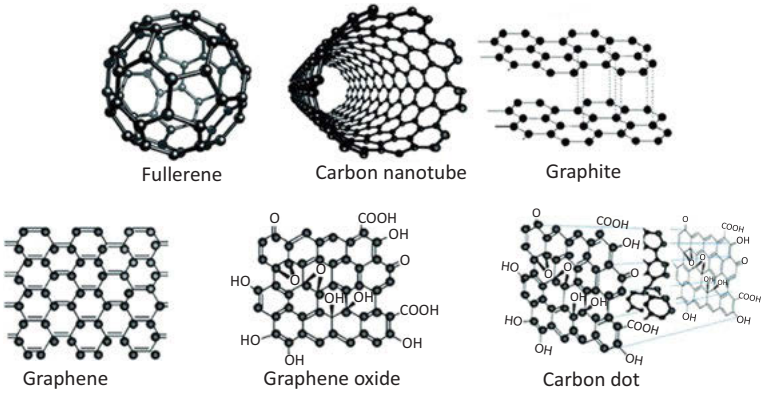

Fig. 4.1: Well-known forms of carbon-based nanomaterials (reprinted with permission from ref. [6]).

4.2 Carbon-based nanomaterials functionalization

Weak dispersibility and insolubility in solvents and matrix have limited the industrial and medical applications of the carbon-based nanomaterials, which can be tuned via appropriate modification, in order to introduce the polar substituents in the structures of these nanomaterials. Carbon allotropes functionalization can be divided into covalent (the covalent attachment of the carbon-based materials to the polar substituents) and noncovalent (weak electrostatic forces (intermolecular van der Waals forces)) approaches.

4.2.1 Covalent approaches

These methods involve the formation of covalent attachment between the carbon-based material and the polar substituents. Carbon allotropes possess some particular site(s), where modification can be carried out via covalent bond. For instance, –COOH (carboxyl), –OH (hydroxyl), and –COC– (epoxide ring) are the sites in graphene and its analogues for covalent modification through condensation and esterification reactions [7–9]. Covalent modification of carbon-based materials can be developed, based on the attachment of peripheral substituents to their molecular structures to extend their applications [10, 11]. However, these sorts of modifications of carbon allotropes can lead to physiochemical changes. For instance, covalent functionalization of CNTs can bring physiochemical changes such as distribution improvement in different media, interfacial adhesion enhancement, reduction of hydrophobicity, reduction of the aggregation ability, mechanical strength reduction, and electrical conductance reduction. A pictorial illustration of commonly used covalent sidewall modification reactions for CNTs is presented in Fig. 4.2. In cycloaddition reaction for covalent functionalization of graphene oxide, sp^2-hybridized carbons converted into sp^3-hydridized, leading to the electron conductance reduction [12]. A pictorial illustration of covalent modification of GO using amination, esterification, and amidation processes is presented in Fig. 4.3.

4.2.2 Noncovalent approaches

These kinds of modifications offer an impressive strategy to functionalize the carbon-based material, without major changes in thermal and electrical properties. π–π stacking, electrostatic interactions, van der Waals intermolecular force of attractions, and hydrophobic interactions are principally used for functionalization of carbon allotropes noncovalently [14–17]. Noncovalent modification using π–π stacking is broadly investigated. Hydrophobic interactions can be regarded as the interaction of carbon allotropes with macromolecules, ionic liquids, and surfactants. The mentioned interactions are mainly employed to disperse carbon-based material in aqueous solvents as well as organic solvents. Interactions between ionic liquids and carbon allotropes mostly require electrostatic interactions such as graphene oxide, which contains several ionic compounds, such as carboxylate and hydroxylate ionic groups. In addition to the mechanism mentioned above, non-covalent modification of carbon-based material can also be carried out by hydrogen attachment [12]. Schematic illustration of noncovalent functionalization of GO is presented in Fig. 4.4.

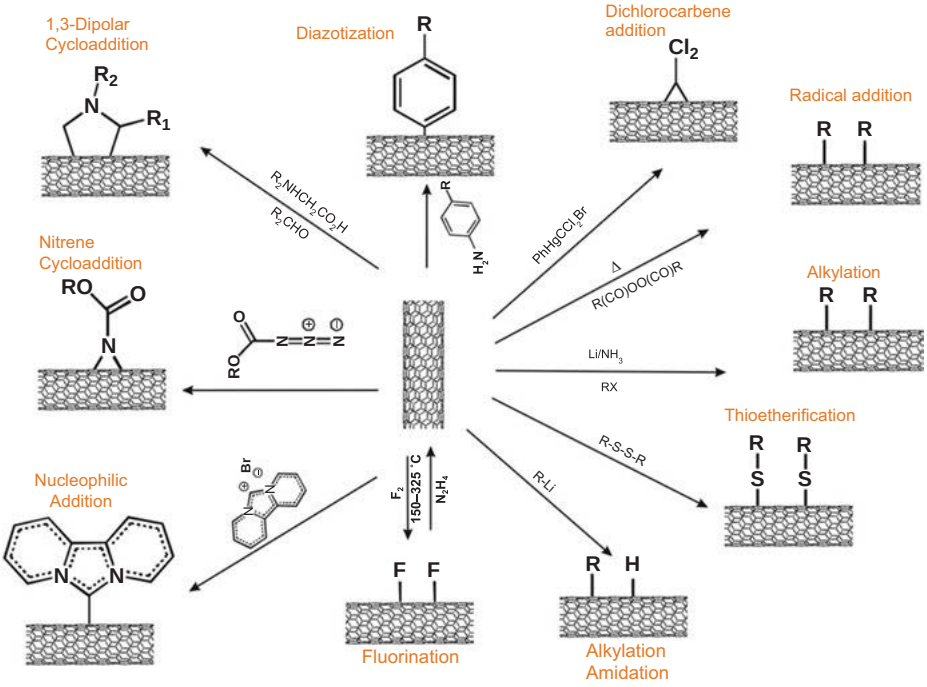

Fig. 4.2: Commonly used covalent sidewall modification reactions for CNTs (reprinted with permission from ref. [13]).

4.3 Carbon allotropes as corrosion inhibitor

Carbon allotropes have been studied for corrosion protection as a suitable alternative to toxic and hazardous inorganic and organic inhibitors [18]. Carbon-based materials offer an eco-friendlier solution, as traditional coatings contain substances that harm aquatic life. The interest in carbon allotropes originates from their magnificent properties including cost parity, abundancy, simple synthesis, lightness, excellent mechanical properties, thermal stability, increased durability, and biocompatibility. Carbon-based materials have been investigated for corrosion protection and showed promising inhibition efficiency [19–21]. Several approaches, such as doping with nitrogen or sulfur, surface functionalization, metals incorporation, or combination with polymers in composites, have been reported to develop appropriate inhibition ability for carbon allomorphs. It is recognized that carbon and its allotropes impede corrosion through a defensive mechanism, the so-called barrier protection, in which carbon-based materials act as a shielding layer, preventing air, salt, and moisture from coming into contact with the substrate [22–24]. Recent advances on carbon nano-

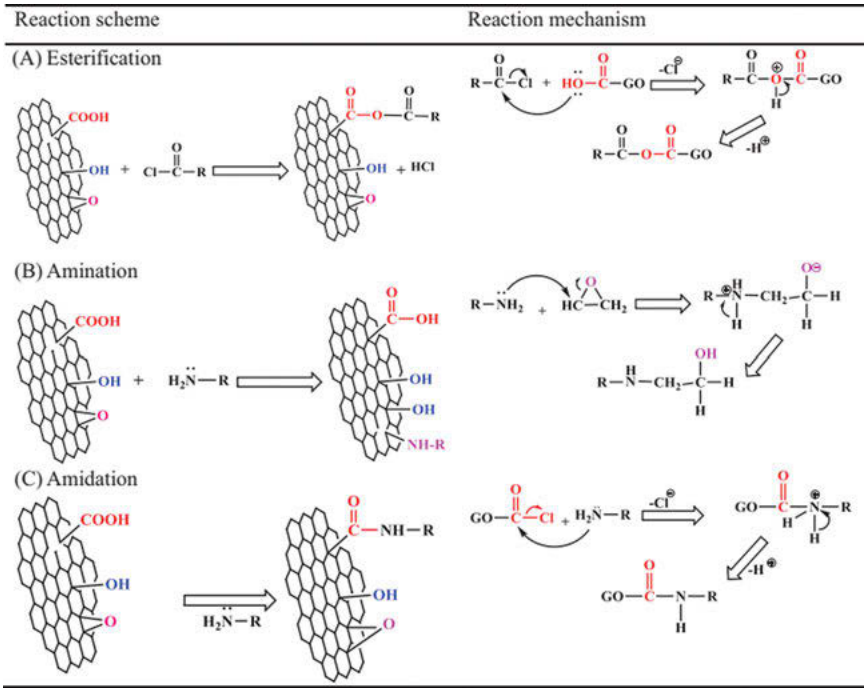

Fig. 4.3: Covalent modification of GO using esterification (A), amination(B), and amidation (C) processes (reprinted from ref. [12], Open Access Article).

allotropes applications in anticorrosive coatings on different metallic surfaces are reviewed in the following.

4.3.1 Carbon nanotubes

Carbon nanotubes (CNTs) have been known to be an excellent choice for conductive fillers due to their large specific surface area, large aspect ratio, and appropriate electrical features [25, 26]. CNTs are categorized as single-walled carbon nanotubes (SWCNTs) and multi-walled carbon nanotubes (MWCNTs). Applying CNTs can positively affect coating features such as stiffness, fracture toughness, Young's modulus, and high thermal stability [27–29]. Based on many studies, remarkable improvement in the corrosive resistance ability of the protective coatings possessing CNTs reflects the electrical current distribution effect on the metallic substrate, which can protect the surface from any localized damage. CNTs reduce the defects and porosities so that compactness of coating can be improved. Not only CNTs can develop proper corrosion resistance in the coatings, they can also enhance the adhesion coatings on metal substrates [30–32].

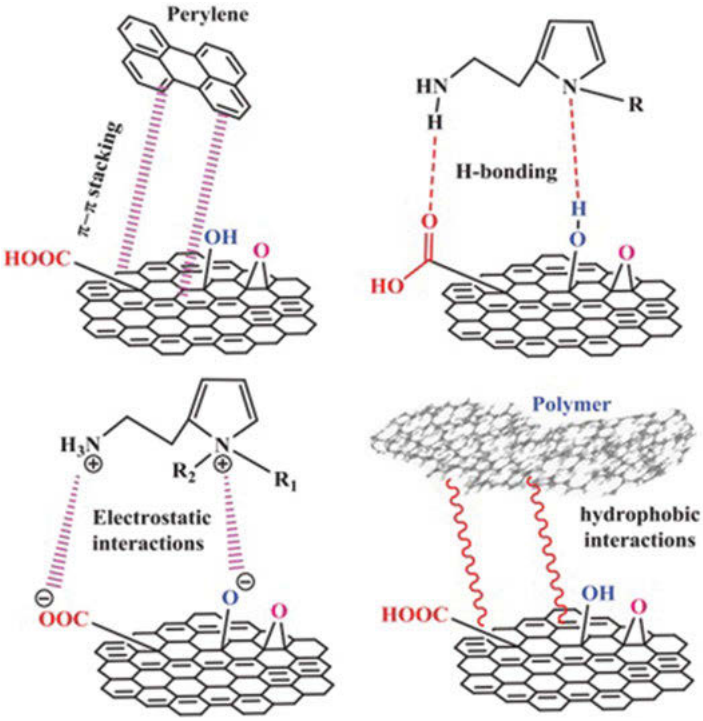

Fig. 4.4: Schematic illustration of noncovalent functionalization of graphene oxide (reprinted from ref. [12], Open Access Article).

A study on the corrosion resistance performance of MWCNTs-reinforced epoxy coatings on aluminum alloys showed that incorporating MWCNTs decreases porosity of coatings and increases the adhesive strength of epoxy composite coatings. Well-distributed MWCNTs in epoxy have decreased the path of ion penetration to the coating and the low-frequency impedance value, indicating overall protection performance. The adhesion and wear resistance of the protective coating were also improved by the addition of MWCNTs, indicating that the bond between the substrate and the epoxy was strengthened. However, it was confirmed that the fracture stress was reduced and that MWCNTs could not improve the mechanical characteristics, because of the weak interaction between the CNTs and the coating structure, which can lead to a reduction in cohesive strength [33].

The excellent distribution of MWCNTs in the polyurethane (PU) matrix showed an enhancement in the barrier features of the nanocomposite coating, since MWCNTs can provide a channel for the conductivity and facilitate the cathodic reactions through the interface of metal and electrolyte. Additionally, the high chemical stability and protection of the coatings in a corrosive environment for long-time exposure can be

achieved, which is related to the barriers fabricated by the polymeric matrix filled with MWNTs, accordingly decreasing corrosive ions diffusion [34].

The dispersion method can be effective on the anti-corrosion features of the epoxy coating. Uniform cluster-free distribution of MWCNTs by a mechanical method involving ultrasonic waves and shear force into the epoxy composite decreases the corrosion rate, since it facilitates cathodic half-reaction by providing high surface area and decreases the oxygen molecule over potential, which can protect metal against corrosion. Fig. 4.5 shows the pathways for corrosive ions in the presence of cluster free distribution of MWCNTs [35].

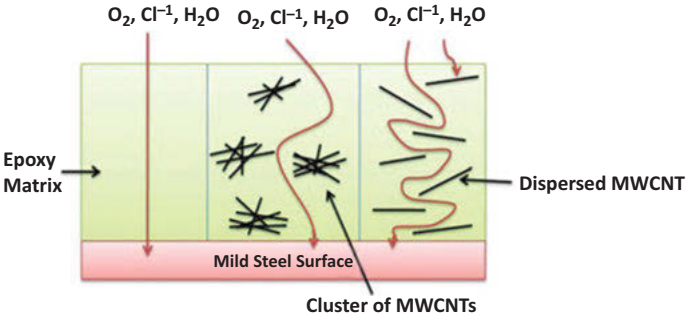

Fig. 4.5: Schematic illustration of proposed path aggressive ions (O_2, chlorine, and H_2O molecules for corrosion protection in blank epoxy and MWCNTs/nanocomposite) (reprinted with permission from ref. [35]).

The anticorrosion mechanism of MWCNTs-filled coating, the high aspect ratio, large incorporated-matrix interfacial zone, and the high corrosive species tortuosity diffusion paths because of its excellent dispersion into the polymeric matrix can be considered for the permeability reduction of coatings [36]. It should be mentioned that MWCNTs incorporation in the nonoptimal value can be harmful for the anticorrosive features of coating due to the MWCNTs agglomeration in the coating [37].

CNTs tend to aggregate because of the high aspect ratio and poor interaction with the coating. CNTs aggregation lowers the mechanical characteristics and corrosion resistance of the protective layer. Different kinds of functionalization are employed to enhance CNTs dispersion in the polymeric coating by enhancing the interfacial interactions between such additive and the polymeric matrix. Physical interactions include the polymer‘s adsorption onto the surface of the nanoparticles, while chemical approaches consist of the polymer chemical bonding on CNTs surfaces [38–40]. The organic groups grafting on the surface of CNTs have been investigated in many studies [41, 42]. Some approaches have been introduced as mechanical functionalization to prevent the aggregation of CNTs and enhance the dispersion of CNTs in the

polymeric matrix. Dispersion through ultrasonic[43, 44] and high-shear mixing [45] can be termed as typical mechanical approaches.

The covalent attachment of the functional groups on the CNTs provides a reaction between nanoparticles and the polymer chains [46]. Oxidation is considered as an approach for modification to introduce functional moieties containing oxygen such as carboxyl, carbonyl, and hydroxyl groups on surfaces of CNTs. The oxidized CNTs enhance the interfacial interaction between the nanoparticles and the different kinds of polymeric matrixes to enhance dispersion of CNTs and cross-link density of the polymer [47]. In addition, the reactive functional groups containing oxygen created by acid treatment are convertible to other types of functional groups such as ester, acryloyl chloride, amine, and silane groups [48]. Silanization is considered to be a traditional technique to enhance the interfacial of CNTs adhesion to the polymeric coating. Organosilanes are known as the most common silane coupling agents with the ability to react with hydroxyl moieties bonded to the CNTs sidewalls, through reduction or oxidation reactions. Proper modification depends on selecting the appropriate organic molecule to provide proper grafting to the CNTs and excellent reactivity for the coating [49].

The nanocomposite coating containing functionalized MWCNTs with carboxyl groups and siloxane-polymethyl methacrylate exhibited higher corrosion performance than the neat coatings, due to better barrier features of the coating, resulting from siloxane covalent bonding and functional groups attached on MWCNTs. The incorporation of carboxyl-functionalized CNTs, known as negatively charged dopant into the polymeric coating, changes the ion transport mechanism to cation-specific property [50].

By adding CNTs to poly (o-phenylenediamine) (POPD), the deposition of polymer on nanotubes was increased, due to a significant number of reaction sites and the high surface area of CNTs. Furthermore, the attached carboxylic and phenolic functional groups on the surface of the CNTs enhanced the adsorption ability of organic compounds. Consequently, the polymerization of POPD as well as its copolymerization with CNTs can be improved, so that the coated substrate passivation in acidic media was enhanced. It was reported that the increase in deposition of polymer for SWCNTs was considerable compared to MWCNTs [50].

Adding polydopamine-wrapped carbon nanotubes to reinforce polyurethane (PU) coatings improved corrosion resistance and adhesion strength. By increasing the CNTs value, the coating's porosity and roughness were increased, which can weaken the PU corrosion resistance, because of the weak dispersion of CNTs. However, Polydopamine (PDA)-wrapped CNTs enhanced CNT dispersion due to better compatibility of PDA with PU, compared to CNTs. Morphological observations proved that PU defects decreased because of the presence of dopamine in CNTs that prevented micro-defects in coatings [51].

Participation of two fillers, including carbon black (CB) and CNTs to reinforce polyurethane polymer can cause an interaction between the additive particles and

hard part of the polyurethane chains. The completely uniform dispersion of filler particles can increase thermal stability and glass transition temperature of the nanocomposite. Adding the fillers can raise the wetting angle and improve the composite's corrosion resistance significantly resulting from increased pathways with more tortuosity for ion diffusion (Fig. 4.6). When the density of cross-links increases, penetration of ion decreases, and improves the barrier's feature [52].

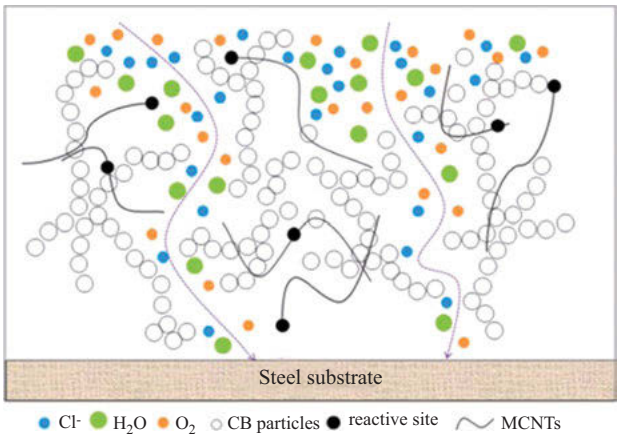

Fig. 4.6: Schematic illustration of corrosion protection process for nanocomposite exposed to 3.5 wt.% NaCl medium at pH = 7 (reprinted with permission from ref. [52]).

A mixture of different types of carbon allotropes can be incorporated into coating material, in order to achieve desirable properties. Investigation of a combination of fullerene and CNTs as filler into resin 22 K BPA-Epoxide Amidoamine showed that incorporating optimal content of such materials could be effective for the nanocomposite coating system's electrical conductivity, water absorption, and anticorrosion properties [53].

Decoration or cladding of CNTs by different kinds of organic particles is an effective method to enhance CNTs distribution, mainly done via the sol-gel method. Incorporation of iron oxide (Fe_3O_4)-decorated CNTs into the epoxy coating can improve CNTs dispersion, due to the interfacial interaction of Fe3O4 particles decorated on the CNTs surface with the coating and mechanical properties of the polymeric coating, due to adhesion strength improvement. Consequently, anticorrosion features and barrier properties of nanocomposite coating can be significantly enhanced [42, 54]. Aluminum oxide (Al_2O_3)-coated MWCNTs/epoxy film also exhibited excellent corrosion resistance. However, Al_2O_3nanoparticles can have inverse effects on the flexibility of coating [55].

Due to the exceptional features, such as doping priority, electrical conductivity, and nontoxicity of CNTs, incorporation of such material into conducting polymers has garnered increasing attention. Barrier feature and electronic interaction related

to the conductive polymer/CNT nanocomposite coatings were proposed as the key mechanisms for protection [56]. Forming a passive layer in the interface of metallic surface and polymeric coating resulting from anodic (oxidation of metal) cathodic (conductive polymer un-doping) reactions can significantly improve the protection process of the metallic substrate from corrosion. Due to high surface area, CNTs nanoparticles can have a cathodic effect in the reoxidation of polymer, which can improve the formation process of oxide film by dissolved oxygen [57]. One of the most important parameters is the aspect ratio of CNTs, which can affect the cathodic effect. Researchers proposed that a high aspect ratio of CNTs can improve the cathodic effect [58]. Polyaniline (PANI) features such as thermal and mechanical properties, and conductivity can be positively improved by CNTs incorporation. In addition, the composition of PANI/CNTs with other polymers, such as epoxy, to prepare ternary nanocomposite is recommended to decrease porosity and improve corrosion resistance of the coating [56, 58, 59]. Adding CNTs into the PANI matrix can create an interwoven fibrous structure that can act as a conductive pathway and improve corrosion protection. In addition to porosities reduction in coating and isolation improvement of the substrate against corrosive species, the presence of CNTs can enhance adherence of polyaniline coating to the substrate surface. Results showed that by increasing the concentration of CNTs, inhibition efficiency improved, due to a significant decrease in the permeability of polymeric coating [25, 60].

4.3.2 Graphene-based materials

Graphene (G) and its derivative materials, including graphene oxide (GO), and reduced graphene oxide (rGO) nanosheets are known as graphene-based materials, which have received increasing attention recently due to their magnificent mechanical, electrical, and thermal properties, and inhibitive features [61–64]. G and its derivation can considerably improve corrosion protection performance of coatings with proper durability compared to conventional ones. Their layered structure, large surface area, and high aspect ratio are the main reasons for their high potential in acting as effective barriers against the penetration of corrosive ions [65–67]. Employing chemical vapor deposition (CVD) to grow the G layer on the metallic substrate was reported to have barrier and anticorrosive features [68]. However, defect-free and large-scale production of G films is still the most important challenge [69].

GO functionalized by silanization process (3-Aminopropyl)triethoxysilane (APTES)) was added to the epoxy coating on magnesium substrate through complex processes, including hydroxylation, silanization, and dip coating. Nucleophilic substitution of the amine groups of silanes with groups of epoxy on the surface of GO occurred during the dip coating process, and a layer was uniformly synthesized on

the surface of substrate (amino-silylation Magnesium) (Fig. 4.7). The corrosion protection performance of the nanocomposite coating was significantly enhanced compared to neat silane coating because the layer containing carbon can decrease the charge transfer approaching the magnesium substrate [70].

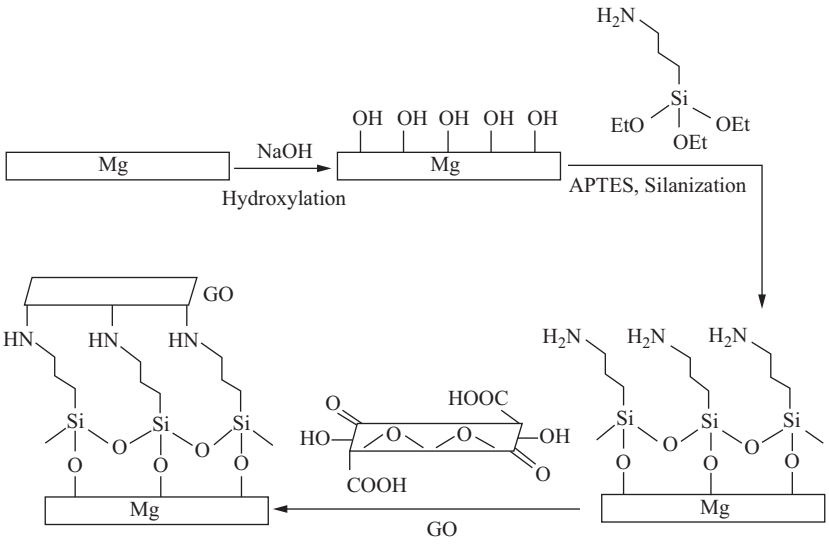

Fig. 4.7: Schematic illustration of the assembly process of GO on (3-Aminopropyl)-triethoxysilane (APTES)-modified Mg surface (reprinted with permission from ref. [70]).

rGO incorporation into Polyurethane (PU) matrix can significantly decrease moisture permeability, due to the self-alignment of rGO sheets during the preparation of nanocomposites. In contrast, G nanosheets perpendicularly align to moisture diffusion, which can increase penetration pathway [71]. GO and rGO incorporation into the PU coating showed better distribution state compared to functionalized graphene with titanate coupling agents, resulting in better corrosion protection performance [72].

The aspect ratio of GO can affect the anticorrosive properties of epoxy coated mild steel. The presence of GO significantly reduces the cracks and micropores of the polymeric coating resulting from the preparation process. Consequently, the corrosive ions penetration path can be remarkably decreased, so that the corrosion protection performance of nanocomposite coating can be improved. Results showed that incorporating a higher aspect ratio of GO could effectively improve barrier properties and reduce the penetration channels for corrosive electrolytes [73].

In fluorographene (graphene fluoride), sp^3 bonds can be created through the reaction of carbon's π-orbitals with p-orbitals of Fluorine. As a result, modification of graphene charge density occurs, and conductivity can be reduced by raising conduction scattering centers. A study of fluorographene incorporation into the polyvinyl

butyral (PVB) coated on copper substrate showed that micro-galvanic corrosion could be restricted in metal and coating interface resulting from the insulating features of the fluorographene [74].

Due to the high surface area, π–π stacking, and van der Waals interactions, graphene and materials derived from graphene tend to aggregate or restack, which leads to a negative impact on their distribution into polymeric coating. In fact, it is almost impossible to apply the graphene-based nanosheets in the composite coatings without enhancing the dispersion and exfoliation [75]. In fact, applying graphene without functionalization into polymeric coating increases the corrosion rate of the substrate on exposure to the corrosive media [69]. There are several functionalization methods such as in situ polymerization and nanoparticles cladding to improve dispersion of such filler and increase the corrosion inhibition efficiency [76].

The chemical functionalization of graphene-based materials effectively reduces their tendency to aggregation, and causes the interfacial interaction enhancement of such materials with polymeric coating through covalent or noncovalent attachments, to provide a simple technique to produce multi-functional coating with excellent barrier properties [77, 78].Applying silane coupling agents in order to functionalize graphene oxide was investigated in several studies. Investigations on using (3-Aminopropyl)triethoxysilane (APTES) saline to modify GO structure for better distribution showed that adding GO modified by APTES into silane coating on steel substrate could improve cross-link of silanol groups of the coating and enhance barrier properties, when compared to the blank silane [79].

Incorporation of G and GO functionalized by APTES into polyurethane (PU) coated on cast iron can remarkably increase the barrier properties of protective film. The results showed that the presence of functionalized-GO and functionalized-G in such polymeric coating can effectively reduce the number of debris formed during friction, so that straight pathways for corrosive ions can be changed into tortuous ones, decreasing the corrosive species diffusion (Fig. 4.8). In addition, FGO showed better distribution compared to FG, due to a considerable number of oxygenated groups on GO sheets. However, adding FG to coating showed better barrier properties, since the mentioned oxygenated groups in FGO can destroy graphene lattice structure and reduce corrosion resistance [80].

Modification of GO by p-phenylenediamine (P) can considerably improve the distribution of such nanoparticles into the epoxy coating. As a result of this modification, GO finds hydrophobic properties that can remarkably enhance the dispersion state and show better corrosion resistance. In addition, the mentioned FGO can prevent penetration of corrosive ions as they earn negative charges in the alkaline media, which can adsorb cations selectively, avoid Cl^- anions penetration into the coating, and decrease hydrolytic degradation (Fig. 4.9) [81].

Decoration of GO nanosheets with inorganic nanoparticles (NP) is an excellent method to decrease the tendency of the GO sheets to agglomerate and improve the corrosion protection of the coatings significantly at a low nanofiller content by filling

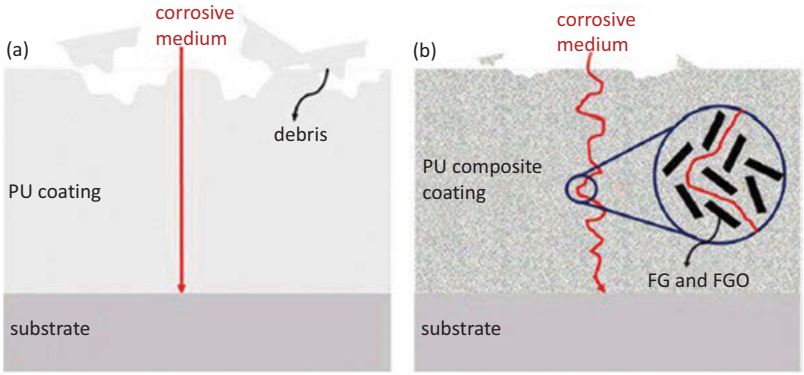

Fig. 4.8: Schematic illustration of pure PU (a), and PU composite coatings with the presence of FG and FGO (b),during tribological and corrosion process (reprinted with permission from ref. [80]).

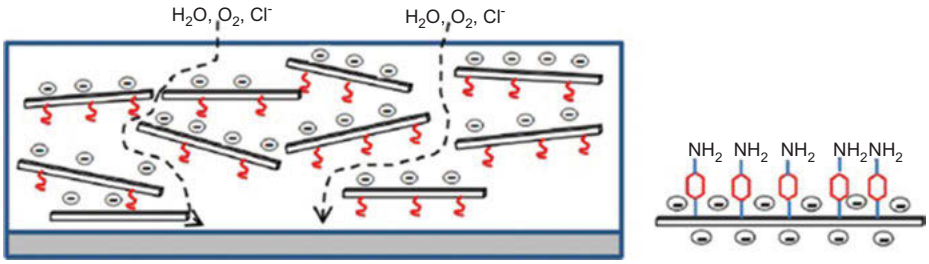

Fig. 4.9: Schematic representation of negative charge creation on the FGO surface, which leads to cation selectivity and the prohibition of anions from diffusing into the coating (reprinted with permission from ref. [81]).

cavities and defects [82]. Nanoparticles such as silica (SiO_2), zinc oxide (ZnO), aluminum oxide (Al_2O_3), titanium oxide (TiO_2), calcium carbonate ($CaCO_3$), and iron oxide (Fe_3O_4) are widely used to decorate GO nanosheets. The results demonstrated that incorporation of GO decorated by such nanoparticles can cause a considerable enhancement in corrosion protection in the epoxy coating, due to homogenous distribution without any aggregation, and a hydrophobic property that prevents water penetration into the substrate [81, 83–85]. The presence of GO sheets, Fe_3O_4 nanoparticles, and Fe_3O_4–GO hybrids to reinforce epoxy coating was investigated. The incorporation of Fe_3O_4–decorated GO demonstrated homogenous distribution without any aggregation in the epoxy coating, which increased the protection capability, compared to epoxy coating filled by GO sheets and Fe_3O_4 nanoparticles, individually (Fig. 4.10) [86].

Although chemical functionalization of graphene-based materials can cause advantages, it can lead to structural defects and changes in physical properties. Noncovalent modification has obtained increasing attention among all methods, due to its controllable capability, outstanding performance, and the minimum

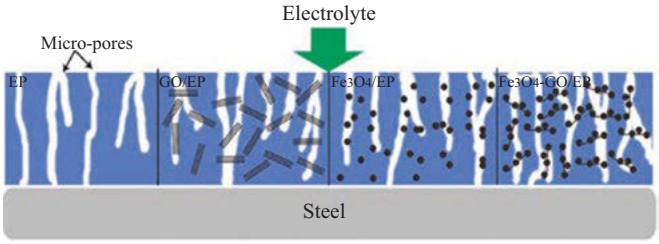

Fig. 4.10: Schematic illustration of the corrosion protection process of the epoxy nanocomposite coatings (reprinted with permission from ref. [86]).

negative effects on the structure of graphene-based materials [87]. Polyaniline (PANI) [88], poly (sodium 4-styrene sulfonate) (PSS) [89], and pyrene butyric acid derivative [90] were successfully used to modify GO nanosheets and provide an aqueous solution with well-distributed GO via π–π interactions. Some aromatic molecules, including phthalocyanine derivatives, pyrene derivatives, and doxorubicin hydrochloride, have also offered capability of a coupling reaction with GO by π–π stacking [91]. In situ polymerization is one the most effective methods to enhance GO dispersion in the coating matrixes.

Incorporating of functionalized-GO into polyetherimide (PEI) and polystyrene (PS) coating through in situ polymerization can effectively enhance additive dispersion and increase barrier properties. GO layer can be exfoliated into polymeric coating due to the chemical bonding between functional groups and π–π interactions of GO [92, 93]. Incorporation of G into polyurethane (PU) enriched by zinc can improve the coating's cathodic protection, as- increasing active zinc content results from electrical conductivity of G nanosheets. In fact, formation of $Zn_5(OH)_8Cl_2$ corrosion product can significantly improve corrosion resistance of Zn nanoparticles (Fig. 4.11) [94].

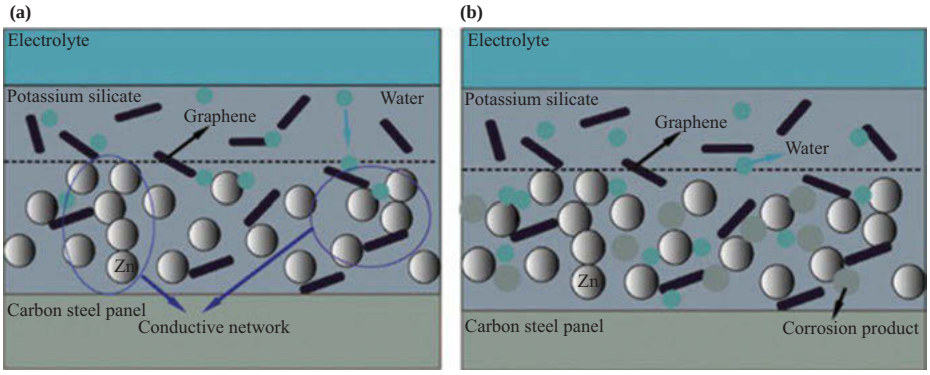

Fig. 4.11: Sketch map for protection process at the cathodic protection stage (a) and barrier protection stage (b) (reprinted with permission from ref. [94]).

Composition of graphene-based materials into conductive polymers, including polyaniline (PANI), polythiophene (PTh), polypyrrole (PPy), and polycarbazole has been widely used in metallic substrates from corrosive media. There are several mechanisms for corrosion protection in such coating that mainly depend on substrate material, physical, and chemical properties of the polymeric matrix [95–98]. PANI Polymerization on G and GO is one of the well-known approaches in order to modify and improve distribution of such materials in polymeric coating. A considerable number of studies have been carried out relating to the mentioned method to improve barrier features and anticorrosive properties of coating on different substrates. Carbon quantum dots (CQDs) are also suitable for chemical functionalization and surface passivation with several polymeric, organic, biological, or inorganic materials. Surface passivation can improve the fluorescence and physical properties of CQDs [99–102].

4.3.3 Carbon quantum dots

CQDs are a new category of carbon-based nanomaterials that has obtained considerable attention due to their superior features [103–106]. Typically, CQDs are spherical nanoparticles with nanocrystalline (ordered) cores, surrounded by anamorphous (disordered) outer layer. Like graphene oxide, CQDs are also suitable for functionalization, since there are several carboxyl, carbonyl and, hydroxyl functional groups on the CQD surface, which provide hydrophilic features and increase distribution in a variety of solvents [107–109].Recently, carbon dots were used as a self-healing agent in different kinds of polymeric coatings to enhance corrosion resistance. Low toxicity and large-scale production capability are the main features of CQDs that are useful in corrosion resistance applications.

Hydrophilic functional groups attached to CQDs can adsorb H_2O and trap oxygen and reduce it to H_2O via four-electron pathways, which can suppress the corrosion process [110]. Graphene oxide quantum dots (GOQDs) have particles of smaller sizes than G and GO, which can be very effective in controlling the impermeability of coatings by filling any defects and cavities to remove the corrosive ions pathways in the coating [111, 112]. Recent investigations demonstrated that heteroatom doping is an impressive approach to improve the electronic and optical properties of CQDs. N-CQDs (Doping N-containing atom) are considered effective corrosion inhibitors because of the strong electronegativity and capability of electron donation of N atoms. In addition, functional groups of the N-CDs can make a strong concoction between N-CDs and coating to prevent or control the growth and initiation of cracks [113–116]. Although adding such nanoparticle scan reduces the defects and fills the porosities, incorporation of N-CDs in polymeric coating should be optimized, since excessive addition of N-CDs can spoil the coating structure and reduce corrosion resistance [117].

Functionalized CQDs can be used as intercalators to improve the distribution of graphene, with the ability to perfectly disperse in water and achieve proper interfacial compatibility in a polymeric matrix. The well-dispersed G can considerably enhance the barrier properties of the blank polymeric coating and provide self-healing ability to it. Despite the fact that the G incorporation can prevent corrosive electrolytes diffusion, the G nanosheets can be aggregated easily in the matrix and limit barrier ability due to the high specific surface area and interlayer forces. In contrast, G modified by CQDs filled the porosities to improve the density of the matrix and could be well dispersed. Furthermore, the adsorbed CQDs on the surface of steel by the coordinate covalent bond can act as a self-healing agent [118].

For Graphene quantum dot (GQDs) functionalization to facilitate their interaction with the polymeric coating, silane coupling agents can be used, which acts as a bridging ligand between nanoparticle and coating and enhances the distribution state of GQDs in the polymeric matrix. Adding an optimal value of modified GQDs (f-GQDs) can decrease the diffusion of corrosive ions through the polymeric coating and decrease the epoxy coating cavities. Additionally, because of the enhanced compatibility of f-GQDs with coating and a considerable reduction in defects, the corrosion rate decreases considerably, compared to neat epoxy coating [112].

The ultrathin graphene oxide quantum dots (GOQDs) nanosheets can improve the mechanical features of the epoxy coating when compared to G, due to better interfacial interactions, which can significantly control crack propagation in the polymeric coating [111]. Incorporation of PANI-modified GOQDs into an epoxy coating significantly improved corrosion protection performance. The obtained results demonstrated that such composition could control the diffusion of aggressive species into the coating. GOQDs-PANI coating showed excellent corrosion protection after long exposure period, due to the low hydrophilicity and excellent compatibility of GOQDs with coating. In addition, the coating can be highly compacted by applying modified GOQDs, resulting in fewer defects and cavities and providing high corrosion resistance. Moreover, filling epoxy coating with GOQDs-PANI can create active inhibition and improve the steel interfacial adhesion in wet conditions. The results proved that the presence of GOQDs-PANI increased the epoxy coating's hydrophobicity and controlled the penetration of water molecules (Fig. 4.12) [119].

A bio-based epoxy nanocomposite was fabricated through in situ polymerization incorporating polyaniline (PANI)-CQDs nanohybrid (PC). Fig. 4.13 demonstrates the interaction between the different kinds of functional moieties of the polymeric matrix (epoxy) and the additives. The CQDs structure, which contains oxygenous groups and the polymeric backbone containing nitrogen of PANI nanofiber in nanohybrid, provide strong secondary bonds with the polar functional moieties of the hyperbranched polymeric matrix (epoxy). Results proved the excellent corrosion resistance performance of nanocomposite coatings compared to blank epoxy coating because of blocking the cathodic and anodic site, due to the presence of conductive PANI-CQDs nanohybrid. Furthermore, the aggressive ions penetration

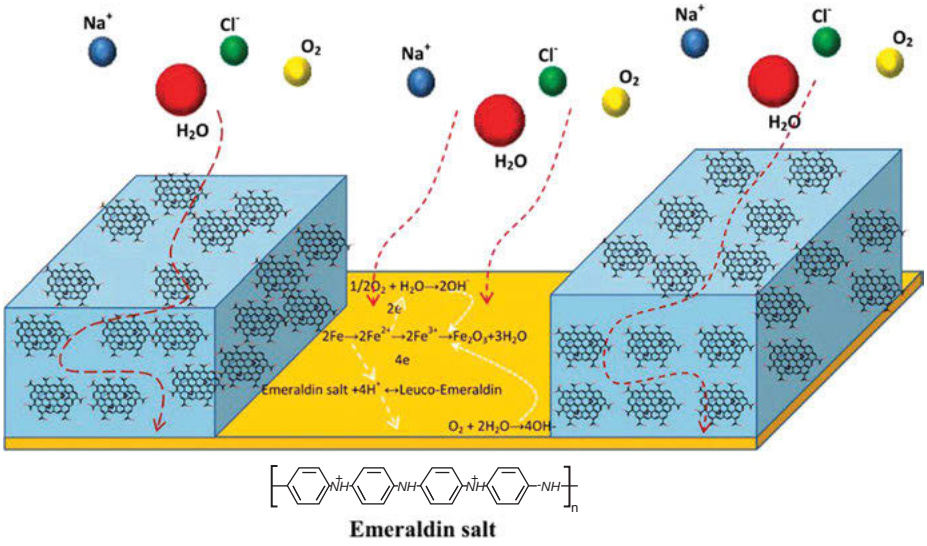

Fig. 4.12: Schematic illustration of proposed mechanism for corrosion protection performance of GOQD-PANI in the polymeric coating (epoxy) (reprinted with permission from ref. [119]).

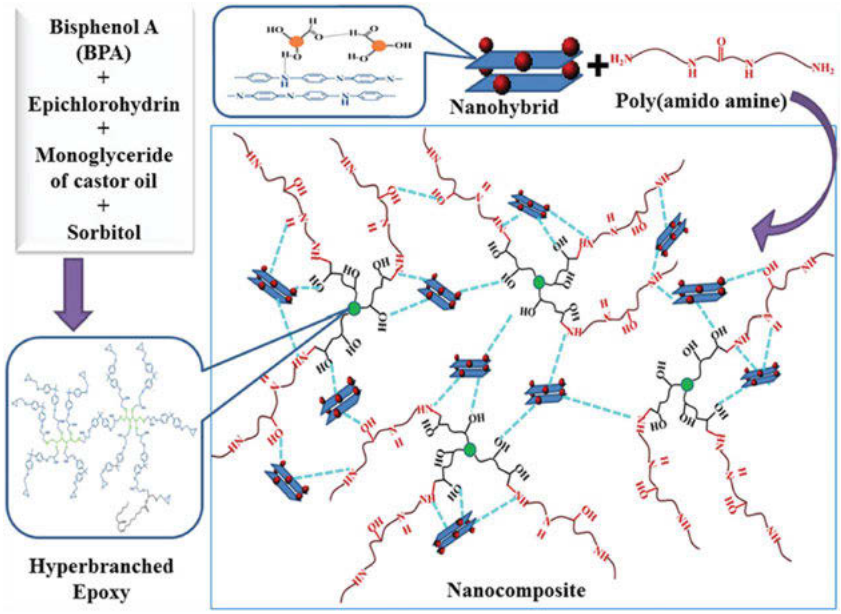

Fig. 4.13: Schematic illustration of in situ preparation of bio-based epoxy nanocomposites using PC nanohybrid (reprinted with permission from ref. [120]).

can be prevented by blocking the active sites and providing tortuous paths, resulting from the cross-linked structure of the coating [120].

4.4 Carbon black

Nanocomposite reinforced by Carbon black (CB) particles are considered as effective as materials to enhance corrosion protection performance, due to their magnificent properties, including high specific surface area and involving the interfacial connection of polymeric and metallic surfaces. [121]. Well-dispersed particles fill the cavities of coatings prevent crack initiation and progression, and increase coating integrity [122, 123]. Therefore, the packing density of the composite can be enhanced, and agglomeration can be prevented, to improve coating homogeneity and barrier properties against corrosive species [124, 125]. Due to the high electric conduction of CB, incorporation of such material into epoxy coating can significantly improve corrosion protection. In fact, the provided conducting pathway creates electrical contact between the metallic surface and coating layer, affecting the barrier properties of nanocomposite coating [126, 127]. In addition, CB nanoparticles can prevent electron localizing in coating defects and limit coating disbanding due to reduction of oxygen because of formation of OH^- species on the interface. Decreasing oxygen reduction rate can improve corrosion protection of coating [128].

Like other carbon allotropes, the most important challenge in incorporating CB in polymeric coatings is aggregation tendency. Applying a surfactant is a known traditional method to provide an electrostatic barrier and prevent the agglomeration of nanoparticles [129]. Attaching different kinds of functionalities, including carboxylic acid and phenolic compounds on CB's surface can act as interaction sites with the agents of the dispersant. Sodium dodecyl sulfate (SDS) is one of the well-known surfactants used for proper CB distribution in epoxy coating. The interaction of CB nanoparticles and their hydrophilic parts with SDS can prevent them from aggregation in coating The functionalized CB nanoparticles can be appropriately distributed in the polymeric matrix and decrease microspores and defects to reduce corrosive ions diffusion, improving corrosion resistance (Fig. 4.14) [130, 131].

4.5 Challenges, opportunities, and future

Recently, carbon nanostructures have been widely incorporated in anticorrosive coatings among different nanomaterials owing to their magnificent properties. Carbon-based nanofillers have the potential to be used extensively in all industries to provide effective corrosion protection properties in coatings, with a good lifetime and reasonable cost. The extraordinary properties of carbon-based coatings, including

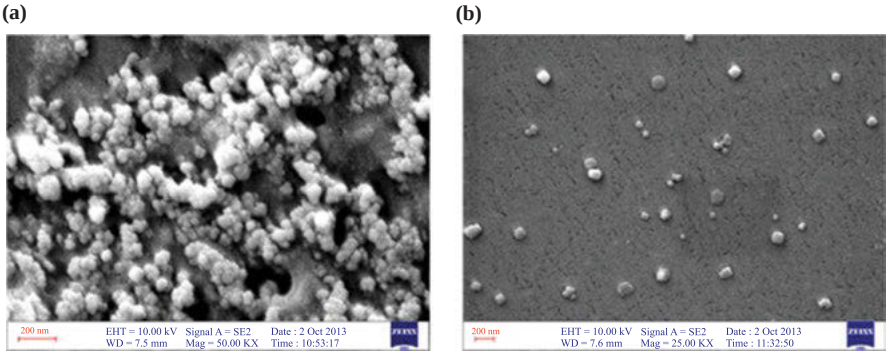

Fig. 4.14: FESEM images of polymeric coating containing nonmodified CB (a) and coating containing SDS-functionalized CB nanoparticles (b) (reprinted with permission from ref. [130]).

mechanical stability, thermal conductivity, flexibility, and easy surface functionalization, present them as ecofriendly alternatives to harmful organic and inorganic corrosion inhibitors. The excellent barrier properties can improve inhibition efficiency by blocking the species penetration effectively. In addition to the aforementioned, since carbon allotropes are abundant, cost-effective, and light materials, they have obtained increasing attention in use as anticorrosive materials in the last decade and have been included in the industry. Adding low amounts of carbon nanofillers into nanocomposite coatings can decrease the anticorrosive inhibitive pigments usage and provide high strength-to-weight ratio. It should be noted that further progress in polymer-based coatings incorporated by carbon-based nano-allotropes can be obtained through enhancing the distribution of nano-sized fillers in polymeric matrixes and low-cost techniques. However, there are still some challenges and possible perspectives that should be addressed in parallel.

Carbon-based nanomaterials production such as graphene should be scaled up using advanced large engineering technologies. It should be noted that the optimum parameters for large-scale production of carbon materials and optimization of their inhibition efficiency on the industrial level are different from the optimized conditions on the lab scale. Consequently, study and investigation to develop efficient coatings and upscaling the application of such coatings should be carried out, in parallel. Due to the nanosize of carbon allotropes, especially carbon fibers and carbon nanotubes, they may penetrate into the cells, so that these materials can be considered toxic. However, the safety risks of carbon allotropes depend entirely on the kind of carbon nanostructure, surface chemistry, shape, size, and the method that is applied. Research efforts should be made to explore the long-term health effect and the fate of these materials in the environment.

The conductivity of graphite and graphene films vary greatly depending on the surface defects, orientation, synthesis procedure, and purity, which causes various reaction rates at the surface. Therefore, challenges related to the quality control of

carbon allotropes, especially graphene and carbon nanotubes, and their influential role in the inhibition efficiency still remain unclear. Furthermore, nanostructures aggregation is still problematic and current strategies to mitigate this effect should be optimized.

4.6 Conclusion

The extraordinary properties of carbon-based coatings provide excellent barrier properties and improve inhibition efficiency by blocking the corrosive ions penetration effectively. Carbon-based nanofillers have the potential to be used extensively in all industries to provide effective corrosion protection properties in coatings with a long lifetime and low cost. However, some issues, including poor dispersion in the matrix, stable quality, and mass production of such nanoparticles, should be addressed, in parallel.

References

[1] Zhang, C.; He, Y.; Xu, Z.; Shi, H.; Di, H.; Pan, Y.; Xu, W. Fabrication of Fe3O4@SiO2 nanocomposites to enhance anticorrosion performance of epoxy coatings. Polym. Adv. Technol. 2016, 27, 740–747, https://doi.org/10.1002/pat.3707.

[2] Elhalawany, N.; Mossad, M.A.; Zahran, M.K. Novel water based coatings containing some conducting polymers nanoparticles (CPNs) as corrosion inhibitors. Prog. Org. Coatings. 2014, 77, 725–732, https://doi.org/10.1016/j.porgcoat.2013.12.017.

[3] Beiro, M.; Collazo, A.; Izquierdo, M.; Nóvoa, X.R.; Pérez, C. Characterisation of barrier properties of organic paints: The zinc phosphate effectiveness. Prog. Org. Coatings. 2003, 46, 97–106, https://doi.org/10.1016/S0300-9440(02)00216-3.

[4] Zin, I.M.; Howard, R.L.; Badger, S.J.; Scantlebury, J.D.; Lyon, S.B. The mode of action of chromate inhibitor in epoxy primer on galvanized steel. Prog. Org. Coatings. 1998, 33, 203–210, https://doi.org/10.1016/S0300-9440(98)00056-3.

[5] McCoy, T.M.; Brown, P.; Eastoe, J.; Tabor, R.F. Noncovalent magnetic control and reversible recovery of graphene oxide using iron oxide and magnetic surfactants. ACS Appl. Mater. Interfaces. 2015, 7, 2124–2133, https://doi.org/10.1021/am508565d.

[6] Yan, Q.L.; Gozin, M.; Zhao, F.Q.; Cohen, A.; Pang, S.P. Highly energetic compositions based on functionalized carbon nanomaterials. Nanoscale. 2016, 8, 4799–4851, https://doi.org/10.1039/c5nr07855e.

[7] Xu, Z.; Wang, S.; Li, Y.; Wang, M.; Shi, P.; Huang, X. Covalent functionalization of graphene oxide with biocompatible poly(ethylene glycol) for delivery of paclitaxel. 2014.

[8] Pham, T.A.; Kumar, N.A.; Jeong, Y.T. Covalent functionalization of graphene oxide with polyglycerol and their use as templates for anchoring magnetic nanoparticles. Synth. Met. 2010, 160, 2028–2036, https://doi.org/10.1016/j.synthmet.2010.07.034.

[9] Yang, Q.; Pan, X.; Clarke, K.; Li, K. Covalent functionalization of graphene with polysaccharides. 2012, 310–317, https://doi.org/10.1021/ie201391e.

[10] Mohammad, S.; Karim, R. Proton conductors produced by chemical modifications of carbon allotropes, perovskites and metal organic frameworks. J. Mater. Chem. A Mater. Energy Sustain. 2017, 5, 7243–7256, https://doi.org/10.1039/C6TA10923C.
[11] Chem, J.M.; Liu, J.; Gooding, J.J. Strategies for chemical modification of graphene and applications of chemically modified graphene. 2012, 12435–12452, https://doi.org/10.1039/c2jm31218b.
[12] Verma, C.; Quraishi, M.A.; Ebenso, E.E.; Hussain, C.M. Recent advancements in corrosion inhibitor systems through carbon allotropes: Past, present, and future. Nano Sel. 2021, 2, 2237–2255, https://doi.org/10.1002/nano.202100039.
[13] Syrgiannis, Z.; Melchionna, M.; Prato, M. Covalent carbon nanotube functionalization, Springer Berlin Heidelberg, Berlin, Heidelberg, 2020, https://doi.org/10.1007/978-3-642-36199-9.
[14] Georgakilas, V.; Tiwari, J.N.; Kemp, K.C.; Perman, J.A.; Bourlinos, A.B.; Kim, K.S.; Zboril, R. Noncovalent functionalization of graphene and graphene oxide for energy materials, biosensing, catalytic, and biomedical applications. 2016, https://doi.org/10.1021/acs.chemrev.5b00620.
[15] Chen, D.; Feng, H.; Li, J. Graphene oxide: Preparation, functionalization, and electrochemical applications. 2012, https://doi.org/10.1021/cr300115g.
[16] Georgakilas, V.; Otyepka, M.; Bourlinos, A.B.; Chandra, V.; Kim, N.; Kemp, K.C.; Hobza, P.; Zboril, R.; Kim, K.S. Functionalization of graphene: covalent and non-covalent approaches, derivatives and applications. 2012.
[17] Gohari, M.S.; Rezaei, S.A.; Rashidi, A.; Saremi, M.; Ebadzadeh, T. The effect of mullite coating and microwave sintering on high temperature oxidation resistance of MWCNTs. Ceram. Int. 2022, 1–7, https://doi.org/10.1016/j.ceramint.2022.01.316.
[18] Cui, G.; Bi, Z.; Zhang, R.; Liu, J.; Yu, X.; Li, Z. A comprehensive review on graphene-based anti-corrosive coatings. Chem. Eng. J. 2019, 373, 104–121, https://doi.org/10.1016/j.cej.2019.05.034.
[19] Galal, A.; Amin, K.M.; Atta, N.F.; Abd El-Rehim, H.A. Protective ability of graphene prepared by γ-irradiation and impregnated with organic inhibitor applied on AISI 316 stainless steel. J. Alloys Compd. 2017, 695, 638–647, https://doi.org/10.1016/j.jallcom.2016.11.081.
[20] Hong, M.S.; Park, Y.; Kim, T.; Kim, K.; Kim, J.G. Polydopamine/carbon nanotube nanocomposite coating for corrosion resistance. J. Mater. 2020, 6, 158–166, https://doi.org/10.1016/j.jmat.2020.01.004.
[21] Atta, N.F.; Amin, K.M.; Abd El-Rehim, H.A.; Galal, A. Graphene prepared by gamma irradiation for corrosion protection of stainless steel 316 in chloride containing electrolytes. RSC Adv. 2015, 5, 71627–71636, https://doi.org/10.1039/c5ra11287g.
[22] Prasannakumar, R.S.; Chukwuike, V.I.; Bhakyaraj, K.; Mohan, S.; Barik, R.C. Electrochemical and hydrodynamic flow characterization of corrosion protection persistence of nickel/multiwalled carbon nanotubes composite coating. Appl. Surf. Sci. 2020, 507, 145073, https://doi.org/10.1016/j.apsusc.2019.145073.
[23] Chilkoor, G.; Sarder, R.; Islam, J.; ArunKumar, K.E.; Ratnayake, I.; Star, S.; Jasthi, B.K.; Sereda, G.; Koratkar, N.; Meyyappan, M.; Gadhamshetty, V. Maleic anhydride-functionalized graphene nanofillers render epoxy coatings highly resistant to corrosion and microbial attack. Carbon N. Y. 2020, 159, 586–597, https://doi.org/10.1016/j.carbon.2019.12.059.
[24] Tian, Y.; Xie, Y.; Dai, F.; Huang, H.; Zhong, L.; Zhang, X. Ammonium-grafted graphene oxide for enhanced corrosion resistance of waterborne epoxy coatings. Surf. Coatings Technol. 2020, 383, 125227, https://doi.org/10.1016/j.surfcoat.2019.125227.
[25] Xiong, Z.; Yun, Y.S.; Jin, H.J. Applications of carbon nanotubes for lithium ion battery anodes. Materials (Basel). 2013, 6, 1138–1158, https://doi.org/10.3390/ma6031138.

[26] Han, Z.; Fina, A. Thermal conductivity of carbon nanotubes and their polymer nanocomposites: A review. Prog. Polym. Sci. 2011, 36, 914–944, https://doi.org/10.1016/j.progpolymsci.2010.11.004.
[27] Gojny, F.H.; Wichmann, M.H.G.; Köpke, U.; Fiedler, B.; Schulte, K. Carbon nanotube-reinforced epoxy-composites: Enhanced stiffness and fracture toughness at low nanotube content. Compos. Sci. Technol. 2004, 64, 2363–2371, https://doi.org/10.1016/j.compscitech.2004.04.002.
[28] Eder, D. Carbon nanotube–inorganic hybrids. Chem. Rev. 2010, 110, 1348–1385, https://doi.org/10.1021/cr800433k.
[29] Khare, R.; Suryasarathi, B. Carbon nanotube based composites- a review. Compr. Compos. Mater. II. 2018, 4, 201–229, https://doi.org/10.1016/B978-0-12-803581-8.10012-8.
[30] Jeon, H.R.; Park, J.H.; Shon, M.Y. Corrosion protection by epoxy coating containing multi-walled carbon nanotubes. J. Ind. Eng. Chem. 2013, 19, 849–853, https://doi.org/10.1016/j.jiec.2012.10.030.
[31] Yang, L.H.; Liu, F.C.; Han, E.H. Effects of P/B on the properties of anticorrosive coatings with different particle size. Prog. Org. Coatings. 2005, 53, 91–98, https://doi.org/10.1016/j.porgcoat.2005.01.003.
[32] Ganguli, S.; Aglan, H.; Dennig, P.; Irvin, G. Effect of loading and surface modification of MWCNTs on the fracture behavior of epoxy nanocomposites. J. Reinf. Plast. Compos. 2006, 25, 175–188, https://doi.org/10.1177/0731684405056425.
[33] Khun, N.W.; Troconis, B.C.R.; Frankel, G.S. Effects of carbon nanotube content on adhesion strength and wear and corrosion resistance of epoxy composite coatings on AA2024-T3. Prog. Org. Coatings. 2014, 77, 72–80, https://doi.org/10.1016/j.porgcoat.2013.08.003.
[34] Wei, H.; Ding, D.; Wei, S.; Guo, Z. Anticorrosive conductive polyurethane multiwalled carbon nanotube nanocomposites. J. Mater. Chem. A. 2013, 1, 10805–10813, https://doi.org/10.1039/c3ta11966a.
[35] Kumar, A.; Ghosh, P.K.; Yadav, K.L.; Kumar, K. Thermo-mechanical and anti-corrosive properties of MWCNT/epoxy nanocomposite fabricated by innovative dispersion technique. Compos. Part B Eng. 2017, 113, 291–299, https://doi.org/10.1016/j.compositesb.2017.01.046.
[36] Jeevanandam, J.; Barhoum, A.; Chan, Y.S.; Dufresne, A.; Danquah, M.K. Review on nanoparticles and nanostructured materials: History, sources, toxicity and regulations. Beilstein J. Nanotechnol. 2018, 9, 1050–1074, https://doi.org/10.3762/bjnano.9.98.
[37] Zachariah, S.; Liu, Y.L. Nanocomposites of polybenzoxazine-functionalized multiwalled carbon nanotubes and polybenzoxazine for anticorrosion application. Compos. Sci. Technol. 2020, 194, 108169, https://doi.org/10.1016/j.compscitech.2020.108169.
[38] Rout, T.K.; Jha, G.; Singh, A.K.; Bandyopadhyay, N.; Mohanty, O.N. Development of conducting polyaniline coating: A novel approach to superior corrosion resistance. Surf. Coatings Technol. 2003, 167, 16–24, https://doi.org/10.1016/S0257-8972(02)00862-9.
[39] Fukuda, H.; Szpunar, J.A.; Kondoh, K.; Chromik, R. The influence of carbon nanotubes on the corrosion behaviour of AZ31B magnesium alloy. Corros. Sci. 2010, 52, 3917–3923, https://doi.org/10.1016/j.corsci.2010.08.009.
[40] Maeda, S.; Armes, S.P. Preparation and characterisation of novel polypyrrole-silica colloidal nanocomposites. J. Mater. Chem. 1994, 4, 935–942, https://doi.org/10.1039/JM9940400935.
[41] Xue, C.H.; Zhou, R.J.; Shi, M.M.; Gao, Y.; Wu, G.; Bin Zhang, X.; Chen, H.Z.; Wang, M. A green route to water soluble carbon nanotubes and in situ loading of silver nanoparticles. Nanotechnology. 2008, 19, https://doi.org/10.1088/0957-4484/19/32/325605.
[42] He, Y.; Chen, C.; Zhong, F.; Chen, H.; Qing, D. Synthesis and properties of iron oxide coated carbon nanotubes hybrid materials and their use in epoxy coatings. Polym. Adv. Technol. 2015, 26, 414–421, https://doi.org/10.1002/pat.3470.

[43] Li, J.; Wong, P.S.; Kim, J.K. Hybrid nanocomposites containing carbon nanotubes and graphite nanoplatelets. Mater. Sci. Eng. A. 2008, 483–484, 660–663, https://doi.org/10.1016/j.msea.2006.08.145.
[44] Dos Santos, A.S.; Leite, T.D.O.N.; Furtado, C.A.; Welter, C.; Pardini, L.C.; Silva, G.G. Morphology, thermal expansion, and electrical conductivity of multiwalled carbon nanotube/epoxy composites. J. Appl. Polym. Sci. 2008, 108, 979–986, https://doi.org/10.1002/app.27614.
[45] Gojny, F.H.; Wichmann, M.H.G.; Fiedler, B.; Schulte, K. Influence of different carbon nanotubes on the mechanical properties of epoxy matrix composites – A comparative study. Compos. Sci. Technol. 2005, 65, 2300–2313, https://doi.org/10.1016/j.compscitech.2005.04.021.
[46] Barrera, E.V. Key methods for developing single-wall nanotube composites. Jom. 2000, 52, 38–42, https://doi.org/10.1007/s11837-000-0197-7.
[47] Ding, K.; Jia, Z.; Ma, W.; Tong, R.; Wang, X. Polyaniline and polyaniline-thiokol rubber composite coatings for the corrosion protection of mild steel. Mater. Chem. Phys. 2002, 76, 137–142, https://doi.org/10.1016/S0254-0584(01)00518-1.
[48] Shinde, V.; Sainkar, S.R.; Gangal, S.A.; Patil, P.P. Synthesis of corrosion inhibitive poly(2,5-dimethylaniline) coatings on low carbon steel. J. Mater. Sci. 2006, 41, 2851–2858, https://doi.org/10.1007/s10853-006-2375-7.
[49] Ezzeddine, A.; Chen, Z.; Schanze, K.S.; Khashab, N.M. Surface modification of multiwalled carbon nanotubes with cationic conjugated polyelectrolytes: fundamental interactions and intercalation into conductive poly(methyl methacrylate) composites. ACS Appl. Mater. Interfaces. 2015, 7, 12903–12913, https://doi.org/10.1021/acsami.5b02540.
[50] Hammer, P.; Dos Santos, F.C.; Cerrutti, B.M.; Pulcinelli, S.H.; Santilli, C.V. Carbon nanotube-reinforced siloxane-PMMA hybrid coatings with high corrosion resistance. Prog. Org. Coatings. 2013, 76, 601–608, https://doi.org/10.1016/j.porgcoat.2012.11.015.
[51] Cai, G.; Hou, J.; Jiang, D.; Dong, Z. Polydopamine-wrapped carbon nanotubes to improve the corrosion barrier of polyurethane coating. RSC Adv. 2018, 8, 23727–23741, https://doi.org/10.1039/c8ra03267j.
[52] Hou, L.; Zhou, M.; Wang, S. Synthesis, thermal and anticorrosion performance of WPU nanocomposites with low carbon-black content by adding amine-modified multiwall carbon nanotube. Diam. Relat. Mater. 2018, 90, 166–171, https://doi.org/10.1016/j.diamond.2018.10.010.
[53] Meng, L.; Soucek, M.D. Comparison of the carbon additives on the conductivity, thermomechanical, and corrosion properties for TEOS oligomer modified epoxy-amine coating systems. Prog. Org. Coatings. 2019, 130, 168–181, https://doi.org/10.1016/j.porgcoat.2019.01.060.
[54] Pham, G.V.; Trinh, A.T.; To, T.X.H.; Nguyen, T.D.; Nguyen, T.T.; Nguyen, X.H. Incorporation of Fe3O4/CNTs nanocomposite in an epoxy coating for corrosion protection of carbon steel. Adv. Nat. Sci. Nanosci. Nanotechnol. 2014, 5, 2–9, https://doi.org/10.1088/2043-6262/5/3/035016.
[55] Yi, H.; Chen, C.; Zhong, F.; Xu, Z. Preparation of aluminum oxide-coated carbon nanotubes and the properties of composite epoxy coatings research. High Perform. Polym. 2014, 26, 255–264, https://doi.org/10.1177/0954008313509390.
[56] Pandey, J.K. Handbook of polymer nanocomposites processing, performance and application. 2015, https://doi.org/10.1007/978-3-642-45232-1.
[57] Salam, M.A.; Al-Juaid, S.S.; Qusti, A.H.; Hermas, A.A. Electrochemical deposition of a carbon nanotube-poly(o-phenylenediamine) composite on a stainless steel surface. Synth. Met. 2011, 161, 153–157, https://doi.org/10.1016/j.synthmet.2010.11.014.
[58] Martina, V.; De Riccardis, M.F.; Carbone, D.; Rotolo, P.; Bozzini, B.; Mele, C. Electrodeposition of polyaniline–carbon nanotubes composite films and investigation on

their role in corrosion protection of austenitic stainless steel by SNIFTIR analysis. J. Nanoparticle Res. 2011, 13, 6035–6047, https://doi.org/10.1007/s11051-011-0453-5.
[59] Yu, Y.; Che, B.; Si, Z.; Li, L.; Chen, W.; Xue, G. Carbon nanotube/polyaniline core-shell nanowires prepared by in situ inverse microemulsion. Synth. Met. 2005, 150, 271–277, https://doi.org/10.1016/j.synthmet.2005.02.011.
[60] Deyab, M.A.;;. Corrosion protection of aluminum bipolar plates with polyaniline coating containing carbon nanotubes in acidic medium inside the polymer electrolyte membrane fuel cell. J. Power Sources. 2014, 268, 50–55, https://doi.org/10.1016/j.jpowsour.2014.06.021.
[61] Zhang, Z.; Zhang, W.; Li, D.; Sun, Y.; Wang, Z.; Hou, C.; Chen, L.; Cao, Y.; Liu, Y. Mechanical and anticorrosive properties of graphene/epoxy resin composites coating prepared by in-situ method. Int. J. Mol. Sci. 2015, 16, 2239–2251, https://doi.org/10.3390/ijms16012239.
[62] Ho, C.Y.; Huang, S.M.; Lee, S.T.; Chang, Y.J. Evaluation of synthesized graphene oxide as corrosion protection film coating on steel substrate by electrophoretic deposition. Appl. Surf. Sci. 2019, 477, 226–231, https://doi.org/10.1016/j.apsusc.2017.10.129.
[63] Liu, S.; Gu, L.; Zhao, H.; Chen, J.; Yu, H. Corrosion resistance of graphene-reinforced waterborne epoxy coatings. J. Mater. Sci. Technol. 2016, 32, 425–431, https://doi.org/10.1016/j.jmst.2015.12.017.
[64] Tang, L.C.; Wan, Y.J.; Yan, D.; Pei, Y.B.; Zhao, L.; Li, Y.B.; Wu, L.B.; Jiang, J.X.; Lai, G.Q. The effect of graphene dispersion on the mechanical properties of graphene/epoxy composites. Carbon N. Y. 2013, 60, 16–27, https://doi.org/10.1016/j.carbon.2013.03.050.
[65] Ramezanzadeh, B.; Ghasemi, E.; Mahdavian, M.; Changizi, E.; Mohamadzadeh Moghadam, M.H. Covalently-grafted graphene oxide nanosheets to improve barrier and corrosion protection properties of polyurethane coatings. Carbon N. Y. 2015, 93, 555–573, https://doi.org/10.1016/j.carbon.2015.05.094.
[66] Rajabi, M.; Rashed, G.R.; Zaarei, D. Assessment of graphene oxide/epoxy nanocomposite as corrosion resistance coating on carbon steel. Corros. Eng. Sci. Technol. 2015, 50, 509–516, https://doi.org/10.1179/1743278214Y.0000000232.
[67] Zhou, Z.; Ji, X.; Pourhashem, S.; Duan, J.; Hou, B. Investigating the effects of g-C3N4/Graphene oxide nanohybrids on corrosion resistance of waterborne epoxy coatings. Compos. Part A Appl. Sci. Manuf. 2021, 149, 106568, https://doi.org/10.1016/j.compositesa.2021.106568.
[68] Prasai, D.; Tuberquia, J.C.; Harl, R.R.; Jennings, G.K.; Bolotin, K.I. Graphene: Corrosion-inhibiting coating. ACS Nano. 2012, 6, 1102–1108, https://doi.org/10.1021/nn203507y.
[69] Schriver, M.; Regan, W.; Gannett, W.J.; Zaniewski, A.M.; Crommie, M.F.; Zettl, A. Graphene as a long-term metal oxidation barrier: Worse than nothing. ACS Nano. 2013, 7, 5763–5768, https://doi.org/10.1021/nn4014356.
[70] Neupane, M.P.; Lee, S.J.; Kang, J.Y.; Park, I.S.; Bae, T.S.; Lee, M.H. Surface characterization and corrosion behavior of silanized magnesium coated with graphene for biomedical application. Mater. Chem. Phys. 2015, 163, 229–235, https://doi.org/10.1016/j.matchemphys.2015.07.034.
[71] Yousefi, N.; Gudarzi, M.M.; Zheng, Q.; Lin, X.; Shen, X.; Jia, J.; Sharif, F.; Kim, J.K. Highly aligned, ultralarge-size reduced graphene oxide/polyurethane nanocomposites: Mechanical properties and moisture permeability. Compos. Part A Appl. Sci. Manuf. 2013, 49, 42–50, https://doi.org/10.1016/j.compositesa.2013.02.005.
[72] Li, J.; Cui, J.; Yang, J.; Li, Y.; Qiu, H.; Yang, J. Reinforcement of graphene and its derivatives on the anticorrosive properties of waterborne polyurethane coatings. Compos. Sci. Technol. 2016, 129, 30–37, https://doi.org/10.1016/j.compscitech.2016.04.017.
[73] Jiang, F.; Zhao, W.; Wu, Y.; Dong, J.; Zhou, K.; Lu, G.; Pu, J. Anti-corrosion behaviors of epoxy composite coatings enhanced via graphene oxide with different aspect ratios. Prog. Org. Coatings. 2019, 127, 70–79, https://doi.org/10.1016/j.porgcoat.2018.11.008.

[74] Yang, Z.; Sun, W.; Wang, L.; Li, S.; Zhu, T.; Liu, G. Liquid-phase exfoliated fluorographene as a two dimensional coating filler for enhanced corrosion protection performance. Corros. Sci. 2016, 103, 312–318, https://doi.org/10.1016/j.corsci.2015.10.039.
[75] Kuila, T.; Bose, S.; Mishra, A.K.; Khanra, P.; Kim, N.H.; Lee, J.H. Chemical functionalization of graphene and its applications. Prog. Mater. Sci. 2012, 57, 1061–1105, https://doi.org/10.1016/j.pmatsci.2012.03.002.
[76] Navalon, S.; Dhakshinamoorthy, A.; Alvaro, M.; Garcia, H. Carbocatalysis by graphene-based materials. Chem. Rev. 2014, 114, 6179–6212, https://doi.org/10.1021/cr4007347.
[77] Yu, B.; Wang, X.; Xing, W.; Yang, H.; Song, L.; Hu, Y. UV-Curable functionalized graphene oxide/Polyurethane acrylate nanocomposite coatings with enhanced . . .. Ind. Eng. Chem. Res. 2012, 51, 14629–14636.
[78] Pourhashem, S.; Rashidi, A.; Alaei, M.; Moradi, M.A.; Maklavany, D.M. Developing a new method for synthesizing amine functionalized g-C3N4 nanosheets for application as anti-corrosion nanofiller in epoxy coatings. SN Appl. Sci. 2019, 1, 1–11, https://doi.org/10.1007/s42452-018-0123-7.
[79] Ahmadi, A.; Ramezanzadeh, B.; Mahdavian, M. Hybrid silane coating reinforced with silanized graphene oxide nanosheets with improved corrosion protective performance. 2016, https://doi.org/10.1039/c6ra04843a.
[80] Mo, M.; Zhao, W.; Chen, Z.; Yu, Q.; Zeng, Z.; Wu, X.; Xue, Q. Excellent tribological and anti-corrosion performance of polyurethane composite coatings reinforced with functionalized graphene and graphene oxide nanosheets. RSC Adv. 2015, 5, 56486–56497, https://doi.org/10.1039/c5ra10494g.
[81] Ramezanzadeh, B.; Niroumandrad, S.; Ahmadi, A.; Mahdavian, M.; Mohamadzadeh Moghadam, M.H. Enhancement of barrier and corrosion protection performance of an epoxy coating through wet transfer of amino functionalized graphene oxide. Corros. Sci. 2016, 103, 283–304, https://doi.org/10.1016/j.corsci.2015.11.033.
[82] Ramezanzadeh, B.; Haeri, Z.; Ramezanzadeh, M. A facile route of making silica nanoparticles-covered graphene oxide nanohybrids (SiO2-GO); fabrication of SiO2-GO/epoxy composite coating with superior barrier and corrosion protection performance. Chem. Eng. J. 2016, 303, 511–528, https://doi.org/10.1016/j.cej.2016.06.028.
[83] Huang, L.; Zhu, P.; Li, G.; Lu, D.; Sun, R.; Wong, C. Core-shell SiO2@RGO hybrids for epoxy composites with low percolation threshold and enhanced thermo-mechanical properties. J. Mater. Chem. A. 2014, 2, 18246–18255, https://doi.org/10.1039/c4ta03702b.
[84] Ramezanzadeh, B.; Ahmadi, A.; Mahdavian, M. Enhancement of the corrosion protection performance and cathodic delamination resistance of epoxy coating through treatment of steel substrate by a novel nanometric sol-gel based silane composite film filled with functionalized graphene oxide nanosheets. Corros. Sci. 2016, 109, 182–205, https://doi.org/10.1016/j.corsci.2016.04.004.
[85] Pourhashem, S.; Vaezi, M.R.; Rashidi, A. Investigating the effect of SiO2-graphene oxide hybrid as inorganic nanofiller on corrosion protection properties of epoxy coatings. Surf. Coatings Technol. 2017, 311, 282–294, https://doi.org/10.1016/j.surfcoat.2017.01.013.
[86] Di, H.; Yu, Z.; Ma, Y.; Li, F.; Lv, L.; Pan, Y.; Lin, Y.; Liu, Y.; He, Y. Graphene oxide decorated with Fe3O4 nanoparticles with advanced anticorrosive properties of epoxy coatings. J. Taiwan Inst. Chem. Eng. 2016, 64, 244–251, https://doi.org/10.1016/j.jtice.2016.04.002.
[87] Sayin, C.S.; Toffoli, D.; Ustunel, H. Covalent and noncovalent functionalization of pristine and defective graphene by cyclohexane and dehydrogenated derivatives. Appl. Surf. Sci. 2015, 351, 344–352, https://doi.org/10.1016/j.apsusc.2015.05.123.
[88] Zhang, X.; Yan, X.; Guo, J.; Liu, Z.; Jiang, D.; He, Q.; Wei, H.; Gu, H.; Colorado, H.A.; Zhang, X.; Wei, S.; Guo, Z. Polypyrrole doped epoxy resin nanocomposites with enhanced mechanical

properties and reduced flammability. J. Mater. Chem. C. 2015, 3, 162–176, https://doi.org/10.1039/c4tc01978d.

[89] Gao, L.; Ren, W.; Xu, H.; Jin, L.; Wang, Z.; Ma, T.; Ma, L.P.; Zhang, Z.; Fu, Q.; Peng, L.M.; Bao, X.; Cheng, H.M. Repeated growth and bubbling transfer of graphene with millimetre-size single-crystal grains using platinum. Nat. Commun.2012, 3, 697–699, https://doi.org/10.1038/ncomms1702.

[90] Sun, W.; Wang, L.; Wu, T.; Pan, Y.; Liu, G. Synthesis of low-electrical-conductivity graphene/pernigraniline composites and their application in corrosion protection. Carbon N. Y. 2014, 79, 605–614, https://doi.org/10.1016/j.carbon.2014.08.021.

[91] Xu, L.Q.; Wang, L.; Zhang, B.; Lim, C.H.; Chen, Y.; Neoh, K.G.; Kang, E.T.; Fu, G.D. Functionalization of reduced graphene oxide nanosheets via stacking interactions with the fluorescent and water-soluble perylene bisimide-containing polymers. Polymer (Guildf). 2011, 52, 2376–2383, https://doi.org/10.1016/j.polymer.2011.03.054.

[92] Yu, Y.H.; Lin, Y.Y.; Lin, C.H.; Chan, C.C.; Huang, Y.C. High-performance polystyrene/graphene-based nanocomposites with excellent anti-corrosion properties. 2014, https://doi.org/10.1039/c3py00825h.

[93] Alhumade, H.; Abdala, A.; Yu, A.; Elkamel, A.; Simon, L. Corrosion inhibition of copper in sodium chloride solution using polyetherimide/graphene composites. Can. J. Chem. Eng. 2016, 94, 896–904, https://doi.org/10.1002/cjce.22439.

[94] Cheng, L.; Liu, C.; Han, D.; Ma, S.; Guo, W.; Cai, H.; Wang, X. Effect of graphene on corrosion resistance of waterborne inorganic zinc-rich coatings. J. Alloys Compd. 2019, 774, 255–264, https://doi.org/10.1016/j.jallcom.2018.09.315.

[95] Deshpande, P.P.; Jadhav, N.G.; Gelling, V.J.; Sazou, D. Conducting polymers for corrosion protection: A review. J. Coatings Technol. Res. 2014, 11, 473–494, https://doi.org/10.1007/s11998-014-9586-7.

[96] Gospodinova, N.; Terlemezyan, L. Conducting polymers prepared by oxidative polymerization: Polyaniline. Prog. Polym. Sci. 1998, 23, 1443–1484, https://doi.org/10.1016/S0079-6700(98)00008-2.

[97] Jiang, S.; Liu, Z.; Jiang, D.; Cheng, H.; Han, J.; Han, S. Graphene as a nanotemplating auxiliary on the polypyrrole pigment for anticorrosion coatings. High Perform. Polym. 2016, 28, 747–757, https://doi.org/10.1177/0954008316647469.

[98] Pourhashem, S.; Vaezi, M.R.; Rashidi, A.; Bagherzadeh, M.R. Exploring corrosion protection properties of solvent based epoxy-graphene oxide nanocomposite coatings on mild steel. Corros. Sci. 2017, 115, 78–92, https://doi.org/10.1016/j.corsci.2016.11.008.

[99] Amrollahi, S.; Ramezanzadeh, B.; Yari, H.; Ramezanzadeh, M.; Mahdavian, M. Synthesis of polyaniline-modified graphene oxide for obtaining a high performance epoxy nanocomposite film with excellent UV blocking/anti-oxidant/ anti-corrosion capabilities, Elsevier Ltd, 2019, https://doi.org/10.1016/j.compositesb.2019.05.015.

[100] Chang, C.H.; Huang, T.C.; Peng, C.W.; Yeh, T.C.; Lu, H.I.; Hung, W.I.; Weng, C.J.; Yang, T.I.; Yeh, J.M. Novel anticorrosion coatings prepared from polyaniline/graphene composites. Carbon N. Y. 2012, 50, 5044–5051, https://doi.org/10.1016/j.carbon.2012.06.043.

[101] Jafari, Y.; Ghoreishi, S.M.; Shabani-Nooshabadi, M. Polyaniline/Graphene nanocomposite coatings on copper: Electropolymerization, characterization, and evaluation of corrosion protection performance. Synth. Met. 2016, 217, 220–230, https://doi.org/10.1016/j.synthmet.2016.04.001.

[102] Jafari, Y.; Ghoreishi, S.M.; Shabani-Nooshabadi, M. Electrochemical deposition and characterization of polyaniline-graphene nanocomposite films and its corrosion protection properties. J. Polym. Res. 2016, 23, https://doi.org/10.1007/s10965-016-0983-8.

[103] Shen, J.; Zhu, Y.; Yang, X.; Li, C. Graphene quantum dots: Emergent nanolights for bioimaging, sensors, catalysis and photovoltaic devices. Chem. Commun. 2012, 48, 3686–3699, https://doi.org/10.1039/c2cc00110a.
[104] Zhang, Z.; Zhang, J.; Chen, N.; Qu, L. Graphene quantum dots: An emerging material for energy-related applications and beyond. Energy Environ. Sci. 2012, 5, 8869–8890, https://doi.org/10.1039/c2ee22982j.
[105] Shin, Y.; Lee, J.; Yang, J.; Park, J.; Lee, K.; Kim, S.; Park, Y.; Lee, H. Mass production of graphene quantum dots by one-pot synthesis directly from graphite in high yield. Small. 2014, 10, 866–870, https://doi.org/10.1002/smll.201302286.
[106] Shkirskiy, V.; Keil, P.; Hintze-Bruening, H.; Leroux, F.; Vialat, P.; Lefèvre, G.; Ogle, K.; Volovitch, P. Factors affecting MoO42- inhibitor release from Zn2Al based layered double hydroxide and their implication in protecting hot dip galvanized steel by means of organic coatings. ACS Appl. Mater. Interfaces. 2015, 7, 25180–25192, https://doi.org/10.1021/acsami.5b06702.
[107] Demchenko, A.P.; Dekaliuk, M.O. Novel fluorescent carbonic nanomaterials for sensing and imaging. Methods Appl. Fluoresc. 2013, 1, https://doi.org/10.1088/2050-6120/1/4/042001.
[108] Yang, S.T.; Cao, L.; Luo, P.G.; Lu, F.; Wang, X.; Wang, H.; Meziani, M.J.; Liu, Y.; Qi, G.; Sun, Y.P. Carbon dots for optical imaging in vivo. J. Am. Chem. Soc. 2009, 131, 11308–11309, https://doi.org/10.1021/ja904843x.
[109] Lim, S.Y.; Shen, W.; Gao, Z. Carbon quantum dots and their applications. *Chem. Soc. Rev.* 2015, *44*, 362–381, https://doi.org/10.1039/c4cs00269e.
[110] Zhu, C.; Fu, Y.; Liu, C.; Liu, Y.; Hu, L.; Liu, J.; Bello, I.; Li, H.; Liu, N.; Guo, S.; Huang, H.; Lifshitz, Y.; Lee, S.T.; Kang, Z. Carbon dots as fillers inducing healing/self-healing and anticorrosion properties in polymers. Adv. Mater. 2017, 29, 1–8, https://doi.org/10.1002/adma.201701399.
[111] Karimi, B.; Ramezanzadeh, B. A comparative study on the effects of ultrathin luminescent graphene oxide quantum dot (GOQD) and graphene oxide (GO) nanosheets on the interfacial interactions and mechanical properties of an epoxy composite. J. Colloid Interface Sci. 2017, 493, 62–76, https://doi.org/10.1016/j.jcis.2017.01.013.
[112] Pourhashem, S.; Ghasemy, E.; Rashidi, A.; Vaezi, M.R. Corrosion protection properties of novel epoxy nanocomposite coatings containing silane functionalized graphene quantum dots, Elsevier B.V., 2018, https://doi.org/10.1016/j.jallcom.2017.10.150.
[113] Liu, Z.; Ye, Y.W.; Chen, H. Corrosion inhibition behavior and mechanism of N-doped carbon dots for metal in acid environment. J. Clean. Prod. 2020, 270, https://doi.org/10.1016/j.jclepro.2020.122458.
[114] Lv, J.; Fu, L.; Zeng, B.; Tang, M.; Li, J. Synthesis and acidizing corrosion inhibition performance of N-doped carbon quantum dots. Russ. J. Appl. Chem. 2019, 92, 848–856, https://doi.org/10.1134/S1070427219060168.
[115] Ye, Y.; Yang, D.; Chen, H.; Guo, S.; Yang, Q.; Chen, L.; Zhao, H.; Wang, L. A high-efficiency corrosion inhibitor of N-doped citric acid-based carbon dots for mild steel in hydrochloric acid environment. J. Hazard. Mater. 2020, 381, 121019, https://doi.org/10.1016/j.jhazmat.2019.121019.
[116] Ren, S.; Cui, M.; Zhao, H.; Wang, L. Effect of nitrogen-doped carbon dots on the anticorrosion properties of waterborne epoxy coatings. Surf. Topogr. Metrol. Prop. 2018, 6, https://doi.org/10.1088/2051-672X/aab588.
[117] Wang, J.; Du, P.; Zhao, H.; Pu, J.; Yu, C. Novel nitrogen doped carbon dots enhancing the anticorrosive performance of waterborne epoxy coatings. Nanoscale Adv. 2019, 1, 3443–3451, https://doi.org/10.1039/c9na00155g.

[118] Ye, Y.; Chen, H.; Zou, Y.; Zhao, H. Study on self-healing and corrosion resistance behaviors of functionalized carbon dot-intercalated graphene-based waterborne epoxy coating. J. Mater. Sci. Technol. 2021, 67, 226–236, https://doi.org/10.1016/j.jmst.2020.06.023.
[119] Ramezanzadeh, B.; Karimi, B.; Ramezanzadeh, M.; Rostami, M. Synthesis and characterization of polyaniline tailored graphene oxide quantum dot as an advance and highly crystalline carbon-based luminescent nanomaterial for fabrication of an effective anti-corrosion epoxy system on mild steel. J. Taiwan Inst. Chem. Eng. 2019, 95, 369–382, https://doi.org/10.1016/j.jtice.2018.07.041.
[120] Saikia, A.; Sarmah, D.; Kumar, A.; Karak, N. Bio-based epoxy/polyaniline nanofiber-carbon dot nanocomposites as advanced anticorrosive materials. J. Appl. Polym. Sci. 2019, 136, 1–11, https://doi.org/10.1002/app.47744.
[121] Guo Zhang, W.; Li, L.; Wei Yao, S.; Qin Zheng, G. Corrosion protection properties of lacquer coatings on steel modified by carbon black nanoparticles in NaCl solution. Corros. Sci. 2007, 49, 654–661, https://doi.org/10.1016/j.corsci.2006.06.017.
[122] Lam, C.K.; Lau, K.T. Localized elastic modulus distribution of nanoclay/epoxy composites by using nanoindentation. Compos. Struct. 2006, 75, 553–558, https://doi.org/10.1016/j.compstruct.2006.04.045.
[123] Dietsche, F.; Thomann, Y.; Thomann, R.; Mülhaupt, R. Translucent acrylic nanocomposites containing anisotropic laminated nanoparticles derived from intercalated layered silicates. J. Appl. Polym. Sci. 2000, 75, 396–405, https://doi.org/10.1002/(SICI)1097-4628(20000118)75:3<396::AID-APP9>3.0.CO;2-E.
[124] Crosky, A.; Kelly, D.; Li, R.; Legrand, X.; Huong, N.; Ujjin, R. Improvement of bearing strength of laminated composites. Compos. Struct. 2006, 76, 260–271, https://doi.org/10.1016/j.compstruct.2006.06.036.
[125] Becker, O.; Varley, R.; Simon, G. Morphology, thermal relaxations and mechanical properties of layered silicate nanocomposites based upon high-functionality epoxy resins. Polymer (Guildf). 2002, 43, 4365–4373, https://doi.org/10.1016/S0032-3861(02)00269-0.
[126] Foyet, A.; Wu, T.H.; Kodentsov, A.; van der Ven, L.G.J.; de With, G.; van Benthem, R.A.T.M. Corrosion protection and delamination mechanism of epoxy/carbon black nanocomposite coating on AA2024-T3. J. Electrochem. Soc. 2013, 160, C159–C167, https://doi.org/10.1149/2.086304jes.
[127] Wei, Y.H.; Zhang, L.X.; Ke, W. Evaluation of corrosion protection of carbon black filled fusion-bonded epoxy coatings on mild steel during exposure to a quiescent 3% NaCl solution. Corros. Sci. 2007, 49, 287–302, https://doi.org/10.1016/j.corsci.2006.06.018.
[128] Grundmeier, G.; Schmidt, W.; Stratmann, M. Corrosion protection by organic coatings: Electrochemical mechanism and novel methods of investigation. Electrochim. Acta. 2000, 45, 2515–2533, https://doi.org/10.1016/S0013-4686(00)00348-0.
[129] Smiechowski, M.F.; Lvovich, V.F. Characterization of non-aqueous dispersions of carbon black nanoparticles by electrochemical impedance spectroscopy. J. Electroanal. Chem. 2005, 577, 67–78, https://doi.org/10.1016/j.jelechem.2004.11.015.
[130] Ghasemi-Kahrizsangi, A.; Neshati, J.; Shariatpanahi, H.; Akbarinezhad, E. Effect of SDS modification of carbon black nanoparticles on corrosion protection behavior of epoxy nanocomposite coatings. Polym. Bull. 2015, 72, 2297–2310, https://doi.org/10.1007/s00289-015-1406-4.
[131] Ghasemi-Kahrizsangi, A.; Shariatpanahi, H.; Neshati, J.; Akbarinezhad, E. Corrosion behavior of modified nano carbon black/epoxy coating in accelerated conditions. Appl. Surf. Sci. 2015, 331, 115–126, https://doi.org/10.1016/j.apsusc.2015.01.038.

Gokul Ram Nishad*, Ashwani Kumar Sharma,
Dakeshwar Kumar Verma

Chapter 5
Carbon allotropes: mechanism of corrosion prevention and control

Abstract: Many methods are used to protect the corrosion occurring in metallic materials, out of which the corrosion inhibitors are mainly used at present. In addition to the traditionally used inhibitors for corrosion inhibition, the practice of smart coating materials has increased in the last few decades, in which carbon allotropes and their composites are being used mainly at present. Some of their characteristics, such as thermal stability and stable protective layer formation, resist to corrosive attack and keep them in the category of special type of corrosion inhibitor. In the present work, description has been given about carbon allotropes-based materials and their corrosion inhibition mechanism and experimental techniques.

Keywords: corrosion inhibitor, adsorption, carbon allotropes, metallic materials, electrochemical analysis, computational calculations

5.1 Introduction

Corrosion is a natural phenomenon in which metallic materials convert into their most stable forms such as oxides, chlorides and sulphates etc. due to environmental conditions. Metallic materials such as steel, aluminum, copper, zinc, and its alloys are mainly used in industries such as construction, petroleum, power plants, nuclear power plants, and aerospace [1–3]. Before use, these metals undergo a process like acid picking and descaling to remove the accumulated rust or scull, in which hydrochloric acid, sulphuric acid, nitric acid, etc. are prominently used as acidic solutions [4, 5]. After removing the rust that has accumulated on the metal surface, this corrosive solution starts consuming by attacking the base metal surface. To prevent this loss, a small amount of substance is added to the electrolytic medium, which is called corrosion inhibitor, because it damages the metal surface. By depositing above, they

*Corresponding author: **Gokul Ram Nishad,** Department of Chemistry, Govt. Digvijay Autonomous Postgraduate College, Rajnandgaon, Chhattisgarh 491441, India, e-mail: nishadgokul505@gmail.com
Ashwani Kumar Sharma, Dakeshwar Kumar Verma, Department of Chemistry, Govt. Digvijay Autonomous Postgraduate College, Rajnandgaon, Chhattisgarh 491441, India

https://doi.org/10.1515/9783110782820-005

protect them from further corrosion [6, 7]. imidazole derivatives [8], thioglycoluril derivatives [9, 10] supramolecule derivatives [11, 12], and drug molecules [13].

Due to their long synthesis process and environmental threats, there is a need for such inhibitors which are green and stable. Graphene, graphene oxide, graphene composites, carbon nanotubes (CNTs), fullerene, and carbon quantum dots (CQDs) are mainly used [14, 15]. All these allotropes behave like smart anticorrosive material, and being stable even in an aggressive environment, forming a protective layer on the metal surface protects the metallic surface from further corrosion. Mainly experimental tools, surface study, and theoretical calculation are predominant for corrosion monitoring techniques. The present review work is mainly focused on the corrosion inhibition mechanism of carbon allotropes. Additionally Fig. 5.1 demonstrated the key characteristics of carbon allotropes.

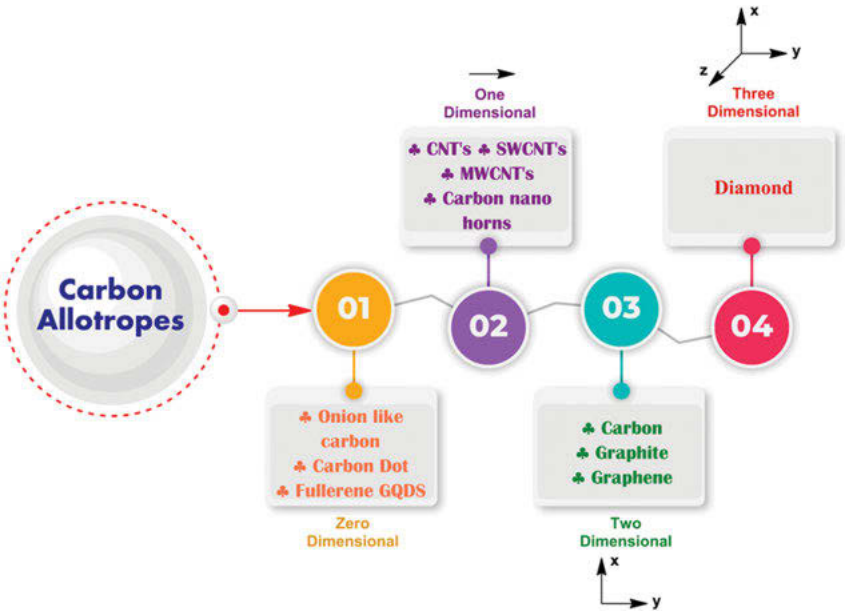

Fig. 5.1: Important characteristics of carbon allotropes [14].

5.2 General corrosion reaction mechanism

– *Electrochemical reactions*

Corrosion on metal surface considered as electrochemical process which involved two half cell reactions i.e. cathodic and anodic. Usually in the oxidation reaction electron has been produced while in reduction reaction electron is involved as reactant. There are mainly two types of electrochemical reactions:

i) *Anodic reaction*: Anodic reaction is also considered as oxidation reaction as it involves the increase in oxidation state of metal ion by loosing electron(s) i.e. electron can be produced during the reaction, for example:

$$M(s) \longrightarrow M^{n+}{}_{(aq)} + ne^-$$

where M = Fe, Al, Zn, Cu
$N = 0, 1, 2, 3, 4$, etc.

Anodic reaction in metal complexes:

$$Fe(CN)_6{}^{4-}(aq) \longrightarrow Fe(CN)_6{}^{3-} + e^-$$

ii) *Cathodicreaction*: In this reaction oxidation number of species decreases due to gain electrons i.e. it can be considered as reduction reaction. Here species gain electron at cathodic side, and this reaction is termed as hydrogen evolution reaction. If the electrolytic solution is acidic, for example:

$$2H^+(aq) + 2e^- \longrightarrow H_2(g) \uparrow$$

Cathodic reactions also exist in neutral or basic solution. In this case dissolved oxygen is reduced to hydroxyl ions as given below:

$$O_2(g) + 2H_2O + 4e^- \longrightarrow 4OH^-(aq)$$

– *Overall electrochemical process*
In acidic electrolytic medium, both anodic and cathodic reactions take together at coupled manner on metal surface.

Formation of potential difference on the metal surface can be considered as the driving force for the course of corrosion. Additionally, Fig. 5.2 shows the coupled reaction on metal surface. Overall process can be representation as follows:

– *Electrochemical analysis*
Corrosion is electrochemical phenomenon, which is generated due to the potential difference in metallic surface. The analysis of corrosion behavior and corrosion rates is done by electrochemical studies. Mainly three electrode cell assembly uses for electrochemical analysis i.e. working electrode, reference electrode, and counter electrode. As working electrode, that metal is taken for which corrosion study is done, such as iron, aluminum, copper, and zinc electrode. Calomel electrode is mainly used for reference electrode, and platinum electrode is mainly used for counter electrode. Electrochemical impedance spectroscopy (EIS) and potentiodynamic polarization are studied under electrochemical techniques.

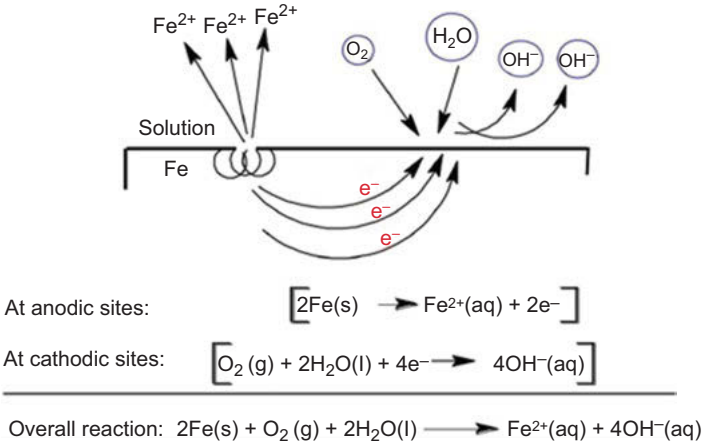

Fig. 5.2: Coupled reactions occurring on metal surface at different electrolytic medium [16].

– *Open circuit potential*

Open circuit potential (OCP) is a passive technique, also known as rest potential, open circuit voltage, equilibrium potential, corrosion potential, and zero potential. It is mainly used to determine the resting potential of the system from which further experiments depend on. Mainly with EIS the potential is set against the OCP, not against the reference electrode. The resting potential between the working electrode and the reference electrode is measured by OCP.

Information about the stability of the electrochemical system in the electrolytic medium is also obtained through the OCP. Overall it can be considered that OCP is simply the potential difference between reference electrode and working electrode.

$$E_{ocp} = E_{working} - E_{ref}$$

Hence the potential can be used as normal voltameter to measure the potential difference between two difference sites or points.

– *Electrochemical impedance spectroscopy*

EIS techniques are used to explain the effect of the corrosion process on surface inhomogeneity. Electrochemical AC and DC techniques are used for performing electrochemical processes in a method to determine corrosion rates.

5.3 Corrosion inhibitors: Past to present perspective

Generally good corrosion inhibitors should have the following properties [17]:

i) Inhibiting molecules having functional group containing different heteroatoms and electron-rich unsaturated bond is present.
ii) Highly water soluble.
iii) Eco-friendly, zero-toxic, and should be cost-effective.
iv) Stable in electrolytic solution.
v) From the methods of making it to the application in it, the process is zero dangerous.

5.3.1 Inorganic corrosion inhibitors

Inorganic inhibitors, such as chromate, phosphate, and silicate, were mainly used as inhibitors a few decades ago, based on the above properties of inhibitors. But due to the ill-effects of living beings, their use started to decrease. A few decades ago, organic corrosion inhibitors were mainly used as replacements for inorganic corrosion inhibitors. Most of the effective inorganic corrosion inhibitors are chromate, phosphate, sulphate, nitrite, and silicates salts of various metals like zinc, copper, and nickel. The inorganic salts mentioned here react with the metal cations present on the surface, and this further gets deposited on the metal surface in the form of a protective layer that prohibits further corrosion [18, 19]. Chromate salts especially $SrCrO_4$ have shown effective inhibition properties by forming a thin stable protective film on the metal surface even without depending upon the environmental parameters like the presence of O_2 and pH [20].

A. I. Munoz and his coworkers examined the copper, nickel, and two copper-nickel (Cu90/Ni10, Cu70/Ni30) alloys in 850 g/L LiBr solution in the absence and presence of chromate (CrO42–), molybdate (MoO42–), and tetraborate (B4O72–) inhibitors. The efficiency was measured using poteniodynamic and cyclic voltametry, and they found that chromate is the most effective inhibitor among the three [21].

B. Ramezanzadeh, E. Ghasemi, F. Askari, and Mahadavian analyzed corrosion-inhibitive pigments based on zinc acetate/bentriazole in 3.5 wt% NaCl solution on mild steel samples by polarization test and EIS. They found that the zinc acetate/benzotriazole is a good inhibitor, and it also decreases the dissolution rate of steel [22].

Q. H. Zhang and his coworkers have studied the corrosion inhibition properties of combined corrosion inhibitors LHD + PT made by mixing amino acid (L-histadine) and 1-phenylthiourea and a modified inhibitor PT-HD (phenylcarbamothioylhistadine) for the corrosion of carbon steel in CO_2-saturated formation water. Experimental data prove that PT-HD is better inhibitor as compared to LHD + PT (inhibition efficiency of 99.2% for 0.4 mM LHD + PT and 99.3% for 0.4 mM PT-HD).

5.3.2 Organic corrosion inhibitors

Organic corrosion inhibitors mainly functional groups of diffusion present electron-rich centers by which they interact with the metal surface. The use of organic corrosion inhibitors has several advantages over inorganic inhibitors such as electron-rich center, less hazardous, green in nature, highly soluble, nontoxic, and eco-friendly. [23, 24]. Molecules are mainly used as organic corrosion inhibitors in aliphatic, aromatic, heterocyclic, carbocyclic, ionic liquids, etc. Organic corrosion inhibitors mainly pharmaceutical molecules, imidazole derivatives [25], indole derivatives [26], thiophene derivatives [27], pyrazine derivatives [28], benzothiazole derivatives [29], etc. have been mainly used by the former researchers. But due to the complex process ranging from synthesis methods to applications of organic corrosion inhibitors, it has also attracted the attention of scientific and researchers toward biomass-based materials in search of alternative inhibitors. Ahmed and coworkers (2022) studied nonanedioic acid toward anticorrosive material for mild steel in 1 M HCl aggressive solution. They reported maximum inhibition efficiency of 97% according to experimental technique at temperature ranging from 303 to 333 K [30]. Due to the toxic, harmful behavior toward the environment, the use of inorganic inhibitors is being reduced. Heteroatoms like S, N, O, and P are present in organic inhibitors. Their two properties viz. higher basicity and electron-donor abilities make them center for absorption on a metal surface.

Palaniappan N. and team members have successfully examined the 4,5-diphenyl -imidazole-functionalized CNTs in 1 M H_2SO_4 as a corrosion-inhibiting barrier layer on nickel alloy surfaces [31]. Abrishami, Naderi, and Ramezanzadeh have synthesized many organic/inorganic using zinc acetylacetonate and organic compounds such as Utrica Dioica leave extracts (ZnAA-U.D). They have examined the synthesized pigments in corrosion control in 3.5 wt.% NaCl solutions and found that the synthesized pigments showed excellent corrosion inhibition properties at pH = 4 [32].

Yujie Qiang and his team have studied corrosion inhibition properties of indazole (IA) and 5-aminoindazole (AIA) for copper in NaCl solution, and they found these compounds very effective corrosion inhibitors with inhibition efficiency order AIA > IA [33].

5.3.3 Biomass materials

Biomass-based corrosion inhibitor I mainly comes across from algae, fungi, bacteria, plant extracts, etc. Materials based on plant extracts include various parts such as bark, root, leaves, flower, fruit, and seed rind, which are currently being used as green rust inhibitors. Plant extract mainly contains a variety of phytoconstituents such as flavonoids, terpenoids, alkaloids, and cholesterol. All these phytoconstituents are electron rich with different diffusion function groups. Plants extract corrosion-resistant, cost-effective, environment-friendly, and are nonhazardous [34, 35].

Biomasses specially extracted from plants have also shown excellent corrosion inhibition properties. The corrosion inhibition potential of the green inhibitors depends upon the structure of the active ingredient. The use of naturally occurring substances as green corrosion inhibitors has been successfully reported in both the acidic as well as basic medium by many researchers.

O. K. Abiola and his coworkers have studied the corrosion inhibition properties of aluminum in hydrochloric acid solutions of *Delonix regia* extract in hydrochloric acid solutions [36], and rosemary leaves were examined by M. Kliskic et al. as corrosion inhibitor for the Al + 2.5 Mg alloy in a 3% NaCl solution at 25 °C [37]. Honey [38] and opuntia extracts [39] were examined by El-Etre as a corrosion inhibitor for copper and aluminum, respectively.

The corrosion inhibition activity of R. communis extract against reinforcing steel corrosion in concrete in 3.5% NaCl media has been studied successfully by S. P. Palanisamy et al. The layer of R. communis on reinforcing steel in concrete also increases the compressive strength and splitting tensile strength [40]. Xin Lai et al. have examined chitosan derivatives for corrosion inhibition properties on aluminum alloy. The corrosion inhibition activities were checked at different concentrations. The maximum inhibition efficiency of chitosan derivatives reaches 94.5% at 200 PPM after being immersed in 3.5 wt% NaCl solution for 72 h [41]. Watermelon extract:Zn complex has been studied in a 3.5% NaCl solution on mild steel (MS) and found that it controls 96% of MS corrosion [42].

5.4 Carbon allotropes as anticorrosive materials

The revolution of materials science facilitates the development of a new generation of effective materials for applications. Compared to other anticorrosive materials, carbon allotropes are among the most preferred materials in the field of corrosion protection due to their characteristics such as large surface area, excellent mechanical properties, light weight and easy synthesis process, and other synergistic behavior.

5.4.1 Graphene, graphene oxide (GO), and its composites as anticorrosive materials

Prasai et al. [43] reported graphene coating on various metals such as Zn and Ni as a protective coating that prevents corrosion. They used electrochemical methods to study the corrosion inhibition of copper and nickel by growing graphene on either of these metals. They found that the graphene coating effectively suppresses metal oxidation and oxygen reduction by cyclic voltammetry measurements. Their EIS measurements showed that while graphene itself is not damaged, the metal beneath

it corrodes over cracks in the graphene film. They reported using chemical vapor deposition (CVD) for graphene coating the corrosion rate of copper films is seven times slower in aerated Na_2SO_4 solution than in bare copper. They reported that nickel with multilayer graphene film corrosives is 20 times slower than nickel surface coated with four layers of mechanically transferred graphene, i.e. four times slower than bare nickel. They were ultimately found to establish graphene as the thinnest known corrosion-protecting coating [43]. Zhang et al. [44] proposed graphene as a biocompatible protective film for metal with potential for biomedical applications and also confirmed that graphene effectively protects Cu surface from corrosion in various biological aqueous environment stops. Their various tests showed that graphene greatly reduces the toxicity of Cu by inhibiting corrosion and reducing the concentration of Cu^{2+} ions produced. They demonstrated that additional thiol derivatives assembled on graphene-coated Cu surface can significantly enhance the stability of the only graphene protection limited by defects in the graphene film [44]. Necolau et al. [45] explained the most recent progress in the field of anticorrosive coatings based on graphene oxide nanostructures as an active filler. With regard to graphene-based coatings, synthesis methods, protective functions, anticorrosion mechanisms, feasibility problems, and some ways to improve the overall properties were highlighted. With regard to the contribution of nanostructures to be used to improve the material's capability, the synergistic effect of graphene is demonstrated primarily with the oxide-refining effect of graphene as being functional with other compounds [45]. Mostly scientists explain that all the revolutionary material can be used in the synthesis of advanced composite coatings by combining the capability of restricting the permeability of water and aggressive species with other extraordinary features of polymeric materials. There is a considerable number of published works on GO polymer composites for anticorrosive applications, and the recent ones focused on the possibility of tailoring and modifying the surface features of graphene oxide in order to obtain advanced materials by various strategies, most of them based on both chemical and physical interactions [46–49].

Graphene oxide has the capability of ensuring the coatings when used as filler with hydrophobic features and can also diminish the adsorption and migration of corrosive media, which effectively improve the corrosion resistance of the composite coating. Ramezanzadeh et al. (2020) developed a nanoplatform with superior anticorrosive action built up through a one-pot synthesis method of zeoliticimidazolate framework-8 (ZIF-8) on the graphene oxide sheets. The particles applied on a steel sample showed a corrosion inhibition efficiency of about 79% when immersed in an NaCl solution by polarization tests. Zhu et al. [50] synthesized functionalized graphene oxide (GO-PPy) by in-situ process to grow polypyrrole (PPy) film on GO surface as shown in Fig. 5.3. This nanocomposites were characterized by FI-TR, XRD, Raman, and FESEM techniques. They also explained that $GP_{0.}05\%$ coating showed the best impermeable and corrosion protection performance compared to other coatings according to EIS (Fig. 5.4) [50].

Fig. 5.3: Schematic representation of synthesis of graphene oxide-polypyrrole [50].

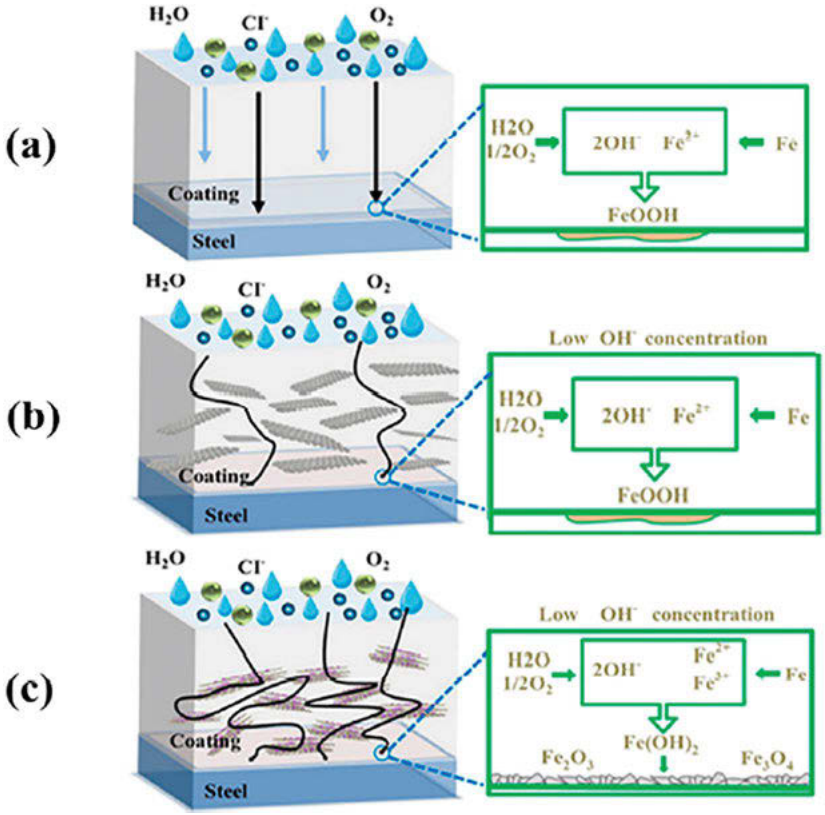

Fig. 5.4: The protective mechanism of graphene oxide-polypyrrole in corrosion protection formulations [50].

5.4.2 Carbon dots, carbon quantum dots, and their composites as anticorrosive materials

The unique properties of carbon dots (CDs) such as rapid solubility in water, biocompatibility, low toxicity, excellent anti-bacterial agent, chemically stable, and high thermal and nonflammable establish it as a versatile material at present, that the corrosion of metal materials in aggressive acidic, saline, CO_2-saturated saline, and microbiological solutions continues in the oil, gas, and other organic chemical industry.Which is in quick need of corrosion protection, for which the use of CDs and their derivatives is an ecological and environmentally efficient method? It contains more pyrrole-like-N, pyridine-N, graphitic N atoms, and O atoms, in which lone electron pairs promote CDs that become efficient corrosion inhibitors.

Saraswat et al. [51] prepared CQDs CD1 and CD2 anticorrosive material for MS in 15% HCl aggresive solution. They reported the maximum protection degree 96.4% and 90%, respectively, according to experimental techniques [51].Cui et al. [52] synthesized nitrogen-doped CDs (NCDs) toward anticorrosive material for Q235 carbon steel in 0.1 M HCl aggressive solution by microwave synthesis. They reported maximum protection degree 89.98% at 500 ppm according to various experimental techniques and characterized by spectroscopic method [52].

Continuously Cen et al. [53] also synthesized N and S co-doped CDs as effective corrosion inhibitors for 5,052 alluminium alloy in 0.1 M HCl anticorrosive solution. They explained their maximum protection degree 89.9%5 mg/L by experimental techniques. Also Fig. 5.5 demonstrated the 2D and 3D AFM images of inhibitor on metallic surface [53]. p-CDs and o-CDs novel nitrogen-doped CDs corrosion inhibitors are prepared by Cui and coworkers (2018) for Q235 carbon steel in 1 M HCl aggressive solution. The maximum protection degree of this material found 97% by various experimental techniques and characterized by spectroscopic method [54]. Ye et al.

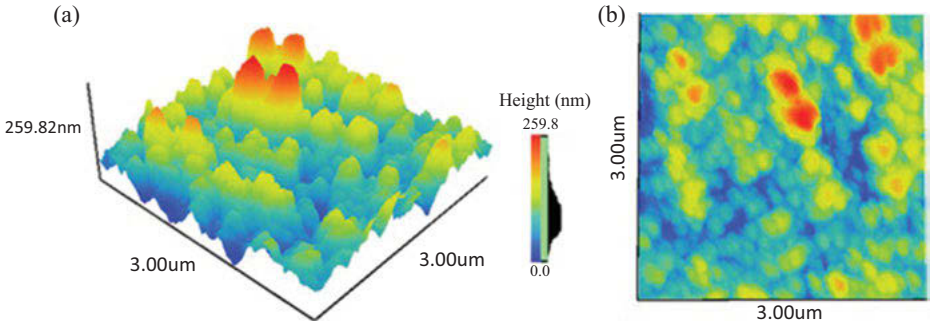

Fig. 5.5: Surface morphology of Al-alloy after immersion with 5 mg L – 1 N, S-CDs for (a) 3D AFM image and (b) 2D AFM image.

[55] prepared green and effective corrosion inhibitor of functionized CDs for Q235 steel in 1 M HCl aggressive solutio. They reported maximum protection degree 90% at 100 mg/L according to the experimental techniques [55].

5.5 Carbon nanotubes and its composites as anticorrosive materials

CNTs and its the derivative are very useful at present due to its specific properties i.e. good conductors of heat and electricity, including high dispersibility, excellent mechanical strength, good mechanical property, high thermal and chemical resistance, high surface-to-volume ratio, and excellent ability to interact with metal surfaces. Alongwith their corrosion inhibition properties, CNTs and their derivatives are successfully applied as catalysts. Salvetat et al. [58] prepared CNTSs from various methods including CVD, thermal synthesis process, and arc discharge evaporation [56–59]. Additionally, Fig. 5.6 shows the SEM and TEM microphotographs of carbon allotropes with their composites on metallic surface.

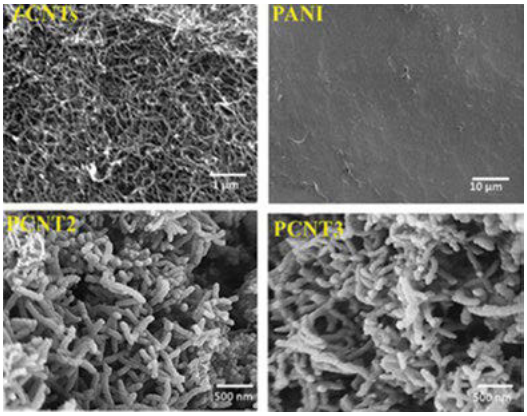

Fig. 5.6: SEM and TEM microphotographs of carbon allotropes with their composites on metallic surface [60].

Ionita et al. [61] explained the mechanical properties of (PPy)/polyaminobenzenesulfonic acid-functionalized single-walled CNT-(PABS) and PPy/carboxylic acid-functionalized single-walled CNT-(CA) using molecular mechanics and molecular dynamics approaches [61]. In another study they found that the PPy film, CNT-PABS, and CNT-CA were used as anticorrosive composite coatings for carbon steel (OL 48–50) alloys in 3.5% NaCl. Potentiodynamic polarization, SEM, and TEM techniques were used to measure the anticorrosive effect of various formulations [62].

5.6 Corrosion inhibition mechanism

In general, corrosion inhibition is acid-base interaction chemistry, in which the inhibitor molecules act as Lewis bases. Whereas metal/alloy surface behaves like Lewis acid. Corrosion inhibitors generally contain various types of hetero-atoms such as O, S, N, P, and pi-electrons as functional groups, which are generally rich in electrons. Whereas on the metal surface, the metal cations generally reside above in the form of M^{n+}, which behave as electron acceptors [12, 63, 64]. Electron-rich centers are present in carbon-based materials and many composites. These molecules are highly stable, blocking the metal surface and protecting the metal surface from further corrosion. Corrosion inhibitors are deposited on the surface of the metal mainly through chemisorption and physisorption mechanisms, with chemisorption being stronger because there is a direct interaction between the metal surface and the inhibitor molecule [65–67]. Additionally, Fig. 5.7 demonstrates the interaction mechanism of CDs on the steel surface.

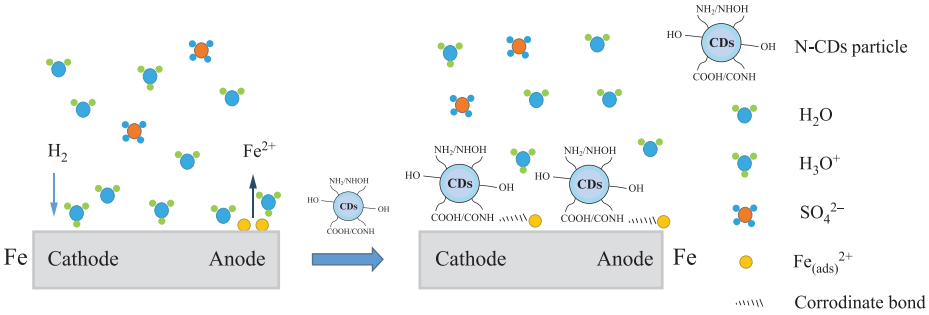

Fig. 5.7: Demonstrated the interaction mechanism of carbon dots on the steel surface [15].

5.7 Conclusion

Carbon allotropes namely graphene, GOs, CNTs, carbon nanorods, fullerenes, and their composite materials with polymers and nanomaterials exhibited broad applications in various fields. Their some unique properties such as small size, large surface area, hydrophobic nature, nano-filler, high temperature stability, and resistance to corrosive environment make them suitable for multiple applications. In this regards, carbon allotropes are used widely as smart anticorrosive materials toward metallic materials in various aggressive electrolytic media. Carbon allotropes are very stable towards corrosive environment to protect metallic surface from further attack. Since the nature of carbon-based materials are very stable and rigid, it can enhance the protection property. Because of their polymeric nature, these materials are associated with

huge intermolecular (Van der Waals) force of attraction they readily undergo agglomeration inside the polymer matrix that adversely affect their uniform distribution and ultimately their corrosion inhibition performance. Recently various reports are published in which covalently and non-covalently modified carbon allotropes have been evaluated as corrosion inhibitors.

References

[1] Jawad, A.Q., et al. Synthesis, characterization, and corrosion inhibition potential of novel thiosemicarbazone on mild steel in sulfuric acid environment. Coatings 2019, 9(11), 729.

[2] Abbaszadegan, A., et al. The effect of charge at the surface of silver nanoparticles on antimicrobial activity against gram-positive and gram-negative bacteria: A preliminary study. J. Nanomater. 2015, 2015.

[3] Haldhar, R., et al. Corrosion inhibitors: Industrial applications and commercialization. In: Sustainable corrosion inhibitors II: Synthesis, design, and practical applications, ACS Publications, 2021, 219–235.

[4] Verma, D., et al. Inhibition performance of Glycine max, Cuscuta reflexa and Spirogyra extracts for mild steel dissolution in acidic medium: Density functional theory and experimental studies. Results Phys. 2018, 10, 665–674.

[5] Abd El-Lateef, H.M.; Abdallah, Z.A.; Ahmed, M.S.M. Solvent-free synthesis and corrosion inhibition performance of Ethyl 2-(1, 2, 3, 6-tetrahydro-6-oxo-2-thioxopyrimidin-4-yl) ethanoate on carbon steel in pickling acids: Experimental, quantum chemical and Monte Carlo simulation studies. J. Mol. Liq. 2019, 296, 111800.

[6] Verma, D.K.; Khan, F. Corrosion inhibition of mild steel in hydrochloric acid using extract of glycine max leaves. Res. Chem. Intermed. 2016, 42(4), 3489–3506.

[7] Verma, D.K., et al. Gravimetric, electrochemical surface and density functional theory study of acetohydroxamic and benzohydroxamic acids as corrosion inhibitors for copper in 1 M HCl. Results Phys. 2019, 13, 102194.

[8] Berdimurodov, E., et al. New and green corrosion inhibitor based on new imidazole derivate for carbon steel in 1 M HCl medium: Experimental and theoretical analyses. Int. J. Eng. Res. Afr. 2022. Trans Tech Publ.

[9] Berdimurodov, E., et al. Thioglycoluril derivative as a new and effective corrosion inhibitor for low carbon steel in a 1 M HCl medium: Experimental and theoretical investigation. J. Mol. Struct. 2021, 1234, 130165.

[10] Berdimurodov, E.T., et al. Novel glycoluril pharmaceutically active compound as a green corrosion inhibitor for the oil and gas industry. Available at SSRN 3951074.

[11] Berdimurodov, E., et al. Novel cucurbit [6] uril-based [3] rotaxane supramolecular ionic liquid as a green and excellent corrosion inhibitor for the chemical industry. Colloids Surf. A Physicochem. Eng. Asp. 2022, 633, 127837.

[12] Berdimurodov, E., et al. Novel bromide–cucurbit [7] uril supramolecular ionic liquid as a green corrosion inhibitor for the oil and gas industry. J. Electroanal. Chem. 2021, 901, 115794.

[13] Verma, D.K., et al. Experimental and theoretical studies on mild steel corrosion inhibition by the grieseofulvin in 1 M HCl. Eur. Chem. Bull. 2017, 6(1), 21–30.

[14] Berdimurodov, E., et al. The recent development of carbon dots as powerful green corrosion inhibitors: A prospective review. J. Mol. Liq. 2021, 118124.

[15] Cao, S., et al. Nitrogen-doped carbon dots as high-effective inhibitors for carbon steel in acidic medium. Colloids Surf. A Physicochem. Eng. Asp. 2021, 616, 126280.
[16] Verma, D.K. Density functional theory (DFT) as a powerful tool for designing corrosion inhibitors in aqueous phase. Adv. Eng. Test. 2018, 87.
[17] Verma, D.K., et al. Heteroatom-based compounds as sustainable corrosion inhibitors: An overview. J. Bio- Tribo-Corros. 2021, 7(1), 1–18.
[18] Deyab, M., et al. Experimental evaluation of new inorganic phosphites as corrosion inhibitors for carbon steel in saline water from oil source wells. Desalination 2016, 383, 38–45.
[19] Raja, P.B., et al. Reviews on corrosion inhibitors: A short view. Chem. Eng. Commun. 2016, 203(9), 1145–1156.
[20] Sinko, J. Challenges of chromate inhibitor pigments replacement in organic coatings. Prog. Organ. Coat. 2001, 42(3–4), 267–282.
[21] Muñoz, A.I., et al. Inhibition effect of chromate on the passivation and pitting corrosion of a duplex stainless steel in LiBr solutions using electrochemical techniques. Corros. Sci. 2007, 49(8), 3200–3225.
[22] Ramezanzadeh, B., et al. Synthesis and characterization of a new generation of inhibitive pigment based on zinc acetate/benzotriazole: Solution phase and coating phase studies. Dyes Pigm. 2015, 122, 331–345.
[23] Brycki, B.E., et al. Organic corrosion inhibitors. Corros. Inhibit. Principles Recent Appl. 2018, 3, 33.
[24] Verma, C., et al. Adsorption behavior of glucosamine-based, pyrimidine-fused heterocycles as green corrosion inhibitors for mild steel: Experimental and theoretical studies. J. Phys. Chem. C 2016, 120(21), 11598–11611.
[25] Kumar, D.; Jain, V.; Rai, B. Imidazole derivatives as corrosion inhibitors for copper: A DFT and reactive force field study. Corros. Sci. 2020, 171, 108724.
[26] Lebrini, M., et al. Electrochemical and quantum chemical studies of some indole derivatives as corrosion inhibitors for C38 steel in molar hydrochloric acid. Corros. Sci. 2010, 52(10), 3367–3376.
[27] Arrousse, N., et al. Thiophene derivatives as corrosion inhibitors for 2024-T3 aluminum alloy in hydrochloric acid medium. RSC Adv. 2022, 12(17), 10321–10335.
[28] Li, X.; Deng, S.; Fu, H. Three pyrazine derivatives as corrosion inhibitors for steel in 1.0 M H2SO4 solution. Corros. Sci. 2011, 53(10), 3241–3247.
[29] Fouda, A., et al. Benzothiazole derivatives as corrosion inhibitors for carbon steel in 1 M phosphoric acid (H3PO4) solution. Afr. J. Pure Appl. Chem. 2013, 7(2), 67–78.
[30] Al-Amiery, A.A., et al. Experimental and theoretical study on the corrosion inhibition of mild steel by nonanedioic acid derivative in hydrochloric acid solution. Sci. Rep. 2022, 12(1), 1–21.
[31] Palaniappan, N., et al. Experimental and DFT studies of carbon nanotubes covalently functionalized with an imidazole derivative for electrochemical stability and green corrosion inhibition as a barrier layer on the nickel alloy surface in a sulphuric acidic medium. RSC Adv. 2019, 9(66), 38677–38686.
[32] Abrishami, S.; Naderi, R.; Ramezanzadeh, B. Fabrication and characterization of zinc acetylacetonate/Urtica Dioica leaves extract complex as an effective organic/inorganic hybrid corrosion inhibitive pigment for mild steel protection in chloride solution. Appl. Surf. Sci. 2018, 457, 487–496.
[33] Qiang, Y., et al. Experimental and theoretical studies on the corrosion inhibition of copper by two indazole derivatives in 3.0% NaCl solution. J. Colloid Interface Sci. 2016, 472, 52–59.
[34] Verma, C., et al. An overview on plant extracts as environmental sustainable and green corrosion inhibitors for metals and alloys in aggressive corrosive media. J. Mol. Liq. 2018, 266, 577–590.

[35] Zucchi, F.; Omar, I.H. Plant extracts as corrosion inhibitors of mild steel in HCl solutions. Surf. Technol. 1985, 24(4), 391–399.
[36] Abiola, O., et al. Eco-friendly corrosion inhibitors: The inhibitive action of Delonix Regia extract for the corrosion of aluminium in acidic media. Anti-Corros. Methods Mater. 2007.
[37] Kliškić, M., et al. Aqueous extract of Rosmarinus officinalis L. as inhibitor of Al–Mg alloy corrosion in chloride solution. J. Appl. Electrochem. 2000, 30(7), 823–830.
[38] El-Etre, A.; Abdallah, M. Natural honey as corrosion inhibitor for metals and alloys II. C-steel in high saline water. Corros. Sci. 2000, 42(4), 731–738.
[39] El-Etre, A. Inhibition of aluminum corrosion using Opuntia extract. Corros. Sci. 2003, 45(11), 2485–2495.
[40] Annaamalai, M., et al. Investigation of corrosion inhibition of welan gum and Neem gum on reinforcing steel embedded in concrete. Int. J. Electrochem. Sci. 2018, 13, 9981–9998.
[41] Lai, X., et al. Chitosan derivative corrosion inhibitor for aluminum alloy in sodium chloride solution: A green organic/inorganic hybrid. Carbohydr. Polym. 2021, 265, 118074.
[42] Mofidabadi, A.H.J.; Dehghani, A.; Ramezanzadeh, B. Investigating the effectiveness of Watermelon extract-zinc ions for steel alloy corrosion mitigation in sodium chloride solution. J. Mol. Liq. 2022, 346, 117086.
[43] Prasai, D., et al. Graphene: Corrosion-inhibiting coating. ACS Nano 2012, 6(2), 1102–1108.
[44] Zhang, W., et al. Use of graphene as protection film in biological environments. Sci. Rep. 2014, 4(1), 1–8.
[45] Necolau, M.-I.; Pandele, A.-M. Recent advances in graphene oxide-based anticorrosive coatings: An overview. Coatings 2020, 10(12), 1149.
[46] Calovi, M., et al. Effect of functionalized graphene oxide concentration on the corrosion resistance properties provided by cataphoretic acrylic coatings. Mater. Chem. Phys. 2020, 239, 121984.
[47] Nayak, S.R.; Mohana, K.N.; Hegde, M.B. Anticorrosion performance of 4-fluoro phenol functionalized graphene oxide nanocomposite coating on mild steel. J. Fluor. Chem. 2019, 228, 109392.
[48] Zhang, F., et al. The effect of functional graphene oxide nanoparticles on corrosion resistance of waterborne polyurethane. Colloids Surf. A Physicochem. Eng. Asp. 2020, 591, 124565.
[49] Zhao, Z., et al. Polydopamine functionalized graphene oxide nanocomposites reinforced the corrosion protection and adhesion properties of waterborne polyurethane coatings. Eur. Polym. J. 2019, 120, 109249.
[50] Zhu, Q., et al. Epoxy coating with in-situ synthesis of polypyrrole functionalized graphene oxide for enhanced anticorrosive performance. Prog. Organ. Coat. 2020, 140, 105488.
[51] Saraswat, V.; Yadav, M. Carbon dots as green corrosion inhibitor for mild steel in HCl solution. ChemistrySelect 2020, 5(25), 7347–7357.
[52] Cui, M., et al. Microwave synthesis of eco-friendly nitrogen doped carbon dots for the corrosion inhibition of Q235 carbon steel in 0.1 M HCl. Int. J. Electrochem. Sci. 2021, 16, 151019.
[53] Cen, H., et al. Carbon dots as effective corrosion inhibitor for 5052 aluminium alloy in 0.1 M HCl solution. Corros. Sci. 2019, 161, 108197.
[54] Cui, M.; Li, X. Nitrogen and sulfur Co-doped carbon dots as ecofriendly and effective corrosion inhibitors for Q235 carbon steel in 1 M HCl solution. RSC Adv. 2021, 11(35), 21607–21621.
[55] Ye, Y.; Yang, D.; Chen, H. A green and effective corrosion inhibitor of functionalized carbon dots. J. Mater. Sci. Technol. 2019, 35(10), 2243–2253.
[56] Peng, Y.G., et al. Preparation of poly (m-phenylenediamine)/ZnO composites and their photocatalytic activities for degradation of CI acid red 249 under UV and visible light irradiations. Environ. Prog. Sustain. Energy 2014, 33(1), 123–130.

[57] Olad, A.; Rashidzadeh, A.; Amini, M. Preparation of polypyrrole nanocomposites with organophilic and hydrophilic montmorillonite and investigation of their corrosion protection on iron. Adv. Polym. Technol. 2013, 32(2).
[58] Salvetat, J.-P., et al. Mechanical properties of carbon nanotubes. Appl. Phys. A 1999, 69(3), 255–260.
[59] Lu, J.P. Elastic properties of carbon nanotubes and nanoropes. Phys. Rev. Lett. 1997, 79(7), 1297.
[60] Kumar, A.M.; Gasem, Z.M. In situ electrochemical synthesis of polyaniline/f-MWCNT nanocomposite coatings on mild steel for corrosion protection in 3.5% NaCl solution. Prog. Organ. Coat. 2015, 78, 387–394.
[61] Ioniţă, M.; Prună, A. Polypyrrole/carbon nanotube composites: Molecular modeling and experimental investigation as anti-corrosive coating. Prog. Organ. Coat. 2011, 72(4), 647–652.
[62] Ganash, A. Electrochemical synthesis and corrosion behaviour of polypyrrole and polypyrrole/carbon nanotube nanocomposite films. J. Compos. Mater. 2014, 48(18), 2215–2225.
[63] Dewangan, Y.; Dewangan, A.K.; Verma, D.K. Carbon nanotubes as corrosion inhibitors. Org. Corros. Inhib. 2021, 371–385.
[64] Dewangan, A.K., et al. Synthetic environment-friendly corrosion inhibitors. In: Environmentally sustainable corrosion inhibitors, Elsevier, 2022, 71–95.
[65] Dewangan, A.; Dewangan, Y.; Verma, D. Pyrazine derivatives as green corrosion inhibitors. Theory Appl. Green Corros. Inhib. 2021, 86, 161–182.
[66] Dewangan, Y., et al. Ionic liquids as green corrosion inhibitors. In: Environmentally sustainable corrosion inhibitors, Elsevier, 2022, 219–244.
[67] Aslam, R., et al. Corrosion inhibition of steel using different families of organic compounds: Past and present progress. J. Mol. Liq. 2021, 118373.

Omar Dagdag*, Rajesh Haldhar, Seong-Cheol Kim,
Elyor Berdimurodov*, Chandrabhan Verma, Ekemini D. Akpan,
Eno E. Ebenso*

Chapter 6
Graphene and graphene oxide as nanostructured corrosion inhibitors

Abstract: The purpose of this chapter is to remind the reader of the bibliographic information required to define the context of our chapter. We begin by discussing the phenomenon of corrosion and its social and economic implications. Corrosion losses have significant economic and environmental impact on the entire global infrastructure, accounting for 3–4% of the GDP of industrialized countries. The use of corrosion inhibitors is probably the simplest, most cost-effective, and most practical anticorrosion strategy commonly used in the industry. Graphene and graphene oxide, having a nanostructure geometry, have a high potential for corrosion inhibition. This chapter briefly describes the principles, types, structures, and applications of graphene and graphene oxide as nanostructured corrosion inhibitors.

Keywords: corrosion, graphene, graphene oxide, nanostructured corrosion inhibitor

Author Contribution Statement: Equal contribution by all the authors.

*Corresponding authors: **Omar Dagdag, Eno E. Ebenso,** Institute of Nanotechnology and Water Sustainability, College of Science, Engineering and Technology, University of South Africa, Johannesburg 1710, South Africa, e-mails: dagdao@unisa.ac.za, ebensee@unisa.ac.za;
Elyor Berdimurodov, Faculty of Chemistry, National University of Uzbekistan, Tashkent, 100034, Uzbekistan, e-mail: elyor170690@gmail.com
Rajesh Haldhar, Seong-Cheol Kim, School of Chemical Engineering, Yeungnam University, Gyeongsan 38541, Republic of Korea
Chandrabhan Verma, Center of Research Excellence in Corrosion, Research Institute, King Fahd University of Petroleum and Minerals, Dhahran 31261, Saudi Arabia
Ekemini D. Akpan, Institute of Nanotechnology and Water Sustainability, College of Science, Engineering and Technology, University of South Africa, Johannesburg 1710, South Africa

https://doi.org/10.1515/9783110782820-006

6.1 Introduction

6.1.1 Corrosion and corrosion inhibitors

For a long time, steel is the widely used construction material in several industries, including food, petroleum, power production, etc. [1–3]. Its excellent mechanical property and low cost makes it viable to be used in different sectors [4]. Corrosion is one of the main problems associated with steel, as it readily dissolves in both acidic and basic mediums [5]. Corrosion proceeds both by oxidation and reduction processes, and metal corrosion is the result of the oxidation process. The aggressive acidic solutions (used in industries involving acid pickling, acid cleaning, acid descaling, and oil-well acidizing) and basic solutions (marine field) easily corrode the constructed materials [6]. Therefore, it is essential to prevent metal/iron dissolution by using corrosion inhibitors [7]. The organic compounds containing nitrogen, sulfur, and oxygen atoms act as corrosion inhibitors [8, 9]. Generally, these compounds interact with the metal surface through adsorption and prevent/inhibit the dissolution of the metal [10]. When the metal is coated with a thin layer of organic material, the coating acts as a physical layer and prevents the metal from getting corroded by the surrounding atmosphere [11]. High inhibition efficiency, low price, low toxic nature, and ease of production are some of the valuable advantages of an inhibitor [12]. There have been advancements in modifying corrosion inhibitors in recent years, where nanocomposite organic coatings are used as inhibitors. The nanoparticles present in the nanocomposites occupy the gap between the large particles and prevent diffusion of the corrosive medium, thereby preventing the corrosion of the metal more effectively [13]. Over the last two decades, nanotechnology has had a good impact on the environment, as it is more efficient to prevent the metal surface from corrosion, and several modifications in this field are being targeted by researchers worldwide. The National Association of Corrosion Engineers (NACE) initiated international measures to prevent and examine the role of corrosion in industrial sectors [14]. The report says that around $2.5 trillions have been spent worldwide with respect to corrosion, which is almost equal to 3.4% of the total GDP. Hence, by implementing several control measures, one can expect to save between 15–35% of the total cost [15]. If there is a proper implementation of the corrosion management system at the industry level, more benefits can be obtained without any accidents, failures, and production loss. One effective way to implement a corrosion management system is to make use of innovative technology in the automotive industry. Even though it may not bring about tremendous improvement in a short period, continuous implementation over a long period with respect to corrosion-related design and processing will result in low manufacturing costs, less operating costs, and a longer lifetime of the automobiles.

6.1.2 Introduction to graphene

Graphene is the crystalline molecular element of carbon atoms, forming a copper hexagonal structure of the sp^2 hybridization compound with the electrical configuration $1s^2 2s^2 2p^2$. In the case of another large carbon allotropy, the lattice structure of graphene is the main building block as shown in Fig. 6.1.

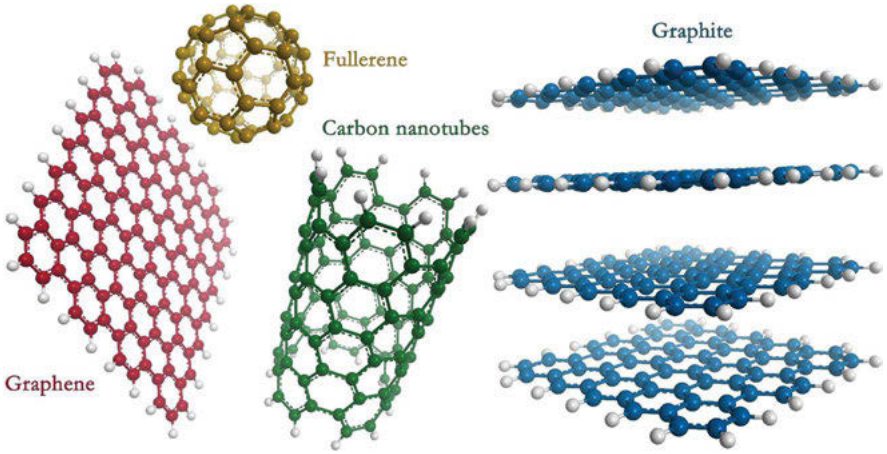

Fig. 6.1: The outlines of carbon allotropy (miniature) are graphene (two dimensions), carbon nanotubes (one dimensional), and fullerene (zero-dimensional). Reprinted with permission from [16], © 2018 Elsevier Publications.

6.2 Graphene fabrication properties, methods, and usage

Fig. 6.2 A schematic model, strategy, and implementation of a graphene production system.

6.3 Anticorrosion mechanism of graphene

As shown in Fig. 6.3, metal corrosion rate can be greatly reduced by using a graphene foil for impact resistance [18]. Even if the graphene film is severely damaged from corrosive materials, it can block corrosive particles, cracks, and defects in the graphene film, which can otherwise cause significant corrosion of the metal. Therefore, the protective properties of the graphene film are shown through cracks,

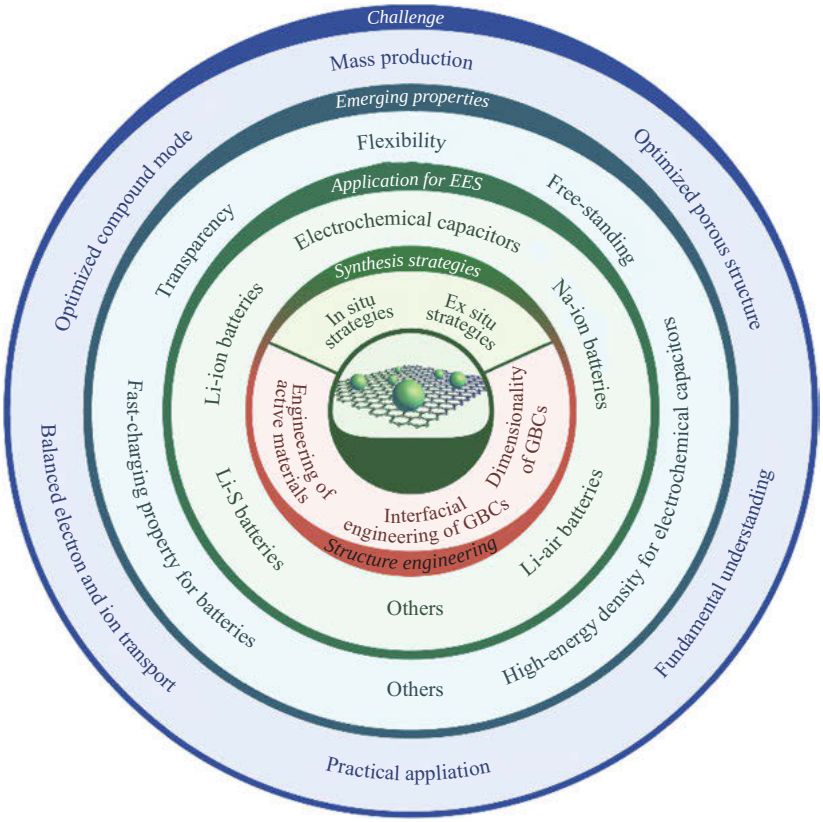

Fig. 6.2: Graphene-based alloy project with production, materials, and applications. Reprinted with permission from [17], © 2020 Elsevier Publications.

blemishes, and creases. As stated in [18], it is therefore important to correct the error by nuclear deposition technology to improve the protection of the graphene film.

6.4 Graphene oxide (GO) and graphene-based organic coatings for corrosion resistance

Graphene has many uses in corrosion protection in various metals. It is one of the most used methods. Graphene and/or its derivatives are added as a filler. The use of graphene improves corrosion resistance as shown in Fig. 6.4 [19].

Fig. 6.5 shows the difference between graphite and graphite oxide layers.

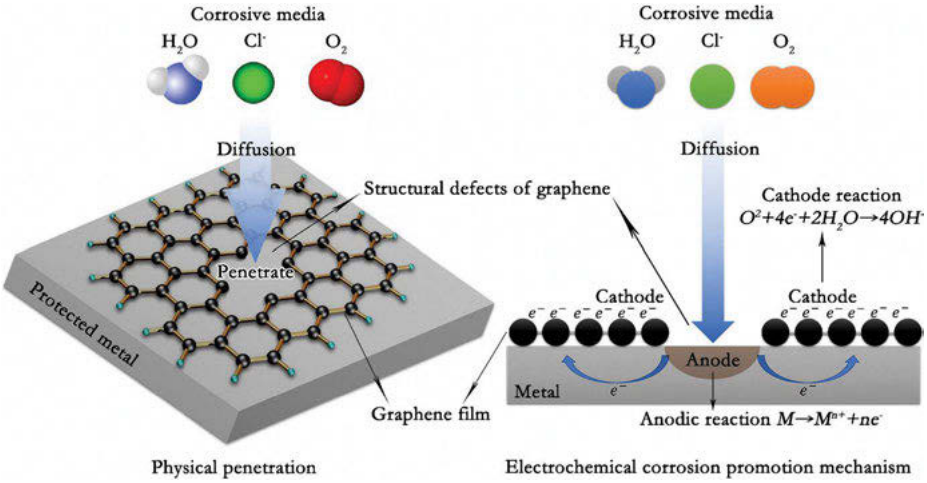

Fig. 6.3: Schematic model of graphene film barrier effect on corrosive medium. Reprinted with permission from [16], © 2018 Elsevier Publications.

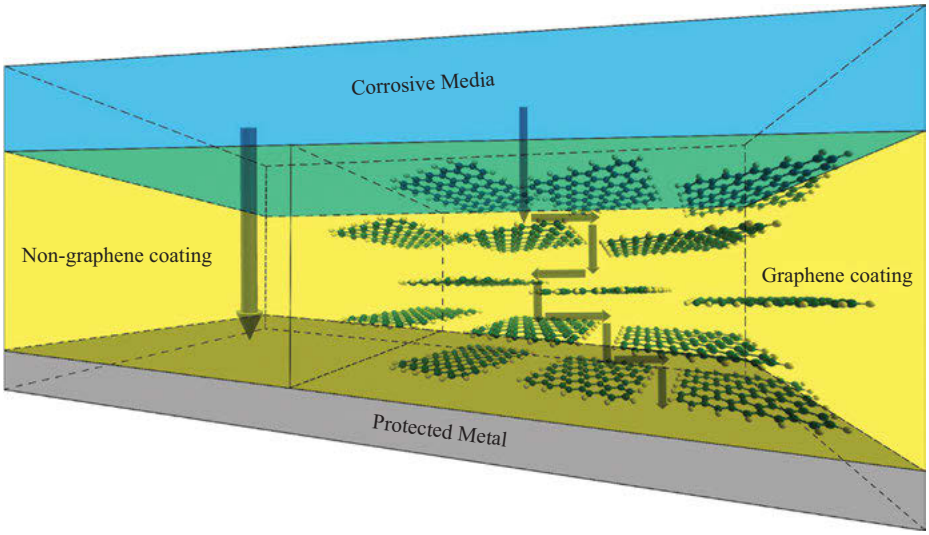

Fig. 6.4: Graphs showing the results of exposure to different aggressive process media. Reprinted with permission from [19], © 2018 Elsevier Publications.

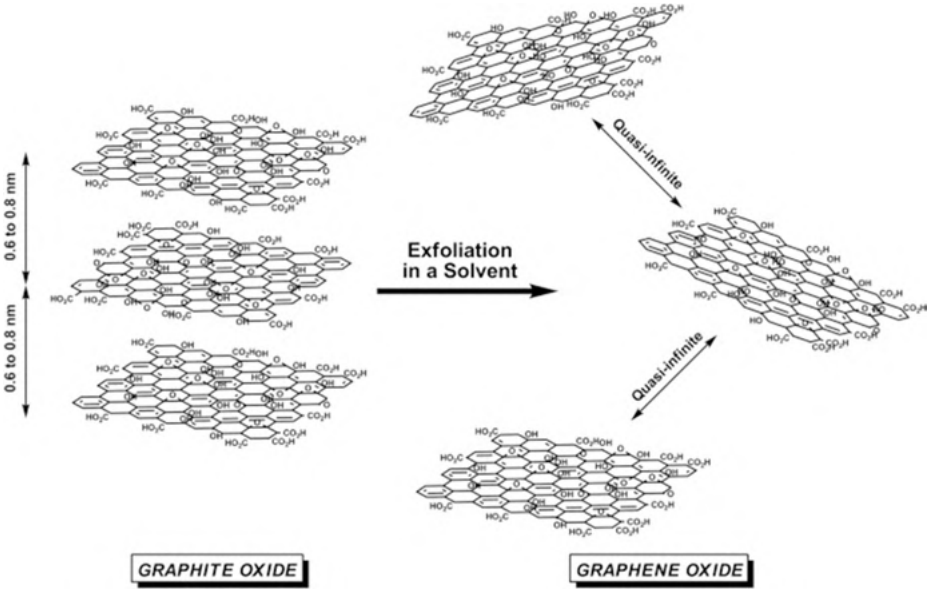

Fig. 6.5: Schematic diagram of the chemical structure of graphite oxide and the plate structure of treated and refined GO. Reprinted with permission from [20], © 2011 Elsevier Publications.

6.5 Graphene oxide/Graphene-based corrosion inhibitors for corrosion protection

6.5.1 Graphene-based corrosion inhibitors for corrosion protection applications

Haddadi et al. [21] developed a new graphene capsule using hollow carbon spheres (HCS) synthesized by the silicon template method. Inhibitor Encapsulation Assessment 2-mercaptobenzimidazole (MBI) in HCS and its inhibitory effects small metal saline solution with discharge resistance. The effect of surface changes on silicon templates of the HCS model was studied using FE-SEM, TEM, and XRD spectroscopy. In addition, TGA and UV mapping methods were used to measure MBI. The associated corrosion protection of KGS was tested by PDP and EIS methods. Results showed the harmonious structure of the amorphous carbon coating and the graphene structure due to the corrosive properties of the amorphous carbon coating. In addition, MBS released by HCS is pH-based and successfully protects small metals from corrosion.

Diagram of the preparation of hollow carbon spears (HCS) with inhibitors. 2-mercaptobenzimidazole (MBI) deposited on the HCS silica template to prevent corrosion is shown in Fig. 6.6.

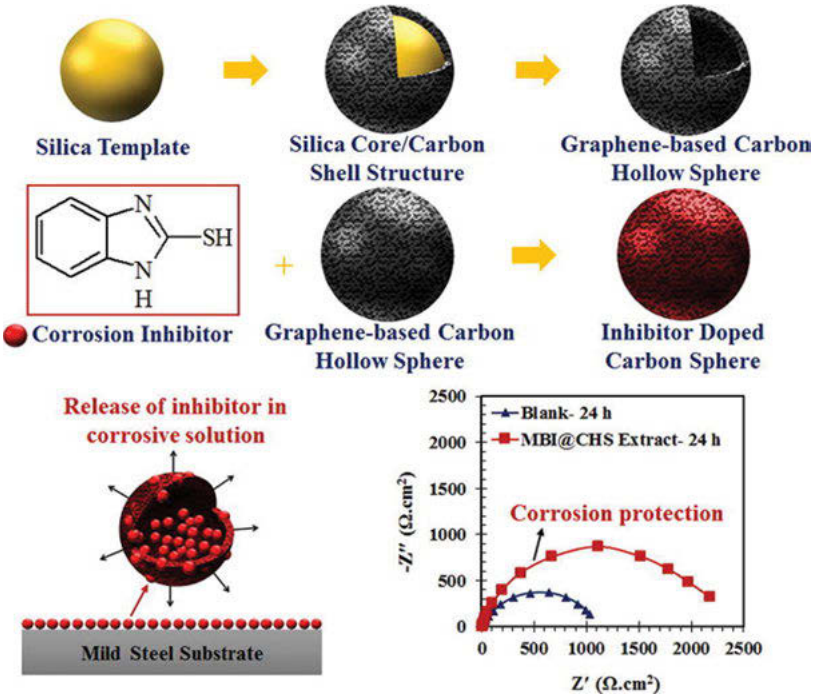

Fig. 6.6: The fabrication process and characteristics of graphene-based hollow carbon spheres for encapsulating organic corrosion inhibitors. Reprinted with permission from [21], © 2018 Elsevier Publications.

Fig. 6.7 schematically shows CGS doped with MBI and the adsorption of MBI in the form of thiolate and thione on a soft metal surface. The permeable CHC structure allows for the gradual release of MBI through the porous CHC structure, which inhibits corrosion. The inhibitor is released at different pH ranges. At local pH values, the inhibitor reacts with metal surfaces, and thereby inhibits corrosion.

6.5.2 Graphene oxide-based corrosion inhibitors for corrosion protection applications

Ansari et al. [22] demonstrated the corrosion inhibition effect of B2AA, a chemically modified GO. Inhibitory ability was assessed using EIS and PDP methods. The outcomes of the experiment were further confirmed by field analysis using FTIR and AFM. B2AA-GO outperforms other nanocomposites in oleic acid. Inhibitory activity improved with increasing B2AA-GO concentrations, to 91.1% at 50 mg/L. EIS studies have shown that the addition of B2AA-GO increases the exchange rate resistance. PDP measurements show a decrease in corrosion current, and the inhibitor is the

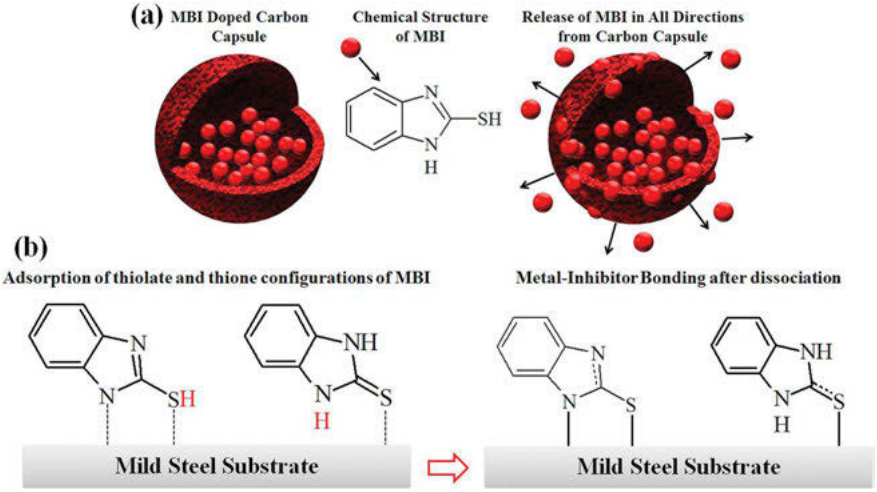

Fig. 6.7: MBI release from CHSs (a) and the subsequent adsorption of MBI thiolate and thione configurations on the MS surface (b). Reprinted with permission from [21], © 2018 Elsevier Publications.

most common cathode type. Angle measurements show an increase in the hydrophobicity of the metal surface when B2AA-GO is added to the corrosive electrolyte. The surface morphology recorded by AFM studies confirms the formation of inhibitory films on the metal surface. The results of the FTIR-ATR measurement also confirm the formation of the protective film on the metal surface.

Fig. 6.8 represents the B2AA-GO model. The structure is mostly flat, which covers the metal better. The B2AA-GO inhibitor is soluble in water.

Javidparvar et al. [23] synthesized graphene oxide using the modified hammer method and then modified it by Ce cations. GO-Ce nanocomposites were characterized and compared by analysis using ICP, HR-TEM, FT-IR, XRD, XPS, EDS, UV-wise, and Zeta potentials. The results showed phosphorus and chemisorption from the GO surface. OCP, PDP, and EIS methods, including FE-SEM and EDS, were used to measure the corrosion protection of the GO-Ce system. The results showed that the formation of a cerium oxide/hydroxide film on the cathode surface retards the absorption of small metals into the chloride. The above procedures are shown in Fig. 6.9.

The pattern of NaCl paraffin desorption and corrosion inhibition due to the release of cations in GO nanoparticles is shown in Fig. 6.10.

Kasaeian et al. [24] observed that the functionalized GO nanofilms are not covalently bound to 1 H-benzimidazole (BIM) molecules. The morphology and chemical

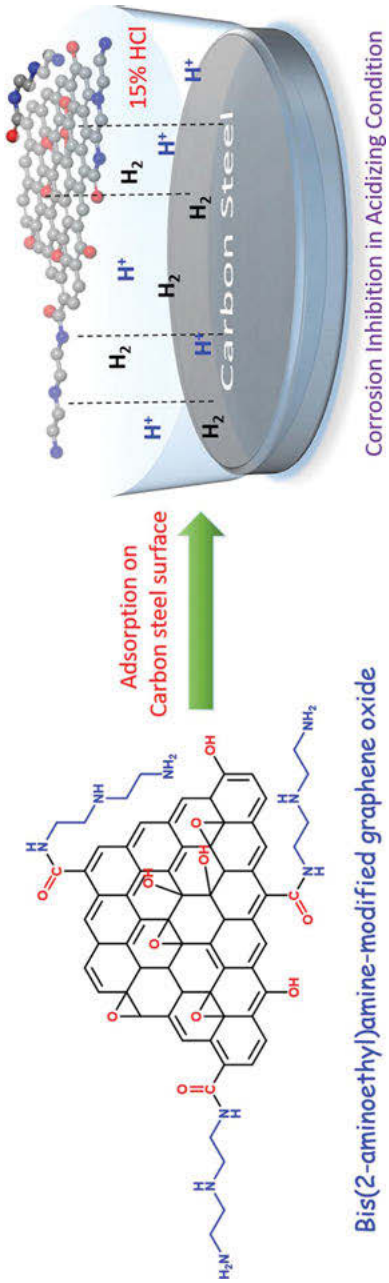

Fig. 6.8: Structure of B2AA-GO inhibitors and the adsorption of B2AA-GO in the acidified state on the CS surface. Reprinted with permission from [22], © 2020 Elsevier Publications.

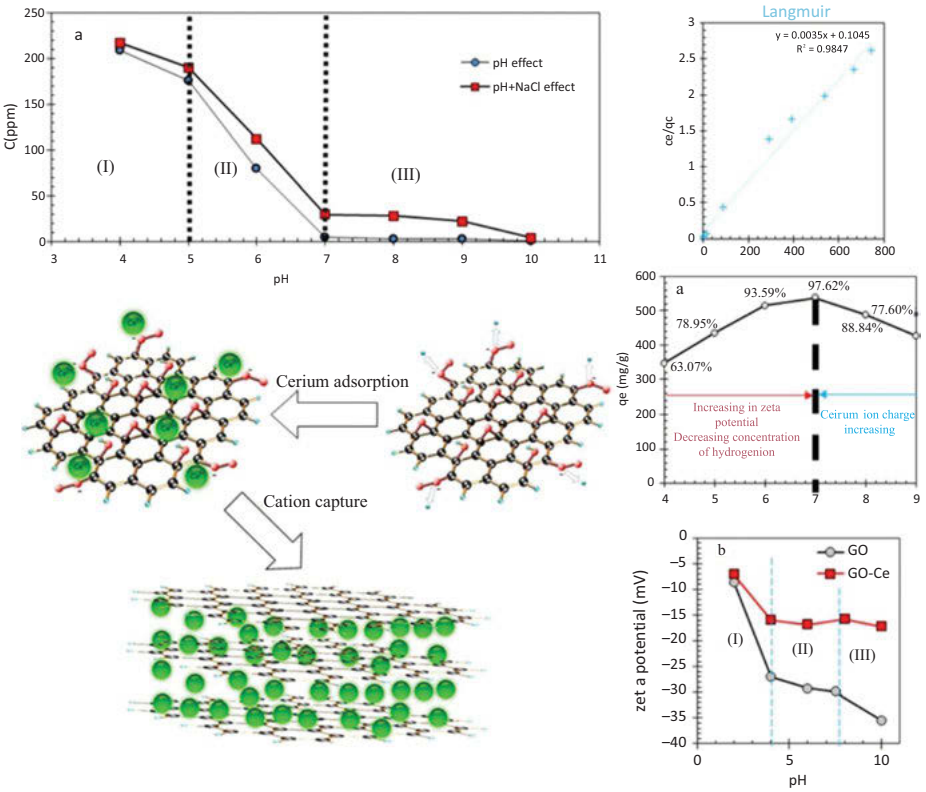

Fig. 6.9: A schematic for GO deprotonation and paraffin adsorption onto deprotonated GO nanoparticles, and the cation capture from GO flocs. Reprinted with permission from [23], © 2019 Elsevier Publications.

composition of GO-BIM compounds were examined by FE-SEM, EDS, XPS, and Raman spectroscopy. The results of the electrochemical analysis show that the integration of 0.1% GO-BIM in the epoxy coating provides a good corrosion-resistant ability with improved blocking and damping properties.

Fig. 6.11 shows the interaction process of GO-BIM at different pH values and the schematic construction of the epoxy coating with GO-BIM to provide both blocking and corrosion protection.

6.6 Future scope

Heteroatom-containing molecules are by and large viewed as successful and known inhibitors for metal corrosion in acidic media. In the oil refining industry, foundational

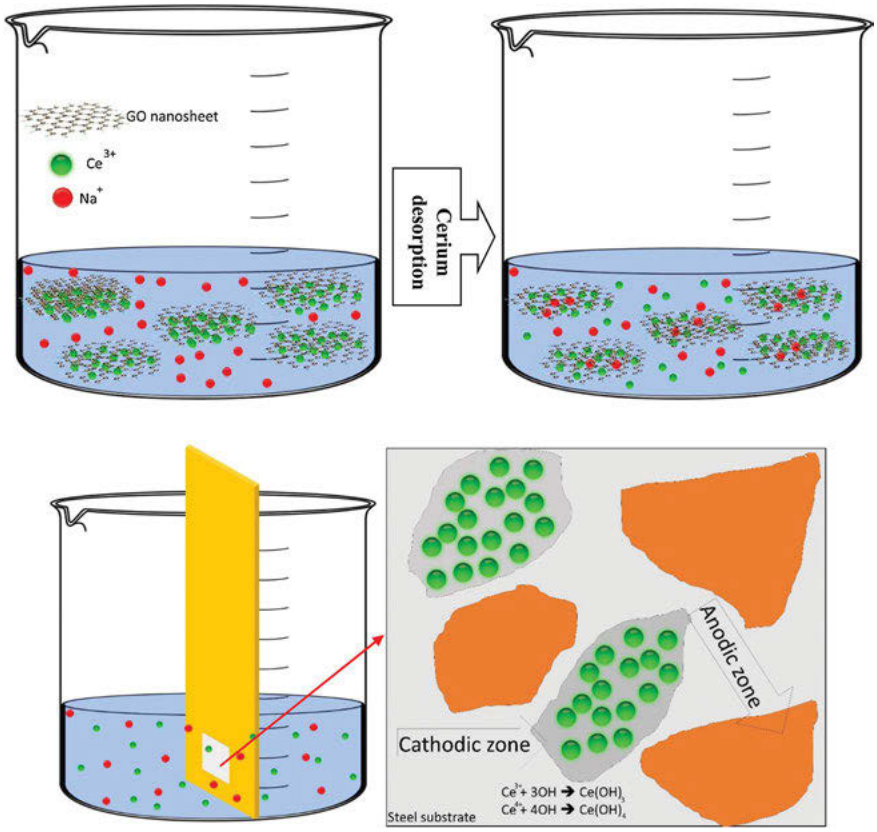

Fig. 6.10: A proposed model for corrosion inhibition of steel specimen in 3.5% NaCl solution with cerium ions released from GO nanosheets. Reprinted with permission from [23], © 2019 Elsevier Publications.

corrosion happens in a few streams, particularly at high temperatures. A few investigations have been carried out in the field of corrosion counteraction, so there is as yet a requirement for better information about inhibitors that are successful in petroleum and gas industries. The ideal choices are heterocyclic natural mixtures, compound atoms, composites, nanomaterials, and carbon-based materials. Inhibitors in this class are stable at room temperature, which is a significant necessity for a fuel refining framework.

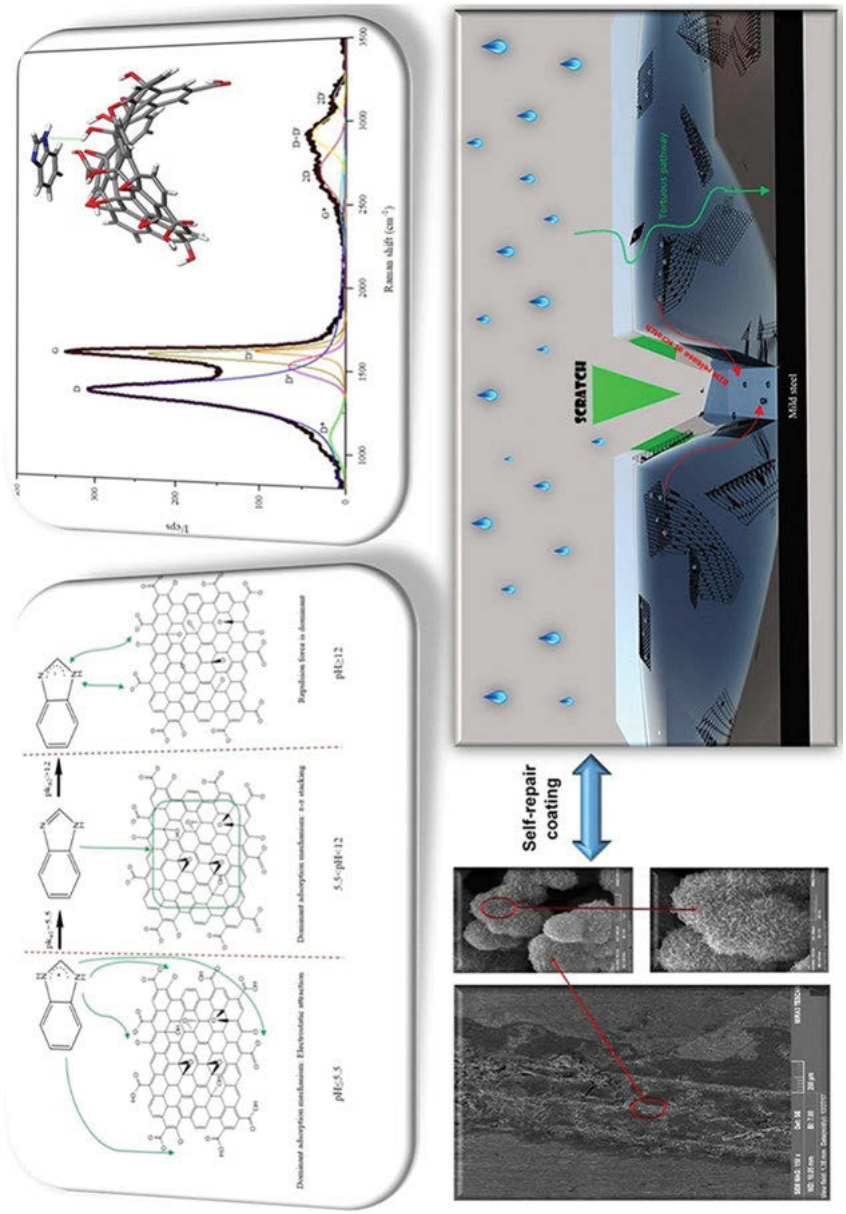

Fig. 6.11: Schematic representation of the interaction between benzimidazole nanowires and graphene oxide at different pH values and a schematic pattern of a scratched epoxy coating with GO-BIM, while providing a barrier and active corrosion protection. Reprinted with permission from [24], © 2018 Elsevier Publications.

6.7 Conclusions

This chapter includes the fundamental information related to the corrosion process, and the economic and social impact of corrosion on the modern world. Graphene and graphene oxide can be used as potential nanostructured corrosion inhibitors. The general introduction of graphene, its production, various techniques, and applications in different fields have been discussed. The chapter also includes the mechanism of corrosion protection by graphene and graphene oxide. The application of graphene and graphene oxide as organic coatings for corrosion protection has been deeply reviewed. Therefore, this chapter offers a spotlight for a better understanding of graphene and graphene oxide, and their applications in the corrosion inhibition sector.

Abbreviations

GDP	Gross domestic product
NACE	National Association of Corrosion Engineers
GO	Graphene oxide
FE-SEM	Field Emission Scanning Electron Microscopes
TEM	Transmission electron microscopy
XRD	X-ray diffraction
TGA	Thermogravimetric analysis
UV	Ultraviolet
PDP	Potentiodynamic polarization
EIS	Electrochemical impedance spectroscopy
OCP	Open circuit potential
EDS	Energy dispersive spectroscopy
XPS	X-ray photoelectron spectroscopy
B2AA-GO	Bis(2-aminoethyl)amine-modified graphene oxide

References

[1] Berdimurodov, E.; Kholikov, A.; Akbarov, K.; Guo, L.; Kaya, S.; Verma, D.K.; Rbaa, M.; Dagdag, O. Novel glycoluril pharmaceutically active compound as a green corrosion inhibitor for the oil and gas industry. J. Electroanal. Chem. 2022, 116055.

[2] Berdimurodov, E.; Kholikov, A.; Akbarov, K.; Guo, L.; Kaya, S.; Katin, K.P.; Verma, D.K.; Rbaa, M.; Dagdag, O.; Haldhar, R. Novel gossypol–indole modification as a green corrosion inhibitor for low–carbon steel in aggressive alkaline–saline solution. Colloids Surf. A Physicochem. Eng. Asp. 2022, 128207.

[3] Prasad, D.; Dagdag, O.; Safi, Z.; Wazzan, N.; Guo, L. Cinnamoum tamala leaves extract highly efficient corrosion bio-inhibitor for low carbon steel: Applying computational and experimental studies. J. Mol. Liq. 2022, 347, 118218.

[4] Berdimurodov, E.; Kholikov, A.; Akbarov, K.; Guo, L.; Kaya, S.; Katin, K.P.; Verma, D.K.; Rbaa, M.; Dagdag, O.; Haldhar, R. Novel bromide–cucurbit [7] uril supramolecular ionic liquid as a green corrosion inhibitor for the oil and gas industry. J. Electroanal. Chem. 2021, 901, 115794.
[5] Berdimurodov, E.; Kholikov, A.; Akbarov, K.; Guo, L.; Kaya, S.; Verma, D.K.; Rbaa, M.; Dagdag, O. New and green corrosion inhibitor based on new imidazole derivate for carbon steel in 1 M Hcl Medium: Experimental and theoretical analyses. 11–44.
[6] Abdellattif, M.H.; Alrefaee, S.H.; Dagdag, O.; Verma, C.; Quraishi, M. Calotropis procera extract as an environmental friendly corrosion Inhibitor: Computational demonstrations. J. Mol. Liq. 2021, 337, 116954.
[7] Haldhar, R.; Kim, S.-C.; Prasad, D.; Bedair, M.; Bahadur, I.; Kaya, S.; Dagdag, O.; Guo, L. Papaver somniferum as an efficient corrosion inhibitor for iron alloy in acidic condition: DFT, MC simulation, LCMS and electrochemical studies. J. Mol. Struct. 2021, 1242, 130822.
[8] Hsissou, R.; Dagdag, O.; Abbout, S.; Benhiba, F.; Berradi, M.; El Bouchti, M.; Berisha, A.; Hajjaji, N.; Elharfi, A. Novel derivative epoxy resin TGETET as a corrosion inhibition of E24 carbon steel in 1.0 M HCl solution. Experimental and computational (DFT and MD simulations) methods. J. Mol. Liq. 2019, 284, 182–192.
[9] Dagdag, O.; Safi, Z.; Erramli, H.; Wazzan, N.; Guo, L.; Verma, C.; Ebenso, E.; Kaya, S.; El Harfi, A. Epoxy prepolymer as a novel anti-corrosive material for carbon steel in acidic solution: Electrochemical, surface and computational studies. Mater. Today Commun. 2020, 22, 100800.
[10] Haldhar, R.; Prasad, D.; Nguyen, L.T.; Kaya, S.; Bahadur, I.; Dagdag, O.; Kim, S.-C. Corrosion inhibition, surface adsorption and computational studies of Swertia chirata extract: A sustainable and green approach. Mater. Chem. Phys. 2021, 267, 124613.
[11] Haldhar, R.; Prasad, D.; Mandal, N.; Benhiba, F.; Bahadur, I.; Dagdag, O. Anticorrosive properties of a green and sustainable inhibitor from leaves extract of Cannabis sativa plant: Experimental and theoretical approach. Colloids Surf. A Physicochem. Eng. Asp. 2021, 614, 126211.
[12] Haldhar, R.; Prasad, D.; Bahadur, I.; Dagdag, O.; Kaya, S.; Verma, D.K.; Kim, S.-C. Investigation of plant waste as a renewable biomass source to develop efficient, economical and eco-friendly corrosion inhibitor. J. Mol. Liq. 2021, 335, 116184.
[13] Haldhar, R.; Prasad, D.; Kamboj, D.; Kaya, S.; Dagdag, O.; Guo, L. Corrosion inhibition, surface adsorption and computational studies of Momordica charantia extract: A sustainable and green approach. SN Appl. Sci. 2021, 3(1), 1–13.
[14] Bhardwaj, N.; Sharma, P.; Guo, L.; Dagdag, O.; Kumar, V. Molecular dynamic simulation and Quantum chemical calculation of phytochemicals present in Beta vulgaris and electrochemical behaviour of Beta vulgaris peel extract as green corrosion inhibitor for stainless steel (SS-410) in acidic medium. Colloids Surf. A Physicochem. Eng. Asp. 2022, 632, 127707.
[15] Bhardwaj, N.; Sharma, P.; Guo, L.; Dagdag, O.; Kumar, V. Molecular dynamic simulation, quantum chemical calculation and electrochemical behaviour of Punica granatum peel extract as eco-friendly corrosion inhibitor for stainless steel (SS-410) in acidic medium. J. Mol. Liq. 2022, 346, 118237.
[16] Ding, R.; Li, W.; Wang, X.; Gui, T.; Li, B.; Han, P.; Tian, H.; Liu, A.; Wang, X.; Liu, X. A brief review of corrosion protective films and coatings based on graphene and graphene oxide. J. Alloys Compd. 2018, 764, 1039–1055.
[17] Wang, B.; Ruan, T.; Chen, Y.; Jin, F.; Peng, L.; Zhou, Y.; Wang, D.; Dou, S. Graphene-based composites for electrochemical energy storage. Energy Storage Mater. 2020, 24, 22–51.
[18] Kumar, S.S.A.; Bashir, S.; Ramesh, K.; Ramesh, S. New perspectives on Graphene/Graphene oxide based polymer nanocomposites for corrosion applications: The relevance of the Graphene/Polymer barrier coatings. Progr. Org. Coat. 2021, 154, 106215.

[19] Ding, R.; Zheng, Y.; Yu, H.; Li, W.; Wang, X.; Gui, T. Study of water permeation dynamics and anti-corrosion mechanism of graphene/zinc coatings. J. Alloys Compd. 2018, 748, 481–495.
[20] Potts, J.R.; Dreyer, D.R.; Bielawski, C.W.; Ruoff, R.S. Graphene-based polymer nanocomposites. Polymer. 2011, 52(1), 5–25.
[21] Haddadi, S.; Ramazani, S.; Mahdavian, M.; Taheri, P.; Mol, J. Fabrication and characterization of graphene-based carbon hollow spheres for encapsulation of organic corrosion inhibitors. Chem. Eng. J. 2018, 352, 909–922.
[22] Ansari, K.; Chauhan, D.S.; Quraishi, M.; Saleh, T.A. Bis (2-aminoethyl) amine-modified graphene oxide nanoemulsion for carbon steel protection in 15% HCl: Effect of temperature and synergism with iodide ions. J. Colloid Interface Sci. 2020, 564, 124–133.
[23] Javidparvar, A.A.; Naderi, R.; Ramezanzadeh, B.; Bahlakeh, G. Graphene oxide as a pH-sensitive carrier for targeted delivery of eco-friendly corrosion inhibitors in chloride solution: Experimental and theoretical investigations. J. Ind. Eng. Chem. 2019, 72, 196–213.
[24] Kasaeian, M.; Ghasemi, E.; Ramezanzadeh, B.; Mahdavian, M.; Bahlakeh, G. Construction of a highly effective self-repair corrosion-resistant epoxy composite through impregnation of 1H-Benzimidazole corrosion inhibitor modified graphene oxide nanosheets (GO-BIM). Corros. Sci. 2018, 145, 119–134.

Sanjukta Zamindar, Manilal Murmu, Naresh Chandra Murmu, Priyabrata Banerjee*

Chapter 7
Chemically modified graphene and graphene oxides as corrosion inhibitors

Abstract: Graphene and graphene oxide (GO) have grabbed special attention in the domain of corrosion mitigation due to their superior characteristics such as large surface coverage, chemical, as well as mechanical stability and chemical resistivity. GO exhibits high water dispersibility due to presence of oxygen functional groups within its scaffold, which makes it hydrophilic, to some extent. Further, chemical functionalization of GO increases its water dispersibility nature, the extended π-conjugation, and the presence of heteroatoms assist in good adsorption of chemically functionalized GO (fGO) on the metallic surfaces. This phenomenon facilitates the use of fGO as an efficient corrosion inhibitor in solution phase, where fGO forms a protective layer on the metallic substrates and acts as a barrier, inhibiting the diffusion of corrosive species like water, oxygen, chloride ions, etc. This chapter features the major works regarding chemical functionalization of GO as a new class of highly efficient corrosion inhibitors used in aqueous solutions. Additionally, the key objective of this chapter is to explore various adsorption and associated corro-

Acknowledgement: PB is very thankful to Department of Higher Education, Science & Technology and Biotechnology, Govt. of West Bengal, India for providing financial assistance vide sanction order no. 78(Sanc.)/ST/P/S&T/6G-1/2018 dated 31.01.2019 and project no. GAP-225612. MM acknowledges Ministry of Tribal Affairs, Govt. of India, New Delhi, India for National Fellowship for Higher Education of Schedule Tribes Students [Erstwhile known as Rajiv Gandhi National Fellowship of Schedule Tribes Students (RGNFST) from University Grants Commission, Govt. of India, New Delhi, India] vide reference no. F1-17.1/2014-15/RGNF-2014-15-ST-JHA-71559/(SA-III/Website) dated: February 2015.

*Corresponding author: **Priyabrata Banerjee**, Surface Engineering & Tribology Group, CSIR-Central Mechanical Engineering Research Institute, Mahatma Gandhi Avenue, Durgapur, 713209, West Bengal, India; Academy of Scientific and Innovative Research (AcSIR), CSIR-HRDC Campus, Sector-19, Kamla Nehru Nagar, Ghaziabad, 201002, India,
Web: www.priyabratabanerjee.in and www.cmeri.res.in, e-mail: pr_banerjee@cmeri.res.in
Sanjukta Zamindar, Manilal Murmu, Naresh Chandra Murmu, Surface Engineering & Tribology Group, CSIR-Central Mechanical Engineering Research Institute, Mahatma Gandhi Avenue, Durgapur, 713209, West Bengal, India; Academy of Scientific and Innovative Research (AcSIR), CSIR-HRDC Campus, Sector-19, Kamla Nehru Nagar, Ghaziabad, 201002, India

https://doi.org/10.1515/9783110782820-007

sion inhibition mechanisms of fGO on metallic surface, in an exquisite way. Furthermore, the futuristic aspects of multiple functionalization of graphene and GO for their efficient application as corrosion inhibitors in adverse and extreme environmental conditions have been outlined.

Keywords: graphene and graphene oxide, chemical functionalization, corrosion, corrosion inhibitor, adsorption, barrier properties

7.1 Introduction

In the present scenario, metallic materials have an enormous application in several industries such as oil and gas industries, marine industries, petroleum production industries, chemical industries, etc., as well as in domestic purposes [1, 2]. Several harsh acidic solutions like HCl, H_2SO_4, etc. are used for the cleaning purposes such as oil well acidizing, acid pickling, acid cleansing, acid descaling, etc., which leads to deterioration of the metallic surfaces due to further corrosive attack of the acids, after completion of its cleansing purposes [3, 4]. Corrosion, a natural process by which the metal wants to convert to its more stable oxide, hydroxide, and sulfide forms by chemical or electrochemical reactions through the gradual destruction of the metal, has become a global issue, due to its massive destructive consequences [5, 6]. There are several types of corrosion, viz., uniform corrosion, galvanic corrosion, pitting and crevice formation, intergranular corrosion, erosion corrosion, selective leaching, etc. [7]. Recently, it has been reported that the global loss due to corrosion is ~ 3.4% of the world's GDP (approx. $2.5 trillion). The amount of economic loss due to the natural catastrophe, corrosion, is ~$360 billion per year, whereas in India, the amount is ~$100 billion per year, which is a true concern to Indian economy [8, 9]. Here lies the need for corrosion inhibitors to mitigate the solution state corrosion of metallic bodies. Of the several corrosion inhibition processes, application of inhibitors and anticorrosive coating are most approved. Corrosion scientists and researchers have figured out solution-state corrosion inhibitors. It has been reported that the organic compounds containing polar functional groups such as carboxyl, carbonyl, amide, nitrile, imine, hydroxyl, methoxy, amino, nitro, ester, acid chloride, diazo, aromatic ring, multiple bonds, etc. are chosen as preferred corrosion inhibitors due to their excellent surface protection ability via physisorption or chemisorption or back-donation [10]. But one of the biggest lacunas of using organic heterocyclic molecules is low protection capability, due to their high molecular surface. Accordingly, researchers have driven the research field to find alternatives for organic heterocycles. Recently, focus has been shifted to graphene and GO-based corrosion inhibitors. Graphene and GOs have grabbed special attention as coating materials, due to their fascinating characteristics, such as large surface coverage, high chemical and thermal stability, high water dispersibility, etc. [11]. Additionally, graphene and GO have been

used in several coating materials due to their unique features [12–14]. But, the presence of hydrophobicity made graphene and GO vulnerable to be used as solution phase corrosion inhibitors. Further modification of graphene and GO made them hydrophilic to some extent, making them dispersible in aqueous solutions and susceptible to adsorption on metal surface, in order to provide protection from the aqueous phase corrosion. Apart from these, use of graphene is gathering interest owing to its cost-effectiveness and environment-friendly nature [15]. From literature survey, it has been observed that there are few numbers of modified GO that have been reported as anticorrosive additives in solution phases. In this chapter, emphasis has been made on the chemically modified or functionalized GO-based corrosion inhibitors, which could provide superior corrosion effectiveness in solution phase.

7.2 Graphene and graphene oxide

A new field in science has been unveiled by the discovery of graphene by Geim and Novoselov, in the year of 2004. Graphene is a two-dimensional sheet within which sp^2-hybridized carbon atoms are arranged in a hexagonal array [16–18]. Graphene and its derivatives, such as GO and reduced GO have versatile applications in several fields. Graphene and GO possess fascinating characteristics such as chemical and thermal stability, large surface coverage, etc., which have made them find use as efficient corrosion inhibitors in solid phase [19–21]. Because of the hydrophobic nature and limited solubility of graphene and GO, the use of graphene and GO as solution-phase corrosion inhibitors was limited [22]. But it has been found that after functionalization of GO, water dispersibility increases along with increasing hydrophilic nature of GO, to some extent. After modification of GO, incorporation of several groups, chemically functionalized GO (fGO) can interact with the metallic surface more efficiently than previously unmodified GO via physisorption, chemisorption, and retro-donation. There are several approaches for synthesizing GO, using green precursors [23]. Till date, to the best of our knowledge, no solution-phase corrosion inhibitor based on modified graphene has been obtained from literature survey. In the present scenario, focus has been shifted to functionalization of GO and its application as anticorrosive materials.

7.3 Chemical modification of graphene and graphene oxide

Graphene contains sp^2-hybridized carbon atoms in its skeleton with perfect planarity; hence graphene prefers to interact with small aromatic molecules, which obviously

shows hydrophobic interaction. On the other hand, GO possesses nonaromatic structure with sp^3-hybridized carbon atoms in addition to the sp^2-hybridized carbon atoms in its molecular structure, and non-planarity within its structures, which facilitates its hydrophilic character. GO contains hydroxyl (-OH) and carboxylic (-COOH) groups, which are likely to be functionalized more easily than graphene. Consequently, GO intends to undergo hydrogen bonding or ionic interaction with incoming modifier [24, 25].The best change in the characteristics of graphene and GO after modification, that is, functionalization, is the change in their solubility in different solvents [26]. Chemically modified GO are obtained via covalent functionalization and non-covalent functionalization. Covalent functionalization involves covalent attachment, whereas non-covalent functionalization involves weak non-covalent interactions like van der Waals interaction [27, 28].

7.3.1 Covalent functionalization of GO

Covalent functionalization of GO involves covalent interaction. Esterification, amination, amidation, and condensation are the common reactions that can be achieved by modifying the hydroxyl, carboxylic, or epoxy functional groups present in GO [29]. For covalent functionalization of GO, several primary amines, polythiophenes, porphyrins, phthalocyanines, and several organic compounds are utilized [30]. The functionalization of GO includes acylation, esterification, nucleophilic epoxide ring opening reaction, diazotization, cycloaddition, etc. The functionalization process of GO is schematically depicted in Fig. 7.1.

In esterification process, the carbonyl chloride group reacts with carboxylic group of GO via nucleophilic attack, and then, esterified fGO is obtained after deprotonation, as shown in Fig. 7.1(a). In amidation process, the amine group of incoming molecule attacks the epoxy ring, and ring opening takes place due to this nucleophilic attack. fGO is obtained via deprotonation as shown in Fig. 7.1(b). Fig. 7.1(c) shows the functionalization via amination, which occurs in two steps. In the first step, the nucleophilic attack of carboxylic group occurs in nucleophilic sulfur center. After that, the removal of the leaving group followed by a second nucleophilic attack, the lone pair of electrons situated on amine nitrogen and release of leaving group takes place; and, finally, deprotonation leads to form fGO product [31–33].

7.3.2 Non-covalent functionalization of GO

Non-covalent functionalization of GO includes weak non-covalent interactions like van der Waals interaction, hydrogen bonding, electrostatic interaction, hydrophobic interaction, π-π interaction, etc. [34]. The non-covalent functionalization of GO

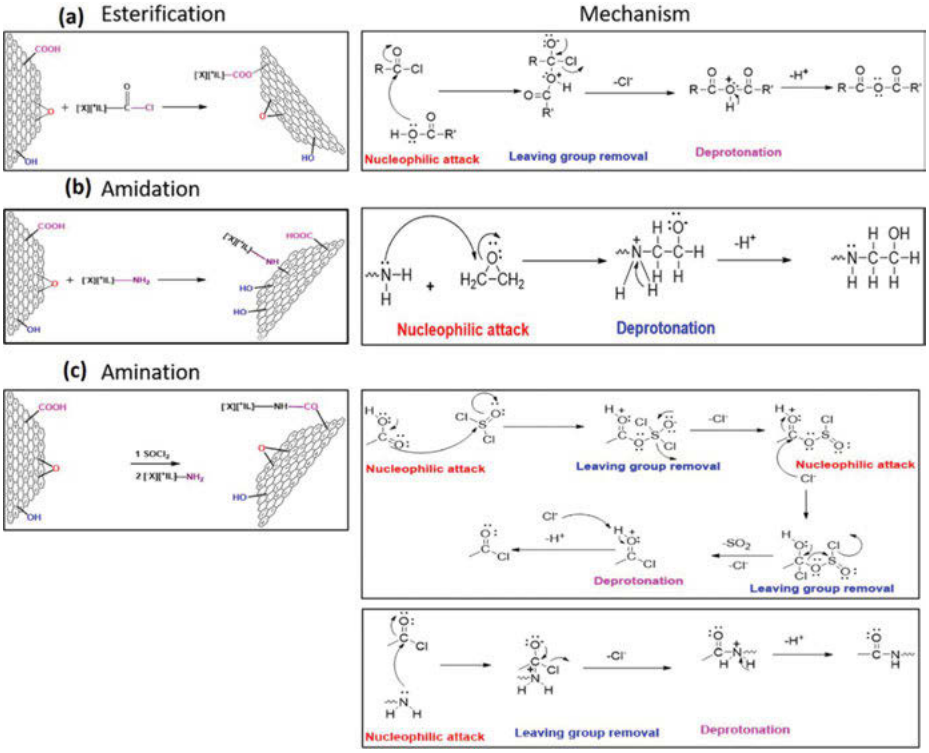

Fig. 7.1: Schematic representation of covalent modification of GO via (a) esterification, (b) amidation, and (c) amination (Reproduced with permission from ref. [11], Copyright © 2020 Elsevier B. V.).

has been schematically presented in Fig. 7.2. In π-π interaction, the π-electron cloud of organic molecules, such as perylene, interact with the π-electron cloud of GO. Thus, fGO is obtained via π-π stacking interaction [35].This mechanism is highly affected by electron acceptance and donation phenomena. In addition to this, electronegative hetero atoms, **like** oxygen and nitrogen, help in hydrogen bonding with the functional groups present within GO molecule[36].The functional groups such as carboxylic and hydroxyl groups of GO that contain negative charges interact with ionic species more strongly via electrostatic interaction[37]. On the other hand, several polymers interact hydrophobically with GO [38].

7.4 Chemically modified graphene as corrosion inhibitor

Graphene acquires a lot of excellent characteristic properties such as chemical and thermal stability, wear and tear resistivity, antioxidant property and hydrophobicity, which have made it a superior material for anticorrosive coating synthesis. Graphene provides a physical barrier toward metal surface and creates blockage against corrosive species, as shown in Fig. 7.3(a). Li et al. reported high-quality and uniform graphene films on copper foils with large surface area [39].

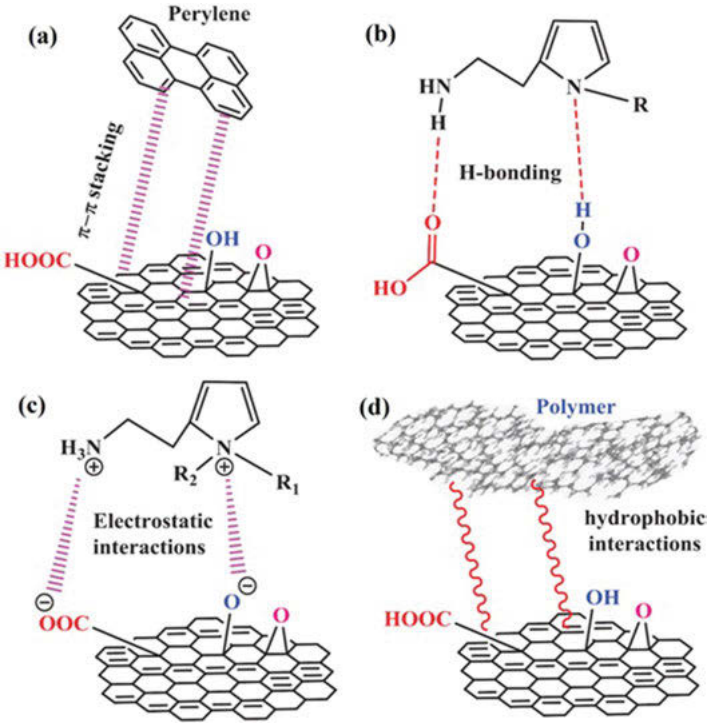

Fig. 7.2: Schematic representation of non-covalent modification of GO via (a) π-π stacking interaction, (b) hydrogen bonding interaction, (c) electrostatic interaction, and (d) hydrophobic interaction (Reproduced from ref. [34]).

Though there are a few defects in the graphene film, it provided corrosion protection. Zhang et al. reported a new two-step method of graphene growth at low temperature on electropolished copper foil. At 600°C, graphene monolayer was obtained uniformly and continuously with superior transparency against corrosion [40]. But there are several different perspectives regarding the protective nature of graphene film towards corrosion.

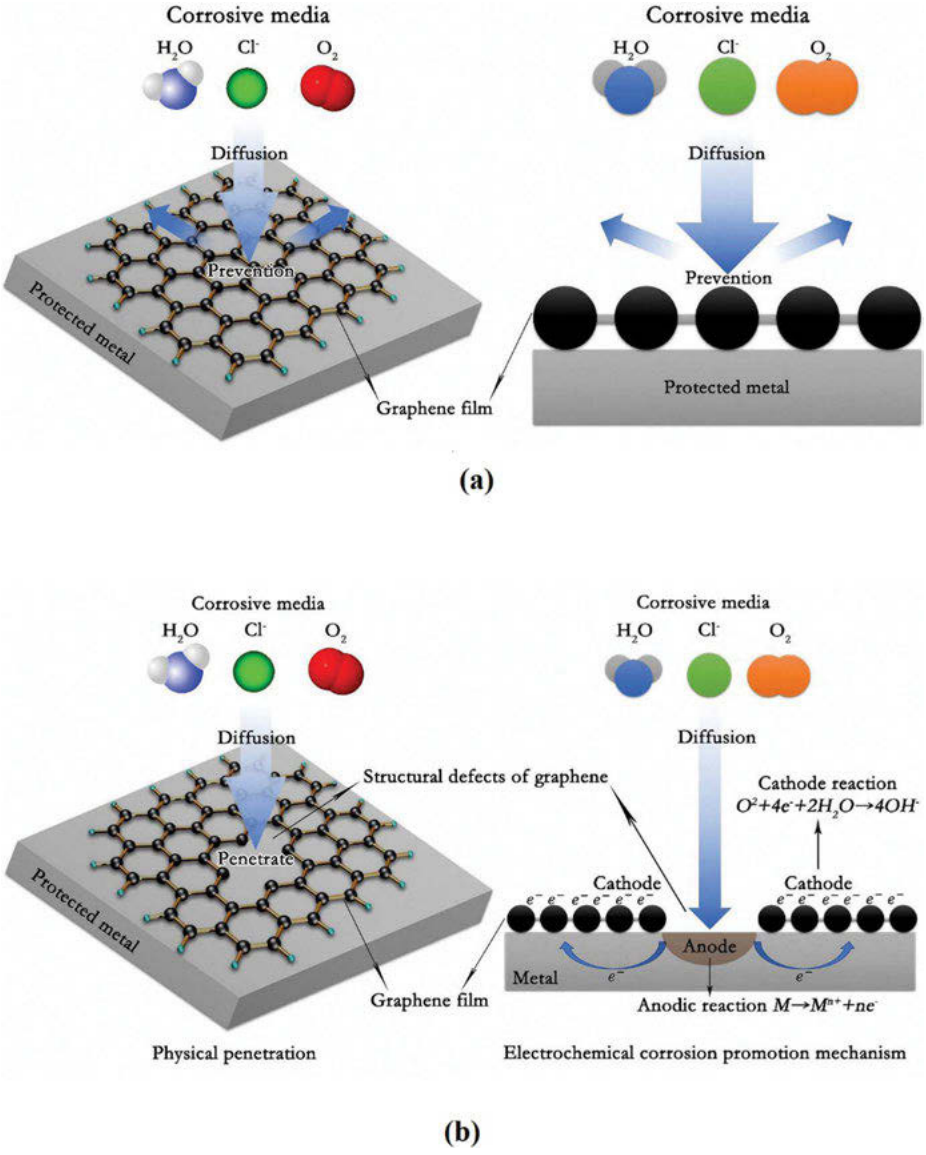

Fig. 7.3: Schematic representation of (a) protection performance of graphene and (b) corrosion occurrence due to graphene (Reproduced with permission from ref. [44], Copyright © 2018 Elsevier B. V.).

In a few researches, graphene has not been considered as an efficient corrosion protective barrier, as completely defect-free GO synthesis is almost impossible [41]. These defects, specially, due to fast cooling, lead to poor long-term barrier performance. Even, in some research, graphene has almost been denied the status of a

corrosion inhibitor, due to its excellent conductive nature that facilitates the electrochemical corrosion of metals, as shown in Fig. 7.3(b) [42]. Lee et al. evaluated the corrosion protection performance of graphene nano sheet on iron metal surface in saline medium by monitoring quartz crystal microbalance (QCM) [43]. It was observed that overall impermeability of graphene into liquids and gases facilitates the use of graphene as the thinnest anticorrosive coating; but ultimately, due to conductive nature of graphene, corrosion on iron surface is facilitated. Again, when the concentration of graphene is increased, chloride ions are trapped near the iron surface, which facilitates further corrosion. The corrosion-promoting nature of graphene was proved by two consecutive phenomena; firstly, the gain in weight due to oxidized product formation after corrosion in iron surface, and secondly, loss in weight due to the detachment of the after-corrosion oxidized product.

7.5 Chemically modified graphene oxide as corrosion inhibitor

Chemically modified graphene oxide has been introduced as a new class of solution phase corrosion inhibitor in various corrosive environments. Patel et al. reported polyurethane functionalized sulfonated graphene oxide (GO) and studied its anticorrosive effectiveness on mild steel in 0.5 M sulfuric acid medium [45]. Nano hybrids exhibited higher order self-assembly phenomena than that of pure polymer. A better surface coverage was obtained from polyurethane-functionalized sulfonated GO. Consequently, this as-synthesized functionalized GO (fGO) provided superior anticorrosive effectiveness. Later on, Gupta et al. synthesized a new aminoazobenzene (AAB) and diaminoazobenzene (DAB)-functionalized GO [46]. The synthesis procedure of AAB-GO followed a two-step path. The first step was the diazotization process, in which *o*-phenylenediamine was reacted with sodium nitrite solution in HCl medium at 0–5°C to obtain a diazotized product; and, in the second step, coupling of aminobenzene with GO occurred in presence of sodium hydroxide at 2°C via sonication. The synthesis of DAB-GO was carried out by simple stirring of *o*-phenylenediamine with GO at 80°C, in presence of methanol solvent. The synthetic routes of AAB-GO and DAB-GO have been schematically represented in Fig. 7.4. It was reported that 25 mgL^{-1} of AAB-GO in 1 M HCl medium exhibited better inhibition (94.65%) on mild steel surface than the other. And, it was reported that the barrier property of fGOs increased with increase in the concentration of fGOs. Theoretical calculations were carried out, and it admirably validated the experimental findings.

Furthermore, this group worked on finding the anticorrosive performance of diazo pyridine (DAZP) and diamino pyridine (DAMP) functionalized GO on mild steel

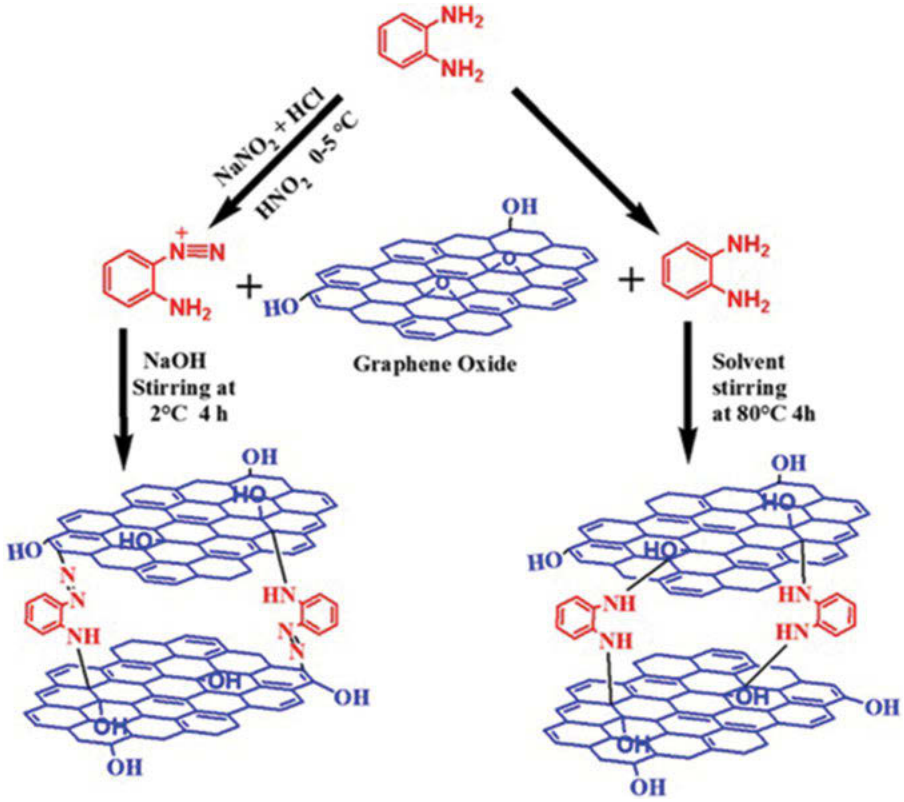

Fig. 7.4: Schematic representation of the synthetic pathway of AAB-GO and DAB-GO (Reproduced with permission from ref. [46], Copyright © 2017 Elsevier B. V.).

surface, in the same acidic medium [47]. Corrosion inhibition property of DAZP-GO was evaluated to protect mild steel in the same acidic medium. DAZP-GO exhibited 96.73% of corrosion inhibition efficiency, which was better than DAMP-GO. Electrochemical studies revealed that the as-produced fGOs act as a mixed type inhibitor with cathodic predominance. SEM, EDX, XRD, and AFM techniques were executed to understand the protective film forming ability of the fGOs. Furthermore, quantum chemical calculations were also carried out to corroborate the experimental findings with the theoretical outcomes. In 2019, further modification of GO was carried out by this research group, and it reported p-aminophenol (PAP) functionalized GO [48]. It was found that the newly synthesized fGO exhibited excellent corrosion inhibition efficiency and inhibition efficiency of the as-produced inhibitor increased with increase in the concentration of the fGO. Along with experimental findings such as characterization, corrosion inhibition studies, etc., theoretical studies, viz., DFT and MD were also executed to corroborate the experimental results. Thus, the functionalization of GO continues. Recently, Baiget et al. synthesized diethylenetriamine (DETA)

functionalized GO [49]. Its protective properties against corrosion of mild steel in HCl medium were evaluated, using EIS and PDP techniques. It was observed that it formed protective films. This protective film possessed mixed type corrosion inhibiting character with cathodic predominance. Later on, Javidparvar et al. reported another organic–inorganic compound-based inhibitor using benzimidazole (BI) and Cerium (Ce) to get GOBICe. This BI and Ce-functionalized GO showed superior film forming ability on mild steel surface and was able to protect the surface from aggressive saline solutions [50]. The interaction of BI on GO surface was pH-dependent, as shown in Fig. 7.5. At lower range of pH, that is, at pH < 4, BI molecules get protonated and electrostatically interact with negatively charged GO, as shown in Fig. 7.5(a). Additionally, π-π interaction between BI and GO leads to better adsorption of BI on GO surface. And with increasing pH, higher electrostatic interaction between GO and cerium cations further strengthens the adsorption phenomenon, as depicted in Fig. 7.5(b).

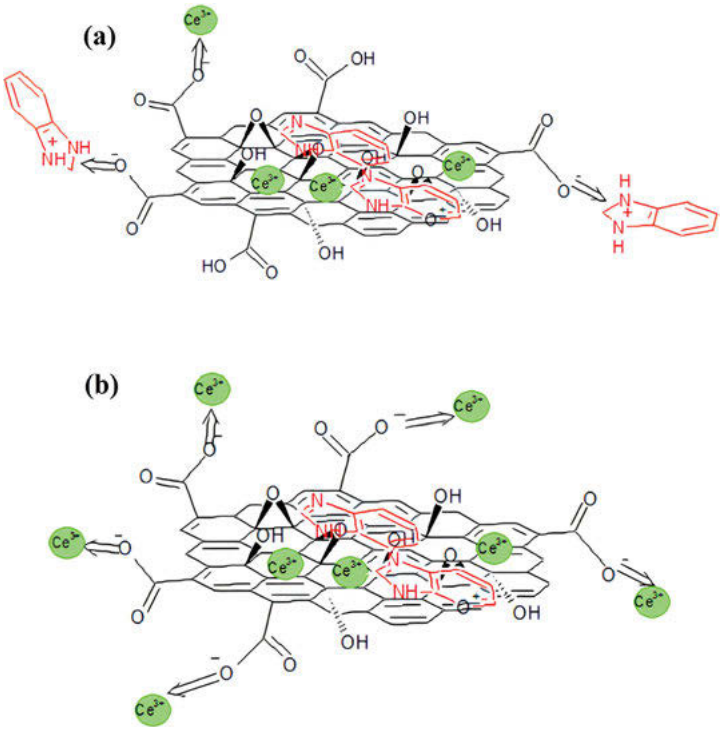

Fig. 7.5: Schematic representation of pH dependency of BI and Ce sorption on GO surface (a) at pH < 4 and (b) at pH > 4 (Adapted with permission from ref. [50], Copyright © 2019 Elsevier B. V.).

Organic and inorganic parts of the fGO exhibited synergic effect, leading to its strong adsorption. The BI molecules interact with cerium cations as well as with the iron cations produced due to anode reaction via cation-π interaction. In another

way, it can be said that the BI molecules donate their lone pairs, situated on N, to the vacant f-orbital of cerium cations or vacant d-orbital of iron cations. Consequently, organic–inorganic complex forms a protective layer by forming precipitation on anodic region, in order to hinder the anodic reaction, that is, deterioration of Fe-metallic surface and the anode. Contrarily, the hydroxyl ions (OH^-) produced in the cathodic region increases the pH, which leads in precipitation of cerium cations in cathodic site to prohibit cathodic reaction. In this way, both the cathodic and anodic regions of steel surface are protected from corrosion synergistically, as demonstrated in Fig. 7.6.

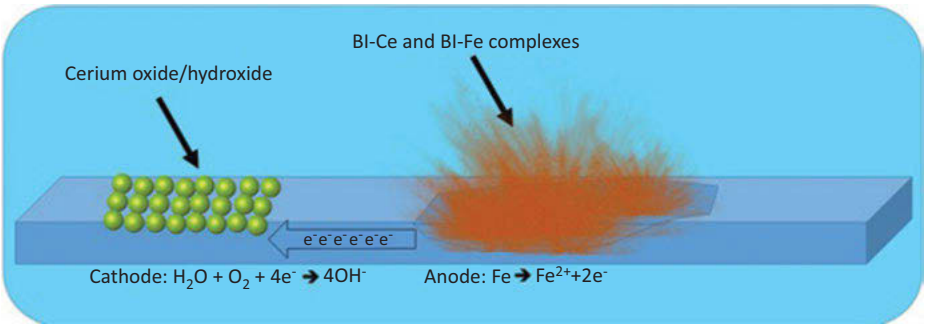

Fig. 7.6: Schematic illustration of film formation mechanism of GOBICe to hinder cathodic and anodic reactions synergistically (Reproduced with permission from ref. [50], Copyright © 2019 Elsevier B. V.).

Haruna et al. utilized cost-effective waste graphene to synthesize GO and further functionalized it with cyclodextrin (CD) [51]. CD-GO was evaluated to protect X60 carbon steel from corrosion in acidic medium via weight loss test and electrochemical measurements. It was found that CD-GO molecules were adsorbed well on carbon steel surface via physisorption and chemisorption, as shown in Fig. 7.7. In chemisorption process, the CD-GO molecules donate the lone pairs of electrons from oxygen to the vacant d-orbital of iron, which leads to the formation of coordinate covalent bond or π-electron metal d-orbital interaction between CD-GO and the metal surface atom lead to form a thin protective film on the metal surface, which, in turn, prohibit the dissolution of iron in anodic zone. On the other hand, acidic environment makes the carbon steel surface to be positively charged. In physisorption process, chloride ions (Cl^-) in hydrated state get adsorbed on positively charged carbon steel surface, and a negatively charged surface is thus created on positively charged carbon steel surface. Accordingly, protonated CD-GO molecules in acidic medium get adsorbed on the negatively charged surface via electrostatic interaction. Thus, hydrogen evolution in cathodic site is hindered by the adsorbed CD-GO. Subsequently, the corrosion on carbon steel surface is also impeded.

This research team further modified GO via incorporation of N,N′-Bis-(2-aminoethyl) piperazine (NAEP) and evaluated its anticorrosive activities on X60 carbon steel in 15%

HCl medium [52]. They used waste disposal to synthesize graphene from which GO was produced; and then, NAEP was grafted on the synthesized GO nano sheet. By this new functionalization, corrosion inhibition efficiency of the inhibitor was increased almost 7% from their previous experiment (vide [51]). Several techniques such as FTIR and Raman were conducted for characterization; in addition to it, techniques like SEM/EDS, TEM, AFM, and EDX were executed for surface analysis. This fGO acted as mixed type inhibitor with cathodic predominance. Adsorption of inhibitor molecules on the metallic surface mainly followed three mechanisms, viz., physisorption, chemisorption, and retro-donation.

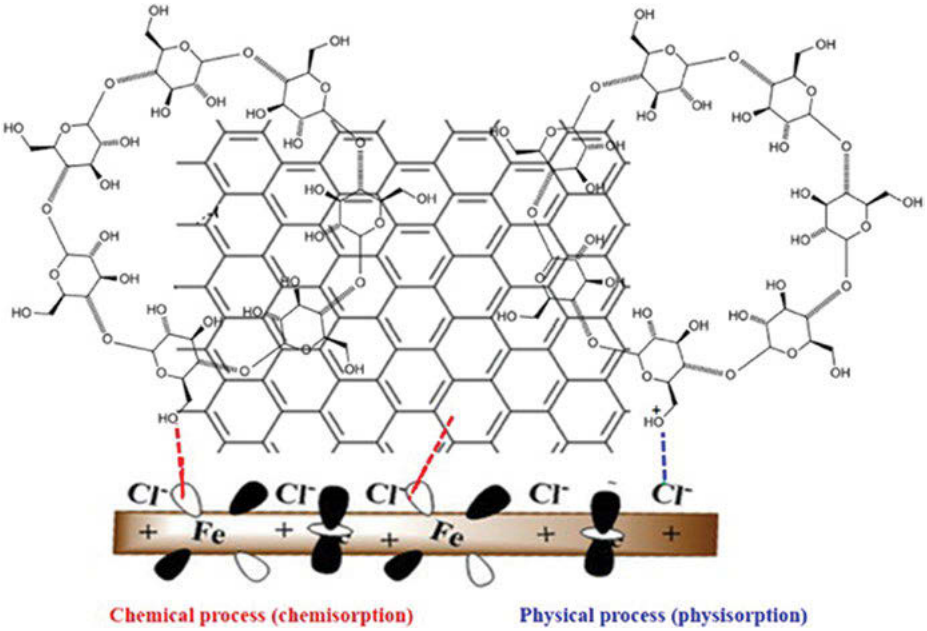

Fig. 7.7: Schematic representation of absorption (chemisorption and physisorption) process of CD-GO on CS surface (Reproduced with permission from ref. [51], Copyright © 2018 Elsevier B. V.).

Radey et al. reported aminoethanol-modified GO (GON) and 2-mercapto ethanol-modified GO (GOS). The corrosion inhibition properties on carbon steel were explored in HCl medium [53]. N,N'-dicyclohexylcarbodiimide (DCC) was used as coupling agent during the synthesis of fGOs. Characterization of the as-produced fGOs was carried out by FTIR, FESEM, and XRD techniques. From SEM images, it was found that GON forms very thin and stacked sheet on carbon steel, whereas, GOS forms wrinkles or crumps on the surface of carbon steel. Both inhibitors obeyed Langmuir adsorption isotherm. However, it is noteworthy to mention that both inhibitors acted as mixed type inhibitor, wherein GON exhibited better corrosion mitigation performance [53]. In 2020, Ansari et al. synthesized polyethyleneimine (PEI)-functionalized GO and

reported its mixed inhibitive nature with cathodic predominance [54]. The as-produced fGO is shown in Fig. 7.8(a). It has been reported that in presence of KI, PEI-GO can provide superior corrosion inhibition effectiveness, around 95.77%, synergistically on carbon steel in highly acidic medium. FTIR, TEM, and SEM were executed for characterization of as-synthesized PEI-GO. 3D profilometry and static contact angle measurements were carried out for surface analysis, and good surface smoothness and hydrophobicity were obtained, as shown in Fig. 7.8(b). From contact angle measurement, it has been found that the contact angle value significantly increased for PEI-GO indicating a hydrophobic film formation on iron surface, wherein, after addition of KI, the hydrophobicity of the iron surface is increased. Thus, the hydrophobic nature of the PEI-GO will inhibit the diffusion of aqueous solutions, which contain corrosive species. The KI interacts synergistically with GO and facilitates its adsorption onto the metal substrates. This adsorption phenomenon ultimately leads to form the protective layer, which provides better barrier property and shows better corrosion inhibition behavior. Electrochemical frequency modulation (EFM), PDP, and weight loss tests were carried

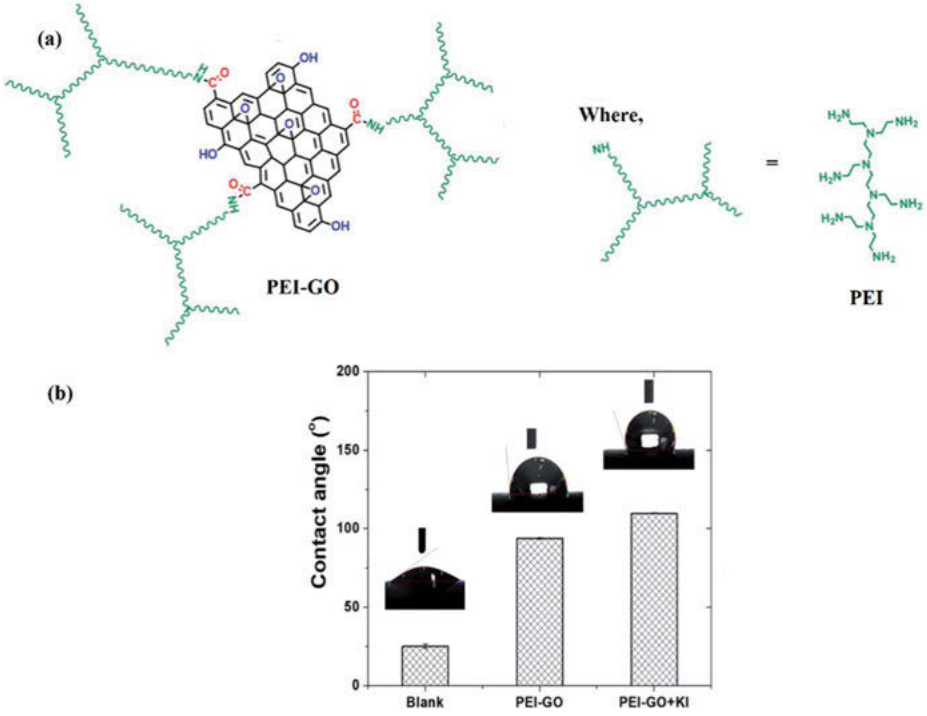

Fig. 7.8: Schematic presentation of (a) as-synthesized fGO, PEI-GO and (b) contact angles of blank iron surface, iron surface after addition of PEI-GO, and iron surface after addition of PEI-GO and KI (Reproduced from ref. [54]).

out to evaluate anticorrosion effectiveness. DFT-based computational studies were also implemented to corroborate the experimental findings [54].

Furthermore, Ansari et al. functionalized GO with bis(2-aminoethyl)amine (B2AA) and evaluated its anticorrosive effectiveness on carbon steel surface in HCl medium [55]. It was obtained that the as-synthesized B2AA-GO acted as mixed type inhibitor with prevalently cathodic nature, and the addition of KI introduced synergic increase in the barrier property of fGO. Admirably, this B2AA-GO exhibited better corrosion inhibition efficiency (~ 96.84% @50 mg/L) than that of the previously reported PEI-GO (~95.77% @50 mg/L) [54]. To evaluate the corrosion effectiveness of this as-synthesized fGO, the EIS, PDP, EFM, and weight loss tests were carried out. From the EIS study, a depressed capacitive semi-circle with a single time constant in the Nyquist plot was obtained, which suggested that the adsorption of the inhibitor, B2AA-GO, followed charge transfer-controlled mechanism. The deviations in Nyquist plot from the ideal semicircular curve are reported as a cause of surface roughness and nonuniformity of the surface due to corrosion during acidization. And, it has been found that impedance of the circuit was increased with increase of the concentration of the inhibitor, that is, surface protection efficacy of this nano emulsion from corrosion increased with increasing concentration of the inhibitor, as illustrated in Fig. 7.9(a). Again, in PDP study, it was found that the addition of B2AA-GO into electrolyte could suppress the anodic reaction that is, dissolution of metal and cathodic reaction, that is, hydrogen evolution, wherein cathodic curve of the Tafel plot showed a greater extent of suppression, as shown in Fig. 7.9(b). From contact angle measurement study, it was obtained that the formed protective film possessed hydrophobic nature.

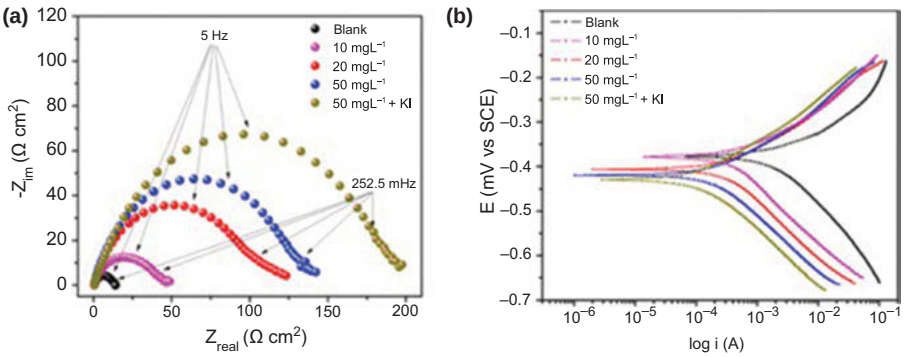

Fig. 7.9: Schematic representation of (a) Nyquist plot obtained from EIS study and (b) Tafel plot obtained from PDP study (Adapted with permission from ref. [55], Copyright © 2019 Elsevier Inc.).

Naser et al. functionalized GO by urea and thiourea and named the functionalized products as GOA and GOB, respectively [56]. The protective nature of the as-produced fGOs was evaluated on C1025 carbon steel surface in highly acidic medium. The fGOs formed protective film on metal substrate by physisorption and exhibited mixed

inhibitive nature. It was found that urea functionalized GO more uniformly in comparison to thiourea. Consequently, GOA acted as an effective and better corrosion inhibitor than GOB. In the same year, Saleh et al. reported octanoate (SO)-grafted GO and evaluated its corrosion inhibition effectiveness for the protection of X60 carbon steel in 1% HCl medium [57]. The adsorption of the fGO on metal surface proceeded via both physisorption and chemisorption mechanisms. Additionally, it was reported that the d-orbitals of iron are capable of donating their extra electrons to the vacant π^*-molecular orbitals of SO-GO. Thus, it leads to back bond formation through this retro-donation mechanism. And it was observed that SO-GO acted as cathodic type inhibitor in acidic solution. Recently, in 2021, 3-amino-1,2,4-triazole (ATA)-functionalized GO was synthesized and characterized by Cen et al., and its anticorrosive performance on carbon steel was evaluated in CO_2-saturated NaCl medium [58]. ATA-GO exhibited excellent corrosion inhibition along with hydrophobic film formation. Adsorption as well as inhibitive mechanism of ATA-GO is depicted in Fig. 7.10. After the addition of ATA-GO into the corrosive solution, the ATA-GO gets closer to the surface via diffusion effect. N-containing heterocycles form coordinate bonds with the iron surface via chemisorption. Owing to the agglomeration effect of ATA-GO, particle deposition and accumulation on metal surface takes place via hydrogen bonding interaction and electrostatic interaction, as shown in Fig. 7.10. Accordingly, a local micro-nano structured outgrowth is formed. This outer layer formed is hydrophobic in nature as it is one of the natural characteristics of nano carbon materials. Consequently, the metal surface is isolated from the surrounding corrosive electrolyte solution.

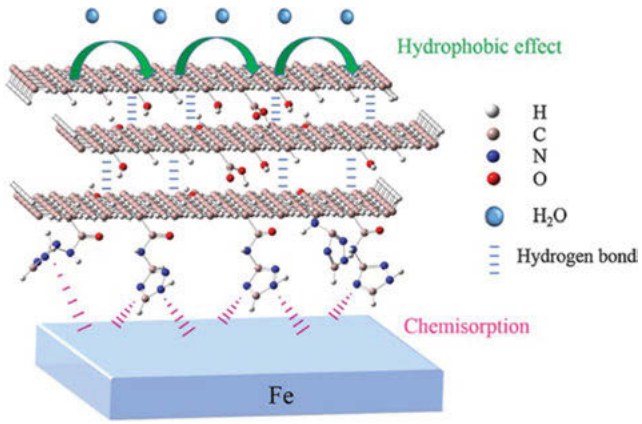

Fig. 7.10: Schematic representation of protection of steel surface by the inhibitive activity of ATA-GO (Reproduced with permission from ref. [58], Copyright © 2021 Elsevier B. V.).

Here, it was found that the corrosion inhibition efficiency primarily followed proportional relation with concentration of the added inhibitor, but after a certain limit, corrosion inhibition efficiency decreased with increase in the concentration of fGO. This was due to agglomeration of the nanoparticles with increasing concentration of fGO, as well as because ferrous ions in electrolytic solution encouraged the sedimentation of fGO. Haruna et al. reported dopamine (DA)-functionalized GO, which showed superior anticorrosive effectiveness on carbon steel in highly acidic medium [59]. Characterization and surface analysis were carried out using several sophisticated techniques such as FTIR, SEM/EDX, AFM, and TEM, and corrosion inhibitive property of the as-produced fGO was evaluated by weight loss test, EFM, EIS, PDP, and LPR techniques. Adsorption of the as-produced DA-GO on metal surface proceeded through physisorption, chemisorption, and retro-donation. The organic aromatic ring donates its electrons to the low-lying vacant orbital of iron to facilitate chemical bonding, that is, chemisorption, whereas, protonated DA-GO interacts with Cl^- on steel surface via physisorption; and iron can also donate its extra electrons to the empty orbitals of DA-GO via retro-donation. These were evidenced by EDX spectra in which no spectra was obtained for heteroatoms in DA-GO inhibited solution and FTIR spectra of the DA-GO surface film after adsorption, in which additional Fe-C-O band was observed. It was observed that DA-GO acted as a mixed type inhibitor with cathodic predominance. The noteworthy characteristic features of most significant fGO, as corrosion inhibitor in solution phase briefed herein, have been tabulated in Tab. 7.1.

7.6 Mechanism of corrosion inhibition by fGO

The fGO exhibits its corrosion inhibition behavior by initially adsorbing in the targeted metal surface atoms, which are exposed towards the corrosive solution in which the fGO is well dispersed. The adsorption of fGO is accomplished either by undergoing physisorption, chemisorption, or retro-donation (back donation of electrons), as shown in Fig. 7.11. When the organic species or additives as corrosion inhibitors are added into the corrosive media, there is a greater possibility of the protonation of some of the active sites present in the fGO, even at mild acidic conditions. These protonated sites of the fGO might interact with the previously adsorbed chloride ions at the surface of the metal substrates. These sorts of interactions arising due to the oppositely charged organic species and the metal centers give rise to adsorption of the organic species through physical interaction, also known as physisorption. The electrons present in the unsaturated π-bonds of the organic aromatic ring are donated to the available d-orbitals of metal surface atoms, giving rise to chemical bond formation, which is also known as chemisorption. Furthermore, the lone pairs of electrons preset in the hetero atoms like nitrogen and oxygen present in the skeleton of fGO are also donated to the vacant d-orbitals of the metal atoms preset at the

Tab. 7.1: Chemically modified graphene oxide as corrosion inhibitor in solution phase.

Sl. No.	Chemically modified product	Substrate	Medium	Studies performed	Remarks*	Inhibition efficiency	Ref.
1	Polyurethane-functionalized sulfonated GO	Mild steel	0.5 M H_2SO_4	FTIR, 1 H-NMR, UV-Vis study, XRD, TGA, TEM, AFM, gravimetric measurement, EIS, PDP, Fluorescence imaging,	Nano hybrid showed best corrosion inhibition property than that of pure polymer than that of sulfonated GO due to homogeneous dispersion of inhibitor in corrosive solution	87.0% @200ppm	[45]
2	Aminoazobenzene (AAB) and diaminoazobenzene (DAB)- functionalized GO	Mild steel	1 M HCl	FTIR, XRD, TEM, Raman spectroscopy, XPS, SEM, EDX, EIS, PDP, DFT	AAB-GO exhibited better corrosion inhibition efficiency	94.65% @25 mg/L	[46]
3	diazo pyridine (DAMP) and diamino pyridine (DAZP)- functionalized GO	Mild steel	1 M HCl	FTIR, SEM, EDX, AFM, XRD, quantum computational calculations, EIS, PDP	DAZP-GO showed better corrosion inhibition efficiency and barrier performance increased with increasing concentration of fGO	96.73% @25 mg/L	[47]
4	p-aminophenol (PAP)-functionalized GO	Mild steel	1 M HCl	FTIR, XRD, TEM, XPS, SEM, EDX, Raman spectroscopy, EIS, PDP, DFT, MD	PAP-GO exhibited better corrosion inhibition efficiency and inhibition efficiency increased with increasing concentration of fGO	92.86% @25 mg/L	[48]
5	Diethylenetriamine (DETA) -functionalized GO	Mild steel	1 M HCl	FTIR, SEM, ATR- FTIR, TEM, EIS, PDP, DFT	DETA-GO acted as mixed type inhibitor with cathodic predominance	92.67% @25 mg/L	[49]

(continued)

Tab. 7.1 (continued)

Sl. No.	Chemically modified product	Substrate	Medium	Studies performed	Remarks*	Inhibition efficiency	Ref.
6	Cereum (Ce)-benzimidazole (BI)-GO	Mild steel	Saline medium	FE-SEM, EDX, FTIR, XRD, XPS, EIS, PDP	GOBICe exhibited better anticorrosive performance	72.37% @ (1:1 Ce and BI)	[50]
7	Cyclodextrin (CD)-based functionalized GO	X60 carbon steel	1 M HCl	SEM, EDX, FTIR, UV-Vis, weight loss test, EIS, PDP, EFM, LPR	CD-GO prohibited cathodic hydrogen evolution as well as acted as mixed type inhibitor	81.17% @15 W/V %	[51]
8	N,N′-Bis-(2-aminoethyl)piperazine (NAEP)-functionalized GO	X60 carbon steel	15% HCl	FTIR, Raman, TEM, SEM/EDS, AFM, EDX, weight loss test, LPR, EIS, PDP	NAEP-GO acted as mixed type inhibitor with cathodic predominance	88.94% @25ppm	[52]
9	Aminoethanol based GO (GON) and 2-mercapto ethanol-based GO (GOS)	Carbon steel rod	1 M HCl	FTIR, XRD, FESEM, PDP,	Both of GON and GOS showed mixed inhibitor character wherein GON exhibited better inhibition efficiency	96.96% @6ppm	[53]
10	Polyethyleneimine (PEI)-grafted GO	carbon steel	15% HCl	FTIR, SEM, TEM, 3D profilometry, WCA, DFT, EFM, PDP, weight loss test,	PEI-GO acted as mixed type inhibitor with cathodic predominance and exhibited synergic effect in presence of KI @65°C	95.77% @50 mg/L	[54]
11	Bis(2-aminoethyl) amine (B2AA)-modified GO	carbon steel	15% HCl	FTIR, SEM, TEM, WCA, AFM, weight loss test, EIS, EFM, PDP,	B2AA-GO exhibited synergic effect in presence of KI @65 °C and excellent interfacial corrosion inhibition as a nano-emulsion	96.84% @50 mg/L	[55]

12	Urea and thiourea-functionalized GO	C1025 carbon steel	0.1 M HCl	Raman, XRD, FESEM, EDX, PDP	Urea functionalized GO more uniformly than thiourea hence more protective property of GO was achieved by using urea	91.7% @100ppm	[56]
13	Octanoate (SO)-grafted GO	X60 carbon steel	15% HCl	FTIR, FT-Raman, TEM, NMR, WCA, SEM/EDS, AFM, EIS, EFM, PDP	SO-GO acted as cathodic type inhibitor	73.31% @25ppm	[57]
14	3-Amino-1,2,4-triazole (ATA)- functionalized GO	carbon steel	CO_2 saturated NaCl solution	FTIR, TGA, XRD, TEM, SEM, EDS, EIS, AFM, XPS, WCA, weight loss test, EIS, PDP	ATA-GO exhibited excellent corrosion inhibition along with hydrophobic film formation	83.4% @20 mg/L	[58]
15	Dopamine (DA)-functionalized GO	carbon steel	15% HCl	FTIR, SEM/EDX, AFM, TEM, weight loss test, EFM, EIS, PDP, LPR	DA-GO acted as mixed type inhibitor with cathodic predominance	95.02% @5ppm	[59]

* AFM = atomic force microscopy; ATR-FTIR = attenuated total reflection Fourier transform infra-red spectroscopy; DFT = density functional theory; EDS = energy dispersive spectroscopy; EDX = energy dispersive X-ray; EFM = electrochemical frequency modulation; EIS = electrochemical impedance spectroscopy; FE-SEM = field-emission scanning electron microscopy; FTIR = Fourier-transform infrared spectroscopy; LPR = linear polarization resistance; MD = molecular dynamic simulation; NMR = nuclear magnetic resonance; PDP = potentiodynamic polarization; SEM = scanning electron microscopy; TEM = transmission electron microscopy; TGA = thermogravimetric analysis; UV-Vis study = UV – Visible spectroscopy study; WCA = water contact angle measurement; XPS = X-ray photoelectron spectroscopy; XRD = X-ray diffraction.

periphery of the metallic substrates and form coordinate bonds, which also facilitates chemisorptions. The chemical bonding gives rise to comparatively strong adhesion of the organic species onto the metal surface atoms. On the other hand, the excess electrons present in the metal d-orbitals are sometimes also back donated towards the available orbitals of the fGO. This process is called retro-donation. Thus, the adsorption of fGO follows either pathway of adsorption or the under adsorption; following these two or all three pathways gives rise to strong adsorption (Fig. 7.11). The adsorbed fGOs act as a barrier that retards the diffusion of the corrosive species towards the vulnerable metal surface atoms; thereby, it protects the metal from further oxidative dissolution in the corrosive media [59].

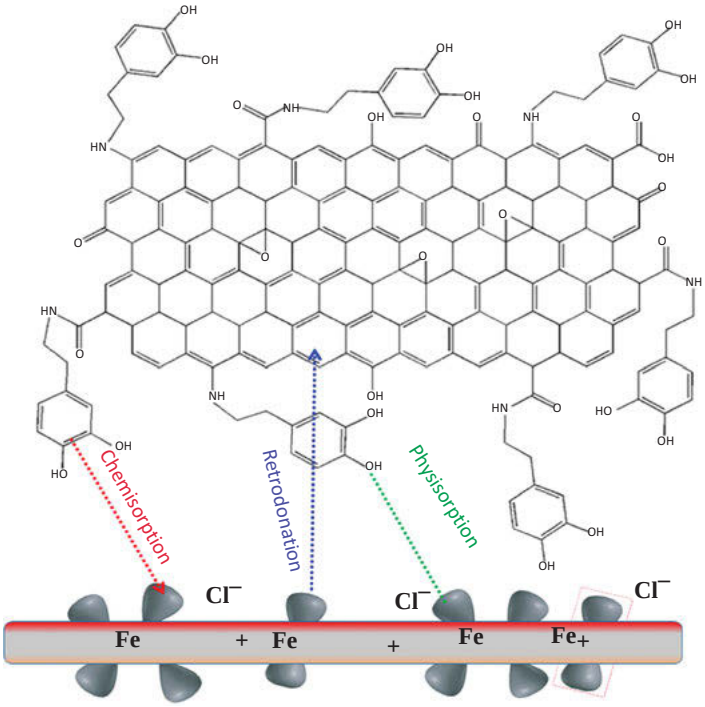

Fig. 7.11: Schematic representation of DA-GO adsorption mechanism on carbon steel surface (Reproduced with permission from ref. [59], Copyright © 2021 Elsevier B. V.).

7.7 Summary and outlook

The unique physical and chemical properties of fGO have led to unprecedented research advances in the synthesis of novel anticorrosive inhibitors as a next generation solution. GO are generally hydrophobic, but after target-specific functionalization of

GO, the as-produced fGO achieve few excellent characteristics such as hydrophilicity, increased water dispersibility, etc. Owing to its extended geometrical structure, it covers greater surface area upon its adsorption onto the metal surface atoms. The strong adsorption onto metal surface via physisorption, chemisorption, and retro-donation exhibited by fGOs gives rise to hydrophobic film formation on metal substrate in solution phase. Hence, fGOs have been considered as a blooming corrosion inhibitor in the solution phase. Obviously, the concentration of fGOs added into the corrosive media plays an important role in impeding corrosion in solution phase.

In future, the heteroatom-doped GOs, which are supposed to provide more effective barrier against corrosion in solution phase, are to be explored. Furthermore, extensive functionalization of GO with various ionic liquids and its utilization as corrosion inhibitor is yet to be explored. Since the fGO and the ionic liquids separately exhibit anticorrosive property, the combined forms are expected to retain, and/or further enhance the anticorrosive properties of the ionic liquids-functionalized GO. The innovative functionalization of graphene and GO might be the "next generation solution" in the field of corrosion mitigation for several types of metals and metallic alloys in various corrosive fields or extreme corrosive environments, such as formation water in oil and gas industries, high temperature corrosion in petroleum petrochemical industries, and so on, that are yet to be explored.

References

[1] Saha, S.K.; Murmu, M.; Murmu, N.C.; Obot, I.B.; Banerjee, P. Molecular level insights for the corrosion inhibition effectiveness of three amine derivatives on the carbon steel surface in the adverse medium: A combined density functional theory and molecular dynamics simulation study. Surf. Interfaces. 2018, 10, 65–73, doi:https://doi.org/10.1016/j.surfin.2017.11.007.

[2] Tripathy, D.B.; Murmu, M.; Banerjee, P.; Quraishi, M.A. Palmitic acid based environmentally benign corrosion inhibiting formulation useful during acid cleansing process in MSF desalination plants. Desalination. 2019, 472, 114128, doi:10.1016/j.desal.2019.114128.

[3] Murmu, M.; Saha, S.K.; Murmu, N.C.; Banerjee, P. Effect of stereochemical conformation into the corrosion inhibitive behavior of double azomethine based Schiff bases on mild steel surface in 1 mol L–1 HCl medium: An experimental, density functional theory and molecular dynamics simulation study. Corros. Sci. 2019, 146, 134–151, doi:http://doi.org/10.1016/j.corsci.2018.10.002.

[4] Sastri, V.S. Challenges in Corrosion: Costs, causes, consequences and control, John Wiley & Sons, 2015, ISBN: 9781118522103.

[5] Quraishi, M.A.; Chauhan, D.S.; Saji, V.S. Heterocyclic organic corrosion inhibitors: Principles and applications, Elsevier Inc., Amsterdam, 2020, ISBN: 9780128185582.

[6] Saha, S.K.; Murmu, M.; Murmu, N.C.; Banerjee, P. Evaluating electronic structure of quinazolinone and pyrimidinone molecules for its corrosion inhibition effectiveness on target specific mild steel in the acidic medium: A combined DFT and MD simulation study. J. Mol. Liq. 2016, 224, 629–638, doi:http://dx.doi.org/10.1016/j.molliq.2016.09.110.

[7] Sastri, V.S. Green corrosion inhibitors: Theory and practice, John Wiley & Sons, 2012.
[8] Nine, M.J.; Cole, M.A.; Tran, D.N.H.; Losic, D. Graphene: A multipurpose material for protective coatings. J. Mater. Chem. A. 2015, 3, 12580–12602, doi:https://doi.org/10.1039/C5TA01010A.
[9] Umoren, S.A.; Solomon, M.M.; Saji, V.S. Corrosion inhibitors in the oil and gas industry, Wiley-VCH Verlag GmbH & Co. KGaA, 2020, 229, ISBN: 978-3-527-34618-9.
[10] Sengupta, S.; Murmu, M.; Murmu, N.C.; Banerjee, P. Adsorption of redox-active Schiff bases and corrosion inhibiting property for mild steel in 1 molL–1 H2SO4: Experimental analysis supported by ab initio DFT, DFTB and molecular dynamics simulation approach. J. Mol. Liq. 2021, 326, 115215, doi:https://doi.org/10.1016/j.molliq.2020.115215.
[11] Chauhan, D.S.; Quraishi, M.A.; Ansari, K.R.; Saleh, T.A. Graphene and graphene oxide as new class of materials for corrosion control and protection: Present status and future scenario. Prog. Org. Coat. 2020, 147, 105741, doi:https://doi.org/10.1016/j.porgcoat.2020.105741.
[12] Amirazodi, K.; Sharif, M.; Bahrani, M. Polypyrrole doped graphene oxide reinforced epoxy nanocomposite with advanced properties for coatings of mild steel. J. Polym. Res. 2019, 26, 244, doi:https://doi.org/10.1007/s10965-019-1905-3.
[13] Nayak, S.R.; Mohana, K.N.; Hegde, M.B. Anticorrosion performance of 4-fluoro phenol functionalized graphene oxide nanocomposite coating on mild steel. J. Fluor. Chem. 2019, 228, 109392, doi:https://doi.org/10.1016/j.jfluchem.2019.109392.
[14] Zhu, Q.; Huang, Y.; Li, Y.; Zhou, M.; Xu, S.; Liu, X.; Liu, C.; Yuan, B.; Guo, Z. Aluminum dihydric tripolyphosphate/polypyrrole-functionalized graphene oxide waterborne epoxy composite coatings for impermeability and corrosion protection performance of metals. Adv. Compos. Hybrid Mater. 2021, 4, 780–792, doi:https://doi.org/10.1007/s42114-021-00265-6.
[15] Allen, M.J.; Tung, V.C.; Kaner, R.B. Honeycomb carbon: A review of graphene. Chem. Rev. 2010, 110(1), 132–145, doi:https://doi.org/10.1021/cr900070d.
[16] Lee, X.J.; Zhang, H.B.Y.; Lai, K.C.; Lee, L.Y.; Gan, S.; Gopakumar, S.T.; Rigby, S. Review on graphene and its derivatives: Synthesis methods and potential industrial implementation. J. Taiwan Inst. Chem. Eng. 2019, 98, 163–180, doi:https://doi.org/10.1016/j.jtice.2018.10.028.
[17] Geim, A.K.; Novoselov, K.S. The rise of graphene, nanoscience and technology: A collection of reviews from nature journals. World Sci. 2009, 11–19, doi:https://doi.org/10.1142/9789814287005_0002.
[18] Singh, V.; Joung, D.; Zhai, L.; Das, S.; Khondaker, S.I.; Seal, S. Graphene based materials: Past, present and future. Prog. Mater. Sci. 2011, 56, 1178–1271, doi:http://dx.doi.org/10.1016/j.pmatsci.2011.03.003.
[19] Kirkland, N.; Schiller, T.; Medhekar, N.; Birbilis, N. Exploring graphene as a corrosion protection barrier. Corros. Sci. 2012, 56, 1–4, doi:http://dx.doi.org/10.1016/j.corsci.2011.12.003.
[20] Yu, L.; Lim, Y.-S.; Han, J.H.; Kim, K.; Kim, J.Y.; Choi, S.-Y.; Shin, K. A graphene oxide oxygen barrier film deposited via a self-assembly coating method. Synth. Met. 2012, 162, 710–714, doi:https://doi.org/10.1016/j.synthmet.2012.02.016.
[21] Zhao, C.; Xu, X.; Chen, J.; Yang, F. Effect of graphene oxide concentration on the morphologies and antifouling properties of PVDF ultrafiltration membranes. J. Environ. Chem. Eng. 2013, 1, 349–354, doi:https://doi.org/10.1016/j.jece.2013.05.014.
[22] Kharisov, B.I.; Kharissova, O.V. Carbon allotropes: Metal-complex chemistry, properties and applications, Springer, 2019, pp, ISBN 978-3-030-03504-4.
[23] Singhal, K.; Mehtab, S.; Pandey, M.; Zaidi, M.G.H. Sustainable development of graphene oxide from pine leaves for electrochemical energy storage and corrosion protection. Curr.

Res. Green Sustain. Chem. 2022, 5, 100266, doi:https://doi.org/10.1016/j.crgsc.2022.100266.
[24] Wahid, M.H.; Stroeher, U.H.; Eroglu, E.; Chen, X.; Vimalanathan, K.; Raston, C.L.; Boulos, R.A. Aqueous based synthesis of antimicrobial-decorated graphene. J. Colloid Interface Sci. 2015, 443, 88–96, doi:https://doi.org/10.1016/j.jcis.2014.11.043.
[25] Georgakilas, V.; Tiwari, J.N.; Kemp, K.C.; Perman, J.A.; Bourlinos, A.B.; Kim, K.S.; Zboril, R. Noncovalent functionalization of graphene and graphene oxide for energy materials, biosensing, catalytic, and biomedical applications. Chem. Rev. 2016, 11, 5464–5519, doi:https://doi.org/10.1021/acs.chemrev.5b00620.
[26] Kharisov, B.I.; Kharissova, O.V.; Gutierrez, H.L.; Méndez, U.O. Recent advances on the soluble carbon nanotubes. Ind. Eng. Chem. Res. 2009, 48, 572, doi:https://doi.org/10.1021/ie800694f.
[27] Marcia, M.; Hirsch, A.; Hauke, F. Perylene-based non-covalent functionalization of 2D materials. FlatChem 2017, 1, 89, doi:https://doi.org/10.1016/j.flatc.2017.01.001.
[28] Englert, J.M.; Dotzer, C.; Yang, G.; Schmid, M.; Papp, C.; Gottfried, J.M.; Steinrück, H.-P.; Spiecker, E.; Hauke, F.; Hirsch, A. Covalent bulk functionalization of graphene. Nat. Chem. 2011, 3, 279, doi:https://doi.org/10.1038/nchem.1010.
[29] Xu, Z.; Wang, S.; Li, Y.; Wang, M.; Shi, P.; Huang, X. Covalent functionalization of graphene oxide with biocompatible poly(ethylene glycol) for delivery of paclitaxel. ACS Appl. Mater. Interfaces. 2014, 6, 17268, doi:https://doi.org/10.1021/am505308f.
[30] Yang, H.; Li, F.; Shan, C.; Han, D.; Zhang, Q.; Niu, L.; Ivaska, A. Covalent functionalization of chemically converted graphene sheets via silane and its reinforcement. J. Mater. Chem. 2009, 19, 4632–4638, doi:https://doi.org/10.1039/B901421G.
[31] Stankovich, S.; Piner, R.D.; Nguyen, S.T.; Ruoff, R.S. Synthesis and exfoliation of isocyanate-treated graphene oxide nanoplatelets. Carbon. 2006, 44, 3342–3347, doi:https://doi.org/10.1016/j.carbon.2006.06.004.
[32] Mo, M.; Zhao, W.; Chen, Z.; Yu, Q.; Zeng, Z.; Wu, X.; Xue, Q. Excellent tribological and anti-corrosion performance of polyurethane composite coatings reinforced with functionalized graphene and graphene oxide nanosheets. RSC Adv. 2015, 5, 56486–56497, doi:https://doi.org/10.1039/C5RA10494G.
[33] Liu, Z.-B.; Xu, Y.-F.; Zhang, X.-Y.; Zhang, X.-L.; Chen, Y.-S.; Tian, J.-G. Porphyrin and fullerene covalently functionalized graphene hybrid materials with large nonlinear optical properties. J. Phys. Chem. B. 2009, 113, 9681–9686, doi:https://doi.org/10.1021/jp9004357.
[34] Verma, C.; Quraishi, M.A.; Ebenso, E.E.; Hussain, C.M. Recent advancements in corrosion inhibitor systems through carbon allotropes: Past, present, and future. Nano Select. 2021, 2, 2237–2255, doi:https://doi.org/10.1002/nano.202100039.
[35] Su, Q.; Pang, S.; Alijani, V.; Li, C.; Feng, X.; Müllen, K. Composites of graphene with large aromatic molecules. Adv. Mater. 2009, 21, 3191–3195, doi:https://doi.org/10.1002/adma.200803808.
[36] Alwarappan, S.; Boyapalle, S.; Kumar, A.; Li, C.-Z.; Mohapatra, S. Comparative study of single-, few-, and multilayered graphene toward enzyme conjugation and electrochemical response. J. Phys. Chem. C. 2012, 116, 6556–6559, doi:https://doi.org/10.1021/jp211201b.
[37] Shown, I.; Ganguly, A. Non-covalent functionalization of CVD-grown graphene with Au nanoparticles for electrochemical sensing application. J. Nanostruct. Chem. 2016, 6, 281, doi:https://doi.org/10.1007/s40097-016-0201-6.
[38] Lee, D.Y.; Khatun, Z.; Lee, J.-H.; Lee, Y.-K.; In, I. Blood compatible graphene/heparin conjugate through noncovalent chemistry. Biomacromolecules. 2011, 12, 336–341, doi:https://doi.org/10.1021/bm101031a.

[39] Li, X.; Cai, W.; An, J.; Kim, S.; Nah, J.; Yang, D.; Piner, R.; Velamakanni, A.; Jung, I.; Tutuc, E. Large-area synthesis of high-quality and uniform graphene films on copper foils. Science 2009, 324, 1312–1314, doi:https://doi.org/10.1126/science.1171245.
[40] Zhang, B.; Lee, W.H.; Piner, R.; Kholmanov, I.; Wu, Y.; Li, H.; Ji, H.; Ruoff, R.S. Low temperature chemical vapor deposition growth of graphene from toluene on electropolished copper foils. ACS Nano 2012, 6, 2471–2476, doi:https://doi.org/10.1021/nn204827h.
[41] Schriver, M.; Regan, W.; Gannett, W.J.; Zaniewski, A.M.; Crommie, M.F.; Zettl, A. Graphene as a long-term metal oxidation barrier: Worse than nothing. ACS Nano. 2013, 7, 5763–5768, doi: https://doi.org/10.1021/nn4014356.
[42] Zhou, F.; Li, Z.; Shenoy, G.J.; Li, L.; Liu, H. Enhanced room-temperature corrosion of copper in the presence of graphene. ACS Nano. 2013, 7, 6939–6947, doi:10.1021/nn402150t.
[43] Lee, J.; Berman, D. Inhibitor or promoter: Insights on the corrosion evolution in a graphene protected surface. Carbon. 2018, 126, 225–231, doi:https://doi.org/10.1016/j.carbon.2017.10.022.
[44] Ding, R.; Li, W. A brief introduction to corrosion protective films and coatings based on graphene and graphene oxide. J. Alloys Compd. 2018, 764, 1039–1055, doi:https://doi.org/10.1016/j.jallcom.2018.06.133.
[45] Patel, D.K.; Senapati, S.; Mourya, P.; Sing, M.M.; Aswal, V.K.; Ray, B.; Maiti, P. Functionalized graphene tagged polyurethanes for corrosion inhibitor and sustained drug delivery. ACS Biomater. Sci. Eng. 2017, 3(12), 3351–3363, doi:10.1021/acsbiomaterials.7b00342.
[46] Gupta, R.K.; Malviya, M.; Verma, C.; Quraishi, M.A. Aminoazobenzene and diaminoazobenzene functionalized graphene oxides as novel class of corrosion inhibitors for mild steel: Experimental and DFT studies. Mater. Chem. Phys. 2017, 198, 360–373, doi: https://doi.org/10.1016/j.matchemphys.2017.06.030.
[47] Gupta, R.K.; Malviya, M.; Verma, C.; Gupta, N.K.; Quraishi, M.A. Pyridine-based functionalized graphene oxides as a new class of corrosion inhibitors for mild steel: An experimental and DFT approach. RSC Adv. 2017, 7, 39063, doi:https://doi.org/10.1039/C7RA05825J.
[48] Gupta, R.K.; Malviya, M.; Ansari, K.R.; Lgaz, H.; Chauhan, D.S.; Quraishi, M.A. Functionalized graphene oxide as a new generation corrosion inhibitor for industrial pickling process: DFT and experimental approach. Mater. Chem. Phys. 2019, 236, 121727, doi:https://doi.org/10.1016/j.matchemphys.2019.121727.
[49] Baig, N.; Chauhan, D.S.; Saleh, T.A.; Quraishi, M.A. Diethylenetriamine functionalized graphene oxide as a novel corrosion inhibitor for mild steel in hydrochloric acid solutions. New J. Chem. 2019, 43(5), doi:https://doi.org/10.1039/C8NJ04771E.
[50] Javidparvar, A.A.; Naderi, R.; Ramezanzadeh, B. Designing a potent anti-corrosion system based on graphene oxide nanosheets non-covalently modified with cerium/benzimidazole for selective delivery of corrosion inhibitors on steel in NaCl media. J. Mol. Liq. 2019, 284, 415–430, doi:https://doi.org/10.1016/j.molliq.2019.04.028.
[51] Haruna, K.; Saleh, T.A.; Obot, I.B.; Umoren, S.A. Cyclodextrin-based functionalized graphene oxide as an effective corrosion inhibitor for carbon steel in acidic environment. Prog. Org. Coat. 2019, 128, 157–167, doi:https://doi.org/10.1016/j.porgcoat.2018.11.005.
[52] Haruna, K.; Saleh, T.A. N,N′-Bis-(2-aminoethyl)piperazine functionalized graphene oxide (NAEP-GO) as an effective green corrosion inhibitor for simulated acidizing environment. J. Environ. Chem. Eng. 2021, 9, 104967, doi:https://doi.org/10.1016/j.jece.2020.104967.
[53] Radey, H.H.; Khalaf, M.N.; Al-Sawaad, H.Z. novel corrosion inhibitors for carbon steel alloy in acidic medium of 1N HCl synthesized from graphene oxide. Open J. Org. Polym. Mater. 2018, 8, 53, doi:https://doi.org/10.4236/ojopm.2018.84005.

[54] Ansari, K.R.; Singh Chauhan, D.; Quraishi, M.A.; Adesina, A.Y.; Saleh, T.A. The synergistic influence of polyethyleneimine grafted graphene oxide and iodide for the protection of steel in acidizing conditions. RSC Adv. 2020, 10, 17739, doi:https://doi.org/10.1039/D0RA00864H.

[55] Ansari, K.R.; Chauhan, D.S.; Quraishi, M.A.; Saleh, T.A. Bis(2-aminoethyl)amine-modified graphene oxide nanoemulsion for carbon steel protection in 15% HCl: Effect of temperature and synergism with iodide ions. J. Colloid Interface Sci. 2020, 564, 124–133, doi:https://doi.org/10.1016/j.jcis.2019.12.125.

[56] Naser, A.A.; Sawaad, H.Z.A.; Mubarak, A.S.A. Novel graphene oxide functionalization by urea and thiourea, and their applications as anticorrosive agents for carbon steel alloy in acidic medium. J. Mater. Environ. Sci. 2020, 11(3), 404–420.

[57] Saleh, T.A.; Haruna, K.; Mohammed, A.-R.I. Octanoate grafted graphene oxide as an effective inhibitor against oil well acidizing corrosion. J. Mol. Liq. 2021, 325, 115060, doi:https://doi.org/10.1016/j.molliq.2020.115060.

[58] Cen, H.; Chen, Z. Amide functionalized graphene oxide as novel and effective corrosion inhibitor of carbon steel in CO2-saturated NaCl solution. Colloids Surf. A Physicochem. Eng. Asp. 2021, 615, 126216, doi:https://doi.org/10.1016/j.colsurfa.2021.126216.

[59] Haruna, K.; Alhems, L.M.; Saleh, T.A. Graphene oxide grafted with dopamine as an efficient corrosion inhibitor for oil well acidizing environments. Surf. Interfaces. 2021, 24, 101046, doi:https://doi.org/10.1016/j.surfin.2021.101046.

Manilal Murmu, Sanjukta Zamindar, Naresh Chandra Murmu,
Priyabrata Banerjee*

Chapter 8
Polymer composites of graphene and graphene oxides as corrosion inhibitors

Abstract: Interest in using graphene and graphene oxide (GO)-based polymer composites as effective corrosion inhibitors is mounting due to their fascinating characteristics such as large surface area coverage, good adhesion property, chemical resistivity, hydrophobicity, chemical and mechanical stability, and so on. The major works based on anticorrosive performances of polymeric composites containing graphene and GO are the focus of this chapter. The key objective of this chapter is to outline recently developed and explored polymeric composites of graphene and GO, the detailed explanation of the corrosion inhibition mechanism, and their use as effective anti-corrosive coating for protecting mild steels exposed to various corrosive electrolytic solutions.

Keywords: Graphene, graphene oxide, polymer composite, mild steel, adsorption, barrier property, corrosion inhibition

Acknowledgement: PB is very thankful to Department of Higher Education, Science & Technology and Biotechnology, Govt. of West Bengal, India for providing financial assistance *vide* sanction order no. 78 (Sanc.)/ST/P/S&T/6G-1/2018 dated 31.01.2019 and project no. GAP-225612. MM acknowledges Ministry of Tribal Affairs, Govt. of India, New Delhi, India for National Fellowship for Higher Education of Schedule Tribes Students [Erstwhile known as Rajiv Gandhi National Fellowship of Schedule Tribes Students (RGNFST) from University Grants Commission, Govt. of India, New Delhi, India] *vide* reference no. F1-17.1/2014-15/RGNF-2014-15-ST-JHA-71559/(SA-III/Website) dated: February 2015.

*Corresponding author: **Priyabrata Banerjee,** Surface Engineering and Tribology Group, CSIR-Central Mechanical Engineering Research Institute, Mahatma Gandhi Avenue, Durgapur 713209, India; Academy of Scientific and Innovative Research (AcSIR), CSIR-HRDC Campus, Sector-19, Kamla Nehru Nagar, Ghaziabad 201002, India, Web: www.priyabratabanerjee.in and www.cmeri.res.in, e-mail: pr_banerjee@cmeri.res.in
Manilal Murmu, Sanjukta Zamindar, Naresh Chandra Murmu, Surface Engineering and Tribology Group, CSIR-Central Mechanical Engineering Research Institute, Mahatma Gandhi Avenue, Durgapur 713209, India; Academy of Scientific and Innovative Research (AcSIR), CSIR-HRDC Campus, Sector-19, Kamla Nehru Nagar, Ghaziabad 201002, India

https://doi.org/10.1515/9783110782820-008

8.1 Introduction

Metals have versatile applications in several industries such as marine industries, oil and gas transportation industries, petroleum industries, chemical industries, as well as in domestic purposes, etc. [1, 2] In industrial areas, several aqueous acidic solutions of HCl, H_2SO_4, and other acids are used for acid pickling, acid cleansing, acid descaling, rust removal, etc. [3, 4]. During the application of such acidic solutions, the main purposes of the adoption of these techniques are accomplished, but the nascent form of the metal surface is prone to further corrosive attack of the acid, which initiates the oxidative dissolution of the concerned metallic materials. That is, these acidic solutions lead to electrochemical reactions with the metal, which results in several damages on the metal surface. Besides these, when the metallic materials are exposed to adverse conditions or the humid environment, the elevation or fluctuation of temperature, air pollution, or contaminations such as aggressive environments are also the cause of the degradation of metallic bodies. Metallic corrosion results in a huge loss in economy as well as loss of lives [5, 6]. In the present scenario, the global loss due to corrosion is reported to be ~3.4% of the world's GDP, which is approximately $2.5 trillion. A recent study has revealed that the amount of economic loss due to corrosion is ~$360 billion/year. A true concern for the Indian economy is that the amount of economic loss in India due to corrosion is ~$100 billion/year [7, 8]. It is noteworthy to mention that corrosion, a natural catastrophe, has raised a genuine concern all over the world due to its impending devastating nature, so, several precautions have been taken for the protection purpose of metals, among which coating technology has grabbed top attention for industrial use [9–11]. By comparing the current trends after literature survey, it has been observed that there is an increased interest in the application of polymeric composite coatings for the protection of metals, whereas polymeric composite coating incorporated with graphene and/or GO have possessed a special demand for the protection of metal and their alloys [12–14]. Among several metals and metal alloys, mild steel has a multipurpose application in industries due to its high mechanical strength, ease of fabrication, high conductivity, and cost-effectiveness [15]. Hence, the focus of the present chapter has been on corrosion and its mitigation on mild steel. In this chapter, graphene and GO-based polymeric nanocomposite synthesis and their application as anticorrosive materials for the protection of mild steels have been outlined elegantly.

8.2 Graphene and graphene oxide as anticorrosive materials

In 2004, Geim and Novoselov unveiled a new era in the field of science by discovering graphene. Graphene is the thinnest allotropic form of carbon in which carbon

atoms are sp^2-hybridized, and they are arranged in a honey-comb like array, that is, in a hexagonal arrangement [16–18]. Several unputdownable characteristics, for instance, large surface area coverage, high adhesion capability, thermal and chemical stability, hydrophobic nature, chemical inertness, etc. of graphene and its congeners have made them significant in use as efficient anticorrosive materials [19–21]. Effective barrier properties against the penetration of water, oxygen, chloride ions, and other corrosive species are shown by graphene and GO-based polymeric coatings applied on the metal surfaces [8]. The closely packed and dense morphology of the polymeric composite coating further act as physical traps for diffusion of water or other electrolytes through the coating. Consequently, the metal surfaces get protected from the harsh and corrosive environment for long period of time [22].

8.3 Polymer composites of graphene as corrosion inhibitors

Polymer composites of graphene applied onto metal surface are reported to efficiently retard the corrosion of the materials exposed in the corrosive media. Recently, Chang et al. developed hydrophobic epoxy/graphene composite (HEGC) nanocomposite by using the nanocasting method [23]. Epoxy coating provides physical barrier property, but the inclusion of graphene nanosheet reinforced within HEGC increased the barrier property of the coating in a significantly high aspect ratio. The *Xanthosoma sagittifolium* leaves papillae were incorporated onto the surface of the epoxy/graphene composite coating. The pictorial representation of *Xanthosoma sagittifolium* leaf is shown in Fig. 8.1(a). The surface of the leaves of *Xanthosoma sagittifolium* are enriched with small papillary hill-like structures, which are clearly visible from SEM images of the leaves, as shown in Fig. 8.1(b), which causes this leaf to be hydrophobic in nature, with contact angle value of 146° (as shown in Fig. 8.1(b) inset). At first, bisphenol A diglycidyl ether was cured with poly(propylene glycol) bis(2-aminopropyl ether). The GO synthesized by Hummers' method was used to get carboxyl graphene by thermal exfoliation method. This thermally exfoliated GO was then mixed with cured epoxy resin to obtain EGC composite. On the other hand, liquid PDMS was casted on a fresh leaf of *Xanthosoma sagittifolium* to obtain PDMS templates that possessed the hydrophobic surface property of *Xanthosoma sagittifolium* leaf. After that, EGC-coated steel surface was covered with the as-produced PDMS templates and was cured at room temperature. After curing, the PDMS templates were removed from the steel surface in order to obtain HEGC with hydrophobic nature, and the contact angle value of HEGC coated surface was found to be ~127°, which was significantly greater than pure epoxy coated surface (~82°). From the SEM images of the as-synthesized HEGC coating, papillary hill-like shapes were found, as shown in Fig. 8.1(c). The hydrophobic nature of the coating does not allow moisture to penetrate through the coating. It was found that

there was an increase in impedance in the case of HEGC-coated cold rolled steel; accordingly, corrosion rate was nicely mitigated on steel surface, immerged in 3.5 wt. % NaCl solution. It was also observed that the diffusion length for oxygen diffusion through the coating was lower than that of normal epoxy coating, as presented in Fig. 8.1(d).

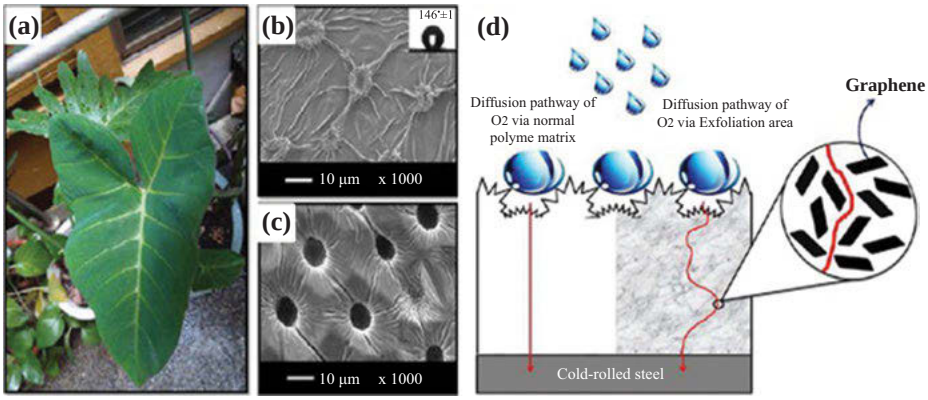

Fig. 8.1: Pictorial representation of (a) *Xanthosoma sagittifolium* leaf, (b) high resolution SEM image of the fresh leaf of *Xanthosoma sagittifolium* along with the contact angle value of the surface of the leaf in the inset, (c) high resolution SEM image of the as-produced HEGC coated surface, and (d) diffusion pathway of oxygen through normal epoxy polymeric matrix and through HEGC coating (Reproduced with permission from ref. [23], Copyright © 2013 Elsevier Ltd.).

In 2016, Alam et al. reported polypyrrole (PPy)/ graphene nano sheets (GNS)/ rare earth elements (RE^{3+})/ dodecyl benzene sulfonic acid (DBSA) nanocomposite, which showed high corrosion inhibition effectiveness on carbon steel in 0.1 M HCl medium [24].The salts of rare earth elements, namely, La^{3+}, Sm^{3+}, and Nd^{3+} were used as passivating agents. It was found that the hybrid nanocomposite containing Sm^{3+} provided better protection, followed by Nd^{3+}, and then, La^{3+} containing hybrid composite. The formulated coating became impenetrable due to π-π interaction between graphene nanosheet and PPy impregnated into the coating. Presence of DBSA within the coating system makes the nanocomposite soluble in organic solvents as well as acts as inhibitor. When corrosion takes place, the hydroxide ions are generated in the cathodic sites. The rare earth elements react with the hydroxide ions and produce $RE(OH)_3$ vide eq. (8.1). The as-formed $RE(OH)_3$ protects both cathodic and anodic sites. Sometimes, dehydration of the rare earth (RE) hydroxides takes place, which results in the formation of rare earth oxides, as shown in eq. (8.2). These rare earth oxides also form a passive layer on the metal surface and provide anticorrosive barrier properties towards the underlying metal. Again, in presence of corrosive media, herein, HCl, the rare earth hydroxides react with chloride ions to form rare earth chloride salts. In this way, the concentration of chloride ions in corrosive solution is reduced. But there is a

tendency towards backward reaction indicating the stability of the $RE(OH)_3$ in acidic medium, vide eq. (8.3). The stability of oxides of REs bears a proportional relation with the corrosion inhibition efficiency. That is why PPy/GNS/Sm^{3+}/DBSA shows better corrosion inhibition property than PPy/GNS/Nd^{3+}/DBSA.

$$RE^{3+} + 3OH^- \rightarrow RE(OH)_3 \tag{8.1}$$

$$2RE(OH)_3 \rightarrow RE_2O_3 + 3H_2O \tag{8.2}$$

$$RE(OH)_3 + 3HCl \leftrightarrow 2RECl_3 + 3H_2O \tag{8.3}$$

Similarly, a new type of hybrid nanocomposite of poly(2-butylaniline), that is, P2BA-functionalized graphene and epoxy was formulated by Chen et al. in 2017 [25]. This as-synthesized coating showed excellent corrosion resistivity on Q235 steel in 3.5 wt. % NaCl solution. UV- visible spectroscopy study, X-ray photoelectron spectroscopy (XPS), scanning electron microscopy (SEM), energy dispersive spectroscopy (EDS), transmittance electron microscopy (TEM), atomic force microscopy (AFM), and X-ray diffraction(XRD) studies were performed for structural or coating characterization. Generally, the graphene tends to aggregate due to its strong interlayer van der Waal interaction and high aspect ratio. It was found that agglomeration and precipitation of graphene take place in the organic solvent media. Herein, the tetrahydrofuran (THF) could be avoided, while P2BA can be preferably used as solvent for dispersing graphene owing to the non-covalent π-π interaction between graphene and P2BA, facilitating its easy dispersion (*vide* Fig. 8.2**)**. These well-dispersed graphene sheets synergistically exhibited superior barrier property against the diffusion of corrosive species towards the metal surface. In addition to it, P2BA exhibited redox catalytic capability. This newly formulated nanocomposite was applied successfully on Q235

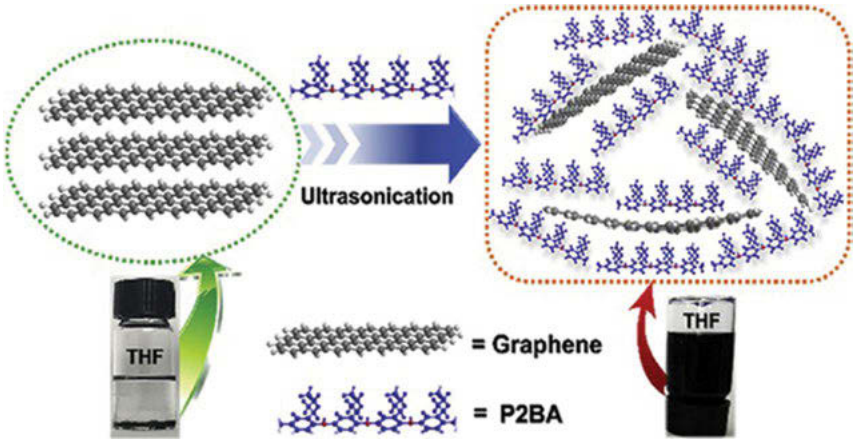

Fig. 8.2: Dispersion of graphene in THF and P2BA dispersant (Reproduced with permission from ref. [25], Copyright © 2016 Elsevier Ltd.).

steel as anticorrosive and anti-wear property, with low friction coefficient. The hybrid epoxy composite containing 0.5 wt.% P2BA and 0.5 wt.% graphene showed best corrosion inhibition efficiency.

The excellent barrier property of graphene-based composite was also obtained by polycrystalline graphene (PG)-reinforced epoxy coating as reported by Pourhashem et al. [26]. Corrosion inhibition performance of the as-formulated coating was evaluated with different percentage of PG. From EIS study, it was revealed that the hybrid composite with 0.05 wt.% PG exhibited better result. From high resolution FE-SEM images, it was found that with increasing concentration of PG, small river-like structures were obtained due to agglomeration. It was also found that with increasing the PG concentration within the epoxy matrix, the agglomeration increased and diminished the corrosion inhibition efficiency. Quantum chemical calculations were also performed to corroborate the theoretical outcomes with the experimental findings. Xu et al. emphasized ball milling method to coat stainless steel (SS) balls with graphene (Gr) with coating thickness 10 nm, and its anticorrosive property in 3.5 wt.% NaCl was established successfully [27]. It was observed that Gr-SS coating was strongly intact on the metallic surface due to the formation of chemical bond between chromium (Cr) and the carbon atoms of the graphene, that is, Cr-C bonds. This Cr-C bond formation enhances the adhesion of the coating on metallic surface, resulting in a slower rate of corrosion (3.14×10^{-3} mm/year), compared to that of bare steel (57.74×10^{-3} mm/year). Additionally, this Gr-SS coating reduced the coefficient of friction value as well as showed enhanced wear resistivity at room temperature. This research group further innovated the coating on the mild steel (MS) surface with Cr-powder, which was then coated with graphene by using the ball-milling method [28]. It was found that this multi-layered graphene coating on Cr-MS surface provided high anticorrosive property in 3.5 wt. % NaCl medium, along with superior wear resistance property and low friction coefficient value. This superior barrier property was facilitated by the formation of Cr-C bond as the Cr-C bond formation is more facile than Fe-C bond formation. Later, similar experiments were carried out to realize the anticorrosive activity of graphene coating on MS surface, which was previously coated with Ti power [29]. Another polymeric epoxy coating composite of silanzied trianiline(SAT)-functionalized graphene sheets (G) namely, SAT-G was synthesized by Ye et al. [30]. SAT was formed by the reaction of aniline trimer (AT) and triethoxysilylpropyl isocyanate (TESPIC), under N_2 environment. After that, a particular amount of graphene was added to the as-produced SAT followed by acetic acid and ethanol. Finally, SAT-G was obtained after sonication and respective stirring of the reacting mixture followed by centrifugation of the obtained product. The synthetic procedure of SAT-G is shown schematically in Fig. 8.3.

From Raman, FTIR, and UV-Visible study, the occurrence of π-π interaction between SAT and G was confirmed. Additionally, the successful implementation of AT within G was confirmed by SEM, TEM, and scanning probe microscopy (SPM). The

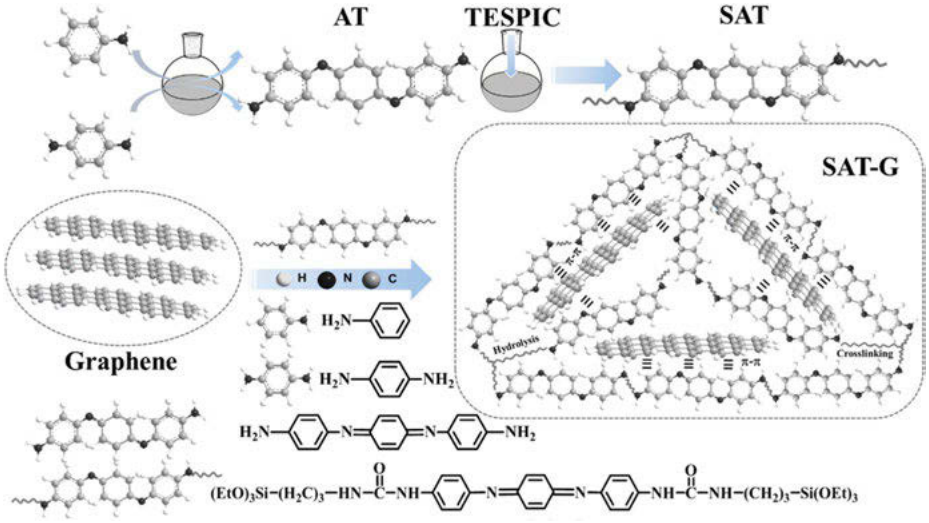

Fig. 8.3: Schematic representation of the synthetic procedure of SAT-G (Reproduced with permission from ref. [30], Copyright © 2018 Elsevier Ltd.).

micro-corrosion of the steel sample was investigated using local electrochemical impedance spectroscopy (LEIS) technique. It was found that SAT-G/epoxy coating loaded with 0.5 wt.% G showed better corrosion-impeding efficiency. Corrosive components like water, chlorine, oxygen, etc. could easily penetrate the pure epoxy matrix, which indicates weak barrier property of pure epoxy matrix, vide Fig. 8.4(a), but, when 0.5 wt.% graphene was added into the epoxy matrix, the corrosion inhibition property was increased to some extent, as shown in Fig. 8.4(b). But, in case of SAT-G/epoxy composite coating, a superior anticorrosive effectiveness was observed. When electrolytic solvent comes in contact with the metallic substrate, corrosion takes place. At this time, ferric ions and electrons are generated through anodic reaction on metal surface. These as-generated electrons are captured by AT resulting the conversion of pernigraniline base to leucoemeraldine base. Concomitantly, Fe^{3+} ions are converted into Fe_2O_3 and Fe_3O_4, which produce a protective film on the underlying metal surface, in order to retard the rate of corrosion. As a result, the SAT-G/epoxy coating acted as superior composite coating to protect the Q235 steel, as shown in Fig. 8.4(c). Meanwhile, AT of leucoemeraldine base could be converted to pernigraniline base via reduction in order to generate hydroxide film, which also provide protection against corrosion. Though there is a problem regarding the agglomeration of graphene when 1 wt.% graphene was embedded within the composite coating, the self-healing ability of SAT could overcome this problem, which is represented in Fig. 8.4(d).

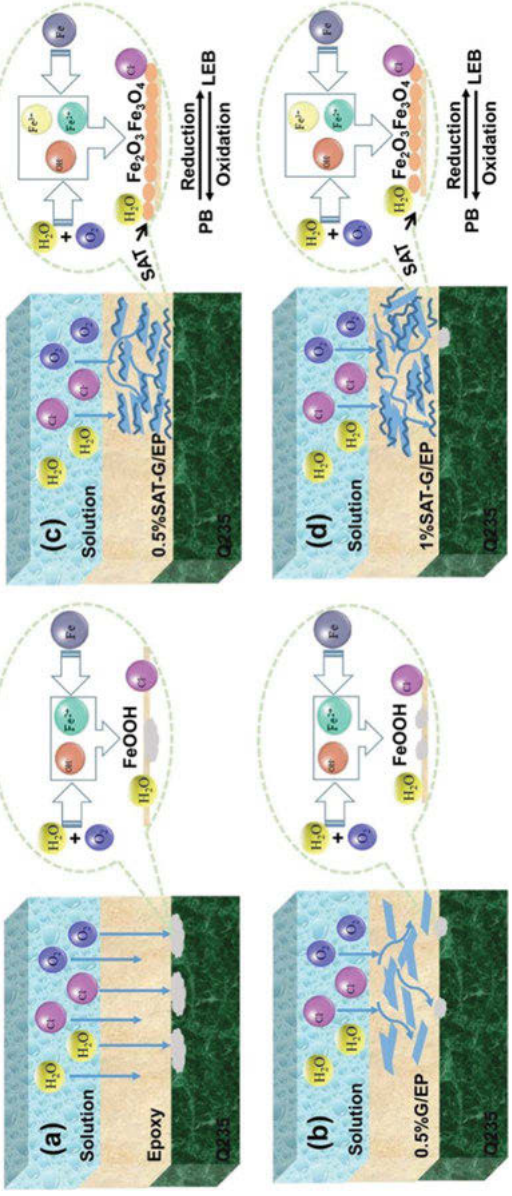

Fig. 8.4: Schematic representation of the protective performance of (a) pure epoxy coating, (b) epoxy coating reinforced with 0.5 wt.% graphene, (c) SAT-G/epoxy coating reinforced with 0.5 wt.% graphene, and (d) SAT-G/epoxy coating reinforced with 1.0 wt.% graphene (Reproduced with permission from ref. [30], Copyright © 2018 Elsevier Ltd.).

Later, this research group further synthesized functionalized graphene/epoxy composite coating, in which graphene was grafted with polyhedral oligomeric silsesquioxane (POSS) and tetra aniline (TA) [31]. This polymeric coating showed excellent corrosion resistivity along with self-healing nature. Its hydrophobic nature was revealed by contact angle measurement. After that, corrosion mitigation property was evaluated for 8-PG-BTA/EP composite coating, which was composed of porous polyhedral oligomeric 8-silsesquioxane framework reinforced within graphene sheet (8-PG) as nanocontainer and benzotriazole (BTA), encapsulated within the pores of the 8-PG to form 8-PG-BTA-made composite with the epoxy matrix (EP) [32]. Recently, in 2020, this research group synthesized functionalized carbon dots (CDs) from citric acid derivative and used it to modify graphene to form CDs-G. Then, the CDs-G was embedded in epoxy matrix to obtain a superior anti-corrosive coating formulation, namely CDs-G/EP [33]. The CDs-G/EP coating composite showed enhanced corrosion inhibition effectiveness, which was attributed to the addition of CDs with graphene as the compactness of the epoxy composite was increased, while, on the other hand, the defects within the pure epoxy coating were reduced significantly. Additionally, the incorporation of CDs facilitated the coordinative bond formation with the hetero-atoms and the Fe-atoms, resulting in self-healing nature. This self-healing property of the as-produced coating was established by scanning vibrating electrode technology (SVET) technique. The oxygen permeability coefficient was found to be high (4.27×10^{-13} cm^3 cm cm^{-2} s^{-1} Pa^{-1}), whereas, the water absorption was found to be low (~ 4.4%) for CDs-G/EP containing 0.5 wt.% CDs-G. CDs-$G_{0.5}$/EP showed efficient barrier property against corrosion, where $G_{0.5}$ represents 0.5 wt.%. of G. But, the barrier property become weaker, with addition of more weight percentage of CDs-G, that is, greater than 0.5 wt.%. Recently, Cui et al. reported a new type of hybrid polymer composite of graphene functionalized with poly(o-phenylenediamine) (Popd) reinforced in epoxy matrix [34]. Its anticorrosive effectiveness was evaluated for Q235 mild steel surface in 3.5 wt. % NaCl solution. The π-π interaction between graphene nanosheet and Ppod nanoparticles resulted in excellent adsorption of Popd nanoparticles within the graphene nanosheet, which resulted in excellent dispersion of G-Popd into epoxy matrix. It was found that G-Popd/epoxy matrix containing 0.5–1.0% of graphene showed excellent barrier property. It has been found that pure epoxy matrix provides poor barrier property; hence, the corrosive molecules or ions could easily penetrate the coating and reach to the metal surface. Consequently, electrochemical reaction starts and metallic corrosion takes place, as shown in Fig. 8.5(a). In anodic site, the Fe^{2+} is generated (anodic reaction: $Fe \rightarrow Fe^{2+} + 2e^-$), and in the cathodic site, OH^- ions are produced (cathodic reaction: $O_2 + 2H_2O + 4e^- \rightarrow 4OH^-$). These as-produced Fe^{2+} and OH^- ions further react with themselves to generate $Fe(OH)_2$. After drying, $Fe(OH)_2$ further produces $Fe(OH)_3$, which again loses water, and an amorphous FeOOH is formed. After crystallization of FeOOH, α and β-FeOOH are formed as the main products, which, in presence of water, are further reduced to Fe^{2+} species that is,

$Fe(OH)_2$, known as green rust as shown in Fig. 8.5(a). It was observed that when graphene nanosheets were added to epoxy matrix, the rate of corrosion retarded to some extent in comparison with pure epoxy coating, as shown in Fig. 8.5(b). Then, it was observed that the addition of Popd nanoparticles increased the corrosion inhibition efficiency of the as-produced SAT-G/epoxy coating. In the cathodic side, the added Popd nanoparticles, that is, Popd(ES) is reduced by taking up the electrons and then converted into Popd (LS). And, the Fe^{2+} reacts with water to produce Fe_2O_3 and Fe_3O_4, which form a passive layer on the metallic surface to prevent corrosion, as shown in Fig. 8.5(c).

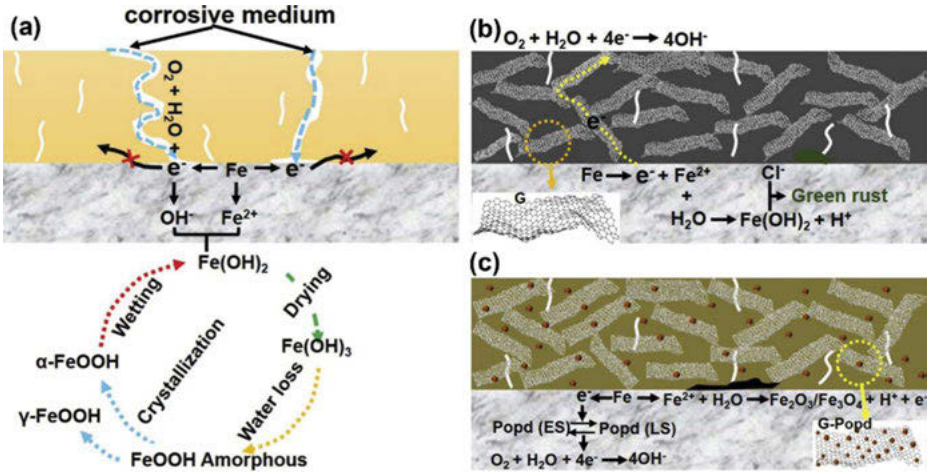

Fig. 8.5: Pictorial representation of the corrosive nature of steel in (a) pure epoxy matrix, (b) epoxy coating reinforced with graphene, and (c) G-Popd/epoxy hybrid composite coating (Reproduced with permission from ref. [34], Copyright © 2019 Elsevier Ltd.).

Recently, Wu synthesized a new waterborne polyurethane (PU)-based coating composite reinforced with sulfonated graphene (SG) and zinc phosphate (ZP) [35]. The electrochemical impedance spectroscopy (EIS) and potentiodynamic polarization (PDP) techniques proved that this as-produced coating provided superior anticorrosive property for the protection of steel surface in 3.5 wt. % NaCl solution. Lv et al. synthesized ZrO_2-encapsulated graphene micro sheet (GZ) via self-assembling and in situ hydrothermal process [36]. Subsequently, the epoxy composite with GZ was formulated. This as-produced GZ-epoxy coating exhibited excellent corrosion inhibition efficiency in highly saline medium.

Further functionalization of graphene and its use as anticorrosive materials continues. In this regard, a new maleic-anhydride functionalized graphene (MAG) embedded in epoxy, namely MAGE was formulated by Chilkoor et al. [37]. The crucial advantage of this MAG adduct was found by its excellent dispersion in epoxy matrix

through the interaction of hydroxyl and carbonyl groups present in MAG. Additionally, tensile strength and hardness of epoxy composite was increased due to the addition of MAG. Surprisingly, this polymeric composite coating provided superior barrier from the effect of sulfur-reducing bacteria, which cause degradation of the polymer through generating bio-film. From the electrochemical measurements, it was clear that the as-generated MAGE polymeric composite could provide protection to the mild steel in both abiotic and biotic conditions. Furthermore, Lin et al. revealed that the polyvinyl alcohol (PVA)-modified graphene can be loaded with cerium hydroxide inhibitor. Its incorporation into the epoxy composite showed excellent corrosion inhibition effectiveness on mild steel in saline medium [38]. Dispersibility of graphene within epoxy matrix was enhanced due to the intercalation of PVA. A new polypyrrole (Ppy)/graphene (G) composite implanted within epoxy matrix was formulated by Liu et al. [39]. It was observed that this Ppy-G polymeric coating provided effective protection of 304 stainless steel in 0.3 M H_2SO_4 mixed with 2ppm hydrofluoric acid. Li et al. modified large CeO_2 nanoflakes with graphene (Gr) and p-aminobenzoic acid (P) and synthesized waterborne acrylic polymeric composite coating Gr-P-CeO_2 [40]. It was observed that Gr-P-CeO_2 composite with 3 wt.% graphene showed effective barrier property against corrosion, as it exhibited high coating resistance along with low corrosion current and strong hydrophobicity. But, hydrophobicity decreased when 5 wt.% graphene was added, as visualized by contact angle measurement. Habibpour et al. reported graphene nanoribbon (GNR)-based polyurethane (PU) coating [41]. It was found that the addition of GNR increased the mechanical properties of the coating along with the corrosion inhibition efficiency on cold rolled steel C1018 in 3.5 wt. % NaCl solution. Similarly, corrosion inhibition effectiveness and corrosion current density were evaluated for epoxy resin embedded with graphene nanoplatelets (GNPs) by Kopsidas et al. [42]. It was found that 0.5 wt.% GNP loaded epoxy could provide superior anticorrosive efficiency. But when more than 0.5 wt.% of GNP was added to epoxy resin, conduction of corrosion increased, which facilitates more corrosion. Zhang et al. formulated a new composite coating from graphene, polyvinyl-butyral (PVB)-epoxy polymer, in which graphene was encapsulated within poly(p-phenylenediamine) (PpPD), in order to reduce its conductive nature [43]. PVB alone could not prevent the penetration of electrolytic solution, but when 0.5 wt.% graphene was encapsulated in PpPD, then the dispersibility of graphene and compactness of the matrix was enhanced. Later on, this research team made further modification on CeO_2-grafted polydopamine (PDA)-wrapped graphene-epoxy composite [44]. The addition of PDA increased the dispersibility of graphene in epoxy matrix, whereas addition of CeO_2 increased the hydrophilicity to some extent. Consequently, the corrosion inhibition property of the coating was improved synergistically, and long-term corrosion inhibition performance was obtained. Mohammed et al. reported poly [N-(pyridine-2-yl) maleamic acid] (PNPM)/graphene and graphene oxide (GO) nanocomposite, which showed excellent protection property against corrosion on low carbon steel in 3.5 wt.% NaCl medium [45]. Polymeric PNPM was synthesized by electro chemical

polymerization from N-(pyridine-2-yl) maleamic acid monomer. FTIR, SEM, AFM, and cyclic voltammetry techniques have been utilized to characterize the polymer along with the polymeric nanocomposite.

8.4 Polymer composites of graphene oxides as corrosion inhibitors

The functionalization of graphene oxide by the organic polymers has also been performed for composite synthesis for its application as anticorrosive coating. Recently, Ramezanzadeh et al. modified graphene oxide (GO) by incorporating polyisocyanate (PI) resin [46]. It was observed that the PI chains were intact with the GO surface via covalent bond formation through hydroxyl and carboxylic groups, as confirmed by XPS, TGA, and XRD data. Consequently, carbamate and ester bond formation took place there. These as-produced PI-GO nanosheets were incorporated within polyurethane (PU) matrix. From XRD analysis, it was revealed that the exfoliation of PI-GO into polyurethane matrix was enhanced. The GO surface become negatively charged when water or other nucleophiles attack the hydroxyl or carboxylic groups of GO nanosheet, as shown in Fig. 8.6(a). Accordingly, when Cl^- or OH^- ions come closer to the GO-coated surface, they are repelled due to the presence of negative charge on the coated surface. So, these anionic species could not penetrate through the coating. But, the molecules of H_2O and O_2 could penetrate normally into the GO coating. But, the diffusion of H_2O and O_2 was restricted, after the incorporation of PI into GO coating, as shown in Fig. 8.6(b). It was observed that the corrosion inhibition effectiveness of the as-synthesized polymeric coating was significantly increased after the incorporation of 0.1 wt.% of PI-GO into the PU matrix.

Later, this research group provided a new strategy in order to provide zinc-rich epoxy composite (ZRC) coating with excellent cathodic protection efficiency [47]. Accordingly, polyaniline (PANI) was grafted within GO nanosheet through in situ polymerization, as shown in Fig. 8.7. Expandable graphite (EG) was used to synthesize GO through modified Hummer's process. After that, aniline monomers were added to GO in 1 M HCl solvent and stirred to obtain GO-PANI nanosheet. During this reaction, aniline attacks the oxygen of the epoxy ring. Then, the ring opening followed by C = C formation takes place. In this way, in situ polymerization proceeds. Highly crystalline and conductive nature of the PANI grown on GO surface was depicted by FT-IR, XRD, and high resolution-transmittance electron microscopy (HR-TEM) analyses. It was observed that the incorporation of 0.1 wt. % of GO and GO-PANI nanosheets within ZRC matrix could enhance the barrier property of the ZRC against corrosion. Oxidation of Zn particles could be diminished due to the addition of PANI. Salt spray analysis, open circuit potential (OCP), and EIS were executed to understand the anticorrosive efficiency of the as-produced GO-PANI-ZRC in 3.5 wt.% NaCl solution for a long time.

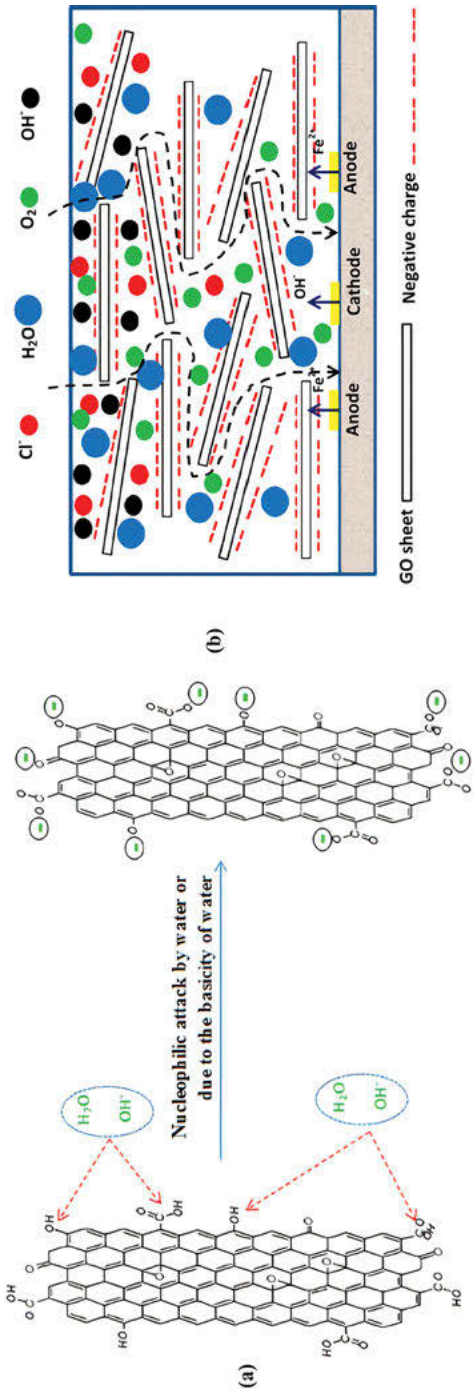

Fig. 8.6: Pictorial representation of (a) nucleophilic attack on the GO surface by water or other basic substance and (b) protective nature of the coating from the harsh saline medium (Reproduced with permission from ref. [46], Copyright © 2013 Elsevier Ltd.).

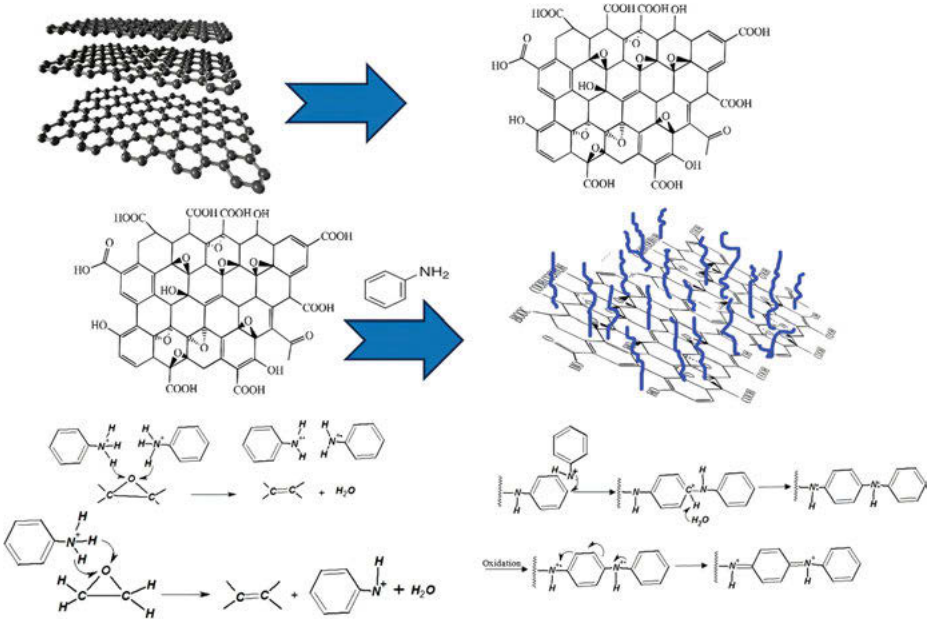

Fig. 8.7: Schematic representation of synthesis of GO and in situ polymerization of PANI on GO (Reproduced with permission from ref. [47], Copyright © 2016 Elsevier Ltd.).

In 2018, this research group further modified GO with polyaniline-cerium oxide (PAni-CeO_2), and it was reinforced into epoxy matrix to obtain a new type of polymeric composite coating [48]. FTIR, TGA, XPS, XRD, UV-Visible spectroscopy, and FE-SEM were used for characterization of the composite. Emeraldine form of polyaniline was used for this study. When electrolytic solution reaches the metal surface, the Fe losses electrons to generate ferric and/or ferrous cations, which further converted into Fe_2O_3. Water is converted into OH^- anions, which react with $Ce(OH)_2^{2+}$. Consequently, CeO_2 and $Ce(OH)_2$ are generated, and a passive layer is formed on the Fe surface, which hinders the cathodic as well as the anodic sites, as shown in Fig. 8.8.

Xia et al. reported a new type of functional graphene oxide/epoxy nanocomposite coating (GEP) for the protection of metals in nuclear industry [49]. In general, epoxy coatings get damaged by the gamma irradiation. But, the incorporation of small amount of GO (0.25 wt.%) within the epoxy matrix, that is, as-synthesized GEP nanocomposite exhibited significant radical scavenger behavior as established by electron spin resonance study. GO was functionalized with γ-(2,3- epoxypropoxy) propytrimethoxysilane (EPTES), and it was found that the dispersibility of functionalized GO in epoxy matrix was more significant than that of GO, as shown in Fig. 8.9. This EPTES-functionalized GO reinforced within epoxy matrix exhibited superior anticorrosive effectiveness, as established by PDP and EIS studies.

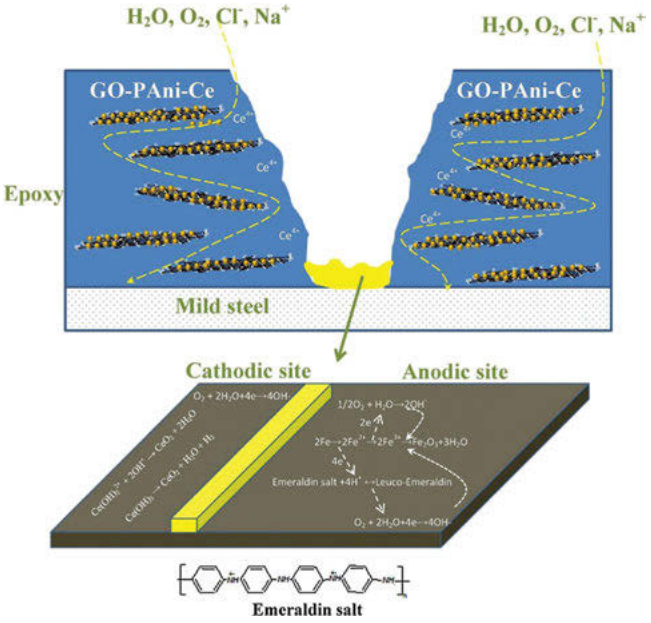

Fig. 8.8: Schematic illustration of the corrosion inhibition mechanism of PAni-CeO_2-epoxy composite coating (Reproduced with permission from ref. [48], Copyright © 2018 Elsevier B. V.).

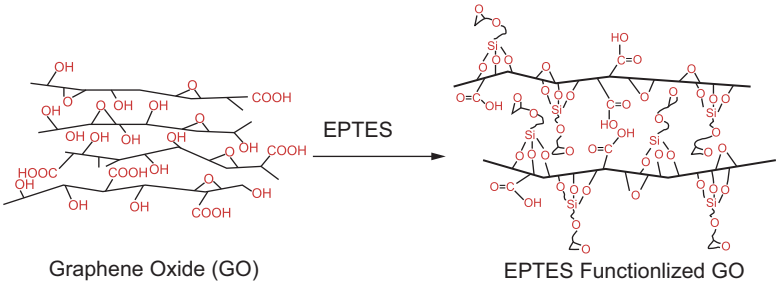

Fig. 8.9: Pictorial representation of functionalization of GO with EPTES (Reproduced with permission from ref. [49], Copyright © 2016 Elsevier Ltd.).

A new type of biopolymer chitosan (CS)-based GO modified with oleic acid (OA) nanocomposite was synthesized by Fayyad et al. [50]. This work highlighted the excellent compatible nature of GO with CS polymer, and use of GO could hinder the permeability of oxygen through the coating. Thus, this as-produced coating exhibited superior anticorrosive nature, along with strong hydrophobicity for the protection of carbon steel surface, in the presence of highly saline medium. Corrosion inhibition efficiency of CS/GO-OA was found to be 100-fold greater than pure CS coating. Di et al. reported GO–zirconia dioxide (ZrO_2)/epoxy composite [51]. FE-SEM, TEM, EDS,

XRD, XPS, and FTIR studies were performed. This polymeric composite coating exhibited superior barrier property, along with specific surface coverage, and thereby, excellent anti-corrosive performance was achieved. Zheng et al. reported epoxy composite coating reinforced with graphene oxide–poly(urea–formaldehyde), through in situ polycondensation [52]. SEM, TEM, FTIR, XRD, and EIS were used for characterization. This as-synthesized composite coating showed excellent corrosion resistance property for carbon steel surface, in presence of 3.5 wt.% NaCl solution. This research group further modified this composite coating by increasing the dispersion of GO sheets. It was found that 8.6 wt.% GO nanosheets-incorporated composite coating exhibited significant corrosion inhibition efficiency [53]. Nikpour et al. fabricated epoxy composite with GO nanosheets functionalized by *Urtica Dioica* (UD) leaf extract [54]. It was observed that at pH-2, this GO-UD showed excellent corrosion inhibition efficiency, whereas at neutral condition, it showed moderate corrosion resistance efficacy. The protection efficacy increased with the addition of zinc cations, since these zinc cations lead to the formation of zinc hydroxide film on the metal surface as well as give rise to chelation formation with UD molecules. Consequently, the rate of both the cathodic and anodic reactions was retarded. DFT analysis confirmed theoretically that the polymeric composite coating gets adsorbed on metal surface via physisorption and chemisorption. The adsorption became facile when the inhibitor got protonated. Again, the pulse current co-deposition technology was used to synthesize polyaniline (PANI)-GO composite coating by Qiu et al. [55]. Higher hydrophobicity and lower porosity of this composite made it an excellent anticorrosive coating. Corrosion inhibition efficiency was found to be 98.4%, while protection efficiency of this PANI-GO coating was found to be 99.3%. Pourhashem et al. studied the corrosion inhibition performance of epoxy coating filled with functionalized GO nanosheets [56]. GO nanosheets were functionalized with 3-aminopropyl triethoxysilane (APTES) and 3-glysidyloxypropyl trimethoxysilane (GPTMS) to produce A-GO and G-GO respectively, as represented in Fig. 8.10(a). As a result of functionalization of GO, the adhesion property of the composite onto the metal surface along with the contact angle of the coated surface increased significantly. When pure epoxy is used, the corrosive electrolyte could penetrate easily due to the poor barrier nature of epoxy, as shown in Fig. 8.10(b). When GO is added to pure epoxy, GO forms bonds with metal surface through oxygen. Consequently, the penetration of electrolytic solvent through the coating is reduced, as shown in Fig. 8.10(c). After the addition of silane-functionalized agents in GO, O-Si-O linkages help in adhesion of the composite, in a more facile way. As a result, contact angle of the surface is increased and electrolytes could not penetrate so easily, as shown in Fig. 8.10(d). The OCP values become more positive when functionalized GO-epoxy coatings were used than that of bare steel, while A-GO showed more positive OCP than that of G-GO. These results indicated better corrosion inhibition efficiency of A-GO than that of G-GO.

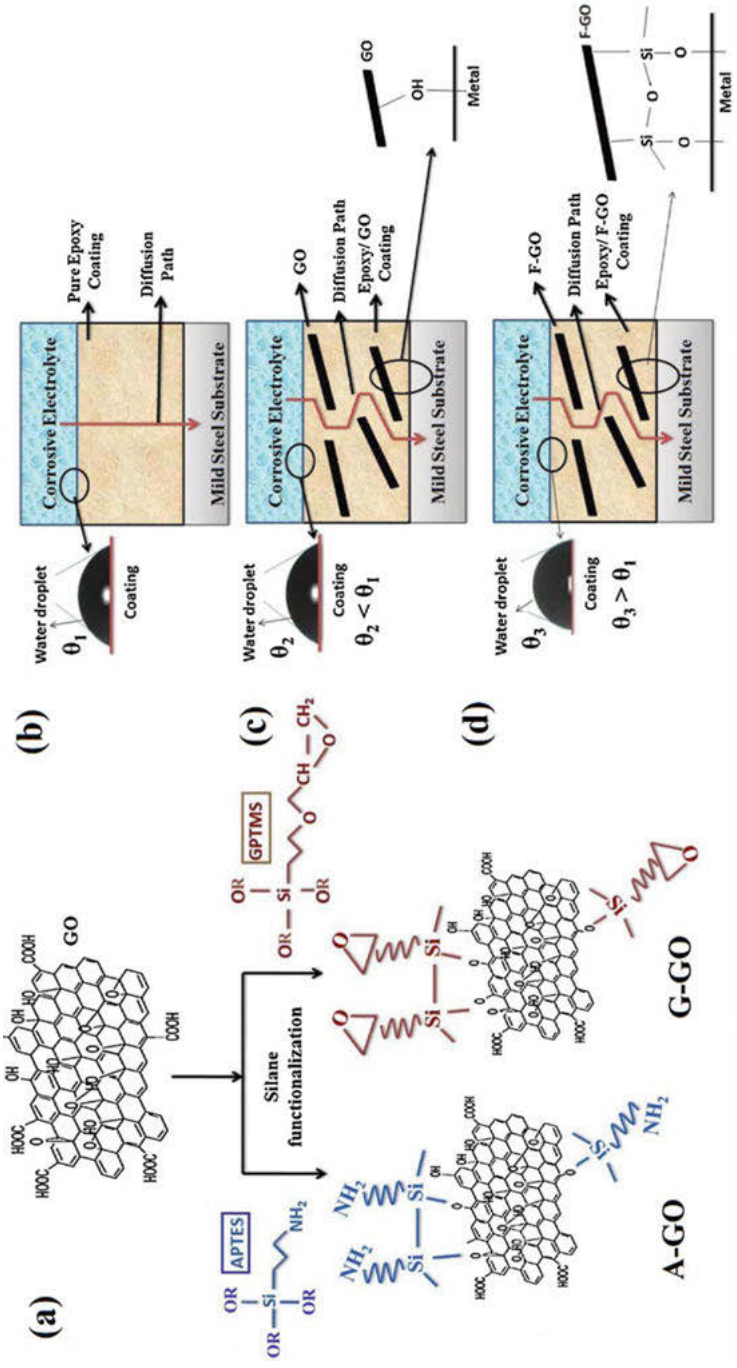

Fig. 8.10: Pictorial representation of (a) functionalization of GO with APTES and GPTMS, contact angle and penetration of electrolytes through (b) pure epoxy coating, (c) GO/epoxy coating and (d) epoxy-functionalized GO composite coating (Reproduced with permission from ref. [56], Copyright © 2017 Elsevier Ltd.).

This research team further modified GO using tetraethyl orthosilicate (TEOS), and its composite with epoxy exhibited excellent corrosive impeding nature on mild steel, in presence of highly saline medium [57]. SiO_2-GO nanocomposite was synthesized in a facile one-step process involving hydrolysis and polycondensation reactions, as shown in Fig. 8.11. XRD, Raman, FTIR, FE-SEM, and AFM results established that SiO_2 nanospheres covered the GO surface via covalent bond formation. Due to the formation of cross-linkage of silane functionality through electrolyte diffusion, the as-produced coating material becomes denser, which further retards the rate of corrosion. Incorporation of minimum amount of hybrid composite, that is, 0.1 wt.%-functionalized GO within epoxy matrix resulted a significantly enhanced corrosion inhibition efficacy, as revealed by EIS, PDP, and salt spray analysis. It was found that corrosion resistance property of the as-produced composite coating was enhanced with increasing immersion time.

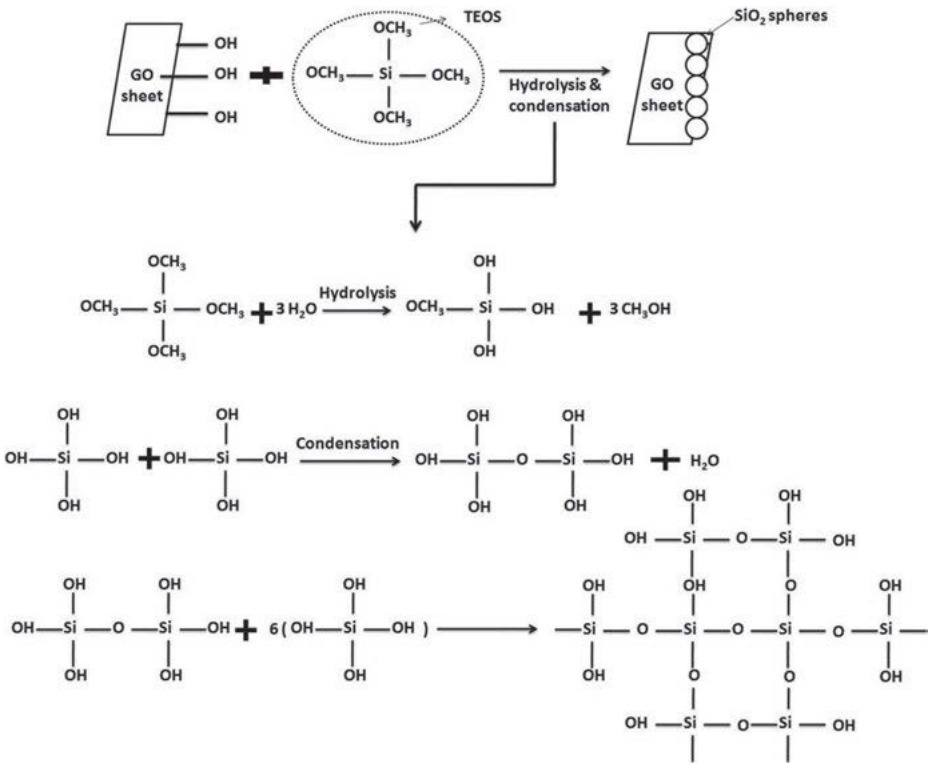

Fig. 8.11: Schematic representation of the synthetic route of GO-SiO_2 nanocomposite (Reproduced with permission from ref. [57], Copyright © 2017 Elsevier Ltd.).

Li et al. reported boric acid (BA)-induced cross-linked poly(vinyl alcohol-co-ethylene) (EVOH)/grafted GO nanocomposite, which provided superior gas-barrier and anticorrosive property [58]. XRD, FTIR, and XPS studies revealed the cross-linkage network between BA, EVOH, and GO within the as-synthesized composite coating. Contact angle measurement was analyzed for the coated steel surface. It was found that the contact angle of pure EVOH-coated steel surface showed contact angle value of 88.1°, while EVOH/BA/GO-coated surface exhibited an increase in the contact angle value. Additionally, it was also found that the contact angle value increased with addition of BA. EVOH/BA/GO composite coating containing 5 wt.% GO and 15 wt.% BA showed maximum contact angle value of 107°, as shown in Fig. 8.12(a). The wettability of the surface became weaker with increasing the amount of BA, that is, with increasing cross-linkage formation. From Tafel and EIS plots, as shown in Fig. 8.12(b, c), respectively, it can be seen that with the increase in the amount of BA, the corrosion current density decreases and impedance increases. The corrosion potential (E_{corr}) value of the coated sample shifted from −280 mV to −102 mV, with the addition of BA. That is, the anticorrosive performance of the as-produced coating increased with the increased amount of BA.

Cui et al. reported polydopamine (PDA)-functionalized GO with eco-friendly waterborne epoxy composite coating, which showed excellent corrosion inhibition efficacy on Q235 carbon steel, in highly saline medium [59]. Mohammadi et al. synthesized *p-tert*-butyl calix[4]arene (BC4A)-modified GO and sodium *p*-sulfonatocalix[4]arene (SC4A)-modified GO to obtain CGO and SGO polymeric composite coatings, respectively (Fig. 8.13) and embedded these in waterborne polyurethane (WPU) matrix, separately [60]. It was observed that after the modification of GO, several benefits were achieved, such as, (i) the dispersibility of GO within WPU matrix was enhanced after modification, that is, coagulation and flocculation problems were solved, (ii) mechanical properties of the composite coating was enhanced after modification, and (iii) adhesion property of the as-synthesized composite enhanced, while CGO-WPU showed better adhesion property than SGO-WPU, thereby increasing the anticorrosive effectiveness. This green coating exhibited 99.8% inhibition efficiency on mild steel in 3.5 wt.% NaCl solution.

Similarly, 1 H-benzimidazole (BIM) corrosion inhibitor-modified GO nanosheets (GO-BIM) incorporated within EPIRAN-01 X-75 epoxy resin was synthesized by Kasaeian et al. [61]. It was reported that 0.1 wt.% GO-BIM incorporated in epoxy composite exhibited superior barrier property. BIM molecules get adsorbed on GO sheets *via* π-π interactions, hydrogen bonding, and/or electrostatic forces. Whenever corrosive solution reaches the metallic surface, corrosive species creates defects on the coating and negatively charged ions get adsorbed on the metallic surface, BIM molecules are released, and get protonated. These protonated BIM molecules get adsorbed on the negatively charged metallic surface and give superior protection against corrosion, as established by EIS. It has been found that the adsorption capability as well as the protective nature of BIM significantly depends upon the pH. At pH = 1, the π-π

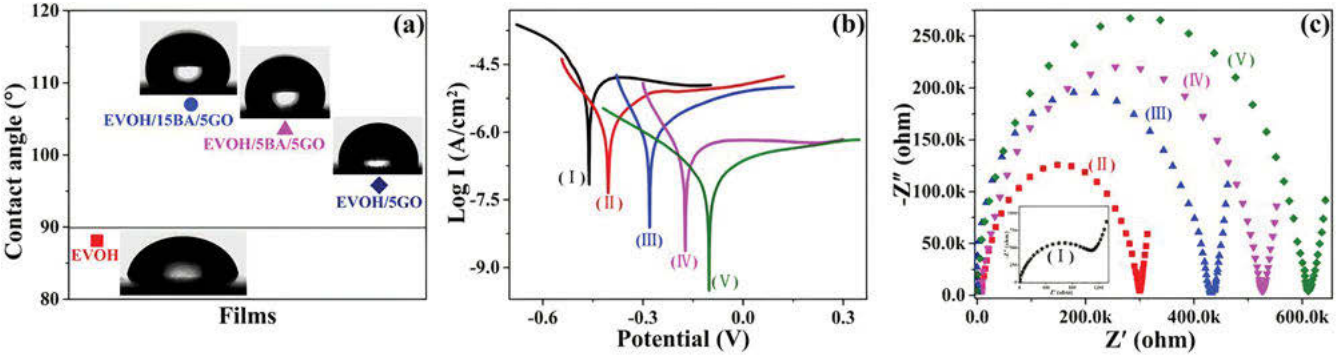

Fig. 8.12: Pictorial representation of (a) contact angle values, (b) Tafel slopes, and (c) Nyquist plots of (I) bare steel sample, (II) EVOH-coated steel, (III) EVOH/BA/GO (containing 5 wt.% GO and 5 wt.% BA) coated steel, (IV) EVOH/BA/GO (containing 5 wt.% GO and 10 wt.% BA)-coated steel, and (V) EVOH/BA/GO (containing 5 wt.% GO and 15 wt.% BA)-coated steel, (Reproduced with permission from ref. [58], Copyright © 2018 Elsevier Ltd.).

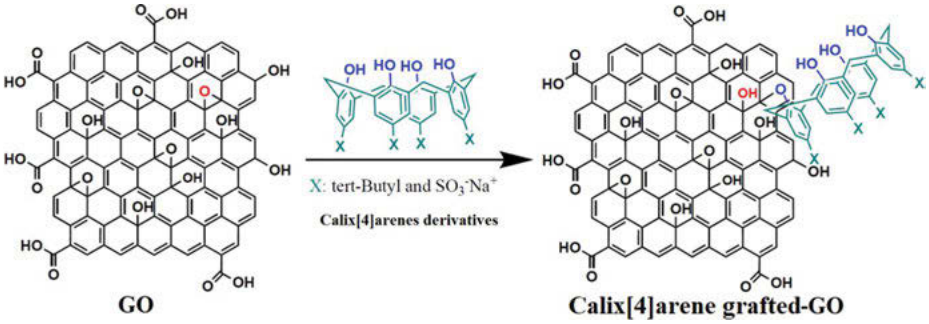

Fig. 8.13: Schematic representation of calix[4]arene grafted GO synthesis (Reproduced with permission from ref. [60], Copyright © 2018 Elsevier B. V.).

interactions predominates between GO and protonated BIM molecules, but at pH = 3, that is, at the optimum pH, electrostatic interactions facilitate the adsorption of BIM on GO. Accordingly, at pH = 3, the GO-BIM provides superior corrosion inhibition efficiency. The protonated BIM forms coordinate bonds as BIM contains electron that reach N-atom, which donates its lone pair of electrons to the empty orbitals of the Fe-metal, and BIM-Fe^{2+} is formed. Thus, this composite coating provided long term corrosion protection effectiveness. Similarly, Parhizkar et al. incorporated cerium nanofillers into GO that was composed of epoxy matrix in order to improve the cathodic disbonding, adhesive nature, and corrosion inhibition effectiveness [62]. The GO was grafted with 3-Aminopropyl triethoxysilane (APTES) to obtain AGO, which nicely adsorbed on Fe surface via Si-O-Fe- and/or -Si-O-Si-covalent bond formation. Additionally, excellent hydrophobicity was exhibited by Ce-AGO coating. This group further modified GO with zinc cations and polyaniline (PAni) [63]. In this case, the cathodic site of corrosion reaction is blocked due to the formation of Zn $(OH)_2$. Again, the anodic sites are blocked by the dense layer formation by the PAni-GO containing metal oxides. Electrostatic interactions and cation-π interactions are feasible between zinc cations and emeraldine forms of PAni. Zhou et al. revealed the grafting polyaniline (PANI) within GO via in situ modulation and incorporated it within waterborne epoxy matrix to obtain a superior anticorrosive coating, with effective water barrier property [64]. Raman, XRD, XPS, TEM, and SEM studies were analyzed for characterization, whereas, EIS and salt spray studies were executed to elucidate the corrosion inhibition effectiveness.

8.5 Summary and outlook

The superior anticorrosive properties of polymeric composite of graphene and graphene oxides have been discussed in this chapter. In addition to it, the synthetic

procedure, adhesion properties, and anticorrosive mechanism have been elucidated nicely. The π-π interactions and electrostatic interactions capability of the graphene and GO within the coating matrix (such as epoxy, polyurethanes, polyanilines, nylon, and bio-polymer) have made their incorporation in the coating formulation possible. The presence of such interactions facilitates good adhesion onto the targeted metal surface. The presence of hydrophobic nature of graphene and GO hinder the penetration of several corrosive species within the coating towards the metal surface atoms. The large surface coverage and densely packed morphology of the as-synthesized polymeric composites containing graphene and GO have made them useful as superior anticorrosive and impermeable composite materials.

In future, the advanced multifunctionalities incorporation into the graphene and GO-based polymeric composites are expected to provide more effective barrier property and remarkably impede the rate of corrosion. Additionally, the incorporation of extreme thermal stability, flame retardancy, and super-hydrophobicity, along with desired mechanical and tribological properties might be explored. A superior techno-economic support as well as a "next generation solution" in the field of corrosion mitigation for several types of metals and metallic alloys is supposed to be achieved by further investigation and synthesis of hitherto unexplored polymeric composites of graphene and GO.

References

[1] Saha, S.K.; Murmu, M.; Murmu, N.C.; Obot, I.B.; Banerjee, P. Molecular level insights for the corrosion inhibition effectiveness of three amine derivatives on the carbon steel surface in the adverse medium: A combined density functional theory and molecular dynamics simulation study. Surf. Interfaces. 2018, 10, 65–73, doi:https://doi.org/10.1016/j.surfin.2017.11.007.

[2] Tripathy, D.B.; Murmu, M.; Banerjee, P.; Quraishi, M.A. Palmitic acid based environmentally benign corrosion inhibiting formulation useful during acid cleansing process in MSF desalination plants. Desalination. 2019, 472, 114128, doi:10.1016/j.desal.2019.114128.

[3] Murmu, M.; Saha, S.K.; Murmu, N.C.; Banerjee, P. Effect of stereochemical conformation into the corrosion inhibitive behaviour of double azomethine based Schiff bases on mild steel surface in 1 mol L–1 HCl medium: An experimental, density functional theory and molecular dynamics simulation study. Corros. Sci. 2019, 146, 134–151, doi:http://doi.org/10.1016/j.corsci.2018.10.002.

[4] Sastri, V.S. Challenges in corrosion: Costs, causes, consequences and control, John Wiley & Sons, 2015, ISBN: 9781118522103.

[5] Li, Y.; Yang, H.; Wang, Y.H.; Wang, F. Superior anticorrosion performance of epoxy based composites with well-dispersed melamine modified graphene oxide. J. Appl. Polym. Sci. 2020, 138, 1–14, doi:https://doi.org/10.1002/app.49866.

[6] Mahato, P.; Banerjee, P.; Murmu, M.; Hirani, H.; Murmu, N.C.; Mishra, S.K. Investigation on multifunctional properties of sputtered Ti-Si-B-C coating with varied thickness over targeted surface. J. Mater. Eng. Perform. 2021, 30, 4432–4444, doi:https://doi.org/10.1007/s11665-021-05633-3.

[7] Verma, C.; Ebenso, E.E.; Quraishi, M.A. Ionic liquids as green and sustainable corrosion inhibitors for metals and alloys: An overview. J. Mol. Liq. 2017, 233, 403–414, doi:http://dx.doi.org/10.1016/j.molliq.2017.02.111.

[8] Nine, M.J.; Cole, M.A.; Tran, D.N.H.; Losic, D. Graphene: A multipurpose material for protective coatings. J. Mater. Chem. A. 2015, 3, 12580–12602, doi:https://doi.org/10.1039/C5TA01010A.

[9] Umoren, S.A.; Solomon, M.M.; Saji, V.S. Corrosion inhibitors in the oil and gas industry, Wiley-VCH Verlag GmbH & Co. KGaA, 2020, 229, ISBN: 978-3-527-34618-9.

[10] Novakovic, J.; Vassiliou, P. Vacuum thermal treated electroless NiP – TiO_2 composite coatings. Electrochim. Acta. 2009, 54, 2499–2503, doi:https://doi.org/10.1016/j.electacta.2008.12.015.

[11] Aubert, A.; Danroc, J.; Gaucher, A.; Terrat, J.P. Hard chrome and molybdenum coatings produced by physical vapor deposition. Thin Solid Films. 1985, 126, 61–67, doi:https://doi.org/10.1016/0040-6090(85.

[12] Chauhan, D.S.; Quraishi, M.A.; Ansari, K.R.; Saleh, T.A. Graphene and graphene oxide as new class of materials for corrosion control and protection: Present status and future scenario. Prog. Org. Coat. 2020, 147, 105741, doi:https://doi.org/10.1016/j.porgcoat.2020.105741.

[13] Amirazodi, K.; Sharif, M.; Bahrani, M. Polypyrrole doped graphene oxide reinforced epoxy nanocomposite with advanced properties for coatings of mild steel. J. Polym. Res. 2019, 26, 244, doi:https://doi.org/10.1007/s10965-019-1905-3.

[14] Zhu, Q.; Huang, Y.; Li, Y.; Zhou, M.; Xu, S.; Liu, X.; Liu, C.; Yuan, B.; Guo, Z. Aluminum dihydric tripolyphosphate/polypyrrole-functionalized graphene oxide waterborne epoxy composite coatings for impermeability and corrosion protection performance of metals. Adv. Compos. Hybrid Mater. 2021, 4, 780–792, doi:https://doi.org/10.1007/s42114-021-00265-6.

[15] Murmu, M.; Saha, S.K.; Murmu, N.C.; Banerjee, P. Amine cured double Schiff base epoxy as efficient anticorrosive coating materials for protection of mild steel in 3.5% NaCl medium. J. Mol. Liq. 2019, 278, 521–535, doi:https://doi.org/10.1016/j.molliq.2019.01.066.

[16] Lee, X.J.; Zhang, H.B.Y.; Lai, K.C.; Lee, L.Y.; Gan, S.; Gopakumar, S.T.; Rigby, S. Review on graphene and its derivatives: Synthesis methods and potential industrial implementation. J. Taiwan Inst. Chem. Eng. 2019, 98, 163–180, doi:https://doi.org/10.1016/j.jtice.2018.10.028.

[17] Geim, A.K.; Novoselov, K.S. The rise of graphene, nanoscience and technology: A collection of reviews from nature journals. World Sci. 2009, 11–19, doi:https://doi.org/10.1142/9789814287005_0002.

[18] Singh, V.; Joung, D.; Zhai, L.; Das, S.; Khondaker, S.I.; Seal, S. Graphene based materials: Past, present and future. Prog. Mater. Sci. 2011, 56, 1178–1271, doi:http://dx.doi.org/10.1016/j.pmatsci.2011.03.003.

[19] Kirkland, N.; Schiller, T.; Medhekar, N.; Birbilis, N. Exploring graphene as a corrosion protection barrier. Corros. Sci. 2012, 56, 1–4, doi:http://dx.doi.org/10.1016/j.corsci.2011.12.003.

[20] Yu, L.; Lim, Y.-S.; Han, J.H.; Kim, K.; Kim, J.Y.; Choi, S.-Y.; Shin, K. A graphene oxide oxygen barrier film deposited via a self-assembly coating method. Synth. Met. 2012, 162, 710–714, doi:https://doi.org/10.1016/j.synthmet.2012.02.016.

[21] Zhao, C.; Xu, X.; Chen, J.; Yang, F. Effect of graphene oxide concentration on the morphologies and antifouling properties of PVDF ultrafiltration membranes. *J. Environ. Chem. Eng*. 2013, 1, 349–354, doi:https://doi.org/10.1016/j.jece.2013.05.014.

[22] George, J.S.; Vijayan P, P.; Paduvilan, J.K.; Salim, N.; Sunarso, J.; Kalarikkal, N.; Hameed, N.; Thomas, S. Advances and future outlook in epoxy/graphene composites for anticorrosive

applications. Prog. Org. Coat. 2022, 162, 106571, doi:https://doi.org/10.1016/j.porgcoat.2021.106571.
[23] Chang, K.-C.; Hsu, M.-H.; Lu, H.-I.; Lai, M.-C.; Liu, P.-J.; Hsu, C.-H.; Ji, W.-F.; Chuang, T.-L.; Wei, Y.; Yeh, J.-M.; Liu, W.-R. Room-temperature cured hydrophobic epoxy/graphene composites as corrosion inhibitor for cold-rolled steel. Carbon. 2014, 66, 144–153, doi:http://dx.doi.org/10.1016/j.carbon.2013.08.052.
[24] Alam, R.; Mobin, M.; Aslam, J. Polypyrrole/graphene nanosheets/rare earth ions/dodecyl benzene sulfonic acid nanocomposite as a highly effective anticorrosive coating. Surf. Coat. Technol. 2016, 307, 382–391, doi:http://dx.doi.org/10.1016/j.surfcoat.2016.09.010.
[25] Chen, C.; Qiu, S.; Cui, M.; Qin, S.; Yan, G.; Zhao, H.; Wang, L.; Xue, Q. Achieving high performance corrosion and wear resistant epoxy coatings via incorporation of noncovalent functionalized graphene. Carbon. 2017, 114, 356–366, doi:http://dx.doi.org/10.1016/j.carbon.2016.12.044.
[26] Pourhashem, S.; Rashidi, A.; Vaezi, M.R.; Yousefian, Z.; Ghasemy, E. The effect of polycrystalline graphene on corrosion protection performance of solvent based epoxy coatings: Experimental and DFT studies. J. Alloys Compd. 2018, 764, 530–539, doi:https://doi.org/10.1016/j.jallcom.2018.06.087.
[27] Xu, H.; Zang, J.; Yuan, Y.; Tian, P.; Wang, Y. In situ preparation of graphene coating bonded to stainless steel substrate via Cr-C bonding for excellent anticorrosion and wear resistant. Appl. Surf. Sci. 2019, 492, 199–208, doi:https://doi.org/10.1016/j.apsusc.2019.06.197.
[28] Xu, H.; Zang, J.; Yuan, Y.; Tian, P.; Wang, Y. Preparation of multilayer graphene coatings with interfacial bond to mild steel via covalent bonding for high performance anticorrosion and wear resistance. Carbon. 2019, 154, 156–168, doi:https://doi.org/10.1016/j.carbon.2019.07.097.
[29] Xu, H.; Zang, J.; Yuan, Y.; Tian, P.; Wang, Y. Fabrication of graphene coating bonded to mild steel via covalent bonding for high anticorrosion performance. J. Alloys Compd. 2019, 805, 967–976, doi:https://doi.org/10.1016/j.jallcom.2019.07.159.
[30] Ye, Y.; Zhang, D.; Liu, T.; Liu, Z.; Pu, J.; Liu, W.; Zhao, H.; Li, X.; Wang, L. Superior corrosion resistance and self-healable epoxy coating pigmented with silanziedtrianiline-intercalated graphene. Carbon. 2019, 142, 164–176, doi:https://doi.org/10.1016/j.carbon.2018.10.050.
[31] Ye, Y.; Yang, D.; Zhang, D.; Chen, H.; Zhao, H.; Li, X.; Wang, L. POSS-tetra aniline modified graphene for active corrosion protection of epoxy-based organic coating. Chem. Eng. J. 2020, 383, 123160, doi:https://doi.org/10.1016/j.cej.2019.123160.
[32] Ye, Y.; Chen, H.; Zou, Y.; Ye, Y.; Zhao, H. Corrosion protective mechanism of smart graphene-based self-healing coating on carbon steel. Corros. Sci. 2020, 174, 108825, doi:https://doi.org/10.1016/j.corsci.2020.108825.
[33] Ye, Y.; Chen, H.; Zou, Y.; Zhao, H. Study on self-healing and corrosion resistance behaviors of functionalized carbon dot-intercalated graphene-based waterborne epoxy coating. J. Mater. Sci. Technol. 2021, 67, 226–236, doi:DOI: https://doi.org/10.1016/j.jmst.2020.06.023.
[34] Cui, M.; Ren, S.; Pu, J.; Wang, Y.; Zhao, H.; Wang, L. Poly(o-phenylenediamine) modified graphene toward the reinforcement in corrosion protection of epoxy coatings. Corros. Sci. 2019, 159, 108131, doi:https://doi.org/10.1016/j.corsci.2019.108131.
[35] Wu, Y.; Wen, S.; Chen, K.; Wang, J.; Wang, G.; Sun, K. Enhanced corrosion resistance of waterborne polyurethane containing sulfonated graphene/zinc phosphate composites. Prog. Org. Coat. 2019, 132, 409–416, doi:https://doi.org/10.1016/j.porgcoat.2019.04.013.
[36] Lv, X.; Li, X.; Li, N.; Zhang, H.; Zheng, Y.-Z.; Wu, J.; Tao, X. ZrO_2 nanoparticle encapsulation of graphene microsheets for enhancing anticorrosion performance of epoxy coatings. Surf. Coat. Technol. 2019, 358, 443–451, doi:https://doi.org/10.1016/j.surfcoat.2018.11.045.

[37] Chilkoor, G.; Sarde, R.; Islam, J.; ArunKumar, K.E.; Ratnayake, I.; Star, S.; Jasthi, B.K.; Sereda, G.; Koratkar, N.; Meyyappan, M.; Gadhamshetty, V. Maleic anhydride-functionalized graphene nanofillers render epoxy coatings highly resistant to corrosion and microbial attack. Carbon. 2020, 159, 586–597, doi:https://doi.org/10.1016/j.carbon.2019.12.059.
[38] Lin, Y.; Chen, R.; Zhang, Y.; Lin, Z.; Liu, Q.; Liu, J.; Wang, Y.; Gao, L.; Wang, J. Sandwich-like polyvinyl alcohol (PVA) grafted graphene: A solid-inhibitors container for long term self-healing coatings. Chem. Eng. J. 2020, 383, 123203, doi:https://doi.org/10.1016/j.cej.2019.123203.
[39] Liu, S.; Pan, T.J.; Wang, R.F.; Yue, Y.; Shen, J. Anti-corrosion and conductivity of the electrodeposited graphene/polypyrrole composite coating for metallic bipolar plates. Prog. Org. Coat. 2019, 136, 105237, doi:https://doi.org/10.1016/j.porgcoat.2019.105237.
[40] Li, H.; Wang, J.; Yang, J.; Zhang, J.; Ding, H. Large CeO2 nanoflakes modified by graphene as barriers in waterborne acrylic coatings and the improved anticorrosion performance. Prog. Org. Coat. 2020, 143, 105607, doi:https://doi.org/10.1016/j.porgcoat.2020.105607.
[41] Habibpour, S.; Um, J.G.; Jun, Y.-S.; Bhargava, P.; Park, C.B.; Yu, A. Structural impact of graphene nanoribbon on mechanical properties and anti-corrosion performance of polyurethane nanocomposites. Chem. Eng. J. 2021, 405, 126858, doi:https://doi.org/10.1016/j.cej.2020.126858.
[42] Kopsidas, S.; Olowojoba, G.B.; Kinloch, A.J.; Taylor, A.C. Examining the effect of graphene nanoplatelets on the corrosion resistance of epoxy coatings. Int. J. Adhes. Adhes. 2021, 104, 102723, doi:https://doi.org/10.1016/j.ijadhadh.2020.102723.
[43] Zhang, J.; Zhang, X.; Zheng, Y. Synthesis of poly(p-phenylenediamine) encapsulated graphene and its application in steel protection. Prog. Org. Coat. 2021, 158, 106330, doi:https://doi.org/10.1016/j.porgcoat.2021.106330.
[44] Zhang, J.; Zheng, Y. CeO2 grafted polydopamine-wrapped graphene to enhance corrosion resistance of coated steel. Prog. Org. Coat. 2022, 164, 106698, doi:https://doi.org/10.1016/j.porgcoat.2021.106698.
[45] Mohammed, R.A.; Saleh, K.A. Advanced anticorrosive coating prepared from poly [N-(Pyridine-2-yl) maleamic acid]/graphene derivatives nanocomposites. Mater. Today: Proc. doi:https://doi.org/10.1016/j.matpr.2021.09.041.
[46] Ramezanzadeh, B.; Ghasemi, E.; Mahdavian, M.; Changizi, E.; Moghadam, M.H.M. Covalently-grafted graphene oxide nanosheets to improve barrier and corrosion protection properties of polyurethane coatings. Carbon. 2015, 93, 555–573, doi:http://dx.doi.org/10.1016/j.carbon.2015.05.094.
[47] Ramezanzadeh, B.; Moghadam, M.H.M.; Shohani, N.; Mahdavian, M. Effects of highly crystalline and conductive polyaniline/graphene oxide composites on the corrosion protection performance of a zinc-rich epoxy coating. Chem. Eng. J. 2017, 320, 363–375, doi:http://dx.doi.org/10.1016/j.cej.2017.03.061.
[48] Ramezanzadeh, B.; Bahlakeh, G.; Ramezanzadeh, M. Polyaniline-cerium oxide (PAni-CeO_2) coated graphene oxide for enhancement of epoxy coating corrosion protection performance on mild steel. Corros. Sci. 2018, 137, 111–126, doi:https://doi.org/10.1016/j.corsci.2018.03.038.
[49] Xia, W.; Xue, H.; Wang, J.; Wang, T.; Song, L.; Guo, H.; Fan, X.; Gong, H.; He, J. Functionalized graphene serving as free radical scavenger and corrosion protection in gamma-irradiated epoxy composites. Carbon. 2016, 101, 315–323, doi:http://dx.doi.org/10.1016/j.carbon.2016.02.004.
[50] Fayyad, E.M.; Sadasivuni, K.K.; Ponnamma, D.; Maadeed, M.A.A. Oleic acid-grafted chitosan/graphene oxide composite coating for corrosion protection of carbon steel. Carbohydr. Polym. 2016, 151, 871–878, http://dx.doi.org/doi:10.1016/j.carbpol.2016.06.001.

[51] Di, H.; Yu, Z.; Ma, Y.; Zhang, C.; Li, F.; Lv, L.; Pan, Y.; Shi, H.; He, Y. Corrosion-resistant hybrid coatings based on graphene oxide–zirconia dioxide/epoxy system. J. Taiwan Inst. Chem. Eng. 2016, 67, 511–520, doi:http://dx.doi.org/10.1016/j.jtice.2016.08.008.
[52] Zheng, H.; Shao, Y.; Wang, Y.; Meng, G.; Liu, B. Reinforcing the corrosion protection property of epoxy coating by using graphene oxide–poly(urea–formaldehyde) composites. Corros. Sci. 2017, 123, 267–277, http://dx.doi.org/doi:10.1016/j.corsci.2017.04.019.
[53] Zheng, H.; Guo, M.; Shao, Y.; Wang, Y.; Liu, B.; Meng, G. Graphene oxide–poly(urea–formaldehyde) composites for corrosion protection of mild steel. Corros. Sci. 2018, 139, 1–12, doi:https://doi.org/10.1016/j.corsci.2018.04.036.
[54] Nikpour, B.; Ramezanzadeh, B.; Bahlakeh, G.; Mahdavian, M. Synthesis of graphene oxide nanosheets functionalized by green corrosion inhibitive compounds to fabricate a protective system. Corros. Sci. 2017, 127, 240–259, doi:http://dx.doi.org/10.1016/j.corsci.2017.08.029.
[55] Qiu, C.; Liu, D.; Jin, K.; Fang, L.; Xie, G.; Robertson, J. Electrochemical functionalization of 316 stainless steel with polyaniline-graphene oxide: Corrosion resistance study. Mater. Chem. Phys. 2017, 198, 90–98, doi:http://dx.doi.org/10.1016/j.matchemphys.2017.05.004.
[56] Pourhashem, S.; Vaezi, M.R.; Rashidi, A.; Bagherzadeh, M.R. Distinctive roles of silane coupling agents on the corrosion inhibition performance of graphene oxide in epoxy coatings. Prog. Org. Coat. 2017, 111, 47–56, doi:http://dx.doi.org/10.1016/j.porgcoat.2017.05.008.
[57] Pourhashem, S.; Vaezi, M.R.; Rashidi, A. Investigating the effect of SiO2-graphene oxide hybrid as inorganic nanofiller on corrosion protection properties of epoxy coatings. Surf. Coat. Technol. 2017, 311, 282–294, doi:http://dx.doi.org/10.1016/j.surfcoat.2017.01.013.
[58] Li, X.; Bandyopadhyay, P.; Guo, M.; Kim, N.H.; Lee, J.H. Enhanced gas barrier and anticorrosion performance of boric acid induced cross-linked poly(vinyl alcohol-co-ethylene) /graphene oxide film. Carbon. 2018, 133, 150–161, doi:https://doi.org/10.1016/j.carbon.2018.03.036.
[59] Cui, M.; Ren, S.; Zhao, H.; Xue, Q.; Wang, L. Polydopamine coated graphene oxide for anticorrosive reinforcement of waterborne epoxy coating. Chem. Eng. J. 2018, 335, 255–266, doi:https://doi.org/10.1016/j.cej.2017.10.172.
[60] Mohammadi, A.; Barikani, M.; Doctorsafaei, A.H.; Isfahani, A.P.; Shams, E.; Ghalei, B. Aqueous dispersion of polyurethane nanocomposites based on calix[4]arenes modified graphene oxide nanosheets: Preparation, characterization, and anticorrosion properties. Chem. Eng. J. 2018, 349, 466–480, doi:https://doi.org/10.1016/j.cej.2018.05.111.
[61] Kasaeian, M.; Ghasemi, E.; Ramezanzadeh, B.; Mahdavian, M.; Bahlakeh, G. Construction of a highly effective self-repair corrosion-resistant epoxy composite through impregnation of 1H-Benzimidazole corrosion inhibitor modified graphene oxide nanosheets (GO-BIM). Corros. Sci. 2018, 145, 119–134, doi:https://doi.org/10.1016/j.corsci.2018.09.023.
[62] Parhizkar, N.; Ramezanzadeh, B.; Shahrabi, T. The epoxy coating interfacial adhesion and corrosion protection properties enhancement through deposition of cerium oxide nanofilm modified by graphene oxide. J. Ind. Eng. Chem. 2018, 64, 402–419, doi:https://doi.org/10.1016/j.jiec.2018.04.003.
[63] Taheri, N.N.; Ramezanzadeh, B.; Mahdavian, M.; Bahlakeh, G. In-situ synthesis of Zn doped polyaniline on graphene oxide for anti-corrosive reinforcement of epoxy coating. J. Ind. Eng. Chem. 2018, 63, 322–339, https://doi.org/doi:10.1016/j.jiec.2018.02.033.
[64] Zhu, X.; Ni, Z.; Dong, L.; Yang, Z.; Cheng, L.; Zhou, X.; Xing, Y.; Wen, J.; Chen, M. In-situ modulation of interactions between polyaniline and graphene oxide films to develop waterborne epoxy anticorrosion coatings. Prog. Org. Coat. 2019, 133, 106–116, doi:https://doi.org/10.1016/j.porgcoat.2019.04.016.

Seyed Ali Rezaei, Maryam Sirati Gohari, Alimorad Rashidi*

Chapter 9
Carbon nanotubes (CNTs) and their composites as nanostructured corrosion inhibitors

Abstract: One of the best strategies to develop appropriate corrosion resistance is the incorporation of nano additives such as CNTs into coatings, in order to prepare a low-cost, lightweight, and environment-friendly nanocomposite coating with proper anti-corrosive properties. Filling coatings by such nano additive can considerably enhance mechanical features and barrier properties and provide reliable durability. CNTs-filled nanocomposites have achieved increasing attention due to their magnificent properties of controlling degradation of the metallic surfaces by providing impermeability of aggressive species. The incorporation of CNTs can effectively improve the corrosion protection performance of Nano coating in both ferrous and nonferrous metals. Different protection mechanisms can be provided due to the presence of CNTs in the anti-corrosive coating, which can result in lengthening the lifetime and enhancing the performance of the protective coating. However, there are some challenges, such as appropriate functionalization in order to provide proper distribution of CNTs in different matrixes, which should be addressed, in parallel.

Keywords: carbon nanotubes (CNTs), composites, corrosion inhibitors, functionalization, mechanism

9.1 Introduction

Corrosion is an undesirable reaction that causes the degradation and destruction of metals and industrial parts due to the presence of aggressive ions in harsh environments, affecting various properties of metallic materials such as mechanical features and durability [1–3]. There are a variety of strategies that address this problematic

*Corresponding author: **Alimorad Rashidi,** Alimorad Rashidi, Nanotechnology Research Center, Research Institute of Petroleum Industry (RIPI), Tehran, Iran, e-mail: rashidiam@ripi.ir
Seyed Ali Rezaei, Research Department of Ceramic, Materials, and Energy Research Center, Alborz, Iran, e-mail: sa.rezaei@merc.ac.ir
Maryam Sirati Gohari, Research Department of Ceramic, Materials, and Energy Research Center, Alborz, Iran, e-mail: m.sirati@merc.ac.ir

https://doi.org/10.1515/9783110782820-009

continuous phenomenon, and among them, coating metallic substrates by nanocomposite containing additive with inhibition role is the most common approach [4–6]. Based on the aggressive environment and substrate, the proper coating material should be chosen, in order to obtain effective corrosion protection. The protection properties and durability of the resistance layers can be reduced due to many reasons such as defects and porosities resulting from the production stage. To address these shortcomings, scientists have focused on the use of nanocomposite coatings, in order to provide novel corrosion-inhibiting systems [7]. The use of different types of nano additives to enhance corrosion resistance efficiency and durability of coatings is a convenient method. Carbon-based nanomaterials have gotten increasing attention due to their inhibition role in corrosion protection [8, 9]. Researchers in this area have reported carbon nanotubes and their composites as major corrosion inhibitors because of their magnificent characteristics such as superior mechanical property, excellent anticorrosion property, thermal and chemical stability, wide surface area, and high conductivity [10]. The mechanical features and barrier properties of coatings can be significantly enhanced by incorporating CNTs in different matrixes. In addition to providing novel properties, low-cost, lightweight, and eco-friendly anticorrosion coatings with reliable durability can be achieved [7]. However, aggregation and poor dispersion of such nanoparticles can be mentioned as the important challenges for their application in anticorrosive films. Numerous researches have been done for the proper functionalization of CNTs in different matrixes, directly affecting the nanocomposite coating properties [11]. This chapter presents a review on methods for CNTs modification to address uncontrolled distribution and limited solubility in different matrixes and some well-known corrosion inhibition mechanisms related to the presence of CNTs in nanocomposite-coated ferrous and nonferrous metals.

9.2 Properties of carbon nanotubes

9.2.1 Mechanical properties

Carbon nanotubes are considered to be the strongest discovered materials in nature, so far. They are the most grounded and adaptable molecular materials due to hexagonal network architecture and carbon-carbon sp^2 covalent bonding to improve the strength of the structure, which affects Young's modulus. The estimated value Young's modulus for CNTs' is 1–1.8 TPa, elongation to failure is 20–30%, and tensile strength, above 100 GPa. Besides the mentioned extraordinary properties, the lightness of such nanoparticles is a leading reason for their broad usage in many industries such as aerospace [12–14].

9.2.2 Electrical properties

Being a 1D carbon nano allotrope and having a peculiar electronic structure are the main reasons for the magnificent electrical properties of CNTs. Due to low electrical resistance, this nanostructure can be superconducting even at low temperatures, with an electrical current flow density of 4×109 A/cm^2. The composition of CNTs with other materials can provide extraordinary properties applicable in many industries [12–14].

9.2.3 Thermal properties

Generally, the thermal conductivity of CNTs depends on the environment and temperature. CNTs possess superior thermal conductivity; they exhibit superconductivity below 20 K (≈ −253 °C) due to the Carbon-Carbon bonds in the structure, which gives quality and stiffness against axial tension, resulting in high adaptability against non-axial strains [12–14].

9.2.4 Chemical properties

Synthesis method and parameter can determine the chemical properties. CNTs are chemically inert, especially when the nanostructure has no defects, which can be mentioned as the leading reason for being chemically stable. In addition, due to its large surface-to-volume ratio, it is considered as an interesting material for hydrogen storage. As the diameter of tubes decreases, the reactivity of CNTs increases. CNTs can react through sidewall and end top [12–14].

9.3 Functionalization of carbon nanotubes

Although CNTs have many magnificent properties, some issues, such as poor distribution in different matrixes limit their application. π–π interactions, known as dominating supramolecular forces, and high surface area are the leading reasons for agglomeration and weak dispersion of such nanoparticles. The two most important strategies to address the mentioned issue and enhance its processability and properties are mechanical and chemical approaches [15, 16]. Although mechanical methods are able to separate CNTs from each other and uniformly disperse in the matrixes, they can also ruin their features by breaking up nanoparticles and decreasing the aspect ratio; more importantly, these are time wasting and ineffectual strategies. However, chemical approaches are employed to modify the surface energy, enhance the adhesion

features, and improve the distribution stability of CNTs. Surface chemistry modification of the carbon nanotubes, either non-covalently (adsorption) or covalently (functionalization), can be mentioned as the main target of these processes (Fig. 9.1). CNTs modification might change various properties (electrical, optical, or mechanical) from the original nanoparticles, which can widen their applications [17, 18].

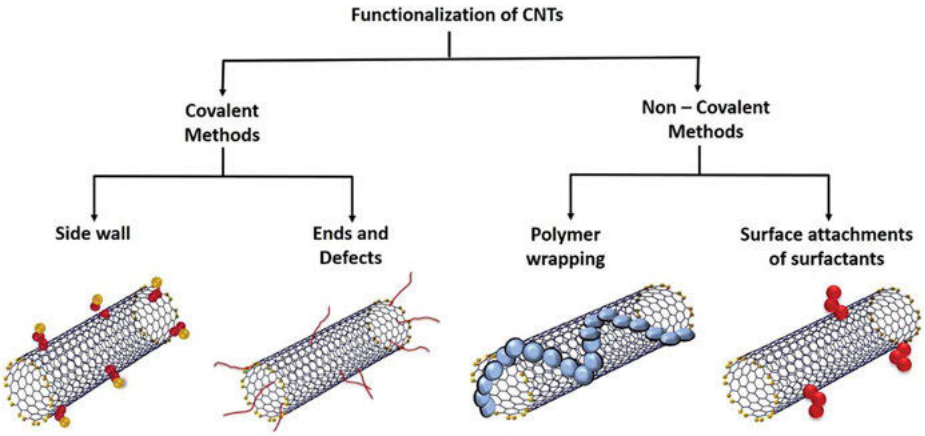

Fig. 9.1: Schematic illustration of Functionalization strategies for carbon nanotubes (Reprinted with permission from ref. [19]).

9.3.1 Covalent functionalization

These kinds of modifications are based on the formation of covalent attachment between functional groups and the nanotubes structure to provide proper distribution of CNTs in the different types of matrixes, such as polymers, which can improve adhesion properties and address the aggregation of the nanoparticles [20, 21] (Fig. 9.2). Covalently modifying CNTs could be categorized into two sections, bonding of functional moieties on the sidewall, including fluorination [22–25], hydrogenation [26], cycloadditions [11, 27–29], electrophilic addition [11, 30], radical additions [31, 32], and indirect chemical functionalization by carboxylic or hydroxyl functional groups on the surface of nanotubes, including carboxylation(amidation and esterification) [33–36] and metallic nanoparticles attachment [37–40]. Although covalent modification has stronger interactions than non-covalent ones, the disruption of the surface-conjugated π network, which can negatively affect electrical conductivity, is considered the main disadvantage for these sorts of functionalizations. The impact of mentioned side effects on mechanical and thermal features of CNTs is limited. However, electrical properties can deteriorate, since each covalent functionalization site acts as an electrons scattering center [41].

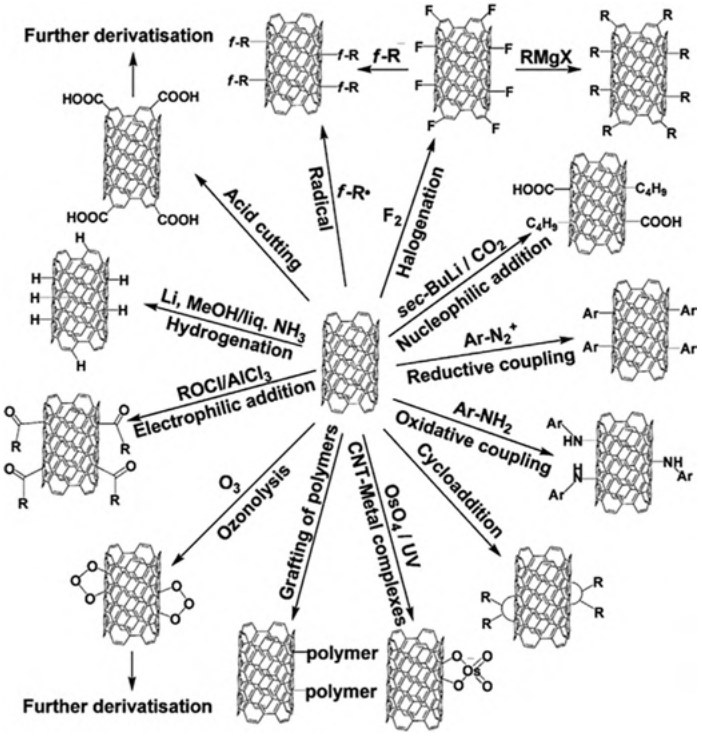

Fig. 9.2: Covalent functionalization of CNTs (Reprinted with permission from ref. [30]).

9.3.2 Non-covalent functionalization

Modifying CNTs non-covalently to adjust the interfacial properties is getting increasing attention due to providing the possibility of adsorbing different functional groups on the CNTs surface and keeping pristine structure and properties intact, without disturbing the π system. These methods are formed by interactions of the hydrophobic section of the adsorbed molecules with nanoparticles sidewalls through van der Waals, π–π, CH–π, and to provide aqueous solubility. The modified surface of CNTs, due to adsorbed ionic molecules, prevents CNTs agglomeration by the electrostatic force between functionalized nanoparticles [17, 41, 42]. The main disadvantage of non-covalent bonding is that the forces between the wrapping molecule and such nanoparticles might be poor and have low load transfer efficiency [43]. Surfactant functionalization [44–52], polymer wrapping [53–58], polymer absorption [59–61], and polymer encapsulation [36, 62–65] are some of the well-known non-covalent functionalization methods.

9.4 CNTs as corrosion inhibitors

Carbon nanotubes have been known as suitable alternative for other fillers due to their large specific surface area, large aspect ratio, and appropriate electrical feature [66, 67]. Applying CNTs can positively affect coating features such as stiffness, Young's modulus, fracture toughness, and high thermal stability [68–70]. Based on many studies, remarkable improvement in the corrosive resistance capability of the coatings possessing CNTs reflects the electrical current distribution effect on the surface of metal, which can protect substrate from any localized damage. CNTs reduce the defects and porosities, so that compactness of coating layer can be developed. Not only can CNTs develop proper corrosion resistance in the coatings, they can also enhance the adhesion coatings on metal substrates [71–73].

CNTs tend to aggregate due to the high aspect ratio and poor interaction with the coating. CNTs aggregation lowers the mechanical characteristics and corrosion resistance of the coating. Different kinds of functionalization are employed to enhance CNTs dispersion in the polymeric coating by enhancing the interfacial interactions between the additive and the polymeric matrix. Physical interactions include the polymer's adsorption onto the surface of the nanoparticles, while chemical approaches consist of the polymer chemical bonding on the surfaces of CNTs. [74–76]. The organic groups grafting on the surfaces of CNTs has been investigated in many studies [77, 78]. Some approaches have been introduced as mechanical functionalization to prevent the CNTs aggregation and enhance CNTs dispersion in the polymeric matrix. Dispersion through ultrasonic [79, 80] and high-shear mixing [81] can be mentioned as typical mechanical approaches.

Because of the exceptional features such as doping priority, electrical conductivity, and nontoxicity of CNTs, incorporation of such material into conducting polymers has obtained increasing attention. Barrier feature and electronic interaction related to the conductive polymer/CNT nanocomposite coatings were proposed as the key mechanisms for protection [82]. Forming a passive layer in the interface of metal and polymer resulting from anodic (oxidation of metal) and cathodic (conductive polymer un-doping) reactions can significantly enhance the protection process of the metallic surface from corrosion. Due to high surface area, CNTs nanoparticles can have a cathodic effect in the reoxidation of polymer, which can improve the formation process of oxide film by dissolved oxygen [83].

9.5 CNTs and their inhibition role in corrosion protection of nonferrous metals

2024 aluminum alloy (Al_2CuMg, AA 2024) is broadly used in various industries, especially aerospace, due to its incredible properties such as lightweight, high strength, and appropriate corrosion protection performance. However, the presence of Cu-rich

particles in such alloys can cause local pitting corrosion, which restricts its application. Applying coating on such alloy is considered as one of the most effective strategies, in order to address the mentioned problem. Bis(triethoxysilylpropyl)tetrasulfide (BTESPT) was coated on AA 2024 (Fig. 9.3), and the effect of adding TiO_2-coated multi-walled carbon nanotubes (MWCNTs) as filler into the coating was investigated. The results showed that incorporating MWCNTs modified by TiO_2 can significantly improve the anticorrosion and barrier properties due to better dispersion of MWCNTs into the coating, which can develop a better cross-linked interfacial layer, accordingly controlling the growth and initiation of cracks. Additionally, due to proper MWCNTs dispersion, accumulated electrons at the interfacial region between substrate and coating might be transmitted, enhancing corrosion inhibition of such alloy. Investigation of surface morphology related to BTESPT, BTESPT/TiO_2, and BTESPT/TiO_2/MWCNTs nanocomposite (Fig. 9.4) demonstrated that coating layer filled by TiO_2/MWCNTs possess smoother and uniform morphology after exposure to seawater compared to other samples, indicating the inhibition role of such filler in the coating [84].

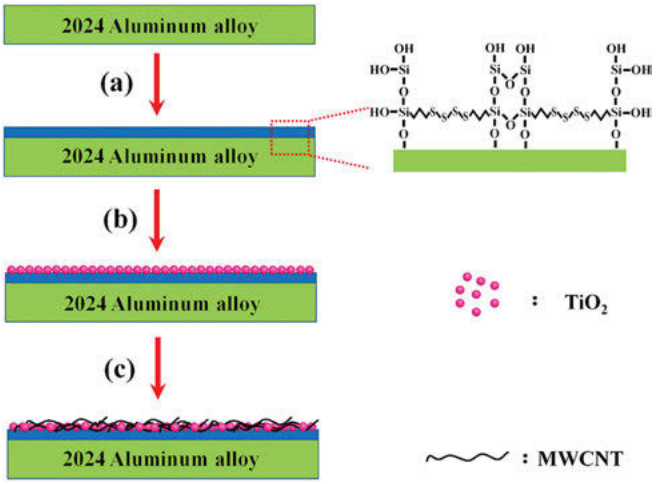

Fig. 9.3: Schematic illustrations of preparation processes for the BTESPT (a), BTESPT/TiO_2 (b), and BTESPT/TiO_2/MWCNT (c) coating on AA 2024 (Reprinted with permission from ref. [84]).

Incorporating CNTs in conductive polymeric matrixes can develop a new class of nanocomposite coating with magnificent features such as synergistic properties. Poly (3-aminobenzoic acid) (P3ABA), a conjugated polymer, is considered as one of the most well-known derivatives of polyaniline (PANI) with proper solubility in organic solvents and poor conductivity. The impact of MWCNTs incorporation into P3ABA protective coating on copper was investigated (Fig. 9.5). The results proved that MWCNTs addition to the polymeric coating could not only improve corrosion

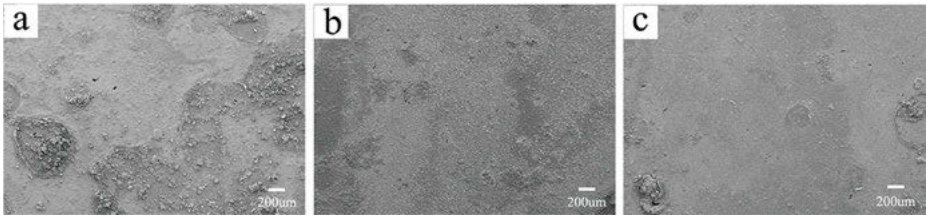

Fig. 9.4: Surface morphologies of BTESPT (a), BTESPT/ TiO_2 (b), and BTESPT/TiO_2/MWCNTs (c) coating on AA 2024, after exposure in seawater (Reprinted with permission from ref. [84], Order License ID: 1197179-1).

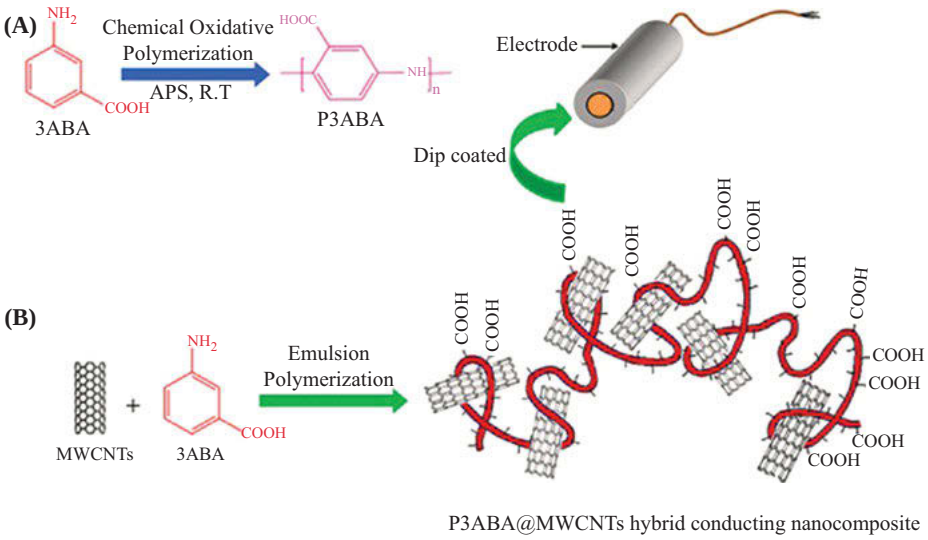

Fig. 9.5: Schematic illustration of production method for P3ABA (A) and P3ABA/MWCNTs composite (B) (Reprinted with permission from ref. [85]).

resistance and barrier properties, but also electrical conductivity, thermal stability, and crystallinity of P3ABA. Recommended mechanisms for considerable reduction of the corrosion rate of P3ABA/MWCNTs coating are associated with the presence of MWCNTs, anodic protection, and electronic barrier protection. Defect and porosity in the P3ABA coating can be remarkably enhanced due to the presence of MWCNTs, which can improve the compactness of coating, prevent penetration of corrosive species, and control the initiation and growth of cracks. Additionally, since P3ABA possesses strong oxidative property, it can act as oxidant to copper [85].

Poly(3,4-ethylenedioxythiophene) nanospheres (PEDOT-NSP) were synthesized on MWCNTs functionalized by carboxyl (PEDOT-NSP/MWCNTs). PEDOT-wrapped MWCNTs with a coaxial structure (PEDOT-COX/MWCNTs) were also prepared without

a surfactant as an anticorrosive coating for aluminum in lithium hexa fluorophosphate ($LiPF_6$) (Fig. 9.6). The results showed that PEDOT-NSP/MWCNTs considerably reduced the corrosion rate of aluminum, compared to PEDOT-COX/MWCNTs. The carboxyl (COOH) group on MWCNTs (negatively charged) can act as dopants for PEDOT through which anion exchange property is minimized (anion transport changes to cation transport property). The more effective protection of such coating is related to the cation exchange of PEDOT and the anion-repulsion of the pristine MWCNTs surface, which can lead to an increase in the electrostatic repulsion. Consequently, pit-causing anions (PF_6^-) cannot diffuse into the coating and initiate the corrosion reaction on the metallic substrate [86].

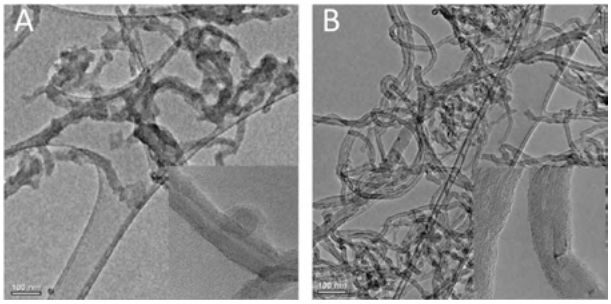

Fig. 9.6: TEM images of PEDOT-NSP/MWNT (A) and PEDOT-COX/MWNT composite synthesized with no surfactant (B) (Reprinted with permission from ref. [86]).

Based on the schematic represented in Fig. 9.7, due to the presence of PEDOT-NSP on MWCNTs, the PF_6^- anions can transport towards the substrate surface, leading to a reduction of corrosion rate. In contrast, due to the absence of surfactant, PEDOT nanospheres cannot be formed so that PEDOT-COX completely covers MWCNTs. As a result, the MWCNTs cannot be exposed to the medium, leading to inferior effectiveness of

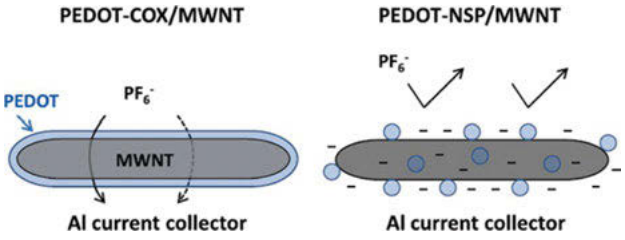

Fig. 9.7: Schematic illustrations related to the synergistic effect concept of PEDOT-NSP and MWNTs on corrosion protection behavior in PEDOT-NSP/MWNTs. In PEDOT-COX/MWNTs, no electrostatic repulsion is expected due to complete coverage of MWNTs with PEDOT (Reprinted with permission from ref. [86]).

PEDOT-COX/MWCNTs. Thus, the optimal value of MWCNTs can sufficiently improve the corrosion protection performance by synergistic effect [86].

Nickel-based alloys are applicable to many industries such as shipbuilding and automobiles. These alloys are known for their proper corrosion resistance in the open-air environment. However, the poor stability of nickel-based alloys was reported in acidic environment due to the diffusion of aggressive ions through their native oxide layer. CNTs modified by 4,5-diphenyl-imidazole (4,5-DPM) (Fig. 9.8) were coated on the nickel alloy, and the corrosion protection efficiency of the mentioned layer was compared with the epoxy coating. Pitting corrosion was observed in the nickel alloy surface coated by epoxy as a result of aggressive spices penetration due to poor passivation protection. In addition, epoxy coating could not protect substrate from long-term exposure in corrosive media due to hydrogen evolution on the metallic substrate, and an increase in anodic nickel alloy dissolution was reported. In contrast, crystalline and tubular structures of 4,5-DPM-functionalized CNT provided proper corrosion protection on the substrate surface due to improvement passivation protection of substrate surface, as a result of hydrogen evolution suppression by the presence of 4,5-DPM-functionalized CNT [87].

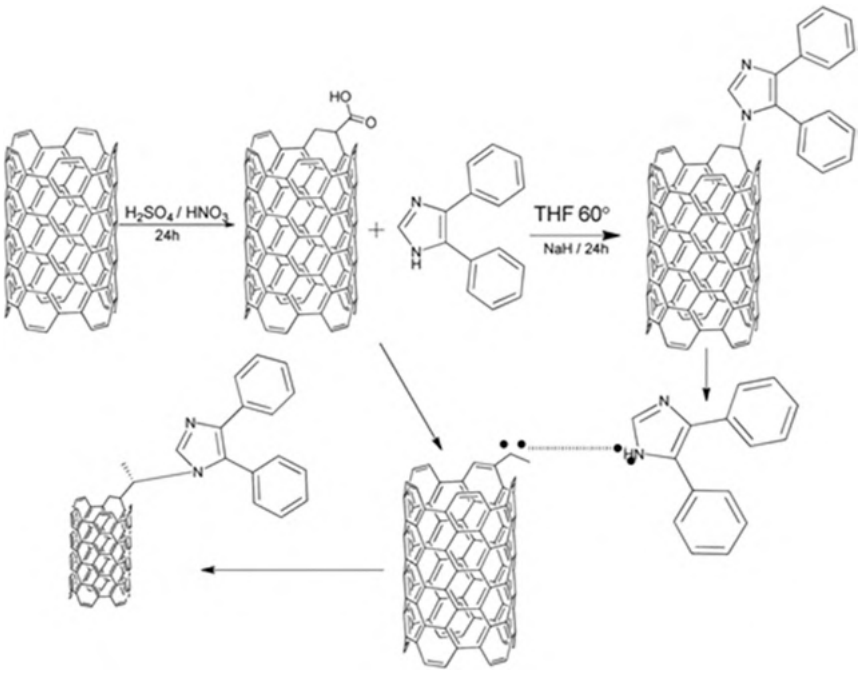

Fig. 9.8: Schematic illustration of possible mechanism for the functionalization of CNTs by 4,5-diphenyl-imidazole (Reprinted with permission from ref. [87]).

Figure 9.9a demonstrates the morphologies of surface related to the epoxy coating and 4,5- DPM-functionalized CNT coating on the nickel alloy after exposure to a harsh environment. Uniform corrosion can be observed in the epoxy coating, which can be related to peeling off the coating from the substrate. However, weak physisorption was observed on the surface of the nickel alloy because of the pitting corrosion initiation. In addition, grain boundaries related to nickel alloy coated by epoxy were intensely affected, owing to the poor stability of coating (Fig. 9.9b). In contrast, a smooth surface can be seen for 4,5-DPM-functionalized CNT-coating with a considerable decrease in localized corrosion. A proper barrier property was provided due to the strong physisorption on the surface of substrate, resulting from the implication of non-bonding electrons related to CNTs in physisorption of coating, and implication of imidazole nitrogen-free electrons in chemisorption on the substrate. No O2 element was detected, since no corrosive oxygen-containing ion was diffused to the coating due to the strong hydrophobic properties of CNTs [87].

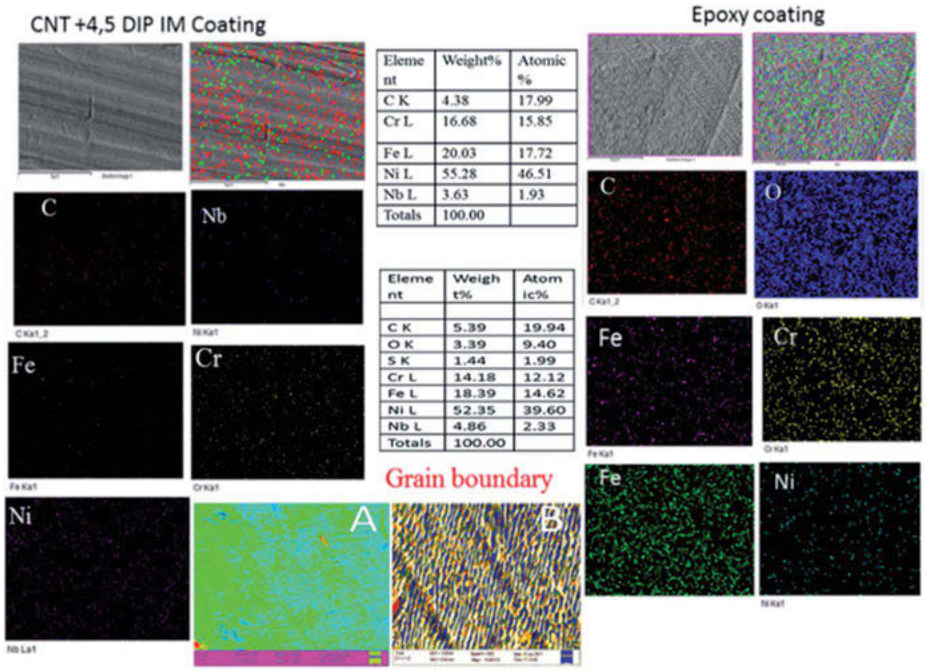

Element	Weight%	Atomic %
C K	4.38	17.99
Cr L	16.68	15.85
Fe L	20.03	17.72
Ni L	55.28	46.51
Nb L	3.63	1.93
Totals	100.00	

Element	Weight%	Atomic%
C K	5.39	19.94
O K	3.39	9.40
S K	1.44	1.99
Cr L	14.18	12.12
Fe L	18.39	14.62
Ni L	52.35	39.60
Nb L	4.86	2.33
Totals	100.00	

Fig. 9.9: The surface morphologies of epoxy coating and 4,5- DPM-functionalized CNT coating on nickel alloy after exposure to a harsh environment (Reprinted with permission from ref. [87]).

The effect of CNTs incorporation on mechanical features, tribological, and passivation behavior of Nickel-Phosphorus (Ni-P)-coated copper substrate was evaluated. Results demonstrated that the presence of CNTs in Ni-P coating can significantly enhance the

anticorrosive properties, resulting from unique mechanical features and superior chemical stability of CNTs. Based on the AFM images (Fig. 9.10), Ni-P-CNT composite coating possesses a streaky surface, with better smoothness and compactness than Ni-P coating. The average roughness of Ni-P coating (192 nm) was decreased after incorporating CNTs (129 nm), indicating the positive effect of CNTs incorporation on the surface morphology of coating [88].

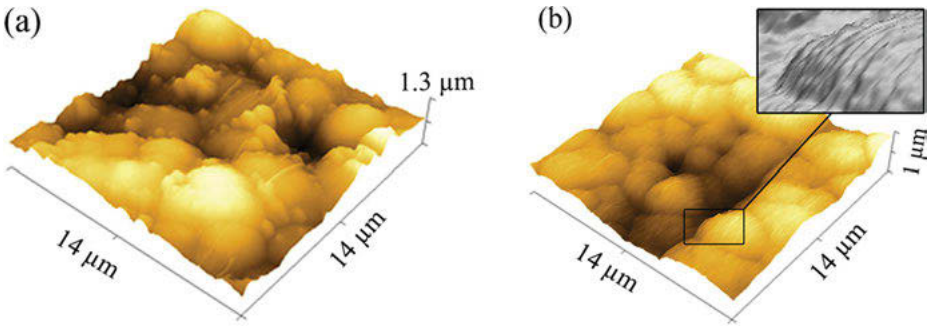

Fig. 9.10: The AFM images of the surface morphology related to Nickel-Phosphorus (a) and Nickel-Phosphorus-CNTs (b) coatings (Reprinted with permission from ref. [88]).

The prepared coatings had undergone heat treatment at 400 °C, followed by evaluation of dynamic friction coefficient and wear resistance. Based on SEM images (Fig. 9.11), considerable plastic deformation observed on the worn surface related to Ni-P coating and a wide wear track with partial irregular pits, micro-cracks and longitudinal grooves, peeling-off, and scuffing were observed. In contrast, smooth and narrow wear track without plastic deformation and crack can be seen on the worn surface related to Ni-P-CNTs composite coating, indicating that friction coefficient of Ni-P coating was higher than the Ni-P-CNTs composite coating [88].

It was indicated that incorporation of CNTs could reduce phosphorus content after heat treatment and nickel was recrystallized and transformed into a nanocrystalline structure, which can lead to increasing the fraction related to the nanocrystalline structure in the Nickel coating. The results showed that the presence of CNTs caused by precipitation of the Ni_3P phase could occur in the matrix, and the existence of such phase can lead to a hardening effect and increase microhardness value. The nanocomposite coating of Ni-P-CNTs showed better corrosion resistance compared to Ni-P coating, due to the presence of CNTs, resulting in the reduction of defects and porosities and the formation of a homogenous and dense Nano coating on the substrate. It was proposed that in addition to low chemical reactivity, CNTs can accelerate the chemical passivation of the substrate, which can affect the corrosion protection performance [88].

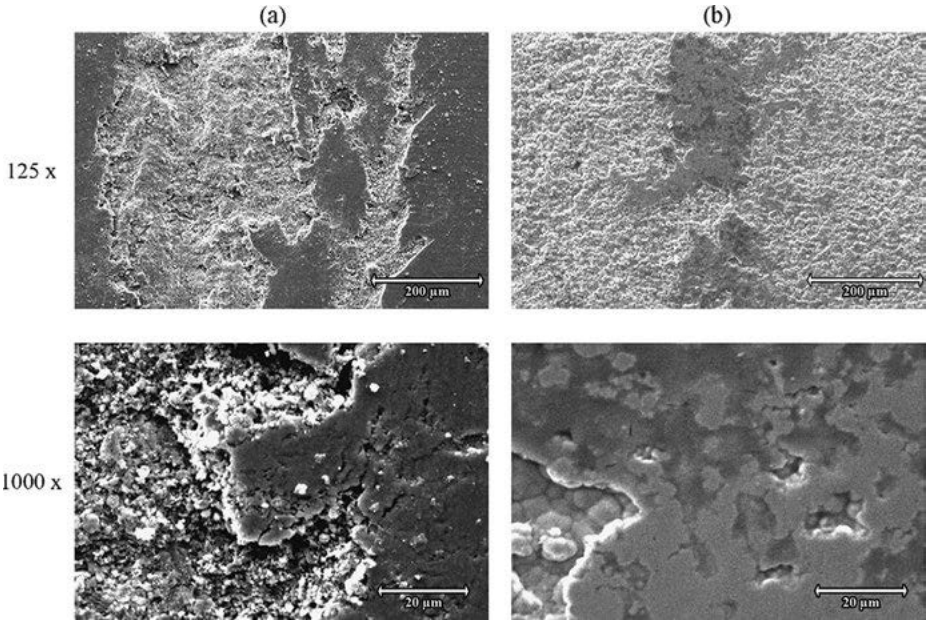

Fig. 9.11: SEM images of the worn surface related to Nickel-Phosphorus (a) and Nickel-Phosphorus-CNTs (b) coatings (Reprinted with permission from ref. [88]).

9.6 CNTs and their inhibition role in corrosion protection for ferrous metals

CNTs-polyaniline (PANI) nanobrushes were synthesized via in situ oxidative polymerization of aniline on carboxylated MWCNTs (c-MWCNTs) (Fig. 9.12). The mass ratio of c-MWNTs to aniline specified the diameter of the final tubular brush-like nanostructures. Based on Fig. 9.13, PANI with short fiber morphology is aggregated drastically, while the PANI chains are properly distributed and attached on CNTs, so that the tubular layer of PANI is homogeneously coated on c-MWCNTs. Excellent corrosion protection performance has been obtained by adding this brush-like nanostructure into epoxy coated carbon steel. Due to the unique morphology of such additive, a new charge transfer bridge is provided via π–π stacking and hydrogen bonding interactions, through which electrochemical activity of coating can be promoted and the application of coating can be extended to a broader range of pH media, compared to neat PANI. The coating provided proper barrier property in the neutral and alkaline corrosion environment and excellent passivation protection in the acidic medium in which a protection layer made of thin oxide is formed on the substrate, resulting from electrochemical interaction of the polymeric coating with the substrate surface [89].

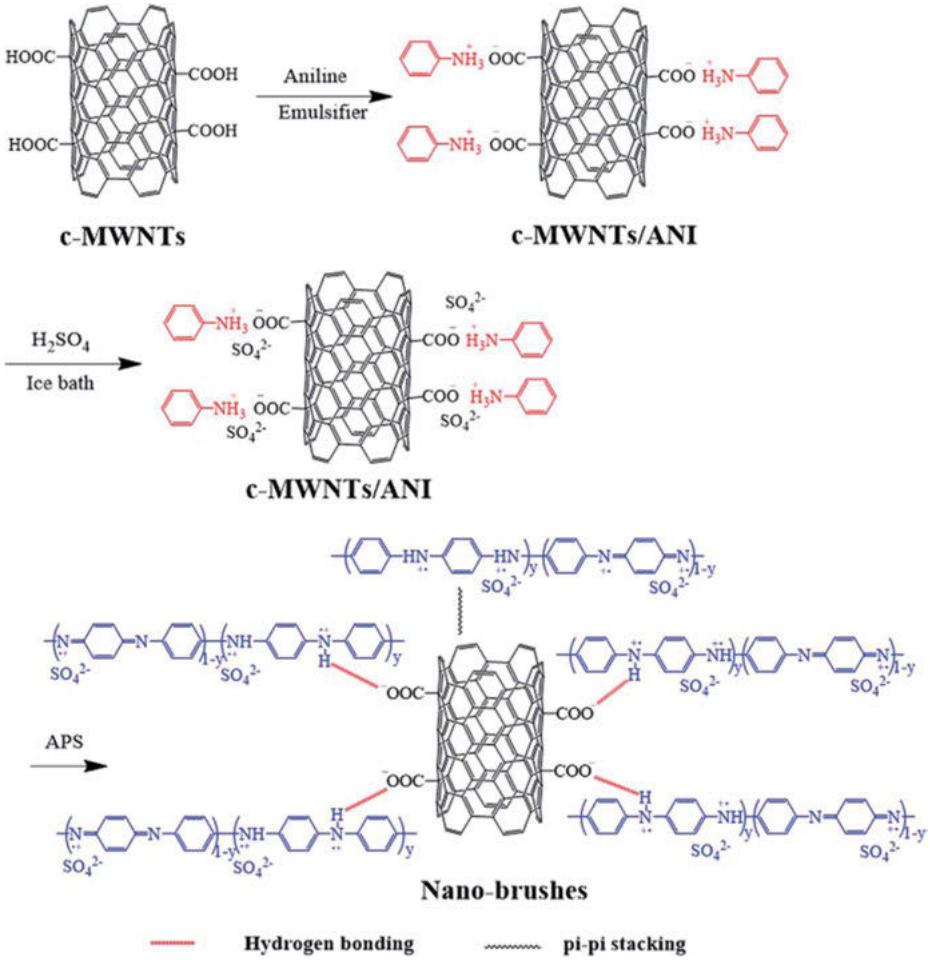

Fig. 9.12: Schematic illustration for c–PANI composite preparation (Reprinted with permission from ref. [89]).

The effect of different aspect ratios on performance of anticorrosive nanocomposite coating made of co-electrodeposited Polyaniline (PANI)–CNTs-coated stainless steel was investigated (Fig. 9.14). In order to prepare such coating, two different types of CNTs, including commercial (d = 110–170 nm, L = 5–9 μm) and home-made (d = 30 nm, L = 5–20 μm) were used. Results demonstrated that regardless of type, incorporating CNTs into PANI matrix can enhance the corrosion resistance of substrate. Based on the obtained results, monomer oxidation can be catalyzed by carbon nanotubes incorporation, and CNTs with high aspect ratio showed better catalytic effect. However, CNTs with low aspect ratio displayed better performance in preventing the penetration of aggressive species to stainless steel. The interaction of CNTs and

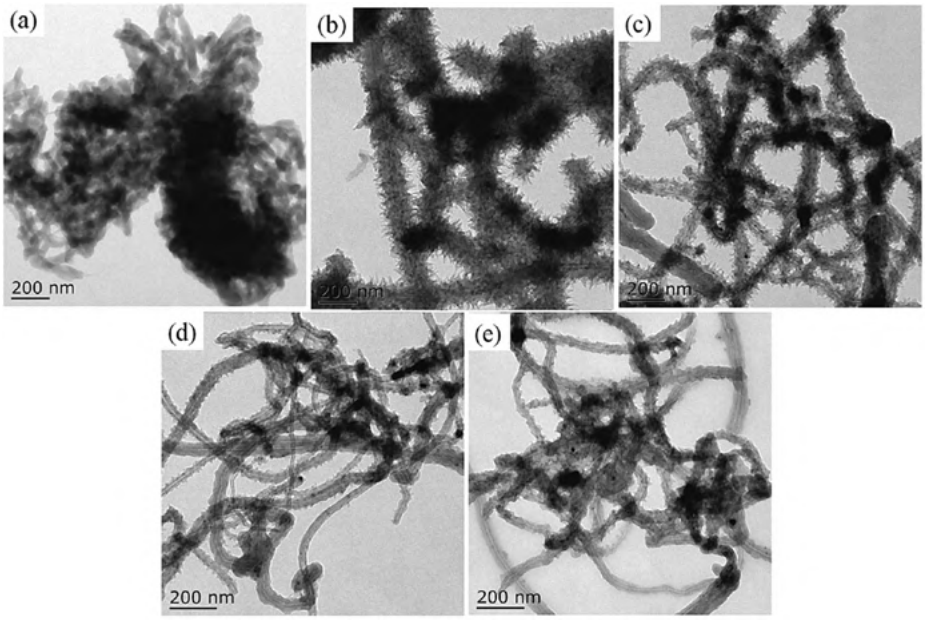

Fig. 9.13: TEM images of PANI (a) and c–PANI brush-like nanostructures synthesized with the different mass ratio of c-MWNTs to aniline 1:8 (b), 1:4 (c), 1:2(d), and 1:1(e) (Reprinted with permission from ref. [89]).

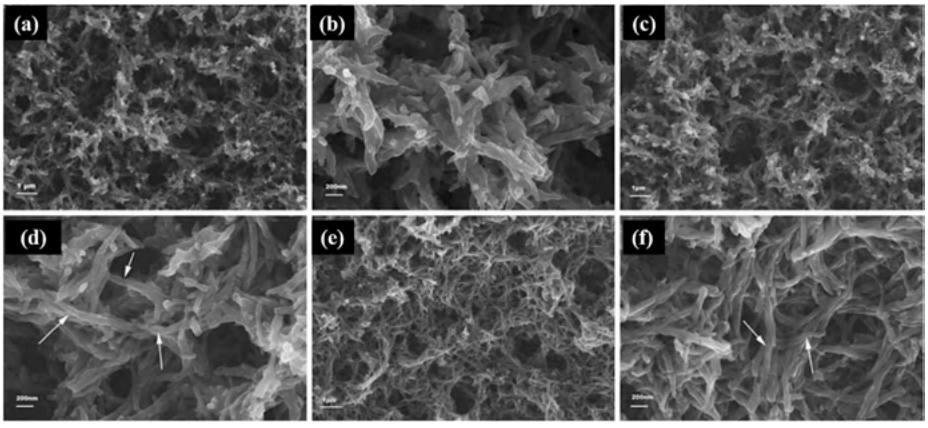

Fig. 9.14: SEM images of Polyaniline (PANI) and CNTs/PANI nanocomposite coating: PANI (a, b), 0.3%v/v CNTc/PANI (c, d), and 0.3%v/v CNThm/PANI (e, f) (Reprinted with permission from ref. [90]).

aniline, which can provide stabilization and protonation of PANI was proposed. In addition, the mentioned interaction can facilitate the charge-transfer process, which can improve electron delocalization. It can also act as condensation nuclei to prevent agglomeration of Polyaniline [90].

Anticorrosive properties of polypyrrole (PPy)/polyaminobenzene sulfonic acid-functionalized single-walled carbon nanotubes (SWCNTs-PABS) and PPy/carboxylic acid-functionalized SWCNTs (SWCNTs-CA)-coated carbon steel were evaluated. Based on SEM images (Fig. 9.15), it can be seen that PPy coating possesses granular type morphology. The morphology of coating remained granular after doping SWCNTs-PABS. The TEM image demonstrated the homogeneous distribution of SWCNTs in the polymeric matrix and revealed the PPy bridges between PPy-coated SWCNTs [91].

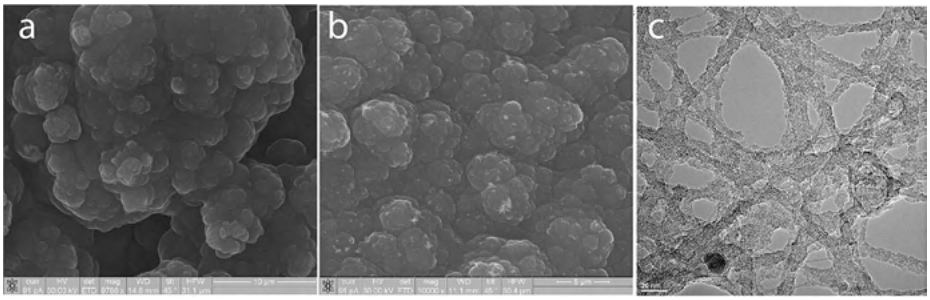

Fig. 9.15: SEM images of neat PPy coating(a) PPy/CNT-PABS nanocomposite coating (b), and TEM image of PPy/CNT-PABS nanocomposite coating (c) (Reprinted with permission from ref. [91]).

The results demonstrated that the SWCNTs-PABS and SWCNTs-CA are well distributed in the polymeric matrix, and the incorporation of these functionalized CNTs considerably improved mechanical properties of the coating, such as Young's modulus. Compared to neat PPy, corrosion resistance performance of coating was considerably enhanced due to the presence of SWCNTs-PABS and SWCNTs-CA. In fact, the presence of CNTs in conductive polymers can increase conductivity, which can lead to an improvement in anticorrosion protection efficiency. Results demonstrated that PPY/SWCNTs-PABS coating displayed better corrosion protection compared to PPY/SWCNTs-CA-coating due to better stability of the polymeric coating. It was proposed that incorporating CNTs in PPy coating can properly promote the electron transfer of the redox reaction and reduce the electrokinetic polarization, and the presence of SWCNTs-PABS is more effective than SWCNTs-CA, in this process [91].

The effect of MWCNTs incorporation into nickel-coated mild steel (MS) on anticorrosive properties was investigated. In order to study the corrosion resistance performance of Ni and Ni-MWCNTs coatings, samples were immersed in static and flow corrosive media. As can be seen in Fig. 9.16, applying a coating can effectively protect MS against corrosion. Based on the results, by increasing the flow corrosion rate was

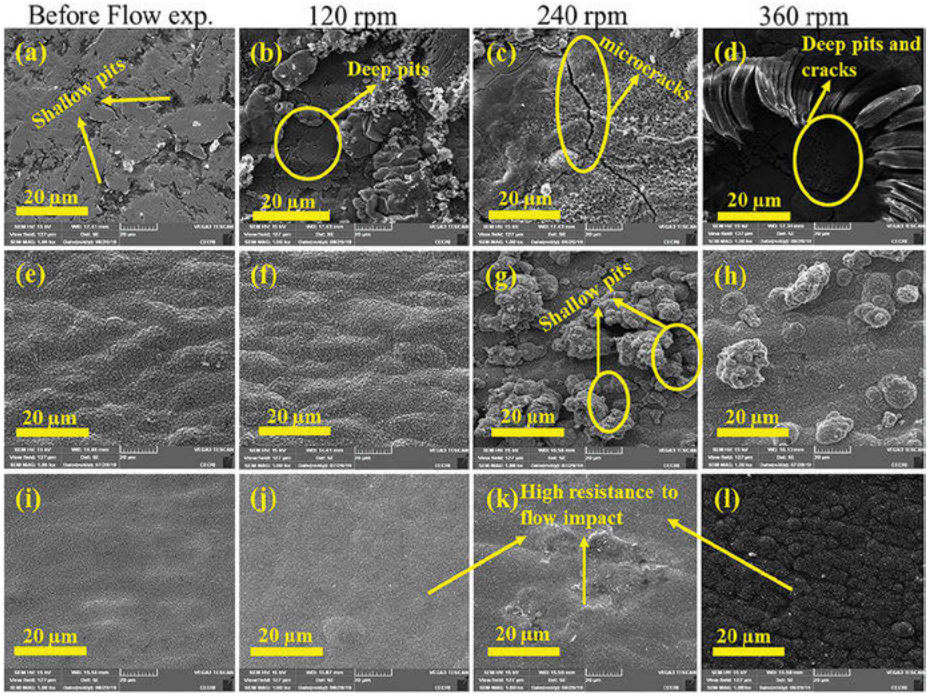

Fig. 9.16: SEM Images of the surface of mild steel immersed in harsh environment; (a–d) Bare, (e–h) Ni-coated and (i–l) Ni-MWCNTs-coated mild steel before and after rotating cage (RC) test (Reprinted with permission from ref. [92]).

also increased in all samples. Ni-MWCNTs coating displayed better performance compared to blank Ni coating in static and flow conditions. It was proposed that filling Ni coating with MWCNTs can improve the compactness and mechanical features, directly affecting the barrier properties. Trapping CNTs in Ni matrix can reduce defects and porosities to control diffusion of corrosive species such as oxygen and chloride [92].

Calcium carbonate ($CaCO_3$)/CNTs were incorporated in Polyaniline (PANI)-coated mild steel, and the effect of two different dopants (Hydroxyethylidene Diphosphonic Acid (HEDP) and Hydrochloric Acid (HCl)) on morphology and corrosion resistance of nanocomposite were investigated. Based on Fig. 9.17b, $CaCO_3$ particles with spherical morphology are uniformly dispersed in CNTs. In order to prepare PANI/CNT nanocomposite via oxidative polymerization of aniline, the system was suspended in an acidic environment, so that $CaCO_3$ could be decomposed to carbon dioxide (CO_2) gas, and a micro-fluid turbulent environment could be formed around CNTs, which can properly enhance distribution of nanoparticles. The morphology of PANI/CNTs composite coating depends on the acid type. By use of HCl as dopant (PANI/CNT (HCl)), Polyaniline grows on carbon nanotubes with dendritic morphology (Fig. 9.17c), while

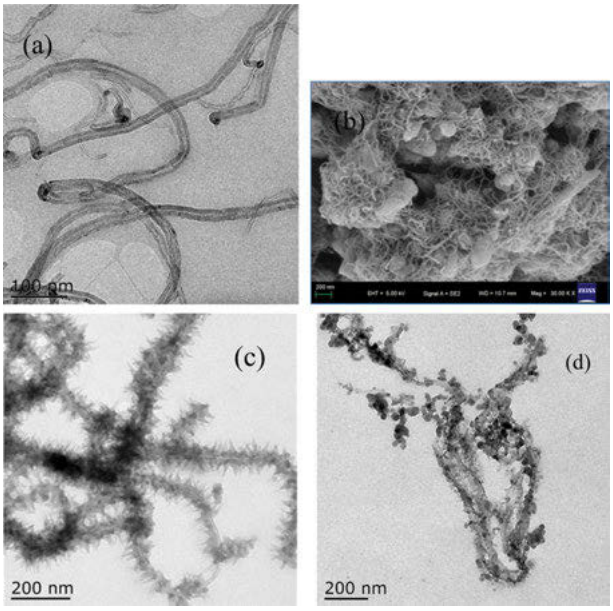

Fig. 9.17: TEM image of CNTs (a), SEM image of CNTs/$CaCO_3$ (b), TEM image of PANI/CNTs/HCl (c), and TEM image of PANI/CNTs/HEDP (d) (Reprinted with permission from ref. [93]).

in PANI/CNT doped by HEDP (PANI/CNT (HEDP)), Polyaniline nanospheres adsorb on carbon nanotubes (Fig. 9.17d) [93].

The results demonstrated that PANI/CNT composite doped by HEDP showed better corrosion resistance compared to PANI/CNT (HCl) composite. Four mechanisms related to corrosion protection for PANI/CNTs were proposed (Fig. 9.18). Porosities and defects in the coating can be removed by incorporating CNTs, which can effectively prevent the diffusion of aggressive ions such as H_2O and O_2 (Nano barrier effect). The next mechanism can be anode protection resulting from protective oxide film formation on the substrate. Due to conductivity enhancement, the electrons can be transferred into nanocomposites coating, so that cathode suppression can be mentioned as another mechanism. Lastly, because of the complex formation between HEDP and Fe^{2+}, the inhibition efficiency of PANI/CNTs (HEDP) is more effective, compared to the PANI/CNTs (HCl) [93].

9.7 Challenges, opportunities, and the future

The extraordinary properties of nanocomposite filled by CNTs provide excellent barrier properties and improve corrosion protection efficiency by developing proper mechanical features and effectively preventing the corrosive species penetration. Appropriate

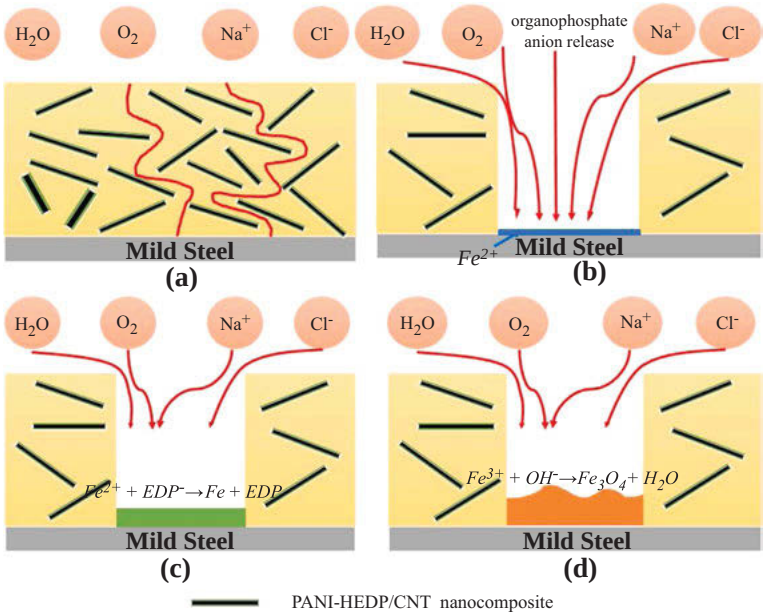

Fig. 9.18: Schematic illustration for corrosion protection mechanism of PANI-HEDP/CNTs composites coated mild steel in corrosive environment. Nano barrier effect (a), Inhibitor role (b), Cathode suppression (c), and Anode protection (d) (Reprinted with permission from ref. [93]).

functionalization is one of the requirements for proper inhibition role of CNTs, which can affect the distribution and adhesion of such nanoparticles in different matrixes. CNTs-filled nanocomposites have great potential in replacing the conventional materials in the anticorrosion coating in all industries. However, there are still some issues and possible perspectives that should be taken into account, in parallel. Large-scale production of CNTs with high quality, high aspect ratio, and proper conductivity in order to improve the inhibition role of such nanomaterial incorporated into different kinds of matrixes should be investigated. More importantly, appropriate dispersion of CNTs is one of the most important concerns that should be investigated, since studies showed that aggregation of such nanoparticles not only cannot improve the protection degree of nanocomposite coating, but can also drastically decrease the lifetime and protection performance of anticorrosive films.

References

[1] Haruna, K.; Obot, I.B.; Ankah, N.K.; Sorour, A.A.; Saleh, T.A. Gelatin: A green corrosion inhibitor for carbon steel in oil well acidizing environment. J. Mol. Liq. 2018, 264, 515–525, https://doi.org/10.1016/j.molliq.2018.05.058.

[2] Ituen, E.; Mkpenie, V.; Dan, E. Surface protection of steel in oil well acidizing fluids using L-theanine-based corrosion inhibitor formulations: Experimental and theoretical evaluation. Surf. Interfaces. 2019, 16, 29–42, https://doi.org/10.1016/j.surfin.2019.04.006.

[3] Singh, A.; Ansari, K.R.; Chauhan, D.S.; Quraishi, M.A.; Lgaz, H.; Chung, I. Comprehensive investigation of steel corrosion inhibition at macro / micro level by ecofriendly green corrosion inhibitor in 15% HCl medium. J. Colloid Interface Sci. 2019, https://doi.org/10.1016/j.jcis.2019.10.040.

[4] Madhusudan Goyal, E.E.E.; Kumar, S.; Bahadur, I.; Verma, C. Organic corrosion inhibitors for industrial cleaning of ferrous and nonferrous metals in acidic solutions: A review. J. Mol. Liq. 2018, https://doi.org/10.1016/j.molliq.2018.02.045.

[5] Saha, S.K.; Dutta, A.; Ghosh, P.; Sukulc, D.; Banerjee, P. Novel Schiff base molecules as efficient corrosion inhibitors for mild steel surface in 1 M HCl medium: Experimental and theoretical approach, 2016, https://doi.org/10.1039/C6CP01993E.

[6] Pourhashem, S.; Saba, F.; Duan, J.; Rashidi, A.; Guan, F.; Nezhad, E.G.; Hou, B. Polymer/Inorganic nanocomposite coatings with superior corrosion protection performance: A review. J. Ind. Eng. Chem. 2020, 88, 29–57, https://doi.org/10.1016/j.jiec.2020.04.029.

[7] Verma, C.; Quraishi, M.A.; Ebenso, E.E.; Hussain, C.M. Recent advancements in corrosion inhibitor systems through carbon allotropes: Past, present, and future. Nano Sel. 2021, 2, 2237–2255, https://doi.org/10.1002/nano.202100039.

[8] Pourhashem, S.; Ghasemy, E.; Rashidi, A.; Vaezi, M.R. Corrosion protection properties of novel epoxy nanocomposite coatings containing silane functionalized graphene quantum dots, Elsevier B.V., 2018, https://doi.org/10.1016/j.jallcom.2017.10.150.

[9] Pourhashem, S.; Vaezi, M.R.; Rashidi, A.; Bagherzadeh, M.R. Distinctive roles of silane coupling agents on the corrosion inhibition performance of graphene oxide in epoxy coatings. Prog. Org. Coatings. 2017, 111, 47–56, https://doi.org/10.1016/j.porgcoat.2017.05.008.

[10] Pourhashem, S.; Ghasemy, E.; Rashidi, A.; Vaezi, M.R. A review on application of carbon nanostructures as nanofiller in corrosion-resistant organic coatings, Springer, US, 2020, https://doi.org/10.1007/s11998-019-00275-6.

[11] Syrgiannis, Z.; Melchionna, M.; Prato, M. Covalent carbon nanotube functionalization, Springer Berlin Heidelberg, Berlin, Heidelberg, 2020, https://doi.org/10.1007/978-3-642-36199-9.

[12] Soni, S.K.; Thomas, B.; Kar, V.R.; Comprehensive, A. Review on CNTs and CNT-reinforced composites: Syntheses, characteristics and applications. Mater. Today Commun. 2020, 25, 101546, https://doi.org/10.1016/j.mtcomm.2020.101546.

[13] Rathinavel, S.; Priyadharshini, K.; Panda, D. A review on carbon nanotube: An overview of synthesis, properties, functionalization, characterization, and the application. Mater. Sci. Eng. B Solid-State Mater. Adv. Technol. 2021, 268, 115095, https://doi.org/10.1016/j.mseb.2021.115095.

[14] Shoukat, R.; Khan, M.I. Carbon nanotubes: A review on properties, synthesis methods and applications in micro and nanotechnology. Microsyst. Technol. 2021, 27, 4183–4192, https://doi.org/10.1007/s00542-021-05211-6.

[15] Huang, Z.; Xi, L.; Subhani, Q.; Yan, W.; Guo, W.; Zhu, Y. Covalent functionalization of multi-walled carbon nanotubes with quaternary ammonium groups and its application in ion chromatography. Carbon N. Y. 2013, 62, 127–134, https://doi.org/10.1016/j.carbon.2013.06.004.

[16] Mallakpour, S.; Soltanian, S. Surface functionalization of carbon nanotubes: Fabrication and applications. RSC Adv. 2016, 6, 109916–109935, https://doi.org/10.1039/c6ra24522f.
[17] Meng, L.; Fu, C.; Lu, Q. Advanced technology for functionalization of carbon nanotubes. Prog. Nat. Sci. 2009, 19, 801–810, https://doi.org/10.1016/j.pnsc.2008.08.011.
[18] Rodney Andrews, T.R.; Jacques, D.; Minot, M. 1Fabrication of carbon multiwall nanotube/polymer composites by shear mixing. Macromol. Mater. Eng 2003, 395–403.
[19] Jun, L.Y.; Mubarak, N.M.; Yee, M.J.; Yon, L.S.; Bing, C.H.; Khalid, M.; Abdullah, E.C. An overview of functionalized carbon nanomaterial for organic pollutant removal. J. Ind. Eng. Chem. 2018, 67, 175–186, https://doi.org/10.1016/j.jiec.2018.06.028.
[20] Koval'chuk, A.A.; Shevchenko, V.G.; Shchegolikhin, A.N.; Nedorezova, P.M.; Klyamkina, A.N.; Aladyshev, A.M. Effect of carbon nanotube functionalization on the structural and mechanical properties of polypropylene/MWCNT composites. Macromolecules. 2008, 41, 7536–7542, https://doi.org/10.1021/ma801599q.
[21] Amiri, A.; Maghrebi, M.; Baniadam, M.; Heris, S.Z. One-pot, efficient functionalization of multi-walled carbon nanotubes with diamines by microwave method. Appl. Surf. Sci. 2011, 257, 10261–10266, https://doi.org/10.1016/j.apsusc.2011.07.039.
[22] Adamska, M.; Narkiewicz, U. Fluorination of carbon nanotubes – a review. J. Fluor. Chem. 2017, 200, 179–189, https://doi.org/10.1016/j.jfluchem.2017.06.018.
[23] Liu, Y.; Jiang, L.; Wang, H.; Wang, H.; Jiao, W.; Chen, G.; Zhang, P.; Hui, D.; Jian, X. A brief review for fluorinated carbon: Synthesis, properties and applications. Nanotechnol. Rev. 2019, 8, 573–586, https://doi.org/10.1515/ntrev-2019-0051.
[24] Bulusheva, L.G.; Fedoseeva, Y.V.; Flahaut, E.; Rio, J.; Ewels, C.P.; Koroteev, V.O.; Van Lier, G.; Vyalikh, D.V.; Okotrub, A.V. Effect of the fluorination technique on the surface-fluorination patterning of double-walled carbon nanotubes. Beilstein J. Nanotechnol. 2017, 8, 1688–1698, https://doi.org/10.3762/bjnano.8.169.
[25] Dubey, R.; Dutta, D.; Sarkar, A.; Chattopadhyay, P. Functionalized carbon nanotubes: Synthesis, properties and applications in water purification, drug delivery, and material and biomedical sciences. Nanoscale Adv. 2021, 3, 5722–5744, https://doi.org/10.1039/d1na00293g.
[26] Talyzin, A.V.; Luzan, S.; Anoshkin, I.V.; Nasibulin, A.G.; Jiang, H.; Kauppinen, E.I.; Mikoushkin, V.M.; Shnitov, V.V.; Marchenko, D.E.; Noréus, D. Hydrogenation, purification, and unzipping of carbon nanotubes by reaction with molecular hydrogen: Road to graphane nanoribbons. ACS Nano. 2011, 5, 5132–5140, https://doi.org/10.1021/nn201224k.
[27] Kumar, I.; Rana, S.; Cho, J.W. Cycloaddition reactions: A controlled approach for carbon nanotube functionalization. Chem A Eur. J. 2011, 17, 11092–11101, https://doi.org/10.1002/chem.201101260.
[28] Singh, P.; Campidelli, S.; Giordani, S.; Bonifazi, D.; Bianco, A.; Prato, M. Organic functionalization and characterization of single-walled carbon nanotubes. Chem. Soc. Rev. 2009, 38, 2214–2230, https://doi.org/10.1039/b518111a.
[29] Tasis, D.; Tagmatarchis, N.; Bianco, A.; Prato, M. Chemistry of carbon nanotubes. Chem. Rev. 2006, 106, 1105–1136, https://doi.org/10.1021/cr050569o.
[30] Wu, H.C.; Chang, X.; Liu, L.; Zhao, F.; Zhao, Y. Chemistry of carbon nanotubes in biomedical applications. J. Mater. Chem. 2010, 20, 1036–1052, https://doi.org/10.1039/b911099m.
[31] Bahr, J.L.; Yang, J.; Kosynkin, D.V.; Bronikowski, M.J.; Smalley, R.E.; Tour, J.M. Functionalization of carbon nanotubes by electrochemical reduction of aryl diazonium salts: A bucky paper electrode. J. Am. Chem. Soc. 2001, 123, 6536–6542, https://doi.org/10.1021/ja010462s.

[32] Bahr, J.L.; Tour, J.M. Highly functionalized carbon nanotubes using in situ generated diazonium compounds. Chem. Mater 2001, 13, 3823–3824, https://doi.org/10.1021/cm0109903.
[33] Hamon, M.A.; Chen, J.; Hu, H.; Chen, Y.; Itkis, M.E.; Rao, A.M.; Eklund, P.C.; Haddon, R.C. Dissolution of single-walled carbon nanotubes. Adv. Mater 1999, 11, 834–840, https://doi.org/10.1002/(SICI)1521-4095(199907)11:10<834::AID-ADMA834>3.0.CO;2-R.
[34] Yeung, C.S.; Tian, W.Q.; Liu, L.V.; Wang, Y.A. Chemistry of single-walled carbon nanotubes. J. Comput. Theor. Nanosci. 2009, 6, 1213–1235, https://doi.org/10.1166/jctn.2009.1171.
[35] Yao, Z.; Braidy, N.; Botton, G.A.; Adronov, A. Polymerization from the surface of single-walled carbon nanotubes – preparation and characterization of nanocomposites. J. Am. Chem. Soc. 2003, 125, 16015–16024, https://doi.org/10.1021/ja037564y.
[36] Zhao, B.; Hu, H.; Yu, A.; Perea, D.; Haddon, R.C. Synthesis and characterization of water soluble single-walled carbon nanotube graft copolymers. J. Am. Chem. Soc. 2005, 127, 8197–8203, https://doi.org/10.1021/ja042924i.
[37] Zhang, W.; Chen, J.; Swiegers, G.F.; Ma, Z.-F.; Wallace, G.G. Microwave-assisted synthesis of Pt/CNT nanocomposite electrocatalysts for PEM fuel cells. Nanoscale. 2010, 2, 282–286, https://doi.org/10.1039/B9NR00140A.
[38] Li, L.; Xing, Y. Pt–Ru nanoparticles supported on carbon nanotubes as methanol fuel cell catalysts. J. Phys. Chem. C. 2007, 111, 2803–2808, https://doi.org/10.1021/jp0655470.
[39] Chen, Z.; Waje, M.; Yan, Y. Durability and activity study of single-walled, double-walled and multi-walled carbon nanotubes supported Pt catalyst for PEMFCs. ECS Meet. Abstr. 2007, MA2007-02, 401–401, https://doi.org/10.1149/MA2007-02/9/401.
[40] Muhammad, A.; Yusof, N.A.; Hajian, R.; Abdullah, J. Decoration of carbon nanotubes with gold nanoparticles by electroless deposition process using ethylene diamine as a cross linker. J. Mater. Res. 2016, 31, 2897–2905, https://doi.org/10.1557/jmr.2016.304.
[41] Moniruzzaman, M.; Winey, K.I. Polymer nanocomposites containing carbon nanotubes. Macromolecules. 2006, 39, 5194–5205, https://doi.org/10.1021/ma060733p.
[42] Zhou, Y.; Fang, Y.; Ramasamy, R.P. Non-covalent functionalization of carbon nanotubes for electrochemical biosensor development. Sensors (Switzerland). 2019, 19, https://doi.org/10.3390/s19020392.
[43] Liu, P. Modifications of carbon nanotubes with polymers. Eur. Polym. J. 2005, 41, 2693–2703, https://doi.org/10.1016/j.eurpolymj.2005.05.017.
[44] Hu, C.; Liao, H.; Li, F.; Xiang, J.; Li, W.; Duo, S.; Li, M. Noncovalent functionalization of multi-walled carbon nanotubes with siloxane polyether copolymer. Mater. Lett 2008, 62, 2585–2588, https://doi.org/10.1016/j.matlet.2007.12.060.
[45] Priya, B.R.; Byrne, H.J. Investigation of sodium dodecyl benzene sulfonate assisted dispersion and debundling of single-wall carbon nanotubes. J. Phys. Chem. C. 2008, 112, 332–337, https://doi.org/10.1021/jp0743830.
[46] Yu, A.; Su, C.C.L.; Roes, I.; Fan, B.; Haddon, R.C. Gram-scale preparation of surfactant-free, carboxylic acid groups functionalized, individual single-walled carbon nanotubes in aqueous solution. Langmuir. 2010, 26, 1221–1225, https://doi.org/10.1021/la902341w.
[47] Duque, J.G.; Cognet, L.; Parra-Vasquez, A.N.G.; Nicholas, N.; Schmidt, H.K.; Pasquali, M. Stable luminescence from individual carbon nanotubes in acidic, basic, and biological environments. J. Am. Chem. Soc. 2008, 130, 2626–2633, https://doi.org/10.1021/ja0777234.
[48] Gohari, M.S.; Rezaei, S.A.; Rashidi, A.; Saremi, M.; Ebadzadeh, T. The effect of mullite coating and microwave sintering on high temperature oxidation resistance of MWCNTs. Ceram. Int. 2022, 1–7, https://doi.org/10.1016/j.ceramint.2022.01.316.

[49] Cui, H.; Yan, X.; Monasterio, M.; Xing, F. Effects of various surfactants on the dispersion of MWCNTs–OH in aqueous solution. Nanomaterials. 2017, 7, https://doi.org/10.3390/nano7090262.
[50] Islam, M.F.; Rojas, E.; Bergey, D.M.; Johnson, A.T.; Yodh, A.G. Solubilization of single-wall carbon nanotubes in water. Nano Lett. 2003, 3, 269–273.
[51] Kharissova, O.V.; Kharisov, B.I.; De Casas Ortiz, E.G. Dispersion of carbon nanotubes in water and non-aqueous solvents. RSC Adv. 2013, 3, 24812–24852, https://doi.org/10.1039/c3ra43852j.
[52] Jiang, L.; Gao, L.; Sun, J. Production of aqueous colloidal dispersions of carbon nanotubes. J. Colloid Interface Sci. 2003, 260, 89–94, https://doi.org/10.1016/S0021-9797(02)00176-5.
[53] O'Connell, M.J.; Boul, P.; Ericson, L.M.; Huffman, C.; Wang, Y.; Haroz, E.; Kuper, C.; Tour, J.; Ausman, K.D.; Smalley, R.E. Reversible water-solubilization of single-walled carbon nanotubes by polymer wrapping. Chem. Phys. Lett. 2001, 342, 265–271, https://doi.org/10.1016/S0009-2614(01)00490-0.
[54] Fujigaya, T.; Nakashima, N. Non-covalent polymer wrapping of carbon nanotubes and the role of wrapped polymers as functional dispersants. Sci. Technol. Adv. Mater. 2015, 16, 24802, https://doi.org/10.1088/1468-6996/16/2/024802.
[55] Tan, S.H.; Suk, K.L.; Goak, J.C.; Hong, S.C.; Kim, J.; Lee, S.; Kim, S.; Seo, Y.; Lee, N. Effect of Poly (2-ethyl-2-oxazoline) on Multi-Walled Carbon Nanotubes Reinforced Poly (vinyl alcohol) Composites 2010, 18, 251–256.
[56] Zheng, M.; Jagota, A.; Semke, E.D.; Diner, B.A.; McLean, R.S.; Lustig, S.R.; Richardson, R.E.; Tassi, N.G. DNA-assisted dispersion and separation of carbon nanotubes. Nat. Mater. 2003, 2, 338–342, https://doi.org/10.1038/nmat877.
[57] Functionalization, N.S.; Carbon, S.; Star, A.; Liu, Y.; Grant, K.; Ridvan, L.; Stoddart, J.F.; Steuerman, D.W.; Diehl, M.R.; Boukai, A.; Heath, J.R. Noncovalent side-wall functionalization of single-walled carbon nanotubes. Macromolecules. 2003, 36, 553–560.
[58] Zhao, W.; Song, C.; Pehrsson, P.E. Water-soluble and optically pH-sensitive single-walled carbon nanotubes from surface modification. J. Am. Chem. Soc. 2002, 124, 12418–12419, https://doi.org/10.1021/ja027861n.
[59] Fernando, K.A.S.; Lin, Y.; Wang, W.; Kumar, S.; Zhou, B.; Xie, S.Y.; Cureton, L.S.T.; Sun, Y.P. Diminished band-gap transitions of single-walled carbon nanotubes in complexation with aromatic molecules. J. Am. Chem. Soc. 2004, 126, 10234–10235, https://doi.org/10.1021/ja047691+.
[60] Chen, R.J.; Zhang, Y.; Wang, D.; Dai, H. Noncovalent sidewall functionalization of single-walled carbon nanotubes for protein immobilization. J. Am. Chem. Soc. 2001, 123, 3838–3839, https://doi.org/10.1021/ja010172b.
[61] Murakami, H.; Nomura, T.; Nakashima, N. Noncovalent porphyrin-functionalized single-walled carbon nanotubes in solution and the formation of porphyrin-nanotube nanocomposites. Chem. Phys. Lett. 2003, 378, 481–485, https://doi.org/10.1016/S0009-2614(03)01329-0.
[62] Xia, H.; Wang, Q.; Qiu, G. Polymer-encapsulated carbon nanotubes prepared through ultrasonically initiated in situ emulsion polymerization. Chem. Mater. 2003, 15, 3879–3886, https://doi.org/10.1021/cm0341890.
[63] Zhou, W.; Lv, S.; Shi, W. Preparation of micelle-encapsulated single-wall and multi-wall carbon nanotubes with amphiphilic hyperbranched polymer. Eur. Polym. J. 2008, 44, 587–601, https://doi.org/10.1016/j.eurpolymj.2008.01.020.
[64] Arnold, M.S.; Guler, M.O.; Hersam, M.C.; Stupp, S.I. Encapsulation of carbon nanotubes by self-assembling peptide amphiphiles. Langmuir. 2005, 21, 4705–4709, https://doi.org/10.1021/la0469452.

[65] Pastine, S.J.; Okawa, D.; Zettl, A.; Fréchet, J.M.J. Chemicals on demand with phototriggerable microcapsules. J. Am. Chem. Soc. 2009, 131, 13586–13587, https://doi.org/10.1021/ja905378v.
[66] Xiong, Z.; Yun, Y.S.; Jin, H.J. Applications of carbon nanotubes for lithium ion battery anodes. Materials (Basel). 2013, 6, 1138–1158, https://doi.org/10.3390/ma6031138.
[67] Han, Z.; Fina, A. Thermal conductivity of carbon nanotubes and their polymer nanocomposites: A review. Prog. Polym. Sci. 2011, 36, 914–944, https://doi.org/10.1016/j.progpolymsci.2010.11.004.
[68] Gojny, F.H.; Wichmann, M.H.G.; Köpke, U.; Fiedler, B.; Schulte, K. Carbon nanotube-reinforced epoxy-composites: Enhanced stiffness and fracture toughness at low nanotube content. Compos. Sci. Technol. 2004, 64, 2363–2371, https://doi.org/10.1016/j.compscitech.2004.04.002.
[69] Eder, D. Carbon nanotube–inorganic hybrids. Chem. Rev. 2010, 110, 1348–1385, https://doi.org/10.1021/cr800433k.
[70] Khare, R.; Suryasarathi, B. Carbon nanotube based composites- a review. Compr. Compos. Mater. II. 2018, 4, 201–229, https://doi.org/10.1016/B978-0-12-803581-8.10012-8.
[71] Jeon, H.R.; Park, J.H.; Shon, M.Y. Corrosion protection by epoxy coating containing multi-walled carbon nanotubes. J. Ind. Eng. Chem. 2013, 19, 849–853, https://doi.org/10.1016/j.jiec.2012.10.030.
[72] Yang, L.H.; Liu, F.C.; Han, E.H. Effects of P/B on the properties of anticorrosive coatings with different particle size. Prog. Org. Coatings. 2005, 53, 91–98, https://doi.org/10.1016/j.porgcoat.2005.01.003.
[73] Ganguli, S.; Aglan, H.; Dennig, P.; Irvin, G. Effect of loading and surface modification of MWCNTs on the fracture behavior of epoxy nanocomposites. J. Reinf. Plast. Compos. 2006, 25, 175–188, https://doi.org/10.1177/0731684405056425.
[74] Rout, T.K.; Jha, G.; Singh, A.K.; Bandyopadhyay, N.; Mohanty, O.N. Development of conducting polyaniline coating: A novel approach to superior corrosion resistance. Surf. Coatings Technol. 2003, 167, 16–24, https://doi.org/10.1016/S0257-8972(02)00862-9.
[75] Fukuda, H.; Szpunar, J.A.; Kondoh, K.; Chromik, R. The influence of carbon nanotubes on the corrosion behaviour of AZ31B magnesium alloy. Corros. Sci. 2010, 52, 3917–3923, https://doi.org/10.1016/j.corsci.2010.08.009.
[76] Maeda, S.; Armes, S.P. Preparation and characterisation of novel polypyrrole-silica colloidal nanocomposites. J. Mater. Chem. 1994, 4, 935–942, https://doi.org/10.1039/JM9940400935.
[77] Xue, C.H.; Zhou, R.J.; Shi, M.M.; Gao, Y.; Wu, G.; Bin Zhang, X.; Chen, H.Z.; Wang, M. A green route to water soluble carbon nanotubes and in situ loading of silver nanoparticles. Nanotechnology 2008, 19, https://doi.org/10.1088/0957-4484/19/32/325605.
[78] He, Y.; Chen, C.; Zhong, F.; Chen, H.; Qing, D. Synthesis and properties of iron oxide coated carbon nanotubes hybrid materials and their use in epoxy coatings. Polym. Adv. Technol. 2015, 26, 414–421, https://doi.org/10.1002/pat.3470.
[79] Li, J.; Wong, P.S.; Kim, J.K. Hybrid nanocomposites containing carbon nanotubes and graphite nanoplatelets. Mater. Sci. Eng. A. 2008, 483–484, 660–663, https://doi.org/10.1016/j.msea.2006.08.145.
[80] Dos Santos, A.S.; Leite, T.D.O.N.; Furtado, C.A.; Welter, C.; Pardini, L.C.; Silva, G.G. Morphology, thermal expansion, and electrical conductivity of multiwalled carbon nanotube/epoxy composites. J. Appl. Polym. Sci. 2008, 108, 979–986, https://doi.org/10.1002/app.27614.

[81] Gojny, F.H.; Wichmann, M.H.G.; Fiedler, B.; Schulte, K. Influence of different carbon nanotubes on the mechanical properties of epoxy matrix composites – A comparative study. Compos. Sci. Technol. 2005, 65, 2300–2313, https://doi.org/10.1016/j.compscitech.2005.04.021.
[82] Pandey, J.K.;, Handbook of Polymer Nanocomposites. Processing, Performance and Application, 2015. https://doi.org/10.1007/978-3-642-45232-1.
[83] Hu, H.; He, Y.; Long, Z.; Zhan, Y. Synergistic effect of functional carbon nanotubes and graphene oxide on the anti-corrosion performance of epoxy coating. Polym. Adv. Technol. 2017, 28, 754–762, https://doi.org/10.1002/pat.3977.
[84] Zhang, Y.; Zhu, H.; Zhuang, C.; Chen, S.; Wang, L.; Dong, L.; Yin, Y. TiO2 coated multi-wall carbon nanotube as a corrosion inhibitor for improving the corrosion resistance of BTESPT coatings. Mater. Chem. Phys. 2016, 179, 80–91, https://doi.org/10.1016/j.matchemphys.2016.05.012.
[85] Zare, E.N.; Lakouraj, M.M.; Moosavi, E. Poly (3-aminobenzoic acid) @ MWCNTs hybrid conducting nanocomposite: Preparation, characterization, and application as a coating for copper corrosion protection. Compos. Interfaces. 2016, 23, 571–583, https://doi.org/10.1080/09276440.2016.1156966.
[86] Richard Prabakar, S.J.; Pyo, M. Corrosion protection of aluminum in LiPF 6 by poly(3,4-ethylenedioxythiophene) nanosphere-coated multiwalled carbon nanotube. Corros. Sci. 2012, 57, 42–48, https://doi.org/10.1016/j.corsci.2011.12.036.
[87] Palaniappan, N.; Cole, I.S.; Kuznetsov, A.E.; Justin Thomas, K.R. Experimental and DFT studies of carbon nanotubes covalently functionalized with an imidazole derivative for electrochemical stability and green corrosion inhibition as a barrier layer on the nickel alloy surface in a sulphuric acidic medium. RSC Adv. 2019, 9, 38677–38686, https://doi.org/10.1039/c9ra08123b.
[88] Alishahi, M.; Monirvaghefi, S.M.; Saatchi, A.; Hosseini, S.M. The effect of carbon nanotubes on the corrosion and tribological behavior of electroless Ni-P-CNT composite coating. Appl. Surf. Sci. 2012, 258, 2439–2446, https://doi.org/10.1016/j.apsusc.2011.10.067.
[89] Qiu, G.; Zhu, A.; Zhang, C. Hierarchically structured carbon nanotube-polyaniline nanobrushes for corrosion protection over a wide pH range. RSC Adv. 2017, 7, 35330–35339, https://doi.org/10.1039/c7ra05235a.
[90] Martina, V.; De Riccardis, M.F.; Carbone, D.; Rotolo, P.; Bozzini, B.; Mele, C. Electrodeposition of polyaniline–carbon nanotubes composite films and investigation on their role in corrosion protection of austenitic stainless steel by SNIFTIR analysis. J. Nanopart. Res. 2011, 13, 6035–6047, https://doi.org/10.1007/s11051-011-0453-5.
[91] Ioni, M.; Prun, A. Polypyrrole/carbon nanotube composites: Molecular modeling and experimental investigation as anti-corrosive coating. Prog. Org. Coatings. 2011, 72, 647–652, https://doi.org/10.1016/j.porgcoat.2011.07.007.
[92] Prasannakumar, R.S.; Chukwuike, V.I.; Bhakyaraj, K.; Mohan, S.; Barik, R.C. Electrochemical and hydrodynamic flow characterization of corrosion protection persistence of nickel/multiwalled carbon nanotubes composite coating. Appl. Surf. Sci. 2020, 507, 145073, https://doi.org/10.1016/j.apsusc.2019.145073.
[93] Rui, M.; Zhu, A. The synthesis and corrosion protection mechanisms of PANI/CNT nanocomposite doped with organic phosphoric acid. Prog. Org. Coatings. 2021, 153, 106134, https://doi.org/10.1016/j.porgcoat.2021.106134.

Avni Berisha

Chapter 10
Chemically modified CNTs as corrosion inhibitors

Abstract: Carbon nanotubes (CNTs) with a wide surface area are gaining importance as anticorrosion coating material due to their exceptional hydrophobicity, chemical resistance, stability, and high mechanical strength. CNT/composite coatings as corrosion inhibitors are a relatively new subject of study for material scientists. This chapter highlights significant studies on the different strategies that use chemically modified CNTs as corrosion inhibitors. The prospect of research on several recently developed CNT/composite materials that are employed in corrosion-protective coatings is discussed.

Keywords: chemically modified CNTs, corrosion inhibition, EIS, coating

10.1 Introduction

Corrosion is seen as a detrimental process that jeopardizes the durability of infrastructures and results in enormous expenses and damage to industrial units and buildings. As a result, engineers now have a substantial difficulty in determining the whole economic and environmental impact of corrosion concerns. Corrosion is an ongoing process that cannot be completely avoided in corrosive environments. Thus, corrosion prevention techniques are limited to decreasing the kinetics and modifying the mechanism of corrosion. Some of these solutions are alloying steel, using corrosion inhibitors, or using a combination of these solutions. Protective coatings are probably as one of the most effective methods of preventing corrosion on metal surfaces. A variety of protective coatings including organic, hybrid organic/inorganic, conversion, and metallic coatings, have been invented to act as a barrier, preventing or delaying metal corrosion by preventing corrosive elements from reaching the metallic substrate. The conventional anticorrosive coatings, which are virtually entirely comprised of heavy-metals-containing species (chromium, phosphate, zinc, and copper-based chemicals), are poisonous and ecologically damaging. As a result, an attempt has been made to identify acceptable nontoxic materials that have a low negative influence on the ecosystem and are

Avni Berisha, Department of Chemistry, Faculty of Natural and Mathematics Science, University of Prishtina, 10000 Prishtina, Kosovo, e-mail: avni.berisha@uni-pr.edu

https://doi.org/10.1515/9783110782820-010

highly successful in preventing metals from corroding. Nowadays, organic coatings are the most common and cost-effective means of protecting metal surfaces against corrosive agents. Organic coatings offer significant physical, protecting characteristics against corrosive species, which can greatly delay the corrosive species' contact with the substrate. Additionally, such coatings can provide protection by sacrificial action or active corrosion inhibition, via the insertion of active/passive entities (inhibitor-like molecules) in the coatings.

It has been demonstrated that the use of different fillers and anticorrosive substances considerably improves corrosion resistance. Over the last two decades, much attention has been given to the incorporation of nanomaterials into organic coatings to enhance their protective efficiency. Among these nanomaterials, CNTs appear to be promising and are now being frequently used for this purpose [1, 2].

10.2 Carbon nanotubes in corrosion

For the purpose of producing a data overview, with descriptive statistics and bibliometric indicators, it was decided to use the RStudio package [3] and Biblioshiny [4], an open-source statistical program. The analysis was performed with a SCOPUS database search ("functionalized" AND "carbon nanotubes "AND "corrosion") on Abstract title, Abstract, and Keywords yields: 154 documents within the timespan of: 2006 to 2022, and presented in Fig. 10.1.

As can be observed from the nearly all-positive trend in the number of articles, the subject is intriguing. In accordance with the analysis of the Author Keywords, CNTs are typically related with investigations that directly involve electrochemical techniques (CV, EIS, and so on), indicating their potential application in corrosion research and electrocatalysis. According to Bradford's Law[5], there are three zones: a central zone consisting of only two journals (Progress in Organic Coatings and ElectrochimicaActa), which published the majority of the articles; an intermediate zone consisting of three journals (Biosensors and Bioelectronics, Surface and Coatings Technology, RCS Advances, Carbon); and a smaller zone consisting of other journals. When shown as a WordCloud graph, the importance of various topics such as CNTs, corrosion, functionalization, and coating, is reflected. Furthermore, it is important to highlight that this field of study is related to a large number of conducting polymers (polypyrrole, polyaniline, and so on).

Despite the fact that humans have been using nano-sized objects for a long time, N. Taniguchi coined the term "nanotechnology" in 1974 [6,7]. Nanostructured materials are recognized to have remarkable mechanical and physical properties. due to their extremely small grain size and high grain boundary volume. CNTs stand out among these materials due to their remarkable mechanical, electrical, thermal, and magnetic characteristics, which have prompted numerous studies.

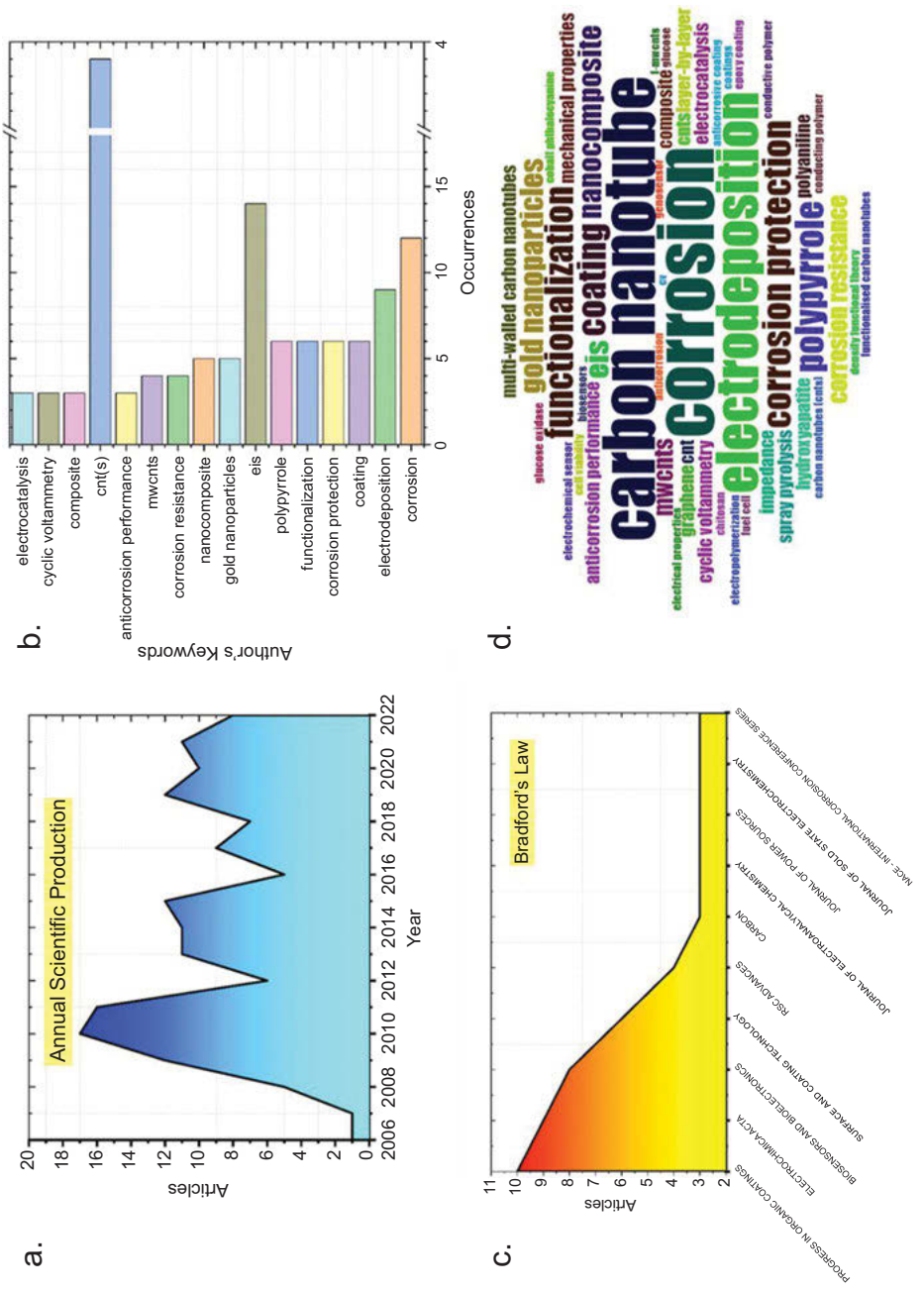

Fig. 10.1: (a) Annual scientific production; (b) Occurrences; (c) Bradford's Law, and (d) WordCloud: Authors' Keywords. Legend: Top-50 Authors' Keywords. Source: R Studio biblioshiny; software: R Studio biblioshiny.

The virtually concentric multiwall carbon nanotubes (c-MWNTs) were the first to be published in 1991 [2], and two years later, the single-wall carbon nanotubes (SWNTs) were concurrently reported by Iijima and Ichihashi [3] and Bethune et al. [4].

Due to their high aspect ratio and limited interfacial contact with the polymeric matrix, conventional CNTs exhibit a pronounced aggregation propensity. Covalent or non-covalent functionalization (Fig. 10.2) are usually followed to facilitate the dispersion of CNTs in the polymeric matrix by improving the interfacial interactions (in the form of physical adsorptions and chemical bondings) between the nanotube and the polymeric matrix [8].

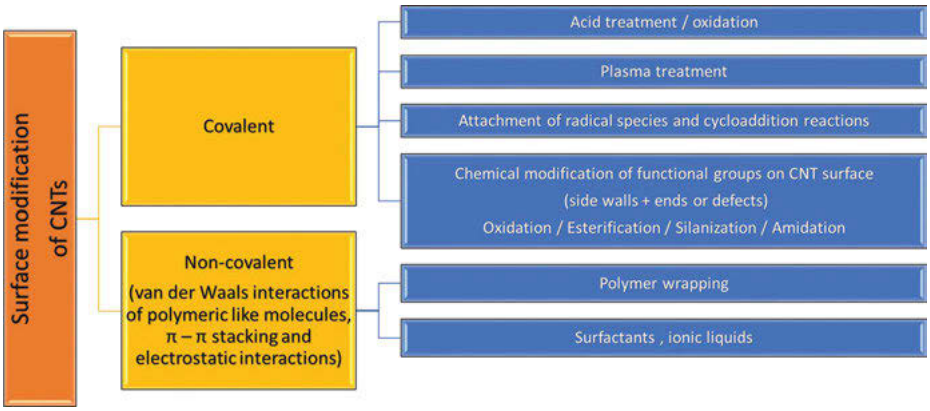

Fig. 10.2: Chart outlining the chemical common modification choices for CNTs.

Non-covalent interactions consist of the adsorption of polymers, oligomers, or molecules to the surface of the nanotubes, and chemical methods involving the chemical bonding of polymer or molecules to the surface of the CNTs [9–11].

10.3 Some of the applied strategies on the use of CNT in corrosion inhibition

Ghahremani et al. presented an interesting path to provide an MWCNT nanocarrier corrosion inhibition (Fig. 10.3) with a remarkable increase in total resistance (Rt). With the inclusion of the composite nanostructures, the oxidized MWCNT framework allows regulated release of polydopamine, chitosan, and zinc (II) ions at the damaged location. The damaged zone developed a protective layer from the released inhibitors, as shown by FE-SEM/EDX. Zn nanocomposite added to epoxy coating increased barrier properties and offered long term corrosion retardation [12].

In another study, the simple ultrasonication process was used to generate nanocomposite-reinforced polyurethane (PU) coatings using polydopamine-wrapped carbon nanotubes (PDA@CNTs) as the nanofiller. Through ageing experiments that comprised salt spraying and solution immersion, the effect of the nanocomposite enhanced PU's corrosion resistance on the Al-alloy as shown by EIS [13].

The poly(2-butylaniline) was used to disperse non-covalently functionalized MWCNs in an epoxy matrix (PBA). Moreover, this dispersion was utilized to create MWCNTs/epoxy (EP) nanocomposites with enhanced corrosion and tribological properties. MWCNTs were included into the epoxy matrix, causing low water absorption and a high impedance modulus. These findings were also consistent with the SEM results after long-term immersion tests [14].

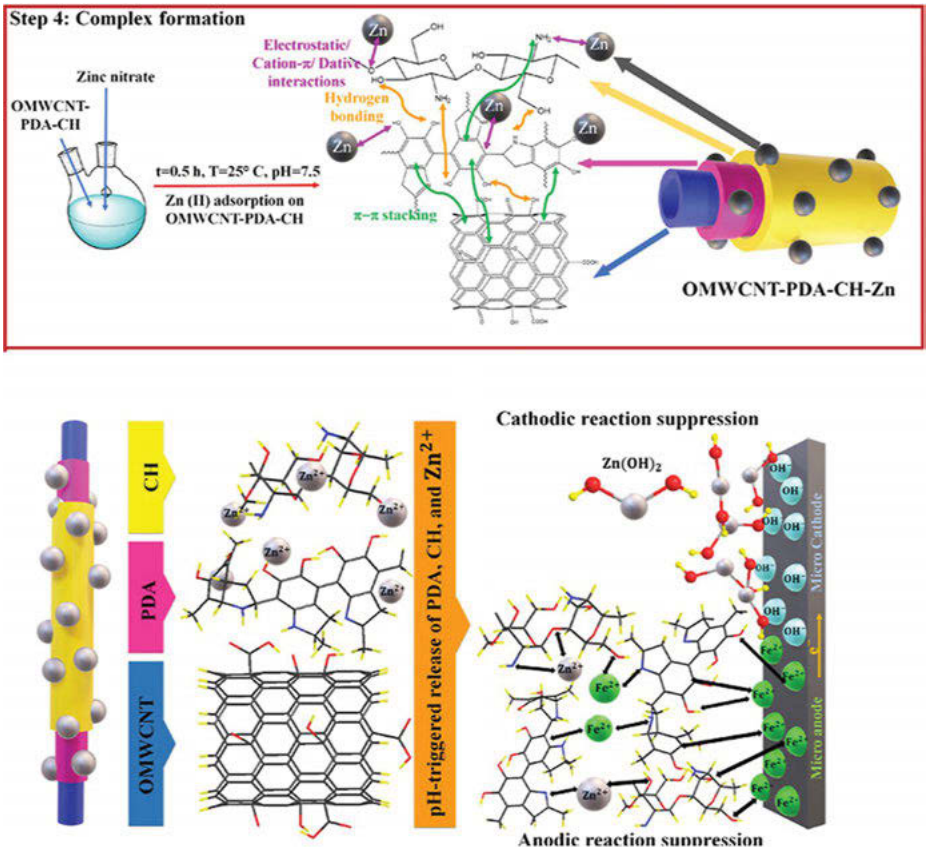

Fig. 10.3: Schematic representation of the multi-functional carbon-based nano-carrier based on multi-walled-CNT-oxide/polydopamine/chitosan for epoxy composite with robust pH-sensitive active anticorrosion properties [12].

Liu et al. revealed that silicon dioxide nanoparticles may be produced in situ on the surface of CNT using tetraethyl orthosilicate. They spread the CNT into the thermoplastic polyurethane (TPU) matrix after treating it with fluorinated silane, forming a super hydrophobic composite layer. They demonstrated that the coating displays outstanding mechanical durability and retains super hydrophobicity following sandpaper abrasion or tape ripping and has a strong adherence to TPU. In addition, the layer inhibits corrosive species from migrating from the solution to the surface, protecting the materials in harsh solution conditions [15].

Chavhan et al. [16] generated electroactive polyamide (EPA)/multiwall carbon nanotube (MWCNT) nanocomposites (NCs) using in situ oxidative coupling polymerization of EPA in the presence of MWCNT and ammonium persulphate as an oxidant. EIS and potentiodynamic polarization techniques revealed that the produced coating has outstanding anticorrosion characteristics for 201 stainless steel. Yan et al. [16] developed highly dispersed silica/carbon nanotube (HAC) to tackle the dispersion and agglomeration issues associated with CNT-based materials. They created a self-healing smart coating layer that protected the materials surface.

Poly(arylene ether nitrile) shown in Fig. 10.4 was used by Xia et al. [16] as a protective coating on P110 steel. They showed that the addition of the cyano-functionalized-MWCNTs (MWCNTs-CN) further increased the PEN coating's corrosion resistance and its mechanical performance.

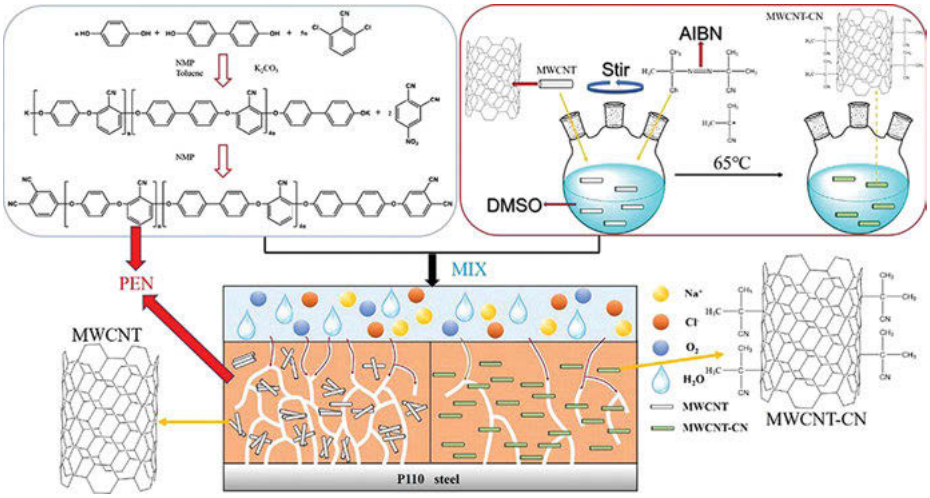

Fig. 10.4: Schematic representation of the MWCNT-CN fillers synthesized by the thermal decomposition of Azobisisobutyronitrile(AIBN) [16].

Bai et al. [17] developed two unique morphologies of poly (3,4-ethylenedioxy thiophene) (PEDOT) composite organic coatings using PEDOT/nanoparticles or PEDOT/carbon nanotubes (PEDOT/CNT). The researchers integrated PEDOT into a

polyvinyl butyral (PVB) matrix and applied it to an iron substrate to generate corrosion-resistant composite coatings. The electrochemical deposition of Ni-P-carbon nanotube (CNT) coatings on mild steel utilizing an electrolyte bath containing varying CNT concentrations led to better-quality corrosion resistance. In comparison to other coatings, the coating generated from electrolyte containing 5 mg/l carbon nanotubes had the highest charge transfer resistance and the lowest corrosion current density value [18].

Chen et al. [19] were able to create a homogeneous dispersion of MWCNTs within fusion-bonded epoxy (FBE) powder coatings by combining ball milling and hot melt extrusion. Prior to its usage as nanofiller in FBE powder coatings, MWCNTs were surface modified using polyvinylpyrrolidone (m-MWCNTs). The corrosion resistance and adhesion strength of the nanocomposite covering were enhanced by m-MWCNTs. The authors proved that the higher coating resistance is mostly due to the even spreading of the nanofiller and the expansion of the pathway for corrosive electrolytes inside the coating matrix.

To protect St37 steel in NaCl solution against corrosion, a hybrid sol–gel coating was created via the reaction of tetraethylorthosilicate and triethoxyvinylsilane. To upturn the corrosion resistance of the intended coating, the authors added two corrosion inhibitors, bromophenol blue and eosin-methylene blue, to the coating[20]. Additionally, the influence of MWCTs used as a surface modifier on the performance of the coating was explored. Corrosion testing was performed using EIS. The results indicated that each inhibitor included in the coating increased corrosion protection by a minor amount. However, the combination of the nanoparticle and inhibitor resulted in a significant increase in the coating's corrosion resistance.

Li et al. [21] employed a two-step technique to introduce a hydrophobic waterborne polyurethane (PU) composite coating, namely using graphene oxide (GO) + carbon nanotubes (CNTs) hybrids as synergistic reinforcement and nano-casting the surface with fresh lotus leaf. The research group established that: a) when compared to pure PU coating, the composite coating demonstrated improved mechanical characteristics as a result of the GO + CNTs hybrid effect, that is, tensile strength was raised; b) the contact angle of the composite coating surface was raised; and c) the composite coating significantly improved corrosion resistance, with an inhibitory effectiveness of > 98 % maintained after 20 days in a 3.5%NaCl solution.

Wu et al. [22] established a durable and quick self-healing coating on steel substrates by incorporating CNTs into the fluid matrix of epoxy resin (EP) or silicone oil.

They enhanced active corrosion resistance of the matrix, by using 1 H, 1 H, 2 H, 2 H-perfluorooctyltriethoxysilane (PTES). The added PTES reacts with the water contained inside the coating. The coating exhibits promising self-healing characteristics when repeatedly scratched on a millimeter scale, as well as high corrosion resistance in an acidic (HCl) or basic (NaOH) aqueous solution. The optimized fluid coating may be employed as a smart corrosion barrier coating for metals owing to its excellent durability and potentially endless self-healing capabilities, paired with a quick response time.

The acid-oxidized multiwall carbon nanotubes (o-MWCNTs) were utilized by Vu et al. [23] acid, as an addition to improve the anticorrosion and mechanical characteristics of an epoxy-based coating.

When compared to pure epoxy coatings and epoxy coatings embedded with pristine MWCNTs, the addition of o-MWCNTs to epoxy coatings increases their anticorrosion properties [24]. Dip-coating was effectively used to coat steel with a bis-[triethoxysilylpropyl] tetrasulfidesilane layer modified with CNT [25]. In terms of anticorrosion performance, the composite coatings outperform the single silane layer.

Shoujie et al. [26] created CNTs-reinforced apatite composite coatings on carbon/carbon composites, by a dual in situ technique consisting of injection chemical vapor deposition and bio mineralization. Prior to coating formulation, carboxyl-functionalized CNTS were formed (through nitric acid treatment). Raman analysis revealed the successful functionalization of carbon nanotubes (Fig. 10.5). Two notable bands can be detected in the recorded Raman spectra of bare carbon nanotubes at 1358 cm^{-1} (the well-known D band) and 1582 cm^{-1} (the G band). The D and G bands of functionalized carbon nanotubes are marginally moved to 1364 and 1596 cm^{-1}. The I_D/I_G ratio (I_D and I_G denote the intensity of the D and G bands, respectively) is used to determine the degree of crystallinity and surface defects in carbon nanotubes, as well as their purity and structural alteration on the sidewall. The researchers demonstrated the effective functionalization of carbon nanotubes by examining the 0.18 value of the I_D to I_G ratio for functionalized CNTs, compared to bare carbon nanotubes.

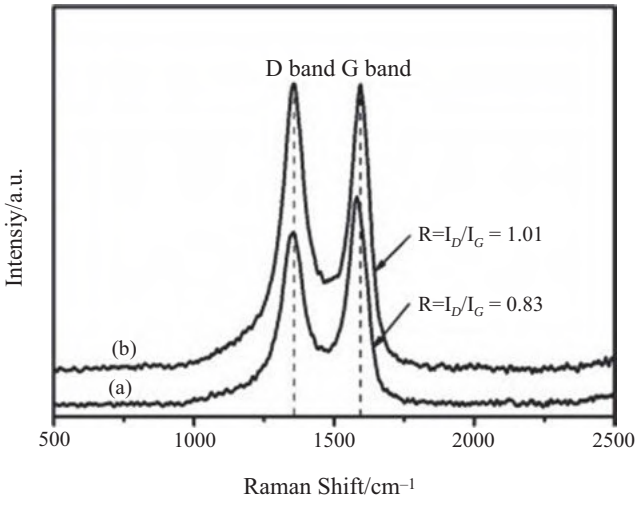

Fig. 10.5: Raman spectra of CNT before (a) and after (b) carboxyl-functionalization [26].

SEM morphology and XPS spectra revealed that CNTs were wrapped in apatite and that the apatite layer got thicker as the immersion period was increased. The corrosion resistance of this apatite composite coating, as determined by electrochemical methods, indicated a tendency toward a more stable coating in simulated bodily fluid with a longer bio mineralization period. The thick apatite layer was estimated to be detrimental to electron conduction, resulting in a low polarization current and a high polarization impedance.

Polyaniline (PANI) and its composites with MWCNT were synthesized using chemical oxidative polymerization. The synthetic composite is prepared as pigments in alkyd resin with varied pigment-binder ratios and evaluated as anticorrosive coatings on carbon steel in acidic media using potentiodynamic polarization and EIS. PANI inhibits corrosion by forming a barrier and acting as a passivate layer on the carbon steel surface. The encapsulation and dispersion of MWCNTs in the PANI matrix improved the anticorrosive capabilities of the alkyd coating [27].

Recently, a sol-gel N-propyl-dimethoxy-silane coating was investigated to improve aluminum's corrosion resistance [28]. The coating was loaded with different numbers of carbon nanotubes having multiple walls (MWCNTs). The nanocomposite coating was applied through drop casting to an Al-alloy substrate. Corrosion resistance of the material was considerably improved when CNT was added to the base coating in seawater. After three days of immersion in the solution, the EIS of the surface coated material persisted. Lou et al. [29] proposed the use of hydrogen bonding-enabled coating materials to significantly reduce electrical resistance. They demonstrated that hydrogen bonding between functionalized carbon nanotubes and ethanol promoted the creation of a dense network of carbon nanotubes that acted as electron channels. Electrochemical testing of the anticorrosion properties of the coating materials generated revealed an outstanding efficiency of up to 99.5 percent in corrosive medium.

By integrating a functionalized multi-walled carbon nanotube/polyindole (f-MWCNT/PIn) nanocomposite into the epoxy resin (EP) matrix, the anticorrosion performance of the EP is improved. The electrochemical approach was used to determine the corrosion resistance of various weight percentages of f-MWCNT/PIn dispersed EP coatings on mild steel (MS) in NaCl solution. EIS and potentiodynamic polarization measurements revealed that a 0.25 % f-MWCNT/PIn nanocomposite coating has outstanding anticorrosion and barrier protection capabilities [29].

Hydrothermally produced functionalized carbon nanotubes (FCNTs) were used as a corrosion inhibitor for carbon steel in a CO_2-saturated NaCl solution. The nanotubes significantly prevent carbon steel corrosion, with inhibition effectiveness close to 90% at a dosage of 100 mg/L. As demonstrated by molecular dynamics simulations, FCNTs may adsorb on carbon steel via functionalized groups and form the hydrophobic layer on the metal surface, which also restricts the diffusion migration of corrosive media (Fig. 10.6) [30].

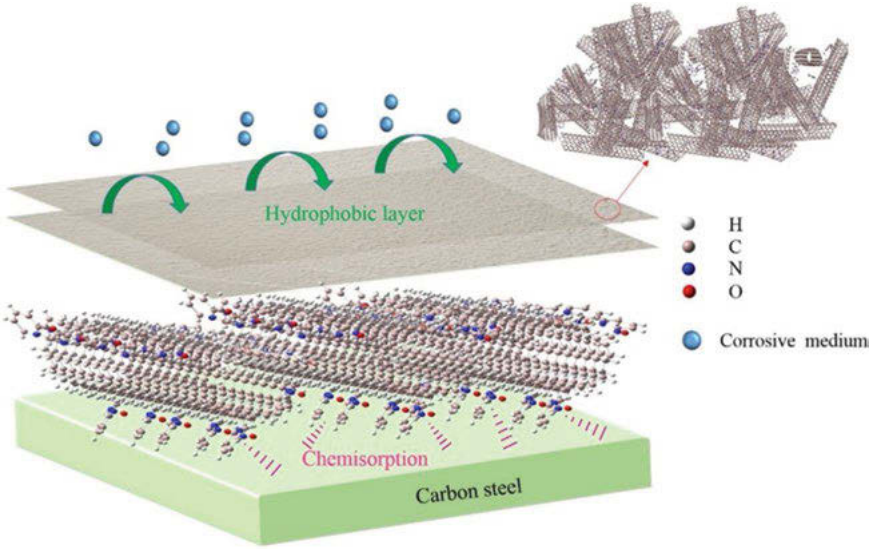

Fig. 10.6: The use of hydrothermally produced functionalized carbon nanotubes as corrosion inhibitors [30].

As Ag has the highest electrical conductivity of all metals, it has been frequently exploited for electrical contact components. Sulfidation is one of the most serious concerns with Ag plating coatings for electrical contact components. The presence of insulating silver sulfide at the contact interface increases the electrical contact resistance of Ag-plated products. The authors demonstrated that following an H_2S gas corrosion test, an Ag/CNT film produced from a non-cyanide plating bath had lower electrical contact resistance than a pure Ag plating layer [31].

Carbon nanotubes functionalized with 3-methoxy-4-(1-phenyl-1 H-benzimidazol -2-yl) phenol were synthesized and used as a corrosion-inhibiting barrier layer on nickel alloy surfaces. On the nickel alloy surface, these functionalized carbon nanotubes exhibited good corrosion prevention [32].

On 316 L stainless steel, a novel spray pyrolysis technique was employed to fabricate a Cu-hydroxyapatite/f-MWCNT 316 L stainless steel. The corrosion current density decreased significantly from 6.8 to 3.8 A, indicating that the Cu replacement hydroxyapatite/f-MWCNT composite coating possessed superior barrier qualities, particularly assisted in the corrosion protection of 316 L stainless steel implants [33].

10.4 Conclusion and future perspective

The study on carbon nanotubes used as anticorrosion coatings is summarized in this chapter. Coatings consisting of CNTs/composites outperform other conventional coatings in terms of corrosion resistance, due to their greater barrier effect. Functionalized CNTs have emerged as a viable alternative to normally expensive and dangerous organic corrosion inhibitors. Chemical functionalization of CNTs is advantageous, because it allows for the dispersion and attachment of other interesting organic molecules (inhibitors) on the surface. When compared to traditional organic corrosion inhibitors, the usage of CNT is simple and, in many cases, more effective. Although there is presently no information on the commercial application of chemically modified carbon nanotubes-based corrosion inhibitors, this is a relatively new area in which significant research is being performed to generate corrosion inhibitor formulations for practical application. Further study will focus on the self-healing and inhibitor release properties of CNT coatings, which might lead to superior combined mechanical and corrosion protection coatings.

References

[1] Verma, C. Nanomaterials as corrosion inhibitors. Handb. Sci. Eng. Green Corros. Inhib. 2022, 261–270, doi:10.1016/B978-0-323-90589-3.00012-4.

[2] Dewangan, Y.; Dewangan, A.K.; Shobha; Verma, D.K. Carbon Nanotubes as Corrosion Inhibitors. *Org. Corros. Inhib*. 2021, 371–385, doi:10.1002/9781119794516.CH16.

[3] Bates, D.; Mächler, M.; Bolker, B.M.; Walker, S.C. Fitting linear mixed-effects models using lme4. J. Stat. Softw. 2015, 67, doi:10.18637/JSS.V067.I01.

[4] Aria, M.; Cuccurullo, C. bibliometrix: An R-tool for comprehensive science mapping analysis. J. Informetr. 2017, 11, 959–975, doi:10.1016/J.JOI.2017.08.007.

[5] Brookes, B.C. Bradford's law and the bibliography of science. Nat.1969 2245223 1969, 224, 953–956, doi:10.1038/224953a0.

[6] Wennersten, R.; Fidler, J.; Spitsyna, A. Nanotechnology: A New Technological revolution in the twenty-first century. Handb. Performability Eng.2008, 943–952, doi:10.1007/978-1-84800-131-2_57.

[7] Pruna, A. Advances in carbon nanotube technology for corrosion applications. Handb. Polym. Nanocomposites. Process. Perform. Appl. Vol. B Carbon Nanotub. Based Polym. Compos.2015, 335–359, doi:10.1007/978-3-642-45229-1_36.

[8] Pruna, A. Advances in carbon nanotube technology for corrosion applications. Handb. Polym. Nanocomposites. Process. Perform. Appl. Vol. B Carbon Nanotub. Based Polym. Compos.2015, 335–359, doi:10.1007/978-3-642-45229-1_36.

[9] Nayak, L., Rahaman, M., Giri, R. (2019). Surface Modification/Functionalization of Carbon Materials by Different Techniques: An Overview. In: Rahaman, M., Khastgir, D., Aldalbahi, A. (eds) Carbon-Containing Polymer Composites. Springer Series on Polymer and Composite Materials. Springer, Singapore. https://doi.org/10.1007/978-981-13-2688-2_2.

[10] Atif, M.; Afzaal, I.; Naseer, H.; Abrar, M.; Bongiovanni, R. Review – surface modification of carbon nanotubes: A tool to control electrochemical performance. ECS J. Solid State Sci. Technol. 2020, 9, 041009, doi:10.1149/2162-8777/AB8929.
[11] Berisha, A.; Chehimi, M.M.; Pinson, J.; Podvorica, F.I. Electrode surface modification using diazonium salts. In: Electroanalytical chemistry; Electroanalytical chemistry: A series of advances, CRC Press, 2015, 115–224, ISBN 978-1-4987-3377-9.
[12] Ghahremani, P.; Mostafatabar, A.H.; Bahlakeh, G.; Ramezanzadeh, B. Rational design of a novel multi-functional carbon-based nano-carrier based on multi-walled-CNT-oxide/polydopamine/chitosan for epoxy composite with robust pH-sensitive active anti-corrosion properties. *Carbon N. Y.* 2022, 189, 113–141, doi:10.1016/J.CARBON.2021.11.067.
[13] Cai, G.; Hou, J.; Jiang, D.; Dong, Z. Polydopamine-wrapped carbon nanotubes to improve the corrosion barrier of polyurethane coating. RSC Adv. 2018, 8, 23727–23741, doi:10.1039/C8RA03267J.
[14] Cui, M.; Ren, S.; Qiu, S.; Zhao, H.; Wang, L.; Xue, Q. Non-covalent functionalized multi-wall carbon nanotubes filled epoxy composites: Effect on corrosion protection and tribological performance. Surf. Coat. Technol. 2018, 340, 74–85, doi:10.1016/J.SURFCOAT.2018.02.045.
[15] Liu, Y.; Cao, X.; Shi, J.; Shen, B.; Huang, J.; Hu, J.; Chen, Z.; Lai, Y. A superhydrophobic TPU/CNTs@SiO2 coating with excellent mechanical durability and chemical stability for sustainable anti-fouling and anti-corrosion. Chem. Eng. J. 2022, 434, 134605, doi:10.1016/J.CEJ.2022.134605.
[16] Chavhan, J.; Rathod, R.; Tandon, V.; Umare, S.; Patil, A. Structural and physico-chemical properties of electroactive polyamide/multi-walled carbon nanotubes nanocomposites. Surf. Interfaces. 2022, 29, 101765, doi:10.1016/J.SURFIN.2022.101765.
[17] Bai, X.; Huang, X.; Zhao, Z.; Hu, X.; Zhou, S.; Liang, Y.; Rohwerder, M. Morphology-dependent delamination performance of poly (3,4-ethylenedioxythiophene) for corrosion protection on iron. J. Electrochem. Soc. 2022, 169, 020549, doi:10.1149/1945-7111/AC5300.
[18] Meshram, A.P.; Kumar, M.K.P.; Srivastava, C. Enhancement in anti-corrosive behavior of Ni-P coatings by incorporation of carbon nanotubes. J. Mater. Eng. Perform. 2022, 31, 1573–1584, doi:10.1007/S11665-021-06260-8.
[19] Chen, S.; Wang, X.; Zhu, G.; Lu, Z.; Zhang, Y.; Zhao, X.; Hou, B. Developing multi-wall carbon nanotubes/Fusion-bonded epoxy powder nanocomposite coatings with superior anti-corrosion and mechanical properties. Colloids Surfaces A Physicochem. Eng. Asp. 2021, 628, 127309, doi:10.1016/J.COLSURFA.2021.127309.
[20] Mohammadzadeh, M.A.; Es'haghi, M. Novel additive-included hybrid sol–gel coatings for practical corrosion protection of carbon steel in a saline medium. J. Mater. Eng. Perform. 2021, 30, 8395–8401, doi:10.1007/S11665-021-05998-5.
[21] Li, S.; Xu, R.; Song, G.; Li, B.; Fang, P.; Fu, Q.; Pan, C. Bio-inspired (GO + CNTs)-PU hydrophobic coating via replication of Lotus leaf and its enhanced mechanical and anti-corrosion properties. Prog. Org. Coatings. 2021, 159, doi:10.1016/J.PORGCOAT.2021.106414.
[22] Wu, Y.; Zhao, W.; Ou, J. Stable, superfast and self-healing fluid coating with active corrosion resistance. Adv. Colloid Interface Sci. 2021, 295, 102494, doi:10.1016/J.CIS.2021.102494.
[23] Vu, C.M.; Bach, Q.V. Oxidized multiwall carbon nanotubes filled epoxy-based coating: Fabrication, anticorrosive, and mechanical characteristics. Polym. Bull. 2021, 78, 2329–2339, doi:10.1007/S00289-020-03218-Z.
[24] Hosseinpour, A.; Rezaei Abadchi, M.; Mirzaee, M.; Ahmadi Tabar, F.; Ramezanzadeh, B. Recent advances and future perspectives for carbon nanostructures reinforced organic coating for anti-corrosion application. Surf. Interfaces. 2021, 23, doi:10.1016/J.SURFIN.2021.100994.

[25] Liu, Y.; Cao, H.; Yu, Y.; Chen, S. Corrosion protection of silane coatings modified by carbon nanotubes on stainless steel. *Int. J. Electrochem. Sci.* 2015, 10, 3497–3509.
[26] Shoujie, L.; Hejun, L.; Leilei, Z.; Shaoxian, L.; Lina, P. The corrosion properties of carbon nanotubes-reinforced apatite composite coating on carbon/carbon composite by a double in situ process. 2018, 35, 96–101, doi:10.1080/02670844.2018.1460537, https://doi.org/10.1080/02670844.2018.1460537.
[27] Farag, A.A.; Kabel, K.I.; Elnaggar, E.M.; Al-Gamal, A.G. Influence of polyaniline/multiwalled carbon nanotube composites on alkyd coatings against the corrosion of carbon steel alloy. Corros. Rev. 2017, 35, 85–94, doi:10.1515/CORRREV-2017-0049/MACHINEREADABLECITATION/RIS.
[28] Calabrese, L.; Khaskoussi, A.; Proverbio, E. Wettability and anti-corrosion performances of carbon nanotube-silane composite coatings. Fibers. 2020, 8, 57, doi:10.3390/FIB8090057.
[29] Lou, D.; Younes, H.; Yang, J.; Jasthi, B.K.; Hong, G.; Hong, H.; Tolle, C.; Bailey, C.; Widener, C.; Hrabe, R. Enhanced electrical conductivity of anticorrosive coatings by functionalized carbon nanotubes: Effect of hydrogen bonding. Nanotechnology. 2022, 33, 155704, doi:10.1088/1361-6528/AC4661.
[30] Cen, H.; Cao, J.J.; Chen, Z. Functionalized carbon nanotubes as a novel inhibitor to enhance the anticorrosion performance of carbon steel in CO2-saturated NaCl solution. Corros. Sci. 2020, 177, 109011, doi:10.1016/J.CORSCI.2020.109011.
[31] Arai, S.; Kikuhara, T.; Shimizu, M.; Horita, M. Superior electrical contact characteristics of Ag/CNT composite films formed in a cyanide-free plating bath and tested against corrosion by H2S gas. Mater. Lett. 2021, 303, 130504, doi:10.1016/J.MATLET.2021.130504.
[32] Jayamoorthy, K.; Saravanan, P.; Rao, V.S.; Rajagopalan, N.R.; Rengarajan, S.; Nisha, P. Carbon nanotubes functionalized with newly synthesized benzimidazole derivative for corrosion inhibition on the nickel alloy surface in a sulfuric acidic medium. Inorg. Nano-Metal Chem. 2021, doi:10.1080/24701556.2021.1984534.
[33] Sivaraj, D.; Vijayalakshmi, K.; Ganeshkumar, A.; Rajaram, R. Tailoring Cu substituted hydroxyapatite/functionalized multiwalled carbon nanotube composite coating on 316L SS implant for enhanced corrosion resistance, antibacterial and bio active properties. Int. J. Pharm. 2020, 590, 119946, doi:10.1016/J.IJPHARM.2020.119946.

Roli Jain, Daniel Amoako Darko, Bhawana Jain, Ruchi Sharma, Reena Rawat*

Chapter 11
Carbon quantum dots (CQDS), carbon nanorods (CNRS), and their composites as nanostructured corrosion inhibitors

Abstract: Metallic corrosion is a serious issue that is focused by all domains of research scientists all over the world. Exposed metallic surfaces corrode not only in the presence of acidic or alkaline environments but they are also attacked by numerous microbes. Such problems are mostly experienced in petrochemical industries. Inorganic inhibitors, containing heavy metals, are harmful to humans and have a negative impact on the environment, Earth's surface, and on ground water quality.

To eradicate such problems, specialty nanomaterials have come to the fore front. Carbon-based nanomaterials (especially carbon quantum dots) are the most common and feasible alternatives because of their easy manufacturing, non-toxic nature, and low cost. Carbon nanoparticles offer good corrosion inhibition efficiency to various metals in different environments. A stable protective coating formed by the nanoparticles on the metal surface help it to protect the metal surface from corrosion damage. In this chapter, corrosion protection and their mechanistic ways have been elucidated, where carbon nanomaterials are the prime inhibitors. Carbon nanomaterials accelerate the chemical bonding to metal surfaces that, consequently, improve the metallic substrate's longevity.

Keywords: metallic corrosion, nanomaterials, carbon quantum dots, protective coating, corrosion inhibitors

*Corresponding author: **Reena Rawat**, Department of Chemistry, Echelon Institute of Technology, Faridabad, Haryana 121101, India, e-mail: renunegi2007@gmail.com
Roli Jain, Department of Chemistry, Dr. Hari Singh Gour University, Sagar, Madhya Pradesh, India
Daniel Amoako Darko, Institute for Environment and Sanitation Studies, University of Ghana, Legon
Bhawana Jain, Department of Chemistry, Govt. V.Y.T. PG. Autonomous College, Durg (C.G.), India
Ruchi Sharma, Department of Chemistry, GGDSD College, Palwal, Haryana 121102, India

https://doi.org/10.1515/9783110782820-011

11.1 Introduction

Corrosion is one of the most serious problems faced by countries due to the significant economic, mechanical, chemical, and health consequences on the development of chemical plants, oil industry, manufacturing, and various metal-using industries. Corrosion in metals and alloys is an electrochemical phenomenon in which the metal surfaces deteriorate by reacting with substances in the environment [1]. Corrosion has a devastating impact on both the financial damage and personal security. The gradual advancements of corrosion inhibitors over the last few decades, and their resultant benefits, are schematically depicted in Fig. 11.1. Corrosion inhibitors are often regarded as the most effective method for preventing corrosion in metals. Primarily, salts of zinc, chromates, nitrates, borates, and phosphates are among the inorganic salts that are employed to protect metallic surfaces against corrosion [2]. Additionally, the selection of a suitable coating material for metallic substances can result in a long service life and offer economic advantages. In order to achieve coating systems with improved performance, a number of factors, including prolonged protective lifetime, low cost, light weight, and long-term sustainability, should be taken into consideration. Metallic coatings (e.g., zinc and chromium) as well as paints are some of the most often used coatings for industrial purposes. The use of chromium-based coatings is prohibited because of the concerns about their environmental impact [3]. Zinc-based coatings, due to their high cost as well as the requirement for heavier coatings, are no longer considered to be realistic options [4]. In this context, the study of heterocyclic compounds [5], plant extracts [6], and polymers [7], is useful, but some of these substances are toxic and hazardous to the environment. Significant factors, such as economic concerns, impact, and environmental considerations, are taken into account while selecting a corrosion inhibitor. Therefore, researchers have concentrated on the development and fabrication of cost-effective, environmentally benign, and low toxic corrosion inhibitors. Thus, advanced technologies are essential for implementation of protection of metal materials from corrosion. Innovations in nanoscience and technology have opened up new possibilities in the different research fields, including environmental and medical [8–10]. For the last few years, carbon-based nanomaterials, for instance fullerene, carbon black, carbon dots, carbon nanorods, carbon nanotubes, graphene, and graphene oxide, are gaining attention as corrosion inhibitors [11]. Among them, carbon dots (CQDs) and carbon nanorods (CNRs) are very popular as corrosion inhibitors [11, 12]. CQDs are an intriguing new class of nanocarbons that consist of discrete, quasispherical nanoparticles with diameters less than 10 nm [13–18]. CQDs are utilized as corrosion inhibitors because of their rigidity, versatility, cost-effectiveness, minimal toxicity, and environmental friendliness [19]. In a report, Hu et al. demonstrated eco-friendly nitrogen and sulfur co-doped CQDs for increasing the anti-corrosion property of Mg alloy in NaCl solution [20]. The nitrogen and sulfur co-doped CQDs could prevent Mg alloy corrosion, with an inhibitory effectiveness of 86.6% at 50 mg/L. Quantum chemistry calculations revealed that these CQDs had significant chemical adsorption on Mg due

to the small energy gap and large dipole moment. Like CQDs, carbon nanorods are another variety of carbon allotropes that also have enormous significance in materials science. Selecting the right catalyst, carbon source, and reaction conditions might influence the structure or morphology and the related characteristics of CNFs during the catalytic manufacturing [21]. It is the crystallographic alignment of graphene (sheet-like graphite) that provides CNFs with a wide range of geometries, such as platelet CNFs and helical CNFs, as well as tubular and cylindrical CNFs [22]. TEM (transmission electron microscope) and SEM (scanning electron microscope) techniques have been used to identify the CNF lattice fringe and overall morphology (scanning electron microscope) [23]. Most CNFs are made up of rod-shaped structural elements. With a unique stacking approach, it should be possible to regulate or create the CNF structure in ways that are advantageous for diverse applications, such as carbon nanorod stacking.

This chapter delivers the ideas of corrosion causes, in brief, and their remediation. The remediation of metallic corrosion described here is based on carbonaceous nanoparticles, especially CQDs. They are very much prone to attach to metallic surfaces. Hence, carbon quantum dots are exploited in various research and development areas to inhibit or delay corrosion dynamics. The detailed corrosion protection mechanism by carbon nanoparticles is depicted in Fig. 11.1.

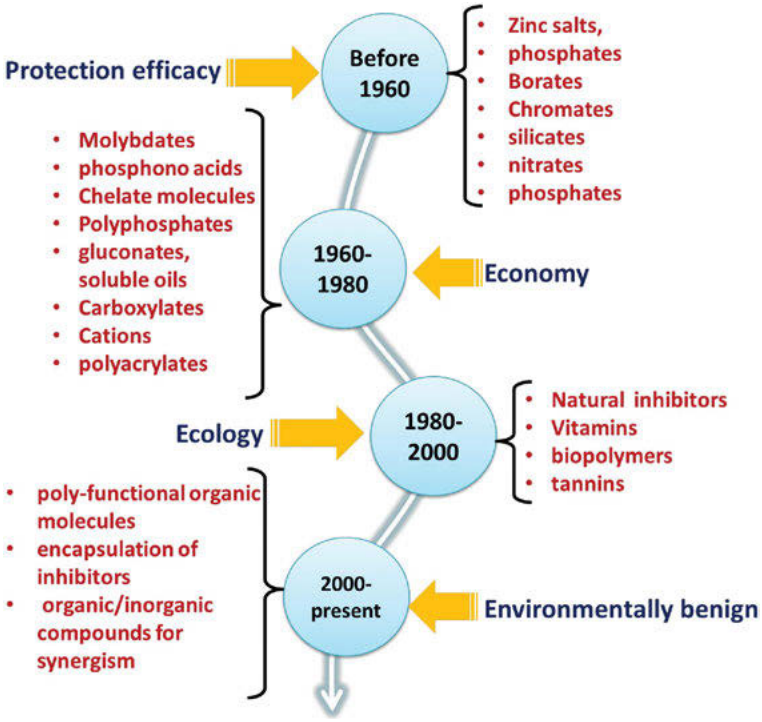

Fig. 11.1: Year-wise developments of corrosion inhibitors and their advantages.

11.2 Corrosion: causes and demerits

Corrosion is described as an attack on metallic substance by means of an electrochemical reaction with the surroundings [1]. As per reports, the yearly GDP loss due to corrosion, to both developing and developed countries, is about 3.4%. For instance, each of China, Japan, and South Africa lost around 310, 9.2, 9.6 billion dollars, respectively, due to corrosion. These losses accounted for 2% of Japan's GDP and 3.34% of China's GDP, which are a developed and developing country, respectively [24]. One of the worst impacts of corrosion behavior is wet corrosion that takes place when chemical reaction occurs in the presence of moisture. Aqueous electrolytes are employed in different sectors and the principal reason for corrosion is organic acids and H_2S gas. Seawater or NaCl is the major electrolytic cause of corrosion in marine industries. Cu, Fe, Al, and brass are the most common metals utilized in diverse industry sectors. Electrolytic media, such as HF, HNO_3, H_2SO_4, HCl, and other strong acidic chemicals, are commonly employed in the course of metallic descaling, acid cleaning, oleation, and pickling [25]. Throughout the acidification process, degradation occurs, often with the metal surface being changed into its chloride, oxide forms, which results in metallic corrosion [26]. Corrosion has a devastating impact on both the financial damage and private safety. Thus, upgraded skills to safeguard metallic products from corrosion must be adopted and developed. Corrosion inhibitors are often regarded as the most efficacious method for preventing corrosion in metals. While selecting a corrosion inhibitor, significant aspects, including financial factors, consequences, and environmental considerations, are taken into account. Generally, corrosion inhibitors react with surfaces of metallic materials and generate protective layers. The structural arrangement and chemical features of the inhibitor control the adsorption process [27]. Organic molecules [28], plant extracts [29], and polymer composites [7] are very useful as corrosion inhibitors, but some of these substances are poisonous and hazardous to the environment. Therefore, carbon-based nanomaterials, such as fullerene, carbon black, derivatives of graphene, carbon dots, carbon nanorods, and carbon nanotubes, are gaining popularity as corrosion inhibitors [11].

11.3 Corrosion inhibitors

In order to protect metal surfaces from corrosive damage, small amounts of corrosion inhibitors, as external materials, are incorporated into hostile fluids during descaling, acid pickling, and oil well refining. Substances with acyclic and cyclic aliphatic and aromatic carbons make up the majority of organic compounds. Heterocyclic compounds are organic molecules that contain atoms such as P, S, N, and O. On the other hand, the most well-known and efficient corrosion inhibitors are organic

substances, whose chemical reactivity and structured orientation are two fundamental characteristics that enable their corrosion inhibition (CI) efficiency.

11.4 Influencing factors of corrosion inhibitors

Researchers examined the inhibitor efficiency, in relation to acid content, temperature, liquid flow rate, and pressure. At greater acid concentrations, certain inhibitors are more potent. At 60 °C, amine compounds provide the best protection. Because of this, agitation has little influence on the rate of corrosion in an uncontrolled acid. Increasing the acid solution pressure reduces the inhibitor's action, but the solubility of metal is lower at higher pressures when an inhibitor is absent.

11.4.1 Temperature effect

The rate of metal corrosion increases as the temperature rises. The efficacy of most inhibitors decreases as the temperature of the metal surface rises, owing to the decreased covering of the metal surface by the adsorbed inhibitors. In contrast, it was proposed that the corrosion rate should be stated as the summation of two rates: $K_1(1-\theta) + K_2\theta$, where θ denotes the portion of the metal coated by inhibitor, K_1 denotes the rate constant for the uninhibited reaction, and K_2 denotes the rate constant for the inhibited system.

When exposed to high temperatures, the efficiency of inhibitors is reduced due to the desorption of the adsorbed inhibitors as well as due to oxygen diminution, in the deficiency of which some non-oxidizing inhibitors, such as sodium benzoate, have no protective effect. Another set of researchers discovered that in the influence of certain inhibitors, such as dibenzyl sulphide, aniline, gelatin, etc., the temperature coefficient and corrosion rate are both reduced. In the presence of an inhibitor, the Arrhenius equation is frequently linear, just as it is in the absence of inhibitors. On the other hand, it was demonstrated that there are three kinds of relationships:

(i) At higher temperatures, corrosion inhibitors lose their ability to slow the process of rusting.
(ii) Even at higher temperatures and in the presence of most inhibitors, the inhibitory action is maintained, and activation energy stays unchanged.
(iii) Some inhibitors have a lower temperature coefficient than without them. At increased temperatures, corrosion delay can be achieved with the use of such inhibitors.

11.4.2 Concentration effect

When it comes to steel corrosion, the number of adsorbed isotopes may be seen to be in correlation to the concentration of organic inhibitors and the corrosion rate of steel in acids. For steel, HCl and gelatin or butylimine polymer or butyric anhydride shows this behavior. At minimal inhibitor doses, this is only apparent. In rare instances, the rate of corrosion can drop to zero or even accelerate at high inhibitor concentrations. In the same way, the protective effect of aliphatic aldehydes on steel in HC1 declines when the aldehyde level is beyond 50 mmol/L. As a result of the conversion of aldehydes to alcohols, their hydrogen depolarizing activity increases.

11.4.3 Agitation speed effect

Excessive agitation frequently reduces the effectiveness of inhibitors. The corrosion rates of carbon steel (CS) in HCl have been found to correlate with the fluid flow speed when industrial inhibitors are present. When agitation increases, the rate of corrosion decreases initially, but then rapidly accelerates, with the minimum recorded at 0.2–2 m/s for corrosion of steel in H_2SO_4 at 0.0043-5 N. Phenylhydrazine, thiourea, or atebrine sustained the corrosion retardation effect on steel in 5 N H_2SO_4, within a particular range of speeds, according to Tulaeva's study [30]. As a result, the corrosion rate was observed to rise practically linearly with the rate of sulfuric acid flow, and the following equation was devised: $p = 0.0026Re^{0.8}$. The acid assault on steel was stronger as the flow rate rose, but it was unaffected by the acid concentration (0.1–6 N H_2SO_4). Steel, in contact with the flowed HCl, hexamine, retained its protection action, but triethanolamine, which inhibited attacks up to 5 N HC1 and in flowing acids of 0.1 and above 5 N HCl, had become an accelerator in 2 to 4 N acid when flowed at this speed.

11.5 Investigation of corrosion-resistant properties of carbon quantum dots (CQDs)

Petroleum sector corrosion is a constant challenge due to the presence of strongly acidic, salty, CO2-saturated, and microbiological fluids. Ecological and environmental advantages of using CQDs in corrosion prevention include their aqueous solubility, cytocompatibility, and nontoxicity, as well as their outstanding bactericidal capabilities and high thermal activity. Assessment of CQDs' activity towards corrosion protection could be delivered in the experimental context as well as in theoretical context. In the following section, both the aspects have been discussed in brief.

11.6 Experimental context

When it comes to determining corrosion and its process in metallic materials, classical experimental approaches are still applied on a wide scale. Weight reduction measurement and electrochemical treatment, including potentiodynamic polarization (PDP) (Fig. 11.2), linear polarization, and electrochemical impedance spectroscopy (EIS), are among the most often used experimental approaches [31]. Weight loss studies are most often the most extensively used technique for determining corrosion inhibitor concentrations in water. Because of its affordability, ease of execution, consistency, and dependability, the weight reduction procedure may be used quickly and simply, and it does not necessitate the use of sophisticated labs, apparatus, or reagents. Anodic and cathodic courses are both involved in the electrochemical process of corrosion. Corrosion may occur in a variety of materials. Corrosion could occur in a number of different contexts. Through the use of the electrochemical approach, it is possible to identify the electrochemical behavior, kinetics, and adsorption process of a material, which are incredibly beneficial and important. During CI, the adsorption and interfacial characteristics of inhibitor molecules may be evaluated using EIS. These characteristics comprise polarization resistance, double-layer capacitance (DLC), and inhibitor effectiveness. EIS is a significant technique for electrochemical study [32]. In addition to the Tafel indices, and anodic and cathodic Tafel slopes, the corrosion current density and corrosion potential may be determined using the potentiodynamic polarization method as well.

Guiand group presented N-doped CQDs (NCQDs) for the corrosion of CS in H_2SO_4system [33]. When evaluating NCQDs as corrosion inhibitors for CS, they used a variety of methods, including electrochemical methods, XRD, TEM, and FTIR (Fourier-transform infrared spectroscopy). This nitrogen-doped CQDs can successfully prevent corrosion of CS in H_2SO_4 solutions, with an inhibition effectiveness of more than 95% at 298 K at 30 mg/L. The remarkable inhibitory feature of the CQDs was ascribed to their unique carbon-rich structure and several polar functionalities present at the surface. Following the Langmuir adsorption concept, the authors discussed that the CQDs can be adsorbed onto the surface of steel, creating a barrier to prevent or decrease corrosion.

According to Yuwei and colleagues (2020), in a 1 M HCl electrolyte, NCQDs based on citric acid (CA) showed good inhibition on an mild steel surface [34]. Electrochemical analysis, SEM, AFM (Atomic force microscopy), etc. were used to determine the material inhibitory performance of CQDs. The surface characterization findings and those from other approaches were found to be in good agreement.

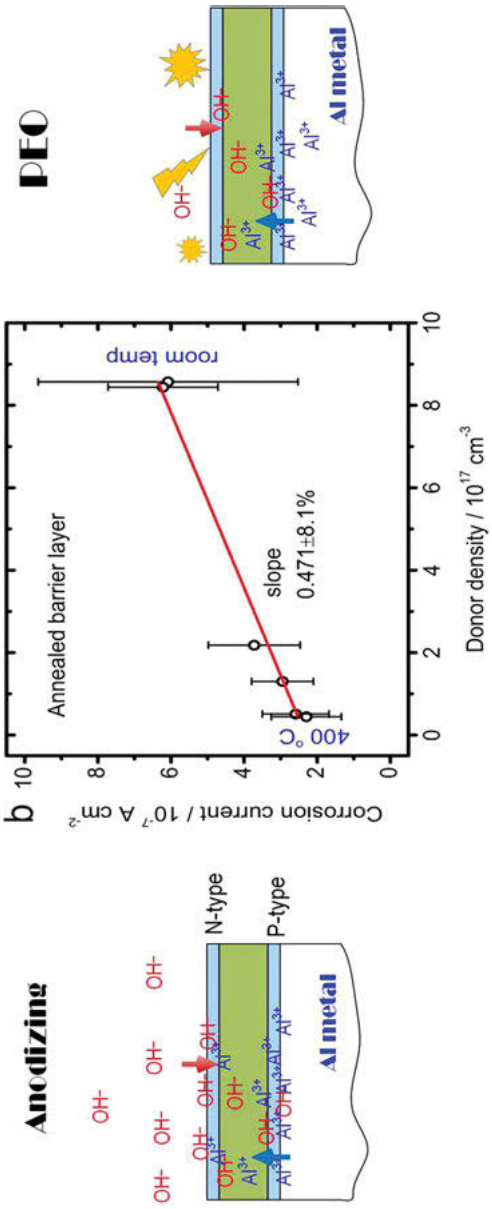

Fig. 11.2: Illustration of potentiodynamic process for anodized metallic aluminum and plasma electrolytic oxidized (PEO) aluminum metal [31].

11.7 Theoretical calculation

The adsorption qualities of an inhibitor may be determined using experimental methods. Test cases make it hard to tell which component of the inhibitor has better capability of intermingling with the metal surface than the other parts of a molecule. The use of molecular modeling and simulations of metal surfaces is critical in understanding the atomistic interactions that occur during corrosion.

Quantum and atomic level computations were performed to gain a better knowledge of the CI process at the molecular and atomic levels. Density function theory (DFT), which is based on quantum chemistry calculations, has been employed extensively in this context in recent years. In addition, molecular software studies, such as molecular dynamic (MD) simulations and Monte Carlo (MC) simulations, have been used in the research. The frontier molecular orbitals (FMOs), as well as the HOMO and LUMO, may be computed with the use of density functional theory. Preliminary studies show that compounds with high values of HOMO may readily donate electrons, whereas molecules with lower values of LUMO can take electrons through electron accepting mechanisms. To study the interaction of corrosion inhibitors with metal in the aqueous medium, MC and MD simulations may be used. The inhibitor-metal interaction alignment and adsorption type may be determined using low-cost, ecofriendly MD and MC calculations. MD is a conceptual molecular modeling system in which the pathway of a chemical may be simply explained by the classical Newtonian process.

As CQDs are zero-dimensional, quantum calculations and molecular modeling of CQDs are not possible. However, because of the organic complex molecules involved in the synthesis of CQDs, DFT, MD, and MC simulation of are possible. Liu and colleagues investigated the anti-corrosion capabilities of three N-doped CQDs in the context of steel corrosion [35]. From DFT calculations, the E_{HOMO}, E_{LUMO}, ΔE, and binding energy were found to be 0.1462 eV, 0.0843 eV, 0.0619 eV, and 188.47 kJ/mol, respectively. Both DFT and MD simulations indicated that N-doped CQDs, with higher HOMO and $E_{Binding}$ energies, have superior inhibitory characteristics. Chen et al. developed NCQDs as green inhibitors from CA and L-histidine for metal corrosion prevention in HCl electrolytes [36]. When compared to CA and L-histidine inhibitors, the inhibitory effectiveness of N-doped CQD was greater than 90% at 100 mg/L. In accordance with the results of theoretical studies, the low energy gap ($\Delta E = 0.0680$ eV) and high binding energy of 190.85 kJ/mol of the CQD indicated that they exhibited strong chemisorption on metal substrates, which completely explained the inhibitory effects at the molecular/atomic level.

11.8 Mechanism of inhibition offered by CQDs

A combination of electrochemical methods, weight loss, spectroscopic, and microscopic evidences is used to examine the inhibitory influence and corrosion mechanism of a corrosion inhibitor. Using isothermal adsorption studies, it has been discovered that CQDs may be found on the surface of CS in two different forms: physical adsorption and chemical adsorption. During the formation of the NCQDs complex, the lone pair electron of the nitrogen atom is coordinated with the vacant 3*d* orbital of the Fe atom. In order to create a very stable chelate, the Fe atom's electron-rich unbonded orbital is countercoordinated with the NCD complex's empty orbital. Because CQDs and free metal ions have electrostatic interactions, they can further adhere and collect on the metal surface. As the percentage of NCDs rises, the adsorption coating on the surface covers a wider area, preventing the metals from reacting with the active ions in the corrosion medium. In summary, the CI mechanism can be thought of as follows: the NCQDs, with the structure of nitrogen oxide graphene, generate electrostatic interaction with the metal surface while at the same time strengthening the adsorption force through the chemical bond, resulting in good CI effectiveness. The adsorption isotherm can be used to look at the adsorption behavior of an inhibitor and figure out how it works. In order to match the adsorption isotherm, the experimental data from PDP were used. It was discovered that the data from PDP fit well with the "Temkin" adsorption isotherm, which can be represented by the following equation:

$$\exp(-2\alpha\theta) = K_{\text{ads}} C_{\text{inh}}$$

Where K_{ads} denotes the adsorption–desorption equilibrium constant, C_{inh} denotes the concentration of inhibitor in the bulk solution, θ denotes the lateral interaction coefficient, and α denotes the surface coverage. For inhibitor molecules in the adsorption layer on a metal surface, the parameter α may be utilized to define the interaction and nonuniformity, taking into account the repulsion ($\alpha < 0$) or attraction ($\alpha > 0$) between the adsorbed particles. Because there is no contact when $\alpha = 0$ (no interaction), the adsorption isotherm equals the Langmuir isotherm.

Now the above equation could be modified to

$$\theta = -\frac{1}{2\alpha}\ln C_{\text{inh}} - \frac{1}{2\alpha}\ln K_{\text{ads}}$$

Using the Temkin adsorption isotherm, the adsorption rates can be evaluated.

11.9 Corrosion prevention efficacy of CQDs in acidic environment

Acidification is used in industries such as gas and oil to eliminate corrosion deposits inside metal pipelines. For acidification, a more acidic solution (HCl and H_2SO_4) is utilized during these operations. Consequently, the surface of the metal components rusts significantly. To preserve the metal substance from corrosion, corrosion inhibitors are added to the acidification solution. CQDs are considered as the most efficient and ecologically friendly corrosion inhibitors. NCQDs have recently been revealed as innovative green CS inhibitors. Cui and coworkers developed new CQDs by using hydrothermal carbonization of aminosalicylic acid as a precursor. When the CQDs were introduced to a corrosion solution, metal corrosion significantly decreased [37]. It has also been reported that the functionalization of CQDs by imidazole can serve as corrosion protection for CS [19]. In another work, Zhang et al. developed NCQDs obtained from amino acid, which was tested against copper, resulting ~ 98% corrosion suppression efficiency [38]. NCQDs react with metal surfaces to create a protecting coating, which restricts the metal and corrosive substances from interacting with erosion. The CI efficacy rises up to 98.5% with increase in NCQDs concentrations. Besides, at higher temperatures the protective effect was still robust, and electrochemical results show the presence of physical adsorption. The application of NCQDs to copper electrodes obeys the Langmuir model, and when paired with evidences of other characterizations, it was ascribed that it is mostly chemical adsorption. Cao et al. proposed functionalized CQDs as outstanding and environmentally safe inhibitors [33]. The presence of these NCQDs significantly inhibited the electrochemical cathodic hydrogen development and anodic steel disintegration. According to the Langmuir adsorption isotherms, NCQDs adsorb onto the steel surface, producing a blockade against corrosive species. Physical adsorption is carried out by graphitic N, whereas chemisorption takes place by pyridinic nitrogen and pyrrole-like nitrogen atoms. Liu et al. reported citric-derived CQDs at various temperatures, which showed corrosion inhibitive efficiency of around 90% [35]. In this study, three types of NCQDs inhibitors were synthesized by decomposing a CA derivative at three different temperatures over two hours. The element N was effectively doped into the CQDs, resulting in pyridinic nitrogen, pyrrole-like nitrogen, and graphitic nitrogen, according to structural characterizations. The ΔG^{O}_{ads} of as-synthesized NCQDs was calculated to be 25.99, 26.94, and 25.78 kJ/mol. These results show that the adsorption film involves both physisorption and chemisorption. Also, the modeling computation revealed that NCQDs were adsorbed parallely on the steel/solution interface. To minimize the corrosion of Q235 steel, NCQDs were derived from amino salicylic acid and histidine by Pan et al. [39]. The results demonstrated that NCDs efficiently inhibited the corrosion of Q235 steel, with an inhibitory efficacy of 93% at a dose of 50 mg/L. The inhibitory mechanism of NCQDs (Fig. 11.3) was investigated using quantum chemistry and molecular dynamics.

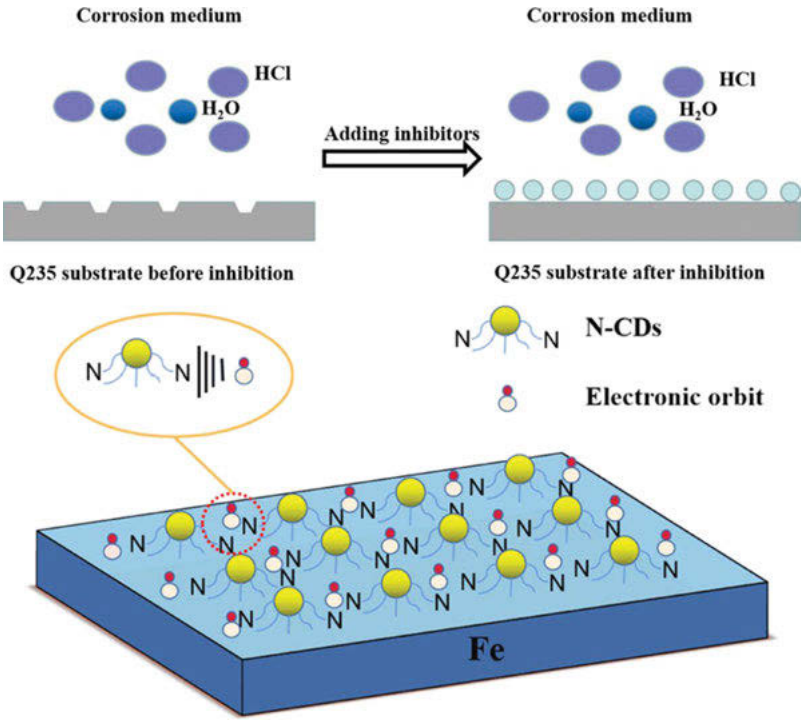

Fig. 11.3: Mechanism of NCDs to inhibit corrosion in acidic environment [39].

11.10 Corrosion inhibition efficacy of CQDs in saline environment

The integration of corrosion inhibitors can successfully reduce corrosion of carbon dioxide in oil fields for CS. Generally, the corrosion inhibitors are electronegative organic chemicals with the elemental composition of N, S, and P that have high adsorption capabilities [40, 41]. Adsorption of these electronegative atoms is mostly determined by physicochemical parameters, particularly e^- density and the properties of donating e^- in the orbital that can establish coordination bonds with the outer track of iron [42]. Currently, most anti-corrosive applications of carbon nanoparticles are dedicated to hydrophobic coating, but few investigations on carbon nanostructures acting as inhibitors in solution have been undertaken [43]. Saline solutions include Cl^- ions, which are hostile and destructive. Metallic goods corrode easily in saline environments. These ions adhere to metallic surface, followed by interaction with metal ions to generate corrosive coating. Some instances of more saline conditions include sea water, ground water, and the aqueous component of crude oil. In these locations, the metallic components decompose in the salty medium. Corrosion inhibitors that are environmentally acceptable,

active, and cheap are necessary in the modern industry. As a result, some studies have proposed that CQDs can be utilized to prevent salt erosion. Cui et al. investigated the corrosion inhibitory influence of NCQDs in 1 M HCl and exhibited the CQD adsorption pattern [44]. N, S-CQDs were expected to be an efficient corrosion inhibitor due to their great electronegativity and electron-donating capabilities of N and S atoms. N, S-codoped CQDs were produced hydrothermally, employing aminosalicylic acid and thiourea as precursor, and applied to examine their CI efficiency [12]. Ashraf and group developed a novel CQD-based corrosion inhibitor in 3.5% NaCl for CS. The CQDs investigated exhibited low toxicity, good chemical stability, high conductivity, thermal stability, and excellent corrosion inhibition that were ecologically beneficial. CQDs become more efficient as a result of these features. The CQDs were created by modifying chitosan with acetic acid [45]. The CV data showed the presence of an oxidation peak of Fe_2O_3 in the corrosive medium at 0.35 V and a reduction peak at 0.90 V. In the presence of CQDs, no oxidation or reduction peaks were seen, showing that the CQD inhibited corrosion on the metallic surface. CA-based CQDs, with imidazole (IM-CQDs), were developed by Yang et al. They tested the inhibition efficacy of Q235 steel in a saline medium [46]. It was discovered that the presence of CQDs blocked the hydrogen charge on the cathodic site. Liu et al. modified the CQDs with zinc molybdenum oxide and reported their potential to prevent CS corrosion in saline conditions after investigation [47]. Polar functionalities like amine and hydroxyl groups were included in this inhibitor, making the CQDs effective corrosion inhibitors. This study states that the presence of modified CQDs in the saline medium elevated the film and electric double layer capacitance (DLC) and charge transfer (CT) resistance, implying that the CQD possess high polarization barrier for steel in the saline environment.

11.11 Corrosion inhibition efficacy of CQDs in aqueous carbonate environments

Carbon dioxide saturation in the water phase of crude oil results in the formation of a more acidic medium and so metallic corrosion is a significant concern in the case of crude oil. As a result, metallic corrosion in carbon dioxide saturated solutions is the most serious issue of chemical industries. Wu et al. used microwave technology to create biocompatible and low cytotoxic functionalized CQDs [48]. Mass loss, study of morphology, elemental analysis, and electrochemical investigations were employed to evaluate the inhibition activity of NCQDs for N80 steel in saturated carbon dioxide saline solution. The results showed that adding NCQDs greatly increased the suppression effectiveness, with inhibition efficacy reaching up to ~ 83% when NCQDs of 600 mg/L were used. In a saturated CO_2 3% NaCl solution, a group of scientists injected NCQD into N80 steel. The amorphous nature, non-toxicity, and good water

solubility of NCQDs were all factors in their selection [49]. Urotropine salt, sulfamic acid, and EDTA were used as precursors for the fabrication of NCQDs. Spectroscopic study of the surface, weight loss, and electrochemical techniques were used to examine the inhibitory features of NCQDs. The NCQDs had improved corrosion protection for N80 steel in the hostile condition, and they were adsorbed on the metallic surface to create a protective coating that guarded the iron from chloride ions, as evidenced in the findings. The results of surface morphology showed that N and S were present on the CS's surface, suggesting that NCQDs may be adsorbed on the CS's surface. In the presence of NCQDs, the film capacitance and DLC dropped, while the CT resistance increased. The NCQDs' lone pair electrons can coordinate with the orbitals of Fe and atmosphere for adsorption on the steel. Guo and coworkers synthesized N,S-CQDs and tested their ability to inhibit steel metal in the NaCl solution [12]. The nitrogen atoms (present in NCQDs), as well as their hydroxyl (-OH) and amino ($-NH_2$) functional groups, benefit in the chemisorption of inhibitors on metal surfaces. Agglomeration was used to create the hydrophobic N,S-CQD film. Because of the intermolecular forces and electrostatic interactions, N,S-CQDs readily combined. Coordinate bonds were generated through e^- transfer between the metal surface (*d*-orbitals) and the CQDs (N atoms).

11.12 Microbiological corrosion inhibition by CQDs

Microbiologically induced corrosion (MIC) is a serious issue in the petroleum industry, resulting in enormous financial and environmental losses. MIC is a term used to describe corrosion caused by the occurrence and action of microbes on surfaces (metallic / non-metallic) [50]. During crude oil transmission, microorganisms in the crude oil and gas damage the interior of metallic pipelines. Bacteria are important species in biological corrosion. Steel pipelines, for example, are rapidly corroded by sulfate-reducing bacteria (SRB) in crude oil. Several antimicrobial treatments are now being employed to prevent microbiological corrosion of metallic objects. Chemical and mechanical modifications as well as manual cleaning are the most prevalent antimicrobial protection strategies.

The most significant species involved in biocorrosion are bacteria [51]. SRB are a well-known bacterial group in the subject of biocorrosion enhancement, and they have been the primary focus of researchers in this field [52]. MIC has been prevented and reduced using a variety of approaches. To obtain a successful outcome in biocorrosion control, a mix of cleaning up, mechanical adjustments, and chemical approaches, such as utilizing biocides, is usually required [53]. The least amount of a biocide required to eradicate microbes, contact time, and biocompatibility are all key biocide properties that might influence the control outcomes [54]. Nanomaterials have distinct and more obvious features, in comparison to bulk; as a result,

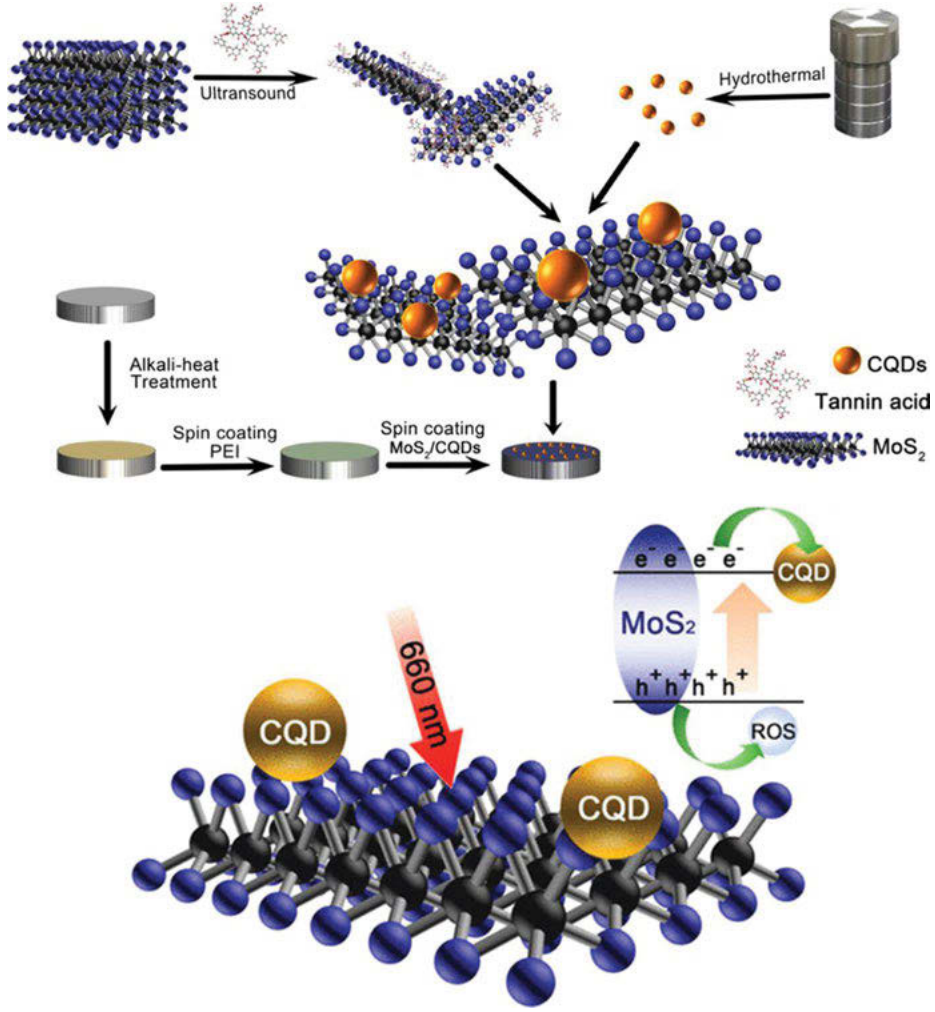

Fig. 11.4: Pictorial representation of the fabrication and enhanced photocatalytic feature of Ti-PEI-MoS_2/CQDs [60].

their employment in a wide range of goods is fast growing, and some of them are used as biocides due to their antibacterial capabilities [55]. Because it is safe and non-invasive, killing bacteria by producing heat and reactive oxygen species (ROS) under light irradiation is an ideal approach [56]. The ROS inside the cell might destroy the bacteria from inside and eventually kill the bacterium [57]. As a result, as a material's photocatalytic capability improves, more ROS are created, and therefore more bacteria are destroyed. Under the irradiation of visible light, molybdenum disulfide, a layered transition-metal disulfide, can create ROS [58]. However, because of the quick recombination of photo-generated e^- and holes, photocatalytic activity of molybdenum

disulfide (MoS_2) is insufficient for an efficient bacteria killing. CDs are a type of frequently used catalyst modification agent [59]. The MoS_2/CQDs combo was created to have effective antibacterial properties as well as minimal toxicity [60]. MoS_2 was selected as the base material because of its photocatalytic and photothermal capabilities (Fig. 11.4). CQDs were introduced to increase MoS_2's photocatalytic activity by acting as an electron transporter, suppressing photo-induced electron–hole recombination and, as a result, improving the photocatalytic ability of MoS_2. In vitro antimicrobial studies demonstrated that the Ti-PEI-MoS2/CQDs composite was capable of completely destroying bacteria after 20 min of 660 nm light irradiation in the presence of bacteria. Kalajahi et al. proposed using Cu-doped CQDs (Cu/CQDs) as an anticorrosion agent for microbiological corrosion protection. FTIR and SEM along with other characterization techniques were used to confirm the nanostructure of Cu/CQDs. Using electrochemical examination methods, the protection against corrosion property of metal-doped CQDs in SRB solutions was tested in this study (EIS and PDP) [61]. Doping of Cu in CQDs resulted in a potential antibacterial activity for X60 steel, according to the findings. The data suggested that the carbon nanoparticles aided in the formation of biofilms on the metallic surface that efficiently protected the steel's surface from biocorrosion system and also eradicated SRB.

11.13 Adsorption dominance in corrosion inhibition mechanism

Both the cathodic and anodic electrochemical processes were positively impacted by the CDs, according to the data. There is a strong correlation between the Gibbs free energy values and the standard enthalpy, for the adsorption and inhibition of CDs on metal surfaces. The inclusion of CD blockers in both acidic and saline environments significantly blocks cathodic hydrogen oxidation and anodic iron reduction, as demonstrated by Langmuir isotherms. It was found that the CQDs produced a thin, protective coating (Fig. 11.5) on the metal substrate, which successfully protected the metallic coating from corrosion.

There is a lot of deterioration on the steel surface because of hydrogen and sulfate ions. An oxidation of hydrogen was carried out at the cathodic site to obtain hydrogen gas. Sulfate ions reduced iron to generate iron sulfate salts. The rate of evolution of H_2 and corrosion of metal (here, steel) is proportional to the amount and temperature of H_2SO_4, therefore an increase in either of these factors will accelerate corrosion. In contrast, in the presence of NCQDs, the catalytic oxidation and anodic reduction processes were shown to be significantly inhibited [62]. Because the NCQDs had several polar functionalities, they were easily chemically interacted with the metal surface, resulting in the formation of coordinating bonds. Because this adsorption process was physical

in nature, it was capable of supporting the inhibitory activity of NCQDs. The NCQDs' charge density and molecular structure architecture influenced the inhibitory mechanism. The investigated inhibitor comprised pyrrole-like nitrogen atoms, pyridinic nitrogen, graphitic nitrogen atoms, and oxygen atoms, among other elements. Covalent bonds were formed when the electron pairs of iron were shared with the unoccupied 3*d* orbitals of the metal. The hydrophobic structure of the NCQDs, which is rich in carbon, served as a shield [63]. As a consequence, the development of a shield enhanced the inhibitor's inhibitory behavior by minimizing the corrosive assaults by sulfate and hydrogen ions on the inhibitor's structure.

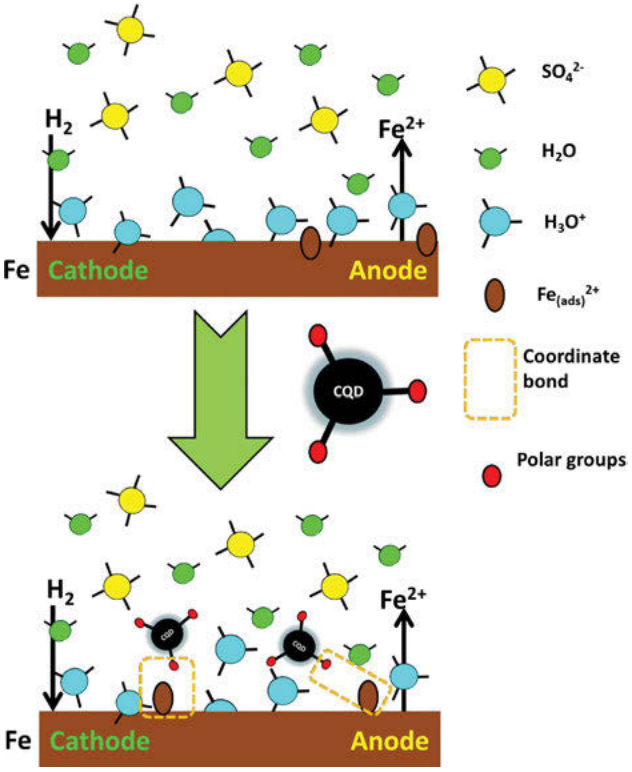

Fig. 11.5: Schematic representation of inhibition mechanism of CQDs on the metallic surface.

11.14 Corrosion inhibition mechanism in various substrates

Doping of CQDs by atoms such as S, N, B, and P may change their physiochemical characteristics, particularly their CI capability. CQDs work similar to typical heterocyclic corrosion inhibitors in that they adsorb and produce a hydrophobic protective coating. Because heteroatoms are abundant in electrons, they should function as active sites for the adsorption process in doped CQDs. As a result, doped CQDs should perform better than undoped CQDs as corrosion inhibitors. Evidently, this form of doping aids in the solubilization of CQDs in polar electrolytes. Once CQDs have been adsorbed to metallic surfaces, corrosion-causing active areas on the surface are thought to be blocked by them. The findings of electrochemical studies and surface research on CQD-based CI have indicated that adsorption is the cause for CI. The anticorrosive properties of CQDs have been determined using methods, including SEM, AFM along with other spectroscopic techniques. After being adsorbed, CQDs are thought to prevent the active sites that cause corrosion on metallic surfaces.

11.15 Corrosion inhibition onto copper substrate

Copper and its alloys are extensively employed in a variety of industrial applications, particularly for maritime equipment. These materials, on the other hand, are extremely corrosive. In marine settings, organic molecules have been recognized as the protective layer against copper corrosion. CQDs are new fangled fellows in the carbon materials family, and their use in many industrial and biological applications is quickly increasing due to their environmentally benign nature and their propensity to solubilize in polar solution. Their anticorrosive aqueous phase use is likewise not far behind. According to literature, N-doped CQDs are frequently employed as corrosion inhibitors for many metallic surfaces. The anticorrosive action of CQDs for copper corrosion in a 1% NaCl solution was first reported by Anindita and group [64]. The UV–visible, IR, and fluorescence spectroscopes were used to examine CQD synthesis. According to IR analysis, CQDs have numerous polar functionalities on their surface, including –OH, C = O, C = S, that helps to dissolve CQDs in marine system and play the role of adsorption sites. At 800 ppm, the most efficient CQDs had an efficiency of 86%. According to the PDP study, CQDs block both anodic and cathodic processes, and operate as inhibitors of mixed varieties.

The CI property of CQDs, produced from green bean coffee powder (GBCP) and urea, was later used as an anticorrosive substance in the copper/1% NaCl system [65]. Zhang et al. created N- and S-codoped CQDs, dubbed N,S-CQDs, with N and S content as high as 17% and 19%, respectively [66]. Several electron microscopy and spectroscopic studies were used to characterize N,S-CQDs. The inhibitory potential of

N,S-CQDs was demonstrated using PDP and EIS investigations. PDP was used to show that N,S-CDs are a mixed-type inhibitor with a minor cathodic preponderance. The N,S-CQDs turn operative by forming a protective coating, according to electrochemical investigations. To characterize N,S-CQDs adsorption, a variety of surface investigation methodologies were used. In the existence of N,S-CQDs, surface morphology was significantly changed, in comparison to a corroded metallic surface, in the absence of CQDs. An SEM experiment for specimens soaked with and without N,S-CQDs for 24 h showed effective inhibition of copper corrosion. This is due to the improved surface morphology caused by CQDs. The AFM analysis confirmed the smoothness of the surface morphology, employing N,S-CQDs as well as their adsorption capabilities for corrosion mitigation. AFM pictures of smoothed and corroded metallic surfaces, with and without N,S-CQDs, as well as the corresponding height profile was evaluated. In the AFM picture of a smoothed surface, the roughness was found to be a mere 4.806 nm. In the absence of N,S-CQDs, copper corrodes and becomes exceedingly rough on the surface, causing it to become excessively corroded and roughened. Metallic surfaces (corroded) revealed a roughness of ~ 40 nm in this condition. Despite this, the creation of an inhibitive coating improves the morphology of corroded surfaces by N,S-CQDs (R_a = 15.363 nm).The adsorption strategy to corrosion protection was further proven by a change in the infrared frequencies of adsorbed carbon nanoparticles, when compared to pure ones. The most important insight into corrosion reduction utilizing the adsorption technique comes from XPS examination. The XPS of Cu2p showed two signals responsible for $Cu2p_{1/2}$ (932.5 eV) and $Cu2p_{3/2}$ (952.3 eV), respectively. The most significant XPS signal was due to the C–C bond; however, there were also weak signals that possibly belonged to C–N, C–O, and C = O. Moreover, Cu-S was responsible for a highly strong peak in the XPS spectra of S2p at 162.5 eV. Based on their findings, the authors hypothesized that N,S-CQDs efficiently adsorb and limit corrosion. The CI potential of NCQDs for copper in sulfuric acid was previously investigated by scientists [38].

11.16 Corrosion inhibition on carbon steel substrate

CS alloys are widely used as building materials owing to their great mechanical superiority, longevity, and inexpensive. Despite this, their lives were cut short due to their potential to corrode in an aggressive environment. Corrosion concerns are exacerbated by acid cleaning techniques for steel alloys, which remove a large amount of metal components. As a result, these cleaning methods make use of external chemicals to eliminate or reduce metallic loss. In such circumstances, the practice of inhibitors that is organic is obviously the most unusual form of corrosion reduction. Application of CQDs as anticorrosive probe for CS has gained popularity in recent years. For the Q235 CS in 1 M HCl system, N-doped CQDs produced from an antibiotic revealed anticorrosive activity [44]. CQDs develop the ability to control both anodic

and cathodic Tafel reactions without causing a significant change in Ecorr. The mixed-type behavior of CQDs was formed as a result of this. CQDs also produce a considerable increase in the value of CT for corrosion, as seen by an increase in the breadth of Nyquist curves. This showed that CQDs operated as interface-type inhibitors, forming a hydrophobic and barrier coating at the interface between Q235 CS and 1 M HCl. The expansion of the degree of phase angle in blocked Bode graphs further supported this thesis. Obviously, an increase in phase angles suggested that the morphology of shielded surfaces had improved. The width of Nyquist curves and the phase angle value increase in proportion with the concentration of CQDs. The polished Q235 surfaces are quite smooth; however they do have minor fractures. The surfaces, on the other hand, are severely damaged after corroding in 1 M HCl, with a mountain-like appearance and fissures. In the absence of CQDs, this may be identified by free acid corrosion. In addition, morphological analysis showed that the Q235 surfaces destroyed in 1 M HCl with CQDs (1 mg/L) was identical to that of one that is not protected. Such a result demonstrated that CQDs were ineffective at lower concentrations. Surface morphologies smoothed out significantly at 5 mg/L concentration. Yang and colleagues [26] reported surface-functionalized CQDs with imidazole (IM-CQDs) and their consequent anticorrosive use in Q235 carbon steel in 1 M HCl and 3.5% sodium chloride solutions. Fig. 11.6 depicts the fabrication of CQDs from CA and the accompanying surface functionalization. Different spectroscopic studies were used to characterize the synthesized functionalized CDs. In both electrolytes, IM-CQDs operated as potential anticorrosive materials. According to polarization studies, at 200 ppm, IM-CQDs demonstrated excellent efficiency in both 1 M HCl (92.60%) and 3.5% sodium chloride solutions (83.45%).

To illustrate the adsorption performance of IM-CQDs, scanning vibrating electrode technology was used, which offers evidence on the local corrosion status. The authors demonstrated the local corrosion findings for Q235 CS corrosion in hydrochloric acid and sodium chloride electrolytes, with and without IM-CQDs. A strong positive current clearly ascribed to a state of high anodic dissolution. Results showed that the corrosion of steel in 1 M hydrochloric acid acquired the maximum + ve current, indicating that the Q235 steel surface was extensively corroded in this condition. Moreover, at 25 mg/L and 200 mg/L concentrations of CQDs, the current swapped to the -ve direction. This study implies that IM-CQDs reduced the local current by constructing a protective covering. In the absence of IM-CQDs, the current density for Q235 CS corrosion in 3.5% sodium chloride was around 0.00 A cm^{-2}. However, in the presence of IM-CQDs doses of 25 and 200 mg/L, the current density changed in the negative direction. The AFM pictures suggested that without IM-CQDs, the metal surface was severely corroded in HCl and sodium chloride solution. However, IM-CQDs, at concentrations of 25 and 200 mg/L, induced substantial surface smoothness. This surface smoothness was much prominent in the presence of higher concentrations of IM-CQDs. In another report, unique NQCDs were prepared from dopamine and investigated as corrosion inhibitors for Q235 CS in 1 M HCl

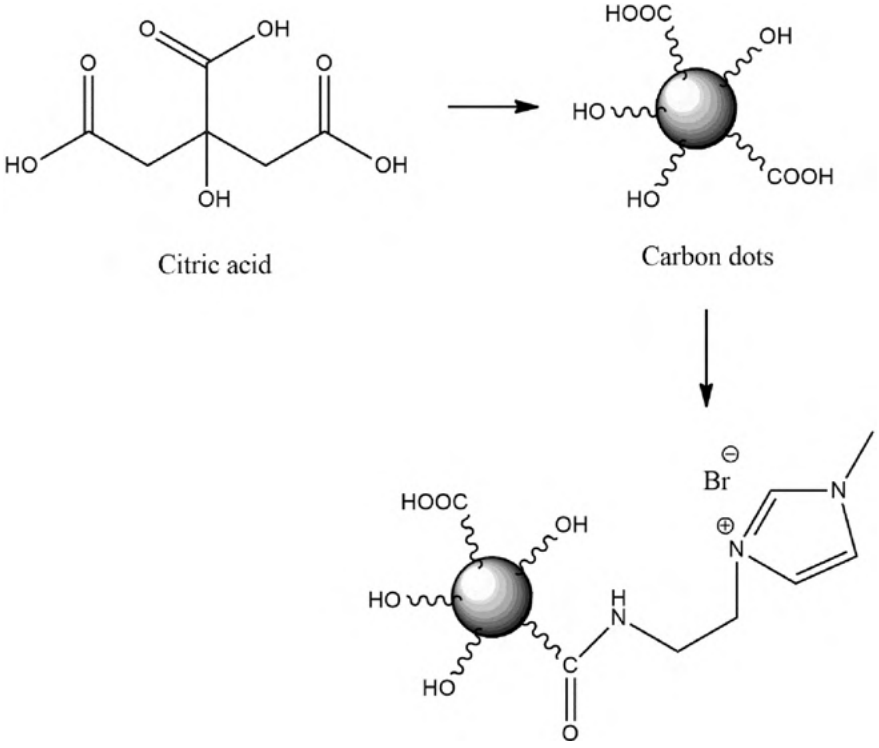

Fig. 11.6: Schematic reaction scheme of CQD functionalization.

solution [67]. The electrochemical results showed that NCQDs operated as a mixed kind of corrosion inhibitor that effectively delayed acid corrosion of CS from 50 to 400 parts per million. In the presence of 400 parts per million of NCQDs at room temperature, the greatest inhibition efficiency was 96.1%. The inhibitory efficiency of NCQDs gradually increased with increasing immersion time, ultimately reaching a stable value. In addition, the inhibitory efficacy was improved proportionally with increasing temperature (298–328 K), ranging from 86.15% to 92.88%. This is because NCQDs can adsorb on the steel surface, thus preventing steel corrosion. The author reported that adsorption of NCQDs on steel surfaces was governed by the adsorption model of Langmuir.

Corrosion of CS in 1 M HCl solution using NCQDs was studied by EIS. In the Nyquist plots (Fig. 11.7a), a depressed capacitive loop and an inductive loop are depicted. The semi-diameter of the capacitive loop upsurges with growing concentrations of NCQDs, suggesting that the presence of NCQDs significantly reduces CT at the steel-solution interface. The fact that all Nyquist graphs had the same depressed shape suggested that NCQDs have no effect on steel corrosion in HCl solution. According to the Bode plots (Fig. 11.7b), at the lowest frequency, the impedance modulus was greater

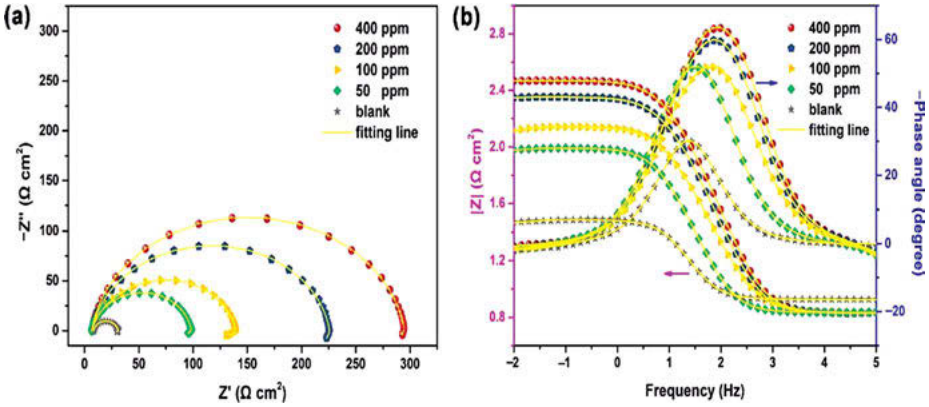

Fig. 11.7: The EIS outcomes of Q235 CS in 1 M HCl solution, with and without NCQDs: (a) Nyquist plots, and (b) Bode plots, respectively [67].

than blank, and the value increases with growing concentrations of NCQDs. The maximum impedance modulus was found to be 295 ohm cm^2 in presence of 400 ppm NCQDs that was ten times greater than the blank solution. Furthermore, when NCQDs were added to the HCl solution, the phase angle peak was higher and wider, and this behavior became more obvious, with increasing concentrations of NCQDs. These data demonstrate that NCQDs had a strong adsorption on the steel surface and showed higher CI effectiveness when used in greater concentrations.

SEM and LSCM were used to examine the surface morphology and roughness of the samples after 60 h of exposure in 1 M HCl solution. Fig. 11.8a showed that prior to being exposed to a corrosive medium, the steel surface was smooth and revealed only a few polished scratches.

In a report, Chen et al. reported functionalized CQDs, derived from imidazole and CA, and evaluated their use as anticorrosive materials for Q235 steel in 1 M HCl [68]. Similar studies of CQDs as corrosion inhibitors were also reported [34, 36]. The steel had a surface roughness (Fig. 11.8b) of around 0.27 μm. It can be seen from Fig. 11.8c that when exposed to 1 M hydrochloric acid solution for 60 h, the steel surface was extensively corroded and became porous. In comparison to steel that is not corroded, the surface roughness (Fig. 11.8d) amplified substantially to 5.18 μm. Fig. 11.8e indicated that when 400 ppm NCQDs were added, the steel surface's corrosion was considerably reduced. The roughness of the corroded metal was only about 1.0 μm, as evident from Fig. 11.8f. These findings demonstrated that the adsorbed NCQDs have a noteworthy consequence toward acid erosion of steel.

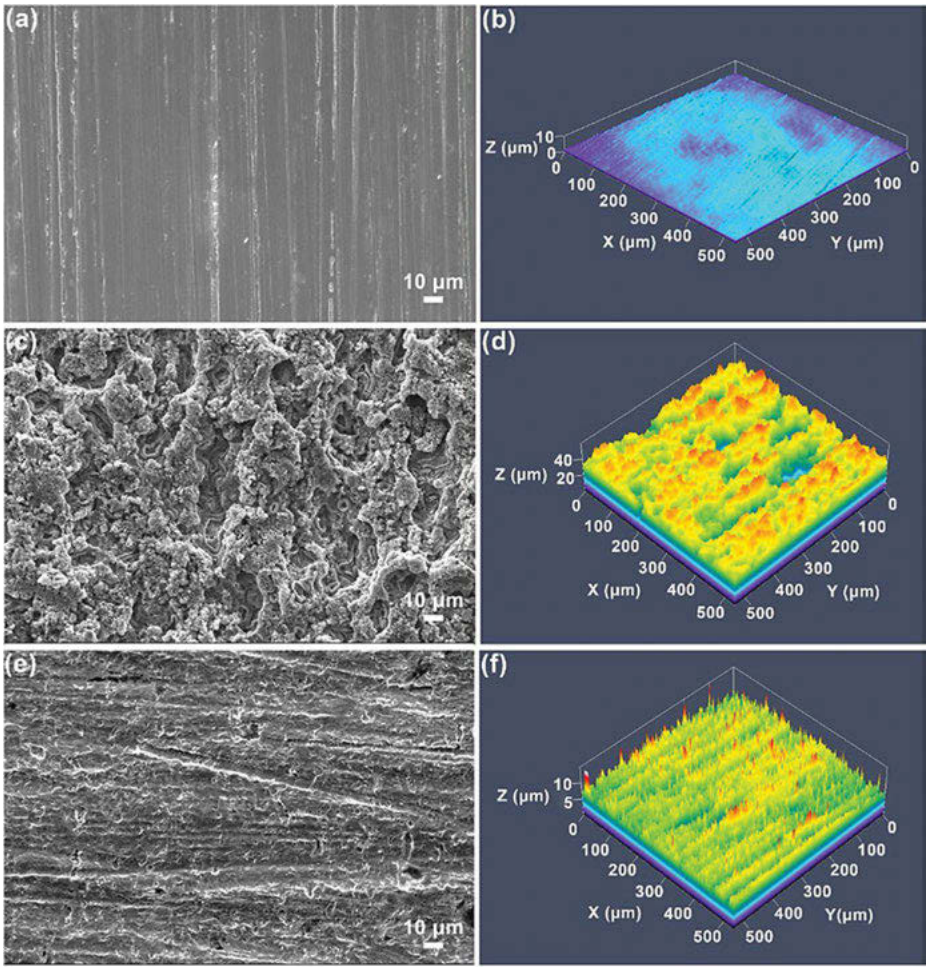

Fig. 11.8: SEM and LSCM pictures of Q235 CS, before and after introduction to 1 M hydrochloric acid solution, with and without NCQDs, (a, b) polished steel, (c, d) blank solution, and (e, f) at 400 ppm NCQDs, respectively [67].

11.17 Corrosion inhibition on mild steel

Mild steel is another iron alloy that has been widely utilized for a variety of domestic and industrial uses for decades. CI in mild steel (MS) is extremely important. According to a review of the literature, there have been some recent reports describing CI of CQDs for MS. In a report, Yadav and coworkers demonstrated the fabrication, properties, and inhibitory effect of N, S co-doped (CD1) and N-doped (CD2) for MS in 15% HCl solution [69]. The CD1 and CD2 were prepared by the solvothermal treatment of

pyromelletic acid in the presence of urea, DETA, and thiourea at a high temperature. The synthesized CDs, with sizes 1.63 –2 nm, contained significant amount of graphitic carbons. The produced CD1 and CD2 inhibited 96.40% and 90.00% at 100 ppm and 303 K, respectively. The EIS studies ascribed that the CT tolerance rises with increasing concentration of CQD1 and CQD2; however, DLC falls with increasing concentration of CQD1 and CQD2. The observed CI was caused by the adsorption of CQDs onto the surface of the MS. Both the CQDs exhibited physisorption mechanism on the surface of the MS steel and adhered to the adsorption isotherm of Langmuir. An analysis of metal surfaces was carried out using several methods of surface characterization. These included corrosion characterization techniques, such as FTIR, SEM, and EDS, as well as AFM, XPS, and XRD. Before and after the administration of inhibitors, the morphological alterations of the metal surface were investigated utilizing these approaches. The 3D metal surface modifications and the bonding energy between the inhibitor and the metal surfaces were studied using AFM and XPS methods, respectively.

Later, the authors also reported hydrothermal synthesis of N, S-CQDs from thiourea, CA, and isoniazid for the application on MS in 15% hydrochloric acid solution [70]. The inhibition efficiency provided through the N, S-CQDs at a dose of 200 mg/L at 303 K was 98.64, which was higher than the majority of similar type previously reported corrosion inhibitors. The CI efficacy of the synthesized N, S-CQDs upsurges with growing concentration and declines with rising temperature. According to electrochemical measurements, N, S-CQDs performed as an inhibitor of mixed kind and revealed significant negative consequence on Tafel reactions. The reduction in current density in the presence of N,S-CQDs showed it to be effective via blocking of active sites, which are responsible for the corrosive damage. Spectroscopic and microscopic studies were used to investigate the adsorption of nanoparticles on the surfaces of metallic substances as well as the influence on CI. Microscopic analysis showed that the introduction of carbon nanoparticles significantly smoothed the surface morphology due to the formation of a corrosion resistant film. An overview of the recently reported anticorrosive outcomes of CQDs for different metal corrosion is represented in Tab. 11.1.

Tab. 11.1: An overview of the CI potential of CQDs for different metallic substances.

Precursors of CQDs	Doping in CQDs	Metallic substances	Electrolyte solution	Inhibition efficiency (%)	Doses (mg/L)	Corrosion rate	Ref.
Serine & CA	N-doped	copper substrate	Sulfuric acid	98.5	200	8.14 MPY	[38]
Aminosalicylic acid	N-doped	CS	Hydrochloric acid	90.9	10	0.4 mg/m^2 h	[44]

Tab. 11.1 (continued)

Precursors of CQDs	Doping in CQDs	Metallic substances	Electrolyte solution	Inhibition efficiency (%)	Doses (mg/L)	Corrosion rate	Ref.
CA & urea	N-doped	CS	sulfuric acid	97.8	30	0.26 mg/ m^2 h^1	[33]
Ammonium citrate	N-doped	MS	Hydrochloric acid	90	200	4.62 MPY	[34]
Aminosalicylic and TU	N,S co-doped	Aluminum alloy	Hydrochloric acid	85	5	1.02 g/m^2 h	[71]
CA, isoniazid & TU	N,S co-doped	MS	Hydrochloric acid	98.07	200	15.6 MPY	[70]
CA & Histidine	N-doped	Steel	Hydrochloric acid	90	100	6.5 MPY	[36]
Aminosalicylic acid and TU	N,S co-doped	CS	Sodium chloride	93	10	0.08 g/m^2 h^1	[12]

CA, citric acid; TU, thiourea; MS, mild steel; CS, carbon steel.

11.18 Conclusions and future perspective

To summarize, CQDs are good corrosion defenders for several metals and alloys in severely robust environmental conditions such as pH, saline, and microbial environments, among other environments. The electrochemical results confirmed that the CQDs had a significant impact on both cathodic and anodic redox processes, where hydrogen was oxidized and iron ions were reduced. Such redox reactions take place in the presence of carbon quantum dots in robust environments. The magnitude of Gibbs' free energy indicated that there was a spontaneous adsorption of CQDs to the exposed metallic substrate. But the usual enthalpy indicated that the adsorption and suppression of CQDs on the substrate were endothermic.

Langmuir adsorption behavior revealed that the CQDs were predominantly blended-type inhibitors, as demonstrated by the results of the experiments. Findings from spectroscopic analysis revealed that the CQDs produced a durable coating on the metal surface, which helped them to shield corrosion damage to a substantial extent. It was discovered that CQDs possessed a higher concentration of atomic nitrogen, pyridinic nitrogen, graphitic nitrogen atoms, and oxygenated moieties, and that the lone pairs of electrons present in these atoms were mostly considered for inhibitory performance of CQDs. In addition, it has been observed that CQDs offer effective antibacterial activity for steel when used in sulfate-reducing microbiological cultures at 50 parts per million (ppm) concentrations. In accordance with the surface morphology results, CQDs developed biofilms on the metal substrate, which were able to

successfully protect steel from bio-corrosive mixture while also killing the SRB. CQDs have the potential to play a major role player in CI in the forthcoming decades, owing to the fact that these small carbonaceous clusters are more effective at low concentrations. Moreover, their easy synthesis from low-cost local items makes them much better chemical probes for corrosion remediation. In addition, CQDs have great water tolerance, cytocompatibility, cause minimal harm, show outstanding antibacterial capabilities, thermal stability, chemical resistance, and the ability to burn without igniting. These features could extrapolate the view of scientists to use carbonaceous materials, especially carbon quantum dots for the protection of metallic surfaces and promote longevity.

Websites

https://www.azonano.com/
https://www.european-coatings.com/articles/archiv/corrosion-protection-of-mild-steel-surfaces
https://oilmanmagazine.com/article/technologies-to-detect-and-mitigate-pipe-corrosion/
https://www.chemistryworld.com/features/the-nanocoatings-holding-back-corrosion/3009097.article

References

[1] Davis, J.R. Corrosion: Understanding the basics, Asm International, 2000.
[2] De Damborenea, J.; Conde, A.; Arenas, M. Corrosion inhibition with rare earth metal compounds in aqueous solutions. In: Rare earth-based corrosion inhibitors, Elsevier, 2014, 84–116.
[3] Aneja, K.S.; Bohm, S.; Khanna, A.; Bohm, H.M. Graphene based anticorrosive coatings for Cr (VI) replacement. Nanoscale. 2015, 7, 17879–17888.
[4] Dennis, R.V.; Patil, V.; Andrews, J.L.; Aldinger, J.P.; Yadav, G.D.; Banerjee, S. Hybrid nanostructured coatings for corrosion protection of base metals: A sustainability perspective. Mater. Res. Express 2015, 2, 032001.
[5] Lgaz, H.; Salghi, R.; Bhat, K.S.; Chaouiki, A.; Jodeh, S. Correlated experimental and theoretical study on inhibition behavior of novel quinoline derivatives for the corrosion of mild steel in hydrochloric acid solution. J. Mol. Liq. 2017, 244, 154–168.
[6] Verma, D.K.; Khan, F. Corrosion inhibition of mild steel in hydrochloric acid using extract of glycine max leaves. Res. Chem. Intermed. 2016, 42, 3489–3506.
[7] Umoren, S.A.; Eduok, U.M. Application of carbohydrate polymers as corrosion inhibitors for metal substrates in different media: A review. Carbohydr. Polym. 2016, 140, 314–341.
[8] Jain, R.; Panday, A. A review of kinetics of nanoparticulated delayed release formulations. J. Nanomed. Nanotechnol. 2015, 6, 2.
[9] Dare, M.; Jain, R.; Pandey, A. Method validation for stability indicating method of related substance in active pharmaceutical ingredients dabigatran etexilate mesylate by reverse phase chromatography. J. Chromatogr. Sep. Tech. 2015, 6, 1.

[10] Jain, R.; Panday, A. COVID-19: A cure and preventive options. Int. J. Immunol. Immunother. 2020, 7, 052.
[11] Verma, C.; Quraishi, M.; Ebenso, E.E.; Hussain, C.M. Recent advancements in corrosion inhibitor systems through carbon allotropes: Past, present, and future. Nano Select. 2021.
[12] Cen, H.; Chen, Z.; Guo, X. N, S co-doped carbon dots as effective corrosion inhibitor for carbon steel in CO2-saturated 3.5% NaCl solution. J. Taiwan Inst. Chem. Eng. 2019, 99, 224–238.
[13] Das, P.; Ganguly, S.; Saha, A.; Noked, M.; Margel, S.; Gedanken, A. Carbon-dots-initiated photopolymerization: An in situ synthetic approach for MXene/poly (norepinephrine)/copper hybrid and its application for mitigating water pollution. ACS Appl. Mater. Interfaces. 2021, 13, 31038–31050.
[14] Das, P.; Ganguly, S.; Margel, S.; Gedanken, A. Immobilization of heteroatom-doped carbon dots onto nonpolar plastics for antifogging, antioxidant, and food monitoring applications. Langmuir. 2021, 37, 3508–3520.
[15] Das, P.; Maruthapandi, M.; Saravanan, A.; Natan, M.; Jacobi, G.; Banin, E.; Gedanken, A. Carbon dots for heavy-metal sensing, pH-sensitive cargo delivery, and antibacterial applications. ACS Appl. Nano Mater. 2020, 3, 11777–11790.
[16] Saravanan, A.; Maruthapandi, M.; Das, P.; Ganguly, S.; Margel, S.; Luong, J.H.; Gedanken, A. Applications of N-doped carbon dots as antimicrobial agents, antibiotic carriers, and selective fluorescent probes for nitro explosives. ACS Appl. Bio Mater. 2020, 3, 8023–8031.
[17] Das, P.; Bose, M.; Das, A.K.; Banerjee, S.; Das, N.C. One-step synthesis of fluorescent carbon dots for bio-labeling assay. In: Macromolecular symposia, Wiley Online Library, 2018, 1800077.
[18] Das, P.; Ganguly, S.; Margel, S.; Gedanken, A. Tailor made magnetic nanolights: Fabrication to cancer theranostics applications. Nanoscale Adv. 2021.
[19] Yang, D.; Ye, Y.; Su, Y.; Liu, S.; Gong, D.; Zhao, H. Functionalization of citric acid-based carbon dots by imidazole toward novel green corrosion inhibitor for carbon steel. J. Clean. Prod. 2019, 229, 180–192.
[20] Pan, L.; Li, G.; Wang, Z.; Liu, D.; Zhu, W.; Zhu, R.; Hu, S. Nitrogen/sulfur co-doped carbon dots for enhancing anti-corrosion performance of Mg alloy in NaCl solution. Chem. Select 2021, 6, 11337–11343.
[21] Rodriguez, N. A review of catalytically grown carbon nanofibers. J. Mater. Res. 1993, 8, 3233–3250.
[22] Rodriguez, N.M.; Chambers, A.; Baker, R.T.K. Catalytic engineering of carbon nanostructures. Langmuir. 1995, 11, 3862–3866.
[23] Lim, S.; Yoon, S.-H.; Mochida, I.; Chi, J.-H. Surface modification of carbon nanofiber with high degree of graphitization. J. Phys. Chem. B. 2004, 108, 1533–1536.
[24] Goyal, M.; Kumar, S.; Bahadur, I.; Verma, C.; Ebenso, E.E. Organic corrosion inhibitors for industrial cleaning of ferrous and non-ferrous metals in acidic solutions: A review. J. Mol. Liq. 2018, 256, 565–573.
[25] Shreir, L.L. Corrosion: Metal/environment reactions, Newnes, 2013.
[26] Daoud, D.; Douadi, T.; Hamani, H.; Chafaa, S.; Al-Noaimi, M. Corrosion inhibition of mild steel by two new S-heterocyclic compounds in 1 M HCl: Experimental and computational study. Corros. Sci. 2015, 94, 21–37.
[27] Verma, D.K.; Ebenso, E.E.; Quraishi, M.; Verma, C. Gravimetric, electrochemical surface and density functional theory study of acetohydroxamic and benzohydroxamic acids as corrosion inhibitors for copper in 1 M HCl. Results Phys. 2019, 13, 102194.

[28] Saha, S.K.; Dutta, A.; Ghosh, P.; Sukul, D.; Banerjee, P. Adsorption and corrosion inhibition effect of Schiff base molecules on the mild steel surface in 1 M HCl medium: A combined experimental and theoretical approach. Phys. Chem. Chem. Phys. 2015, 17, 5679–5690.
[29] Salleh, S.Z.; Yusoff, A.H.; Zakaria, S.K.; Taib, M.A.A.; Seman, A.A.; Masri, M.N.; Mohamad, M.; Mamat, S.; Sobri, S.A.; Ali, A. Plant extracts as green corrosion inhibitor for ferrous metal alloys: A review. J. Clean. Prod. 2021, 127030.
[30] Putilova, I.N.; Balezin, S.A.E.; Barannik, V.P. Metallic corrosion inhibitors, Pergamon Press, 1960.
[31] Lou, H.-R.; Tsai, D.-S.; Chou, -C.-C. Correlation between defect density and corrosion parameter of electrochemically oxidized aluminum. Coatings. 2020, 10, 20.
[32] Garcia, S.; Markley, T.; Mol, J.; Hughes, A. Unravelling the corrosion inhibition mechanisms of bi-functional inhibitors by EIS and SEM–EDS. Corros. Sci. 2013, 69, 346–358.
[33] Cao, S.; Liu, D.; Wang, T.; Ma, A.; Liu, C.; Zhuang, X.; Ding, H.; Mamba, B.B.; Gui, J. Nitrogen-doped carbon dots as high-effective inhibitors for carbon steel in acidic medium. Colloids Surf. A Physicochem. Eng. Asp. 2021, 616, 126280.
[34] Ye, Y.; Yang, D.; Chen, H.; Guo, S.; Yang, Q.; Chen, L.; Zhao, H.; Wang, L. A high-efficiency corrosion inhibitor of N-doped citric acid-based carbon dots for mild steel in hydrochloric acid environment. J. Hazard. Mater. 2020, 381, 121019.
[35] Liu, Z.; Ye, Y.; Chen, H. Corrosion inhibition behavior and mechanism of N-doped carbon dots for metal in acid environment. J. Clean. Prod. 2020, 270, 122458.
[36] Ye, Y.; Zhang, D.; Zou, Y.; Zhao, H.; Chen, H. A feasible method to improve the protection ability of metal by functionalized carbon dots as environment-friendly corrosion inhibitor. J. Clean. Prod. 2020, 264, 121682.
[37] Cui, M.; Ren, S.; Zhao, H.; Wang, L.; Xue, Q. Novel nitrogen doped carbon dots for corrosion inhibition of carbon steel in 1 M HCl solution. Appl. Surf. Sci. 2018, 443, 145–156.
[38] Zhang, Y.; Zhang, S.; Tan, B.; Guo, L.; Li, H. Solvothermal synthesis of functionalized carbon dots from amino acid as an eco-friendly corrosion inhibitor for copper in sulfuric acid solution. J. Colloid Interface Sci. 2021, 604, 1–14.
[39] Pan, L.; Li, G.; Wang, Z.; Liu, D.; Zhu, W.; Tong, C.; Zhu, R.; Hu, S. Carbon dots as environment-friendly and efficient corrosion inhibitors for Q235 steel in 1 M HCl. Langmuir. 2021.
[40] Ahovan, M.; Nasr-Esfahani, M.; Umoren, S.A. Inhibitive effect of 1-[(2-hydroxyethyl) amino]-2-(salicylideneamino) ethane toward corrosion of carbon steel in CO2-saturated 3.0% NaCl solution. J. Adhes. Sci. Technol. 2016, 30, 89–103.
[41] Sığırcık, G.; Yildirim, D.; Tüken, T. Synthesis and inhibitory effect of N, N'-bis (1-phenylethanol) ethylenediamine against steel corrosion in HCl Media. Corros. Sci. 2017, 120, 184–193.
[42] Jjunju, F.P.; Maher, S.; Damon, D.E.; Barrett, R.M.; Syed, S.; Heeren, R.M.; Taylor, S.; Badu-Tawiah, A.K. Screening and quantification of aliphatic primary alkyl corrosion inhibitor amines in water samples by paper spray mass spectrometry. Anal. Chem. 2016, 88, 1391–1400.
[43] Prabakar, S.R.; Hwang, Y.-H.; Bae, E.G.; Lee, D.K.; Pyo, M. Graphene oxide as a corrosion inhibitor for the aluminum current collector in lithium ion batteries. Carbon. 2013, 52, 128–136.
[44] Cui, M.; Ren, S.; Xue, Q.; Zhao, H.; Wang, L. Carbon dots as new eco-friendly and effective corrosion inhibitor. J. Alloys Compd. 2017, 726, 680–692.
[45] Keerthana, A.; Ashraf, P.M. Carbon nanodots synthesized from chitosan and its application as a corrosion inhibitor in boat-building carbon steel BIS2062. Appl. Nanosci. 2020, 10, 1061–1071.

[46] Liu, Z.; Hao, X.; Li, Y.; Zhang, X. Novel Ce@ N-CDs as green corrosion inhibitor for metal in acidic environment. J. Mol. Liq. 2021, 118155.
[47] Liu, X.-R.; Sheng, -X.-X.; Yuan, X.-Y.; Liu, J.-K.; Sun, X.-W.; Yang, X.-H. Research on correlation between corrosion resistance and photocatalytic activity of molybdenum zinc oxide modified by carbon quantum dots pigments. Dyes Pigments. 2020, 175, 108148.
[48] Wu, X.; Li, J.; Lv, J.; Deng, C.; Yang, L. Novel carbon dots for corrosion inhibition of N80 carbon steel in 3% saturated CO2 saline solution. Rus. J. Appl. Chem. 2021, 94, 1111–1121.
[49] Li, J.; Lv, J.; Fu, L.; Tang, M.; Wu, X. New ecofriendly nitrogen-doped carbon quantum dots as effective corrosion inhibitor for saturated CO 2 3% NaCl solution. Rus. J. Appl. Chem. 2020, 93, 380–392.
[50] Eid, M.M.; Duncan, K.E.; Tanner, R.S. A semi-continuous system for monitoring microbially influenced corrosion. J. Microbiol. Methods. 2018, 150, 55–60.
[51] Kakooei, S.; Ismail, M.C.; Ariwahjoedi, B. Mechanisms of microbiologically influenced corrosion: A review. World Appl. Sci. J. 2012, 17, 524.
[52] Enning, D.; Garrelfs, J. Corrosion of iron by sulfate-reducing bacteria: New views of an old problem. Appl. Environ. Microbiol. 2014, 80, 1226–1236.
[53] Magin, C.M.; Cooper, S.P.; Brennan, A.B. Non-toxic antifouling strategies. Mater. Today. 2010, 13, 36–44.
[54] Ranke, J.; Jastorff, B. Multidimensional risk analysis of antifouling biocides. Environ. Sci. Pollut. Res. 2000, 7, 105–114.
[55] Brinch, A.; Hansen, S.F.; Hartmann, N.B.; Baun, A. EU regulation of nanobiocides: Challenges in implementing the biocidal product regulation (BPR). Nanomaterials. 2016, 6, 33.
[56] Cai, Y.; Liang, P.; Tang, Q.; Yang, X.; Si, W.; Huang, W.; Zhang, Q.; Dong, X. Diketopyrrolopyrrole–triphenylamine organic nanoparticles as multifunctional reagents for photoacoustic imaging-guided photodynamic/photothermal synergistic tumor therapy. ACS Nano. 2017, 11, 1054–1063.
[57] Pellieux, C.; Dewilde, A.; Pierlot, C.; Aubry, J.-M. [18] Bactericidal and virucidal activities of singlet oxygen generated by thermolysis of naphthalene endoperoxides. Meth. Enzymol. 2000, 319, 197–207.
[58] Li, Z.; Meng, X.; Zhang, Z. Recent development on MoS2-based photocatalysis: A review. J. Photochem. Photobiol C Photochem. Rev. 2018, 35, 39–55.
[59] Zhang, J.; Yuan, X.; Jiang, L.; Wu, Z.; Chen, X.; Wang, H.; Wang, H.; Zeng, G. Highly efficient photocatalysis toward tetracycline of nitrogen doped carbon quantum dots sensitized bismuth tungstate based on interfacial charge transfer. J. Colloid Interface Sci. 2018, 511, 296–306.
[60] Han, D.; Ma, M.; Han, Y.; Cui, Z.; Liang, Y.; Liu, X.; Li, Z.; Zhu, S.; Wu, S. Eco-friendly hybrids of carbon quantum dots modified MoS2 for rapid microbial inactivation by strengthened photocatalysis. ACS Sustain. Chem. Eng. 2019, 8, 534–542.
[61] Kalajahi, S.T.; Rasekh, B.; Yazdian, F.; Neshati, J.; Taghavi, L. Green mitigation of microbial corrosion by copper nanoparticles doped carbon quantum dots nanohybrid. Environ. Sci. Pollut. Res. 2020, 27, 40537–40551.
[62] Berdimurodov, E.; Kholikov, A.; Akbarov, K.; Guo, L.; Abdullah, A.M.; Elik, M. A gossypol derivative as an efficient corrosion inhibitor for St2 steel in 1 M HCl+ 1 M KCl: An experimental and theoretical investigation. J. Mol. Liq. 2021, 328, 115475.
[63] Das, S.; Ngashangva, L.; Goswami, P. Carbon dots: An emerging smart material for analytical applications. Micromachines. 2021, 12, 84.
[64] Anindita, F.; Darmawan, N.; Mas' Ud, Z.A. Fluorescence carbon dots from durian as an eco-friendly inhibitor for copper corrosion. In: AIP Conference Proceedings, AIP Publishing LLC, 2018, 020008.

[65] Christopher, K.; Mas'ud, Z.A.; Hanif, N. Versatile coffee carbon dots as lead (ii) and copper (ii) ion fluorescence detectors and copper corrosion inhibitor. 2019.
[66] Zhang, Y.; Tan, B.; Zhang, X.; Guo, L.; Zhang, S. Synthesized carbon dots with high N and S content as excellent corrosion inhibitors for copper in sulfuric acid solution. J. Mol. Liq. 2021, 116702.
[67] Cui, M.; Yu, Y.; Zheng, Y. Effective corrosion inhibition of carbon steel in hydrochloric acid by dopamine-produced carbon dots. Polymers. 2021, 13, 1923.
[68] Ye, Y.; Yang, D.; Chen, H. A green and effective corrosion inhibitor of functionalized carbon dots. J. Mater. Sci. Technol. 2019, 35, 2243–2253.
[69] Saraswat, V.; Yadav, M. Carbon dots as green corrosion inhibitor for mild steel in HCl solution. Chem. Select. 2020, 5, 7347–7357.
[70] Saraswat, V.; Yadav, M. Improved corrosion resistant performance of mild steel under acid environment by novel carbon dots as green corrosion inhibitor. Colloids Surf. A Physicochem. Eng. Asp. 2021, 627, 127172.
[71] Cen, H.; Zhang, X.; Zhao, L.; Chen, Z.; Guo, X. Carbon dots as effective corrosion inhibitor for 5052 aluminium alloy in 0.1 M HCl solution. Corros. Sci. 2019, 161, 108197.

Seyyed Arash Haddadi, Saeed Ghaderi,
Mohammad Ebrahim Haji Naghi Tehrani, Bahram Ramezanzadeh*

Chapter 12
Recent advances in carbon allotropes nanostructured as anticorrosive coatings

Abstract: Owing to superior characteristics of carbon allotropes, such as excellent thermo-physical properties, high thermal stability, morphological diversity, and high electrical conductivity, they have found great interest in many applications. It has been demonstrated in the literature that the application of carbon allotropes, including graphene family, carbon nanotubes (CNTs), carbon quantum dots (CQDs) and carbon dots (CDs), fullerene, hollow carbon spheres (HCSs), and nanodiamond (ND), in different corrosion protection coating systems can enhance not only anticorrosion resistance but also the tribological and mechanical properties of the coating systems. In addition, the direct application of carbon allotropes on metallic substrates via different methods, such as layer-by-layer deposition and chemical vapor deposition (CVD), offers promising corrosion inhibition impacts in harsh corrosive conditions. In this chapter, the most recent studies on the application of carbon allotropes in anticorrosion materials have been reviewed.

Keywords: carbon allotropes, graphene family, corrosion, protective coatings, fullerene

12.1 Introduction

Corrosion is an intrinsically natural phenomenon that leads to the deterioration of metals and their conversion to more stable forms such as metal oxides/hydroxides. All small and large industrial units across the world suffer from noticeable costs of damages caused by corrosion [1, 2]. Corrosion of metallic parts in these industrial units not only reduces their efficiency but also puts their human resources in danger and risk. Prevention of corrosion is almost impossible, but decelerating and/or

*Corresponding author: Bahram Ramezanzadeh, Department of Surface Coatings and Corrosion, Institute for Color Science and Technology, P.O. Box 16765-654, Tehran, Iran,
e-mail: ramezanzadeh-bh@icrc.ac.ir
Seyyed Arash Haddadi, Saeed Ghaderi School of Engineering, University of British Columbia, Kelowna, BC V1V 1V7, Canada
Mohammad Ebrahim Haji Naghi Tehrani, Department of Surface Coatings and Corrosion, Institute for Color Science and Technology, P.O. Box 16765-654, Tehran, Iran

https://doi.org/10.1515/9783110782820-012

changing its kinetics is possible [3, 4]. The separation of metals' surfaces from their environment is one of the practical approaches to slowing the rate of corrosion. The application of different types of coatings over metallic surfaces is the most common and cost-effective strategy to limit the interactions between the metallic surfaces and their environment. An intelligent selection of an appropriate coating prolongs the lifetime of metals and saves more financial resources [5, 6].

The incorporation of fillers, such as UV-resistive pigments, anticorrosion pigments, and reinforcing agents, can improve the durability and performance of the coatings. Thanks to nanotechnology, fillers in nanoscales remarkably enhance the overall mechanical, tribological, and anticorrosion properties of the coatings, compared to microscale fillers, due to their large surface area and strong molecular/intermolecular interactions [7, 8]. Among the different types of nanomaterials, carbonaceous fillers have attracted great interest due to their various morphology, good elasticity, and excellent mechanical, electrical, and thermal stabilities. Carbonaceous nanostructures offer remarkable enhancements in lower contents (i.e., 0.1–1 wt.%), in comparison to other organic and inorganic fillers, mostly embedding in high loadings in a range between 5–10 wt.%. Thus, carbon-based materials are well-known lightweight engineered advanced materials [1, 9]. A significant number of studies have demonstrated the role of different carbon allotropes as nanofillers to achieve enhanced mechanical, tribological, and anticorrosion properties. To mitigate the corrosion of metals, carbon allotropes can be incorporated into the base metals, polymeric or metallic matrices of coatings, or can be deposited as thin layers over the metals' surfaces [10, 11]. This chapter aims to present state-of-the-art studies on the application of different types of carbon allotropes, such as the graphene family, CNTs, CQDs and CDs, fullerene, HCSs, and ND, in the field of corrosion protection.

12.2 Graphene family

The carbon materials of graphene, graphene oxide (GO), and graphene quantum dots (GQDs) have become the center of attention from the corrosion protection viewpoint, especially in recent years. Several coatings procedures, such as layer-by-layer deposition, dip/drop-casting, rapid thermal annealing, CVD, electrophoretic deposition/electrodeposition, spin coating, and spray coating, have been proposed for a wide range of substrates [12–19]. Although it is not possible to address all the research on these materials, an attempt has been made by the authors in order to provide the main advancements in this scope.

12.2.1 Graphene

Graphene is a critical class of carbon materials, taken into consideration from the academic and industrial standpoints, with respect to acceptable electrical, mechanical, and thermal properties. Zero- to three-dimensional carbon-based structures can be categorized in the graphene category [20, 21]. Graphene has a honeycomb structure with high strength capability wherein the carbons are at the joint through the σ/π bonds [22]. The ring-like network of the six carbon atoms provides high strength yield and an impermeable shield, which is suitable for protection in harsh environments.

Studies on corrosion protection by employing graphene can be categorized into two main subjects: pure and composite graphene structures. The results indicate that the graphene-based film offers protection for a variety of alloys. Direct fabrication on metallic surfaces is a technique to fabricate the graphene film on the metallic surface. The electrophoretic CVD and laser fabrication methods are some of the well-known methods for this objective [23–27]. Due to the simplicity of the CVD approach and its capability to cover a large area with an acceptable quality film, considerable attention has been given to this methodology [21]. Research on this matter reveals that the graphene film grown through the CVD process hinders the Cu, Cu/Ni alloys from atmospheric oxidation [28]. Copper is one of the nominated substrates by several researchers as a basis to form the anticorrosive graphene film assessed by CVD-based procedures. The records pointed out that the growth of graphene film's multilayer and single layer notably promotes the corrosion-protection life span [27, 29]. The protection of the graphene film was not limited to the metallic surfaces, and Wang et al. [30] proposed the water-shielding function of the graphene film for silicate glass.

The corrosion protection potency of the pure graphene film is under debate [31, 32]; however, the obtained protection yield demands a more extended serving lifetime. This conveys that the structural defects of the graphene film are seen to diminish. The addition of the graphene layer [32–35] and modification of the steps (i.e. doping and atomic layer deposition) [36–40], adjusting of the metal/graphene film interaction [41, 42], optimization of the implemented CVD parameters [13, 43–46], designing of the hybrid CVD/polymer coating [35] have been introduced as a methodology to reduce the undesirable consequence of the defects footprint in the graphene [12, 47]. It is worth mentioning that the existing defects in the graphene film act as susceptible sites for the initiation of localized deteriorative corrosion reactions [48–50]. Nonetheless, some critical issues remain unaddressed by this method. Note that CVD is not applicable for a wide range of alloys. Metallic surfaces, such as steel, magnesium, and aluminum address some of the hurdles in the coating procedure. These hurdles are considered to be the main objections to the use of this method [51–54]. Further, the modifying steps of the mechanical transfer method also induce adverse traces from the contaminations, leading to the appearance of undesirable properties [55, 56].

In order to develop economic/rational anticorrosive graphene-based assemblies, composite graphenes have been established, especially for the fabrication of

reinforced organic coatings. Organic coatings (i.e. epoxy) display remarkable barrier features in corrosive media. However, intense efforts have been made to reach the ultra-protective level of the organic coating. Curing is an imperative process of organic coatings that inevitably leave microcracks/voids inside the matrix. The composite development of organic coatings is one of the feasible/facile approaches for addressing this need [57]. Nevertheless, considering the low dispersion tendency (i.e. graphene sheets), the modification step is a decisive stage in the fabrication of anticorrosive coatings. The high surface/volume ratio of graphene in combination with van der Waals interaction causes the agglomeration tendency for pure graphene. Results have shown that with the support of uniform dispersion of the functionalized/modified graphene structure, a high protection time can be attained. Modification of the graphene structure brings about the generation of the robust/well-dispersed filament in the coating matrix. The formed graphene filament not only covers the defects of the organic coatings but also constructs the complex long diffusion tracks, resulting in prolonging the solution availability. The provision of the organic/inorganic interaction is among the important approaches for enhancing the dispersion. Numerous types of modifying materials, including furan epoxide monomer and poly (2-butyaniline), indicated the acceptable granting of an anticorrosive role to the epoxy resin in NaCl-based corrosive media [58, 59]. In another study, Ye et al. [60] designed the composite epoxy coating, utilizing the silanized trianiline-intercalated graphene. Results have shown that the adopted functional structure of the graphene acts as a potent barrier in the epoxy matrix along with the self-healing capability. In the context of chemical modifying agents, the non-covalent interaction of the poly (2-aminithiazole) intensifies the barrier feature of the epoxy coatings, demonstrated by the electrochemical spectroscopy in a 3.5 wt.% NaCl solution. Besides, the addition of the graphene-poly (2-aminithiazole) provided remarkable wear resistance, compared to the neat epoxy coating [61]. In another detailed study, Ding et al. [62] adopted the hydroxyl epoxy phosphate monomer (PGHEP) as a π-π interactor for graphene structure. The synthesized structure was investigated through the characterization methods, and the corrosion evaluation exams (EIS and salt-spray) exhibited an acceptable performance of the fabricated composite epoxy coatings in the aggressive solution containing NaCl components. Records showed that the development of the barrier, adhesion, and the hydrophobicity state of the coatings are in line with the availability of the complex paths for solution penetration, resulting in pronounced protection, in comparison to neat epoxy. APTES ((3-aminopropyl) triethoxysilane), as the silanizing chemical compound, is a robust candidate for dispersing the graphene well in the coating matrix, such as polyurethane (PU) [63, 64]. The majority of the researches were conducted on coating matrices, such as epoxy and PU, to protect the surface of the steel against the aggressive media attacks. However, there are some reports on the other coating matrix (i.e. polyaniline (PANI)) and other substrates (i.e. brass) being protected in an aggressive solution using graphene [65, 66]. Note that a combination of the modifying components indicated excellent protection, in which the coupling reagent of tannic acid and

γ-(2,3-epoxypropoxy)propytrimethoxysilane delay the deterioration of the epoxy coating from the invasion of the corrosive ions [67]. Table 12.1 lists brief modifying agents of the graphene structure for the corrosion protection application.

Tab. 12.1: Modifying agents applied for awarding corrosion protection of different substrates.

Modifying agent	Protected substrate	Reference
Furan epoxide monomer	Steel	[58]
Poly (2-butyaniline)	Steel	[59]
Aniline trimer/Triethoxysilylpropyl isocyanate	Steel	[60]
Poly (2-aminithiazole)	Steel	[61]
Hydroxyl epoxy phosphate monomer	Steel	[62]
(3-aminopropyl) triethoxysilane	Cast iron	[63]
(3-aminopropyl) triethoxysilane	Cast iron	[64]

12.2.2 GO

To date, numerous studies have been conducted on applying GO as a panacea for enhancing anticorrosive performance. GO offers lower production cost and also provides benefits of an extended protection lifespan, making it a suitable substitute for graphene, for constructing high-efficient anticorrosive setups [60, 68]. The available functional groups on the GO surface (hydroxyl, epoxy, and carboxyl), with the semiplanar structure, can address the two main basic demands for setting up corrosion protective systems. The high surface/volume ratio of the GO serves as a shield from the invasion of corrosive substances. Furthermore, the available functional groups on the GO galleries, by linking capacity, cooperate through the covalent/non-covalent interaction by the reducing/modifying agents. In other words, the GO frameworks can act as a carrier infrastructure for organic/inorganic agents [57].

Similar to graphene, direct fabrication is one of the main strategies to generate the GO film. The electrophoretic/electrodeposition techniques are able to generate the GO film on the metallic surface [69]. Even though the graphene film deposition via the electrophoretic method displays protection enhancement against the corrosive environment up to 3–6 times compared to the blank sample [70, 71], the protection yields have not been significant.

Notably, the organic coating can mediate the destructive corrosion reaction. However, the outstanding protection by this way is concerned with the composites development. The employment of GO in the coating for composite fabrications, especially the polymer matrixes, suffers from nonuniform dispersion [21, 68]. The high surface energy

and the tendency of the GO sheet to agglomerate give rise to low dispersion. The mechanical exfoliation is able to provide the proper dispersion of the GO in the polymeric coatings [72, 73]. Ultrasonic, high-speed magnetic stirring, and ball milling are the main subgroups of the mechanical dispersion approach. Chemical modification can be applied as another potent way to ensure the uniform dispersion. The chemical modification can be implemented through the covalent/non-covalent interactions. The π-π interactions, hydrogen bonds, Van der Waals forces, and electrostatic interactions are considered non-covalent interactions, while doping, free-radical covalent, silane coupling, and condensation reactions are of the covalent interaction kind [74]. Rolling of the oxide state of the metallic element is another alternative for elevating the degree of dispersion. The coated platform through the covalent/non-covalent interaction between the graphene-based structure and the metal-oxide has been recorded as the prominent method for preventing the agglomeration, causing the uniform distribution of the graphene-second phase in the coating. The addition of the second metal-based nano-phases (i.e. TiO_2 [75–77], SiO_2 [78–80] (Fig. 12.1), $CaCO_3$ [81], Al_2O_3 [82, 83], and Fe_3O_4 [84]) were studied and the results suggested that this group of materials can accelerate the dispersion, i.e., ascend the graphene sheet interlayer spaces [29, 51, 85].

A lot of attention has been focused on evaluating the different reagents for modifying the GO dispersion. Towards this, silanized chemical factors were utilized to provide better steel corrosion protection using GO in the epoxy resin [86–88]. Moreover, boosting of the GO dispersion in the epoxy coatings has also been achieved by PVP [88], 3-aminophenoxyphthalonitrile [89],conductive polymers (PANI [90], polypyrrole (PPy) [91], polythiophene [57]), polydopamine(PDA) [92], and N-(3-aminopropyl)-3-decylimidazole ionic liquid [93]. It is worth mentioning that the GO has been investigated on a broader scale, in which some other types of the coating matrices (polyurethane, polyvinylbutyral, and polystyrene) were investigated to provide corrosion protection to steel, copper, and zinc alloys [94–98].

In the abovementioned approaches, the uniform dispersion consequently limits the solution penetration. Meanwhile, the benefit of chemical modification can also take into consideration from other perspectives. Organic/inorganic components, by themselves, profit from their natural ability to offer protection to metals. The organic compounds are able to fabricate an inhibition film via the donor/acceptor mechanism. The available pair electrons of the organic structures can form coordinate bonds with the unoccupied orbitals of the metal surface. The developed inhibiting layer can serve as a potent barrier in corrosive solutions. The mentioned hypothesis, therefore, was verified for active anticorrosion performance of the composite coating. In other words, smart coatings with dual active/passive protection abilities were seen to be enhanced by the inclusion of the functional GO into the coating phase. Regarding the desirable degree of protection, separate or mixed types inhibitors can be loaded via covalent/non-covalent interactions on the GO sheet (Fig. 12.2) [61, 99, 100]. The metronidazole-grafted GO nanocomposites by Yu et al. [101] offered protection at the scratch site of the epoxy coating. It is worth mentioning that GO is

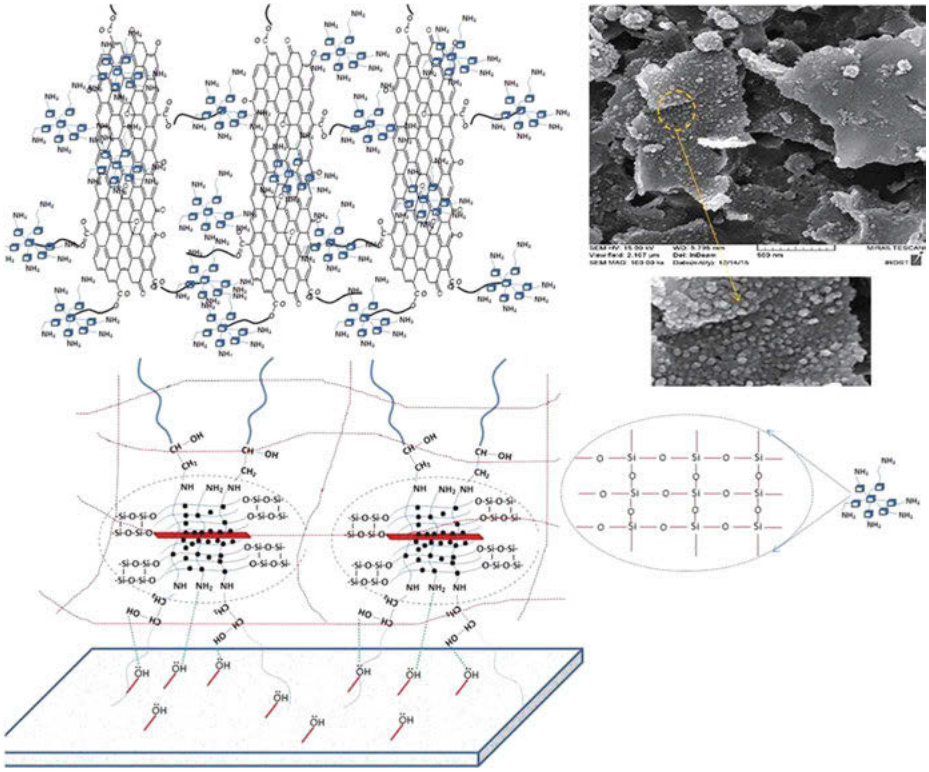

Fig. 12.1: Schematic of shielding performance of SiO_2-GO nanosheets in the epoxy matrix. Copyrighted from [78] by permission.

potentially able to adjust the release of the organic/inorganic loaded agents, resulting in long-term protection [57]. When mechanical damage occurs in the coating matrix, the exposed surface of the metal in the corrosive media contains two main sectors of anodic and cathodic sites. The anodic sites are immune to the destructive corrosion reaction by the organic pair, while the inorganic pair controls the undesirable reaction at the cathodic region [102, 103]. Based on this knowledge, researchers take advantage of the versatility of organic/inorganic agents to design coatings, which are called smart coatings. Diverse classes of chemical compounds with different inorganic substances have been suggested. Results show that the simultaneous application of the organic/inorganic compounds can account for the outstanding higher level of active performance, relying on the provided anodic/cathodic protection at the defect zones [57, 104]. This purpose can be achieved by applying inorganic agents, such as zinc, along with an organic inhibitor or utilizing the structures that consist of both of these factors, such as metal-organic frameworks (MOFs), which consist of the organic ligand and the metal-based cluster [105, 106].

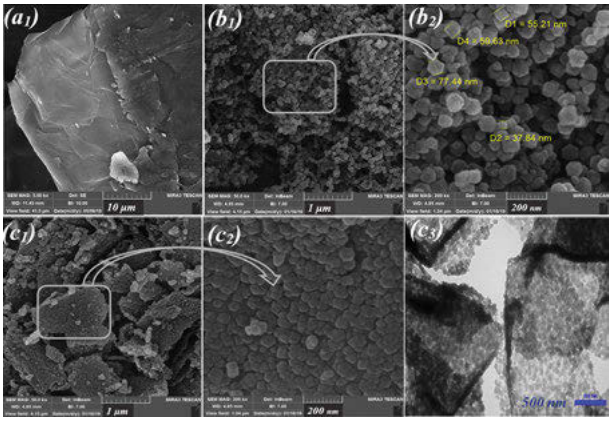

Fig. 12.2: Morphology of the synthesized GO (a), ZIF-8 (b_1, b_2), and GO@ZIF-8 (c_1, c_2) nanocomposites, respectively, and TEM image for GO@ZIF-8 (c3). Copyrighted from [103] by permission.

Although the corrosion protection offered by GO has a high priority in aggressive media, such as marine conditions and acidic solutions, some medical applications have heretofore been conceived to regulate the response of the metallic surfaces (i.e. Titanium). The deposited hydroxyapatite graphene-related structure indicated the promotion of corrosion response, together with properties that stand out from biocompatibility and mechanical perspectives [25, 107, 108]. Besides, employing graphene-based materials has been followed for other objectives, such as improving the protection in the case of microbially induced corrosion and erosion-corrosion conditions [29, 109–111]. Furthermore, the fabrication of superhydrophobic graphene-based coatings is another strategy adopted to design protective systems [112, 113].

12.2.3 GQDs

GQD is another derivation of graphene. GQDs are known as the zero-dimensional type of graphene structure in the < 100 nm scale. The unique properties of GQDs find their way into versatile research fields, including corrosion protection. GQDs are similar to GO, owing to the great tendency in a polar solvent, π-π conjugated network, along with the available functional groups [114–116]. GQDs can be derived from the top-down/bottom-up methods [114].

The study of researchers on the GQDs potential has revealed that GQDs can address anticorrosion issues [117–120]. GQDs also require the modification step to reach the high dispersion degree in the coatings matrix. In this regard, the bridging role of the silane group of the (3-aminopropyl) triethoxysilane (APTES) was enhanced by Pourhashem et al. [121]. The developed structure by this team was characterized in

detail, and the electrochemical records revealed coating protection improvement in the presence of a harsh environment. In another study, the magnesium substrate was protected by the generation of the N-doped GQDs/polymethyltrimethoxysilane by means of the electrodeposition/silane treatment techniques, which offered corrosion mitigation performance 6 times better than bare magnesium alloy [40]. The modified GQD nanostructure, introduced by Rameznzadeh et al. through aniline polymerization, also demonstrated protection capability. The composite epoxy matrix comprised of the modified graphene oxide quantum dot (GOQD) composites experienced acceptable protection in simulated seawater condition [122]. Other studies also mentioned the higher level of coating protection by GQDs. The silane-modified GQDs and TiO_2 nanotubes displayed an acceptable level of protection for epoxy coating [123]. A brief description of the corrosion protection provided by GQDs is reported in Tab. 12.2.

Tab. 12.2: Coating procedures and the modification steps of GQDS applied for corrosion protection.

Nanoparticles	Modifying agent	Coating type	Protected substrate	Reference
GQD	N-doped/ polymethyltrimethoxysilane	Electrodepose/ Silane treated	AZ91D magnesium alloy	[40]
	APTES	Epoxy	Steel	[121]
	TiO_2-APTES	Epoxy	Steel	[123]
GOQD	PANI	Epoxy	Steel	[122]

12.2.4 Mitigation mechanism of graphene-based anticorrosive coatings

The remarkable ability of corrosion protection offered by graphene-based setups to impede destructive corrosion reaction stand on four fundamental panaceas:

(i) Boosting the shielding capability

The high aspect ratio of graphene brings about the generation of the tortuous tracks to govern solution permeation. This feature becomes more detectable in composite coatings. In coatings such as epoxy, graphene can promote anticorrosive behavior from different standpoints. First, the matrix defects roll as a direct channel for subsiding the corrosive substances. These defects mostly arise from the curing stage, leaving microcracks/voids. In this regard, the presence of graphene can impede the formation/propagation of cracks through the absorption of the crack-growth energy, leading to construction of higher intact coating. Simultaneously, the crystalline state of the polymer coating can also be affected by the added graphene-based structure.

The embedded graphene-related particles alter the crystallization, causing higher toughness states [124–128]. Moreover, the filament role of the graphene, through the uniform dispersion in the coating matrix, can diminish or reduce the free pathways of infiltration. In this condition, long-term protection in the intact mode (without artificial damage) can be attained [57, 129–132].

(ii) Scarifying anode regulation
Applying a zinc-rich coating is one of the feasible approaches to conducting the sacrificial anode in the anticorrosive system. However, an intense attempt has been made to promote the efficiency of the zinc-rich coating. Towards this, the addition of the graphene structure can serve as a rational approach by acting as a cathode and intensifying the conductive connection network between the zinc particles. The coupling of graphene allowed the corrosive solution to facile interactions with the accessible zinc/graphene, leading to a rapid disruption of the undesirable corrosion reaction. Subsequently, the generated corrosive product can also potently occupy and execute the permeation paths at the initial stage of corrosion. Besides, the joining of the zinc particles accommodates building up the conductive network of the zinc particle, leading to the extraction of zinc particles from their isolation state, in contrast to the bare zinc-rich coating [133–137].

(iii) Self-healing capacity
As mentioned previously, chemical modification can play a remarkable role by tuning the dispersion in the organic matrix of the coatings. Meanwhile, another beneficial point arises through the modification step. The participated chemical agents can serve as the corrosion inhibition factor in most cases. This is important since the direct implementation of the inhibitor is not applicable in the coating matrix, leading to the appearance of adverse effects from the anticorrosive standpoint [138]. In other words, applying corrosion inhibitors demands a rational approach to fabricate a control-releasing system. In this context, the graphene-based structure benefits from the great potency. In fact, the modification step can provide an outstanding barrier (passive) feature by uniform dispersion. On the other hand, in the case of mechanical damages or notches, the controlled release of the loaded chemical components adsorbed on the graphene-based structure can ensure participation in interacting with the metallic surface through the donor-acceptor mechanism, leading to the generation of the inhibition layer at both the anodic and cathodic sites of the damaged zone [57, 103, 104].

12.3 CQDs/CDs

CQDs/CDs are another class of carbon-based derivations with a high level of importance from the corrosion protection standpoint. The CQDs/CDs show an acceptable

degree of inhibition potency in diverse corrosive conditions for a wide range of alloys. CQDs/CDs, as a feasible/environmentally friendly inhibitor substitution, have been proposed as a protective agent for awarding corrosion retardancy to the metallic surface. More than 95% inhibition efficiency can be achieved by employing these structures. The great protection capacity of CQDs/CDs originated from the pyrrole-like N, pyridine-N, graphitic-N, and the available O atoms. Note that along with the great inhibition capacity, the properties of CQDs/CDs also correspond to some other features such as the green/zero toxic feature and cost-effectiveness [139]. Some of the modified structures of CQDs/CDs can be categorized into single/dual dope [140, 141], polymer-based [142], and ionic liquid [143]. Table 12.3 reports the highlighted research on evaluating the inhibition potency of CQDs/CDs in different corrosive media. It is worth mentioning that there are other considered protection capabilities for CQDs/CDs, such as corrosion inhibition potency, in microbiological environments [144].

On the other hand, CQDs/CDs also promote the protection capability of organic coatings for extended time intervals [1, 145–147]. In this context, the obtained modified boron nitride with amine-functionalized CDs showed unique protection for the copper substrate that is coated by the epoxy, which contains the aforesaid structure [148]. In line with the outstanding inhibition role of the N-doped CQDs/CDs in the aggressive aqueous solution, the inclusion of the N-doped structures can also amplify the protection [147, 149]. The nanofiller acting of the N-doped carbon nanodots was employed, and results revealed the outstanding increment in the service lifetime of the epoxy in the NaCl corrosive media [150, 151]. In another study, the developed microcapsule of ZnO-nitrogen-doped CDs was applied on a waterborne polyacrylate coating. Corrosion evaluations showed that great protection potency was endowed through the fabricated composite coating [152].

Tab. 12.3: Some of the recent advancements in the employment of the CQDs/CDs as an inhibitive agent.

Corrosive media	Additional modification	Solution type(s)	Inhibition efficiency range (%)	Studied substrate(s)	Reference
Acidic	N-doped	HCl-H_2SO_4	81.0–97.8	Steel-Copper	[140, 141, 161, 162, 153–160]
	S, N-doped	HCl	85.9–96.0	Steel-5052 Aluminum	[141, 163]
Saline	N-doped	3.5 wt.% NaCl	88.96	Steel	[159]
	Imidazole functionalization of the citric acid-based CD	3.5 wt.% NaCl	85.7	Steel	[143]

It is worth mentioning that recently, some studies have focused on CQDs/CDs as appropriate options for adjusting/modifying the structural properties, and results have indicated the outstanding enhancement corrosion protection index achievement from the graphene derivations [164] and MXene [165]. In addition, other substrates, such as magnesium, have been targeted for boosting anticorrosive performance and CQDs/CDs strongly addressed this issue [142].

12.4 CNT

CNTs are 1D graphitic tubular-shaped allotropes of carbon classified into single-wall CNT (SWCNT) and multi-wall CNTs (MWCNTs) types [166–168]. The architecture of an SWCNT is a tubular rolled sheet of graphene with the diameter of nanotubes changing from a fraction of a nanometer to several nanometers, and lengths of up to a few centimeters [169, 170]. Synthesis methods of CNTs are arc discharge evaporation, laser ablation, thermal approach, CVD, and plasma-enhanced CVD (PECVD) [171–173]. CNTs have shown desirable physical and chemical properties, including high mechanical strength, physical and chemical resistance, electrical conductivity, and high specific surface area [174–176]. These features make CNTs favorable candidates for a wide range of applications, such as energy storage devices, molecular electronics, conductive coatings, electromagnetic interference shielding, and sensors and actuators [177–180]. Apart from these wide ranges of applications, CNTs have attracted researchers to conduct a plethora of works to investigate the effect and performance of CNTs and their composites in corrosion protection [181]. Incorporating CNTs into complex structures and coatings has led to obtaining high-performance corrosion protective coatings [182].

12.4.1 Application of CNTs in corrosion protection

It is well known that metallic parts are susceptible to corrosion, inevitably. Corrosion of metallic surfaces occurs at large scales, which calls for huge budgets. Different techniques, including anodic/cathodic protection, protective coatings, environmental modifications, changing the pH of the media, and incorporation of inhibitors have been incorporated to reduce the corrosion phenomena [183]. Among these techniques, corrosion protective coatings and inhibitors, or a combination of both of them (inhibitor-loaded coatings) have shown great efficiency in reducing the corrosion rate [184, 185]. The addition of corrosion inhibitors, even at low concentrations, lead to the formation of a thin barrier film on the surface of the exposed metallic surface, obstructing the active corrosion sites [186]. Similarly, covering the surface of metals with a protective coating blocks the paths of corrosive ions to the metal's surface.

Furthermore, the protective coatings, reinforced by inserting high specific surface area corrosion inhibitors (nanocomposite coatings), effectively hinder the reach of aggressive moieties to the surface of the substrate [187, 188].

Recently, CNTs have been introduced as one of the most beneficial nanomaterials to build high-performance and advanced nanocomposites, with improved mechanical, thermal, electrical, and anticorrosion properties [189]. Based on these specifications, CNTs and their derivatives contribute to building multi-functional anticorrosion nanocomposite coatings [190]. Introducing CNTs into corrosion protective coatings leads to enhancing the barrier mechanisms, hindering the aggressive corrosion reactions against metallic substrates [191].

12.4.2 CNTs-based nanocomposites

Taking advantage of all the specific properties of CNTs, they are outstanding reinforcing agents for polymer as well as metallic coatings [192]. Various organic polymers are used to fabricate anticorrosion coatings, such as epoxy, alkyd, epoxy ester, acrylic resins, and polyurethane. It has been shown that the addition of CNTs to epoxy coatings enhanced the adhesion and cohesion strength, wear resistance, mechanical properties, and corrosion resistance of the coating [193, 194]. Alongside polymeric matrices, CNTs have been used to make metallic-based nanocomposites, such as Mg, lead-tin, and nickel coatings. Khun et al. [195] reported that by adding low contents of MWCNTs to epoxy coatings, the corrosion resistance, adhesion to the aluminum alloy AA2024-T3, and tensile strength of the coating increased significantly. They concluded that these interesting findings are due to the 3D dispersion of MWCNTs in the matrix, and thus a decrease in the porosity, which declined the diffusion of the electrolyte into the nanocomposite coating.

As shown in Fig. 12.3, by increasing the concentration of CNTs to up to 0.5 wt.% in the alkyd matrix, the corrosion resistance of the coating on mild steel in the 3.5 wt.% NaCl solution increased by 140%. Obviously, due to the hydrophobic nature of the MWCNTs, the addition of MWCNTs to the coatings increased the hydrophobicity of the resulting nanocomposite coatings [196]. The lower ability of water up-taking contributes to the prolonged protection [196]. Keeping in mind the typical corrosive saline or acidic media, CNTs provide improved anticorrosion properties in a simulated condition, similar to the human body fluid, to protect implantable metals, such as titanium. Gopi et al. [197] investigated that the electrodepositing of CNTs-hydroxyapatite on a titanium substrate brought about enhanced corrosion protection, adhesion strength, and mechanical properties, as well as cell viability.

MWCNTs have shown a synergistic effect, in combination with zinc particles, to improve the cathodic protection of mild steel. By increasing the content of MWCNTs, the formation of a 3D network through the matrix increases, which leads to higher bulk cohesion. The resulting denser nanocomposite prevents the diffusion of

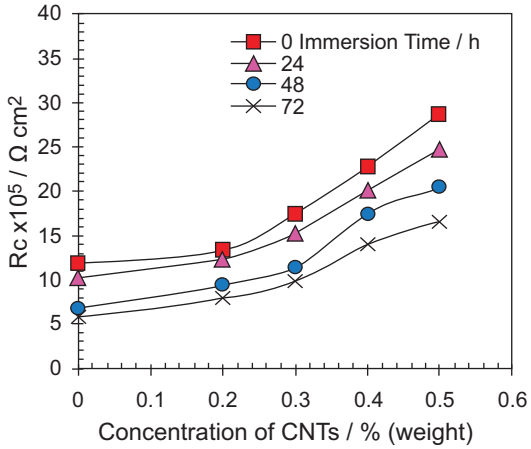

Fig. 12.3: The corrosion resistance of alkyd coating depends on the concentration of CNTs in the nanocomposite coating. Copyrighted from [198] by permission.

aggressive species, as a result of which the formation of rust and blister on the surface of the coated substrate is minimized [199].

Superior performance is predictable when the filler forms strong chemical bonding with the matrix. In a work by Kumar et al. [200], it was reported that the final corrosion protection properties of epoxy-MWCNTs are affected by the MWCNTs' dispersion methodology. They used ultrasonication to disperse MWCNTs in epoxy by applying shear force simultaneously. As shown in Fig. 12.4, a successful dispersion of MWCNTs hinders the diffusion of aggressive species into the coating. Their findings revealed that a well-dispersed epoxy-MWCNTs nanocomposite (0.75 wt.%) indicated a better interfacial interaction, leading to lower corrosion rates. Furthermore, they reported that by increasing the concentration of MWCNTs, the corrosion potential

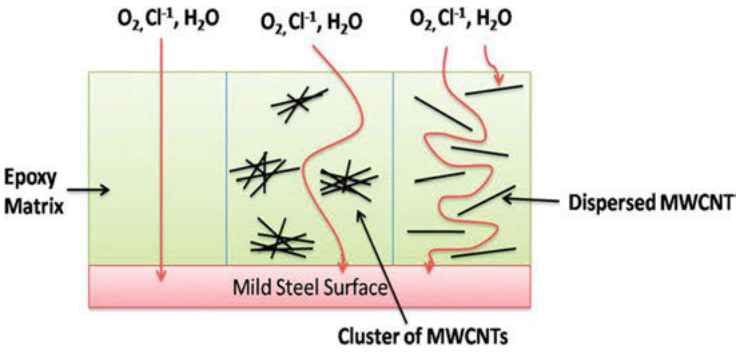

Fig. 12.4: Illustration of the dispersion effect of MWCNTs in an anticorrosion coating on a mild steel substrate. Copyrighted from [200] by permission.

(E_{corr}) shifted to more positive values, compared to the mild steel coated with pure epoxy, confirming the corrosion protection improvement [201].

Wei et al. [202] used in-situ surface-initiated-polymerization of polyurethane (PU) coating containing MWCNTS to protect mild steel substrates in a 3.0 wt.% NaCl electrolyte. Their results noted that the incorporation of MWCNTs into PU enhances the long-term chemical stability of the resulting nanocomposite coating in the corrosive media, increasing the corrosion protection efficiency by ~ 98%. Based on the obtained potentiodynamic polarization curves, their fabricated nanocomposite coatings showed lower corrosion current density (I_{corr}) and more positive E_{corr}.

According to the conducted research, the prominent properties of CNTs that provide improved anticorrosion properties are their high aspect ratio, large specific surface area, and outstanding mechanical properties. These features lead to obtaining strong interfacial interaction with matrix, denser nanocomposite, higher cohesion, and improved adhesion to the substrates [203, 204]. Several methods have been utilized to functionalize CNTs and enhance their nanocomposite properties, which will be discussed in the following sections.

12.4.3 Surface modification of CNTs

Despite the coating reinforcing effects of CNTs, and high electrical and thermal conductivity, employing pristine CNTs in anticorrosion coatings may deteriorate the rate of corrosion of metallic substrates due to their weak dispersion [205]. CNTs-loaded nanocomposite coatings suffer from deficient dispersion, which has imposed great limitations on the employment of CNTs [206]. The inferior dispersion of CNTs stems from the high aspect ratio of the nanotubes and the lack of functional groups on the hydrophobic surface, which induce the formation of aggregation and weak interfacial interaction with the polymeric matrix [207]. Therefore, fabricating a well-dispersed CNT-loaded nanocomposite coating is a significant challenge. To address this issue, novel methods have been used to change the chemistry of CNTs and functionalize them with various functional groups, or combine them into complex structures [208–210]. Surface modification of CNTs can be achieved by building carbon double bonds and graphene edges. Although surface modification improves the dispersability of CNTs in a diverse polymeric matrix, it may result in the emergence of structural defects. Common surface modifications methods that are used to functionalize the surface of CNTs include oxidation, polymer grafting, and silanization [211].

12.4.4 Oxidation technique

One of the reliable techniques to attach a functional group is the oxidation process, which leads to the emergence of oxygen-based groups on the surface of CNTs [212].

The resulting oxygen-containing groups are usually hydroxyl and carboxyl [213]. The oxidized CNTs demonstrate suitable dispersion in organic anticorrosion coatings [214]. Oxidation techniques are based on two methods – liquid and gas phase treatments. In liquid-phase oxidation of CNTs, the functional groups containing oxygen are created on the surface using chemical and electrochemical oxidation. In chemical oxidation, surface modification occurs using oxidant chemicals, such as acids, peroxides, ozone, and potassium permanganate [215]. This method affects the ends of the CNTs with rare structural damages. In electrochemical oxidation systems, surface modification of CNTs happens when a CNTs-coated electrode is placed in a conductive electrolyte. By applying an anodic potential, the CNTs are oxidized on the surface of the electrode [216]. This method is more favorable for preparing oxidized CNTs-coated electrodes.

Gas-phase oxidation of CNTs relies on two techniques – X-ray lithography and plasma oxidation [217]. Although the gas-based oxidation approaches provide high levels of oxidation on the surface of CNTs, the surficial defects on the surface of the modified CNTs are considerable [213].

A very common method to embed carboxylate-functionalized CNTs in polymer nanocomposites is treatment with nitric acid (HNO_3), sulfuric acid (H_2SO_4), or a mixture of both [218, 219]. Exposure to concentrated acids results in the attachment of carboxyl groups to the ends and sidewalls of CNTs [220]. The attachment of carboxyl groups supports the CNTs to form chemical bonds with the other components or the matrix, as a result of which better dispersion and better reinforcing properties are likely to be achieved for the resulting nanocomposite coating [221].

In a work reported by Manh Vu1 and Bach [222], by incorporating MWCNTs and oxidized MWCNTs in epoxy coatings (EP), the corrosion resistance of the coatings increased from 124 to 1,376 and 2,566 kΩ cm^2, respectively. Additionally, the capacitance of the obtained EP coatings reduced from 36.2×10^{-9} to 5.4×10^{-9} and 1.2×10^{-9} F cm^{-2} for EP/MWCNTs and EP/o-MWCNTs coatings, respectively. The observed significant enhancement in the anticorrosion properties represents the role of functionalization of CNTs to fabricate strong bonding between the surface of CNTs and the polymeric matrix. As illustrated in Fig. 12.5, immersing MWCNTs in an acidic mixture of HNO_3/H_2SO_4 results in the appearance of oxygen-containing groups on the surface of the MWCNTs. Alongside the anticorrosion properties of the coatings, load resistance and surface hardness play a key role in formulating durable and strong protective coatings. These features are affected by the cross-linking density of the polymeric matrix; higher the cross-linking value, stiffer is the coating. Functionalized MWCNTs, due to the presence of active sites of functional groups, tend to interact with the functional groups of epoxy resin [223]. The result of the improved interaction between MWCNTs and the matrix is the achievement of a nanocomposite coating with enhanced corrosion protection properties, mechanical strength, and surface hardness.

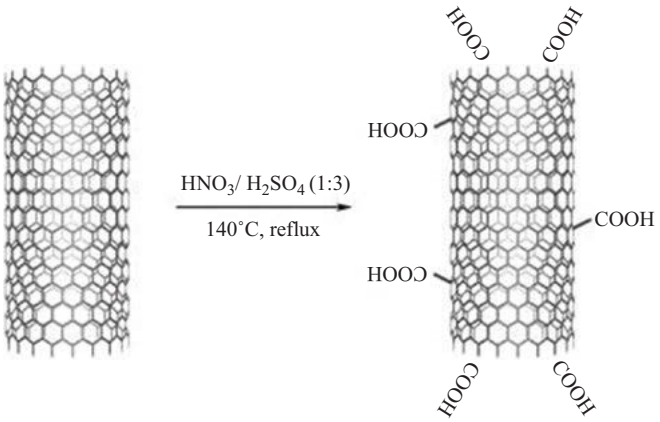

Fig. 12.5: Illustration of a mechanism of acid oxidation of CNT, followed by the addition of alkane groups. Copyrighted from [224] by permission.

More and Mhaske [225] showed that oxidizing MWCNTs by etching acid solution enables the components to form strong chemical bonding, in turn, increasing the protection performance of the coating. Due to the tubular nature of the CNTs, they effectively fill the gaps, lessen the oxygen permeability, and boost the mechanical properties. They claimed that inserting O-MWCNTs results in an increase in the coating compactness, as a result of which the diffusion pathways of the deteriorative specimens, such as ions and oxygen, through the coating are blocked. MWCNTs possess high mechanical strength, indicating that by incorporating them into anticorrosion coatings, they prevent crack formation or propagation, and ameliorate failure resistance under applied shear or load.

Surface oxidization of CNTs can be expedited by employing moderate sonication of CNTs, subjected to an acidic etching solution (HNO_3/H_2SO_4). Xing et al. [226] reported that their sonication-assisted acid-abased oxidation increased the roughness of the surface of the CNTs due to the creation of functional groups on the surface of CNTs. Ferreira et al. [227] showed that the oxidation of CNTs using acidic solutions gives rise to the dispersion of CNTs in polar solvents such as water and ethanol. Furthermore, their findings proved that oxidation, followed by the addition of alkane groups (dodecylamine (DDA) to the oxidized CNTs, provides dispersability of CNTs in xylene.

12.4.5 Polymer grafting on CNTs

Modification of CNTs with polymeric materials has been an interesting subject for many researchers. Polymer grafting of CNTs is performed to increase the dispersion and interfacial adhesion, reduce the hydrophobicity, and change the electrochemical

performance [228]. Additionally, the grafted polymer chains on the surface of CNTs can serve as a potential framework and an active site for designing new CNTs-based hybrid platforms [229, 230]. The polymer grafting technique is a covalent functionalization of CNTs by means of which the atomic sp^2 structure of CNTs transforms into an sp^3 carbonaceous structure. Polymer grafting of CNTs includes two approaches, grafting-to and grafting from [231]. In the grafting-to methodology, the carboxylic functionalized groups on the surface of CNTs react with a pre-formed polymer containing compatible end functional groups, such as hydroxyl and amino moieties [232]. Whereas, in the grafting-from approach, polymer grafting occurs by in-situ polymerization on the surface of CNTs. Controlling the grafting-to technique, due to the hindrance of the neighboring polymer, is challenging, which restricts the number of grafting polymeric chains [230]. Intrinsically, conductive polymers (ICPs) are potent candidates to form CNTs-grafted nanocomposites for anticorrosion applications.

12.4.5.1 Conductive polymers-CNTs

The effectiveness of grafting ICPs on the surface of CNTs has been proven for fabricating high-performance organic corrosion inhibitors. Among the different ICPs, PANI, PPy, PDA, and poly(3,4-ethylene dioxythiophene) (PEDOT) are the most favorable ones [233, 234]. Organic corrosion inhibitors based on CNTs-conductive polymers have shown enhanced mechanical, electrical, and anticorrosion properties, due to the formation of bonding between CNTs and the polymeric chains. In the case of grafting conductive polymers to CNTs, functionalization of CNTs is a prerequisite; while, to prepare core-shell structures, pristine CNTs are favorable. In the following sections, the recent advances in fabricating CNTs-conductive polymers for metals corrosion protection in corrosive environments will be reviewed.

PANI-CNTs. PANI is one of the most studied conductive polymers for a wide range of applications, such as capacitors, batteries, sensors, and actuators because of its adjustable electrical conductivity, nontoxic nature, and electrochemical properties [235–238]. PANI is available in three types – fully oxidized black-colored pernigraniline, half oxidized green-colored emeraldine salt, and fully reduced transparent yellow leucoemeraldine [239]. PANI and its derivatives have shown competitive performance as metal anticorrosion coatings [240]. Protective coatings, based on PANI and its derivatives, have shown different corrosion protection mechanisms, including barrier behavior, corrosion inhibition, passivation protection, and electric field effect [241–243]. The formation of iron oxide and PANI complexes, covering the surface of mild steel, show the passivation protection mechanism of the PANI-based coatings [244, 245]. PANI deprotonation highly depends on the pH of the electrolyte, where at $pH > 4$, its electroactivity and conductivity decline, which restricts its applications in marine and alkaline media ($pH \geq 7$). To address this issue, by doping PANI chains with polyanion components, their electroactivity is improved [246, 247].

One of the reliable techniques to enhance the PANI electrochemical properties is doping with electro-conductive nanomaterials, which are based on a charge transfer mechanism [248]. Zhou et al. [249] reported that synthesizing PANI in the presence of pristine SWCNTs as dopants without any further functionalization results in the formation of an electroactive nanocomposite that possesses rapid electron transfer properties and high chemical stability in neutral and alkaline media [250, 251].

Choudhury and Kar [252] doped PANI with various concentrations of carboxylic-groups-functionalized MWCNTs (fMWCNTs) and measured their electrical conductivity. They showed that by doping PANI to 2 wt.% of fMWCNTs, the electrical conductivity increased by two orders of magnitude from 6.7×10^{-3} to 1.4×10^{-1} S cm^{-1}. This enhancement in electrical conductivity indicates the role of MWCNTs as efficient electron acceptors for charge transfer between the fMWCNTs and PANI through the π-π^* stacking of the carboxylic groups of fMWCNTs and the quinoid rings of PANI. The higher concentrations of fMWCNTs lead to the formation of aggregations, in turn obstructing the formation of the conductive network through the nanocomposite.

Kumar and Gasem [253] first, oxidized the MWCNTs using a mixture of HNO_3/H_2SO_4 solution. Then, they synthesized PANI/o-MWCNTs nanocomposite coating on the surface of mild steel via in-situ polymerization. They reported that the deposited nanocomposite coating of PANI/o-MWCNTs increased the surface hydrophobicity, which led to an increase in corrosion protection efficiency of the coating. As shown in Fig. 12.6, the surface of the PANI/o-MWCNTs nanocomposite coating showed the highest hydrophobicity (higher water contact angle) compared to those of PANI coating and uncoated mild steel specimens. By increasing the concentration of O-MWCNTs in the nanocomposite coating, the contact angle shifted to higher values, confirming an increment in the hydrophobicity of the coating. An increment in the surface hydrophobicity gave rise to enhanced water repulsion, as a result of which the corrosion protection performance was improved.

It has been shown that grafting PANI chains on the surface of carboxylic-functionalized MWCNTs (c-MWCNTs) produce hierarchical nanobrushes, as illustrated in Fig. 12.7 [254].

PANI consists of short fibers that are likely to form agglomeration. Grafting PANI on the tubular surface of c-MWCNTs creates electroconductive nanobrushes, in which PANI chains contribute to the hairbrushes and c-MWCNTs serve as the backbone [255]. Owing to the formation of different chemical bondings between the OCNTs and PANI chains, a grafted nanocomposite is formed. Benzene rings present in the backbone of PANI create π-π stacking interaction with the sidewall of OCNTs. The -N groups of the PANI skeleton establish hydrogen bonds with the carboxylic groups of the OCNTs, forming CNT-C(=O)N-PANI bonding. Furthermore, the induced electrostatic attraction between the positively charged $-NH^+$ in PANI and the negatively charged $-COO^-$, strengthens the grafting of PANI on the OCNTs. The

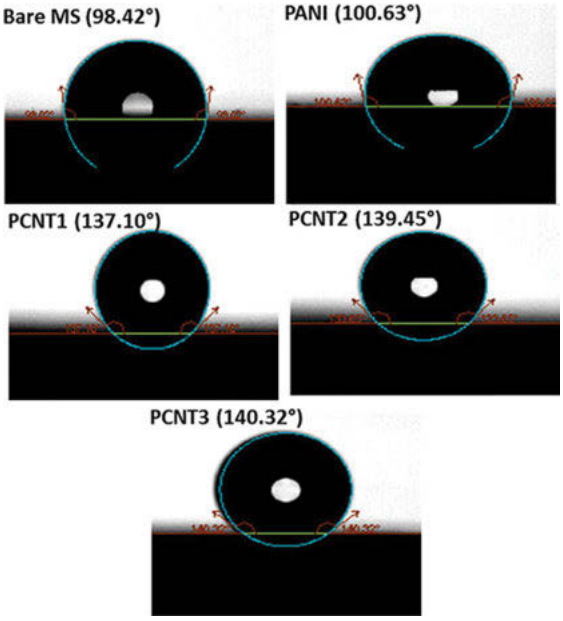

Fig. 12.6: Water contact angle values of bare, PANI-coated, and PANI-CNTs coated mild steel substrates. Copyrighted from [253] by permission.

formation of a PANI on the surface of the OCNTs results in an increase in the diameter of the final nanocomposite [255, 256]. Transmission electron microscopy (TEM) images depict this theory, confirming an increase in the diameter of the c-MWCNTs (Fig. 12.8).

Incorporation of CNTs-PANI nanocomposites into the coatings shifts E_{corr} to higher values, at which, I_{corr} is lower, as a result of which better corrosion protection is obtained [257]. Recently, Rui and Zhu et al. [258] revealed that coatings based on the waterborne acrylic amino resin loaded with 1 wt.% of CNTs-$CaCO_3$-PANI nanocomposite and doped with hydrochloric acid and phosphoric acid showed intelligent and long-lasting function, offering a synergistic effect at the nano-scale barrier, anode protection, cathode suppression, and inhibition mechanisms. Using the potentiodynamic polarization measurements, they reported anodic protection mechanism, which was validated. E_{corr} values of – 0.638, – 0.497, and – 0.427 V were obtained for the unfilled, CNTs-PANI (HCl doped) and CNTs-PANI (HEDP doped) waterborne acrylic coatings, respectively. Their analyses showed that the addition of CNTs-PANI nanocomposites to the coatings increases the density of the coating since nanofiller acts as crosslinker points and reduces the porosity of the coatings. The lower the porosity of the coatings, better is the barrier protection mechanism against diffusion of corrosive species and oxygen. Furthermore, results showed that for artificially scratched coatings immersed in a saline solution, the changes in Tafel slopes are

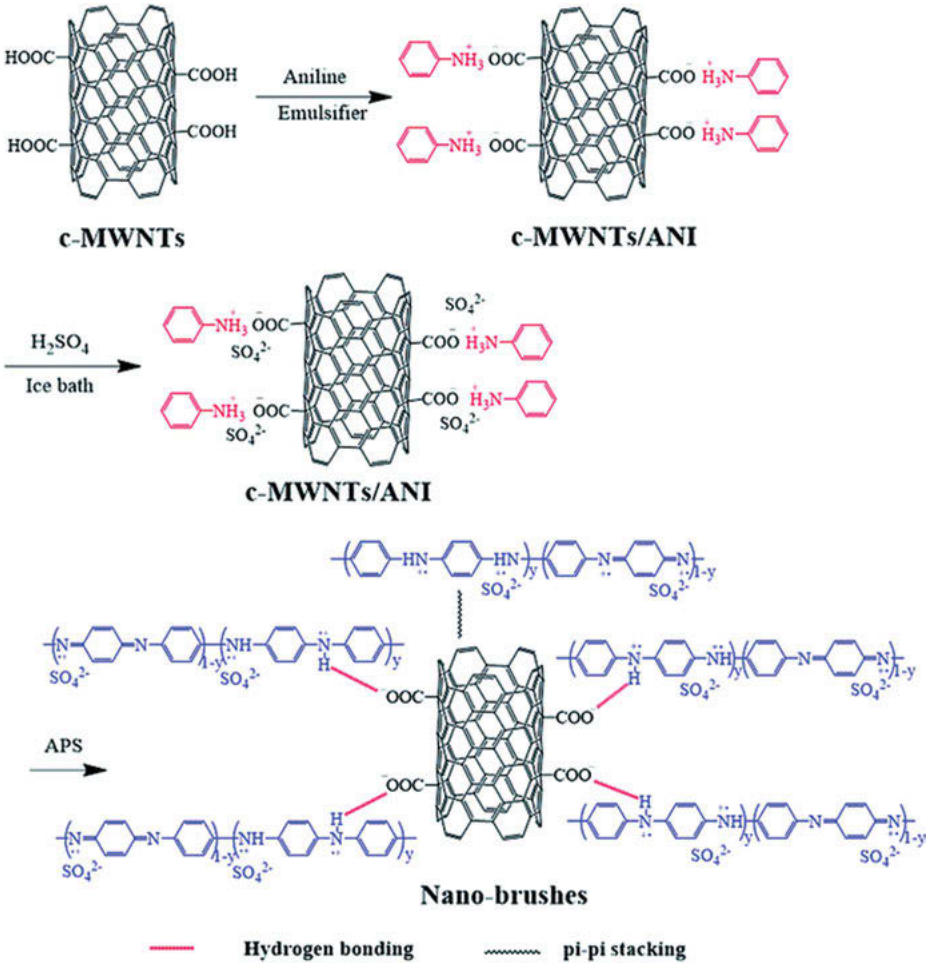

Fig. 12.7: The illustration of the c-MWCNTs-PANI brush-like nanocomposite. Reproduced from [254] with permission from the Royal Society of Chemistry.

intense for the cathodic ones, confirming the formation of a passive thin film covering the defected areas.

These properties support the application of such materials to fabricate a multifunctional smart self-healing coating. The active mechanism of corrosion protection allows the coating to compensate for the created defects and cracks through the system and form a protective layer on the defected areas [259]. Taking advantage of the multi-functional properties of OCNTs-PANI nanocomposites, they are known as high-performance nanofillers that increase the effectiveness of silane coatings in saline media [260, 261]. Silane-based coatings are a new class of coatings that have found applications, instead of chromate conversion coatings. The corrosion protection

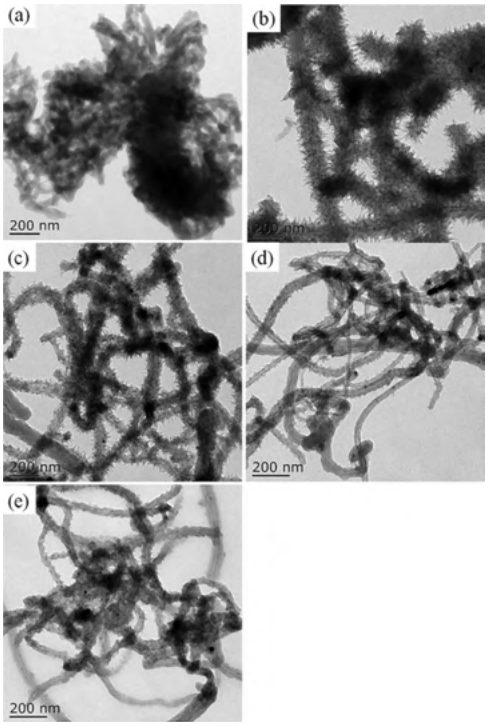

Fig. 12.8: TEM images of the PANI (a) and c-MWCNTs-PANI nanobrush nanocomposites with the c-MWCNTs: PANI ratios of 1:8 (b), 1:4 (c), 1:2 (d), and 1:1 (e). Reproduced from [254] with permission from the Royal Society of Chemistry.

mechanism of the silane coatings relies on their barrier properties. Silane nanocomposite coatings have shown improved durability, adhesion to the substrate, and corrosion barrier characteristics [262].

In the research conducted by Akbarzadeh et al. [263], the grafted PANI on the surface of oxidized CNTs (OCNTs) via in-situ polymerization of aniline monomer loaded into the silane coatings changed the barrier corrosion protection mechanism to a hybrid barrier/active mechanism. These formulated nanocomposite coatings showed the construction of a thin protective layer on the scratched areas of the coating, which means that the presence of OCNTs-PANI in the coatings results in minimizing the attacks of aggressive species on the defects of the coatings. As the FE-SEM micrographs reveal in Fig. 12.9, corrosion products are obvious in the scratched areas of the pristine silane-based coating, while in the presence of OCNTs, the amount of corrosion products decreased. However, by the addition of OCNTs-PANI to the silane coating, a protective layer formed on the metallic surface areas of the scratched zones, blocking the reaching of deteriorative ions to the surface.

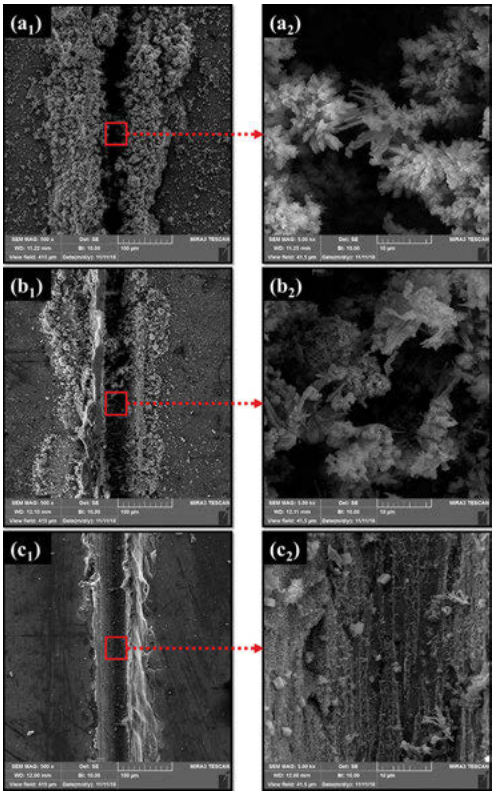

Fig. 12.9: FE-SEM images of artificial scratched pristine silane (a_1,a_2), OCNTs-silane (b_1,b_2), and OCNTs-PANI-silane (c_1,c_2) coatings immersed in a 0.1 M NaCl solution. Copyrighted from [263] by permission.

In addition to direct coating and grafting nanocomposite of CNT-PANI, the core-shell architecture can be fabricated by the oxidative polymerization of the PANI shell on the CNTs' core [264]. Zhang et al. [265] prepared a nano-slurry composed of the synthesized core-shell CNT-PANI dispersed in the aqueous acrylic amino resin and dipped mild steel rods in the mixture. After the completion of coating and processing, the electrochemical impedance measurements showed that the coating contained 0.5 wt.% of PANI/CNT (in a 2:1 ratio), showing the highest corrosion protection performance (33 days), compared to the blank coating (11 days). As illustrated in Fig. 12.10, weak π-π stacking guarantees the adsorption and interaction between the CNT and the aniline monomer to initialize the core-shell oxidative polymerization. Their results indicated that the introduction of core-shell nanocomposite of CNT-PANI into the organic coating increases the corrosion protection efficiency by three preservative mechanisms – nano-barrier effect, anodic protection, and cathodic suppression. Additionally, they claimed that by increasing the ratio of

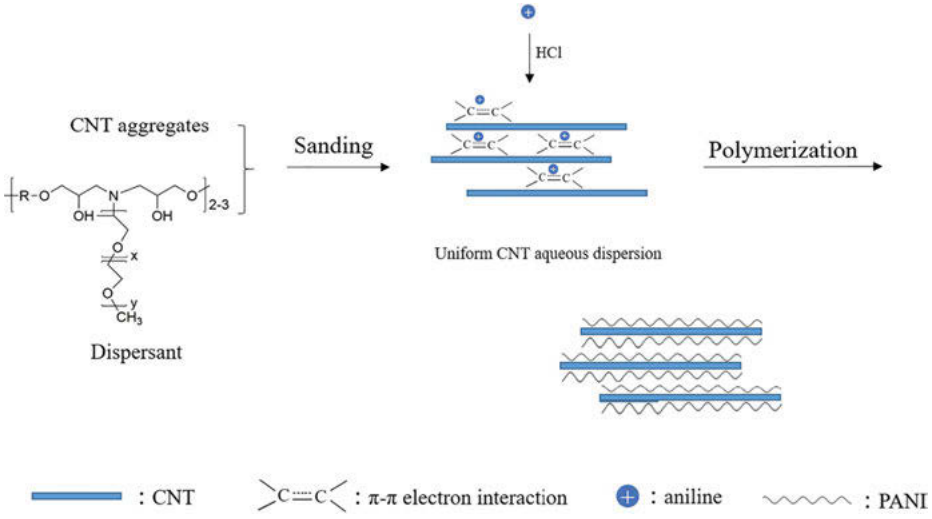

Fig. 12.10: Schematic illustration of the polymerization of core-shell structures of PANI-CNTs nanocomposites. Copyrighted from [265] by permission.

PANI/CNT to 8:1, the nanocomposite coating performed as a smart self-healing coating that resists the corrosion propagation in the defective zones.

In another study, Deshpande et al. [266] synthesized PANI on the MWCNTs surface and loaded the resulting core-shell nanocomposite into a modified epoxy coating as a corrosion inhibitor for a 3.5 wt.% NaCl electrolyte. They showed that the presence of the conductive inhibitors reduces I_{corr} from 21.1 μA cm^{-2} for the low-carbon steel coated with epoxy to 12.6 μA cm^{-2} for the one coated with PANI-MWCNTs-epoxy paint. They discussed that the observed phenomenon leads to a decrease in the corrosion rate from 0.134 mm $year^{-1}$ to 0.037 mm $year^{-1}$ for the low-carbon steel coated with epoxy and PANI-MWCNTs-epoxy coatings, respectively.

All the performed previous studies have shown that the addition of CNTs-PANI nanocomposites enhances the corrosion protection of metallic substrates through synergistic mechanisms.

PPy-CNTs. PPy is a conductive polymer well-known for its high stability, high conductivity, and good electron-transfer properties [267, 268]. PPy has shown great potential as a reliable coating on different substrates using potentiostatically or galvanostatically electropolymerization techniques. Malik et al. deposited PPy on the surface of mild steel to prevent corrosion in the form of pitting in acidic media [269]. Gergely et al. [270] reported that PPy-grafted MWCNTs showed greater interaction with the alkyd matrix and indicated a synergistic effect, showing barrier and anodic meditating mechanism to protect aluminum substrate in saline and acidic solutions.

PEDOT-CNTs. PEDOT is another ICP that can be grafted or wrapped over CNTs with the aim of metal corrosion protection. PEDOT has found numerous applications in organic solar cells, electrochromic displays, photovoltaics, supercapacitors, sensors, and organics electrodes [271]. Its significant conductivity enables the stabilization of the stationary potential at the interface of the PEDOT coating/metal [272]. PEDOT establishes a passive layer on the metallic surface in the polymer/metal interface, thereby shifting E_{corr} to higher values [269, 273]. Similar to PANI, PEDOT can be doped by a negatively charged dopant, such as carboxylic-functionalized MWCNTs (CMWCNTs). Prabakar and Pyo [274] reported that in $LiPF_6$ media, the COO^- groups not only serve as a dopant of PEDOT, but also their negative charge repels the corrosive anions (PF^-_6) approaching the surface of the aluminum. They used Cu_2O-assisted microemulsion polymerization to fabricate coaxial core-shell CNTs-PEDOT (PEDOT-COX/MWCNT) and PEDOT nanosphere-grafted on MWCNT (PEDOT-NSP/MWCNT) architectures, as illustrated in Fig. 12.11. Their measurements reveal that the deposition of a thin film of the prepared nanocomposites on the aluminum surface hinders the formation of corrosion pits in a $LiPF_6$ electrolyte medium. Based on their findings, PEDOT-COX/MWCNT coating showed a corrosion protection performance, similar to that one of pure PEDOT coating. However, PEDOT-NSP/MWCNT indicated the synergistic effect of cation exchange of PEDOT nanospheres and anion repulsion of the MWCNT surface to protect it against the invasion of deteriorative species.

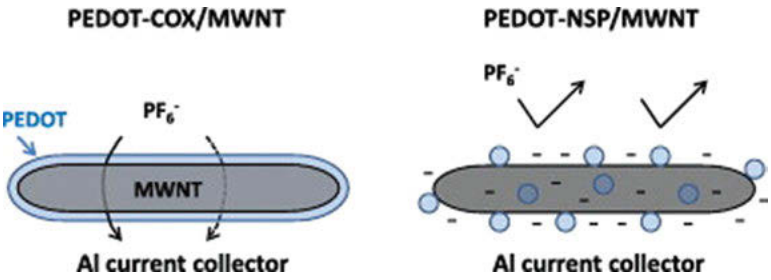

Fig. 12.11: Schematic illustration of the synergistic effects of PEDOT-COX/MWCNT (core-shell) and PEDOT nanosphere-grafted MWCNT nanostructures in the LiPF6 media. Copyrighted from [274] by permission.

12.4.6 Silanization of CNTs

The silanization process using organosilane components is a well-known technique to create functional groups to increase the interfacial interaction of CNTs with the matrix [275]. Organofunctional silane coupling agents are components that provide physical or chemical linkages between two chemicals [276]. Before silanization, using oxidation techniques, carboxyl groups can be created on the surface of CNTs.

The appearing silane coupling agents on the surface of CNTs increase the interfacial interaction, reduces the agglomeration of CNTs, and augments hydrophobicity [277].

Hammer et al. [278] deposited a nanocomposite coating of acid-treated CNTs and siloxane-polymethyl methacrylate using sol acid-catalyzed hydrolytic polycondensation of tetraethylorthosilicate (TEOS) and 3-methacryloxy propyltrimethoxysilane (MPTS) on the surface of mild steel substrates to evaluate the corrosion protection properties of the resulting nanocomposite coatings in saline and acidic media. They obtained a well-dispersed, smooth, and protective coating, which increased the total corrosion impedance and decreased I_{corr} by four and three orders of magnitude, respectively.

12.4.7 Inorganic components-CNTs

Inorganic materials, including metallic-based materials such as Al_2O_3, TiO_2, ZnO, Fe_2O_3, and CeO_2, are a class of corrosion inhibitors used to make anticorrosion coatings [279–281]. The combination of inorganic components with CNTs enhances the dispersion of CNTs in the matrix, thereby increasing the corrosion protective performance of the resulting nanocomposite coating. Cai et al. [282] grafted CeO_2 on the CNTs with an adhesive layer of PDA to fabricate a ternary interfacial layer (CeO_2-PDA-CNTs), dispersed in polyurethane coatings on an aluminum alloy substrate (AA-7075). They attained improved crosslinking density and adhesion strength with the addition of CeO_2-PDACNTs. Their results validated that by incorporating CeO_2-PDACNTs into the PU coating, the long-term corrosion protection performance of the PU coating was enhanced, which was measured using long-term cyclic aging tests. The corrosion resistance of the resulting nanocomposite stayed above 10^8 Ω. cm^2 even after 7 cycles of aging tests, which was three orders of magnitude larger than that of PU coating. Additionally, due to the synergistic effect of the components, the prepared nanocomposite coating showed outstanding corrosion barrier, UV irradiation resistance, and antistriping properties.

CNTs are widely known for their interesting properties, such as electrical, mechanical, and electrochemical properties, for use in corrosion protection applications. CNTs suffer from the lack of functional groups and several techniques have been proposed to attach functional groups to the surface of CNTs to increase their interfacial interaction with the matrix, change their hydrophobicity, enable dispersion in different matrices and solvents, and graft materials. The mentioned methodologies enhance the corrosion protection properties of the CNTs-based nanocomposite coating. Based on the reviewed dopants and grafting materials to link on CNTs, covalent organic frameworks or metal-organic frameworks would be the next class of materials to develop high-performance CNTs-based nanocomposite coatings.

12.5 Fullerene

Fullerene is a carbon allotrope, which has a rolled-up graphene structure, such as closed-caged or partially close-caged carbonaceous hollow spheres, which were discovered by Kroto et al. in 1985 [283]. Fullerene derivatives, with the general formulation of C_n (i.e. C_{94}, C_{80}, C_{70}, and C_{60}) series of carbon atoms, connect via single and double bonds the infused carbon rings with five to seven atoms. The most well-known species of fullerenes is C_{60}, which is highly stable with an average diameter of 0.7–1 nm and a molecular weight of 720 g mol^{-1}. Owing to the interesting properties of fullerenes, i.e. high chemical reactivity, high surface area, excellent thermal, electrochemical, and mechanical stabilities, and small particle size, they find use in many applications such as supercapacitors, energy storage, fuel cells, and corrosion. Based on the functionalities of fullerenes, they can offer a wide range of properties in different media and applications [1, 283, 284].

For the fabrication of fullerene-based nanocomposite materials, the improvement of their dispersion and chemical interactions with polymers is achieved by tailoring the functional groups of fullerenes. Also, surface functionalities of fullerene, such as hydroxyl groups in polyhydroxylated fullerenes ($C_{60}(OH)_n$, are superior active sites for the loading of active agents, grafting of polymers and other surface modifiers, and attachment of secondary nanostructures to design hybridized fullerene-based nanostructures [283]. Liu et al. [285] investigated the effects of modified fullerene (FC_{60}) and graphene (FG) on the tribological and anticorrosion performance of epoxy coatings. 3-Aminopropyltriethoxysine was used as the coupling agent to improve the dispersion and chemical interaction of fullerene nanospheres and graphene nanosheets in the epoxy matrix. Results showed that the epoxy coating containing FC_{60} has more improvement in the tribological properties than the anticorrosion performance, compared to FG-filled epoxy coatings. The coatings containing different concentrations of FC_{60} and FG ranged from 0.25 to 1 wt.% for each filler. Coatings filled with 0.5 wt.% each of FC_{60} and FG showed better corrosion mitigation performance. The better corrosion mitigation performance of FG than FC_{60} was related to the better barrier ability of FG nanosheets, compared to FC_{60} nanospheres, which was achieved by lengthening the diffusion path of the corrosive electrolyte and the ions.

Another strategy to improve the dispersability and chemical interactions of fullerenes with polymeric media is the partial surface oxidization of fullerene nanospheres. Samadianfard et al. [286] studied the effects of different contents of oxidized fullerene (OF), ranging from 25–500 mg L^{-1} on the corrosion mitigation ability of a sol-gel coating, based on tetraethylorthosilicate (TEOS) and (3-glycidyloxypropyl) trimethoxysilane (GPTMS), over AM60B magnesium alloys. The characterization of the nanocomposite coatings proved the chemical interactions of functionalities of OF nanoparticles and the matrix of the sol-gel coating, as illustrated schematically in Fig. 12.12.

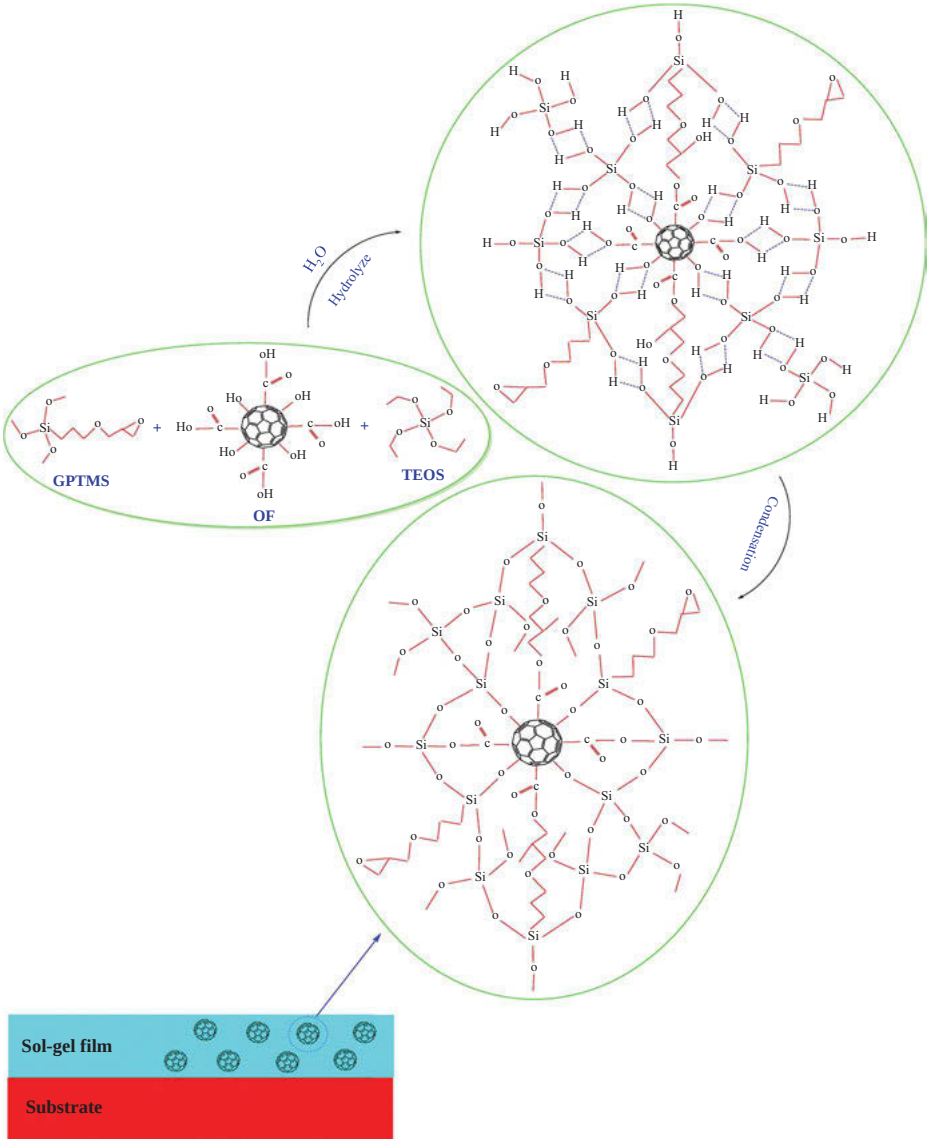

Fig. 12.12: The scheme of chemical interactions between the OF nanoparticles and sol-gel coating. Copyrighted from [286] by permission.

The surface roughness of the sol-gel coating, filled with 100 mg L^{-1} of OF, reduced from 67.5 to 40.3 nm, compared to the neat coating, owing to the improved dispersion and chemical interactions of fullerene nanoparticles after the oxidization. The sol-gel coatings, filled with 25–100 mg L^{-1} of OF, demonstrated the highest value of total corrosion resistance (up to 1,400 min). The addition of 200 and 500 mg L^{-1} of

OF led to a decrease in the anticorrosion performance of the final nanocomposite sol-gel coatings due to the aggregations' formation in coatings, weakening their barrier performance. In another similar study, Samadianfard et al. [287] modified the surface of fullerenes with amine (-NH_2) groups (F-NH_2) and then stabilized them with sodium dodecyl sulfate (SDS) surfactant (F-SDS), as shown schematically in Fig. 12.13.

The active corrosion mitigation of the sol-gel coatings, filled with 500 ppm of F-NH_2 and F-SDS, over AM60B magnesium alloys showed that in almost all immersion times, the F-SDS-filled sol-gel coating exhibited higher total corrosion resistance, owing to the better dispersion of F-NH_2 than F-SDS. The presence of F-NH_2 and F-SDS in the sol-gel coatings decreased the number of microscopic defects in the coating, while they increased the surface roughness of the coatings to some extent. Corrosion mitigation of gas/oil pipelines was achieved by the application of C_{60}/epoxy coatings [288]. Results showed a reinforcement of mechanical properties, such as tensile strength and adhesion strength, by the incorporation of C_{60}. The accelerated corrosion tests (200 h salt spray) showed significant anticorrosion performance of C_{60}-filled epoxy coatings. Also, an intact layer for the mitigation of corrosion was observed for epoxy coatings filled with 0.5 and 1 wt.% C_{60}, with a 50% damage recovery, compared to the unfilled epoxy coating.

Recently, some comparative studies have been conducted on the anticorrosion performance of different carbon allotropes. Wang et al. [11] studied the effects of three different carbon allotropes, including C_{60}, graphene nanoplatelets (GNPs), and CNTs as 0D, 1D, and 2D carbonaceous nanostructures, on tribological, mechanical, and anticorrosion characteristics of the epoxy coatings. Results showed better anticorrosion performances of the epoxy coatings filled with C and GNPs. All C_{60}-, GNPs-, and CNT-filled composites showed enhanced tribological properties, while C_{60} had more impact on the enhancement of tensile properties.

Direct deposition of fullerene nanospheres on metals is another approach for the protection of metallic substrates against corrosion. Sittner et al. [289] deposited a thin layer of fullerene nanospheres on iron substrates, using high vacuum-assisted thermal evaporation. The coated iron substrates were then post-treated via a radiofrequency plasma process under room conditions. In this respect, findings revealed the fabrication of an amorphous carbon network over iron substrates due to the opening of soccer-ball-shaped meshes of fullerenes. Moreover, the electrochemical evaluation of iron substrates, before and after the radiofrequency plasma treatment, presented a better corrosion mitigation performance of the post-treated plates due to the lower level of surface porosity. The deposition of a fullerene-nickel coating on steel substrates led to a decrease in I_{corr} and an increase in anodic dissolution potential, compared to a neat nickel coating in 0.5 M H_2SO_4 [290].

One strategy to alter the characteristics of metals is fabricating lightweight carbon allotropes-reinforced metal matrix composites with enhanced mechanical, tribological, or corrosion mitigation properties. In this respect, Turan et al. [291, 292] developed magnesium metallic composites reinforced with fullerene, GNP, and MWCNT using a

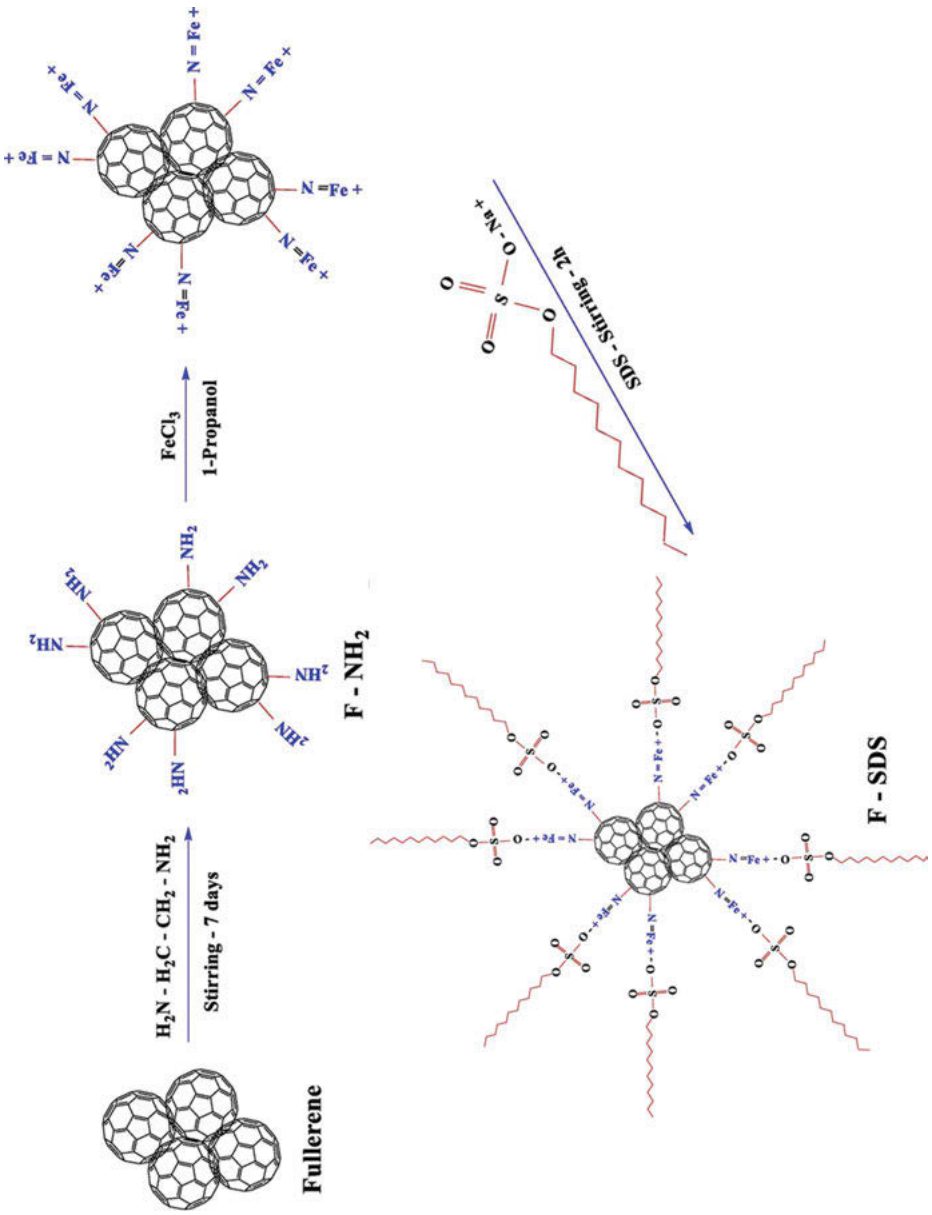

Fig. 12.13: The scheme of the functionalization of fullerenes with -NH_2 and their stabilization with SDS. Copyrighted from [287] by permission.

semi-powder metallurgical method. Results exhibited enhanced wear, compression strength, and hardness properties for the magnesium metallic composites filled with 0.5 wt.% of carbon allotropes, while the corrosion mitigation performance of magnesium metallic composites reduced after the introduction of carbon allotropes. In conclusion, as stated in the literature, the fullerene-filled composites illustrate excellent wear and tribological performance, leading to the decrement of fretting corrosion by reducing the friction coefficient between the metallic surfaces that are in contact with each other [293].

12.6 HCSs

HCSs are another class of carbon nanostructures, which have attracted much interest in many advanced applications, such as catalysis, supercapacitors, fabrication of electrodes, energy storage, batteries, fuel cells, and corrosion protection [294, 295]. Superior characteristics of HCSs, such as excellent thermal and chemical stabilities, tunable shell permeability, surface functionalities, and good dimensional stability, have turned them into potent carbonaceous nanostructures for the aforementioned applications [294, 296, 297]. Based on the synthesis methods of HCSs, they display unique properties, such as specific ratios of surface to volume, engineered shell porosity, and specific structural defects in carbonaceous shells. The synthesis methods of HCSs are classified into soft-templating and hard-templating [294, 298]. In the soft-templating method, soft colloidal templates, such as gas bubbles, micelle, and emulsion droplets, are used as cores. The advantages and disadvantages of the soft-templating methods are ease in the core removal and difficulties in tuning the monodispersity and morphology [298, 299]. On the other hand, in the hard-templating method, in the first step, a rigid scarifying micro/nanotemplate, such as metallic particles, polymeric spheres, and silica particles, is used as the core. In the next step, a thin layer of carbon precursor is applied to the outer surface of the hard template. In the last step, after pyrolysis of the carbon-based shells, HCSs are obtained by removing the hard templates. In these methods, the diameter and monodispersity of templates, the surface chemistry of cores, the thickness of the applied carbon-based shell, the approach of cores removal, and the pyrolysis conditions are the most important synthesis factors [294, 298]. One superior ability of HCSs, compared to other carbon allotropes, is their encapsulation capability. The encapsulation of active components inside the free volume of HCSs makes them a potent candidate for the fabrication of self-healing/active corrosion protective coatings [300, 301]. However, their dispersion in organic corrosion protective coatings can also improve the barrier performance of the fabricated nanocomposite coatings. The evaluation of the application of HCSs in the field of corrosion is still in progress; thus, a few studies have been performed so far.

Li et al. [302] synthesized a novel porous hollow graphitized carbon nanosphere (GCN) loaded with a corrosion inhibitor (M16). The GCNs were synthesized by the ultra-carbonization of hollow PPy/PANI nanospheres at 2,100 °C under an argon stream for 8 h. The schematic illustration of M16-loaded GCNs (GCN@M16) is presented in Fig. 12.14.

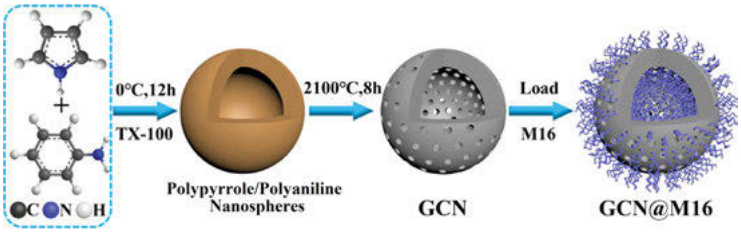

Fig. 12.14: The schematic illustration of the GCN@M16 synthesis. Copyrighted from [302] by permission.

The release of M16 corrosion inhibitors from GCNs accounted for the 94.3% reduction in the antiabrasion index and the corrosion protection of copper plates in a 5 mole HCl electrolyte. The remarkable release of M16 corrosion inhibitors from GCN@M16 carbon capsules and the formation of an M16 thin film over copper plates are responsible for the improved wear and anticorrosion performance. The enhanced anticorrosion performance of the silane coating was obtained by the encapsulation of Zn^{2+} as an inorganic corrosion inhibitor in HCSs (Zn@HCS) [300]. A hard-templating method by silica particles was used for the synthesis of HCSs via the pyrolysis of polysaccharide shells in an inert media. The maximum release of Zn^{2+} from HCSs was observed at pH 4. For the Zn@HCN extract in a 3.5 wt.% NaCl solution, the value of the charge transfer resistance (R_{ct}) of the bare mild steel plate reached 13.3 kΩ cm^2 after 72 h. The impedance characterization of silane coatings with a scratch showed that in the presence of 2.5 wt.% Zn@HCSs as the optimum concentration, R_{ct} increased from 5.7 kΩ cm^2 for the blank coating to 7.7 kΩ cm^2 after 24 h. The encapsulation of mercaptobenzimidazole (MBI) as an organic corrosion inhibitor in HCSs was performed by Haddadi et al. [301, 303] HCSs, with an average particle size of 240 nm, were synthesized via a hard-templating method using amino-functionalized monodisperse silica nanoparticles, the thermal decomposition of polysaccharide shells at 900 °C, and the silica templates removal using 10% HF. Characterization results of the synthesized HCSs revealed that the amino-functionalization of silica templates leads to the formation of crystalline graphene-based carbon shells with sp^2 carbon structures, with enhanced mechanical and dimensional stabilities. The characterization of the core content of MBI-loaded HCS proved the encapsulation of 7.2 wt.% with a maximum release at alkaline pHs. The enhanced corrosion protection of mild steel plates was obtained in the presence of the extract of MBI-loaded HCS in a 3.5 wt.% NaCl

solution. The values of I_{corr} and the total resistance of bare mild steel plates reached from 22.2 μA cm^{-2} and 1.1 kΩ cm^2 to 8 μA cm^{-2} and 2.2 kΩ cm^2 after 24 h. In the coating phase, in the presence of 3 wt.% MBI-loaded HCSs, enhanced barrier and active self-healing performance of the intact and scratched epoxy coating were observed, as presented schematically in Fig. 12.15. In the case of scratched epoxy coatings, the release of MBI from the damaged HCSs accelerated the release of MBI from virgin HCSs around the scratch, with cathodic activities and localized alkaline pHs being responsible for the protective film formation at the interface of steel/coating. Also, the results of the scanning vibrating electrode technique (SVET) proved the reduction of corrosion activities over the scratch for the HCSs-loaded epoxy coating. The incorporation of MBI-loaded HCSs led to the enhancement of scratch hardness modulus from 347.9 to 427.4 MPa and a 58% decrease in the adhesion loss.

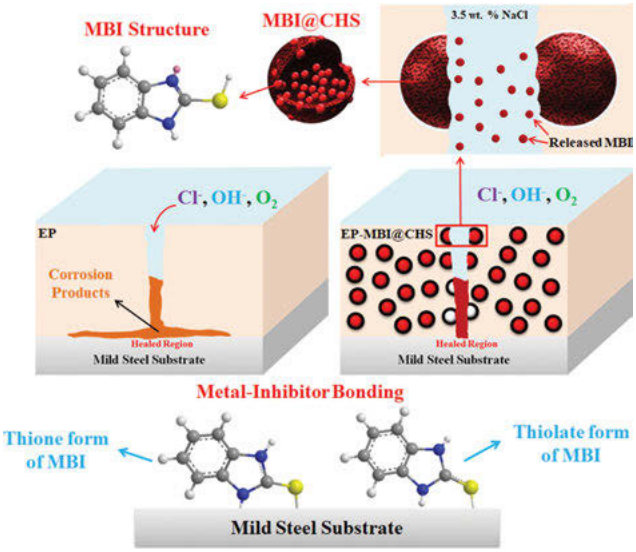

Fig. 12.15: The scheme of active/self-healing mechanism of the epoxy coating containing MBI-loaded HCSs. Copyrighted from [303] by permission.

In another epoxy coating system loaded with 2, 5, and 10 wt.% each of amine (Am-DCS) and epoxy-loaded (Ep-DCS) HCSs as active film-forming agents, enhanced mechanical, barrier, and active/self-healing properties of the epoxy coatings were obtained [304, 305]. The characterization of polyamine and epoxy-doped HCSs showed the successful loading of 44% amine and 39% epoxy in Am-DCSs and Ep-DCSs, respectively. The highest amount of damage recovery was observed for the epoxy coating containing 10 wt.% Am-DCSs and Ep-DCSs, preconditioned for 6 h at room conditions, corresponding to the optimum release and reaction of polyamine and epoxy agents in the scratched zone, as per the scheme shown in Fig. 12.16.

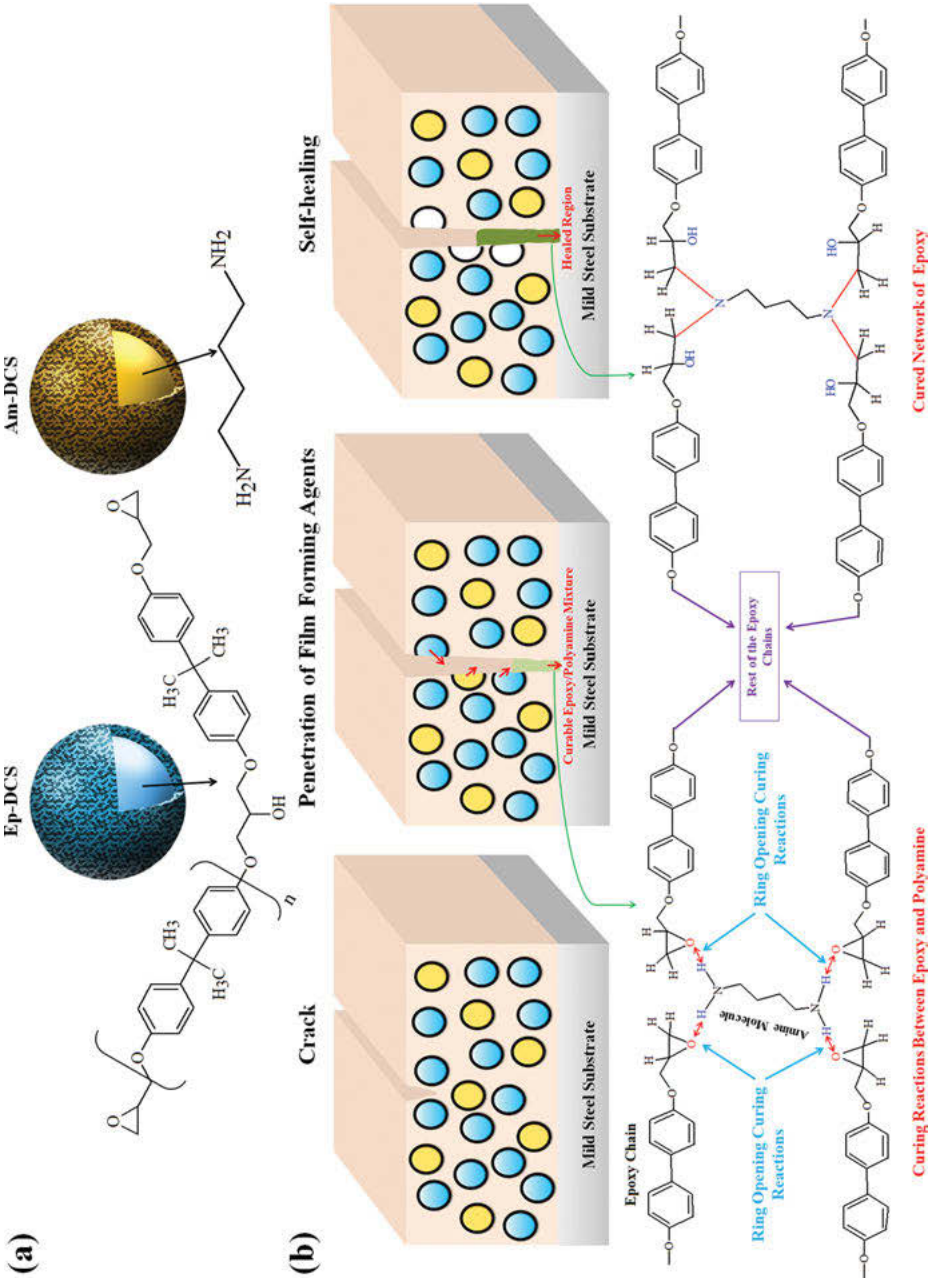

Fig. 12.16: The scheme of amine- and epoxy-loaded HCSs (a) and the film-forming mechanism of the epoxy coating containing amine- and epoxy-loaded HCSs (b). Copyrighted from [304] by permission.

Mechanical characterization of the epoxy coatings filled with different contents of amine- and epoxy-loaded HCSs showed the improvement of tensile strength, Young's modulus, and scratch hardness modulus. In the case of the epoxy coating loaded with 10 wt.% Am-DCSs and Ep-DCSs, the adhesion loss decreased from 52.6% for the blank epoxy coating to 4%.

Mesoporous silica/graphene-based carbon core-shell nanospheres were synthesized via the hard-templating method by Haddadi et al. [306] for the encapsulation of organic components of a walnut green shell extract as green corrosion inhibitors (WE@MCNs). The electrochemical investigation of WE@MCNs in the solution phase revealed an increase of R_{ct} for bare mild steel plates from 0.61 to 4.1 kΩ cm^2 after 24 h immersion in the saline electrolyte. Also, the active anticorrosion performance of the epoxy coating filled with 3 wt.% WE@MCNs increased by 1450%, compared to the blank coating. As stated earlier, HCSs are potent reservoirs for the encapsulation of a wide range of active agents, such as corrosion inhibitors, curing catalysts, film-forming agents, and hydrophobic components. In addition, the incorporation of HCSs into the organic coatings not only improves their barrier/active/self-healing anticorrosion performance but also enhances their mechanical characteristics such as adhesion strength, tensile modulus, and scratch hardness.

12.7 ND

Diamond is a zero-dimension 0-D allotrope of carbon, due to its low dimensional size (1–100 nm), high specific surface area, high thermal and electrical conductivity, and great strength. NDs are preferred to fabricate anticorrosion nanocomposite coatings with enhanced properties [307, 308]. NDs are synthesized with various techniques, such as CVD, plasma-aided CVD, laser-based synthesis, plasma etching, detonation, and irradiation of graphite [309–311].

Functional groups on the surface of ND, including carboxylic acid, ether, ketone, hydroxyl, and anhydride groups, have made ND intrinsically active to form bonding with other components [312]. However, these functional groups interact with each other and result in the agglomeration of ND in the polymeric matrix [313]. Using surface modification techniques, the functionality of ND can be changed [314]. Thermal oxidation by removing the graphitic layer on the surface of ND and creating carboxylic groups, enhances the interaction capability of the resulting modified ND [315]. Various chemical surface treatments has been performed to modify the surface of ND to achieve a strong bonding between ND and the polymer matrix, among which polymer grafting and silanization are of significance [316, 317]. Grafting dodecylamine (DDA) on the surface of the thermally oxidized ND led to better dispersion in the epoxy resin, improved adhesion to the mild steel substrate,

and increased the low-frequency impedance of epoxy coating by an order of magnitude of up to 30 days of immersion in a solution of 3.5 wt.% NaCl [315].

ND-based conductive nanocomposites have shown promising properties for fabricating corrosion protective coatings [318]. Conductive polymers, including PANI, PPy, and polythiophene and their derivatives, have attracted research interest to modify and enhance the properties of ND [319, 320]. It has been shown that grafting PANI on the surface of ND leads to a decrease in the water uptake capacity of the nanocomposite coating [321]. This occurs due to the reduction in the available free volume between the nanoparticles and the grafted polymeric chains, giving rise to lower porosity and higher barrier properties of the coating [322]. In another work [323], a three-step modification of ND, including thermal oxidation of ND detonation, amino functionalization, and PANI grafting, was employed to formulate epoxy-based nanocomposite coatings for anticorrosion purposes. They showed that the epoxy coating loaded with 5 wt.% of PANI/ND presents synergistic corrosion protection due to the combined physical barrier properties and anodic protection.

Nezamdoust et al. [324] showed that hybridizing hydroxylated ND (HND) with silane coatings using a sol-gel technique provides corrosion protection for magnesium alloy (AM60B) in a 0.35 wt.% $(NH_4)_2SO_4$ and 0.05 wt.% NaCl solution. Their findings revealed that the addition of 0.01 wt.% HND to the silane coating increased the compactness of the coating, as a result of the improved barrier properties and improved blockage of the coating's defects. Further to these, the ND can be incorporated for designing superhydrophobic nanocomposite coatings. It was shown that loading fluorosilane-modified NDs into siloxane-acrylic resins presented a contact angle of 154° and an increase in the impedance of the coatings on bare LY12 alloy by two orders of magnitude [325].

12.8 Conclusions and future trends

In recent decades, by developing new classes of carbon allotropes, advanced nanomaterials based on carbon allotropes have become increasingly well-known in the field of corrosion protection. The engineered carbon allotropes illustrated both barrier and active corrosion protection properties in various anticorrosion systems, such as polymeric, metallic, and carbonaceous nanocomposite coatings and films. In the case of polymer nanocomposite anticorrosion systems, the direct incorporation of carbon allotropes, such as graphene, CNTs, and fullerene, is considered a key challenge due to the lack of functionalities. Direct dispersion of the aforementioned carbon allotropes results in the formation of aggregations, poor adhesion to metallic substrates, and the creation of structural microdefects in the polymer matrices. Various treatment methods, such as oxidization, silanization, polymer grafting, and decoration with secondary nanostructures, have been developed to improve their dispersability

and compatibility with the host matrices. Further assessments of the anticorrosion nanocomposite systems filled with surface-treated carbon allotropes revealed enhanced barrier properties, while more modifications are required for self-healing/active corrosion performance. To design/fabricate capsule-based self-healing systems, the loading of corrosion inhibitors in porous structures of carbon nanotubes and/or decoration of secondary nanostructures filled with active agents have been introduced. Direct deposition of carbon allotropes, such as graphene, CNTs, and fullerenes, over the surfaces of metals using rapid thermal annealing, CVD, and electrophoretic deposition/electrodeposition methods can construct protective carbonaceous films. The presence of carbonaceous films not only protects the surface of metals against oxidation but also creates barriers between the metallic surfaces and corrosive environments.

Other important objects for future applications of carbon allotropes in the field of corrosion are cost-effective mass production and commercialization of the different carbon allotropes with various functionalities. Moreover, the combination and optimization of different modification approaches and the application of actual techniques by the consideration of present studies would be at the center of attention for future research.

References

[1] Pourhashem, S.; Ghasemy, E.; Rashidi, A.; Vaezi, M.R. A review on application of carbon nanostructures as nanofiller in corrosion-resistant organic coatings. J. Coat. Technol. Res. 2020, 17, 19–55.
[2] Talbot, D.E.J.; Talbot, J.D.R. Corrosion science and technology, CRC press, 2018.
[3] McCafferty, E. Introduction to corrosion science, Springer Science & Business Media, 2010.
[4] Stewart, R.F.; Masia, M.; Macknick, A.B. Corrosion protection method, 1985.
[5] Schweitzer, P.A. Paint and coatings: Applications and corrosion resistance, CRC press, 2005.
[6] Khanna, A.S. High-performance organic coatings, Elsevier, 2008.
[7] Simpson, C. Improved corrosion-inhibiting pigments. Chemtech 1997, 27.
[8] Sarkodie, B.; Acheampong, C.; Asinyo, B.; Zhang, X.; Tawiah, B. Characteristics of pigments, modification, and their functionalities. Color Res Appl. 2019, 44, 396–410.
[9] Rafiee, M.A.; Yavari, F.; Rafiee, J.; Koratkar, N. Fullerene–epoxy nanocomposites-enhanced mechanical properties at low nanofiller loading. J. Nanoparticle Res. 2011, 13, 733–737.
[10] Santos, M.; Bilek, M.M.M.; Wise, S.G. Plasma-synthesised carbon-based coatings for cardiovascular applications. Biosurf. Biotribol. 2015, 1, 146–160.
[11] Wang, X.; Tang, F.; Cao, Q.; Qi, X.; Pearson, M.; Li, M., et al. Comparative study of three carbon additives: Carbon nanotubes, graphene, and fullerene-c60, for synthesizing enhanced polymer nanocomposites. Nanomaterials 2020, 10, 838.
[12] Prasai, D.; Tuberquia, J.C.; Harl, R.R.; Jennings, G.K.; Bolotin, K.I. Graphene: Corrosion-inhibiting coating. ACS Nano. 2012, 6, 1102–1108.
[13] Raman, R.K.S.; Banerjee, P.C.; Lobo, D.E.; Gullapalli, H.; Sumandasa, M.; Kumar, A., et al. Protecting copper from electrochemical degradation by graphene coating. Carbon N. Y. 2012, 50, 4040–4045.

[14] Kirkland, N.T.; Schiller, T.; Medhekar, N.; Birbilis, N. Exploring graphene as a corrosion protection barrier. Corros. Sci. 2012, 56, 1–4.
[15] Ollik, K.; Lieder, M. Review of the application of graphene-based coatings as anticorrosion layers. Coatings 2020, 10, 883.
[16] Naghdi, S.; Jaleh, B.; Ehsani, A. Electrophoretic deposition of graphene oxide on aluminum: Characterization, low thermal annealing, surface and anticorrosive properties. Bull. Chem. Soc. Jpn. 2015, 88, 722–728.
[17] ETY, L.; TL, L.; Chong, K.F. Facile corrosion protection coating from graphene. Int. J. Chem. Eng. Appl. 2012, 3, 453.
[18] Raza, M.A.; Ali, A.; Ghauri, F.A.; Aslam, A.; Yaqoob, K.; Wasay, A., et al. Electrochemical behavior of graphene coatings deposited on copper metal by electrophoretic deposition and chemical vapor deposition. Surf. Coat. Technol. 2017, 332, 112–119.
[19] Rehman, Z.U.; Raza, M.A.; Ghauri, F.A.; Kanwal, R.; Ahmad, A.; Inam, A. Graphene oxide coatings deposited on steel substrate using electrophoretic deposition and electrochemical evaluation of coatings in saline media. Key Eng. Mater. 2018, 778, Trans Tech Publ, 111–117.
[20] Stankovich, S.; Dikin, D.A.; Dommett, G.H.B.; Kohlhaas, K.M.; Zimney, E.J.; Stach, E.A., et al. Graphene-based composite materials. Nature 2006, 442, 282–286.
[21] Ding, R.; Li, W.; Wang, X.; Gui, T.; Li, B.; Han, P., et al. A brief review of corrosion protective films and coatings based on graphene and graphene oxide. J. Alloys Compd. 2018, 764, 1039–1055.
[22] Yu, W.; Sisi, L.; Haiyan, Y.; Jie, L. Progress in the functional modification of graphene/graphene oxide: A review. RSC Adv. 2020, 10, 15328–15345.
[23] Ye, X.; Long, J.; Lin, Z.; Zhang, H.; Zhu, H.; Zhong, M. Direct laser fabrication of large-area and patterned graphene at room temperature. Carbon N. Y. 2014, 68, 784–790.
[24] Ye, X.; Lin, Z.; Zhang, H.; Zhu, H.; Liu, Z.; Zhong, M. Protecting carbon steel from corrosion by laser in situ grown graphene films. Carbon N. Y. 2015, 94, 326–334.
[25] Shi, Y.Y.; Li, M.; Liu, Q.; Jia, Z.J.; Xu, X.C.; Cheng, Y., et al. Electrophoretic deposition of graphene oxide reinforced chitosan–hydroxyapatite nanocomposite coatings on Ti substrate. J. Mater. Sci. Mater. Med. 2016, 27, 1–13.
[26] Park, J.H.; Park, J.M. Electrophoretic deposition of graphene oxide on mild carbon steel for anti-corrosion application. Surf. Coat. Technol. 2014, 254, 167–174.
[27] Huang, W.-H.; Lin, C.-H.; Lin, B.-S.; Sun, C.-L. Low-temperature CVD graphene nanostructures on Cu and their corrosion properties. Materials (Basel) 2018, 11, 1989.
[28] Chen, S.; Brown, L.; Levendorf, M.; Cai, W.; Ju, S.-Y.; Edgeworth, J., et al. Oxidation resistance of graphene-coated Cu and Cu/Ni alloy. ACS Nano. 2011, 5, 1321–1327.
[29] Wen, G.; Bai, P.; Tian, Y. A review of graphene-based materials for marine corrosion protection. J. Bio-and Tribo-Corrosion 2021, 7, 1–21.
[30] Wang, B.; Cunning, B.V.; S-y, P.; Huang, M.; J-y, K.; RS, R. Graphene coatings as barrier layers to prevent the water-induced corrosion of silicate glass. ACS Nano. 2016, 10, 9794–9800.
[31] Dong, Y.; Liu, Q.; Zhou, Q. Corrosion behavior of Cu during graphene growth by CVD. Corros Sci 2014, 89, 214–219.
[32] Schriver, M.; Regan, W.; Gannett, W.J.; Zaniewski, A.M.; Crommie, M.F.; Zettl, A. Graphene as a long-term metal oxidation barrier: Worse than nothing. ACS Nano. 2013, 7, 5763–5768.
[33] Tiwari, A.; Singh Raman, R.K. Durable corrosion resistance of copper due to multi-layer graphene. Materials (Basel) 2017, 10, 1112.
[34] Zhang, H.; Ren, S.; Pu, J.; Xue, Q. Barrier mechanism of multilayers graphene coated copper against atomic oxygen irradiation. Appl. Surf. Sci. 2018, 444, 28–35.

[35] Yu, F.; Camilli, L.; Wang, T.; Mackenzie, D.M.A.; Curioni, M.; Akid, R., et al. Complete long-term corrosion protection with chemical vapor deposited graphene. Carbon N. Y. 2018, 132, 78–84.
[36] Ren, S.; Cui, M.; Li, W.; Pu, J.; Xue, Q.; Wang, L. N-doping of graphene: Toward long-term corrosion protection of Cu. J. Mater. Chem. A. 2018, 6, 24136–24148.
[37] Hsieh, Y.-P.; Hofmann, M.; Chang, K.-W.; Jhu, J.G.; Li, -Y.-Y.; Chen, K.Y., et al. Complete corrosion inhibition through graphene defect passivation. ACS Nano. 2014, 8, 443–448.
[38] Nair, R.R.; Wu, H.A.; Jayaram, P.N.; Grigorieva, I.V.; Geim, A.K. Unimpeded permeation of water through helium-leak–tight graphene-based membranes. Science (80-) 2012, 335, 442–444.
[39] Du, X.; Skachko, I.; Barker, A.; Andrei, E.Y. Approaching ballistic transport in suspended graphene. Nat. Nanotechnol. 2008, 3, 491–495.
[40] Jiang, B.K.; Chen, A.Y.; Gu, J.F.; Fan, J.T.; Liu, Y.; Wang, P., et al. Corrosion resistance enhancement of magnesium alloy by N-doped graphene quantum dots and polymethyltrimethoxysilane composite coating. Carbon N. Y. 2020, 157, 537–548.
[41] Kyhl, L.; Balog, R.; Cassidy, A.; Jørgensen, J.; Grubisic-čabo, A.; Trotochaud, L., et al. Enhancing graphene protective coatings by hydrogen-induced chemical bond formation. ACS Appl. Nano Mater. 2018, 1, 4509–4515.
[42] Weatherup, R.S.; D'Arsié, L.; Cabrero-Vilatela, A.; Caneva, S.; Blume, R.; Robertson, J., et al. Long-term passivation of strongly interacting metals with single-layer graphene. J. Am. Chem. Soc. 2015, 137, 14358–14366.
[43] Dong, Y.; Liu, Q.; Zhou, Q. Time-dependent protection of ground and polished Cu using graphene film. Corros Sci 2015, 90, 69–75.
[44] Anisur, M.R.; Banerjee, P.C.; Easton, C.D.; Raman, R.K.S. Controlling hydrogen environment and cooling during CVD graphene growth on nickel for improved corrosion resistance. Carbon N. Y. 2018, 127, 131–140.
[45] Nayak, P.K.; Hsu, C.-J.; Wang, S.-C.; Sung, J.C.; Huang, J.-L. Graphene coated Ni films: A protective coating. Thin Solid Films 2013, 529, 312–316.
[46] Zhou, F.; Li, Z.; Shenoy, G.J.; Li, L.; Liu, H. Enhanced room-temperature corrosion of copper in the presence of graphene. ACS Nano. 2013, 7, 6939–6947.
[47] Stoot, A.C.; Camilli, L.; Spiegelhauer, S.-A.; Yu, F.; Bøggild, P. Multilayer graphene for long-term corrosion protection of stainless steel bipolar plates for polymer electrolyte membrane fuel cell. J. Power Sources 2015, 293, 846–851.
[48] Hu, J.; Ji, Y.; Shi, Y.; Hui, F.; Duan, H.; Lanza, M. A review on the use of graphene as a protective coating against corrosion. Ann. J. Mater. Sci. Eng. 2014, 1, 16.
[49] Zhang, Y.H.; Wang, B.; Zhang, H.R.; Chen, Z.Y.; Zhang, Y.Q.; Sui, Y.P., et al. The distribution of wrinkles and their effects on the oxidation resistance of chemical vapor deposition graphene. Carbon N. Y. 2014, 70, 81–86.
[50] Hui, F.; Shi, Y.; Ji, Y.; Lanza, M.; Duan, H. Mechanical properties of locally oxidized graphene electrodes. Arch. Appl. Mech. 2015, 85, 339–345.
[51] Cui, G.; Bi, Z.; Zhang, R.; Liu, J.; Yu, X.; Li, Z. A comprehensive review on graphene-based anti-corrosive coatings. Chem. Eng. J. 2019, 373, 104–121.
[52] Pu, N.-W.; Shi, G.-N.; Liu, Y.-M.; Sun, X.; Chang, J.-K.; Sun, C.-L., et al. Graphene grown on stainless steel as a high-performance and ecofriendly anti-corrosion coating for polymer electrolyte membrane fuel cell bipolar plates. J. Power Sources 2015, 282, 248–256.
[53] Blesman, A.I.; Polonyankin, D.A.; Postnikov, D.V. The influence of the high temperature annealing on the small impurities segregation in J24056 grain steel. Procedia Eng. 2015, 113, 413–417.

[54] Chen, X.-M.; Song, S.-H.; Weng, L.-Q.; Liu, S.-J. Solute grain boundary segregation during high temperature plastic deformation in a Cr–Mo low alloy steel. Mater Sci. Eng. A. 2011, 528, 7663–7668.
[55] Kim, H.H.; Kang, B.; Suk, J.W.; Li, N.; Kim, K.S.; Ruoff, R.S., et al. Clean transfer of wafer-scale graphene via liquid phase removal of polycyclic aromatic hydrocarbons. ACS Nano. 2015, 9, 4726–4733.
[56] Li, Z.; Wang, Y.; Kozbial, A.; Shenoy, G.; Zhou, F.; McGinley, R., et al. Effect of airborne contaminants on the wettability of supported graphene and graphite. Nat. Mater 2013, 12, 925–931.
[57] Tehrani, M.E.H.N.; Ramezanzadeh, M.; Bahlakeh, G.; Ramezanzadeh, B.S. P-codoped rGO-phytic acid-polythiophene core–shell; synthesis, modeling, and dual active–passive anti-corrosion performance of epoxy nanocomposite. J. Ind. Eng. Chem. 2021, 103, 102–117.
[58] Ding, J.-H.; Zhao, H.-R.; Zheng, Y.; Zhao, X.; Yu, H.-B. A long-term anticorrosive coating through graphene passivation. Carbon N. Y. 2018, 138, 197–206.
[59] Chen, C.; Qiu, S.; Cui, M.; Qin, S.; Yan, G.; Zhao, H., et al. Achieving high performance corrosion and wear resistant epoxy coatings via incorporation of noncovalent functionalized graphene. Carbon N. Y. 2017, 114, 356–366.
[60] Ye, Y.; Zhang, D.; Liu, T.; Liu, Z.; Pu, J.; Liu, W., et al. Superior corrosion resistance and self-healable epoxy coating pigmented with salinized trianiline-intercalated graphene. Carbon N. Y. 2019, 142, 164–176.
[61] Qiu, S.; Liu, G.; Li, W.; Zhao, H.; Wang, L. Noncovalent exfoliation of graphene and its multifunctional composite coating with enhanced anticorrosion and tribological performance. J. Alloys Compd. 2018, 747, 60–70.
[62] Ding, J.; Ur Rahman, O.; Peng, W.; Dou, H.; Yu, H. A novel hydroxyl epoxy phosphate monomer enhancing the anticorrosive performance of waterborne graphene/epoxy coatings. Appl. Surf. Sci. 2018, 427, 981–991.
[63] Mo, M.; Zhao, W.; Chen, Z.; Liu, E.; Xue, Q. Corrosion inhibition of functional graphene reinforced polyurethane nanocomposite coatings with regular textures. RSC Adv. 2016, 6, 7780–7790.
[64] Mo, M.; Zhao, W.; Chen, Z.; Yu, Q.; Zeng, Z.; Wu, X., et al. Excellent tribological and anti-corrosion performance of polyurethane composite coatings reinforced with functionalized graphene and graphene oxide nanosheets. RSC Adv. 2015, 5, 56486–56497.
[65] Sun, W.; Wang, L.; Yang, Z.; Zhu, T.; Wu, T.; Dong, C., et al. A facile method for the modification of graphene nanosheets as promising anticorrosion pigments. Mater. Lett. 2018, 228, 152–156.
[66] Chang, C.-H.; Huang, T.-C.; Peng, C.-W.; Yeh, T.-C.; Lu, H.-I.; Hung, W.-I., et al. Novel anticorrosion coatings prepared from polyaniline/graphene composites. Carbon N. Y. 2012, 50, 5044–5051.
[67] He, Y.; Chen, C.; Xiao, G.; Zhong, F.; Wu, Y.; He, Z. Improved corrosion protection of waterborne epoxy/graphene coating by combining non-covalent and covalent bonds. React Funct. Polym. 2019, 137, 104–115.
[68] Hou, W.; Gao, Y.; Wang, J.; Blackwood, D.J.; Teo, S. Recent advances and future perspectives for graphene oxide reinforced epoxy resins. Mater. Today Commun. 2020, 23, 100883.
[69] Rekha, M.Y.; Srivastava, C. Microstructure and corrosion properties of zinc-graphene oxide composite coatings. Corros Sci 2019, 152, 234–248.
[70] Raza, M.A.; Rehman, Z.U.; Ghauri, F.A.; Ahmad, A.; Ahmad, R.; Raffi, M. Corrosion study of electrophoretically deposited graphene oxide coatings on copper metal. Thin Solid Films 2016, 620, 150–159.

[71] Quezada-Rentería, J.A.; Cházaro-Ruiz, L.F.; Rangel-Mendez, J.R. Synthesis of reduced graphene oxide (rGO) films onto carbon steel by cathodic electrophoretic deposition: Anticorrosive coating. Carbon N. Y. 2017, 122, 266–275.
[72] Rajabi, M.; Rashed, G.R.; Zaarei, D. Assessment of graphene oxide/epoxy nanocomposite as corrosion resistance coating on carbon steel. Corros Eng. Sci. Technol. 2015, 50, 509–516.
[73] Chang, K.C.; Ji, W.F.; Li, C.W.; Chang, C.H.; Peng, Y.Y.; Yeh, J.M., et al. The effect of varying carboxylic-group content in reduced graphene oxides on the anticorrosive properties of PMMA/reduced graphene oxide composites. Express Polym. Lett. 2014, 8.
[74] Kulyk, B.; Freitas, M.A.; Santos, N.F.; Mohseni, F.; Carvalho, A.F.; Yasakau, K., et al. A critical review on the production and application of graphene and graphene-based materials in anti-corrosion coatings. Crit. Rev. Solid State Mater. Sci. 2021, 1–48.
[75] Yu, Z.; Di, H.; Ma, Y.; He, Y.; Liang, L.; Lv, L., et al. Preparation of graphene oxide modified by titanium dioxide to enhance the anti-corrosion performance of epoxy coatings. Surf. Coat. Technol. 2015, 276, 471–478.
[76] Kumar, A.; Anant, R.; Kumar, K.; Chauhan, S.S.; Kumar, S.; Kumar, R. Anticorrosive and electromagnetic shielding response of a graphene/TiO 2–epoxy nanocomposite with enhanced mechanical properties. RSC Adv. 2016, 6, 113405–113414.
[77] Liu, J.; Yu, Q.; Yu, M.; Li, S.; Zhao, K.; Xue, B., et al. Silane modification of titanium dioxide-decorated graphene oxide nanocomposite for enhancing anticorrosion performance of epoxy coatings on AA-2024. J. Alloys Compd. 2018, 744, 728–739.
[78] Ramezanzadeh, B.; Haeri, Z.; Ramezanzadeh, M. A facile route of making silica nanoparticles-covered graphene oxide nanohybrids (SiO2-GO); fabrication of SiO2-GO/epoxy composite coating with superior barrier and corrosion protection performance. Chem. Eng. J. 2016, 303, 511–528.
[79] Pourhashem, S.; Vaezi, M.R.; Rashidi, A. Investigating the effect of SiO2-graphene oxide hybrid as inorganic nanofiller on corrosion protection properties of epoxy coatings. Surf. Coat. Technol. 2017, 311, 282–294.
[80] Ma, Y.; Di, H.; Yu, Z.; Liang, L.; Lv, L.; Pan, Y., et al. Fabrication of silica-decorated graphene oxide nanohybrids and the properties of composite epoxy coatings research. Appl. Surf. Sci. 2016, 360, 936–945.
[81] Di, H.; Yu, Z.; Ma, Y.; Pan, Y.; Shi, H.; Lv, L., et al. Anchoring calcium carbonate on graphene oxide reinforced with anticorrosive properties of composite epoxy coatings. Polym. Adv. Technol. 2016, 27, 915–921.
[82] Fan, Y.; Jiang, W.; Kawasaki, A. Highly conductive few-layer graphene/Al2O3 nanocomposites with tunable charge carrier type. Adv. Funct. Mater. 2012, 22, 3882–3889.
[83] Yu, Z.; Di, H.; Ma, Y.; Lv, L.; Pan, Y.; Zhang, C., et al. Fabrication of graphene oxide–alumina hybrids to reinforce the anti-corrosion performance of composite epoxy coatings. Appl. Surf. Sci. 2015, 351, 986–996.
[84] Zhan, Y.; Zhang, J.; Wan, X.; Long, Z.; He, S.; He, Y. Epoxy composites coating with Fe3O4 decorated graphene oxide: Modified bio-inspired surface chemistry, synergistic effect and improved anti-corrosion performance. Appl. Surf. Sci. 2018, 436, 756–767.
[85] Huang, L.; Zhu, P.; Li, G.; Lu, D.D.; Sun, R.; Wong, C. Core–shell SiO 2@ RGO hybrids for epoxy composites with low percolation threshold and enhanced thermo-mechanical properties. J. Mater. Chem. A. 2014, 2, 18246–18255.
[86] Pourhashem, S.; Vaezi, M.R.; Rashidi, A.; Bagherzadeh, M.R. Distinctive roles of silane coupling agents on the corrosion inhibition performance of graphene oxide in epoxy coatings. Prog. Org. Coat. 2017, 111, 47–56.

[87] Pourhashem, S.; Rashidi, A.; Vaezi, M.R.; Bagherzadeh, M.R. Excellent corrosion protection performance of epoxy composite coatings filled with amino-silane functionalized graphene oxide. Surf. Coat. Technol. 2017, 317, 1–9.
[88] Xia, W.; Xue, H.; Wang, J.; Wang, T.; Song, L.; Guo, H., et al. Functionalized graphene serving as free radical scavenger and corrosion protection in gamma-irradiated epoxy composites. Carbon N. Y. 2016, 101, 315–323.
[89] Hu, H.; He, Y.; Long, Z.; Zhan, Y. Synergistic effect of functional carbon nanotubes and graphene oxide on the anti-corrosion performance of epoxy coating. Polym. Adv. Technol. 2017, 28, 754–762.
[90] Zhu, X.; Ni, Z.; Dong, L.; Yang, Z.; Cheng, L.; Zhou, X., et al. In-situ modulation of interactions between polyaniline and graphene oxide films to develop waterborne epoxy anticorrosion coatings. Prog. Org. Coat. 2019, 133, 106–116.
[91] Zhu, Q.; Li, E.N.; Liu, X.; Song, W.; Li, Y.; Wang, X., et al. Epoxy coating with in-situ synthesis of polypyrrole functionalized graphene oxide for enhanced anticorrosive performance. Prog. Org. Coat. 2020, 140, 105488.
[92] Cui, M.; Ren, S.; Zhao, H.; Xue, Q.; Wang, L. Polydopamine coated graphene oxide for anticorrosive reinforcement of water-borne epoxy coating. Chem. Eng. J. 2018, 335, 255–266.
[93] Liu, C.; Qiu, S.; Du, P.; Zhao, H.; Wang, L. An ionic liquid–graphene oxide hybrid nanomaterial: Synthesis and anticorrosive applications. Nanoscale 2018, 10, 8115–8124.
[94] Li, Y.; Yang, Z.; Qiu, H.; Dai, Y.; Zheng, Q.; Li, J., et al. Self-aligned graphene as anticorrosive barrier in waterborne polyurethane composite coatings. J. Mater. Chem. A. 2014, 2, 14139–14145.
[95] Sun, W.; Wang, L.; Wu, T.; Pan, Y.; Liu, G. Synthesis of low-electrical-conductivity graphene/pernigraniline composites and their application in corrosion protection. Carbon N. Y. 2014, 79, 605–614.
[96] Yu, Y.-H.; Lin, -Y.-Y.; Lin, C.-H.; Chan, -C.-C.; Huang, Y.-C. High-performance polystyrene/graphene-based nanocomposites with excellent anti-corrosion properties. Polym. Chem. 2014, 5, 535–550.
[97] Qi, K.; Sun, Y.; Duan, H.; Guo, X. A corrosion-protective coating based on a solution-processable polymer-grafted graphene oxide nanocomposite. Corros Sci 2015, 98, 500–506.
[98] Sun, W.; Wang, L.; Wu, T.; Wang, M.; Yang, Z.; Pan, Y., et al. Inhibiting the corrosion-promotion activity of graphene. Chem. Mater. 2015, 27, 2367–2373.
[99] Hou, P.; Liu, C.; Wang, X.; Zhao, H. Layer-by-layer self-assembled graphene oxide nanocontainers for active anticorrosion application, 2019.
[100] Gupta, R.K.; Malviya, M.; Verma, C.; Quraishi, M.A. Aminoazobenzene and diaminoazobenzene functionalized graphene oxides as novel class of corrosion inhibitors for mild steel: Experimental and DFT studies. Mater Chem. Phys. 2017, 198, 360–373.
[101] Yu, Z.; Lv, L.; Ma, Y.; Di, H.; He, Y. Covalent modification of graphene oxide by metronidazole for reinforced anti-corrosion properties of epoxy coatings. RSC Adv. 2016, 6, 18217–18226.
[102] Feng, L.; Yang, H.; Wang, F. Experimental and theoretical studies for corrosion inhibition of carbon steel by imidazoline derivative in 5% NaCl saturated Ca (OH) 2 solution. Electrochim. Acta. 2011, 58, 427–436.
[103] Ramezanzadeh, M.; Ramezanzadeh, B.; Mahdavian, M.; Bahlakeh, G. Development of metal-organic framework (MOF) decorated graphene oxide nanoplatforms for anti-corrosion epoxy coatings. Carbon N. Y. 2020, 161, 231–251.
[104] Dehghani, A.; Bahlakeh, G.; Ramezanzadeh, B. Synthesis of a non-hazardous/smart anti-corrosion nano-carrier based on beta-cyclodextrin-zinc acetylacetonate inclusion complex decorated graphene oxide (β-CD-ZnA-MGO). J. Hazard Mater. 2020, 398, 122962.

[105] Haeri, Z.; Ramezanzadeh, B.; Ramezanzadeh, M. Recent progress on the metal-organic frameworks decorated graphene oxide (MOFs-GO) nano-building application for epoxy coating mechanical-thermal/flame-retardant and anti-corrosion features improvement. Prog. Org. Coat. 2022, 163, 106645.
[106] Seidi, F.; Jouyandeh, M.; Taghizadeh, M.; Taghizadeh, A.; Vahabi, H.; Habibzadeh, S., et al. Metal-organic framework (MOF)/epoxy coatings: A review. Materials (Basel) 2020, 13, 2881.
[107] Janković, A.; Eraković, S.; Mitrić, M.; Matić, I.Z.; Juranić, Z.D.; Tsui, G.C.P., et al. Bioactive hydroxyapatite/graphene composite coating and its corrosion stability in simulated body fluid. J. Alloys Compd. 2015, 624, 148–157.
[108] Li, M.; Liu, Q.; Jia, Z.; Xu, X.; Shi, Y.; Cheng, Y., et al. Electrophoretic deposition and electrochemical behavior of novel graphene oxide-hyaluronic acid-hydroxyapatite nanocomposite coatings. Appl. Surf. Sci. 2013, 284, 804–810.
[109] Chilkoor, G.; Sarder, R.; Islam, J.; ArunKumar, K.E.; Ratnayake, I.; Star, S., et al. Maleic anhydride-functionalized graphene nanofillers render epoxy coatings highly resistant to corrosion and microbial attack. Carbon N. Y. 2020, 159, 586–597.
[110] Krishnamurthy, A.; Gadhamshetty, V.; Mukherjee, R.; Chen, Z.; Ren, W.; Cheng, H.M., et al. Passivation of microbial corrosion using a graphene coating. Carbon N. Y. 2013, 56, 45–49.
[111] Tamilarasan, T.R.; Sanjith, U.; Shankar, M.S.; Rajagopal, G. Effect of reduced graphene oxide (rGO) on corrosion and erosion-corrosion behaviour of electroless Ni-P coatings. Wear 2017, 390, 385–391.
[112] Nine, M.J.; Cole, M.A.; Johnson, L.; Tran, D.N.H.; Losic, D. Robust superhydrophobic graphene-based composite coatings with self-cleaning and corrosion barrier properties. ACS Appl. Mater. Interfaces 2015, 7, 28482–28493.
[113] Ye, Y.; Zhang, D.; Li, J.; Liu, T.; Pu, J.; Zhao, H., et al. One-step synthesis of superhydrophobic polyhedral oligomeric silsesquioxane-graphene oxide and its application in anti-corrosion and anti-wear fields. Corros Sci 2019, 147, 9–21.
[114] Zhu, S.; Song, Y.; Zhao, X.; Shao, J.; Zhang, J.; Yang, B. The photoluminescence mechanism in carbon dots (graphene quantum dots, carbon nanodots, and polymer dots): Current state and future perspective. Nano Res. 2015, 8, 355–381.
[115] Zhang, X.; Ji, H.; Zhang, X.; Wang, Z.; Xiao, D. Capillary column coated with graphene quantum dots for gas chromatographic separation of alkanes and aromatic isomers. Anal. Methods 2015, 7, 3229–3237.
[116] Al Jahdaly, B.A.; Elsadek, M.F.; Ahmed, B.M.; Farahat, M.F.; Taher, M.M.; Khalil, A.M. Outstanding graphene quantum dots from carbon source for biomedical and corrosion inhibition applications: A review. Sustainability 2021, 13, 2127.
[117] Pourhashem, S.; Rashidi, A.; Vaezi, M.R. Comparing the corrosion protection performance of graphene nanosheets and graphene quantum dots as nanofiller in epoxy coatings. Ind. Lubr. Tribol. 2019.
[118] Bopp, C.; Santhanam, K. Corrosion protection of Monel alloy coated with graphene quantum dots starts with a surge. Chem. Eng. 2019, 3, 80.
[119] Qiu, Z.; Li, L.; Zhu, Q.; Guo, R.; Yao, Y.; Wu, C., et al. Physical stability, rheology, thermal conductivity and optical and corrosion properties of a graphene quantum dot fluid. J. Nanosci. Nanotechnol. 2021, 21, 5312–5318.
[120] Chen, Z.; Wang, M.; Fadhil, A.A.; Fu, C.; Chen, T.; Chen, M., et al. Preparation, characterization, and corrosion inhibition performance of graphene oxide quantum dots for Q235 steel in 1 M hydrochloric acid solution. Colloids Surfaces A. Physicochem Eng. Asp. 2021, 627, 127209.

[121] Pourhashem, S.; Ghasemy, E.; Rashidi, A.; Vaezi, M.R. Corrosion protection properties of novel epoxy nanocomposite coatings containing silane functionalized graphene quantum dots. J. Alloys Compd. 2018, 731, 1112–1118.
[122] Ramezanzadeh, B.; Karimi, B.; Ramezanzadeh, M.; Rostami, M. Synthesis and characterization of polyaniline tailored graphene oxide quantum dot as an advance and highly crystalline carbon-based luminescent nanomaterial for fabrication of an effective anti-corrosion epoxy system on mild steel. J. Taiwan Inst. Chem. Eng. 2019, 95, 369–382.
[123] Ji, X.; Seif, A.; Duan, J.; Rashidi, A.; Zhou, Z.; Pourhashem, S., et al. Experimental and DFT studies on corrosion protection performance of epoxy/graphene quantum dots@ TiO2 nanotubes coatings. Constr. Build. Mater. 2022, 322, 126501.
[124] Zhang, L.; Li, Y.; Wang, H.; Qiao, Y.; Chen, J.; Cao, S. Strong and ductile poly (lactic acid) nanocomposite films reinforced with alkylated graphene nanosheets. Chem. Eng. J. 2015, 264, 538–546.
[125] Wang, J.; Li, C.; Zhang, X.; Xia, L.; Zhang, X.; Wu, H., et al. Polycarbonate toughening with reduced graphene oxide: Toward high toughness, strength and notch resistance. Chem. Eng. J. 2017, 325, 474–484.
[126] Jin, J.; Rafiq, R.; Gill, Y.Q.; Song, M. Preparation and characterization of high performance of graphene/nylon nanocomposites. Eur. Polym. J. 2013, 49, 2617–2626.
[127] Park, Y.T.; Qian, Y.; Chan, C.; Suh, T.; Nejhad, M.G.; Macosko, C.W., et al. Epoxy toughening with low graphene loading. Adv. Funct. Mater. 2015, 25, 575–585.
[128] Wang, J.; Jin, X.; Li, C.; Wang, W.; Wu, H.; Guo, S. Graphene and graphene derivatives toughening polymers: Toward high toughness and strength. Chem. Eng. J. 2019, 370, 831–854.
[129] Papageorgiou, D.G.; Kinloch, I.A.; Young, R.J. Mechanical properties of graphene and graphene-based nanocomposites. Prog. Mater. Sci. 2017, 90, 75–127.
[130] Tan, B.; Thomas, N.L. A review of the water barrier properties of polymer/clay and polymer/graphene nanocomposites. J. Memb. Sci. 2016, 514, 595–612.
[131] Nielsen, L.E. Models for the permeability of filled polymer systems. J Macromol Sci 1967, 1, 929–942.
[132] Pierleoni, D.; Xia, Z.Y.; Christian, M.; Ligi, S.; Minelli, M.; Morandi, V., et al. Graphene-based coatings on polymer films for gas barrier applications. Carbon N. Y. 2016, 96, 503–512.
[133] Ding, R.; Zheng, Y.; Yu, H.; Li, W.; Wang, X.; Gui, T. Study of water permeation dynamics and anti-corrosion mechanism of graphene/zinc coatings. J. Alloys Compd. 2018, 748, 481–495.
[134] Teng, S.; Gao, Y.; Cao, F.; Kong, D.; Zheng, X.; Ma, X., et al. Zinc-reduced graphene oxide for enhanced corrosion protection of zinc-rich epoxy coatings. Prog. Org. Coat. 2018, 123, 185–189.
[135] Marchebois, H.; Keddam, M.; Savall, C.; Bernard, J.; Touzain, S. Zinc-rich powder coatings characterisation in artificial sea water: EIS analysis of the galvanic action. Electrochim. Acta. 2004, 49, 1719–1729.
[136] Marchebois, H.; Savall, C.; Bernard, J.; Touzain, S. Electrochemical behavior of zinc-rich powder coatings in artificial sea water. Electrochim. Acta. 2004, 49, 2945–2954.
[137] Zhou, S.; Wu, Y.; Zhao, W.; Yu, J.; Jiang, F.; Wu, Y., et al. Designing reduced graphene oxide/zinc rich epoxy composite coatings for improving the anticorrosion performance of carbon steel substrate. Mater. Des. 2019, 169, 107694.
[138] Sinko, J. Challenges of chromate inhibitor pigments replacement in organic coatings. Prog. Org. Coat. 2001, 42, 267–282.
[139] Berdimurodov, E.; Verma, D.K.; Kholikov, A.; Akbarov, K.; Guo, L. The recent development of carbon dots as powerful green corrosion inhibitors: A prospective review. J. Mol. Liq. 2021, 118124.

[140] Cao, S.; Liu, D.; Wang, T.; Ma, A.; Liu, C.; Zhuang, X., et al. Nitrogen-doped carbon dots as high-effective inhibitors for carbon steel in acidic medium. Colloids Surfaces A. Physicochem Eng. Asp. 2021, 616, 126280.
[141] Saraswat, V.; Yadav, M. Carbon dots as green corrosion inhibitor for mild steel in HCl solution. ChemistrySelect 2020, 5, 7347–7357.
[142] Zhang, H.D.; Chen, A.Y.; Gan, B.; Jiang, H.; Gu, L.J. Corrosion protection investigations of carbon dots and polydopamine composite coating on magnesium alloy. J. Magnes Alloy. 2021.
[143] Yang, D.; Ye, Y.; Su, Y.; Liu, S.; Gong, D.; Zhao, H. Functionalization of citric acid-based carbon dots by imidazole toward novel green corrosion inhibitor for carbon steel. J. Clean. Prod. 2019, 229, 180–192.
[144] Kalajahi, S.T.; Rasekh, B.; Yazdian, F.; Neshati, J.; Taghavi, L. Green mitigation of microbial corrosion by copper nanoparticles doped carbon quantum dots nanohybrid. Environ. Sci. Pollut. Res. 2020, 27, 40537–40551.
[145] Karak, N. Nanocomposites of epoxy and carbon dots. Sustain. Epoxy Thermosets Nanocomposites, ACS Publications, 2021, 201–233.
[146] Zhu, C.; Fu, Y.; Liu, C.; Liu, Y.; Hu, L.; Liu, J., et al. Carbon Dots as Fillers Inducing Healing/Self-Healing and Anticorrosion Properties in Polymers. Adv. Mater. Weinheim 2017, 29, 1701399.
[147] Wang, J.; Du, P.; Zhao, H.; Pu, J.; Yu, C. Novel nitrogen doped carbon dots enhancing the anticorrosive performance of waterborne epoxy coatings. Nanoscale Adv. 2019, 1, 3443–3451.
[148] Wan, S.; Chen, H.; Cai, G.; Liao, B.; Guo, X. Functionalization of h-BN by the exfoliation and modification of carbon dots for enhancing corrosion resistance of waterborne epoxy coating. Prog. Org. Coat. 2022, 165, 106757.
[149] Wang, X.; Li, C.; Zhang, M.; Lin, D.; Yuan, S.; Xu, F., et al. A novel waterborne epoxy coating with anti-corrosion performance under harsh oxygen environment. Chem. Eng. J. 2022, 430, 133156.
[150] Li, S.; Du, F.; Lin, Y.; Guan, Y.; Qu, W.; Cheng, J., et al. Excellent anti-corrosion performance of epoxy composite coatings filled with novel N-doped carbon nanodots. Eur. Polym. J. 2022, 163, 110957.
[151] Ren, S.; Cui, M.; Zhao, H.; Wang, L. Effect of nitrogen-doped carbon dots on the anticorrosion properties of waterborne epoxy coatings. Surf. Topogr. Metrol Prop. 2018, 6, 24003.
[152] Bao, Y.; Yan, Y.; Wei, Y.; Ma, J.; Zhang, W.; Liu, C. Salt-responsive ZnO microcapsules loaded with nitrogen-doped carbon dots for enhancement of corrosion durability. J. Mater Sci. 2021, 56, 5143–5160.
[153] Luo, J.; Cheng, X.; Zhong, C.; Chen, X.; Ye, Y.W.; Zhao, H., et al. Effect of reaction parameters on the corrosion inhibition behavior of N-doped carbon dots for metal in 1 M HCl solution. J. Mol. Liq. 2021, 338, 116783.
[154] Lv, J.; Fu, L.; Zeng, B.; Tang, M.; Li, J. Synthesis and acidizing corrosion inhibition performance of N-doped carbon quantum dots. Russ. J. Appl. Chem. 2019, 92, 848–856.
[155] Qiang, Y.; Zhang, S.; Zhao, H.; Tan, B.; Wang, L. Enhanced anticorrosion performance of copper by novel N-doped carbon dots. Corros Sci 2019, 161, 108193.
[156] Ye, Y.; Yang, D.; Chen, H.; Guo, S.; Yang, Q.; Chen, L., et al. A high-efficiency corrosion inhibitor of N-doped citric acid-based carbon dots for mild steel in hydrochloric acid environment. J. Hazard Mater. 2020, 381, 121019.
[157] Zhou, Q.; Yuan, G.; Lin, M.; Wang, P.; Li, S.; Tang, J., et al. Large-scale electrochemical fabrication of nitrogen-doped carbon quantum dots and their application as corrosion inhibitor for copper. J. Mater Sci. 2021, 56, 12909–12919.

[158] Cui, M.; Qiang, Y.; Wang, W.; Zhao, H.; Ren, S. Microwave Synthesis of Eco-friendly Nitrogen Doped Carbon Dots for the Corrosion Inhibition of Q235 Carbon Steel in 0.1 M HCl. Int. J. Electrochem Sci. 2021, 16, 151019.
[159] Ye, Y.; Jiang, Z.; Zou, Y.; Chen, H.; Guo, S.; Yang, Q., et al. Evaluation of the inhibition behavior of carbon dots on carbon steel in HCl and NaCl solutions. J. Mater Sci. Technol. 2020, 43, 144–153.
[160] Ye, Y.; Zhang, D.; Zou, Y.; Zhao, H.; Chen, H. A feasible method to improve the protection ability of metal by functionalized carbon dots as environment-friendly corrosion inhibitor. J. Clean. Prod. 2020, 264, 121682.
[161] Ye, Y.; Zou, Y.; Jiang, Z.; Yang, Q.; Chen, L.; Guo, S., et al. An effective corrosion inhibitor of N doped carbon dots for Q235 steel in 1 M HCl solution. J. Alloys Compd. 2020, 815, 152338.
[162] Liu, Z.; Ye, Y.W.; Chen, H. Corrosion inhibition behavior and mechanism of N-doped carbon dots for metal in acid environment. J. Clean. Prod. 2020, 270, 122458.
[163] Cen, H.; Zhang, X.; Zhao, L.; Chen, Z.; Guo, X. Carbon dots as effective corrosion inhibitor for 5052 aluminium alloy in 0.1 M HCl solution. Corros Sci 2019, 161, 108197.
[164] Ye, Y.; Chen, H.; Zou, Y.; Zhao, H. Study on self-healing and corrosion resistance behaviors of functionalized carbon dot-intercalated graphene-based waterborne epoxy coating. J. Mater Sci. Technol. 2021, 67, 226–236.
[165] Ding, J.; Zhao, H.; Yu, H. Structure and performance insights in carbon dots-functionalized MXene-epoxy ultrathin anticorrosion coatings. Chem. Eng. J. 2022, 430, 132838.
[166] Baddour, C.E.; Briens, C. Carbon nanotube synthesis: A review. Int. J. Chem. React Eng. 2005, 3.
[167] Rashad, A.A.; Noaman, R.; Mohammed, S.A.; Yousif, E. Synthesis of carbon nanotube: A review. J. Nanosci Technol. 2016, 155–162.
[168] Vijayaraghavan, V.; Garg, A.; Lam, J.S.L.; Panda, B.; Mahapatra, S.S. Process characterisation of 3D-printed FDM components using improved evolutionary computational approach. Int. J. Adv. Manuf. Technol. 2015, 78.
[169] Anzar, N.; Hasan, R.; Tyagi, M.; Yadav, N.; Narang, J. Carbon nanotube-A review on Synthesis, Properties and plethora of applications in the field of biomedical science. Sensors Int. 2020, 1, 100003.
[170] Plata, D.L.; Hart, A.J.; Reddy, C.M.; Gschwend, P.M. Early evaluation of potential environmental impacts of carbon nanotube synthesis by chemical vapor deposition. Environ. Sci. Technol. 2009, 43, 8367–8373.
[171] Joselevich, E.; Dai, H.; Liu, J.; Hata, K.; Windle, H. A. Carbon nanotube synthesis and organization. Carbon Nanotub. 2007, 101–165.
[172] Harris, P.J.F.; Harris, P.J.F. Carbon nanotube science: Synthesis, properties and applications, Cambridge university press, 2009.
[173] Prasek, J.; Drbohlavova, J.; Chomoucka, J.; Hubalek, J.; Jasek, O.; Adam, V., et al. Methods for carbon nanotubes synthesis. J. Mater. Chem. 2011, 21, 15872–15884.
[174] Yellampalli, S. Carbon nanotubes: Synthesis, characterization, applications, BoD–Books on Demand, 2011.
[175] Xie, S.; Li, W.; Pan, Z.; Chang, B.; Sun, L. Mechanical and physical properties on carbon nanotube. J. Phys. Chem. Solids. 2000, 61, 1153–1158.
[176] Bandaru, P.R. Electrical properties and applications of carbon nanotube structures. J. Nanosci. Nanotechnol. 2007, 7, 1239–1267.
[177] Yang, Z.; Tian, J.; Yin, Z.; Cui, C.; Qian, W.; Wei, F. Carbon nanotube-and graphene-based nanomaterials and applications in high-voltage supercapacitor: A review. Carbon N. Y. 2019, 141, 467–480.
[178] Al-Saleh, M.H. Influence of conductive network structure on the EMI shielding and electrical percolation of carbon nanotube/polymer nanocomposites. Synth. Met. 2015, 205, 78–84.

[179] Cao, Z.; Wei, B.B.Q. A perspective: Carbon nanotube macro-films for energy storage. Energy Environ. Sci. 2013, 6, 3183–3201.
[180] Kamkar, M.; Ghaffarkhah, A.; Hosseini, E.; Amini, M.; Ghaderi, S.; Arjmand, M. Multilayer polymeric nanocomposites for electromagnetic interference shielding: Fabrication, mechanisms, and prospects. New J Chem 2021.
[181] Nayak, S.R.; Mohana, K.N.S.; Hegde, M.B.; Rajitha, K.; Madhusudhana, A.M.; Naik, S.R. Functionalized multi-walled carbon nanotube/polyindole incorporated epoxy: An effective anti-corrosion coating material for mild steel. J. Alloys Compd. 2021, 856, 158057.
[182] Souto, L.F.C.; Soares, B.G. Polyaniline/carbon nanotube hybrids modified with ionic liquids as anticorrosive additive in epoxy coatings. Prog. Org. Coat. 2020, 143, 105598.
[183] Haddadi, S.A.; Ghaderi, S.; Sadeghi, M.; Gorji, B.; Ahmadijokani, F.; AR, S.A., et al. Enhanced active/barrier corrosion protective properties of epoxy coatings containing eco-friendly green inorganic/organic hybrid pigments based on zinc cations/Ferula Asafoetida leaves. J. Mol. Liq. 2020, 114584.
[184] Popoola, A.P.I.; Olorunniwo, O.E.; Ige, O.O. Corrosion resistance through the application of anti-corrosion coatings. Dev Corros Prot. 2014, 13, 241–270.
[185] Sidky, P.S.; Hocking, M.G. Review of inorganic coatings and coating processes for reducing wear and corrosion. Br. Corros. J. 1999, 34, 171–183.
[186] Ghaderi, S.; Haddadi, S.A.; Davoodi, S.; Arjmand, M. Application of sustainable saffron purple petals as an eco-friendly green additive for drilling fluids: A rheological, filtration, morphological, and corrosion inhibition study. J. Mol. Liq. 2020, 315.
[187] Pourhashem, S.; Saba, F.; Duan, J.; Rashidi, A.; Guan, F.; Nezhad, E.G., et al. Polymer/Inorganic nanocomposite coatings with superior corrosion protection performance: A review. J. Ind. Eng. Chem. 2020, 88, 29–57.
[188] Radhamani, A.V.; Lau, H.C.; Ramakrishna, S. Nanocomposite coatings on steel for enhancing the corrosion resistance: A review. J. Compos. Mater. 2020, 54, 681–701.
[189] Eder, D. Carbon nanotube– inorganic hybrids. Chem. Rev. 2010, 110, 1348–1385.
[190] Sharma, V.; Goyat, M.S.; Hooda, A.; Pandey, J.K.; Kumar, A.; Gupta, R., et al. Recent progress in nano-oxides and CNTs based corrosion resistant superhydrophobic coatings: A critical review. Prog. Org. Coat. 2020, 140, 105512.
[191] Khare, R. Carbon nanotube based composites-a review. J. Miner Mater. Charact. Eng. 2005, 4, 31.
[192] Ganguli, S.; Aglan, H.; Dennig, P.; Irvin, G. Effect of loading and surface modification of MWCNTs on the fracture behavior of epoxy nanocomposites. J. Reinf Plast Compos. 2006, 25, 175–188.
[193] Butyrskaya, E.V.; Nechaeva, L.S.; Zapryagaev, S.A. Theoretical study of the corrosion protection mechanism by carbon nanotubes. Comput. Theor. Chem. 2016, 1090, 1–5.
[194] Zachariah, S.; Liu, Y.-L. Nanocomposites of polybenzoxazine-functionalized multiwalled carbon nanotubes and polybenzoxazine for anticorrosion application. Compos. Sci. Technol. 2020, 194, 108169.
[195] Khun, N.W.; Troconis, B.C.R.; Frankel, G.S. Effects of carbon nanotube content on adhesion strength and wear and corrosion resistance of epoxy composite coatings on AA2024-T3. Prog. Org. Coat. 2014, 77, 72–80.
[196] Jeon, H.; Park, J.; Shon, M. Corrosion protection by epoxy coating containing multi-walled carbon nanotubes. J. Ind. Eng. Chem. 2013, 19, 849–853.
[197] Gopi, D.; Shinyjoy, E.; Sekar, M.; Surendiran, M.; Kavitha, L.; Kumar, T.S.S. Development of carbon nanotubes reinforced hydroxyapatite composite coatings on titanium by electrodeposition method. Corros. Sci. 2013, 73, 321–330.

[198] Deyab, M.A. Effect of carbon nano-tubes on the corrosion resistance of alkyd coating immersed in sodium chloride solution. Prog. Org. Coat. 2015, 85, 146–150.
[199] Park, S.; Shon, M. Effects of multi-walled carbon nano tubes on corrosion protection of zinc rich epoxy resin coating. J. Ind. Eng. Chem. 2015, 21, 1258–1264.
[200] Kumar, A.; Ghosh, P.K.; Yadav, K.L.; Kumar, K. Thermo-mechanical and anti-corrosive properties of MWCNT/epoxy nanocomposite fabricated by innovative dispersion technique. Compos. Part B. Eng. 2017, 113, 291–299.
[201] Li, P.; He, X.; Huang, T.-C.; White, K.L.; Zhang, X.; Liang, H., et al. Highly effective anti-corrosion epoxy spray coatings containing self-assembled clay in smectic order. J. Mater. Chem. A. 2015, 3, 2669–2676.
[202] Wei, H.; Ding, D.; Wei, S.; Guo, Z. Anticorrosive conductive polyurethane multiwalled carbon nanotube nanocomposites. J. Mater. Chem. A. 2013, 1, 10805–10813.
[203] Jeevanandam, J.; Barhoum, A.; Chan, Y.S.; Dufresne, A.; Danquah, M.K. Review on nanoparticles and nanostructured materials: History, sources, toxicity and regulations. Beilstein J. Nanotechnol. 2018, 9, 1050–1074.
[204] Hosseinpour, A.; Abadchi, M.R.; Mirzaee, M.; Tabar, F.A.; Ramezanzadeh, B. Recent advances and future perspectives for carbon nanostructures reinforced organic coating for anti-corrosion application. Surf. Interfaces 2021, 23, 100994.
[205] Najmi, P.; Keshmiri, N.; Ramezanzadeh, M.; Ramezanzadeh, B. Highly improving the mechanical-responses/thermal-stability of the epoxy nano-composite using novel highly-oxidized multi-walled carbon nanotubes (OMWCNT) functionalized by Zinc-doped Polyaniline (PANI) nanofibers. J. Taiwan Inst. Chem. Eng. 2021, 119, 245–258, https://doi.org/https://doi.org/10.1016/j.jtice.2021.02.008.
[206] Fukuda, H.; Szpunar, J.A.; Kondoh, K.; Chromik, R. The influence of carbon nanotubes on the corrosion behaviour of AZ31B magnesium alloy. Corros. Sci. 2010, 52, 3917–3923.
[207] Li, J.; Wong, P.-S.; Kim, J.-K. Hybrid nanocomposites containing carbon nanotubes and graphite nanoplatelets. Mater Sci. Eng. A. 2008, 483–484, 660–663.
[208] Xue, C.-H.; Zhou, R.-J.; Shi, -M.-M.; Gao, Y.; Wu, G.; Zhang, X.-B., et al. A green route to water soluble carbon nanotubes and in situ loading of silver nanoparticles. Nanotechnology 2008, 19, 325605.
[209] Gojny, F.H.; Wichmann, M.H.G.; Fiedler, B.; Schulte, K. Influence of different carbon nanotubes on the mechanical properties of epoxy matrix composites – A comparative study. Compos. Sci. Technol. 2005, 65, 2300–2313.
[210] Barrera, E.V. Key methods for developing single-wall nanotube composites. Jom 2000, 52, 38–42.
[211] Rout, T.K.; Jha, G.; Singh, A.K.; Bandyopadhyay, N.; Mohanty, O.N. Development of conducting polyaniline coating: A novel approach to superior corrosion resistance. Surf. Coat. Technol. 2003, 167, 16–24.
[212] Ding, K.; Jia, Z.; Ma, W.; Tong, R.; Wang, X. Polyaniline and polyaniline–thiokol rubber composite coatings for the corrosion protection of mild steel. Mater Chem. Phys. 2002, 76, 137–142.
[213] Chen, C.; Ogino, A.; Wang, X.; Nagatsu, M. Oxygen functionalization of multiwall carbon nanotubes by Ar/H2O plasma treatment. Diam. Relat. Mater. 2011, 20, 153–156.
[214] Ezzeddine, A.; Chen, Z.; Schanze, K.S.; Khashab, N.M. Surface Modification of Multiwalled Carbon Nanotubes with Cationic Conjugated Polyelectrolytes: Fundamental Interactions and Intercalation into Conductive Poly(methyl methacrylate) Composites. ACS Appl. Mater. Interfaces 2015, 7, 12903–12913.
[215] Ovejero, G.; Sotelo, J.L.; Romero, M.D.; Rodríguez, A.; Ocaña, M.A.; Rodríguez, G., et al. Multiwalled Carbon Nanotubes for Liquid-Phase Oxidation. Functionalization,

Characterization, and Catalytic Activity. Ind. Eng. Chem. Res. 2006, 45, 2206–2212, https://doi.org/10.1021/ie051079p.
[216] Shao, Y.; Yin, G.; Zhang, J.; Gao, Y. Comparative investigation of the resistance to electrochemical oxidation of carbon black and carbon nanotubes in aqueous sulfuric acid solution. Electrochim. Acta. 2006, 51, 5853–5857.
[217] Dumée, L.F.; Sears, K.; Marmiroli, B.; Amenitsch, H.; Duan, X.; Lamb, R., et al. A high volume and low damage route to hydroxyl functionalization of carbon nanotubes using hard X-ray lithography. Carbon N. Y. 2013, 51, 430–434.
[218] Li, L.; Xing, Y. Electrochemical Durability of Carbon Nanotubes in Noncatalyzed and Catalyzed Oxidations. J. Electrochem. Soc. 2006, 153, A1823.
[219] Vanyorek, L.; Meszaros, R.; Barany, S. Surface and electrosurface characterization of surface-oxidized multi-walled N-doped carbon nanotubes. Colloids Surfaces A. Physicochem Eng. Asp. 2014, 448, 140–146.
[220] Hiura, H.; Ebbesen, T.W.; Tanigaki, K. Opening and purification of carbon nanotubes in high yields. Adv. Mater. Weinheim 1995, 7, 275–276.
[221] Sun, Y.-P.; Fu, K.; Lin, Y.; Huang, W. Functionalized carbon nanotubes: Properties and applications. Acc. Chem. Res. 2002, 35, 1096–1104, https://doi.org/10.1021/ar010160v.
[222] Vu, C.M.; Bach, Q.-V. Oxidized multiwall carbon nanotubes filled epoxy-based coating: Fabrication, anticorrosive, and mechanical characteristics. Polym. Bull. 2021, 78, 2329–2339.
[223] Ye, J.-S.; Liu, X.; Cui, H.F.; Zhang, W.-D.; Sheu, F.-S.; Lim, T.M. Electrochemical oxidation of multi-walled carbon nanotubes and its application to electrochemical double layer capacitors. Electrochem Commun 2005, 7, 249–255.
[224] Bikiaris, D.; Vassiliou, A.; Chrissafis, K.; Paraskevopoulos, K.M.; Jannakoudakis, A.; Docoslis, A. Effect of acid treated multi-walled carbon nanotubes on the mechanical, permeability, thermal properties and thermo-oxidative stability of isotactic polypropylene. Polym. Degrad. Stab. 2008, 93, 952–967.
[225] More, A.P.; Mhaske, S.T. Anticorrosive coating of polyesteramide resin by functionalized ZnO-Al2O3-Fly ash composite and functionalized multiwalled carbon nanotubes. Prog. Org. Coat. 2016, 99, 240–250.
[226] Xing, Y.; Li, L.; Chusuei, C.C.; Hull, R.V. Sonochemical oxidation of multiwalled carbon nanotubes. Langmuir 2005, 21, 4185–4190.
[227] Ferreira, F.V.; Francisco, W.; de Menezes, B.R.C.; Cividanes, L.D.S.; Dos Reis Coutinho, A.; Thim, G.P. Carbon nanotube functionalized with dodecylamine for the effective dispersion in solvents. Appl. Surf. Sci. 2015, 357, 2154–2159.
[228] Liu, P. Modifications of carbon nanotubes with polymers. Eur. Polym. J. 2005, 41, 2693–2703.
[229] Kar, K.K.; Rana, S.; Pandey, J. Handbook of polymer nanocomposites processing, performance and application, Springer, 2015.
[230] Basheer, B.V.; George, J.J.; Siengchin, S.; Parameswaranpillai, J. Polymer grafted carbon nanotubes – Synthesis, properties, and applications: A review. Nano-Struct. Nano-Objects 2020, 22, 100429.
[231] Homenick, C.M.; Lawson, G.; Adronov, A. Polymer grafting of carbon nanotubes using living free-radical polymerization. Polym. Rev. 2007, 47, 265–290.
[232] Tasis, D.; Tagmatarchis, N.; Bianco, A.; Prato, M. Chemistry of carbon nanotubes. Chem. Rev. 2006, 106, 1105–1136.
[233] Farag, A.A.; Kabel, K.I.; Elnaggar, E.M.; Al-Gamal, A.G. Influence of polyaniline/multiwalled carbon nanotube composites on alkyd coatings against the corrosion of carbon steel alloy. Corros Rev. 2017, 35, 85–94.

[234] Ioniță, M.; Prună, A. Polypyrrole/carbon nanotube composites: Molecular modeling and experimental investigation as anti-corrosive coating. Prog. Org. Coat. 2011, 72, 647–652.
[235] Sen, T.; Mishra, S.; Shimpi, N.G. Synthesis and sensing applications of polyaniline nanocomposites: A review. RSC Adv. 2016, 6, 42196–42222.
[236] Ghasemi, B.; Yaghmaei, S.; Ghaderi, S.; Bayat, A.; Mardanpour, M.M. Effects of chemical, electrochemical, and electrospun deposition of polyaniline coatings on surface of anode electrodes for evaluation of MFCs performance. Biochem. Pharmacol. 2020, 104039.
[237] Tian, Z.; Yu, H.; Wang, L.; Saleem, M.; Ren, F.; Ren, P., et al. Recent progress in the preparation of polyaniline nanostructures and their applications in anticorrosive coatings. RSC Adv. 2014, 4, 28195–28208.
[238] Gilhotra, C.; Chander, M.; Sanjay,. A review: Conducting polyaniline polymer. AIP Conf. Proc., vol. 2142, AIP Publishing LLC; 2019, p. 150008.
[239] Abaci, U.; Guney, H.Y.; Kadiroglu, U. Morphological and electrochemical properties of PPy, PANI bilayer films and enhanced stability of their electrochromic devices (PPy/PAni–PEDOT, PAni/PPy–PEDOT). Electrochim. Acta. 2013, 96, 214–224.
[240] Zarrintaj, P.; Vahabi, H.; Saeb, M.R.; Mozafari, M. Application of polyaniline and its derivatives. In: Fundamental and emerging applications of polyaniline, Elsevier, 2019, 259–272.
[241] Sazou, D.; Deshpande, P.P. Conducting polyaniline nanocomposite-based paints for corrosion protection of steel. Chem. Pap 2017, 71, 459–487.
[242] Qiu, S.; Chen, C.; Cui, M.; Li, W.; Zhao, H.; Wang, L. Corrosion protection performance of waterborne epoxy coatings containing self-doped polyaniline nanofiber. Appl. Surf. Sci. 2017, 407, 213–222.
[243] Zhu, A.; Wang, H.; Sun, S.; Zhang, C. The synthesis and antistatic, anticorrosive properties of polyaniline composite coating. Prog. Org. Coat. 2018, 122, 270–279.
[244] Arefinia, R.; Shojaei, A.; Shariatpanahi, H.; Neshati, J. Anticorrosion properties of smart coating based on polyaniline nanoparticles/epoxy-ester system. Prog. Org. Coat. 2012, 75, 502–508.
[245] Hermas, A.-E.A.; Abdel Salam, M.; Al-Juaid, S.S. In situ electrochemical preparation of multi-walled carbon nanotubes/polyaniline composite on the stainless steel. Prog. Org. Coat. 2013, 76, 1810–1813.
[246] Li, P.; Tan, T.C.; Lee, J.Y. Corrosion protection of mild steel by electroactive polyaniline coatings. Synth. Met. 1997, 88, 237–242.
[247] Armelin, E.; Pla, R.; Liesa, F.; Ramis, X.; Iribarren, J.I.; Alemán, C. Corrosion protection with polyaniline and polypyrrole as anticorrosive additives for epoxy paint. Corros Sci. 2008, 50, 721–728.
[248] Wu, T.-M.; Lin, Y.-W. Doped polyaniline/multi-walled carbon nanotube composites: Preparation, characterization and properties. Polymer (Guildf) 2006, 47, 3576–3582.
[249] Zhou, H.; Lin, Y.; Yu, P.; Su, L.; Mao, L. Doping polyaniline with pristine carbon nanotubes into electroactive nanocomposite in neutral and alkaline media. Electrochem. Commun. 2009, 11, 965–968.
[250] Kinlen, P.J.; Silverman, D.C.; Jeffreys, C.R. Corrosion protection using polyanujne coating formulations. Synth. Met. 1997, 85, 1327–1332.
[251] Sathiyanarayanan, S.; Muthukrishnan, S.; Venkatachari, G.; Trivedi, D.C. Corrosion protection of steel by polyaniline (PANI) pigmented paint coating. Prog. Org. Coat. 2005, 53, 297–301.
[252] Choudhury, A.; Kar, P. Doping effect of carboxylic acid group functionalized multi-walled carbon nanotube on polyaniline. Compos. Part B. Eng. 2011, 42, 1641–1647.

[253] Kumar, A.M.; Gasem, Z.M. In situ electrochemical synthesis of polyaniline/f-MWCNT nanocomposite coatings on mild steel for corrosion protection in 3.5% NaCl solution. Prog. Org. Coat. 2015, 78, 387–394.
[254] Qiu, G.; Zhu, A.; Zhang, C. Hierarchically structured carbon nanotube–polyaniline nanobrushes for corrosion protection over a wide pH range. RSC Adv. 2017, 7, 35330–35339.
[255] Dhand, C.; Arya, S.K.; Singh, S.P.; Singh, B.P.; Datta, M.; Malhotra, B.D. Preparation of polyaniline/multiwalled carbon nanotube composite by novel electrophoretic route. Carbon N. Y. 2008, 46, 1727–1735.
[256] Martina, V.; De Riccardis, M.F.; Carbone, D.; Rotolo, P.; Bozzini, B.; Mele, C. Electrodeposition of polyaniline–carbon nanotubes composite films and investigation on their role in corrosion protection of austenitic stainless steel by SNIFTIR analysis. J. Nanoparticle Res. 2011, 13, 6035–6047.
[257] Rui, M.; Jiang, Y.; Zhu, A. Sub-micron calcium carbonate as a template for the preparation of dendrite-like PANI/CNT nanocomposites and its corrosion protection properties. Chem. Eng. J. 2020, 385, 123396.
[258] Rui, M.; Zhu, A. The synthesis and corrosion protection mechanisms of PANI/CNT nanocomposite doped with organic phosphoric acid. Prog. Org. Coat. 2021, 153, 106134.
[259] Najmi, P.; Keshmiri, N.; Ramezanzadeh, M.; Ramezanzadeh, B. Synthesis and application of Zn-doped polyaniline modified multi-walled carbon nanotubes as stimuli-responsive nanocarrier in the epoxy matrix for achieving excellent barrier-self-healing corrosion protection potency. Chem. Eng. J. 2021, 412, 128637.
[260] Liu, Y.; Cao, H.; Yu, Y.; Chen, S. Corrosion protection of silane coatings modified by carbon nanotubes on stainless steel. Int. J. Electrochem Sci. 2015, 10, 3497–3509.
[261] Calabrese, L.; Khaskoussi, A.; Proverbio, E. Wettability and anti-corrosion performances of carbon nanotube-silane composite coatings. Fibers 2020, 8, 57.
[262] Akbarzadeh, S.; Naderi, R.; Mahdavian, M. Fabrication of a highly protective silane composite coating with limited water uptake utilizing functionalized carbon nano-tubes. Compos. Part B. Eng. 2019, 175, 107109.
[263] Akbarzadeh, S.; Ramezanzadeh, M.; Ramezanzadeh, B.; Mahdavian, M.; Naderi, R. Fabrication of highly effective polyaniline grafted carbon nanotubes to induce active protective functioning in a silane coating. Ind. Eng. Chem. Res. 2019, 58, 20309–20322.
[264] Wu, T.-M.; Lin, Y.-W.; Liao, C.-S. Preparation and characterization of polyaniline/multi-walled carbon nanotube composites. Carbon N. Y. 2005, 43, 734–740.
[265] Zhang, J.; Zhu, A. Study on the synthesis of PANI/CNT nanocomposite and its anticorrosion mechanism in waterborne coatings. Prog. Org. Coat. 2021, 159, 106447.
[266] Deshpande, P.P.; Vathare, S.S.; Vagge, S.T.; Tomšík, E.; Stejskal, J. Conducting polyaniline/multi-wall carbon nanotubes composite paints on low carbon steel for corrosion protection: Electrochemical investigations. Chem. Pap 2013, 67, 1072–1078.
[267] MacDiarmid, A.G. Polyaniline and polypyrrole: Where are we headed?. Synth. Met. 1997, 84, 27–34.
[268] Diaz, A.F.; Castillo, J.I.; Logan, J.A.; Lee, W.-Y. Electrochemistry of conducting polypyrrole films. J. Electroanal. Chem. Interfacial Electrochem. 1981, 129, 115–132.
[269] Malik, M.A.; Włodarczyk, R.; Kulesza, P.J.; Bala, H.; Miecznikowski, K. Protective properties of hexacyanoferrate containing polypyrrole films on stainless steel. Corros. Sci. 2005, 47, 771–783.
[270] Gergely, A.; Pászti, Z.; Hakkel, O.; Drotár, E.; Mihály, J.; Kálmán, E. Corrosion protection of cold-rolled steel with alkyd paint coatings composited with submicron-structure types polypyrrole-modified nano-size alumina and carbon nanotubes. Mater. Sci. Eng. B. 2012, 177, 1571–1582.

[271] Lövenich, W. PEDOT-properties and applications. Polym. Sci. Ser. C. 2014, 56, 135–143.
[272] Zhu, D.; Lu, X.; Lu, Q. Electrically Conductive PEDOT Coating with Self-Healing Superhydrophobicity. Langmuir 2014, 30, 4671–4677.
[273] Tallman, D.E.; Spinks, G.; Dominis, A.; Wallace, G.G. Electroactive conducting polymers for corrosion control. J. Solid State Electrochem 2002, 6, 73–84.
[274] Prabakar, S.J.R.; Pyo, M. Corrosion protection of aluminum in LiPF6 by poly (3, 4-ethylenedioxythiophene) nanosphere-coated multiwalled carbon nanotube. Corros. Sci. 2012, 57, 42–48.
[275] Mohammad Raei Nayini, M.; Bastani, S.; Ranjbar, Z. Synthesis and characterization of functionalized carbon nanotubes with different wetting behaviors and their influence on the wetting properties of carbon nanotubes/polymethylmethacrylate coatings. Prog. Org. Coat. 2014, 77, 1007–1014.
[276] Velasco-Santos, C.; Martínez-Hernández, A.L.; Lozada-Cassou, M.; Alvarez-Castillo, A.; Castaño, V.M. Chemical functionalization of carbon nanotubes through an organosilane. Nanotechnology 2002, 13, 495–498.
[277] Zhou, T.; Wang, X.; Liu, X.H.; Lai, J.Z. Effect of silane treatment of carboxylic-functionalized multi-walled carbon nanotubes on the thermal properties of epoxy nanocomposites. Express Polym. Lett. 2010, 4, 217–226.
[278] Hammer, P.; Dos Santos, F.C.; Cerrutti, B.M.; Pulcinelli, S.H.; Santilli, C.V. Carbon nanotube-reinforced siloxane-PMMA hybrid coatings with high corrosion resistance. Prog. Org. Coat. 2013, 76, 601–608.
[279] Pham, G.V.; Trinh, A.T.; Hang, T.T.X.; Nguyen, T.D.; Nguyen, T.T.; Nguyen, X.H. Incorporation of Fe 3 O 4 /CNTs nanocomposite in an epoxy coating for corrosion protection of carbon steel. Adv. Nat. Sci. Nanosci. Nanotechnol. 2014, 5, 35016.
[280] Yi, H.; Chen, C.; Zhong, F.; Xu, Z. Preparation of aluminum oxide-coated carbon nanotubes and the properties of composite epoxy coatings research. High Perform. Polym. 2013, 26, 255–264.
[281] He, Y.; Chen, C.; Zhong, F.; Chen, H.; Qing, D. Synthesis and properties of iron oxide coated carbon nanotubes hybrid materials and their use in epoxy coatings. Polym. Adv. Technol. 2015, 26, 414–421.
[282] Cai, G.; Xiao, S.; Deng, C.; Jiang, D.; Zhang, X.; Dong, Z. CeO2 grafted carbon nanotube via polydopamine wrapping to enhance corrosion barrier of polyurethane coating. Corros. Sci. 2021, 178, 109014.
[283] Aschberger, K.; Johnston, H.J.; Stone, V.; Aitken, R.J.; Tran, C.L.; Hankin, S.M., et al. Review of fullerene toxicity and exposure–appraisal of a human health risk assessment, based on open literature. Regul. Toxicol. Pharmacol. 2010, 58, 455–473.
[284] Coro, J.; Suarez, M.; Silva, L.S.R.; Eguiluz, K.I.B.; Salazar-Banda, G.R. Fullerene applications in fuel cells: A review. Int. J. Hydrogen Energy 2016, 41, 17944–17959.
[285] Liu, D.; Zhao, W.; Liu, S.; Cen, Q.; Xue, Q. Comparative tribological and corrosion resistance properties of epoxy composite coatings reinforced with functionalized fullerene C60 and graphene. Surf. Coat. Technol. 2016, 286, 354–364.
[286] Samadianfard, R.; Seifzadeh, D.; Habibi-Yangjeh, A.; Jafari-Tarzanagh, Y. Oxidized fullerene/sol-gel nanocomposite for corrosion protection of AM60B magnesium alloy. Surf. Coat. Technol. 2020, 385, 125400.
[287] Samadianfard, R.; Seifzadeh, D.; Habibi-Yangjeh, A. Sol-gel coating filled with SDS-stabilized fullerene nanoparticles for active corrosion protection of the magnesium alloy. Surf. Coat. Technol. 2021, 419, 127292.

[288] Wang, X.; Tang, F.; Qi, X.; Lin, Z.; Battocchi, D.; Chen, X. Enhanced protective coatings based on nanoparticle fullerene C60 for oil & gas pipeline corrosion mitigation. Nanomaterials 2019, 9, 1476.
[289] Sittner, F.; Enders, B.; Ensinger, W. Electrochemical determination of corrosion protection ability of fullerene thin films treated by radiofrequency plasma. Thin Solid Films 2004, 459, 233–236.
[290] Tseluikin, V.N.; Solov'eva, N.D.; Gun'kin, I.F. Electrodeposition of nickel-fullerene C60 composition coatings. Prot. Met. 2007, 43, 388–390.
[291] Turan, M.E.; Sun, Y.; Akgul, Y. Mechanical, tribological and corrosion properties of fullerene reinforced magnesium matrix composites fabricated by semi powder metallurgy. J. Alloys Compd. 2018, 740, 1149–1158.
[292] Turan, M.E.; Sun, Y.; Aydin, F.; Zengin, H.; Turen, Y.; Ahlatci, H. Effects of carbonaceous reinforcements on microstructure and corrosion properties of magnesium matrix composites. Mater Chem. Phys. 2018, 218, 182–188.
[293] Krasnyy, V.A.; The use of nanomaterials to improve the wear resistance of machine parts under fretting corrosion conditions. IOP Conf. Ser. Mater. Sci. Eng., vol. 560, IOP Publishing; 2019, p. 12186.
[294] Li, S.; Pasc, A.; Fierro, V.; Celzard, A. Hollow carbon spheres, synthesis and applications- a review. J. Mater. Chem. A. 2016, 4, 12686–12713.
[295] Liu, T.; Zhang, L.; Cheng, B.; Yu, J. Hollow carbon spheres and their hybrid nanomaterials in electrochemical energy storage. Adv. Energy Mater. 2019, 9, 1803900.
[296] Li, Y.; Li, T.; Yao, M.; Liu, S. Metal-free nitrogen-doped hollow carbon spheres synthesized by thermal treatment of poly (o-phenylenediamine) for oxygen reduction reaction in direct methanol fuel cell applications. J. Mater. Chem. 2012, 22, 10911–10917.
[297] Yang, X.; Li, Y.; Zhang, P.; Sun, L.; Ren, X.; Mi, H. Hierarchical hollow carbon spheres: Novel synthesis strategy, pore structure engineering and application for micro-supercapacitor. Carbon N. Y. 2020, 157, 70–79.
[298] Wang, X.; Feng, J.; Bai, Y.; Zhang, Q.; Yin, Y. Synthesis, Properties, and Applications of Hollow Micro-/Nanostructures. Chem. Rev. 2016.
[299] Zhang, Z.; Qin, M.; Jia, B.; Zhang, H.; Wu, H.; Qu, X. Facile synthesis of novel bowl-like hollow carbon spheres by the combination of hydrothermal carbonization and soft templating. Chem Commun 2017, 53, 2922–2925.
[300] Behgam, R.; Mahdavian, M.; Ramazani, A. Fabrication of Hollow Carbon Spheres Doped with Zinc Cations for Corrosion Protection of Organosilane Coatings. Surf. Interfaces 2020, 100696.
[301] Haddadi, S.A.; Ramazani, S.A.A.; Mahdavian, M.; Taheri, P.; Mol, J.M.C. Fabrication and characterization of graphene-based carbon hollow spheres for encapsulation of organic corrosion inhibitors. Chem. Eng. J. 2018, 352.
[302] Liu, S.; Jing, Y.; Zhang, T.; Zhang, J.; Xu, F.; Song, Q., et al. Excellent tribological and anti-corrosion performances enabled by novel hollow graphite carbon nanosphere with controlled release of corrosion inhibitor. Chem. Eng. J. 2021, 412, 128648.
[303] Haddadi, S.A.; AR, S.A.; Mahdavian, M.; Arjmand, M. Epoxy nanocomposite coatings with enhanced dual active/barrier behavior containing graphene-based carbon hollow spheres as corrosion inhibitor nanoreservoirs. Corros. Sci. 2021, 185, 109428.
[304] Haddadi, S.A.; Ramazani, S.A.A.; Mahdavian, M.; Taheri, P.; Mol, J.M.C.; Gonzalez-Garcia, Y. Self-healing epoxy nanocomposite coatings based on dual-encapsulation of nano-carbon hollow spheres with film-forming resin and curing agent. Compos. Part B. Eng. 2019, 175, https://doi.org/10.1016/j.compositesb.2019.107087.

[305] Haddadi, S.A.; Ramazani, S.A.; Mahdavian, M.; Taheri, P.; Mol, J.M.C. Mechanical and Corrosion Protection Properties of a Smart Composite Epoxy Coating with Dual-Encapsulated Epoxy/Polyamine in Carbon Nanospheres. Ind. Eng. Chem. Res. 2019, 58, 3033–3046.
[306] Haddadi, S.A.; Kohlan, T.B.; Momeni, S.; AR, S.A.; Mahdavian, M. Synthesis and application of mesoporous carbon nanospheres containing walnut extract for fabrication of active protective epoxy coatings. Prog. Org. Coat. 2019, 133, 206–219.
[307] Zhang, Y.; Rhee, K.Y.; Hui, D.; Park, S.-J. A critical review of nanodiamond based nanocomposites: Synthesis, properties and applications. Compos. Part B. Eng. 2018, 143, 19–27.
[308] Karami, P.; Khasraghi, S.S.; Hashemi, M.; Rabiei, S.; Shojaei, A. Polymer/nanodiamond composites-a comprehensive review from synthesis and fabrication to properties and applications. Adv. Colloid Interface Sci. 2019, 269, 122–151.
[309] Shvidchenko, A.V.; Eidelman, E.D.; Vul, A.Y.; Kuznetsov, N.M.; Stolyarova, D.Y.; Belousov, S.I., et al. Colloids of detonation nanodiamond particles for advanced applications. Adv. Colloid Interface Sci. 2019, 268, 64–81.
[310] Amans, D.; Chenus, A.-C.; Ledoux, G.; Dujardin, C.; Reynaud, C.; Sublemontier, O., et al. Nanodiamond synthesis by pulsed laser ablation in liquids. Diam. Relat. Mater. 2009, 18, 177–180.
[311] Kharisov, B.I.; Kharissova, O.V.; Chávez-Guerrero, L. Synthesis techniques, properties, and applications of nanodiamonds. Synth. React Inorganic Met Nano-Metal Chem 2010, 40, 84–101.
[312] Rehman, A.; Houshyar, S.; Wang, X. Nanodiamond-based fibrous composites: A review of fabrication methods, properties, and applications. ACS Appl. Nano Mater. 2021, 4, 2317–2332.
[313] Molavi, H.; Shojaei, A.; Pourghaderi, A. Rapid and tunable selective adsorption of dyes using thermally oxidized nanodiamond. J. Colloid Interface Sci. 2018, 524, 52–64.
[314] Hou, W.; Gao, Y.; Wang, J.; Blackwood, D.J.; Teo, S. Nanodiamond decorated graphene oxide and the reinforcement to epoxy. Compos. Sci. Technol. 2018, 165, 9–17.
[315] Rahmani, P.; Shojaei, A.; Tavandashti, N.P. Nanodiamond loaded with corrosion inhibitor as efficient nanocarrier to improve anticorrosion behavior of epoxy coating. J. Ind. Eng. Chem. 2020, 83, 153–163.
[316] Hajiali, F.; Shojaei, A. Silane functionalization of nanodiamond for polymer nanocomposites-effect of degree of silanization, 2016.
[317] Mochalin, V.N.; Neitzel, I.; Etzold, B.J.M.; Peterson, A.; Palmese, G.; Gogotsi, Y. Covalent incorporation of aminated nanodiamond into an epoxy polymer network. ACS Nano. 2011, 5, 7494–7502.
[318] Schrand, A.M.; Hens, S.A.C.; Shenderova, O.A. Nanodiamond particles: Properties and perspectives for bioapplications. Crit. Rev. Solid State Mater. Sci. 2009, 34, 18–74.
[319] Kausar, A. Review on conducting polymer/nanodiamond nanocomposites: Essences and functional performance. J. Plast Film Sheeting 2019, 35, 331–353.
[320] Gomez, H.; Ram, M.K.; Alvi, F.; Stefanakos, E.; Kumar, A. Novel synthesis, characterization, and corrosion inhibition properties of nanodiamond– polyaniline films. J. Phys. Chem. C 2010, 114, 18797–18804.
[321] Ashassi-Sorkhabi, H.; Es'haghi, M. Corrosion protection of mild steel by nano-colloidal polyaniline/nanodiamond composite coating in NaCl solution. J. Coat. Technol. Res. 2014, 11, 371–380.
[322] Ashassi-Sorkhabi, H.; Bagheri, R.; Rezaei-Moghadam, B. Corrosion protection properties of PPy-ND composite coating: Sonoelectrochemical synthesis and design of experiment. J. Mater. Eng. Perform. 2016, 25, 611–622.

[323] Mohammadkhani, R.; Shojaei, A.; Rahmani, P.; Tavandashti, N.P.; Amouzegar, M. Synthesis and characterization of polyaniline/nanodiamond hybrid nanostructures with various morphologies to enhance the corrosion protection performance of epoxy coating. Diam. Relat. Mater. 2021, 120, 108672.
[324] Nezamdoust, S.; Seifzadeh, D.; Habibi-Yangjeh, A. Nanodiamond incorporated sol– gel coating for corrosion protection of magnesium alloy. Trans Nonferrous Met Soc China 2020, 30, 1535–1549.
[325] Uzoma, P.C.; Wang, Q.; Zhang, W.; Gao, N.; Li, J.; Okonkwo, P.C., et al. Anti-bacterial, icephobic, and corrosion protection potentials of superhydrophobic nanodiamond composite coating. Colloids Surfaces A. Physicochem Eng. Asp. 2021, 630, 127532.

Taiwo W. Quadri*, Lukman O. Olasunkanmi, Omolola E. Fayemi, Eno E. Ebenso

Chapter 13
Industrial corrosion inhibitors: nanostructured carbon allotropes as ideal substitutes

Abstract: Nanostructured carbon allotropes are sought-after materials of interest in several fields. These nanostructures have shown great prospects in the development of efficient, cost-effective and environmentally benign corrosion inhibitors for use in several industries. Their associated facile synthesis, low cost, outstanding anticorrosive properties, and eco-friendliness have drawn much attention in the inhibitor formulation industry. This chapter overviews contemporary applications of carbon-based nanostructures as ideal and sustainable substitutes for traditional organic and inorganic corrosion inhibitors in commercial industries. Attention is paid to the inhibition performances of functionalized forms of carbon dots, graphene oxide, and carbon nanotubes employed as aqueous phase inhibitors of metallic deterioration in acidic and neutral solutions. The limitations and challenges of carbon allotropes as industrial corrosion inhibitors are also briefly outlined. Overall, this chapter establishes that nanostructured carbon allotropes are positioned as the next-generation inhibitors for industrial metals.

Keywords: carbon allotropes, corrosion, industrial corrosion inhibitors, green corrosion inhibitors, industrial metal, carbon dots, carbon nanotubes, graphene oxide

*Corresponding author: **Taiwo W. Quadri,** Department of Chemistry, School of Chemical and Physical Sciences and Material Science Innovation & Modelling (MaSIM) Research Focus Area, Faculty of Natural and Agricultural Sciences, North-West University, Private Bag X2046, Mmabatho 2735, South Africa, e-mail: taiwoquadri27@gmail.com
Lukman O. Olasunkanmi, Department of Chemistry, Faculty of Science, Obafemi Awolowo University, Ile Ife 220005, Nigeria & Department of Chemical Sciences, University of Johannesburg, Doornfontein Campus, P.O. Box 17011, Johannesburg 2028, South Africa
Omolola E. Fayemi, Department of Chemistry, School of Chemical and Physical Sciences and Material Science Innovation & Modelling (MaSIM) Research Focus Area, Faculty of Natural and Agricultural Sciences, North-West University, Private Bag X2046, Mmabatho 2735, South Africa,
Eno E. Ebenso, Institute for Nanotechnology and Water Sustainability, College of Science, Engineering and Technology, University of South Africa, Johannesburg 1710, South Africa

https://doi.org/10.1515/9783110782820-013

13.1 Introduction

Alloys and metals are prone to degradation on exposure to the environment. Their tendency to return to their thermodynamically stable state often depends on several factors such as their physical nature, temperature range, surface impurities, electrolytic solution, and pH level [1, 2]. Material degradation is not exclusive to metallic materials; polymers and ceramics also undergo corrosion in aggressive environments. Metallic corrosion takes several forms including uniform, galvanic, pitting, erosion, microbial, dealloying, stress corrosion cracking, and crevice corrosion. The knowledge of the forms of corrosion is crucial in developing appropriate control systems.

According to Pikaar et al. [3], metallic corrosion accounts for the loss of one-third of steel annually, besides the reported annual global loss of approximately 3% of the world gross domestic product (GDP). In addition to material and economic losses, corrosion poses the risk of environmental hazards, toxicity to human and aquatic lives, and loss of human life due to structural collapse and pipeline bursts [4]. The main industries extremely affected by metallic degradation are depicted in Fig. 13.1. In particular, corrosion is about the greatest challenging problem in the oil, gas, and petroleum industries. The oil industry and its allies have expended a lot of resources to combat the corrosion of pipelines and machinery that are essential to its daily operations. Till date, mitigating corrosion phenomena remains a daunting task for researchers in academia and industry.

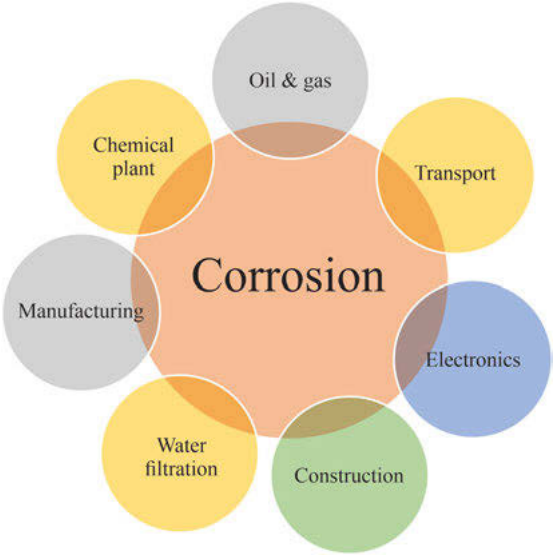

Fig. 13.1: Major industries affected by metallic degradation.

Corrosion management has led to the exploration of several cost-saving and technically efficient options to combat corrosion processes, thereby alleviating its damaging consequences. Innovations in protective coatings, inhibition, cathodic/anodic protection, design modification, and selection of corrosion-resistant materials have been developed in order to mitigate metallic corrosion [4–6]. These methods lessen metallic destruction by modifying the material, procedure, and/or medium of application. As powerful as each of these techniques could be in corrosion management, numerous factors need to be considered before their industrial application. In many cases, it is advisable to adopt one or more of these techniques in lessening the rate of material degradation.

One of the most promising and well-known practical techniques for retarding corrosion processes is the application of corrosion inhibitors. Corrosion inhibitors are chemical additives that are introduced into electrolytic systems in diminutive amounts to retard electrochemical reaction [7]. Over the years, several studies have been conducted to determine the inhibitive potential of different chemical additives in aggressive media [2, 8]. These additives, which are often introduced into corrosive solutions in minute amounts (between 10 and 1,000 mg/L), do not significantly react with the components of the electrolytic medium. As the search for efficient, cost-effective, and eco-friendly inhibiting materials evolves, nanostructured carbon allotropes, which are well-known for their special attributes are being considered by corrosion experts as feasible metallic corrosion inhibitors. This chapter presents a discussion on the main classes of industrial corrosion inhibitors, their mechanisms of action and corrosion of industrial metals. The chapter also overviews recent advancements of novel carbon allotropes as ideal substitutes for conventional inhibitors, in different commonly encountered aggressive media. The limitations and challenges associated with nanostructured carbon allotropes as corrosion inhibitors are also highlighted.

13.2 Industrial corrosion inhibitors and their mechanisms of action

13.2.1 Inorganic and organic industrial inhibitors

Industrial chemical inhibitors can be generally categorized on the basis of their interference on electrochemical half-cell reactions, reaction mechanism, and medium of application [9]. Figure 13.2 gives a graphical representation of the classification of industrial inhibitors based on these three classes. Based on their interference on half-cell reactions, industrial corrosion inhibitors can be subdivided into cathodic or anodic inhibitors (inorganic additives) and mixed inhibitors (organic additives). These classes of inhibitors comprise compounds that possess capabilities to protect

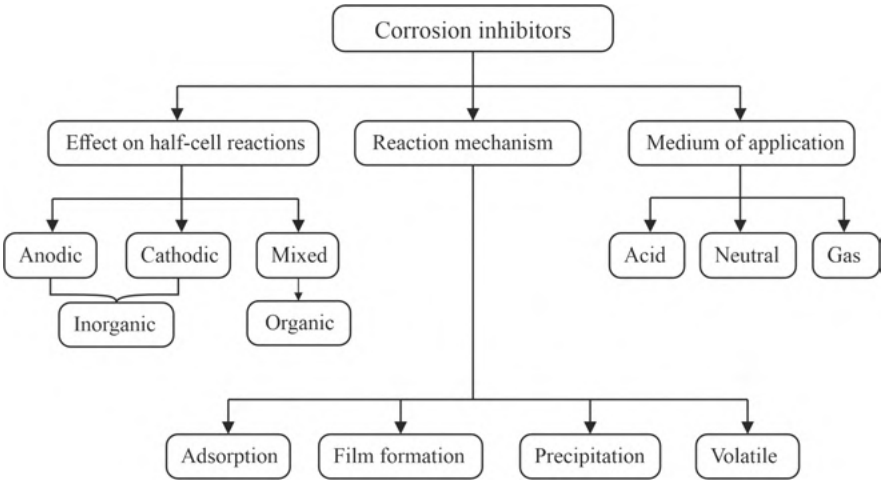

Fig. 13.2: Classification of industrial corrosion inhibitors.

the integrity of metals from degradation in electrolytic media. Inorganic chemical additives often contain crystalline salts such as silicates, nitrites, chromates, and phosphates. On the other hand, organic chemical additives are organic molecules typically possessing one or more polar groups, aromatic rings, heteroatoms (O, N, S, and P) and multiple bonds in their chemical structure [1].

In the past, inorganic chemical additives topped the chart of preferred inhibiting materials in commercial industries because of their numerous advantages. They are known to excellently suppress hydrogen evolution at the cathodic region (cathodic inhibitors) or impede metallic dissolution at the anode (anodic inhibitors). In addition, these traditional inhibitors restrain material deterioration at high temperatures for longer exposure time and are relatively cheaper than organic compounds. Despite these advantages, their further use has been vehemently protested because of their demerits. Their ineffectiveness in strong acid solutions (> 17% HCl), difficulty in combining, formation of sparingly soluble compounds on metals, and most importantly, their environmental toxicity are major considerations for rethinking the use of these compounds in commercial industries [10, 11]. Organic inhibitors have emerged as ready alternatives to toxic inorganic compounds because of their sustainability and effectiveness in corrosive media. These additives often protect the metal by adhering on the corroded surface and deterring the permeation of aggressive ions. Numerous studies have shown that they often interfere with the anodic and cathodic reaction simultaneously; hence, they are popularly referred to as mixed-type inhibitors. It must, however, be noted that not all organic compounds can be classified as highly effective and environment-friendly chemicals. Their high cost, harmful impact of their synthesis, post-application disposal into the environment, and their failure to

protect metals from deterioration at high temperatures are strong limitations to their promotion as ideal substitutes [4, 12, 13].

To overcome these problems, research has shifted focus to the exploration of "green" corrosion inhibitors. Industrial inhibitors are termed "green" if they are cheap, readily available, biodegradable, and nontoxic to man and the environment [5]. These inhibitors can either be sourced naturally (plant extracts, natural polymers) or synthesized following the principles of green chemistry as proposed by Anastas (the father of green chemistry) and Warner in 1998 [14]. Green corrosion-inhibiting materials being reported as alternatives to conventional organic inhibitors include extracts from plant parts [15], polymers [16], drugs [17], and ionic liquids [18]. These green inhibitors have been identified to contain aliphatic chains, aromatic rings, heterocyclic rings, heteroatoms, and polar functional groups. These characteristics facilitate the adhesion of the inhibiting materials to the metallic substrate, thereby restraining the interaction of the metal with the corrosive species.

Factors that are often considered in the selection of industrial chemical additives for corrosion control are as follows [2, 16, 19]:

1. The industrial additive should be dispersible or soluble in the medium of application.
2. Solvent used in dissolving the inhibitor should be cheap, environmentally benign, and nontoxic.
3. The industrial inhibitor should possess a large molecular size, several active chemical groups, and pi-bonds that can block the active sites of degradation.
4. The industrial additive should be capable of forming a chelate with the metallic sample.
5. The inhibitor/metal protective layer should be capable of covering a large surface area and be insoluble in water or organic solvents.
6. The industrial additive should be efficient at high temperatures and flow velocities.
7. The industrial additive should have long range effectiveness.
8. The industrial inhibitor should be environmentally sustainable and nontoxic to man and the environment.
9. The industrial additive should be readily available/cheap/easily synthesized.

In contemporary times, a new group of corrosion-inhibiting additives has emerged which is fast gaining recognition in corrosion science and engineering. This group of compounds is known as nanostructured carbon allotropes. Figure 13.3 displays some of the common nanostructured carbon allotropes [20]. These nano allotropes are low-dimensional materials that have found wide applications in several commercial industries on account of their sterling mechanical, electronic, and optical qualities. Termed as "wonder materials," they have become useful in catalysis, biomedicine, sensor development, and energy storage devices [20, 21]. Recent forays into their anticorrosive properties have shown outstanding results, leading to a rising interest in their synthesis and utilization. These results are not unconnected to

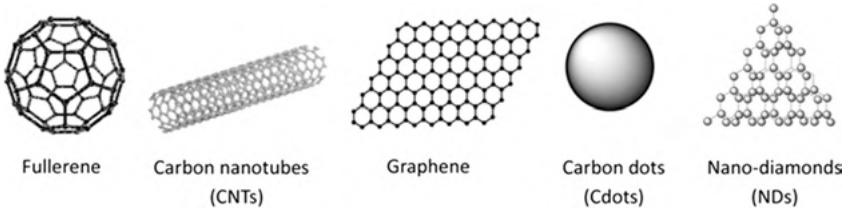

Fig. 13.3: Common nanostructured carbon allotropes [20].

their ready availability, facile synthesis, excellent anticorrosive properties, large molecular size, and eco-friendliness. Based on these qualities, these materials are positioned to become the next-generation industrial inhibiting-materials.

13.2.2 Mechanisms of action of industrial corrosion inhibitors

Corrosion inhibition is a complex process due to numerous factors involved. Generally, industrial corrosion inhibitors including carbon nano allotropes are known to spread on the metal substrate to form a thin film that shields the metal surface from corrosive species in the electrolyte [22]. However, an in-depth investigation into the mechanisms of action of inhibiting materials is of great importance, as it will shed light on how industrial inhibitors behave. Several efforts have been made to understand the inhibition mechanisms of industrial inhibitors with some measure of success achieved.

Traditional and simple testing techniques such as weight loss (WL)/gravimetric, thermometric, and gasometric studies have been reported in the study of inhibitors. These methods provide information on the kinetics and thermodynamics of the corrosion process. Modern equipment have been deployed to conduct electrochemical analyses such as open circuit potential (OCP), linear polarization resistance (LPR), scanning vibrating electrode technique (SVET), electrochemical impedance spectroscopy (EIS), cyclic voltammetry (CV), and potentiodynamic polarization (PDP) in a bid to gain further insights into the corrosion inhibition process. Spectroscopic methods such as Fourier transform infrared (FTIR) spectroscopy, energy dispersive X-ray spectroscopy (EDS), ultraviolet-visible spectroscopy (UV-vis), and Raman spectroscopy are widely used to examine the interaction of inhibitor molecules with the industrial metal. Surface analytical studies, which provide information on the nature of the surface with and without the industrial inhibitors, have been conducted using microscopic techniques such as scanning electron microscopy (SEM), atomic force microscopy (AFM) and laser scanning confocal microscopy (LSCM). Current advancements in computer systems have provided a platform to investigate the mechanisms of action of industrial corrosion inhibitors. Nowadays, molecular modeling is being carried out using density functional theory (DFT) to identify probable

electronic and structural attributes responsible for inhibition and to provide information on the interactions of inhibitor molecules with metallic substrate. In addition, computational algorithms such as Monte Carlo simulation (MCS) and molecular dynamic simulations (MDS) have been put to use in corrosion inhibition systems [23, 24].

Generally, corrosion inhibition has been inferred to depend on the capability of the inhibiting molecules to adhere on the metal substrate using their multiple (double/triple) bonds, or their heteroatoms. The adsorption capabilities are influenced by the charge and the nature of the metal under study, the type of corrosive solution, and chemical structure of the industrial inhibitor (aromaticity, functional groups, possible steric effects, etc.). In most cases, the mode of inhibitor adsorption has been attributed to the electrostatic force of attraction on the charged inhibitor compounds or the interaction of the lone pair electrons with the empty d-orbital of the metal under consideration (coordinate covalent bonding). The former is referred to as physical adsorption, and the latter is recognized as chemical adsorption [25, 26]. Industrial inhibitors adsorb on metallic surfaces via electrostatic interactions, coordinate covalent bonding, or both.

13.3 Degradation of industrial metal in corrosive solutions

13.3.1 Corrosion mechanism of industrial metals

Industrial metals comprising ferrous and nonferrous metals are known to have broad applications in contemporary times. From basic use as home utensils such as spoons and pots to more complex industrial machines, metals continue to be invaluable in all aspects of human life. Ferrous metals are renowned for their numerous applications in the construction, transport, oil, and gas industries. Similarly, aluminum, copper, zinc, and silver are recognized for their importance in the construction, transport, chemical, food packaging, and electronics industries. Figure 13.4 presents an outline of some common industrial metals and their commercial applications.

Steel is extensively used as construction material for large-scale industrial machinery such as cooling systems, storage tanks, pipelines, reaction vessels, boilers, and heat exchangers. They are choice materials because of their eco-friendliness, recyclability, endearing mechanical properties, durability, relatively low cost, and natural abundance [27, 28]. Various grades of steel are being used in the industry owing to their individual properties. Commonly reported grades of steel in inhibition studies are Q235 steel, N80 steel, and X80 steel. It is a well-known fact that steels degrade in various aggressive solutions.

Copper is an industrial metal widely used in both pure and alloyed form because of its special characteristics such as superior mechanical properties, relatively noble

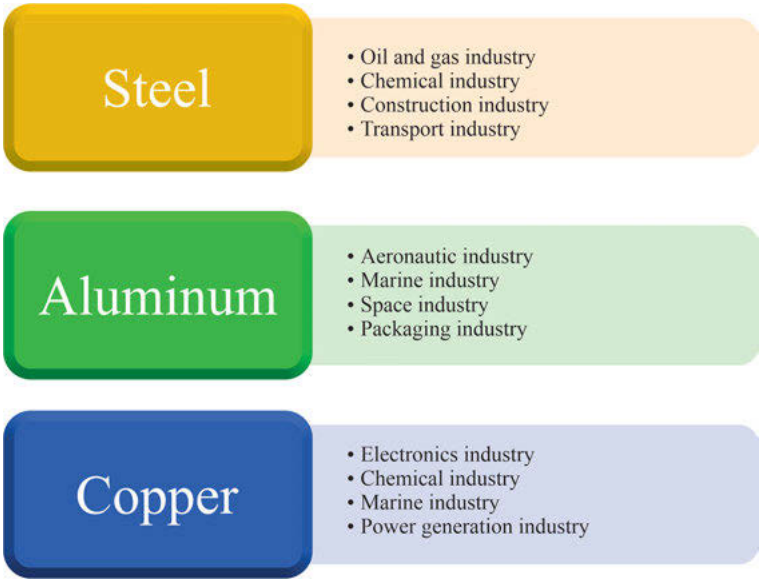

Fig. 13.4: Common industrial metals and their commercial applications.

properties, and high thermal and electrical conductivities. It has proven to be beneficial in chemical, power generation, marine, and electronic industries and is widely used in heating and cooling systems. While copper possesses some corrosion resistance in the atmosphere, it undergoes degradation in strong corrosive solutions. Aluminum is a metal of interest that is extensively studied in corrosion science. It is known to develop a strong passive (oxide) film when exposed to the atmosphere or corrosive solution. However, the passive film gets dissolved in the presence of strong acids and bases, predisposing it to corrosion attack [23].

13.3.2 Commonly encountered corrosive media

Acid solutions have multipurpose applications in commercial industries including acid pickling, oil well acidizing, boiler cleaning, acid descaling, and etching. Metallic materials accumulate rusts, impurities, and carbonates in the exterior part due to extended usage in industry. These are easily removable using strong acids. In the process of eliminating the scales, these acids contribute to the corrosion of the steel structures. The two commonly used acids for removing accumulated rusts and scales are HCl and H_2SO_4. Others include HF, H_3PO_4, formic, and acetic acids. These acids are sometimes used as mixtures in the industries. HCl (5–28% concentration) is a well-reported solution used in acidization, because it forms soluble metal chlorides in aqueous solutions. The impact of solution temperature on industrial metal corrosion

is also noteworthy. During pickling operations, HCl (15–22% concentration) is regarded as the most cost-effective acid for a pickling period of 7–10 min at a temperature range of 30–40 °C. In addition, 5–25% concentration of H_2SO_4 at a temperature of 60–100 °C is considered an appropriate selection for pickling of steel alloys [11, 29]. Owing to the aforementioned, most reported studies on industrial corrosion mitigation focus on HCl and H_2SO_4 solutions.

Several reports have studied the corrosion behavior of different metal substrates in neutral electrolytes (3% and 3.5% NaCl solutions) [30]. Besides, CO_2, which is normally present in crude oil and natural gases leading to failure of pipelines and downhole tubing, has been investigated. CO_2 corrosion, widely known as sweet corrosion, is a common problem in petroleum, oil, and gas industries. The other common type is sour corrosion, which occurs in the presence of H_2S [31]. As a result, most reported inhibitory investigations of nanostructured carbon allotropes targeted at the petrochemical, oil, and gas industries address corrosion in CO_2-saturated NaCl solutions.

13.4 Application of nanostructured carbon allotropes as ideal industrial inhibitors in different corrosive media

13.4.1 Common nanostructured carbon allotropes used as corrosion inhibitors

Modern scholarship has discovered new and powerful carbon allotropes beyond graphite and diamond. Presently, more than ten novel carbon allotropes have been discovered and researched. Common ones among them are the low-dimensional nanostructures that have gained much interest over the past few decades [21, 32]. Methods for fabricating nanostructured carbon allotropes are broadly divided into bottom-up and top-down techniques. Common bottom-up methods include hydrothermal, chemical vapor deposition, sol gel, and green synthesis, while top-down methods include sputtering, thermal evaporation, and laser ablation techniques. Each method is known to have its merits and demerits [33].

Carbon dots (CDs) or carbon quantum dots (CQDs) are unique zero-dimensional carbon nanostructures that have shown excellent and impressive properties in various industrial applications. They are recognized for their fascinating characteristics such as abundant carbon presence, easy preparation, cheap starting materials, high solubility, eco-friendliness, bright photoluminescence, and excellent biodegradability. They have become very useful materials in the fields of biomedicine, chemical sensors, catalysis, as well as corrosion inhibition. Studies show that doping of CDs with heteroatoms such as P, N, and S generally improve their adsorption capabilities

and, hence, their inhibition performances [34, 35]. These heteroatoms possess strong adsorption capabilities that significantly enhance the inhibitive effect of CDs. Graphene is a well-researched nanostructured carbon allotrope because of its attractive properties. Despite its numerous attractive properties, graphene has scarcely been reported as chemical inhibitors because of its non-lipophilic and non-hydrophilic nature. However, graphene oxide (GO) and reduced graphene oxide (rGO), along with their functionalized forms have been assessed as industrial inhibitors due to the presence of carbonyl, epoxides, hydroxyl, and carboxyl groups, which aids their solubility [36]. GO are two-dimensional nanostructures, which are formed from the oxidation of graphene. GO contains functional groups that significantly improve their characteristics resulting in their high chemical reactivity, high solubility, and adjustable band gap [37]. Carbon nanotubes (CNTs) belong to a special class of low-dimensional nanostructured carbon allotropes, which are renowned for their specific physical and electrical characteristics. Only few studies have reported functionalized CNTs (FCNTs) as corrosion inhibitors because they are generally insoluble in aqueous phase. This has promoted their use in anticorrosive coating formulations. In some recent studies, CNTs have been reported to serve as nanofillers to reinforce the corrosion resistance of nanocomposite coatings [38–40]. Until now, CO_2 corrosion has been controlled by the injection of phosphates, thiourea, imidazolines, amides, and Schiff bases. With the imposition of stringent legislation in favor of sustainability and environmental safety, the use of organic inhibitors will be substituted by nanostructured carbon allotropes.

13.4.2 Inhibition of metallic corrosion in HCl solution using nanostructured carbon allotropes

This section overviews investigations on the corrosion inhibition of nanostructured carbon allotropes in HCl environments. Most of the inhibitive assessments carried out using nanostructured carbon allotropes are often conducted in HCl solutions. Ye et al. [41] used N-doped carbon dots (N-CDs) prepared from reacting L-histidine (L-His) and citric acid (CA) as an inhibitor for mitigating Q235 steel dissolution in a 0.1 M HCl medium. Corrosion rate, Tafel, AC impedance, corrosion morphology, and theoretical analyses were employed in studying the inhibitive performance of the N-CDs. The variations of corrosion rate and the corrosion current density (i_{corr}) significantly reduced in the presence of N-CDs, when compared to the L-His and CA. The reduced variation was correlated to the formation of a defensive layer at the steel/acid interface. PDP method gave a maximum protection efficiency of 96% with 200 mg/L, thus establishing that N-CDs were potent in reducing the rate of corrosion significantly. In a more aggressive medium of 1 M HCl, the authors reported a reduced inhibition efficiency (IE) of 94% with 200 mg/L for functionalized CDs (FCDs) prepared from citric acid carbon dots (CA-CDs) and imidazole [42]. Another investigative study conducted by Ye's research group on three specimens of N-doped

citric acid-based CDs using SVET, EIS, PDP, and WL revealed the inhibition potency of the CDs in 1 M HCl. Prior to corrosion studies, the chemical composition of the synthesized CDs was firstly examined using several instruments including scanning probe microscopy (SPM), transmission electron microscopy (TEM), and X-ray photoelectron spectroscopy (XPS). TEM analysis revealed that the three CDs specimens had a size range of 2–15 nm, and SPM images showed the relative uniform dispersion of the three specimens. The electrochemical investigations signified that CDs2 had the best inhibitive effect on Q235 carbon steel (IE = 96.96% at 200 mg/L) and successfully hindered the corrosion pits. This is portrayed in the mechanism of action presented in Fig. 13.5. SEM and AFM were employed to validate the inhibition effect of CDs. The authors discovered that inhibition was due to physical adsorption of graphitic N atoms present in CDs on steel substrate and coordination bonding of pyridine and pyrrole-like N atoms and the steel sample [43].

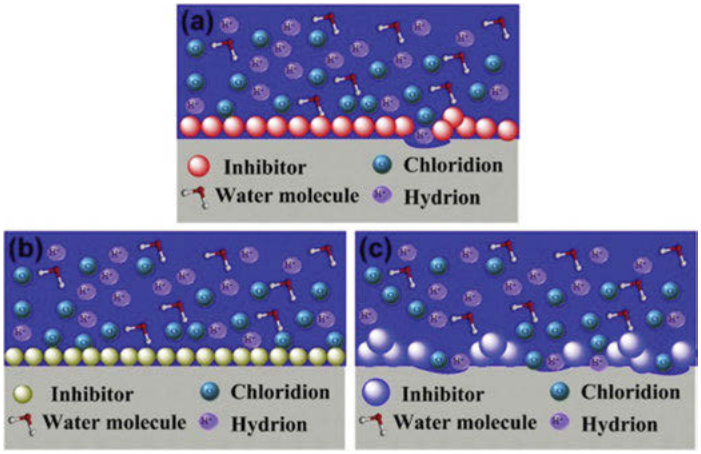

Fig. 13.5: Mechanism of action of (a) CDs1 (b) CDs2 (c) CDs3 on Q235 steel in HCl [43].

An investigative report by Cui et al. [44] revealed that NCDs fabricated from dopamine can suppress Q235 carbon steel degradation in 1 M HCl to the tune of 96.10%, after the inclusion of 400 ppm NCDs at ambient temperature. According to gravimetric analysis, NCDs can impede corrosion at prolonged exposure time and high temperatures. A cursory look at the impedance plots (Fig. 13.6a) revealed that the inclusion of various concentrations of NCDs into the electrolytic system increased the diameter of the semicircle. The value of the charge transfer resistance (R_{ct}) in the blank solution (13.52 Ω cm^2) increased to 221.90 Ω cm^2, with the inclusion of 400 ppm NCDs. In addition, higher and broader peaks were observed in the Bode diagrams as various concentrations of NCDs were added (Fig. 13.6b). These observations indicate a strong adhesion of NCDs to the steel specimen. Furthermore, the

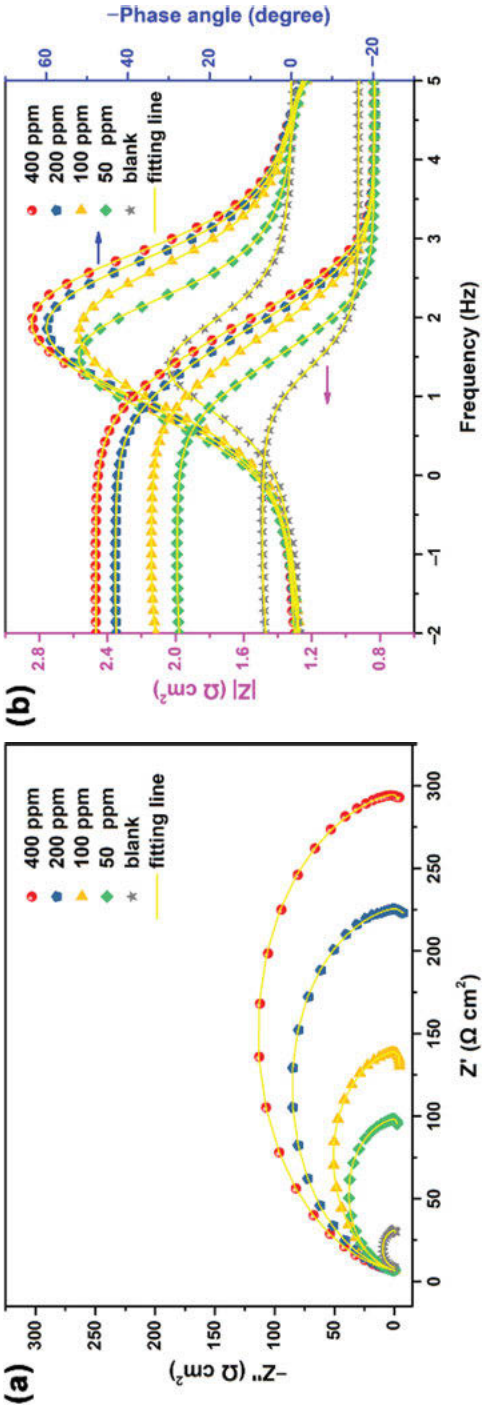

Fig. 13.6: (a) EIS plots and (b) Bode diagrams for Q235 carbon steel degradation in 1 M HCl solution, with and without various amounts of NCDs [44].

authors employed SEM and LSCM to study the inhibitive effect of NCDs and found out that the inclusion of 400 ppm NCDs to the electrolytic system after 60 h exposure drastically reduced surface damage and roughness (Fig. 13.7).

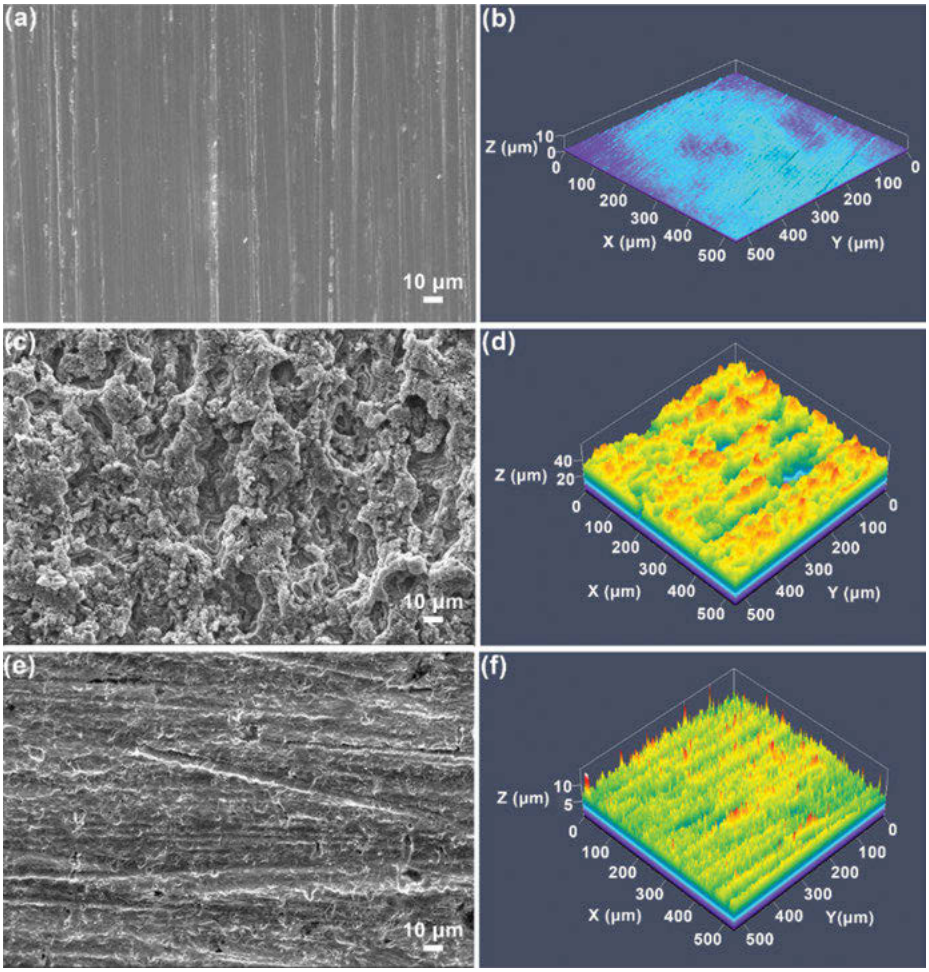

Fig. 13.7: SEM and LSCM diagrams of Q235 carbon steel degradation before and after 60 h immersion in 1 M HCl, without and with 400 ppm NCDs, (a, b) plain steel, (c, d) in blank medium, (e, f) after the inclusion of 400 ppm NCDs [44].

According to Luo et al. [45], varying reaction parameters such as operating temperature and time have a substantial impact on the anticorrosive ability of N-CDs for Q235 steel degradation in 1 mol/L HCl medium. This viewpoint was established by varying reaction temperature (160, 180 and 200 °C) and reaction time (0.5, 1 and 2 h) in studying the inhibition potential of N-CDs fabricated from tryptophan. N-CDs

attained optimum protection performance of 94% at 180 °C and 1 h with 200 mg/L. The surface roughness of the metal specimen in the inhibitor and in the blank solution was examined by SEM, LSCM and XPS, and the results obtained agreed with the experimental electrochemical analyses. Table 13.1 presents other recent inhibition studies conducted in 1 M HCl medium using CDs prepared from eco-friendly sources for Q235 steel degradation. At a concentration range of 100–400 mg/L, the different authors obtained inhibition performances of 94–99%. According to the various reports, all the CDs acted as mixed-type additives and their mechanism of action on steel substrate complied with the Langmuir adsorption model.

To enhance the production of crude oil, oil well acidization is often carried out in petroleum industries by passing 15% HCl through steel cylinders to remove scales and deposits in the flow channels. Modeling this highly acidic environment, Saraswat et al. examined the inhibition behavior of eco-friendly N-CDs and N,S-CDs for the dissolution of mild steel [27, 46, 47]. The authors reported maximum IE ranging from 90–99% at very low concentrations, thus showing the excellent performance of CDs for industrial operations. Studies showing the excellent inhibitive characteristics of CDs for X80 steel in 0.1 M HCl [48] and N80 steel in 1 M HCl [49] have been documented.

Tab. 13.1: Inhibition performances of carbon dots for Q235 steel degradation in 1 M HCl.

No	Carbon dots	Precursors	Conc.	Highest IE	Refs
1.	N-doped carbon dots	4-aminosalicyclic acid (ASA)	100 mg/L	96.00%	[50]
2.	N-doped carbon dots	Natural citric acid	200 mg/L	97.43%	[51]
3.	N-doped carbon dots	p-phenylenediamine (p-PD) and o-phenylenediamine (o-PD)	200 mg/L	94.00%	[52]
4.	N-doped carbon dots	Methacrylic acid and ethyl (methyl)amine	200 mg/L	93.93%	[53]
5.	N-doped carbon dots	Methacrylic acid and n-butylamine	200 mg/L	99.35%	[54]
6.	N-doped carbon quantum dots	Folic acid and o-phenylenediamine	150 mg/L	95.40%	[55]
7.	Ce@ N-doped carbon dots	Cerium nitrate hexahydrate and citric acid	200 mg/L	96.40%	[56]
8.	Imidazole ionic liquid modified carbon dots	Citric acid and imidazole ionic liquid	200 mg/L	92.60%	[57]

Chen et al. [58] examined the potency of graphene oxide quantum dots (GOQDs) to suppress Q235 steel deterioration in 1 M HCl using mass loss and electrochemical

assessments. Chemical analysis of the prepared GOQDs via FTIR and XPS revealed the presence of aldehyde, carboxyl, and hydroxyl groups, which are reputed to form adsorption film on metal specimens. GOQDs impeded both anodic and cathodic half-reactions with a pronounced anodic effect. Information from the AFM images revealed that the adhesion of GOQDs on the steel substrate occasioned the reduction of average roughness from 12.0 nm in HCl to 8.6 nm in the presence of GOQDs. Furthermore, DFT studies revealed that GOQDs acted as the electron donor to the steel substrate.

Shirazi prepared a new type of nanocomposite from poly (o-anthranilic acid) (PAA) to mitigate the degradation of stainless steel in 2 M HCl. Graphene oxide (GO) and functionalized multi-walled carbon nanotubes (f-MWCNT), which have been well reported for their special characteristics were incorporated into the fabricated PAA to augment the protection abilities of PAA. The successful synthesis of the new nanocomposite was established, using different modern analytical instruments. From electrochemical studies, an optimum 70 ppm PAA/GO/f-MCNT yielded an excellent IE of 91.87%, which outperformed PAA, PAA/f-MWCNT 4%, and PAA/GO 5% alone. The adsorption of the nanocomposite was best explained using the Langmuir adsorption model [59].

To restrain the deterioration of steel in oil-well acidizing conditions, Ansari utilized bis(2-aminoethyl)amine-modified graphene oxide (B2AA) to functionalize GO. Analytical methods such as SEM, TEM, and FTIR were employed to confirm the fabricated B2AA-GO. After successful confirmation, the nanostructured carbon allotrope was applied to serve as a protective blanket over carbon steel surface in 15%

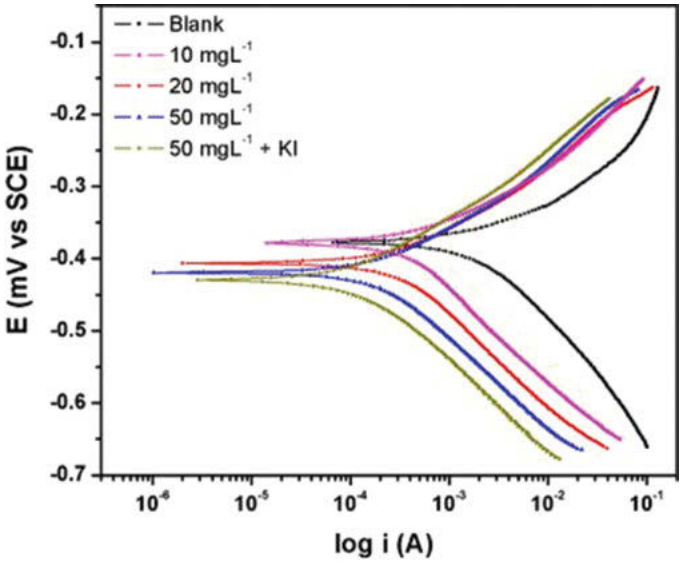

Fig. 13.8: Tafel curves for the carbon steel degradation with the introduction and exclusion of B2AA-GO and with 5 mM KI in HCl [63].

HCl. The study achieved its aim to the tune of 90.27% at 65 °C. Synergistic studies were further carried out using iodide ions, and the IE was significantly enhanced to 96.77%. The Tafel curves (Fig. 13.8) showed inhibition occurred at both anode and cathode regions, with a cathodic prevalence. In another study, GO modified with polyethyleneimine (PEI) was documented as an excellent additive to suppress oil well acidization. The study reported a protection efficiency of 88.24% with 50 mg/L PEI-GO and a further improvement of 95.77%, with the addition of 5 mM KI [60]. The computational study revealed that PEI-GO acts in both the protonated and neutral forms. On their protection mechanisms, the neutral PEI-GO molecules chemisorbed by sharing of their lone pairs of electrons, while the protonated molecules physisorbed via electrostatic interactions. To protect aluminum from corrosive ions in HCl, ball-type metallophthalocyanines (MPcs) were combined with reduced GO nanosheets (rGONS). Electrochemical study conducted on the inhibitors achieved an exceptional inhibition performance above 97% surface morphology at the maximum studied concentration. The study was supported by computational analyses [61]. Another study developed nano inhibitor of rGO and mixed metal oxide nanocomposite for the degradation of mild steel in 0.1 M HCl and obtained IE of 80% [62]. Table 13.2 displays other functionalized graphene oxides that have been assessed for their surface protection of mild steel in 1 M HCl.

Tab. 13.2: Inhibition performances of functionalized graphene oxide for mild steel in 1 M HCl.

No	Functionalized graphene	Optimum conc.	Maximum IE	Refs
1.	Diazo pyridine functionalized graphene oxide (DAZP-GO)	25 ppm	96.73%	[64]
2.	Diamino pyridine functionalized graphene oxide (DAMP-GO)	25 ppm	95.08%	[64]
3.	Aminoazobenzene functionalized graphene oxide (AAB-GO)	25 ppm	94.65%	[65]
4.	Diaminobenzene functionalized graphene oxide (DAB-GO)	25 ppm	92.05%	[65]
5.	p-aminophenol functionalized graphene oxide (PAP-GO)	25 ppm	92.86%	[36]
6.	Diethylenetriamine functionalized graphene oxide (DETA-GO)	25 ppm	92.67%	[66]

Tab. 13.2 (continued)

No	Functionalized graphene	Optimum conc.	Maximum IE	Refs
7.	Sodium dodecyl sulfate modified graphene oxide (GO-SDS)	200 ppm	95.50%	[67]
8.	Sodium propyl sulfate modified graphene oxide (GO-SPS)	200 ppm	88.00%	[67]

In an interesting study, Yousefi et al. showed that CNTs functionalized with two, biodegradable Gemini surfactants, namely dodecyl betainate gemini (BT) and dodecyl ester quat gemini (ET) have the potency to inhibit steel degradation in 2 M HCl solution. The study discovered that better dispersion of the surfactant at higher concentrations resulted in stronger adsorption on the steel substrate. The maximum IE of 93% was obtained for BT with 2.5 mM. The study was further supported with corrosion morphology tests and DFT calculations [68].

13.4.3 Inhibition of metallic corrosion in H_2SO_4 solution using nanostructured carbon allotropes

A few conducted studies have revealed the ability of CDs to retard industrial corrosion processes in the presence of sulfuric acid solutions. Results obtained from these studies generally indicate that CDs satisfactorily provide surface protection to the different studied metal, to the tune of 91.1–99.8%, at a minute concentration range of 30–200 mg/L. The inhibition mechanisms were found to align with the Langmuir adsorption model in all the studied cases.

An intent to gain adequate understanding of the mechanistic action of N-doped CDs on copper substrate propelled Qiang et al. [69] to synthesize and characterize novel and eco-friendly N-CDs. Examination of the anticorrosive ability of the prepared CDs for copper in 0.5 M H_2SO_4 using Tafel analysis showed that IE of 91.1% was attained at a minute dosage of 50 mg/L. The study obtained a ΔG_{ads} ranging from −33 to −34 kJ/mol, which indicated that adsorption occurred via mixed adsorption mechanism with a predominant chemisorption. A study by Zhang et al. [70] assessed the suppressive ability of functionalized N-CDs prepared from L-serine and citric acid for copper degradation in H_2SO_4. The authors reported an IE of 98.5% after 24 h exposure. Impedance studies suggest the adherence of N-CDs on the active sites of the copper substrate, which restricts the transport of aggressive species.

Cao et al. [71] provided an interpretation for the inhibition mechanism of eco-friendly N-doped functionalized CDs (N-CDs) for the degradation of carbon steel in

0.5 M H_2SO_4. The efficiency of N-CDs was credited to the successful retardation of iron dissolution and hydrogen evolution at the anode and cathode, respectively, sequel to the addition of 10–30 mg/L N-CDs. The incremental introduction of N-CDs into the acidic electrolyte produced a pronounced reduction in the i_{corr}. At 298 K, the team reported an IE of 97.8% with 30 mg/L. Results from all the study methods concurred. The adhesion of N-CDs molecules on the steel sample was via electrostatic interaction and coordinate covalent bonding. In addition, it was reported that the net positive charge on the steel surface in sulfuric acid adsorbs the SO_4^{2-} and creates an excess negative charge, which favors cation adsorption. The team conclusively attributed the efficiency and excellent adsorption of N-CDs to the presence of multiple functional groups and their carbon-rich structure. The corrosion protection mechanism of N-CDs has also been established by a recent study conducted by Xu et al. [72], using techniques such as Raman spectroscopy, AFM, FTIR, XPS, UV, SEM, and EDS. The authors opined that the results from these techniques reveal that N-CDs chelate with copper ion in solution to create a defensive film on the metal substrate, which is composed of the aggregation of the N-CDs.

In a study conducted in 2021, novel N-doped carbon quantum dots (N-CQDs) were applied as powerful inhibiting materials for Q235 steel degradation in sulfuric acid solution for the first time [73]. Amino guanidine hydrochloride (AG) and citric acid (CA) were used as raw materials in the hydrothermal preparation of the N-CQDs. The synthetic process was modified to simplify the purification process and save processing time as well as ramp up the functional group density of CDs. High resolution TEM (HRTEM) revealed that the CQDs particle size was 2.5 ± 0.8 nm with a spherical shape. Successful formation of N-CQDs was confirmed by the presence of C-N, C=N, and C=C bonds from the FTIR analysis. Also, an absorption peak around 330 nm from UV-vis analysis and chemical composition report of 19.24% at % N, 58.53 at% C and 22.22% at% O from XPS spectrum corroborated successful fabrication. Corrosion studies were conducted using WL, AC impedance test, Tafel analysis, and surface analyses (AFM, XPS and SEM), coupled with quantum chemical studies. The authors reported that a maximum protection performance of 95.30% was recorded from mass loss technique, with 200 mg/L after 60 h exposure time. The precursors (AG and CA) were also reported to have an intangible effect on the protection performance of the CQDs, as depicted in Tab. 13.3. Inferences from the obtained DFT quantum parameters confirmed that N-doped CQDs donated more electrons than CQDs on account of the N-doping, thereby leading to their increased inhibitive effect. The presented HOMO-LUMO distribution showed uniform and wide distribution of the frontier orbitals on the entire N-CQDs molecules, as compared to the CQDs, as well as the planarity of N-CQDs (Fig. 13.9).

Co-doping has the potential to enhance the inhibitive effect of CDs in sulfuric medium. In a recent study, Zhang et al. demonstrated that co-doped CDs with higher molecular size are better inhibiting compounds than pure or doped CDs. The team prepared and performed an electrochemical study on the corrosion protection of copper

Tab. 13.3: Anticorrosion performance of different additives on Q235 steel surface in 0.5 M H_2SO_4 corrosive electrolyte solution at 298 K, after 24 h exposure period [73].

Inhibitors	Weight loss (mg)	Corrosion rate ($mg.cm^{-2}h^{-1}$)	IE
Blank	385	61.46	–
GA	280	44.70	27.3
CA	351	56.03	8.8
N-CQDs	30	4.79	92.2

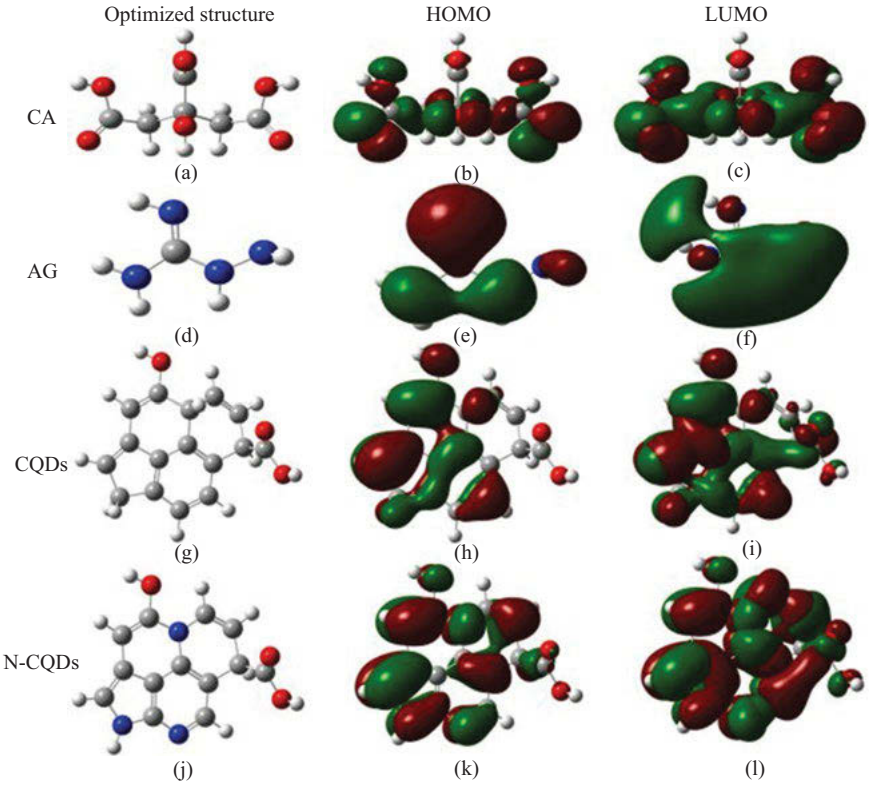

Fig. 13.9: Geometrically optimized molecular structures and HOMO/LUMO distribution of N-CQDs [73].

in sulfuric acid using CDs containing 19% S and 17% N, which yielded 99.83%, with as little as 50 mg/L [74]. The presence of N,S-CDs in the corrosive solution suppressed electrochemical reactions at both anodic and cathodic regions, with a predominant suppression observed at the cathodic region. Authors speculate that N,S-CDs protect

the metal substrate by substituting the water molecules at the copper/solution interface, thereby retarding electron transport. The results obtained from the study were supported by surface analytical techniques.

The corrosion of niobium (Nb) and tantalum (Ta) metals is scarcely reported in literature. Mehmeti and Podvorica explored the corrosion behavior of these metals in the presence of carboxylated graphene oxide (GO-COOH)/0.1 M H_2SO_4 electrolyte using OCP, Tafel, DFT, and MDS techniques. PDP plots showed a predominant anodic inhibition in both metals and a decrease in i_{corr}, as a result of the formation of adherence layers by GO-COOH. Authors reported an IE of 70.22 and 64.07% for Nb and Ta in GO-COOH, respectively. Interaction of Nb and Ta surfaces with GO-COOH was extensively studied by MDS and MCS and was found to agree with the experimental evaluation.

13.4.4 Inhibition of metallic corrosion in (CO_2-saturated) NaCl solution using nanostructured carbon allotropes

Nanostructured carbon allotropes have been reported as excellent chemical additives in mitigating metallic deterioration in NaCl and CO_2-saturated NaCl solutions by several authors. For instance, Zeng et al. [75] fabricated functionalized CDs (Me-CDs) from modified melamine via hydrothermal method. The chemical analyses of the synthesized structures were performed using FTIR, TEM, AFM, and XPS. Five concentrations (50–200 mg/L) of Me-CDs were prepared in NaCl solution, and their pH and conductivity value was measured. The adsorption capabilities of the various prepared amounts of Me-CDs for carbon steel corrosion in 3.5 wt% NaCl electrolyte were investigated using OCP, AC impedance, and Tafel analyses. Protection capacities of 92.91, 92.36, and 93.10% were achieved from WL, AC impedance, and Tafel analyses, respectively. Successful reaction between the amidogen of melamine and the carboxyl of CDs to form Me-CDs was confirmed by the absorption peak at 16,341 cm^{-1}, which is credited to the N-C = O bond. Diameter size of 10–30 nm and uniformly dispersed spherical nanomaterials were obtained from HRTEM. SEM images revealed a smoother steel surface after the inclusion of Me-CDs, compared to the steel immersed in NaCl medium. The observed smoothness was credited to the coverage of the steel substrate by the molecules of Me-CDs. Similarly, hydrothermally prepared, glucose-based FCDs were employed by Wan et al. [75] to suppress copper degradation in 3.5% NaCl electrolyte using SVET, EIS, and PDP techniques. With 70 ppm, FCDs suppressed both half-cell reactions and complied with the Langmuir adsorption model. The study recorded an optimal IE of 88.15%, which was credited to the coverage of adherence film on the copper substrate.

Non-toxic functionalized N-CDs prepared via microwave method were utilized to suppress the degradation of N80 steel exposed to CO_2-saturated 3.5 wt% NaCl. The chemical structures of the prepared N-CDs were confirmed using FTIR, XRD, and UV-vis. Further characterization was done using XPS and TEM. The N-CDs were

reported to be spherically shaped and uniformly dispersed in solution, with a particle size range of 10–24 nm. Tafel analysis revealed that as little as 50 mg/L inhibited degradation to the tune of 83.5%. Peak inhibition performance of 95.4% was attained with 200 mg/L in NaCl medium. The inhibiting material acted primarily as an anodic inhibitor. The protective effect of N-CDs was further established by the reduction observed in the degree of surface coarseness of the steel exposed to the corrosive electrolyte, in the presence of the N-CDs [76].

Cen et al. [77] assessed the anticorrosive effect of N,S co-doped CDs for carbon steel degradation in CO_2-saturated NaCl medium. As expected, increase in the inhibitor dosage reduced weight loss and corrosion rate at 50 °C, until the peak IE of 93.0% was obtained with 50 mg/L. The presence of N, S, O, C, and Fe on the steel surface as seen in the full-range XPS spectrum of the steel surface indicates the adsorption of the co-doped CDs (Fig. 13.10). Measuring the water contact angle provides information on the hydrophobicity and inhibition performance of the studied inhibitors, besides the wettability of the surface. In this study, inclusion of N,S-CDs increased the water contact angle from 43° to 92°, which was higher than the contact angle of the precursors, 4-aminosalicylicacid (26°), and thiourea (61°) under the same testing conditions. Investigation into the mechanism of action of N,S-CDs revealed that the nanoparticles and functional groups present in N,S-CDs can form hydrophobic covering and adsorb onto the substrate by chemical adsorption, respectively.

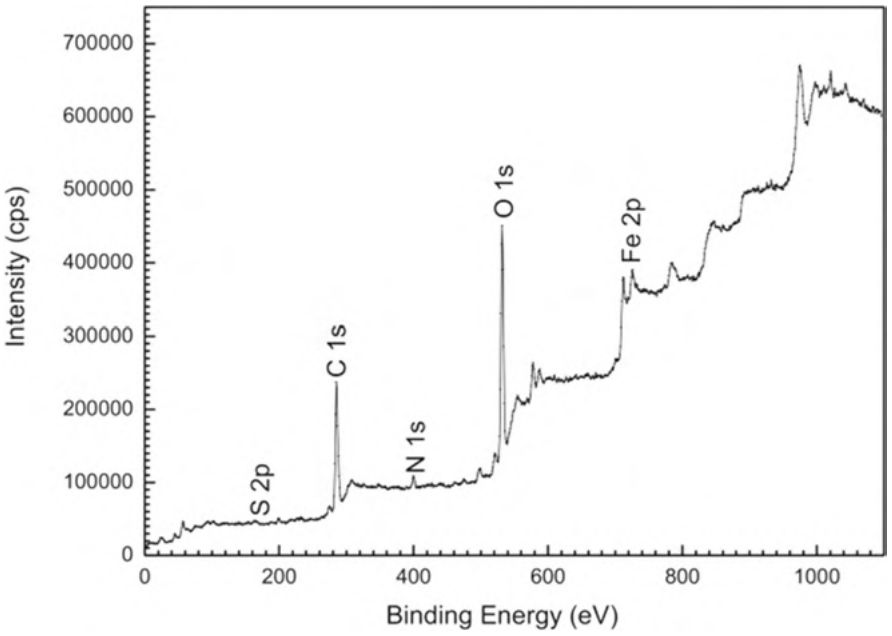

Fig. 13.10: Full range XPS image of carbon steel surface in the presence of 50 mg/L N,S-CDs [77].

Functionalized GO (FGO) was fabricated with 3-amino-1,2,4-triazole (ATA) using cross-linking method and analyzed by XPS, FTIR, XRD, EDS, Raman spectroscopy, and thermogravimetric analysis (TGA). Morphological analyses of the synthesized FGO were confirmed by SEM and TEM. Using WL, electrochemical, and surface analytical techniques, Cen and Chen [37] investigated the inhibitive effect of FGO in CO_2-saturated 3.5 wt% NaCl medium for N80 steel degradation. From gravimetric analysis, a peak IE of 83.4% was achieved with a minute concentration of 20 mg/L FGO in the studied electrolyte. The drastic increment of the R_{ct} from 78.8 to 362.4 Ω cm^2 after the addition of 20 mg/L at 303 K indicated effective film formation of FGO to protect N80 steel. AFM tests indicated the thickness of the protective film was between 60–100 nm. Furthermore, inhibition action was attributed to the hydrophobic covering formed by the lamellar nanoparticles present in FGO.

In another study, Cen et al. [78] established the inhibitory effect of FCNTs for carbon steel degradation in CO_2-saturated 3.5 wt% NaCl medium. CNTs were chemically functionalized using the hydrothermal method by adding 0.2 g uniformly dispersed CNTs to 2 g 2-aminopyridine (AP) by magnetic stirring. The obtained mixture was subjected to heating for 9 h at 180 °C, after which natural cooling and filtration were done. Filtrate was purified, and FCNTs were collected and freeze-dried under vacuum. Figure 13.11 presents the schematic diagram of the synthetic procedure. WL experiments showed that a little dosage of 100 mg/L achieved a maximum IE of 89.2%. Comparatively, FCNTs (78.9%) inhibited corrosion better than CNTs (13.9%) and AP (70.4%) with 60 mg/L at 298 K. Quantum chemical calculations and MDS were further employed to study the inhibition mechanism of FCNTs.

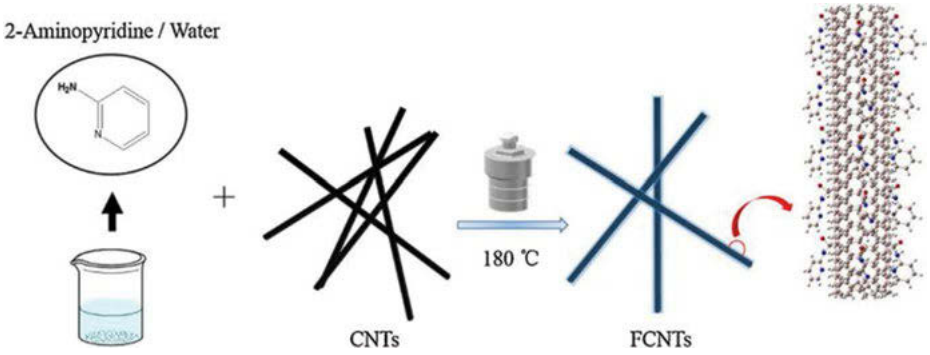

Fig. 13.11: Schematic diagram of FCNTs synthesis [78].

13.5 Limitations and challenges of nanostructured carbon allotropes as industrial inhibitors

It is true that much progress has been recorded in less than a decade on the development of nanostructured carbon allotropes as ideal substitutes for traditional inhibitors. However, certain pertinent problems need to be outlined and addressed to effectively combat corrosion, using nanostructured carbon allotropes. To a large extent, most of the studies on the inhibition of industrial metals by nanostructured carbon allotropes are still at the laboratory scale. Efforts should be geared towards large-scale applications of nanostructured carbon allotropes to replace the conventional inhibitors that have been certified unsafe for the environment. Besides, there is only a superficial understanding of the process by which nanostructured carbon allotropes inhibit metallic corrosion in various corrosive solutions. There is need for further robust study to unravel the mechanistic action by which these nanostructures protect metals. This knowledge will furnish the scientific community and the industry with information necessary in taking key decisions in the field of corrosion inhibition [25]. Furthermore, most inhibition studies of nanostructured carbon nano allotropes are focused on steel corrosion in HCl. It is understandable that steel is a preferred industrial metal, and HCl is about the most commonly used industrial acid; hence, the several reports focused in the direction. Nonetheless, investigations into the corrosion of other important industrial metals such as aluminum and zinc in the presence of other corrosive media are essential.

13.6 Conclusions and future perspectives

In the present chapter, a panoramic view of chemical additives utilized in commercial industries for suppressing corrosion processes in their machinery has been provided. The degradation of industrial metals such as steel, copper, and aluminum were examined in common corrosive solutions. The mechanisms of action were briefly discussed in view of the different adopted electrochemical, spectroscopic, microscopic, and computational methods. The uniqueness of nanostructured carbon allotropes as green industrial inhibitors in modern corrosion systems was emphasized. Case studies on the inhibition of functionalized and eco-friendly nano allotropes were discussed. Functionalized carbon dots, graphene oxide, and carbon nanotubes were found to effectively suppress metallic degradation in different electrolytic media. The limitations and challenges of using nanostructured carbon allotropes as industrial inhibitors are also highlighted. Based on the foregoing discussion in this chapter, it is believed that further advancements in the research on nanostructured carbon allotropes will yield astounding industrial inhibitors that will outperform most inorganic and organic inhibitors currently in use. The intense search for effective, sustainable, and inexpensive inhibiting

materials will hopefully lead to a strong consideration of nanostructured carbon allotropes as inhibitors of industrial metals, since they possess desirable characteristics needed to position them as future industrial corrosion inhibitors.

References

[1] Hossain, N.; Asaduzzaman Chowdhury, M.; Kchaou, M. An overview of green corrosion inhibitors for sustainable and environment friendly industrial development. J. Adhes. Sci. Technol. 2021, 35(7), 673–690.
[2] Palanisamy, G. Corrosion inhibitors, Intechopen, 2019.
[3] Pikaar, I.; Sharma, K.R.; Hu, S.; Gernjak, W.; Keller, J.; Yuan, Z. Reducing sewer corrosion through integrated urban water management. Science. 2014, 345(6198), 812–814.
[4] Quadri, T.W.; Olasunkanmi, L.O.; Fayemi, O.E.; Ebenso, E.E. Nanomaterials and nanocomposites as corrosion inhibitors. In: Sustainable corrosion inhibitors II: Synthesis, design, and practical applications, ACS Publications, 2021, 187–217.
[5] Haldhar, R.; Kim, S.-C.; Berdimurodov, E.; Verma, D.K.; Hussain, C.M. Corrosion inhibitors: Industrial applications and commercialization. In: Sustainable corrosion inhibitors II: Synthesis, design, and practical applications, ACS Publications, 2021, 219–235.
[6] Panchal, J.; Shah, D.; Patel, R.; Shah, S.; Prajapati, M.; Shah, M. Comprehensive review and critical data analysis on corrosion and emphasizing on green eco-friendly corrosion inhibitors for oil and gas industries. J. Bio- Tribo-Corros. 2021, 7(3), 1–29.
[7] Quadri, T.W.; Olasunkanmi, L.O.; Fayemi, O.E.; Ebenso, E.E. Utilization of ZnO-based materials as anticorrosive agents: A review. In: Inorganic anticorrosive materials, 2022, 161–182.
[8] Serdaroğlu, G.; Kaya, S. Organic and inorganic corrosion inhibitors: A comparison. In: Organic corrosion inhibitors: Synthesis, characterization, mechanism, and applications, 2021, 59–73.
[9] Hughes, A.E.; Mol, J.M.; Zheludkevich, M.L.; Buchheit, R.G. Active protective coatings. Active protective coatings: New-generation coatings for metals, Springer series in materials science, Vol. 233, ISBN 978-94-017-7538-0, Springer Science+ Business Media, Dordrecht, 2016.
[10] Tamalmani, K.; Husin, H. Review on corrosion inhibitors for oil and gas corrosion issues. Appl. Sci. 2020, 10(10), 3389.
[11] Finšgar, M.; Jackson, J. Application of corrosion inhibitors for steels in acidic media for the oil and gas industry: A review. Corros. Sci. 2014, 86, 17–41.
[12] Verma, C.; Quraishi, M. Gum Arabic as an environmentally sustainable polymeric anticorrosive material: Recent progresses and future opportunities. Int. J. Biol. Macromol. 2021.
[13] Verma, C.; Quraishi, M.; Ebenso, E.E.; Hussain, C.M. Recent advancements in corrosion inhibitor systems through carbon allotropes: Past, present, and future. Nano Select. 2021.
[14] Anastas, P.; Eghbali, N. Green chemistry: Principles and practice. Chem. Soc. Rev. 2010, 39(1), 301–312.
[15] Verma, C.; Ebenso, E.E.; Bahadur, I.; Quraishi, M.A. An overview on plant extracts as environmental sustainable and green corrosion inhibitors for metals and alloys in aggressive corrosive media. J. Mol. Liq. 2018, 266, 577–590.

[16] Umoren, S.A.; Solomon, M.M. Protective polymeric films for industrial substrates: A critical review on past and recent applications with conducting polymers and polymer composites/nanocomposites. Prog. Mater. Sci. 2019, 104, 380–450.
[17] Shamnamol, G.; Sreelakshmi, K.; Ajith, G.; Jacob, J.M., editors. Effective utilization of drugs as green corrosion inhibitor–A review. AIP Conference Proceedings, 2020, AIP Publishing LLC.
[18] Verma, C.; Alrefaee, S.H.; Quraishi, M.; Ebenso, E.E.; Hussain, C.M. Recent developments in sustainable corrosion inhibition using ionic liquids: A review. J. Mol. Liq. 2021, 321, 114484.
[19] Umoren, S.A.; Eduok, U.M. Application of carbohydrate polymers as corrosion inhibitors for metal substrates in different media: A review. Carbohydr. Polym. 2016, 140, 314–341.
[20] Liu, Z.; Liang, X.-J. Nano-carbons as theranostics. Theranostics. 2012, 2(3), 235.
[21] Tiwari, S.K.; Kumar, V.; Huczko, A.; Oraon, R.; Adhikari, A.D.; Nayak, G. Magical allotropes of carbon: Prospects and applications. Crit. Rev. Solid State Mater. Sci. 2016, 41(4), 257–317.
[22] Quadri, T.W.; Olasunkanmi, L.O.; Fayemi, O.E.; Solomon, M.M.; Ebenso, E.E. Zinc oxide nanocomposites of selected polymers: Synthesis, characterization, and corrosion inhibition studies on mild steel in HCl solution. ACS Omega. 2017, 2(11), 8421–8437.
[23] Quadri, T.W.; Akpan, E.D.; Olasunkanmi, L.O.; Fayemi, O.E.; Ebenso, E.E. Fundamentals of corrosion chemistry. In: Environmentally sustainable corrosion inhibitors, Elsevier, 2022, 25–45.
[24] Quadri, T.W.; Olasunkanmi, L.O.; Fayemi, O.E.; Akpan, E.D.; Verma, C.; Sherif, E.-S.M., et al. Quantitative structure activity relationship and artificial neural network as vital tools in predicting coordination capabilities of organic compounds with metal surface: A review. Coord. Chem. Rev. 2021, 446, 214101.
[25] Marzorati, S.; Verotta, L.; Trasatti, S.P. Green corrosion inhibitors from natural sources and biomass wastes. Molecules. 2018, 24(1), 48.
[26] Quadri, T.W.; Olasunkanmi, L.O.; Akpan, E.D.; Alfantazi, A.; Obot, I.; Verma, C., et al. Chromeno-carbonitriles as corrosion inhibitors for mild steel in acidic solution: Electrochemical, surface and computational studies. RSC Adv. 2021, 11(4), 2462–2475.
[27] Saraswat, V.; Yadav, M. Carbon dots as green corrosion inhibitor for mild steel in HCl solution. Chem. Select. 2020, 5(25), 7347–7357.
[28] Quadri, T.W.; Olasunkanmi, L.O.; Akpan, E.D.; Ebenso, E.E. Indole and its derivatives as corrosion inhibitors. In: Organic corrosion inhibitors: Synthesis, characterization, mechanism, and applications, 2021, 167–220.
[29] Verma, C.; Quraishi, M.; Ebenso, E. Corrosive electrolytes. Int. J. Corros. Scale Inhibit. 2020, 9(4), 1261–1276.
[30] Aslam, R.; Mobin, M.; Aslam, A.; Zehra, S.; Aslam, J. Corrosion inhibitors for neutral environment. In: Environmentally sustainable corrosion inhibitors, Elsevier, 2022, 147–164.
[31] Verma, C.; Quadri, T.W.; Ebenso, E.E.; Quraishi, M. Polymer nanocomposites as industrially useful corrosion inhibitors: Recent developments. In: Handbook of polymer nanocomposites for industrial applications, 2021, 419–435.
[32] Nasir, S.; Hussein, M.Z.; Zainal, Z.; Yusof, N.A. Carbon-based nanomaterials/allotropes: A glimpse of their synthesis, properties and some applications. Materials. 2018, 11(2), 295.
[33] Abid, N.; Khan, A.M.; Shujait, S.; Chaudhary, K.; Ikram, M.; Imran, M., et al. Synthesis of nanomaterials using various top-down and bottom-up approaches, influencing factors, advantages, and disadvantages: A review. Adv. Colloid Interface Sci. 2021, 102597.
[34] Zhou, Q.; Yuan, G.; Lin, M.; Wang, P.; Li, S.; Tang, J., et al. Large-scale electrochemical fabrication of nitrogen-doped carbon quantum dots and their application as corrosion inhibitor for copper. J. Mater. Sci. 2021, 56(22), 12909–12919.

[35] Verma, C.; Alfantazi, A.; Quraishi, M. Quantum dots as ecofriendly and aqueous phase substitutes of carbon family for traditional corrosion inhibitors: A perspective. J. Mol. Liq. 2021, 343, 117648.
[36] Gupta, R.K.; Malviya, M.; Ansari, K.R.; Lgaz, H.; Chauhan, D.S.; Quraishi, M.A. Functionalized graphene oxide as a new generation corrosion inhibitor for industrial pickling process: DFT and experimental approach. Mater. Chem. Phys. 2019, 236, 121727.
[37] Cen, H.; Chen, Z. Amide functionalized graphene oxide as novel and effective corrosion inhibitor of carbon steel in CO2-saturated NaCl solution. Colloids Surf A Physicochem. Eng. Asp. 2021, 615, 126216.
[38] Deyab, M.; Awadallah, A.E. Advanced anticorrosive coatings based on epoxy/functionalized multiwall carbon nanotubes composites. Prog. Org. Coat. 2020, 139, 105423.
[39] Nayak, S.R.; Mohana, K.N.S.; Hegde, M.B.; Rajitha, K.; Madhusudhana, A.M.; Naik, S.R. Functionalized multi-walled carbon nanotube/polyindole incorporated epoxy: An effective anti-corrosion coating material for mild steel. J. Alloys Compd. 2021, 856, 158057.
[40] Hong, M.-S.; Park, Y.; Kim, T.; Kim, K.; Kim, J.-G. Polydopamine/carbon nanotube nanocomposite coating for corrosion resistance. J. Materiomics 2020, 6(1), 158–166.
[41] Ye, Y.; Zhang, D.; Zou, Y.; Zhao, H.; Chen, H. A feasible method to improve the protection ability of metal by functionalized carbon dots as environment-friendly corrosion inhibitor. J. Clean. Prod. 2020, 264, 121682.
[42] Ye, Y.; Yang, D.; Chen, H. A green and effective corrosion inhibitor of functionalized carbon dots. J. Mater. Sci. Technol. 2019, 35(10), 2243–2253.
[43] Ye, Y.; Yang, D.; Chen, H.; Guo, S.; Yang, Q.; Chen, L., et al. A high-efficiency corrosion inhibitor of N-doped citric acid-based carbon dots for mild steel in hydrochloric acid environment. J. Hazard. Mater. 2020, 381, 121019.
[44] Cui, M.; Yu, Y.; Zheng, Y. Effective corrosion inhibition of carbon steel in hydrochloric acid by dopamine-produced carbon dots. Polymers. 2021, 13(12), 1923.
[45] Luo, J.; Cheng, X.; Zhong, C.; Chen, X.; Ye, Y.W.; Zhao, H., et al. Effect of reaction parameters on the corrosion inhibition behavior of N-doped carbon dots for metal in 1 M HCl solution. J. Mol. Liq. 2021, 116783.
[46] Saraswat, V.; Kumari, R.; Yadav, M. Novel carbon dots as efficient green corrosion inhibitor for mild steel in HCl solution: Electrochemical, gravimetric and XPS studies. J. Phys. Chem. Solids. 2022, 160, 110341.
[47] Saraswat, V.; Yadav, M. Improved corrosion resistant performance of mild steel under acid environment by novel carbon dots as green corrosion inhibitor. Colloids Surf. A Physicochem. Eng. Asp. 2021, 627, 127172.
[48] Niu, F.; Zhou, G.; Zhu, J.; Zhang, X.; Shi, Y.; Lu, G., et al. Inhibition behavior of nitrogen-doped carbon dots on X80 carbon steel in acidic solution. J. Mol. Liq. 2021, 339, 117171.
[49] Lv, J.; Fu, L.; Zeng, B.; Tang, M.; Li, J. Synthesis and acidizing corrosion inhibition performance of N-doped carbon quantum dots. Rus. J. Appl. Chem. 2019, 92(6), 848–856.
[50] Cui, M.; Ren, S.; Xue, Q.; Zhao, H.; Wang, L. Carbon dots as new eco-friendly and effective corrosion inhibitor. J. Alloys Compd. 2017, 726, 680–692.
[51] Liu, Z.; Ye, Y.; Chen, H. Corrosion inhibition behavior and mechanism of N-doped carbon dots for metal in acid environment. J. Clean. Prod. 2020, 270, 122458.
[52] Cui, M.; Ren, S.; Zhao, H.; Wang, L.; Xue, Q. Novel nitrogen doped carbon dots for corrosion inhibition of carbon steel in 1 M HCl solution. Appl. Surf. Sci. 2018, 443, 145–156.
[53] Ye, Y.; Jiang, Z.; Zou, Y.; Chen, H.; Guo, S.; Yang, Q., et al. Evaluation of the inhibition behavior of carbon dots on carbon steel in HCl and NaCl solutions. J. Mater. Sci. Technol. 2020, 43, 144–153.

[54] Ye, Y.; Zou, Y.; Jiang, Z.; Yang, Q.; Chen, L.; Guo, S., et al. An effective corrosion inhibitor of N doped carbon dots for Q235 steel in 1 M HCl solution. J. Alloys Compd. 2020, 815, 152338.
[55] Zhu, M.; Guo, L.; He, Z.; Marzouki, R.; Zhang, R.; Berdimurodov, E. Insights into the newly synthesized N-doped carbon dots for Q235 steel corrosion retardation in acidizing media: A detailed multidimensional study. J. Colloid Interface Sci. 2022, 608, 2039–2049.
[56] Liu, Z.; Hao, X.; Li, Y.; Zhang, X. Novel Ce@ N-CDs as green corrosion inhibitor for metal in acidic environment. J. Mol. Liq. 2022, 349, 118155.
[57] Yang, D.; Ye, Y.; Su, Y.; Liu, S.; Gong, D.; Zhao, H. Functionalization of citric acid-based carbon dots by imidazole toward novel green corrosion inhibitor for carbon steel. J. Clean. Prod. 2019, 229, 180–192.
[58] Chen, Z.; Wang, M.; Fadhil, A.A.; Fu, C.; Chen, T.; Chen, M., et al. Preparation, characterization, and corrosion inhibition performance of graphene oxide quantum dots for Q235 steel in 1M hydrochloric acid solution. Colloids Surf. A Physicochem. Eng. Asp. 2021, 127209.
[59] Shirazi, Z.; Golikand, A.N.; Keshavarz, M.H. A new nanocomposite based on poly (o-anthranilic acid), graphene oxide and functionalized carbon nanotube as an efficient corrosion inhibitor for stainless steel in severe environmental corrosion. Compos. Commun. 2020, 22, 100467.
[60] Ansari, K.; Chauhan, D.S.; Quraishi, M.; Adesina, A.; Saleh, T.A. The synergistic influence of polyethyleneimine-grafted graphene oxide and iodide for the protection of steel in acidizing conditions. RSC Adv. 2020, 10(30), 17739–17751.
[61] Nnaji, N.; Nwaji, N.; Mack, J.; Nyokong, T. Ball-type phthalocyanines and reduced graphene oxide nanoparticles as separate and combined corrosion inhibitors of aluminum in HCl. J. Mol. Struct. 2021, 1236, 130279.
[62] Kumar, H.; Sharma, R.; Yadav, A.; Kumari, R. Synthesis, characterization and influence of reduced Graphene Oxide (rGO) on the performance of mixed metal oxide nano-composite as optoelectronic material and corrosion inhibitor. Chem. Data Collect. 2020, 29, 100527.
[63] Ansari, K.R.; Chauhan, D.S.; Quraishi, M.A.; Saleh, T.A. Bis(2-aminoethyl)amine-modified graphene oxide nano emulsion for carbon steel protection in 15% HCl: Effect of temperature and synergism with iodide ions. J. Colloid Interface Sci. 2020, 564, 124–133.
[64] Gupta, R.K.; Malviya, M.; Verma, C.; Gupta, N.K.; Quraishi, M.A. Pyridine-based functionalized graphene oxides as a new class of corrosion inhibitors for mild steel: An experimental and DFT approach. RSC Adv. 2017, 7(62), 39063–39074.
[65] Gupta, R.K.; Malviya, M.; Verma, C.; Quraishi, M.A. Aminoazobenzene and diaminoazobenzene functionalized graphene oxides as novel class of corrosion inhibitors for mild steel: Experimental and DFT studies. Mater. Chem. Phys. 2017, 198, 360–373.
[66] Baig, N.; Chauhan, D.S.; Saleh, T.A.; Quraishi, M.A. Diethylenetriamine functionalized graphene oxide as a novel corrosion inhibitor for mild steel in hydrochloric acid solutions. New J. Chem. 2019, 43(5), 2328–2337.
[67] Ansari, K.R.; Chauhan, D.S.; Quraishi, M.A.; Saleh, T.A. Surfactant modified graphene oxide as novel corrosion inhibitors for mild steels in acidic media. Inorg. Chem. Commun. 2020, 121, 108238.
[68] Yousefi, A.; Javadian, S.; Sharifi, M.; Dalir, N.; Motaee, A. An experimental and theoretical study of biodegradable Gemini surfactants and surfactant/carbon nanotubes (CNTs) mixtures as new corrosion inhibitor. J. Bio- Tribo-Corros. 2019, 5(4), 1–15.
[69] Qiang, Y.; Zhang, S.; Zhao, H.; Tan, B.; Wang, L. Enhanced anticorrosion performance of copper by novel N-doped carbon dots. Corros. Sci. 2019, 161, 108193.

[70] Zhang, Y.; Zhang, S.; Tan, B.; Guo, L.; Li, H. Solvothermal synthesis of functionalized carbon dots from amino acid as an eco-friendly corrosion inhibitor for copper in sulfuric acid solution. J. Colloid Interface Sci. 2021, 604, 1–14.
[71] Cao, S.; Liu, D.; Wang, T.; Ma, A.; Liu, C.; Zhuang, X., et al. Nitrogen-doped carbon dots as high-effective inhibitors for carbon steel in acidic medium. Colloids Surf. A Physicochem. Eng. Asp. 2021, 616, 126280.
[72] Xu, Q.; Ge, K.; Zhang, S.; Tan, B. Understanding the adsorption and inhibitive properties of Nitrogen-Doped Carbon Dots for copper in 0.5 M H2SO4 solution. J. Taiwan Inst. Chem. Eng. 2021, 125, 23–34.
[73] Xu, X.; Wei, H.; Liu, M.; Shen, G.; Li, Q.; Hussain, G., et al. Nitrogen-doped carbon quantum dots for effective corrosion inhibition of Q235 steel in concentrated sulfuric acid solution. Mater. Today Commun. 2021, 29, 102872.
[74] Zhang, Y.; Tan, B.; Zhang, X.; Guo, L.; Zhang, S. Synthesized carbon dots with high N and S content as excellent corrosion inhibitors for copper in sulfuric acid solution. J. Mol. Liq. 2021, 116702.
[75] Zeng, Y.; Kang, L.; Wu, Y.; Wan, S.; Liao, B.; Li, N.; Guo, X. Melamine modified carbon dots as high effective corrosion inhibitor for Q235 carbon steel in neutral 3.5 wt% NaCl solution. J. Mol. Liq. 2022, 349, 118108.
[76] Wan, S.; Chen, H.; Liao, B.; Guo, X. Adsorption and anticorrosion mechanism of glucose-based functionalized carbon dots for copper in neutral solution. J. Taiwan Inst. Chem. Eng. 2021, 129, 289–298.
[77] Wu, X.; Li, J.; Deng, C.; Yang, L.; Lv, J.; Fu, L. Novel carbon dots as effective corrosion inhibitor for N80 steel in 1 M HCl and CO2-saturated 3.5 wt% NaCl solutions. J. Mol. Struct. 2022, 1250, 131897.
[78] Cen, H.; Chen, Z.; Guo, X. N, S co-doped carbon dots as effective corrosion inhibitor for carbon steel in CO2-saturated 3.5% NaCl solution. J. Taiwan Inst. Chem. Eng. 2019, 99, 224–238.
[79] Cen, H.; Cao, J.; Chen, Z. Functionalized carbon nanotubes as a novel inhibitor to enhance the anticorrosion performance of carbon steel in CO2-saturated NaCl solution. Corros. Sci. 2020, 177, 109011.

Navid Hosseinabadi

Chapter 14
Carbon allotropes-based materials as ideal substitutes for industrially useful self-healing coatings: recent advancements and future proponents

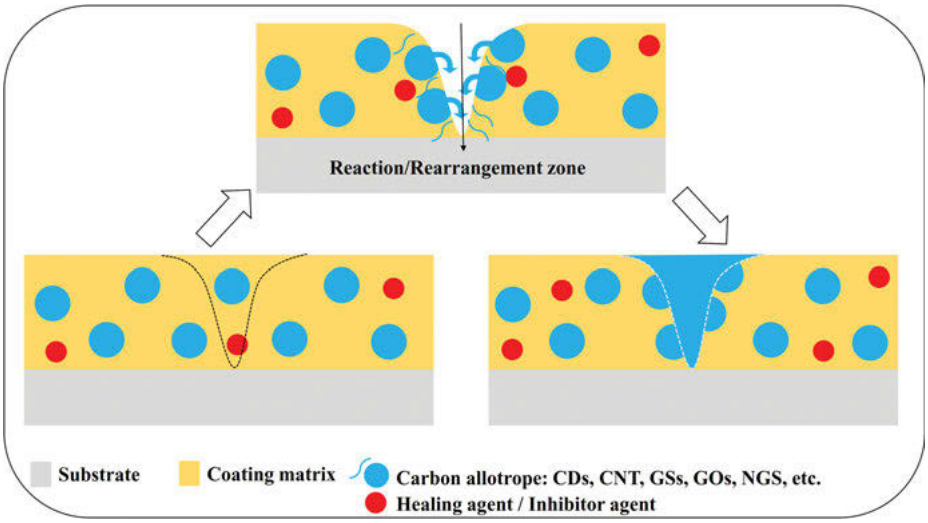

Graphical Schematic.

Overview: Self-healing (self-repairing) materials as outer surface (coatings) are gaining scientific and industrial interests due to their efficiency in detecting and self-healing surface deteriorations. This capability can improve the surface and tribological quality of service materials (mostly metals), specially towards surface-active chemical phenomena (corrosion). Synthetic carbon allotropes, such as, fullerenes, nanotubes, graphene, and the like, have the potential to participate in this application as a base-material or polymer matrix composite-reinforcement material for coatings. This ability is rooted in their high affinity for reaction with healing agents (polymers), environmental gases (carbon dioxide), humidity (water droplets and water aerosols), and by converting

Navid Hosseinabadi, Assistant Professor, Department of Materials Engineering and Metallurgy, Faculty of Engineering2, Shiraz Branch, Islamic Azad University, Shiraz 74731-71987, Iran, The abadeh school of higher education, Shiraz university, Shiraz, Pobox: 71946-84334 Iran, e-mail: Navid.Hosseinabadi@iau.ac.ir

https://doi.org/10.1515/9783110782820-014

these solids/liquids/gases into a carbon-based material, which is able to reinforce and heal itself. The self-healing proficiency of these coatings depends on the polymer matrix modification, carbon allotropes functionality, carbon allotropes free surface area, carbon allotropes' access to the surrounding atmosphere, availability of certain reacting elements, composite processing methods, and matrix-carbon nanofiller interaction/compatibility. In the following chapter, special consideration is given to the self-healing efficiency of polymer-based carbon allotropes-reinforced nanocomposites in the technical field of metal anticorrosive coatings, and the related critical issues and challenges associated with self-healing nanocomposites with different sample systems. The role of these materials as electrolyte diffusion paths for self-healing / blocking agents and crack/pit filling materials are considered; the response sensitivity of these materials to outer external stimulus, as the main mechanism trigger, is reviewed; and some of the characterization techniques that can be used for offline and online evaluation of the healing efficiency of the proposed systems are discussed. Among the different systems, the environmentally-friendly self-healing anticorrosion coatings will be reviewed.

Keywords: self-healing, carbon allotropes, nanocomposite, polymer, coating

14.1 Self-healing coating as an anticorrosive method

Among the different routes available to fight and control surface corrosion, the use of coatings and corrosion inhibitors (with large molecular size for better surface coverage and protection efficiency) are the most common and a combination/incorporation of the two is constantly evolving [1]. It is widely accepted that the application of coatings is the most applicable and cost-effective method of improving surface quality against corrosion and, consequently, the durability of metallic structures. The main role of a coating in corrosion protection is to provide a dense barrier against corrosive agents such as O^{2-}, Cl^{-}, etc. [2] for various metallic materials, such as aluminum alloys, magnesium alloys, steel, and zinc-coated steel, and their metal matrix composites (MMC) that are used in automobile parts, building structures, home appliances, etc. The partial blocking of the pathways to corrosive species very often does not mean an effective inhibiting of corrosion. Therefore, coatings are the major protective measure, accounting for up to 90% of expenditure on corrosion protection via organic-based surface treatments. The protection mechanism for metal surfaces exhibited by the coating is related to the adsorption between the contact surfaces and the material involved in the process, and also to the chemical processes that occur when the system is exposed to aggressive conditions and erosive environments [3]. In addition to the protective and decorative purposes, researchers have focused their attention on developing functional coatings, capable of delivering

additional functions simultaneously, such as anticorrosive, super hydrophobic, antifouling, self-healing, thermal-resistant, and antimicrobial capabilities. These coatings have become more effective in the presence of organic corrosion inhibitors by adsorbing on the metallic surface using their electron-rich centers (multiple bonds and functional groups). The adsorption mechanism of organic corrosion inhibitors follows chemical, physical, or physiochemical-type, that in most cases includes adsorption of organic corrosion inhibitors, and follows the physio-chemisorption mechanism [4].

Another important aspect that needs to be considered is the diffusion pathway for the corrosive species as well as the corrosion rate [5]. The application of various sealants or coatings (metals, non-metals, organic inhibitors, biopolymers, primers, or others) can change the surface composition and add more strength to the structure. The organic coating matrix is an efficient solution to protect the metallic substrates by building a physical border between them and the environmental conditions that sustain the deterioration of the reactive materials [6]. However, there are still some deficiencies, such as local defects, pinholes, micro cracks, or pores, which can allow the small ions to diffuse within the polymeric coating and induce corrosion.

Self-healing materials have attracted scientific attention for offering a wide range of applications in conjunction with a long-lasting performance [7], which involve self-healing techniques, such as layer-by-layer method, microvascular networks, ion exchange method, reversible crosslinks, and shape-memory-assisted self-healing [8]. The term 'self-healing' in materials science is often associated with self-recovery of the initial properties of the material, following damage caused by the external environment or internal stresses (such as stress-corrosion cracking). The same definition is also applicable to functional coatings. However, a partial recovery of the main functionality of the material can also be considered as a self-healing ability. Thus, in the case of corrosion protective coatings, the term 'self-healing' can be interpreted in different ways. Coating systems, based on an active corrosion protection mechanism, can also be considered as 'self-healing' coatings, since the main function of the protection system, namely corrosion protection, is recovered during the operation [9].

However, defects may appear in the protective films during the operation of the coated structures, allowing direct access of corrosive agents to the metallic surface. The corrosion processes develop faster after the disruption of the protective barrier. Therefore, active 'self-healing' of defects in coatings is necessary to provide long-term protection. Self-healable systems, as coatings, contain lightweight, high thermo-mechanical performance, excellent adhesion, good chemical resistance, and corrosion resistance; with low susceptibility toward scratches and micro cracks as the main routes for the transport of corrosive materials along the metal's surface. This property is a major concern while dealing with new corrosive environments [10]. The smart anticorrosion coating restores its protective properties after being damaged by the surrounding environment, which is attributed with technical terms such as self-healing / repairing and shielding effects [11]. Corrosion can occur beneath these coatings, even if and where defects have been healed or sealed if the electrolyte has penetrated to

the substrate when the defect was induced [12]. As the coating is broken, the self-healing mechanism can be activated to restore the coating defect or when the metal is corroded at the defect of coating; the self-healing agent would form a protective film at the location of defect [13]. There is a good self-healing possibility in most polymer-based micro/nanocapsules of carbon allotropes. The strong adsorption of the material leads to a protective hydrophobic shield against the harmful impact of corrosive species on the metal surface, making this microcapsule combination an excellent candidate for environments that are humid. A polymer-shelled microcapsule, suspended in a solution with the corresponding catalyst, would be applied to a surface with carbon-allotrope reinforcement. When the surface experiences a crack or a rupture, the microcapsules would also experience this effect, thereby exposing the core materials to the catalyst (See Fig. 14.1). As the catalyst and the core materials interact, polymerization occurs and bonds the crack to close it [14]. The core materials or healing agents for micro and nanocapsules are able to react with multiple kinds of exposures after being ruptured, including, the coating matrix and carbon allotropes. The core materials should generate viscoelastic substances that have intrinsic self-healing capabilities [15].

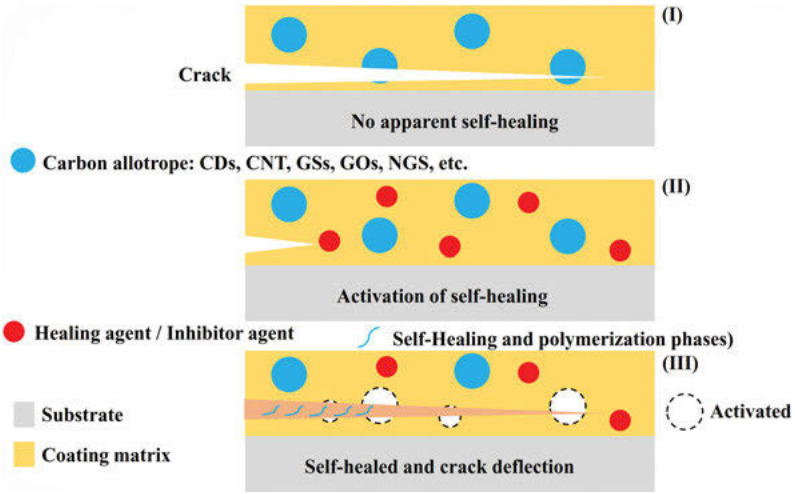

Fig. 14.1: The activation of self-healing carbon allotropes in matrix with (I) and without (II) agents and after activation (III).

The general self-healing coating activation mechanisms involve:

- Converting the physical energy of the crack and pit formation (residual stress energy) or thermal expansion stress energy to chemical energy, to heal the damaged area;
- Blocking the infiltration of the corrosive medium via dense medium-phobic outer-layer;

- Triggering an activation via certain parameters, such as pH fluctuation, due to metal ion hydrolysis at anodes (pH decrease) and oxygen reduction to hydroxides (pH increase);
- Self-repairing and self-healing due to adsorption or reactions; and
- Forming reversible network structures via physical or chemical interactions [16];

Some physical interactions (i.e., intermolecular interaction, hydrophobic interaction, ionic bonding, etc.) often result in limited healing efficiency without an external activation [17]. Therefore, most researches are mainly focused on the extrinsic self-healing coatings for anticorrosion applications. The key activators in this type of self-healing coatings are the micro/nanocapsules and the matrix [18], in which the anticorrosion healing agent is typically encapsulated in the micro/nanocontainer as the core content (healing performance evaluation of a self-healing carbon fiber/epoxy composite [19]). As an example, the self-healing carbon nanotubes in nanocomposite coatings can be designed using epoxy, polyurethane, poly(methyl methacrylate), and rubbers [20] as the matrix. The nano-sized carbon allotropes; particularly graphene (*G*), graphene oxide (*GO*), single- and multi-walled carbon nanotubes (single-walled CNT and multi-walled) (*CNTs*, *SWCNTs*, and *MWCNTs*), graphene oxide microcapsules (*GOMCs*), and their chemically modified derivatives are widely used in anticorrosive coating formulations. Generally, carbon allotropes acquire a nanofiller property and a high hydrophobicity, which make them ideal anticorrosive materials [21]. Carbon allotropes, such as Graphene oxide (*GO*), have the capability of guaranteeing the coating integrity, when used as filler with hydrophobic characteristics, and can also reduce the adsorption and migration of corrosive media, which effectively enhances the corrosion resistance of the composite coating. Even a defect-free monolayer of graphene oxide sheet is almost impermeable against water, oxygen, and corrosive ions. There are many reports on the use of graphene oxide sheets in polymer composites for the enhancement of the barrier properties [22].

At the same time, the chemical arrangement of certain carbon-based allotropes and structures, such as Graphene oxide contains two-dimensional sheet of a semi aromatic network made of sp^2 carbon atoms, organized in an ideal structure. The basis of its outstanding properties resides in its chemical configuration, which consists of a two-dimensional sheet of a semi aromatic network made of sp^2carbon atoms organized in an ideal hexagonal pattern. The very significant distinctiveness of most carbon-based allotrope materials is the existence of numerous defects on its basal plane, such as the different oxygen-containing functional groups, including epoxide, carboxyl, and hydroxyl [23]. These oxygenated groups are responsible for many benefits, such as increased solubility, hydrophilicity, and the ability to form a stable colloidal solution, and they also provide the possibility of performing various functionalization reactions on the basal plane [21]. As another example, the combination of CNTs with conducting polymers in coatings can remarkably improve the corrosion protection performance of such coatings. This could be due to a synergistic

effect between both components in their mixture. If a self-healing coating suffers mechanical damage and the corrosive species in the environment begins to degrade, the bare metal surface, the damaged surface, is automatically repaired by a chemical component of the coating [24]. In this case, (a) the damage triggers the healing mechanism by rupturing the micro or nanocapsules filled with healing agents (b) transport of the healing agent to the failure site, (c) closure and formation of the barrier at the damaged site by the healing agent, (d) immobilization by physical or chemical interactions [25]. These coatings are mostly quantified by the healing efficiency values (η_e), which is defined by the percentage recovery of a certain property, relative to the original value [26]:

$$\eta_e = \frac{Property\ value_{healed}}{Property\ value_{Initial}} \tag{14.1}$$

The classical understanding of self-healing is based on the complete recovery of the coating functionalities due to the real healing of the defect, which restores the initial integrity of the coating, even at atmospheric conditions, by a combination of water molecules and carbon dioxide with polymethacrylamide (*PAM*) and cross-linked polyurethane (*PUR*) matrix [27, 28]. However, the main function of the anticorrosion coatings is protection of a metallic substrate against environmentally-induced corrosion attack. Thus, it is not obligatory to recover all of the properties of the film in this case. The hindering of corrosion activity at a defect by the coating itself, by whatever means, is enough to constitute self-healing, because the corrosion protective system recovers its main function, namely protection against corrosion, after being damaged [29]. These applications are suitable for polymer micro/nano capsules, including protecting the inner surfaces of aircraft fuel tanks, transport lines, and reservoirs. The enhanced functionality can be achieved when smart coatings are applied to military equipment and industrial gas turbines in which the encapsulated self-healing agent, in microcapsules, can be dispersed into the coating [30].

Some self-healing systems can be categorized as physical self-healing gels, formed through non-covalent interactions among the molecular gelation agents (e.g., hydrophobic interactions, hydrogen bonding), and chemical self-healing gels assembled via dynamic covalent bond formation. Self-healing covalent gels generally exhibit greater resilience and mechanical stabilities compared to the non-covalent counterparts [31].

The transfer of the self-healing approaches used for bulk materials to coatings is very complicated since the self-healing system should be embedded in a thin sub-millimeter polymer layer [32]. The idea of a coating that is capable of reflow-healing of defects is the main challenge for introducing self-healing carbon allotrope coatings. On this note, the immobilization of various nanomaterials in self-healing medium, such as graphene oxide and carbon nanotubes, is the basis for many self-healing mixtures in these systems [33]. The self-healing micro and nanocapsules show optimum performance at or above room temperature, but low temperature self-healing capabilities are also in high demand for use in cold climates. For aerospace applications, temperatures

can be as low as −60 °C; therefore, self-healing coatings, with temperature-tolerant capabilities, would be excellent additions at these temperatures [34]. These coatings can be evaluated via local electrochemical impedance spectroscopy (*LEIS*) and the anti-permeability of coating by the oxygen permeability test (P_{O_2}) [35]. The composite self-healing coatings are expanded to laminate reinforced carbon allotrope systems, such as carbon nano fiber/epoxy (Hexcel T300/914), arranged with Quasi-isotropic (QI) plates (laminates) of $(-45°/90°/45°/0°)_{2S}$ and hollow fibers, which is a combination of one and two dimensional reinforcement with 75% healing efficiency [36].

14.2 Carbon allotropes as self-healing means of corrosion inhibition

The utilization of carbon nano/micro sized allotropes for incorporating self-healing properties in coatings can be categorized into different methods. The most common and promising are:

14.2.1 The inhibitor healing method

Corrosion control can be achieved by the application of nanocontainers such as Poly (urea-formaldehyde) (PUF), poly(melamine formaldehyde) microcapsules (*PMF*), cellulose nanofibers (*CNF*/*HNT*), etc. along with carbon allotropes in the structure of coating, which are loaded with corrosion inhibitors, resulting in autonomous healing without the need for a catalyst [37]. The corrosion inhibitor can be added to the different parts of the coating system since the corrosion protection coating is usually a complex system that comprises several layers. The inhibiting compounds can be incorporated in the pre-treatment layer, the primer or the top coat, using different strategies. The component containing the corrosion inhibitor serves as a reservoir from which inhibitors may leach out during its service life. The following part of the paper provides an overview of the different strategies for the incorporation of the inhibitor into the corrosion protective systems to achieve self-healing and active corrosion protection. For intrinsic self-healing, the inhibitor dispersed in the coating composite matrix offers benefits, such as inherent healing ability, non-requirement of catalyst; and multiple healing capabilities; however, the main drawback is the need for an external stimulus such as pH or temperature to initiate the crack healing process. The intrinsic self-healing by this method is due to the physical and chemical interactions of the material by itself. The physical interactions could be attained by blending with polymers that can achieve reversible 'sacrificial bonds' (especially hydrogen bonds). The presence of such sacrificial bonds in the polymers is responsible for the local fusion and rejoining of the cracks, around and along the carbon allotropes.

The strong chemical interactions cause reversible covalent and non-covalent bonds that create rapid conformational changes and result in the fast healing of the cracks [38]. For the extrinsic self-healing-inhibitor-induced composite coatings, the inhibitors are encapsulated or embedded in certain forms within the coating matrix. The external stimulus causes a rupture in the shell of the micro/nanocontainer, releases the inhibitor to heal the corrosion (an external stimulus is needed to induce cross-linking or volume swelling), and seals the damage from corrosion in wet and/or dry conditions [39]. It can also be activated by the aid of an external healing agent that is encapsulated in carbon microcapsules, mesoporous carbon allotrope fillers, and carbon fibers, which can flow via capillary action to the damaged site to fill the cracks [40]. The healing agent in these systems should be mobile enough to flow to the damage sites and the catalyst or crosslinker must be uniformly dispersed in the composite matrix for better healing of the cracks along the carbon allotrope reinforcements. The advantages of this system includes a simple self-healing model and easy encapsulation of healing agents; while the drawbacks are limited to one-time crack repairing and high costs of the necessary catalysts [41].

The coating choices of the polymer matrix can also improve the coating behavior. A conducting polymer and an organic semiconductor, such as polyaniline, shows a significant dependence on the protection efficiency on the redox state, and can also create certain passivating effect on small defects in the presence of larger defects, where the coating is no longer able to provide passivation. The consequence, in this situation, is a rapid coating degradation, followed by delamination [42]. The corrosion inhibitor can be introduced by simply mixing it into the coating formulation. The corrosion inhibiting chemicals can be effective only if their solubility in the corrosive environment is in a certain range. A very low solubility leads to a lack of active agent at the defect site and, consequently, to a weak self-healing ability. If the solubility is too high, the substrate will be protected but for only a relatively short time, since the inhibitor will be rapidly leached out from the coating [43]. The corrosion inhibitors may even interact chemically with the components of the coating formulation, weakening the barrier properties of the final coating. The slight possibility of a degradation of the barrier properties, resulting from the addition of an inhibitor, is the main concern in the development of active corrosion protection systems. The possible interactions between the inhibitor and the components of the coating (i.e., polymer matrix and carbon allotropes) can lead to a complete deactivation of its inhibiting activity and self-healing abilities of the matrix. The situation is different in the hybrid organosiloxane-based film systems. The production of self-healing hybrid films, doped with organic and inorganic corrosion inhibitors, results in thin hybrid films. These systems are suggested as alternative pre-treatments or primers for different metallic substrates. The incorporation of inorganic or organic corrosion inhibitors into the hybrid films can significantly improve the corrosion protection properties of aluminum alloys, magnesium alloys, galvanized steel, and stainless-steel substrates [44].

14.2.2 The polymeric healing method

This application of carbon allotropes involves the crosslinking reaction between the monomer (healing agent) and the curing agent at the damage site, which retains the properties of the original coating. In this method, the healing agents are polymerized as epoxy, DCPD etc. with hardeners or catalyst loaded in same or different containers, and dispersed in the epoxy matrix-reinforced coatings to protect the metal surface [45].

14.2.3 The ion exchange method

This technique is developed to release the corrosion inhibitors into the defective site. Here, the species containing ion exchangers that are dispersed in the epoxy matrix can release inhibiting ions, upon demand, alongside carbon allotropes-reinforcement phases [46]. The use of carbon nanotube's surface as an inhibitor carrier is an applicable route to adsorb the inorganic corrosion-inhibiting anions onto the particle surface by an ion-exchange mechanism. The corrosion inhibitors are released from the particle surfaces by a subsequent ion exchange with anions or cations (e.g., chlorides, sulfates, sodium ions) that are transported into the coating from the environment via water that penetrates through the coating. However, this mechanism can also lead to an undesirable release of the inhibitor, initiated by the presence of harmless ions in the surrounding environment [47]. The corrosion-inhibiting inorganic cations can be incorporated as exchangeable ions that are associated with cation-exchange solids. The benefits of this approach are that the cation exchange materials are completely insoluble in polar mediums. Using anion-exchange materials to immobilize the anionic inhibitors causes the release of inhibitor anions, which can be provoked by aggressive corrosive ions, such as chloride. The anion exchange can act as an absorbing agent for harmful ions, releasing the inhibiting ions in response [48].

14.2.4 The reversible crosslinks method

This method provides multiple healing capabilities, without the need for catalysts or healing agents, and only an external stimulus for self-healing is required. The self-healing of graphite epoxy laminate substrate by using 'mendomer' powder is an example of this method. They are polymer matrix coatings that are mendable through heating. The powder used has dicyclopentadiene units in the polymer. Due to defects such as internal fracture, the dicyclopentadiene breaks and results in two cyclopentadiene terminal groups. The cyclopentadiene units will recombine upon heating. The graphite fibers in these composite coatings act as electric conductors to provide the necessary heat for the self-healing process [49].

14.2.5 The shape-memory-assisted self-healing method

According to the dominant mechanism of this system, the composite coating experiences a complete healing and retains the structural properties. Self-healing in this system is assisted by the shape-memory effect of the epoxy matrix. The shape-memory effect brings the cracks closer to each other, while the melting of the PCL fibers heals the cracks around the carbon allotropes reinforcements [50, 51].

14.2.6 The reflow-based self-healing coatings method

These protective coatings provide low-weight structures, with enhanced service life – a combination of traditional engineering approaches with biological self-healing mechanisms and a demonstration of coatings that are able to heal or seal defects by mechanical blocking via polymerization or precipitation mechanisms around the carbon allotropes [3]. The physical integrity of the composite coating is partially recovered due to these processes.

In carbon allotropes-reinforced self-healing coatings, an epoxy-based system heals cracks and autonomically pits the polymer bulk material, which contains a microencapsulated healing agent that is released upon crack initiation. Then, the healing agent is polymerized, after contact with the embedded catalyst. Next, it bonds the crack faces and recovers the integrity of the material [52]. Similarly, in the presence of hollow reinforcement carbon fibers that are used in carbon fiber-reinforced plastic matrix and embedded in a liquid resin, the repair process is triggered after impact loading of the material [53]. The hollow carbon fibers ranging in diameters of 30 to 100 μm can be filled with uncured resin systems that bleed into a damage site upon fiber fracture. After being cured, they provide a method of crack blocking and recovery of mechanical integrity [54]. By employing a self-healing system that is capable of autonomous repairing of repeated damage events, the composite substrate delivers the healing agent to the cracks in a polymer coating via a three-dimensional microvascular network that is embedded into the substrate. The cracked and defective coating can be repaired by repeatedly mimicking a biological system. This approach for most corrosion protection applications is rare since the microvascular network formation of the adsorbed surface coating on most metal substrates is technologically difficult. Although, coatings capable of reflow-healing of defects in protective coatings can be designed with in-situ self-repair ability after being damaged by stressful environments, the repair can be achieved through microencapsulated polymerizable agents that are incorporated into the carbon allotrope-reinforced coating matrix, as in the case of the bulk composites. If the coating is damaged, the ruptured microcapsules release the film-forming components in the immediate vicinity of the damage. The fluid flows over the exposed areas of the metal surface and fills any defects or cracks in the coating, recovering the protective barrier [29]. The

introduction of the different types of capsules, loaded with coating repair compounds and corrosion inhibitors, can be used as the other approach. For instance, the efficacy of 'self-healing' corrosion protection coatings with urea-formaldehyde and microcapsules (50–150 μm diameter), containing several types of film-forming agents, has been studied. The microcapsules stay intact for a long time in the dry coatings and are ruptured only by a damage that released the core constituents to the defect. The chosen microcapsules are stable [55]. These systems can be designed as a self-healing coating, integrated with cathodic protection systems. The specific film-formers, sensitive to pH and electrical field, can be introduced into the coatings applied on metal structures, under cathodic protection and be reinforced with carbon allotropes. The pH-dependent triggered release mechanism involves the release of organic molecular species from the hybrid coating matrix and can be described by the pH-dependent activation of the desorption processes, which can provide an 'intelligent' release of the corrosion inhibitor, only in places of local pH changes, originating from localized corrosion processes (hybrid films with 2-mercaptobenzothiazole and 2-mercaptobenzimidazole incorporated as corrosion inhibitors) [56]. Many water-soluble and self-curable epoxy electro additions that can be deposited as fillers (up to 30 *wt*.%) can be used as organic film formers. The significant reduction in the current, necessary for cathodic protection, is the indication of the self-healing ability of the coatings. The barrier properties in these composite coatings are significantly increased, in comparison to scratched reference samples [57]. Although these carbon allotrope composite coatings are based on polymerization of a healing agent in the defects with barrier recovering properties of the protective coatings, the barrier properties of a damaged coating can also be restored by simple blocking of the defects with insoluble precipitates. These deposits in cracks can originate from the reaction of a corrosive medium or corrosion products with components of the coating [58].

The concepts relating to carbon allotropes as inhibitor and healing agent nanocontainers can be classified into two groups –encapsulation with different types of shells, and immobilization on the surface of or inside the carriers [59]. (i) A nano porous reservoir is designed for storing the corrosion inhibitors at the metal/coating interface. The nanostructured porous character of the mesoporous carbon nanocontainers can provide a highly effective surface area for the adsorption of the inhibitor. The adsorbed inhibitor can be leached out from the porous layer to the defect, healing the cracks and pits in the coating. Further, (ii) the integration of nanoscale containers (carriers) that are loaded with active inhibiting compounds and healing agents helps in dispersal within the conventional coatings. These systems are based on 'passive' host– 'active' guest structures. Nanocontainers (i.e., carbon-based nanotubes and particles) are uniformly distributed in the passive matrix, keeping the active species in a certain position. This removes the possibility of excessive inhibitor leaching. When the local environment changes or if a corrosion process starts at a coating defect, the nanocontainers respond to this signal and release the immobilized active material. This inhibitor entrapment is based on the

complexation of organic molecules by cyclodextrin, known complexation agents, which can play the role of hosts, forming inclusion complexes with various organic guest molecules that fit within the cyclodextrin cavities. The similar organic aromatic and heterocyclic compounds are usually the main candidates for the inclusion complexation reaction [60]. The nanocontainers, with polymer shells, can be successfully applied to water-borne polymer coatings, to be used for the protection of metals. The mixture of the two types of nanocontainers in one coating can increase the performance of the coating (See Fig. 14.2) by the inner and inter distribution of corrosion inhibition and healing agents. The use of mesoporous ceramic with carbon allotropes (nanotubes) is a mechanism that involves the nanotube to open first for the epoxy pre-polymers to react with the amine curing agent. Because the coating is immersed in an electrolyte solution, the nanotubes slowly start releasing the epoxy pre-polymer. The polymer comes in contact with the amine curing agent and begins the self-healing process. It was proven that this coating recovered 57% of the anticorrosive property [61].

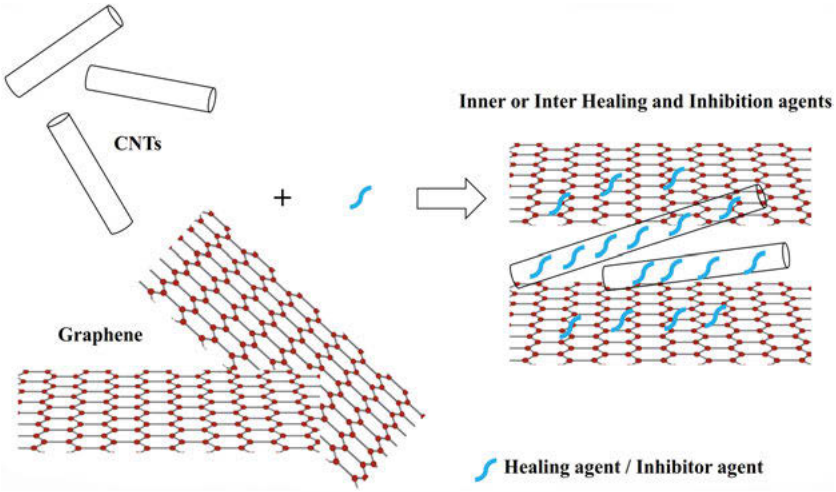

Fig. 14.2: The hybrid allotrope as an inner and inter agent transport system.

The microemulsion polymerization method is a process designed for the production of micron-sized capsules and doping of the system with a corrosion inhibitor, which has low solubility in water and hence can lead to preferential distribution in the organic polymer matrix phase in carbon allotropes-reinforced self-healing coatings. The formation of polymer shells around the organic micro-drops forms microcapsules, containing an organic core and loaded with corrosion inhibitor / healing agents. In the case of a defect / pit formation in the organic film, the capsules are disrupted and they release the water-displacing fluid, which removes the electrolyte and covers the

scratch area. Furthermore, the inhibitors are delivered to active sites to passivate the surface and suppress the development and propagation of corrosion [62].

The Layer-by-Layer (LbL) assembled shells can also facilitate self-healing by controllable leaching, triggered by corrosion and defects-related stimuli. The nanocontainers, with specially designed storage/release of the inhibitor and healing agents, can be formed with nano-sized dimensions, and create the layer-by-layer deposition approach. The nanocontainers are formed with a step-by-step deposition of the oppositely charged substances from their aqueous and non-aqueous solutions on the surface of a template material, forming LbL shells. The LbL films, containing one or several polyelectrolyte monolayers, assembled on the surface of a sacrificial template possess control of shell permeability towards ions and small organic molecules [63]. The storage of corrosion inhibitors and healing agents in the polyelectrolyte multilayers has three advantages: (i) it isolates the inhibitor, avoiding its negative effect on the integrity of the coating; (ii) it provides an intelligent release of the corrosion inhibitor, regulating the permeability of the polyelectrolyte assemblies by changing the local pH and humidity, and (iii) it regulates the release of polymer matrix healing agent. The change of pH is the most preferred trigger to initiate the release of the inhibitor, as corrosion activity leads to local changes in pH near the cathodic and anodic defects. Therefore, smart coating, containing polyelectrolyte containers, can detect the beginning of the corrosion and start the self-healing process in the corrosion defects and scratches in carbon allotropes-reinforced self-healing coatings [3]. The carbon nanotubes, hollow tubular structure in the submicron range, and a strong surface charge on the tubules can be exploited for designing nano-organized multilayers using the layer-by-layer method, similar to Halloysite nanotubes [64].

14.3 Carbon allotropes-reinforced self-healing composite coating systems

The carbon-based materials (allotropes), as the reinforcement phase for self-healing composite coatings, offer an eco-friendly approach to corrosion inhibition and healing agent transport and release in coatings than most traditional formulations. The important specification and importance of these materials originates from (i) cost efficiency; (ii) abundancy and availability; (iii) environmental friendly; (iv) simple synthesis; (v) lightness and excellent mechanical stability (especially for graphene); (vi) thermal stability; (vii) increased durability and (viii) biocompatibility [65]. Carbon-based materials (allotropes) have been investigated for corrosion prevention and have shown promising inhibition efficiency. To further improve the inhibition ability of carbon allomorphs, several approaches, such as doping with nitrogen or sulfur, surface functionalization, incorporation of metals or combination with polymers in

composites, have been reported [66]. It is recognized that carbon and its allotropes, especially graphene, hinder corrosion via a defensive mechanism, called barrier protection. In this mechanism, graphene, for example, in the coating acts as a shielding layer, preventing air, salt, and moisture from coming into contact with the underlying metal or alloy [67].

Carbon and its allotropes can be classified according to their geometry/dimension into the following widely known categories [68],

i) Zero-dimensional materials such as carbon dots, fullerene, onion-like, and nanodiamond
ii) One-dimensional materials such as carbon nanotubes, carbon nanowires, naonohorn, multi walled nanotubes
iii) Two-dimensional materials such as graphene, graphene oxide, graphite sheets, and nanoribbons
iv) Three-dimensional materials such as graphite and diamond in which the zero- to two-dimensional are the main candidates as additives in composite polymers

14.3.1 Zero-dimensional: carbon dots and fullerene-based self-healing anticorrosion coatings

Carbon dots (CDs) have received increasing attention due to their superior properties, including low toxicity, high water solubility, unique photoluminescence, and biocompatibility, allowing them to be used in a wide range of applications [69]. The structure of functionalized Carbon dots offers both multiple bonds and electronegative atoms (such as O, S and N), shows low cytotoxicity, and can be used as eco-friendly corrosion inhibitors for many metals in different corrosive environments [70]. The carbon dots, as interface inhibitors, have three modes of action: (i) blocking active sites; (ii) geometric blocking; and (iii) electrocatalytic effect. Carbon dots have been incorporated in epoxy resin, poly (methylmethylacrylate), polyurethane, polyvinylalcohol, and methyl/phenyl-triethoxysilane (MTES/PTES). The focus of many researches has been on the enhancement of anticorrosion protection of carbon dots via the use of S and N co-doped carbon dots (N, S-CDs). The utilization of these allotropes with enhanced protection and inhibition efficiency has increased as N, S-CDs contents increased (up to 93% at 50 mg/L). The results show a decrease in the corrosion current, which is related to the ability of these materials to be adsorbed on the metal (such as steel) surface through their functional groups, while N, S-CDs nanoparticles form a hydrophilic barrier extra thin film (about 40 nm) over the steel surface. This film has shown strong hydrophobicity when the contact angle increased from 43° to 92° [71].

Fullerene structures, which are considered as zero-dimensional analogues of benzene, are carbon-enriched molecules, generally of ellipsoidal and spherical morphology. Fullerene has a lubricating behavior, which helps in its use in tribology

and industrial applications. This behavior arises from its strong intermolecular bonding and spherical morphology [72]. The Oxidized Fullerene (OF) nanoparticles, used in a hybrid composite coating with silane, decrease the roughness, which can be related to the formation of a dense layer, as a result of the interaction between the coating and the Oxidized Fullerene nanoparticles [73]. Bhattacharya et al. have developed Self-Healing Carbon Dot – Polymer coating systems by reacting carbon dots produced from aldehyde precursors with branched polyethylenimine. The self-healing mixtures can be formed through the Schiff base reaction between the aldehyde units. They have deduced that imine bonds can be generated on the carbon dots' surface and on primary amine residues within the polyethylenimine network. The dynamic covalent imine bonds between the carbon dots and polymeric matrix provides the mixtures with both excellent self-healing properties as well as high mechanical strength [33]. The spray coating of the silane-functionalized graphene quantum dots (f-GQDs) in solvent-based epoxy coatings also increases the protection capability and lowers the corrosion rate [74].

14.3.2 One-dimensional: carbon nanotubes, nanowires, and naonohorn-based self-healing anticorrosion coatings

The anticorrosion carbon nanotubes (CNTs) / wire / horns are basically graphene sheets rolled up to form seamless tubes and cylinders. They are considered as superior reinforcing materials for different composites because of their excellent mechanical properties, such as stiffness, modulus, and strength, compared to other existing materials [75]. Carbon nanotubes have also shown electrochemical behavior different from the other carbon allotropes. The enhancement in corrosion resistance provided by CNTs for different metals is associated to the modification of the surface by filling and blocking the crevices and holes [76]. The addition of different surfactants to the solution, ball milling process, and functionalization mostly helps in preventing the aggregation and in improving the dispersability, to decrease the great tendency to aggregate in solutions because of the high length-to-diameter ratio. The resultant coatings have decreased the corrosion rate by 77.3%, which is attributed to the formation of spinels on the surface [77]. The enhanced hydrophobicity and corrosion protection can be induced by the incorporation of different concentrations of multi-walled carbon nanotube (MWCNT). These allotropes are covalently functionalized to gain the desirable anticorrosive properties to achieve physiochemical changes, such as increase in dispersion. The introduction of these allotropes has resulted in an increase in the interfacial adhesion ability, a decrease in the hydrophobicity, a decrease in the agglomeration ability, a decrease in the mechanical strength, and a decrease in the electrical conductance [78]. The excellent corrosion protection ability of conducting polymers, such as polyaniline (PANI), mainly arises from passivation of catalysis and electron transmission on metal surfaces, which in turn relies on the redox activity of the PANI materials

[42]. Therefore, enhancing the protection ability of such materials through the formation of carbon allotropes nanocomposites to control the structure and morphology and to increase the redox activity, is promising [79]. In PANI/CNT core-shell nanocomposites systems, an excellent redox activity in both acidic and neutral medium can be achieved via oxidative polymerization of aniline on the surface of calcium carbonate and CNT nanocomposites. The anticorrosion behavior involves a gradual increase in the radius of the single-capacity arc, which demonstrates the formation of a dense oxide film on the metal surface. The formed layer acts as an efficient physical barrier to the corrosive ion and an increase in the charge-transfer resistance (R_{ct}) from 2,172 to 10,300 $\Omega\, cm^2$ [80]. The CNT-PABS (Poly-M-Amino Benzene Sulphonic Acid) & CNT-CA (Carbon Aerogel-Carbon Nanotube) systems cause the decrease in i_{corr} from 2 to 1.3 $10^{-5} A cm^{-2}$ (Carbon steel) [81]. The application of MWCNT in Ppy (polypyrrole)/MWCNT composite coating showed an increase in R_{ct} from 12.5 to 25,000 $\Omega\, cm^2$on 304 stainless steel substrates [82]. The reinforcing self-healing PANI-based anticorrosion composites show decrease in *CR* from 2.93 to 0.00155 mpy for PANI/f-CNT on mild steel substrates [83], increase in R_{ct} from 151 to $10^4 \Omega\, cm^2$ for PANI/MWCNT system on carbon steel substrates [80], and a decrease in i_{corr} from 6.98 to 4.38 for PANI–CNT systems on mild steel substrates [84]. This approach in MWNT/PU (Polyurethane) system leads to the decrease in i_{corr} from 1.62 to 0.076 $10^{-6} A cm^{-2}$ and increase in R_{ct} from 0.07 to 3 $10^6 \Omega\, cm^2$ on stainless steel substrates [85]. The replacement of the matrix barely affects the result, as in the HA(hydroxyapatite)/f-MWCNT system, a decrease in i_{corr} from 7.3 to 6 $\mu A cm^{-2}$ of 316 L on stainless steel substrates can be expected [86]. The incorporation of nanotubes in epoxy/carbon nanotube composite coating system with an amine curing/self-healing agent, like diglycidyl ether of bisphenol A (DGEBA) and multi-walled carbon nanotube (0.25–0.75 wt.%-MWCNT), activates the healing mechanisms. The intrinsic self-healing occurs by creating electrically percolating nanotube network, which recognizes the damaged area [87] and the carbon nanotubes create the spontaneous healing to the epoxy resins after the matrix cracking phenomenon. The reversible bonding self-healing mechanism is created in polyurethane/carbon nanotube using a heal material, such as polytetrahydrofuran and aliphatic triisocyanate and carbon 2 wt.% MWCNT nanotube / and even oxidized CNT (ox-CNT). The intrinsically-activated self-healing occurs by an electrical percolation network (conducting) and a thermo-reversible and electrically-healable network. The modified carbon nanotube improves the interfacial interactions with the polymer [88]. The carbon encapsulation in poly (methyl methacrylate) (PMMA)/ carbon nanotube (15–20 wt.%) involves capsules in an epoxy matrix with 93.5% healing efficiency via plasticizing action from the microcapsules and interactions in the system due to the high surface area. The microcapsules act as healing agents to heal the cracked or damaged area [89]. Base coating of self-healing superhydrophobic in PAH(polycyclic aromatic hydrocarbon)–SPEEK (Sulfonated poly(ether ether ketone))/PAA(Polyacrylic acid) system with corrosion-resistant, antiadhesive, and drag-reduction capabilities is due to the Layer-by-layer

(LbL) assembly [90]. The crack healing efficiency is considerable in systems with polyethylene-co-methacrylic acid (EMAA) and polyethylene-co-glycidyl methacrylate (PEGMA), and two non-reactive thermoplastics (ethylene vinyl acetate (EVA) and acrylonitrile butadiene styrene (ABS)), with about 50 vol.% carbon nanofiber in the epoxy resin network with heal de-laminations efficiency up to 35% [91]. In epoxy resin (diglycidyl ether of bisphenol A:DGEBPA, E-51) with 13 wt.% TETA(Triethylene-tetramine) curing agent and 15 wt.% CNT microcapsules, an ~ 83% healing efficiency via the rough microcapsule's shell edge inlaid into the matrix can be observed, which is caused by the release of the healing agent and leaving an empty microcapsule's shell. Besides, the high strength interface joint between the microcapsules and the matrix is due to the mechanical engagement of the microcapsule's shell that possesses a rough outside [92]. The application of other healing mechanisms has proven to create considerable efficiency. The delivering of epoxy-based healing agents containing short carbon fibers (SCFs) to cracks through an embedded vascular system is a promising method in these systems. The cracks in the matrix are created through the carbon fiber layer of carbon fiber–reinforced composite specimens. The short carbon fibers in the released healing agents can be aligned in a local electric field, if available. The alignment reconnects the structural carbon fibers (14 vol.%) with 47.3% healing efficiency [93]. The hollow vessels can contain a liquid healing agent mixed with SCFs. The vessels and structural fibers can be aligned with one another throughout the matrix. When some of the structural fibers rupture or degrade via corrosion phenomena, the same happens to nearby vessels, causing them to release the healing agent, which then flows to fill the gaps between the broken fibers. As short carbon fibers are electrically conductive, they can be aligned to an electrical field, generated across the gaps, by connecting a power supply to the carbon fiber–reinforced composite material. The healing agent in the gap starts to solidify, freezing the location of the SCFs, and enabling them to form permanent links between the broken fibers [93].

The basic and similar principles can be applied to thermoplastic polymers as a coating matrix [76]. The thermoplastic poly(ethylene-co-methyl acrylate) (EMA) and poly(ethylene-co-methacrylic acid) (EMAA) with carbon fiber (35 wt.%) in the epoxy resin network composite system is a good example. The small patches of EMA and EMAA films in the interlayer region create about 39–46% healing efficiency for EMA and 36–88% for EMAA [94]. Similarly, 10 wt.% addition of reactive thermoplastic additives (polyethylene-co-methacrylic acid (EMAA) and polyethylene-co-glycidyl methacrylate (PEGMA)), and two non-reactive thermoplastics (ethylene vinyl acetate (EVA) and acrylonitrile butadiene styrene (ABS)), can used as matrix healing agents in the epoxy resin network with 50–60 wt.% carbon fibers content. The healing efficiency (η_e) of the thermoplastics increases in the order of ABS (lowest-η_e : 15%), PEGMA, EVA, and EMAA (highest-η_e : 36%). The carbon-reinforced composite coating healing occurs by the reactive EMAA and PEGMA thermoplastics, which involves a unique pressure delivery mechanism, whereas healing by the non-reactive EVA thermoplastic is controlled by its viscosity and adhesion to the

fracture surfaces to obtain a considerable healing efficiency (η_e : 35%). ABS was ineffective as a healing agent in the composite due to its high viscosity, which impeded the flow into the delamination crack [95].

14.3.3 Two-dimensional: graphite sheet, graphene and graphene oxide-based self-healing anticorrosion coatings

Natural graphite sheet (NGS), Graphene, and Graphene oxide are the bases for 2D carbon allotrope reinforcement of self-healing composites or chemically modified allotropes. Graphene in composite materials shows advantages due to its distinguished highly specific surface area, mechanical, electrical, and thermal properties, with minor drawbacks such as costs generated by the production methods, poor solubility, and its tendency to agglomerate. Overall, graphite derivatives, such as graphene and graphene oxide, are considered as promising anticorrosion coatings for metals due to their superior properties, including lightweight, impermeability, inertness, wear resistance, and mechanical stability. Their chemical inertness is considered as one of the strongest justifications for their use as anticorrosion coatings alongside their high affinity for self-healing. Spray coating GO/epoxy self-healing composite coatings cause the corrosion potential for GO/EP composite coatings to change towards more positive values with and lower the i_{corr} values, indicating high corrosion resistance for epoxy composite coatings [96]. Spray coating alkyd/exfoliated graphene oxide nanosheet composite, with well-distributed GO nanosheets (0.5 wt.%) filled alkyd formulation, exhibits more resistance to corrosion than monolithic composite coating. The mixed formulations of spray coating composites, such as GO-Fe_3O_4@ poly (DA + KH550) hybrid/epoxy, in the presence of potential penetrating of O_2 and H_2O through the micropores of the coating can reduce its functionality. Yet, in the presence of graphene within the epoxy matrix, the coating performance improves. The anticorrosion behavior of the coating was greatly enhanced due to the high aspect ratio of graphene oxide and the synergistic effect of graphene oxide and magnetite nanoparticles [97].

Graphite-based materials have also shown enhanced potential as fillers for polymeric matrices, which can be efficiently used as a barrier or protective layer for most of metals against corrosion (polyurethane/graphene self-healing nanocomposites) [98]. The graphene-based smart anticorrosion coating loaded with an inhibitor not only maintains the excellent barrier properties of graphene (passive anticorrosion), but also enhances the smart anticorrosion performance of the inhibitor in the presence of active anticorrosion and amino-acid-based (11-(4-(pyrene-1-yl)butanamidoundecanoic acid. The system ensures self-repairing, which contains carbon allotropes (graphene and single wall carbon nanotubes) [99]. The indirect graphene coating on steel, copper, and carbon steel has benefits, such as cost effectiveness, uniform deposition, good control of coating thickness, and anti-corrosion applications; and drawbacks such as poor adhesion of GO to the substrate [100]. An effective distribution of such

materials into the polymer matrix can be achieved by different ways, including surface functionalization and selection of a polymer with suitable functional groups that can interact with graphite derivatives to form some kind of physical or chemical bonding [101]. In the exfoliated graphite sheet /polyetherimide (UFG/PEI) nanocomposite systems, the applied coatings show long-term corrosion protection for the metal and this can be attributed to the inclusion of the exfoliated graphite into the polymeric matrix, with a high chance of self-repairing [102]. The electronic transport properties of graphite-based materials mainly depend on the thickness of the forming layers, while the barrier properties are mainly controlled by reducing the ion transport, which is preserved even for the multilayer graphene and the functionalized graphene derivatives, and can create protection efficiency in the graphite intercalation compound, GIG (up to 76%) [103].

The graphene healing ability evolves around two main mechanisms: (i) the healing induced by high temperatures (the kinetic energy available at room temperature is not enough to allow free atoms to overcome the energetic barriers and trigger the healing process) and; (ii) heating effects where the creation of a hole in the graphene structures generate significant modifications in the energy landscape, experienced by atoms with up to 150 meV energy barrier. This behavior is necessary in order to reach the interior of the defect and to initiate the healing process after the atoms are trapped inside the hole. The presence of this barrier can confine them, favoring their reaction with the membrane edges, and contributing to the healing process [104]. The graphene oxide can be an alternative due to the strength of its structural similarities with graphite. This oxidized form of graphene possesses superior mechanical strength, chemical, and thermal stability. Graphene oxide has been considered a promising nanomaterial in barrier applications. This molecule does not allow the diffusion of small atoms or compounds due to the high density of the constituent electrons of the honeycomb-like structures from the planar sheet [103]. The non-covalent surface treatment of graphene oxide can modify the hybridization of the carbon structure from sp^2 to sp^3, which increases the number of defects on the basal plane and impacts the mechanical properties of the GO nanosheets [105]. Graphite derivatives can enhance the corrosion protection through other approaches. They can play a key role in improving the adhesion of the different coatings, especially for coatings that suffer from brittleness and weak resistance to crack corrosion, such as reinforcing the epoxy composite coatings by the different concentrations of reduced graphene oxide (RGO) [106]. The GO nanosheets can be assembled into three-dimensional layered sheets, which keep the integrity of the coating by mitigating the exchange of volatile compounds with the external environment. In addition to its chemical inertness, electrical conductivity, and intrinsic impermeability, the size of the graphene flakes has a considerable influence over the performance of the coating [107]. Javidparvar et al. [108] used graphene oxide as a platform to load the corrosion inhibitor (BTA (benzotriazole) and cerium) to form a controlled release system, and found that the corrosion degree of metal substrate was greatly suppressed. Liu et al. [109] successfully attached the cyclodextrin nanocontainer to the surface of GO by

strong hydrogen bonding, and then loaded BTA into the cyclodextrin nanocontainer to prepare a smart graphene-based protective coating. The study found that the BTA in the cyclodextrin nanocontainer could be effectively released, forming a protective film on the surface of substrate to prevent further corrosion when the pH in the external environment was changed. These researches have emphasized the importance of the distribution of graphene oxide (GO) in solvent-based epoxy coatings for superior protection. The better corrosion performance of GO sheets was correlated to the high aspect ratio of graphene oxides in its structure. The composite coatings containing GO provides a substantial barrier against corrosion by blocking the diffusion path of corrosive ions toward the substrate [110].

Systems, including graphene sheets, containing porous polyhedral oligomeric silsesquioxane (POSS) framework can be synthesized as nanocontainer for self-healing organic coating. Ye et al. [111] prepared such a system with BTA loaded into the porous graphene sheets and then embedded into epoxy coating to form a composite coating. The spontaneous release from graphene-based nanocontainer leads to the self-healing. They also dispersed the GO in DMSO (Dimethyl sulfoxide) via ultrasonication, infiltrated with 8-POSS and paraformaldehyde, loaded with BTA molecules in 8-POSS porous structure, and coated with epoxy resin (E-44). The BTA loading and release kinetics indicate the self-healing behavior [112]. While the mixture in 8-PG(propylene glycol)-BTA/EP(Ethylene propylene) specimen displays a higher impedance than EP and 8-PG/EP specimens, the corrosion reaction processes will be significantly inhibited. Besides, the impedance difference at the defect and intact region can be measured to evaluate the self-healing ability of the coatings. The released BTA forms a protective film ($\alpha - FeOOH$) with the metal ions to restore the defect region and inhibit the redox reaction at the interface. The EIS results indicate that the impedance (Z) value and the formation of a protective film on the steel surface are caused by the release of BTA. This film can block the direct contact between the corrosive medium, showing high R_c and R_{ct} values during that time. The BTA coating can fill the defect and further enhance the compactness of the coating, causing a decrease in oxygen permeability (P_{O_2}) form $1.876 \times 10^{-12} cm^3.cm/cm^2.s.Pa$ to $1.127 \times 10^{-13} cm^3.cm/cm^2.s.Pa$, with about three times lower medium (water) uptake. As the GO causes pH response, the change of local pH would trigger the release of BTA. In the process of BTA adsorption and deposition, the 8-PG exhibits an excellent barrier property, which could greatly reduce the longitudinal diffusion of the corrosive media and improve the self-healing efficiency of the coating [29]. Ye et al. reported that the spray coating of graphene with novel aniline trimer (AT) creates the functionalized graphene sheets (SAT-G) structure. These precursors can be applied to create composite coatings with 0.5 and 1 wt.% of SAT-G as 0.5% SAT-G/EP and 1% SAT-G/EP. As a result, the large diameter of the capacitive arc in the obtained EIS results suggests an excellent barrier property of the fabricated coatings. The hybrid functionalized graphene sheets that are well dispersed in the epoxy matrix, provide a superior anticorrosion property with promising self-healing and shielding

effects [113]. The use of polyaniline nanofibers (PANI) modified graphene oxide (GO) in epoxy coating system creates an anticorrosion system through a layer-by-layer (L-b-L) assembly technique. The Polyaniline nanofibers can be functionalized with GO sheets by different methods. In the most common method, the polymerization of aniline on GO can be carried out in the presence of an initiator (ammonium persulfate). This process creates GO-Pani-GI (green corrosion inhibitors) nanosheets, which decrease i_{corr} from 11.5 to 2.6 ($\mu A/cm^2$) in mild steel substrates [114]. In the self-healing composite system developed by Zhao et al., the metal organic frameworks (MOFs) were in situ grown on the graphene oxide (GO) sheets to fabricate GO/MOFs nanocontainers for both active and passive corrosion protection. The encapsulating benzotriazole embedded in polyvinyl butyral (PVB) resin helps the increase in R_{ct} from $10^5$to $10^{10}\Omega\, cm^2$ for pure copper or archaized bronze substrates. The GO/MOFs nanocontainers play a shielding role, which makes the path of the corrosion media intruding into the coatings, more twisted, which in return prolongs the protection time. Containers release the corrosion inhibitor in demand with external stimulation to perform the self-healing effect intelligently [115]. In the composite system of epoxy/polyamide and benzimidazole loaded on graphene oxide, the increase in R_{ct} from 5,000 to 25,000 $\Omega\, cm^2$ on mild steel substrates can be achieved. The barrier performance of polymer coatings is the main reason for the corrosion protection in the case of EP and GO/EP samples. In these two samples, the epoxy-based composites postpone accessing of the corrosive agents (water, oxygen, and ions) to the substrate surface. The graphene oxide, incorporated into the epoxy coating formulation, improves the corrosion resistance of the nanocomposite by blocking the diffusion pathway in the polymeric film. The improvement in the barrier performance of the nanocomposites directly depends on the dispersion quality of the GO into the polymer film. Therefore, the non-covalent surface modifications of the nanosheets by benzimidazole complexes may enhance the dispersion of nanosheets in the epoxy film and improve the barrier function [116].

Similar systems such as β-cyclodextrin/graphene (CD-G) (1 vol.%) in epoxy resin (E51) benefit from graphene-epoxy supramolecular elastomer, with intrinsic self-healing underwater and superior anticorrosion properties, to mitigate corrosion and promote self-repairing. The self-healing function derives from the graphene-assisted host-guest chemistry. The host molecules (β-CD) are attached to the graphene surfaces to generate the CD-G, which acts as the macro-crosslinker. Bode phase studies show that CD-G have high a phase angle (close to – 90º) at high frequencies, while this value for neat medium coating decreases to – 50º, showing that the impermeable graphene nanosheets inhibit the penetration of electrolyte and further enhance the self-healing efficiency to near 55%. According to LEIS results, the effective self-healing property of CD-G-reinforced elastomer coatings hinders corrosion propagation and decreases the localized corrosion activity at the exposed interface. The permeability coefficient of oxygen (P_{O_2}) decreases from $2.38\times10^{-12}cm^3.cm/cm^2.s.Pa$ to $1.84\times10^{-14}cm^3.cm/cm^2.s.Pa$ [117]. Graphene oxide microcapsules (GOMCs) can be embedded in polyurethane matrix, enabling

the fabrication of self-healing coating on hot dipped galvanized steel (HDGS). These parts act as microcontainers impacting properties, including mechanical stability, physical impermeability, compatibility between the shell and the coating matrix, and effective storage of the healing agent. The oxygen containing functional groups on the GO shell creates good compatibility GOMCs and PU matrix. The monolithic and reinforced coatings show a decrease of the arc radius of the Nyquist plot after a long duration of exposure, which corresponds to decrease in the impedance modulus of the coatings and the diffusion of the electrolytes in the organic coatings. The impedance modulus in this system increases10^5 times. The possible crack initiation via thermal cycling, coupling stress, accumulation of the corrosion products under the organic coating, and the mechanical damage are the main degradation reasons. After the oxidation/polymerization reaction, the healing agent solidifies and heals the cracks. As a result, cracks propagate autonomously through the microcapsules, instead of the interface between GOMCs and PU matrix [118].

14.4 The conclusion and future scope

The potential utilization of inert carbon nano allotropes as self-healing anticorrosive substitutes for conventional coatings can be achieved due to their general properties, such as high aspect ratio, high strength, flexibility, and low density; combined with medium-activated self-repairing properties, such as chemically, mechanically, mechano-chemical activation, and reinforced with corrosion inhibition agents. The most common designs in these systems involves carbon nanoallotropes in hybrid with other anticorrosive substances in a synergic application, which includes principal barrier formation by carbon allotrope(s) and surrounding the polymer materials matrix against corrosive agents (bipolar hydrophobic action) in the presence of healing and corrosion inhibition agents. The carbon allotropes facilitate the agents transfer to the necessary zone via their self-containment (CNTs), micro capsulation, inter-layer, and surface adsorption (graphene and graphene oxides) in monolithic, composite, or hybrid capacities.

The increasing trends in carbon allotrope offer large scale production and application (CNTs, graphene and hybrid carbon-based nanomaterials), and the increase in their availability facilitates their corrosion inhibition efficiency through research studies and on-site applications. The estimates of market domination of carbon allotropes (such as graphene's market size valued at $91.3 million in 2019, which is projected to reach $1,369.1 million by 2027), growing at a CAGR (compound annual growth rate) of 40.2% from 2020 to 2027 and CNTs projected to grow from USD 876 million in 2021 to USD 1,714 million by 202, at a CAGR of 14.4% [119]) shows the potential of application as coating and corrosion inhibition, although this usage cannot compete with electrical and electro-thermal application of carbon nano allotropes.

References

[1] Kokalj, A. Molecular modeling of organic corrosion inhibitors: Calculations, pitfalls, and conceptualization of molecule–surface bonding. Corros. Sci. 2021, 193, 109650.

[2] Ramakrishnan, T.; Raja Karthikeyan, K.; Tamilselvan, V.; Sivakumar, S.; Gangodkar, D.; Radha, H., et al. Study of various epoxy-based surface coating techniques for anticorrosion properties. Adv. Mater. Sci. Eng. 2022, 2022.

[3] Zhang, F.; Ju, P.; Pan, M.; Zhang, D.; Huang, Y.; Li, G., et al. Self-healing mechanisms in smart protective coatings: A review. Corros. Sci. 2018, 144, 74–88.

[4] Fouda, -A.E.-A.S.; El-Askalany, A.H.; Molouk, A.F.; Elsheikh, N.S.; Abousalem, A.S. Experimental and computational chemical studies on the corrosion inhibitive properties of carbonitrile compounds for carbon steel in aqueous solutions. Sci. Rep. 2021, 11(1), 1–24.

[5] Sun, J.; Wang, Y.; Li, N.; Tian, L. Tribological and anticorrosion behavior of self-healing coating containing nanocapsules. Tribol. Int. 2019, 136, 332–341.

[6] Zhang, M.Q.; Rong, M.Z.; Yin, T. Self-healing polymers and polymer composites. Self-Healing Mater. Fund. Des. Strat. Appl. 2008, 29–71.

[7] Yan, D.; Wang, Y.; Liu, J.; Song, D.; Zhang, T.; Liu, J., et al. Self-healing system adapted to different pH environments for active corrosion protection of magnesium alloy. J. Alloys Compd. 2020, 824, 153918.

[8] Wypych, G. Self-healing materials, Ontario M1E 1C6, ChemTec Publishing, Canada, 2019.

[9] Karaxi, E.K.; Kartsonakis, I.A.; Charitidis, C.A. Assessment of self-healing epoxy-based coatings containing microcapsules applied on hot dipped galvanized steel. Front. Mater. 2019, 222.

[10] Fedrizzi, L.; Fürbeth, W.; Montemor, F. Self-healing properties of new surface treatments (EFC 58), Institute of Materials. Minerals and Mining, 2011.

[11] González-García, Y.; García, S.J.; Hughes, A.E.; Mol, J.M.C. A combined redox-competition and negative-feedback SECM study of self-healing anticorrosive coatings. Electrochem. Commun. 2011, 13(10), 1094–1097.

[12] Lutz, A.; van den Berg, O.; Wielant, J.; De Graeve, I.; Terryn, H. A multiple-action self-healing coating. Front. Mater. 2016, 2.

[13] Zhang, Y.; Yu, M.; Chen, C.; Li, S.; Liu, J. Self-healing coatings based on stimuli-responsive release of corrosion inhibitors: A review. Front. Mater. 2022, 8.

[14] Islam, S.; Bhat, G. Progress and challenges in self-healing composite materials. Mater. Adv. 2021, 2(6), 1896–1926.

[15] Bekas, D.G.; Tsirka, K.; Baltzis, D.; Paipetis, A.S. Self-healing materials: A review of advances in materials, evaluation, characterization and monitoring techniques. Compos. Part B Eng. 2016, 87, 92–119.

[16] Thostenson, E.T.; Chou, T.-W. Carbon nanotube networks: Sensing of distributed strain and damage for life prediction and self healing. Adv. Mater. 2006, 18(21), 2837–2841.

[17] Jiang, X.; Xi, M.; Bai, L.; Wang, W.; Yang, L.; Chen, H., et al. Surface-initiated PET-ATRP and mussel-inspired chemistry for surface engineering of MWCNTs and application in self-healing nanocomposite hydrogels. Mater. Sci. Eng. C. 2020, 109, 110553.

[18] Khan, A.; Jawaid, M.; Asiri, A.M.A. Self-healing composite materials. 2020.

[19] Wu, X.-F.; Rahman, A.; Zhou, Z.; Pelot, D.D.; Sinha-Ray, S.; Chen, B., et al. Electrospinning core-shell nanofibers for interfacial toughening and self-healing of carbon-fiber/epoxy composites. J. Appl. Polym. Sci. 2013, 129(3), 1383–1393.

[20] Kausar, A. Self-healing polymer/carbon nanotube nanocomposite: A review. J. Plast. Film Sheeting. 2021, 37(2), 160–181.

[21] Verma, C.; Quraishi, M.A.; Ebenso, E.E.; Hussain, C.M. Recent advancements in corrosion inhibitor systems through carbon allotropes: Past, present, and future. Nano Select. 2021, 2(12), 2237–2255.
[22] Su, Y.; Kravets, V.; Wong, S.; Waters, J.; Geim, A.K.; Nair, R.R. Impermeable barrier films and protective coatings based on reduced graphene oxide. Nat. Commun. 2014, 5(1), 1–5.
[23] Deline, A.R.; Frank, B.P.; Smith, C.L.; Sigmon, L.R.; Wallace, A.N.; Gallagher, M.J., et al. Influence of oxygen-containing functional groups on the environmental properties, transformations, and toxicity of carbon nanotubes. Chem. Rev. 2020, 120(20), 11651–11697.
[24] Yabuki, A. Self-healing coatings for corrosion inhibition of metals. Modern Appl. Sci. 2015, 9(7), 214.
[25] Kötteritzsch, J.; Schubert, U.S.; Hager, M.D. Triggered and self-healing systems using nanostructured materials. Nanotechnol. Rev. 2013, 2(6), 699–723.
[26] Tan, P.; Somashekar, A.; Casari, P.; Bhattacharyya, D. Healing efficiency characterization of self-repairing polymer composites based on damage continuum mechanics. Compos. Struct. 2019, 208, 367–376.
[27] Kwak, S.Y.; Giraldo, J.P.; Lew, T.T.S.; Wong, M.H.; Liu, P.; Yang, Y.J., et al. Polymethacrylamide and carbon composites that grow, strengthen, and self-repair using ambient carbon dioxide fixation. Adv. Mater. 2018, 30(46), 1804037.
[28] Yang, Y.; Urban, M.W. Self-repairable polyurethane networks by atmospheric carbon dioxide and water. Angew. Chem. 2014, 126(45), 12338–12343.
[29] Palumbo, G. Smart coatings for corrosion protection by adopting microcapsules. Phys. Sci. Rev. 2016, 1, 5.
[30] Ulaeto, S.B.; Rajan, R.; Pancrecious, J.K.; Rajan, T.; Pai, B. Developments in smart anticorrosive coatings with multifunctional characteristics. Prog. Org. Coat. 2017, 111, 294–314.
[31] Strandman, S.; Zhu, X. Self-healing supramolecular hydrogels based on reversible physical interactions. Gels 2016, 2(2), 16.
[32] Samadzadeh, M.; Boura, S.H.; Peikari, M.; Kasiriha, S.; Ashrafi, A. A review on self-healing coatings based on micro/nanocapsules. Prog. Org. Coat. 2010, 68(3), 159–164.
[33] Bhattacharya, S.; Phatake, R.S.; Nabha Barnea, S.; Zerby, N.; Zhu, -J.-J.; Shikler, R., et al. Fluorescent self-healing carbon dot/polymer gels. ACS Nano 2019, 13(2), 1433–1442.
[34] Kim, D.-M.; Cho, Y.-J.; Choi, J.-Y.; Kim, B.-J.; Jin, S.-W.; Chung, C.-M. Low-temperature self-healing of a microcapsule-type protective coating. Materials 2017, 10(9), 1079.
[35] Liu, T.; Zhao, H.; Mao, F.; Li, J. Electrochemical investigation of graphene on the corrosion of scratched polyurea-based organic coating. Mater. Res. Express 2019, 6(12), 125619.
[36] Williams, G.; Trask, R.; Bond, I. A self-healing carbon fibre reinforced polymer for aerospace applications. Compos. Part A Appl. Sci. Manuf. 2007, 38(6), 1525–1532.
[37] Yabuki, A.; Shiraiwa, T.; Fathona, I.W. pH-controlled self-healing polymer coatings with cellulose nanofibers providing an effective release of corrosion inhibitor. Corros. Sci. 2016, 103, 117–123.
[38] Hammer, L.; Van Zee, N.J.; Nicolaÿ, R. Dually crosslinked polymer networks incorporating dynamic covalent bonds. Polymers. 2021, 13(3), 396.
[39] Shchukina, E.; Shchukin, D.G. Nanocontainer-based active systems: From self-healing coatings to thermal energy storage. Langmuir. 2019, 35(26), 8603–8611.
[40] Liang, C.; Li, Z.; Dai, S. Mesoporous carbon materials: Synthesis and modification. Angew. Chem. Int. Ed. 2008, 47(20), 3696–3717.
[41] Aïssa, B.; Therriault, D.; Haddad, E.; Jamroz, W. Self-healing materials systems: Overview of major approaches and recent developed technologies. Adv. Mater. Sci. Eng. 2012, 2012.

[42] Beygisangchin, M.; Abdul Rashid, S.; Shafie, S.; Sadrolhosseini, A.R.; Lim, H.N. Preparations, properties, and applications of polyaniline and polyaniline thin films – A review. Polymers. 2021, 13(12), 2003.
[43] Kuznetsov, Y.I.; Redkina, G.V. Thin protective coatings on metals formed by organic corrosion inhibitors in neutral media. Coatings. 2022, 12(2), 149.
[44] Yan, R.; He, W.; Zhai, T.; Ma, H. Anticorrosion organic–inorganic hybrid films constructed on iron substrates using self-assembled polyacrylic acid as a functional bottom layer. Electrochim. Acta. 2019, 295, 942–955.
[45] Vijayan, P.P.; Hany El-Gawady, Y.M.; Al-Maadeed, M.A.S. Halloysite nanotube as multifunctional component in epoxy protective coating. Ind. Eng. Chem. Res. 2016, 55(42), 11186–11192.
[46] Dong, Y.; Wang, F.; Zhou, Q. Protective behaviors of 2-mercaptobenzothiazole intercalated Zn–Al-layered double hydroxide coating. J. Coat. Technol. Res. 2014, 11(5), 793–803.
[47] Taghavikish, M.; Dutta, N.K.; Roy Choudhury, N. Emerging corrosion inhibitors for interfacial coating. Coatings. 2017, 7(12), 217.
[48] Sahin, S.; Dykstra, J.E.; Zuilhof, H.; Zornitta, R.L.; de Smet, L.C.P.M. Modification of cation-exchange membranes with polyelectrolyte multilayers to tune ion selectivity in capacitive deionization. ACS Appl. Mater. Interfaces. 2020, 12(31), 34746–34754.
[49] Park, J.S.; Takahashi, K.; Guo, Z.; Wang, Y.; Bolanos, E.; Hamann-Schaffner, C., et al. Towards development of a self-healing composite using a mendable polymer and resistive heating. J. Compos. Mater. 2008, 42(26), 2869–2881.
[50] Luo, X.; Mather, P.T. Shape memory assisted self-healing coating. ACS Macro Lett. 2013, 2(2), 152–156.
[51] Shojaei, A. Modeling of self-healing smart composite materials. Li G, editor, Elsevier, Cambridge, CB22 3HJ, UK, 2015.
[52] Kessler, M.; Sottos, N.R.; White, S. Self-healing structural composite materials. Compos. Part A Appl. Sci. Manuf. 2003, 34(8), 743–753.
[53] Mphahlele, K.; Ray, S.S.; Kolesnikov, A. Self-healing polymeric composite material design, failure analysis and future outlook: A review. Polymers. 2017, 9(10), 535.
[54] Mahmood, H.; Dorigato, A.; Pegoretti, A. Healable carbon fiber-reinforced epoxy/cyclic olefin copolymer composites. Materials. 2020, 13(9), 2165.
[55] Paolini, N.A.; Cordeiro Neto, A.G.; Pellanda, A.C.; Carvalho Jorge, A.; Barros Soares, B.; Floriano, J.B., et al Evaluation of corrosion protection of self-healing coatings containing tung and copaiba oil microcapsules. Int. J. Polym. Sci. 2021, 2021.
[56] Snihirova, D.; Lamaka, S.V.; Cardoso, M.M.; Condeço, J.A.; Ferreira, H.E.; de Fatima Montemor, M. pH-sensitive polymeric particles with increased inhibitor-loading capacity as smart additives for corrosion protective coatings for AA2024. Electrochim. Acta 2014, 145, 123–131.
[57] Sauvant-Moynot, V.; Gonzalez, S.; Kittel, J. Self-healing coatings: An alternative route for anticorrosion protection. Prog. Org. Coat. 2008, 63(3), 307–315.
[58] Andreeva, D.V.; Shchukin, D.G. Smart self-repairing protective coatings. Mater. Today. 2008, 11(10), 24–30.
[59] Tabish, M.; Yasin, G.; Anjum, M.J.; Malik, M.U.; Zhao, J.; Yang, Q., et al. Reviewing the current status of layered double hydroxide-based smart nanocontainers for corrosion inhibiting applications. J. Mater. Res. Technol. 2021, 10, 390–421.
[60] Keshmiri, N.; Najmi, P.; Ramezanzadeh, M.; Ramezanzadeh, B.; Bahlakeh, G. Ultrastable porous covalent organic framework assembled carbon nanotube as a novel nanocontainer for anti-corrosion coatings: Experimental and computational studies. ACS Appl. Mater. Interfaces. 2022.
[61] Shchukina, E.; Wang, H.; Shchukin, D.G. Nanocontainer-based self-healing coatings: Current progress and future perspectives. Chem. Commun. 2019, 55(27), 3859–3867.

[62] Dennis, R.V.; Patil, V.; Andrews, J.L.; Aldinger, J.P.; Yadav, G.D.; Banerjee, S. Hybrid nanostructured coatings for corrosion protection of base metals: A sustainability perspective. Mater. Res. Express. 2015, 2(3), 032001.
[63] Mateos-Maroto, A.; Fernández-Peña, L.; Abelenda-Núñez, I.; Ortega, F.; Rubio, R.G.; Guzmán, E. Polyelectrolyte multilayered capsules as biomedical tools. Polymers. 2022, 14(3), 479.
[64] Cavallaro, G.; Milioto, S.; Lazzara, G. Halloysite nanotubes: Interfacial properties and applications in cultural heritage. Langmuir. 2020, 36(14), 3677–3689.
[65] Hughes, A.E.; Cole, I.S.; Muster, T.H.; Varley, R.J. Designing green, self-healing coatings for metal protection. NPG Asia Mater. 2010, 2(4), 143–151.
[66] Gómez, I.J.; Vázquez Sulleiro, M.; Mantione, D.; Alegret, N. Carbon nanomaterials embedded in conductive polymers: A state of the art. Polymers. 2021, 13(5), 745.
[67] Amin, H.M.; Galal, A. Corrosion protection of metals and alloys using graphene and biopolymer based nanocomposites, CRC Press, 2021.
[68] Hirsch, A. The era of carbon allotropes. Nat. Mater. 2010, 9(11), 868–871.
[69] Nasir, S.; Hussein, M.Z.; Zainal, Z.; Yusof, N.A. Carbon-based nanomaterials/allotropes: A glimpse of their synthesis, properties and some applications. Materials. 2018, 11(2), 295.
[70] Pan, L.; Li, G.; Wang, Z.; Liu, D.; Zhu, W.; Tong, C., et al. Carbon dots as environment-friendly and efficient corrosion inhibitors for Q235 steel in 1 M HCl. Langmuir. 2021, 37(49), 14336–14344.
[71] Parvate, S.; Dixit, P.; Chattopadhyay, S. Superhydrophobic surfaces: Insights from theory and experiment. J. Phys. Chem. B. 2020, 124(8), 1323–1360.
[72] Thakral, S.; Mehta, R. Fullerenes: An introduction and overview of their biological properties. Ind. J. Pharm. Sci. 2006, 68(1), 13.
[73] Samadianfard, R.; Seifzadeh, D.; Habibi-Yangjeh, A.; Jafari-Tarzanagh, Y. Oxidized fullerene/sol-gel nanocomposite for corrosion protection of AM60B magnesium alloy. Surf. Coat. Technol. 2020, 385, 125400.
[74] Pourhashem, S.; Ghasemy, E.; Rashidi, A.; Vaezi, M.R. Corrosion protection properties of novel epoxy nanocomposite coatings containing silane functionalized graphene quantum dots. J. Alloys Compd. 2018, 731, 1112–1118.
[75] Rajak, D.K.; Pagar, D.D.; Kumar, R.; Pruncu, C.I. Recent progress of reinforcement materials: A comprehensive overview of composite materials. J. Mater. Res. Technol. 2019, 8(6), 6354–6374.
[76] Zhang, L.; Chao, Y.; Yang, K.; Xue, D.; Zhou, S. Recent advances in metal/alloy nano coatings for carbon nanotubes based on electroless plating. Front Chem. 2022, 9, 782307.
[77] Kania, A.; Cesarz-Andraczke, K.; Brytan, Z.; Reimann, Ł.; Smolarczyk, P. The influence of casein coatings on the corrosion behavior of Mg-based alloys. Materials. 2022, 15(4), 1399.
[78] Norizan, M.N.; Moklis, M.H.; Demon, S.Z.N.; Halim, N.A.; Samsuri, A.; Mohamad, I.S., et al. Carbon nanotubes: Functionalisation and their application in chemical sensors. RSC Adv. 2020, 10(71), 43704–43732.
[79] Reddy, K.R.; Sin, B.C.; Ryu, K.S.; Noh, J.; Lee, Y. In situ self-organization of carbon black–polyaniline composites from nanospheres to nanorods: Synthesis, morphology, structure and electrical conductivity. Synth. Met. 2009, 159(19–20), 1934–1939.
[80] Farag, A.A.; Kabel, K.I.; Elnaggar, E.M.; Al-Gamal, A.G. Influence of polyaniline/multiwalled carbon nanotube composites on alkyd coatings against the corrosion of carbon steel alloy. Corros. Rev. 2017, 35(2), 85–94.
[81] Ioniţă, M.; Prună, A. Polypyrrole/carbon nanotube composites: Molecular modeling and experimental investigation as anti-corrosive coating. Prog. Org. Coat. 2011, 72(4), 647–652.
[82] Ganash, A. Electrochemical synthesis and corrosion behaviour of polypyrrole and polypyrrole/carbon nanotube nanocomposite films. J. Compos. Mater. 2014, 48(18), 2215–2225.

[83] Kumar, A.M.; Gasem, Z.M. In situ electrochemical synthesis of polyaniline/f-MWCNT nanocomposite coatings on mild steel for corrosion protection in 3.5% NaCl solution. Prog. Org. Coat. 2015, 78, 387–394.
[84] Rajyalakshmi, T.; Pasha, A.; Khasim, S.; Lakshmi, M.; Murugendrappa, M.; Badi, N. Enhanced charge transport and corrosion protection properties of polyaniline–carbon nanotube composite coatings on mild steel. J. Electron. Mater. 2020, 49(1), 341–352.
[85] Wei, H.; Ding, D.; Wei, S.; Guo, Z. Anticorrosive conductive polyurethane multiwalled carbon nanotube nanocomposites. J. Mater. Chem. A 2013, 1(36), 10805–10813.
[86] Sivaraj, D.; Vijayalakshmi, K. Novel synthesis of bioactive hydroxyapatite/f-multiwalled carbon nanotube composite coating on 316L SS implant for substantial corrosion resistance and antibacterial activity. J. Alloys Compd. 2019, 777, 1340–1346.
[87] Liu, Y.; Zhao, J.; Zhao, L.; Li, W.; Zhang, H.; Yu, X., et al. High performance shape memory epoxy/carbon nanotube nanocomposites. ACS Appl. Mater. Interfaces. 2016, 8(1), 311–320.
[88] Wang, X.; Zhao, J.; Chen, M.; Ma, L.; Zhao, X.; Dang, Z.-M., et al. Improved self-healing of polyethylene/carbon black nanocomposites by their shape memory effect. J. Phys. Chem. B. 2013, 117(5), 1467–1474.
[89] Li, Q.; Mishra, A.K.; Kim, N.H.; Kuila, T.; Lau, K.-T.; Lee, J.H. Effects of processing conditions of poly(methylmethacrylate) encapsulated liquid curing agent on the properties of self-healing composites. Compos. Part B Eng. 2013, 49, 6–15.
[90] Li, Y.; Li, L.; Sun, J. Bioinspired self-healing superhydrophobic coatings. Angew. Chem. Int. Ed. 2010, 49(35), 6129–6133.
[91] Pingkarawat, K.; Bhat, T.; Craze, D.A.; Wang, C.H.; Varley, R.J.; Mouritz, A.P. Healing of carbon fibre–epoxy composites using thermoplastic additives. Polym. Chem. 2013, 4(18), 5007–5015.
[92] Wang, R.; Hu, H.; Liu, W.; Dai, C.; He, X.; Wang, S. Preparation and properties of self-healing carbon fiber reinforced epoxy composite. 18th International Conference on composite materials, 2015.
[93] Wang, Y.; Edgell, J.; Graham, N.; Jackson, N.; Liang, H.; Pham, D.T. Self-healing of structural carbon fibres in polymer composites. Cogent Eng. 2020, 7(1), 1799909.
[94] Wang, C.H.; Sidhu, K.; Yang, T.; Zhang, J.; Shanks, R. Interlayer self-healing and toughening of carbon fibre/epoxy composites using copolymer films. Compos. Part A Appl. Sci. Manuf. 2012, 43(3), 512–518.
[95] Pingkarawat, K.; Bhat, T.; Craze, D.; Wang, C.; Varley, R.J.; Mouritz, A. Healing of carbon fibre–epoxy composites using thermoplastic additives. Polym. Chem. 2013, 4(18), 5007–5015.
[96] Chen, L.; Liu, H.; Liu, Z.; Song, Q. Thermal conductivity and anti-corrosion of epoxy resin based composite coatings doped with graphene and graphene oxide. Compos. Part C Open Access. 2021, 5, 100124.
[97] Zhu, Q.; Li, E.; Liu, X.; Song, W.; Zhao, M.; Zi, L., et al. Synergistic effect of polypyrrole functionalized graphene oxide and zinc phosphate for enhanced anticorrosion performance of epoxy coatings. Compos. Part A Appl. Sci. Manuf. 2020, 130, 105752.
[98] Hamilton, A.R.; Sottos, N.R.; White, S.R. Pressurized vascular systems for self-healing materials. J. Royal Soc. Interface. 2012, 9(70), 1020–1028.
[99] Roy, S.; Baral, A.; Banerjee, A. An amino-acid-based self-healing hydrogel: Modulation of the self-healing properties by incorporating carbon-based nanomaterials. Chem. Eur. J. 2013, 19(44), 14950–14957.
[100] Mišković-Stanković, V.; Jevremović, I.; Jung, I.; Rhee, K. Electrochemical study of corrosion behavior of graphene coatings on copper and aluminum in a chloride solution. Carbon. 2014, 75, 335–344.
[101] Potts, J.R.; Dreyer, D.R.; Bielawski, C.W.; Ruoff, R.S. Graphene-based polymer nanocomposites. Polymer. 2011, 52(1), 5–25.

[102] Ding, R.; Li, W.; Wang, X.; Gui, T.; Li, B.; Han, P., et al A brief review of corrosion protective films and coatings based on graphene and graphene oxide. J. Alloys Compd. 2018, 764, 1039–1055.
[103] Smith, A.T.; LaChance, A.M.; Zeng, S.; Liu, B.; Sun, L. Synthesis, properties, and applications of graphene oxide/reduced graphene oxide and their nanocomposites. Nano Mater. Sci. 2019, 1(1), 31–47.
[104] Botari, T.; Paupitz, R.; da Silva Autreto, P.A.; Galvao, D.S. Graphene healing mechanisms: A theoretical investigation. Carbon. 2016, 99, 302–309.
[105] Huang, X.-M.; Liu, L.-Z.; Zhou, S.; Zhao, -J.-J. Physical properties and device applications of graphene oxide. Front. Phys. 2020, 15(3), 1–70.
[106] Zhu, L.; Feng, C.; Cao, Y. Corrosion behavior of epoxy composite coatings reinforced with reduced graphene oxide nanosheets in the high salinity environments. Appl. Surf. Sci. 2019, 493, 889–896.
[107] Necolau, M.-I.; Pandele, A.-M. Recent advances in graphene oxide-based anticorrosive coatings: An overview. Coatings. 2020, 10(12), 1149.
[108] Javidparvar, A.A.; Naderi, R.; Ramezanzadeh, B. Designing a potent anti-corrosion system based on graphene oxide nanosheets non-covalently modified with cerium/benzimidazole for selective delivery of corrosion inhibitors on steel in NaCl media. J. Mol. Liq. 2019, 284, 415–430.
[109] Liu, C.; Zhao, H.; Hou, P.; Qian, B.; Wang, X.; Guo, C., et al. Efficient graphene/cyclodextrin-based nanocontainer: Synthesis and host–guest inclusion for self-healing anticorrosion application. ACS Appl. Mater. Interfaces. 2018, 10(42), 36229–36239.
[110] Fang, Z.; Huang, L.; Fu, J. Research status of graphene polyurethane composite coating. Coatings. 2022, 12(2), 264.
[111] Ye, Y.; Chen, H.; Zou, Y.; Ye, Y.; Zhao, H. Corrosion protective mechanism of smart graphene-based self-healing coating on carbon steel. Corros. Sci. 2020, 174, 108825.
[112] Olivieri, F.; Castaldo, R.; Cocca, M.; Gentile, G.; Lavorgna, M. Innovative silver-based capping system for mesoporous silica nanocarriers able to exploit a twofold anticorrosive mechanism in composite polymer coatings: Tailoring benzotriazole release and capturing chloride ions. ACS Appl. Mater. Interfaces 2021, 13(40), 48141–48152.
[113] Ye, Y.; Zhang, D.; Liu, T.; Liu, Z.; Pu, J.; Liu, W., et al. Superior corrosion resistance and self-healable epoxy coating pigmented with silanzied trianiline-intercalated graphene. Carbon. 2019, 142, 164–176.
[114] Ramezanzadeh, B.; Kardar, P.; Bahlakeh, G.; Hayatgheib, Y.; Mahdavian, M. Fabrication of a highly tunable graphene oxide composite through layer-by-layer assembly of highly crystalline polyaniline nanofibers and green corrosion inhibitors: Complementary experimental and first-principles quantum-mechanics modeling approaches. J. Phys. Chem. C 2017, 121(37), 20433–20450.
[115] Zhao, Y.; Jiang, F.; Chen, Y.-Q.; Hu, J.-M. Coatings embedded with GO/MOFs nanocontainers having both active and passive protecting properties. Corros. Sci. 2020, 168, 108563.
[116] Javidparvar, A.A.; Naderi, R.; Ramezanzadeh, B. Manipulating graphene oxide nanocontainer with benzimidazole and cerium ions: Application in epoxy-based nanocomposite for active corrosion protection. Corros. Sci. 2020, 165, 108379.
[117] Liu, C.; Li, J.; Jin, Z.; Hou, P.; Zhao, H.; Wang, L. Synthesis of graphene-epoxy nanocomposites with the capability to self-heal underwater for materials protection. Compos. Commun. 2019, 15, 155–161.
[118] Li, J.; Feng, Q.; Cui, J.; Yuan, Q.; Qiu, H.; Gao, S., et al. Self-assembled graphene oxide microcapsules in Pickering emulsions for self-healing waterborne polyurethane coatings. Compos. Sci. Technol. 2017, 151, 282–290.
[119] Research and markets. Graphene Market by Type, and Application: Global Opportunity Analysis and Industry Forecast 2020–2027, May 2020 [Available from: https://www.researchandmarkets.com/reports/5125464/graphene.

Abhinay Thakur, Praveen Kumar Sharma, Ashish Kumar*

Chapter 15
Economics and commercialization of carbon allotropes nanostructured corrosion inhibitors

Abstract: Corrosion is an expensive and destructive issue in several industries as it can damage materials used to construct bridges and buildings, automobiles, water pipeline systems, petroleum constructions (e.g., pipelines, refineries), and so on. Annually, billions of dollars are invested in infrastructure replacement and corrosion control methods, resulting in losses of 3–4% of the Gross domestic product (GDP) in developed countries. The putative utilization of various nanostructured substances in corrosion protection, mitigation, and regulation is a matter of growing attention, in this regard. Due to their exceptional characteristics such as huge surface area, excellent mechanical properties, light weight, easy synthesis, and synergistic behavior with other materials, carbon allotropes (i.e., carbon black, fullerene, carbon nanotubes, carbon dots, graphene and graphene oxide) nanostructures coatings have become extremely important as an effective corrosion inhibitor. The goal of this chapter is to explore the economic and commercial growth and strategies used by various industries and countries around the world to employ carbon allotropes nanostructures-based corrosion inhibitors. As per current data, the worldwide corrosion inhibitor market was $6 billion (USD) in 2013, $7.7 billion (USD) in 2020, and is predicted to hit $10 billion (USD) by 2027. This chapter also throws light on carbon allotropes nanostructures-based coatings, economics, and commercialization of these carbon allotropes nanostructure-based corrosion inhibitors. Furthermore, morphological investigations of metal surfaces are provided.

Keywords: carbon allotropes, nanomaterials, anticorrosion, corrosion inhibitors, commercialization, sustainability

15.1 Introduction

Metals and their alloys are considered to be the industry's foundation, and they are employed in a broad range of applications in our daily lives, including industrial

*Corresponding author: **Ashish Kumar,** NCE, Department of Science and Technology, Government of Bihar, India, e-mail: drashishchemlpu@gmail.com
Abhinay Thakur, Praveen Kumar Sharma, Department of Chemistry, Faculty of Technology and Science, Lovely Professional University, Phagwara, Punjab, India

https://doi.org/10.1515/9783110782820-015

machinery, structural engineering, energy, electronics, petroleum refining, water purification, and so on. Metals, on the other hand, are thermodynamically unstable in extremely harsh conditions and corrode. Metallic corrosion causes annual financial damage of billions of dollars, around the globe [1–3]. Corrosion of metallic structures has become a terrible issue that has spread to a variety of disciplines. Corrosion causes loss of reliability, spillages of products, damage to metallic appliances, inability to utilize metallic components, and loss of valuable components like pipe obstruction, mechanical stress to groundwater pipes, and fatalities caused by mechanical loss of metallic bridges, cars, and airplanes, to name a few [4–8]. A corrosion inhibitor is commonly used as a corrosion control technique for its simplicity of usage, effectiveness, and low cost. Corrosion inhibitors could adhere to metal surfaces or interact with corrosion products such as metallic ions to form insoluble compounds that prevent subsequent corrosion. Corrosion inhibitors, on the other hand, have some limits in terms of innovation and implementation. Throughout the operating procedure, a corrosion inhibitor might hydrolyze and degrade. As a result, the quantity of inhibitors used in this strategy might be excessive in the beginning and very minimal, later. Not only is it a squandering of supplies, but also reduces production and servicing time. As a result, it is critical to construct another inhibitor, wherein a discharge mechanism can be engaged when corrosion occurs and maintains the amount in a moderate range, over time [9, 10]. When constructing an intelligent controlled-discharge inhibitor device, it is vital to include a smart on-off switch that can manage the inhibitor's discharge, based on environmental stimuli. Smart materials are smart coatings enclosing specific materials that show a rapid or piecemeal alteration in their dynamically adjusting swelling qualities, including a change in outer environment variables (such as pH, temperature). Organic coatings are an excellent way to prevent corrosion in metals and alloys. Nonetheless, even if there are no faults, a substantial percentage of hostile ions might permeate the covering over time, causing corrosion at the interaction. In any event, defects in the covering caused by an external attack, such as the impacts of pebbles or abrasion, are more dangerous. Organic/inorganic composite coatings provide long-term safety and durability. The organic portion of the coating provides the protective impact and self-healing characteristics to preserve the underneath substrate of metals, whereas, the inorganic pigment portion, which is typically used as an inhibitor, protects against corrosion [9, 11, 12]. The pigments that include chromates are most efficient. One of the most extensive and rigorous restrictions is on lead and hexavalent chromium. These constraints have prompted substantial research into the development of environment-friendly corrosion inhibitors and organic coating sections. An excellent corrosion inhibitor also should offer a number of benefits, including high inhibitory efficiency, low cost, low cytotoxicity, and ease of manufacture. The use of nanomaterial compounds in anticorrosive coatings and corrosion inhibitors could have a positive effect on the ecosystem. The nanomaterial compounds could remove the need for harmful solvents and have

also proved to be a suitable option to the toxic phosphate–chromate pretreatment of metallic substrates, which contains toxic hexavalent chromium.

According to the National Aeronautics and Space Administration (NASA) corrosion technology industry, the expense of corrosion to the United States is expected to be around $276 billion, each year. By the end of the year, the overall cost of corrosion would have surpassed $1 trillion [1, 13]. The National Association of Corrosion Engineers (NACE) studied the corrosion costs of the American economy, which is divided into five sectors. The research goes on to detail how much corrosion costs each business in terms of money:

- **Transportation:** $29.7 billion
- **Infrastructure:** $22.6 billion
- **Government:** $20.1 billion
- **Production and Manufacturing:** $17.6 billion
- **Utilities:** $47.9 billion

According to both NACE.org and NASA research, optimum corrosion treatment strategies could save organizations around 25% and 35% of yearly corrosion-related costs. Corrosion protection is critical for avoiding both direct and indirect costs. The money spent on restoring corroded materials is referred to as direct costs. Indirect costs include expenses caused as a result of manufacturing delays, environmental and health concerns, and legal responsibilities. In the United States alone, these two operational expenditures total $552 billion [14, 15]. The expense of corrosion in the manufacturing and production business is $17.6 billion per year. Here's how much revenue every sector loses because of corrosion:

- **Petroleum Refining:** $3.7 billion
- **Pulp and Paper:** $6 billion
- **Food Processing:** $2.1 billion
- **Oil and Gas Exploration and Production:** $1.4 billion
- **Chemical, Petrochemical, and Pharmaceutical:** $1.7 billion
- **Home Appliances:** $1.5 billion
- **Mining:** $0.1 billion
- **Agricultural:** $1.1 billion

Corrosion has several direct costs including capital, which entails the restoration of structures, equipment, and machines; construction and regulation entailing materials choice, corrosion permits, special treatments (e.g., acid cleaning), regulating chemicals, repair and restoration; degradation and financial losses, which entails products and loss of production, tech assistance; and supplementary reserve and insurance that are indirect corrosion expenses. According to assessments conducted in the United Kingdom and the United States, the total direct and indirect costs of corrosion amount to about 4.5% of the gross national product (GNP) [16–18]. This equates to around $500 per year per capita for the populous of developed countries. In addition,

it is projected that around 10% of the world's steel output, or nearly 5×10^{-7}tons per year, is produced to replace rusted steel. One ton of steel is rusted every 90 s in the United Kingdom, according to statistics. Apart from metal waste, the energy required to produce one ton of steel using iron ore is sufficient to power a typical household for three months. Corrosion would also result in higher energy consumption, health problems due to toxic components, and even fatality due to explosions or deterioration of conveyance (aircraft). The Corrosion Atlas case history 01.11.06.06 documented a disastrous event caused by distillation pipeline failures, which culminated in a fire and overall refinery facility damage. As a result, efficient corrosion prevention and management could assist in minimizing economic, societal, and physical losses. Each of these implications raised societal pressure to maintain corrosion and protect the natural environment. Considering the thermodynamic rationale for corrosion, it is not surprising that the costs associated with corrosion are substantial. Based on numerous studies performed over the last 30 years, the average direct cost of corrosion to an industrial economy is roughly 3.1% of the country's GNP. In the United States, this equates to about $276 billion per year. The Ministry of Defense solely spends $20 billion on corrosion [19–21]. Given the huge financial, security, and historical implications of corrosion on civilization, and the premise that corrosion of metals is an electrochemical method, it is not strange that the Corrosion Department is one of the oldest departments. Although the Section was founded in 1942, corrosion has been a major topic of discussion in Society since 1903. Uhlig wrote reviews of the early literature and history of the Section during the Society's 50th and 75th anniversaries, while Isaacs released a centenary assessment, much later. Uhlig's Corrosion Handbook is recommended for anyone looking for a comprehensive source of corrosion literature. The global corrosion inhibitor market is predicted to grow at a CAGR of 4.9% between 2021 and 2026, approaching USD 7.9 billion in 2021 and USD 10.1 billion in 2026. The marketplace for corrosion inhibitors is being driven by rising consumption from multiple end industries, as well as stringent regulatory and sustainability demands addressing the ecosystem [9, 14, 22, 23]. We have addressed the commercialization and economic possibilities of corrosion inhibitors in this chapter, with a focus on carbon allotropes based on nanostructures.

15.2 Carbon allotropes nanostructures (CAN)-based corrosion inhibitors

Carbon is found in a variety of monomeric allotropes, including diamond, graphite, graphene, fullerene, carbon nanohorns and carbon nanotubes (CNTs), among others. The solubility of carbon allotropes could be improved by properly functionalizing them and adding polar substituents to their molecular geometries. Covalent and noncovalent functionalization techniques could both be used to functionalize carbon

allotropes [24–26]. Covalent functionalization comprises covalent bonding among carbon allotropes along with their polar substituents, whereas non-covalent functionalization comprises weak intermolecular (van der Waals forces) among carbon allotropes, along with their polar substituents. On average, allotropes of carbon contain one or more particular sites, wherein functionalization by covalent linkage could be accomplished. For instance, graphene analogs could be functionalized with –OH (hydroxyl), –COC– (epoxide ring), and –COOH (carboxyl) using esterification and condensation processes. Although covalent functionalization of > C=C is challenging, a free radical technique, such as dienophile assault, could be used. Among the common covalent functionalizations of graphene, analogs are esterification, cycloaddition, isocyanate, acylation, diazotization, and ring rearrangement, under the action of a nucleophile [27, 28]. Figure 15.1 shows the various carbon nanostructures existing in a variety of shapes and sizes [29].

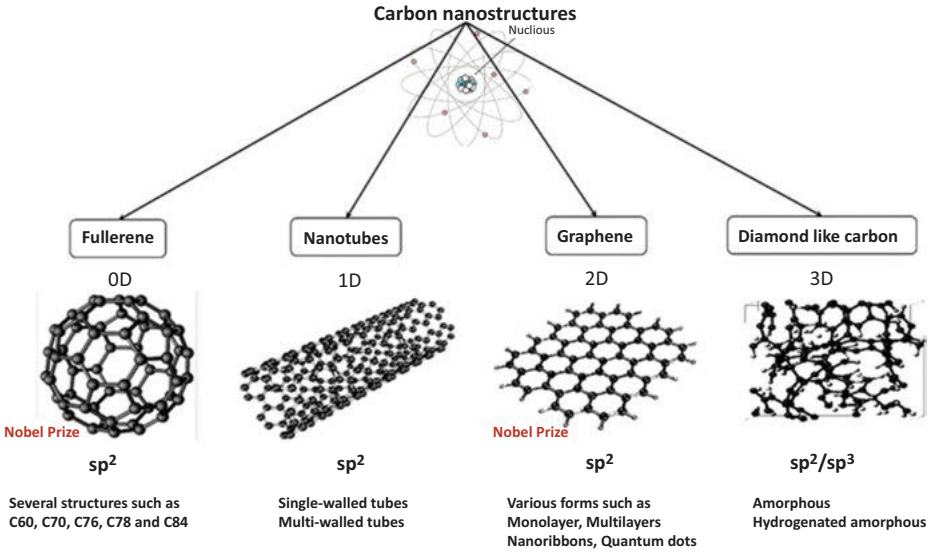

Fig. 15.1: Carbon nanostructures come in a variety of shapes and sizes. Adapted with permission from Ref. [29]. Based on the Creative common attribution-based license CCBY.

Several primary amines, porphyrins, polythiophenes, phthalocyanines, and amine-terminated numerous organic compounds, particularly C60 fullerene, have been used to covalently functionalize carbon allotropes via the above chemical processes. Epoxide ring-opening reactions with alcohol and amine ($R\text{-}NH_2$) could also be used to functionalize the graphene oxide (GO) (R-OH). The poly(vinyl alcohol) and poly(allylamine) moieties are commonly attached to aromatic rings using similar processes [30–32]. The cycloaddition reaction catalyzed by free radicals could be used to functionalize > C=C. (Diels-Alder type reaction). The cycloaddition step converts sp^2-hybridized

carbons to sp^3-hydridized carbons, lowering the GO's electron conductivity capability. Carbon nanotubes (CNTs) are carbon tubes having dimensions estimated in nanometers (nm). Single-walled carbon nanotubes (SWCNTs) and multi-walled carbon nanotubes (MWCNs) are two types of carbon nanotubes (MWCNTs). In 1993, Ichihashi and Iijima and Bethune et al. discovered and isolated carbon nanotubes. Van der Waals interactions were used to join two or more rings of CNTs in MWCNTs. CNTs and their derivatives (functionalized CNTs) are frequently utilized in material science for a range of biochemical and manufacturing uses due to their outstanding strength properties, mechanical strength, and nano-sized architecture.

However, as CNTs have high electrical conductivity, they accelerate the rate of corrosion in aqueous media by boosting the electron transfer process. As a result, despite their numerous advantages, use of CNTs as corrosion inhibitors (CIs), particularly in the aqueous environment, is severely limited. However, they must be covalently functionalized in order to get the desired anticorrosive characteristics. Numerous chemical transformations could be used to covalently functionalize SWCNTs and MWCNTs. Different allotropes of carbon, like GO and CNTs could be covalently functionalized with diverse chemical entities to expand their physiological and industrial uses. Non-covalent functionalization of carbon allotropes, on the other hand, is mostly accomplished through hydrophobic contacts, electrostatic interactions, pie-pie stacking, and van der Waals intermolecular force of attraction. Non-covalent functionalization, on the other hand, is an intriguing approach for functionalizing carbon allotropes because it preserves the majority of their features, particularly thermal and electrical capabilities. The use of pie-pie stacking to non-covalently functionalize carbon allotropes, particularly graphene analogs and CNTs (SWCNTs and MWCNTs), has been frequently described. The π-electron cloud of the aromatic ring(s) (e.g., pyrene and perylene) interacts with the π-electron cloud of the carbon allotropes in this sort of interaction. Aromatic compounds may engage to carbon allotropes via π-πstacking; meanwhile, carbon allotropes (G, GO, CNTs, etc.) could interface with surfactants, macromolecules, and ILs via hydrophobic interactions. These interactions are mostly used in aqueous and organic solvents to disperse carbon allotropes [33–35]. Electrostatic interactions among ionic liquids and GO (and potentially other allotropes) are primarily involved because GO contains a variety of ionic groups, particularly hydroxylate and carboxylate ionic groups. Non-covalent functionalization of CNT can be achieved by establishing π-π interactions, electrostatic interactions, and CH-π interactions between CNTs and biomolecules. Figure 15.2 shows the physical deposition, self-assembly, consequent healing, layer-by-layer deposition, and sol-gel methods are the mechanisms by which graphene and graphene oxide films are formed [36].

Nanomaterials have unique physicochemical and mechanical capabilities, making them ideal substances for a range of biochemical and industrial functions. At low concentrations, nanomaterials offer superior corrosion resistance. Nanomaterials and their derivatives give extremely large surface coverage, as opposed to standard macroscopic substances, owing to their incredibly significant surface-to-volume ratio. This

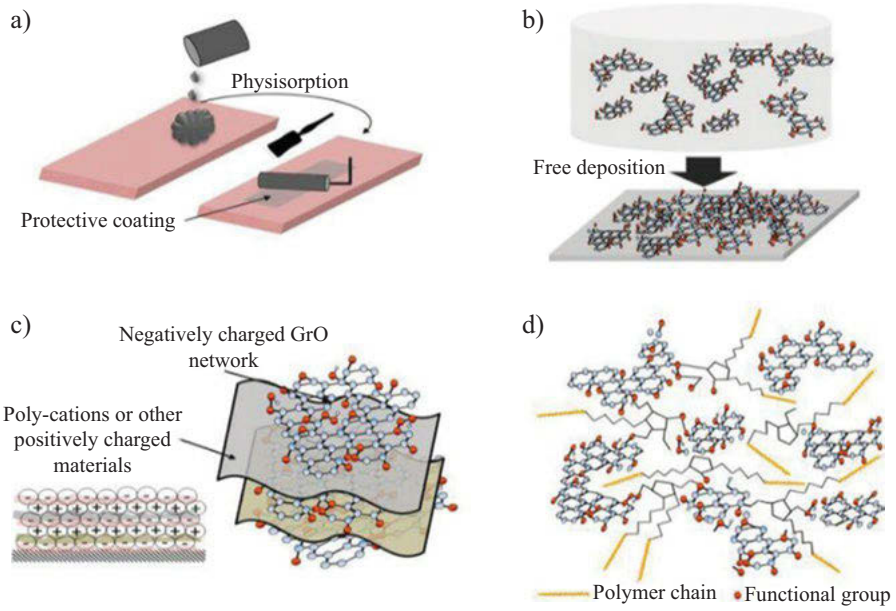

Fig. 15.2: (a) Physical deposition and consequent healing, (b) Self-assembly, (c) Layer-by-layer deposition, and (d) Sol-gel method are the mechanisms by which graphene and graphene oxide films are formed. Adapted with permission from Ref. [36]. Based on the Creative common attribution-based license CCBY.

results in great protective efficiency. The creation of water-soluble nanomaterials carbon allotropes and their derivatives is the focus of present corrosion scientific and technological study. The covalent and/or non-covalent surface functionalization of nanomaterials is among the most prevalent and widely utilized approaches [37–39]. Typically, polar substituents like –OH (hydroxyl), epoxide, and –COOH (carboxyl) are formed as a consequence of this sort of functionalization. By improving the interaction among nanomaterial compounds and aqueous electrolytes, these polar substituents improve the functionalized nanomaterials' dispersibility/solubility. This form of chemical modification is commonly employed to bind heterocyclic moieties to nanomaterial surfaces. It is worth noting that, in addition to improving nanomaterial solubility in aqueous solutions, polar substituents could also serve as an adsorption center amid metal-inhibitor interactions.

As maritime fouling-release (FR) surfaces, Selim et al. [31] developed two novel super hydrophobic nanocomposite sets using reduced graphene oxide (RGO) and graphene oxide/boehmite nanorods (GO-γ-AlOOH) nanofillers in polydimethylsiloxane (PDMS). Controlling the forms and distribution of nanofillers in silicone frameworks changed the self-cleaning and anti-fouling properties. γ-AlOOH nanorods had a singular crystallinity and had a mean diameter of 10–20 nm and a width of 200 nm. RGO was created by a hydrothermal procedure, while GO-γ-AlOOH nanocomposites

were created through a chemical deposition method and used as fouling-release coating constituents. To investigate the symbiotic influences of graphene-based materials upon the interfacial, structural, and FR features, these nanofillers were dispersed in the silicone matrices using the solution casting approach. The PDMS/GO-γ-AlOOH composite, exhibiting maximum hydrophobicity (WCA of 151°1°), packed roughness (RMS of6.43 nm), and FR characteristics were made with homogeneity of the distribution (3 wt%). Throughout a wide pH range, this nanocoating provided excellent physical endurance, corrosion resilience, and thermal characteristics. It also demonstrated excellent pH stability, as well as super hydrophobicity retention, following thermal stimulation and salt fog resistance. When tested against gram-positive and gram-negative bacteria and fungi, it had the lowest percentages of biodegradability and microbiological endurance, as well as the highest cell viability. It was compared to a number of commercially available and well-studied antifouling coatings, and the GO-γ-AlOOH(3 wt%) nanofiller surpassed them in terms of surface self-cleaning. This research reveals that a nanocomposite covering of PDMS/GO-γ-AlOOH (3 wt%) has the ability to efficiently inhibit biofouling microorganisms in the marine ecosystem. A field trial in genuine sea water verified the findings, with the homogeneously distributed GO-γ-AlOOH (3 wt%) nanofillers exhibiting the optimum FR efficiency.

Verma et al. [9] presented a discussion about the covalent and non-covalent functionalization of various carbon allotropes and how they may be utilized as corrosion inhibitors in various coating compositions and the aqueous environment. They concluded that these ingredients are commonly used in electrolytes as coating formulations for a variety of metals and alloys. Because of their filling capabilities and strong hydrophobicity, these materials are used as nanofillers in polymer matrixes. Due to the obvious significant intermolecular force of attraction, these materials are less diffusible. They are easily agglomerated, which has an unfavorable influence on their dispersion characteristics and corrosion resistance. The dispersibility of these materials could be improved by appropriately functionalizing them with organic molecules. Magnetic stirring, ball milling, ultrasonic mixing and shear emulsification could all be utilized to improve their dispersion.

David et al. [2] investigated MWCNTs using various forms of nanoparticles (NPs) to create hybrid substances exhibiting superior antibacterial and anticorrosion properties. The nanotubes adorned using zinc oxide (ZnO) nanoparticles (NPs) had a restricted size variation of NPs, measuring 7–13 nm, 15–33 nm for nanotubes decorated with silver (Ag) NPs, and 20–35 nm for nanotubes decorated with hydroxyapatite (HAp) NPs, correspondingly. The water dissemination of the resultant nanomaterials was improved for all the decorated MWCNTs, as demonstrated by the relative absorbance fluctuation in the duration of the water-dispersed nanomaterials. The antibacterial activity of the nanomaterials generated was outstanding; however, adding NPs to the surface of MWCNTs improved the nanocomposites' efficiency. The use of HAp, ZnO, and Ag NPs to decorate MWCNTs was confirmed by ESEM data. As can be observed, the NPs have developed and coated the surface of

MWCNTs, to a great extent (Fig. 15.3). It is probable that the MWCNTs structure will be significantly altered after purification, which entails acid treatments, and that certain bundles will be delaminated and coiled. The obtained results by TEM, on the other hand, demonstrate that the structure of MWCNTs is largely intact after decorating. In all cases, the NPs have adhered to the surface of MWCNTs, and the produced outer layer embraces the MWCNTs equally, notably in the event of MWCNTs-Ag. In Fig. 15.3a, the exterior layer of rod-like HAp NPs entirely conceals the nanotubes, with conglomerations of particles visible in some areas. ZnO NPs did not completely cover the surface of nanotubes, resulting in aggregates of various irregular forms on sections of the nanotube surface (Fig. 15.3b), whereas MWCNTs Ag (Fig. 15.3c) indicates that nanoparticles uniformly coated the whole

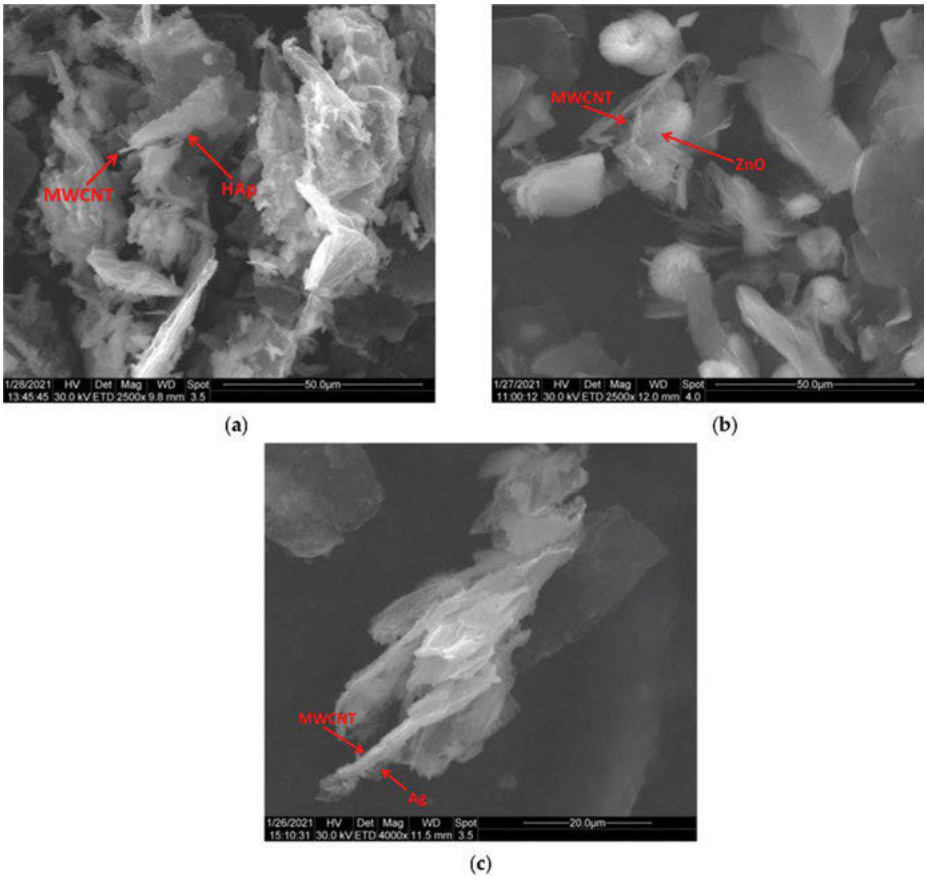

Fig. 15.3: SEM images depicting the adoration of MWCNTs with HAp (a), ZnO (b) and Ag (c) NPs. Adapted with permission from Ref. [2]. Based on the Creative common attribution-based license CCBY.

surface of MWCNTs. The NP agglomeration implies that the MWCNTs perform a supportive function as a deposition center for the clusters.

Figure 15.4 shows the Raman spectra of MWCNTs HAp, MWCNTs ZnO, and MWCNTs Ag. At 1,348, 1,606 and 2,698 cm^{-1}, correspondingly, three bands belonging to the crystalline carbon D (band D – disorder), G band (graphite band), and G' band (D overtone) characteristic of MWCNTs were detected.

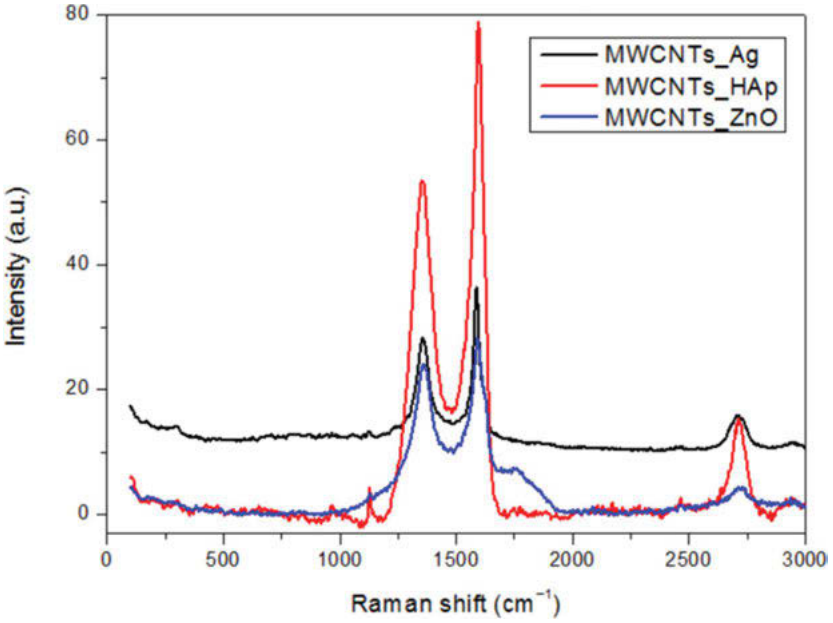

Fig. 15.4: Raman spectra of MWCNTs with NPs on them. Adapted with permission from Ref. [2]. Based on the Creative common attribution-based license CCBY.

15.3 Economics and commercialization of CAN

Metal treatment, water treatment and lubricants, and oil and gas production are the three main markets for corrosion inhibitors. Water treatment offers a 44% market share, followed by metal treatment/lubricants/fuels, which offers a 32% market share. The residual corrosion inhibitor consumption, at 24%, is accounted for by oil and gas production. The demand for water remediation is steady, and it would continue to follow regional economic trends. By 2024, the worldwide corrosion inhibitor industry for water treatments is expected to grow at a modest pace. Machine production and maintenance have a significant impact on metal treatment usage. Corrosion inhibitor consumption in this industry is predicted to be low over the next five years. The price of crude oil determines the need for corrosion inhibitors

in the oil and gas industry. The crude oil price is expected to remain stable around a midpoint for the next five years. As a consequence, the progression of growth of corrosion inhibitors will be slow [40–42].

Corrosion inhibitors can help reduce unit closures and heat loss, extend the life of equipment, eliminate contamination, and give a clean appearance. Other techniques of corrosion resistance include linings and coatings, material design and cathodic protection, in addition to corrosion inhibitors. The bulk of corrosion inhibitors is sold by their primary producers to commercial firms that make end-use products for water remediation, lubricant and biofuels, metal treatment (particularly metallurgical fluids and rust-preventive lubricants), and oil and gas field operations. End-use goods frequently contain additional functional constituents, as well as significant volumes of dispersants and solvents. Even though these specialized firms are more actively engaged in the practice of resolving corrosion issues than basic producers, corrosion control techniques and applications are only a small part of their entire company. From 2016 to 2019, global usage of corrosion inhibitors increased at a rate of more than 2% per year on average [43–45]. During the period 2019–24, consumption is predicted to expand at a rate of less than 2% per year on average. Corrosion inhibitors are expected to rise at a somewhat slow pace, reflecting the stability of most basic sectors in developed nations. They also represent the industries' substitution of plastics, ceramic, and corrosion-resistant alloys for steel. Industries frequently use corrosion inhibitors quite efficiently by implementing superior monitoring and management systems, in order to limit discharge in industrial effluents and ecological harm.

After plunging in 2014 and 2016, the mean annual expansion rate of corrosion inhibitors in North America increased to roughly 2% in 2016–19, owing mostly to the significant decline in crude oil prices in 2014. Drilling activity in 2015 and 2016 was hampered by the falling crude oil price. Consequently, in North America the corrosion inhibitor usage will be will increase at a steady rate between 2019 and 2024. A sluggish economy in China would also lead to decreased corrosion inhibitor expansion, particularly in the industrial sector. Sluggish economies and uncertain political conditions will also hamper progress in other regions, such as Brazil. The position of significant Western water treatment enterprises like GE, Ecolab and Ashland, in China, represents an important market development. Other significant developments in this industry are due to regulatory and environmental challenges that might result in the substitution of particular products with less hazardous or ecologically dangerous alternatives. These problems could be caused by CI themselves or by changes in the end-use market sector, where they have been applied.

15.3.1 Inorganic corrosion inhibitors market overview

As per the American Galvanizer's Association, oxidation and galvanic corrosion affect roughly 85% of total steel output. Metals like copper, aluminum, and zinc,

which are frequently utilized in industries for a variety of applications including machinery, containers, systems, pipelines, bridges, and many others, corrode and oxidize naturally, when subjected to the aspects and humidity in the air and soil. The rising need for corrosion-affinity metals in numerous industries, coupled with the lack of robust substitutes, necessitates anticorrosion chemicals for layering or coating reasons, according to an Industry ARC analyst. As a result, these industries rely on low-cost inorganic compounds that are commonly accessible as anticorrosive bases on industrial metals. The global market for inorganic corrosion inhibitors was valued at $6.45 billion in 2018. The United States is rising as a global oil and gas exporter, implying an increase in the amount of pipes and machinery installed for oil drilling and processing processes. Furthermore, according to the International Energy Agency, the United States is the world's second-largest renewable energy market, engaging heavily in the management and upkeep of turbines, gearboxes, pipes, and other equipment. Furthermore, a huge manufacturing market and a stable home economy could promote the expansion of anticorrosive agents in North America, resulting in a regional share of 38% in 2018 [46].

Due to the negative impacts of lead and chromium inhibitors, advancements in this field allow room for alternative CAN corrosion inhibitors to grow. In addition, the anticorrosion coatings market generated $8.91 billion in sales in 2018, indicating the worldwide market's great potential and desire for effective corrosive inhibitors. According to the study, the global market for inorganic CI will increase at a 4.45% compound annual growth rate (CAGR) from 2015 to 2025. Inorganic corrosion inhibitors produce a protective coating on/in pipelines that prevents corrosion caused by oxidation by soil, air, or water contact, resulting in significant interest in wastewater treatment centers and the oil and gas sector. The power generation industry has been rapidly growing in recent years, with a large potential for the future market in terms of revenue. During the forecast timeframe of 2019–2025, this category is expected to produce significant demand for inorganic corrosion inhibitors, supporting market growth at a CAGR of 4.89%.

– **Inorganic corrosion inhibitors market growth drivers**

Corrosion cost the US Navy Division $3,430 million in aviation and missiles, $489 million in ground vehicles, and $3,534 million in vessels in 2016. This accounts for a significant amount of money spent on maintenance and repair, creating a strong need for inorganic corrosion inhibitors. Anodic inhibitors are used extensively in docks, harbors, bridges, and onshore oil drilling sites to passivate the corrosion process and reduce unintended dangers such as bridge failure and loss of human lives. The worldwide inorganic corrosion inhibitor market has been growing in recent years, as a result of the benefits associated. Inorganic corrosion inhibitors are increasingly used in machinery, turbines, metal parts, and a variety of instruments and devices as a consequence of rising industrialization and the quantification of renewable energy plants. As a result, the market is expected to generate significant revenue during the forecast timeframe.

– **Inorganic corrosion inhibitors market key players**

Champion Technologies Inc., AkzoNobel, Solutia Inc., BASF SE, Suez S.A., Chemtreat Inc., GE Water and Process Technologies, DowDuPont, Ashland Inc., Solenis, Ecolab Inc., and Cortec Corporation lead the global inorganic corrosion inhibitor market. AkzoNobel is a global coatings firm that provides antifouling, concrete protection, and corrosion protection to a variety of industrial and noncommercial clients. Water-based acrylic, primers and priming finishes, surface tolerance, and other products are among the company's contributions to the niche market.

– **Inorganic corrosion inhibitors market trends**

Chrome plating in industrial applications has been linked to harmful side effects, prompting several major corporations to invest in research and development (R&D) to develop new components as corrosion inhibitors. Hexigone Inhibitors Ltd. just released Intelli-ion AXs, a novel corrosion inhibitor that is both environmentally friendly and beneficial in the industrial sector.

– **Inorganic corrosion inhibitors market: industry coverage**

Formulation, type, treatment, and application are the four segments of the worldwide inorganic corrosion inhibitors market. Chromate, Molybdate, Nitrite, and Others are some of the formulation segments. Anodic inhibitor and cathodic inhibitor are two types of inhibitors. Sprays, coatings, and Others are the different classifications based on the treatment. Oil and Gas, Chemicals and Petrochemicals, Water Treatment, and Others are the application segments in this market [47–49].

15.3.2 Organic corrosion inhibitors market overview

Organic corrosion inhibitors are expected to achieve US$4.5 billion by 2027, after rising at a CAGR of 4.8% from 2022 to 2027, due to their widespread use in different end-use industries like building construction, oil and gas, electricity production, and others. By adsorbing corrosive elements, such compounds may build a protective coating over metal surfaces, minimizing corrosion and metal breakdown. Organic Amines, which include various H_2SO_4 solutions such as quaternary ammonium salt, urea, and others, are the most common organic compounds used to resist corrosion. As the degree of unsaturation rises, aldehydes become more defensive. The construction industry's explosive growth has created a requirement for organic corrosion inhibitors, propelling the market forward. Additionally, during the forecast timeframe, the expanding oil and gas industry is predicted to significantly fuel the organic corrosion inhibitors market. Also, as per the Energy Information Administration, crude oil supply in the United States will exceed 14.0 million barrels per day (b/d) by 2022. The International Trade Administration estimates that expenditures in Indonesia's oil and gas industry totaled USD 12.3 billion in 2018 and USD 12 billion in 2019.

– **Organic corrosion inhibitors market, by product type**

In 2021, the Amines sector held 28% of the market share, and it is expected to increase rapidly over the projected period. Amines have a number of benefits, including being environmentally benign, nontoxic, recyclable, and very inexpensive. Water systems, power plants, boilers, metallurgical fluids, distilleries, and other places benefit from the amine-based organic corrosion inhibitor. Companies are turning to much more eco-friendly chemicals to manufacture organic corrosion inhibitors. During the projected timeframe, the Benzotriazoles segment is anticipated to increase rapidly. Benzotriazoles are employed in three ways: as a corrosion inhibitor, an ultraviolet light stabilizer for polymers, and as a photography antifogging agent. Benzotriazoles are used in high quantities as corrosion inhibitors in the majority number of situations, and as a consequence, they become an environmental pollutant. At concentrations of 0.01–2.0%, they are used as corrosion inhibitors and fire retardants in antifreeze.

– **Organic corrosion inhibitors market, by application**

Due to the rising use of CAN corrosion inhibitors in the oil and gas industry, the oil and gas segment owned the highest share in the organic corrosion inhibitors market in 2021 and is expanding at a CAGR of 3.6%. Corrosion is a basic occurrence in oil and gas pipelines. Pipelines are always subjected to corrosion threats due to their role as a means of transferring oil and gas from wellheads to production plants, from the period of commissioning until deactivation. Global oil stockpiles averaged 1.8 million barrels per day (b/d) in the first half of 2021, as per the Energy Information Administration. The global average utilization of petroleum and liquid fuels has reached 97.4 million barrels per day by 2021, up 5.0 million barrels from 2020, and an incremental 3.6 million barrels per day in 2022.

– **Organic corrosion inhibitors market, by geography**

Due to the growing oil and gas sectors in the region, the Asia Pacific province owned the highest share of the organic corrosion inhibitors market in 2021, up to 35%. The oil and gas business in the province is growing due to increased infrastructure development and urbanization. The International Association of Oil and Gas Producers (IOGP) estimates that the Asia Pacific produced 7.6 million barrels of oil per day in 2018, accounting for 8% of global production. China is the region's greatest producer, producing half of the region's oil. Other notable Asia Pacific exporters included India and Indonesia, which each had an 11% share, Malaysia, which had 9%, Thailand, which had 6%, Australia, which had 5%, and Vietnam, which had 4%. The top importers were Japan, China, and South Korea. As a result of the growing oil and gas industry, consumption of organic corrosion inhibitors is expected to rise, propelling the organic corrosion inhibitors market in the Asia Pacific region.

– **Organic corrosion inhibitors market key drivers**

The annual cost of corrosion to the oil and gas industry in the United States is estimated to be USD 27 billion, according to NACE International. Costs could be reduced by using corrosion-resistant materials and corrosion-related processes, quite frequently. Corrosion inhibitors could be used to decrease or eliminate metal corrosion. Insulating metals and alloys or delaying corrosion induced by cathodic and anodic processes protect them. Corrosion inhibitors are used in various sectors to decrease repair and maintenance costs, lengthen equipment lifespan, and minimize output loss due to corrosion. Corrosion inhibitors are thus an essential component in lowering corrosion expenses. The advancement of the National Strategic Project Development, that is, the Cirebon Power Unit 2 with a capacity of 11,000 MW, achieved 39% in February 2019 and is expected to be operational by February 2022. The requirement for organic corrosion inhibitors will rise dramatically as oil and gas and power generation projects expand. Thus, over the projected period, the rising oil and gas and power generating projects serve as a promoter for the organic corrosion inhibitors market.

– **Organic corrosion inhibitors market landscape**

Competitors in the CAN corrosion inhibitors market use a variety of methods, including technology releases, acquisitions, and R&D. The organic corrosion inhibitors market is dominated by the following companies:

1. Arteco N.V.
2. Afton chemical Limited
3. BengKuang Marine Limited
4. CIMCOOL Fluid Technology, LLC,
5. BASF
6. Cortec Corporation
7. ChemTreat Inc.
8. CRC Industries Inc.
9. Akzonobel N.V. Angus Chemical Company
10. Australian Organic Coolants

– **Corrosion inhibitors market, by product**

Organic CI addressable market led the global industry in 2015, and it is expected to continue to rise at a rapid pace throughout the forecast period. Because of their excellent stability and other qualities, organic amines, benzotriazole, phosphonates, tolyltriazole, and mercaptobenzothiazole are the most commonly utilized organic goods in the business. Furthermore, increased worries about inorganic products and their related negative environmental effects will help the segment's rise by 2023 [50, 51]. The market for inorganic corrosion inhibitors is expected to grow at a moderate rate of more than 3% CAGR over the forecast period. Depending on its mechanism on metals such as magnesium, zinc, and nickel, the inorganic industry can be divided into

anodic and cathodic products. Due to its improved stability under tough environmental circumstances, the product is extensively utilized.

– **Corrosion inhibitors market, by application**

In 2015, the water-based CI market led the overall business. The segment's rise is mostly influenced by the increasing demand for water treatment chemicals. Additionally, expanding industries such as refining, manufacturing, quarrying, and energy production are expected to have a beneficial impact on global industry growth over the forecast period. By 2023, the corrosion inhibitors market for total oil/solvent is expected to increase at a rate of more than 4%. Copper, steel, zinc, aluminum, cast iron, and alloys are among the oil/solvent-based uses. Oil/solvent-based coatings offer consistent efficacy over a long period, which is expected to drive market growth by 2023. Furthermore, due to its higher flammability properties, the application has a restricted range when functioning over complex systems, which may have a detrimental impact on sales.

– **Corrosion inhibitors market, by end-use**

In 2015, the global CI market for power generation was estimated to be worth around USD 1.5 billion. The product is widely used in generation units, including gas turbines, switch gears, pumps, and electronics equipment. As the world's population grows, so does the world's energy needs. This tendency will benefit the power generation end-use industry, as a whole. Over the forecast period, the global CI market size for oil and gas is termed to grow at a CAGR of more than 5.5%. The increasing oil and gas industry will be the main driver of global industry growth by 2023. As oil and gas exploration equipment is subjected to harsh environmental conditions and requires corrosion protection, the commodity is widely used in the industry. In addition, by 2023, shale gas exploration in the United States and Russia will augment business expansion.

– **Corrosion inhibitors market, by region**

In 2015, the CI market in North America, driven by the United States, was estimated at over USD 1.5 billion. One of the primary factors leading to business expansion is the good perspective of the regional construction industry, following the 2008 economic downturn. Moreover, by 2023, the thriving oil and gas industry of the United States will drive product demand.

In 2015, the Asia Pacific, driven by India and China, controlled the worldwide corrosion inhibitors market and is expected to grow at the fastest rate, throughout the forecast period. Increased building expenditure for commercial and domestic projects is credited for the region's growth. Furthermore, by 2023, growing government investment in infrastructure facilities would significantly support regional economic expansion.

– **Competitive market share**

In 2015, the global corrosion inhibitors market was relatively fragmented, including key players such as Ecolab, GE, BASF, and Ashland accounting for less than half of the entire market share. DuPont, Champion Technologies, Dow, AkzoNobel, Daubert, Dai-Ichi, Henkel, Halox, Lubrizol, Eastman, Cytec, and Cortec are some of the other major industry share providers. In order to enhance their global position, these industry groups are heavily engaged in strategic growth operations like capacity acquisitions, expansion and mergers, and the development of new products.

15.4 COVID-19 impact on global corrosion inhibitor market

As a consequence of the rapid emergence of the COVID-19 epidemic, nations throughout the world adopted lockdown laws, halting the import and export of Organic (CAN) Corrosion Inhibitors. Owing to the pandemic, which has severely impacted the organic corrosion inhibitors business, fewer people are eager to acquire products and commodities on a global scale. To curb the transmission of the infection, large sections of people and governments have been prohibited from traveling. Restrictions on travel and lockdown have had a significant influence on the sector, making it difficult to market the goods abroad. Economists think that the COVID-19 epidemic will result in a global recession similar to the Economic Crisis [52, 53]. Finally, the crisis may be over once all restrictions have been repealed. The global economy may see a rapid rebound due to the high rate of recovery. Many factors influence this type of economic recovery; for instance, reducing supply to match reduced demand may lead to a shortage and price inflation in the long term. Corrosion expenses in end-use industries are a major element driving the market for CI. Total corrosion costs comprise the cost of construction, building, or production, as well as the cost of corrosion-related management, repairs, and restoration, and the expense of depreciation or restoration of structures damaged by corrosion. Depending on the industry, these rates vary. According to NACE International, the annual cost of corrosion in the oil and gas industry in the United States is expected to be USD 27 billion. By adopting corrosion-resistant materials and corrosion-related technical processes more widely, the cost of corrosion-resistant materials and processes could be reduced. Corrosion inhibitors prevent or slow down metal corrosion. They serve as a shield for metals or alloys, generating an absorbent layer or delaying corrosion-causing anodic and cathodic processes. Corrosion inhibitors minimize maintenance and repair costs, increase the usable equipment life, and minimize output loss due to corrosion damage, in various sectors. This lowers the cost of corrosion and stimulates the market for CI. The World Bank estimates that developing nations will have to invest roughly 4.5% of their GDP to attain long prosperity. In the next five years, infrastructure growth

connected to energy, freshwater, energy, transit, and industrial requirements are predicted to enhance the market for corrosion inhibitors. According to Oxford Economics, global infrastructure expenditure will exceed USD 94 trillion by 2040, with an extra USD 3.4 trillion needed to meet the United Nations' Sustainable Development Goals for power and water. As per Oxford Economics analysis, APAC countries including Malaysia, India, China, Indonesia, the Philippines, Vietnam, and Thailand will account for more than half of the global infrastructure spending by 2040. Manufacturers will be able to provide a broad array of CI to distinct applications, in particular, to prevent them from corrosion, as the use of industrial water in developing countries grows.

15.5 Challenges and future outlooks

Corrosion investigation gives information on the fundamental dynamics and equipment used in the corrosion process. Nanocoating contains ultrafine elements, which would have an effect on the outcome surface in terms of the lattice structure, size distribution, permeability, dispersal of intermetallic particles, surfaces condition, and so on. Smoothing the surface, for example, increases its characteristics and reduces the possibility of pit formation on such surfaces. Meanwhile, coating the surface with nanoparticles leads to excessive smoothness, which could compromise the coating's adhesion and produce distinctions in areas of the covering. Additionally, decreasing surface roughness might enhance the chances of selective intergranular corrosion, allowing for the formation of a damaged and porous coating around the triple-intersection grain borders. As these two methodologies allow CAN nanoparticles to interact with the surface in a variety of methods, it is difficult to determine which forecast is correct. Furthermore, the integrity of such nanomaterials surrounding the perimeter of the substrate controls oxide generation; as a result, the surface state development process alters and is difficult to identify. The surface state shift from passivation to pit onset, and ultimately to film disintegration, is impacted. The new state is determined by the uncoated surface's fundamental states and the cleanliness of the preceding coated surface, both of which might influence uniform field corrosion. The nonuniform distribution of nanoparticles on the coated substrate's exterior may cause particles to aggregate and generate unstable sites with higher potential, which can lead to pit formation. In contrast, an accumulated coating may physically insulate the substrate surface from electrolyte particles. Predicting the progression of the process is difficult, and further corrosion study is needed.

15.6 Conclusion

Carbon allotropes, particularly carbon nanotubes (CNTs), graphene (G), graphene oxide (GO), etc., have been discussed as excellent nano-sized alternatives to existing molecular CI. The significant impact of their corrosion inhibitors on a variety of metals has led to a large increase in their global use by a number of developing countries and businesses. These materials are frequently employed in electrolytes as coating compositions for a variety of metals and alloys. These compounds are used as nanofillers in polymer matrixes because of their filling capabilities and strong hydrophobicity. Due to the obvious significant intermolecular force of attraction, these materials are visibly less dispersible. They are easily agglomerated, which has an unfavorable influence on their dispersion characteristics and corrosion inhibition. The dispersibility of these materials could be improved by appropriately functionalizing them with organic molecules. Physical procedures such as magnetic stirring and shear emulsification could also be used to improve their dispersion. Organic substances are being used to try to chemically change them. As modified carbon allotropes are highly soluble in polar electrolytes, they can be employed as aqueous phase CI. As a result, future research should focus on developing and synthesizing soluble carbon allotrope derivatives. In light of the foregoing, it is suggested that high-impact tactics be used to commercialize the CAN-based CI internationally, without any significant limits.

Link of few potent websites related to the discussed chapter

https://www.materialsperformance.com/articles/coating-linings/2016/04/chromate-primer-alternative-uses-carbon-nanotubes
https://www.corrosion
https://www.nace.org/home
https://corrosion
https://eoncoat.com/corrosion

References

[1] Hossain, N.; Asaduzzaman Chowdhury, M.; Kchaou, M. An overview of green corrosion inhibitors for sustainable and environment friendly industrial development. J. Adhes. Sci. Technol. 2021, 35, 673–690.

[2] David, M.E.; Ion, R.M.; Grigorescu, R.M.; Iancu, L.; Holban, A.M.; Nicoara, A.I., et al. Hybrid materials based on multi-walled carbon nanotubes and nanoparticles with antimicrobial properties. Nanomaterials. 2021, 11, 1–22.

[3] Panchal, J.; Shah, D.; Patel, R.; Shah, S.; Prajapati, M.; Shah, M. Comprehensive review and critical data analysis on corrosion and emphasizing on green eco-friendly corrosion inhibitors for oil and gas industries. J. Bio- Tribo-Corros. 2021, 7, 1–29.
[4] Thakur, A.; Kumar, A.; Kaya, S.; Vo, D.V.N.; Sharma, A. Suppressing inhibitory compounds by nanomaterials for highly efficient biofuel production: A review. Fuel 2022, 312, 122934.
[5] Thakur, A.; Kumar, A. Sustainable inhibitors for corrosion mitigation in aggressive corrosive media: A comprehensive study, vol. 7, Springer International Publishing,2021.
[6] Bashir, S.; Thakur, A.; Lgaz, H.; Chung, I.-M.; Kumar, A. Computational and experimental studies on Phenylephrine as anti-corrosion substance of mild steel in acidic medium. J. Mol. Liq. 2019, 293, 111539.
[7] Bashir, S.; Thakur, A.; Lgaz, H.; Chung, I.-M.; Kumar, A. Corrosion inhibition performance of acarbose on mild steel corrosion in acidic medium: An experimental and computational study. Arab. J. Sci. Eng. 2020, 45, 4773–4783.
[8] Bashir, S.; Thakur, A.; Lgaz, H.; Chung, I.M.; Kumar, A. Corrosion inhibition efficiency of bronopol on aluminum in 0.5 M HCl solution: Insights from experimental and quantum chemical studies. Surf. Interfaces. 2020, 20, 100542.
[9] Verma, C.; Quraishi, M.A.; Ebenso, E.E.; Hussain, C.M. Recent advancements in corrosion inhibitor systems through carbon allotropes: Past, present, and future. Nano Sel. 2021, 2, 2237–2255.
[10] Smajic, J.; Alazmi, A.; Wehbe, N.; Costa, P.M.F.J. Electrode–electrolyte interactions in an aqueous aluminum–carbon rechargeable battery system. Nanomaterials. 2021, 11.
[11] Soleymani Eil Bakhtiari, S.; Bakhsheshi-Rad, H.R.; Tavakoli, M.; Razzaghi, M.; Ismail, A.F.; Ramakrishna, S.; Berto, F. Polymethyl methacrylate-based bone cements. Polymers (Basel). 2020.
[12] Wu, W.; Pan, Y.; Liu, Z.; Du, C.; Li, X. Electrochemical and stress corrosion mechanism of submarine pipeline in simulated seawater in presence of different alternating current densities. Materials (Basel). 2018, 11.
[13] Azarniya, A.; Safavi, M.S.; Sovizi, S.; Azarniya, A.; Chen, B.; Hosseini, H.R.M., et al. Metallurgical challenges in carbon nanotube-reinforced metal matrix nanocomposites. Metals (Basel). 2017, 7.
[14] Pourhashem, S.; Ghasemy, E.; Rashidi, A.; Vaezi, M.R. A review on application of carbon nanostructures as nanofiller in corrosion-resistant organic coatings, vol. 17, Springer, US, 2020.
[15] Verma, C.; Quraishi, M.A.; Rhee, K.Y. Present and emerging trends in using pharmaceutically active compounds as aqueous phase corrosion inhibitors. J. Mol. Liq. 2021, 328, 115395.
[16] Krishnan, M.A.; Aneja, K.S.; Shaikh, A.; Bohm, S.; Sarkar, K.; Bohm, H.L.M., et al. Graphene-based anticorrosive coatings for copper. RSC Adv. 2018, 8, 499–507.
[17] Calovi, M.; Rossi, S.; Deflorian, F.; Dirè, S.; Ceccato, R.; Guo, X., et al. Effects of graphene-based fillers on cathodic delamination and abrasion resistance of cataphoretic organic coatings. Coatings. 2020, 10.
[18] Mitura, K.; Kornacka, J.; Kopczyńska, E.; Kalisz, J.; Czerwińska, E.; Affeltowicz, M., et al. Active carbon-based nanomaterials in food packaging. Coatings. 2021, 11, 1–31.
[19] Maas, M. Carbon nanomaterials as antibacterial colloids. Materials (Basel). 2016, 9, 1–19.
[20] Cui M; Li, X. Nitrogen and sulfur Co-doped carbon dots as ecofriendly and effective corrosion inhibitors for Q235 carbon steel in 1 M HCl solution. RSC Adv. 2021, 11, 21607–21621.
[21] Harb, S.V.; Pulcinelli, S.H.; Santilli, C.V.; Knowles, K.M.; Hammer, P. A comparative study on graphene oxide and carbon nanotube reinforcement of PMMA-siloxane-silica anticorrosive coatings. ACS Appl. Mater. Interfaces. 2016, 8, 16339–16350.
[22] Bordin, E.S.; Wrenn, C.G. A comprehensive review. J. Higher Educ. 1953, 24, 164.

[23] Ryl, J. Special issue: Recent advances in corrosion science. Materials (Basel). 2020, 13, 15–16.
[24] Wu, J.; Sharifi, T.; Gao, Y.; Zhang, T.; Ajayan, P.M. Emerging carbon-based heterogeneous catalysts for electrochemical reduction of carbon dioxide into value-added chemicals. Adv. Mater. 2019, 31, 1–24.
[25] Zhang, R.; Yu, X.; Yang, Q.; Cui, G.; Li, Z. The role of graphene in anti-corrosion coatings: A review. Constr. Build. Mater. 2021, 294, 123613.
[26] Cheng, F.; Chen, J. Metal–air batteries: From oxygen reduction electrochemistry to cathode catalysts. Chem. Soc. Rev. 2012, 41, 2172–2192.
[27] Rana, A.; Khan, I.; Saleh, T.A. Advances in carbon nanostructures and nanocellulose as additives for efficient drilling fluids: Trends and future perspective-A review. Energy Fuels. 2021, 35, 7319–7339.
[28] Tang, X.; Liu, D.; Wang, Y.J.; Cui, L.; Ignaszak, A.; Yu, Y., et al. Research advances in biomass-derived nanostructured carbons and their composite materials for electrochemical energy technologies. Prog. Mater. Sci. 2021, 118, 100770.
[29] Al-Jumaili, A.; Alancherry, S.; Bazaka, K.; Jacob, M.V. Review on the antimicrobial properties of Carbon nanostructures. Materials (Basel). 2017, 10, 1–26.
[30] Njeumen, C.A.; Ejuh, G.W.; Assatse, Y.T.; Kamsi, R.A.Y.; Ndjaka, J.M.B. Computational studies of reactivity descriptors, electronic and nonlinear optical properties of multifunctionalized fullerene ylide with acetylsalicylic acid. J. Mol. Model. 2021, 27.
[31] Selim, M.S.; Fatthallah, N.A.; Higazy, S.A.; Hao, Z.; Jing, M.P. A comparative study between two novel silicone/graphene-based nanostructured surfaces for maritime antifouling. J. Colloid Interface Sci. 2022, 606, 367–383.
[32] Jahdaly BA, A.; Elsadek, M.F.; Ahmed, B.M.; Farahat, M.F.; Taher, M.M.; Khalil, A.M. Outstanding graphene quantum dots from carbon source for biomedical and corrosion inhibition applications: A review. Sustain. 2021, 13, 1–33.
[33] Tamalmani, K.; Husin, H. Review on corrosion inhibitors for oil and gas corrosion issues. Appl. Sci. 2020, 10.
[34] Frigione, M.; Lettieri, M. Recent advances and trends of nanofilled/nanostructured epoxies. Materials (Basel). 2020, 13, 1–24.
[35] Al-Otaibi, J.S.; Almuqrin, A.H.; Mary, Y.S.; Mary, Y.S.; Van, A.C. DFT and molecular docking studies of self-assembly of sulfone analogues and graphene. J. Mol. Model. 2020, 26.
[36] Ola, S.K.; Soni, S.; Dhayal, V.; Singh Shekhawat, D. A review: Graphene modified polymer coatings for corrosion protection. IOP Conf. Ser.: Earth Environ. Sci. 2021, 796.
[37] Babaei, K.; Fattah-alhosseini, A.; Molaei, M. The effects of carbon-based additives on corrosion and wear properties of Plasma electrolytic oxidation (PEO) coatings applied on Aluminum and its alloys: A review. Surf. Interfaces. 2020, 21, 100677.
[38] Technology, V. New advances in vehicular technology and automotive engineering. 2012.
[39] Elnaggar, E.M.; Kabel, K.I.; Farag, A.A.; Al-Gamal, A.G. Comparative study on doping of polyaniline with graphene and multi-walled carbon nanotubes. J. Nanostruct. Chem. 2017, 7, 75–83.
[40] Mazumder, M.A.J. Global impact of corrosion: Occurrence, cost and mitigation. Glob. J. Eng. Sci. 2020, 5, 0–4.
[41] Chauhan, D.S.; Quraishi, M.A.; Ansari, K.R.; Saleh, T.A. Graphene and graphene oxide as new class of materials for corrosion control and protection: Present status and future scenario. Prog. Org. Coat. 2020, 147.
[42] Wan, S.; Chen, H.; Zhang, T.; Liao, B.; Guo, X. Anti-corrosion mechanism of parsley extract and synergistic iodide as novel corrosion inhibitors for carbon steel-Q235 in acidic medium by electrochemical, XPS and DFT methods. Front Bioeng. Biotechnol. 2021, 9, 1–15.

[43] Lima, R.M.A.P.; Alcaraz-Espinoza, J.J.; Da Silva, F.A.G.; De Oliveira, H.P. Multifunctional wearable electronic textiles using cotton fibers with polypyrrole and carbon nanotubes. ACS Appl. Mater. Interfaces. 2018, 10, 13783–13795.
[44] Roy, A.; Ghosh, A.; Bhandari, S.; Sundaram, S.; Mallick, T.K. Realization of poly(methyl methacrylate)-encapsulated solution-processed carbon-based solar cells: An emerging candidate for buildings' comfort. Ind. Eng. Chem. Res. 2020, 59, 11063–11071.
[45] Şengül, H.; Theis, T.L.; Ghosh, S. Toward sustainable nanoproducts: An overview of nanomanufacturing methods. J. Ind. Ecol. 2008, 12, 329–359.
[46] Perathoner, S.; Gangeri, M.; Lanzafame, P.; Centi, G. Nanostructured electrocatalytic Pt-carbon materials for fuel cells and CO2 conversion. Kinet Catal. 2007, 48, 877–883.
[47] Merchan-Merchan, W.; Saveliev, A.V.; Kennedy, L.; Jimenez, W.C. Combustion synthesis of carbon nanotubes and related nanostructures. Prog. Energy Combust. Sci. 2010, 36, 696–727.
[48] Mirzaee, M.; Rashidi, A.; Zolriasatein, A.; Rezaei Abadchi, M. Corrosion properties of organic polymer coating reinforced two-dimensional nitride nanostructures: A comprehensive review, vol. 28, Springer, Netherlands, 2021.
[49] Bacakova, L.; Grausova, L.; Vacik, J.; Kromka, A.; Biederman, H.; Choukourov, A., et al. Nanocomposite and nanostructured carbon-based films as growth substrates for bone cells. Adv. Divers Ind. Appl. Nanocomp. 2011.
[50] Kumar, V.S.; Mary, Y.S.; Pradhan, K.; Brahman, D.; Mary, Y.S.; Serdaroğlu, G., et al. Conformational analysis and quantum descriptors of two new imidazole derivatives by experimental, DFT, AIM, molecular docking studies and adsorption activity on graphene. Heliyon. 2020, 6.
[51] Wilson, P.M.; Zobel, A.; Lipatov, A.; Schubert, E.; Hofmann, T.; Sinitskii, A. Multilayer graphitic coatings for thermal stabilization of metallic nanostructures. ACS Appl. Mater. Interfaces. 2015, 7, 2987–2992.
[52] Subekti, N.; Soedarsono, J.W.; Riastuti, R.; Sianipar, F.D. Development of environmental friendly corrosion inhibitor from the extract of areca flower for mild steel in acidic media. Eastern-European J. Enterp. Technol. 2020, 2, 34–45.
[53] Pérez-Rodríguez, S.; Rillo, N.; Lázaro, M.J.; Pastor, E. Pd catalysts supported onto nanostructured carbon materials for CO2 valorization by electrochemical reduction. Appl. Catal B Environ. 2015, 163, 83–95.

Authorlist

Bhawana Jain
Siddhachalam Laboratory
Raipur
Chhattisgarh 493221
India

Reena Rawat
Department of Chemistry
Echelon Institute of Technology
Faridabad 121101
Haryana
India

Daniel Amoako Darko
Institute for Environment and Sanitation Studies
University of Ghana
Legon

Alimorad Rashidi
Nanotechnology Research Center
Research Institute of Petroleum Industry (RIPI)
Tehran
Iran

Maryam Sirati Gohari
Research Department of Ceramic Materials and Energy Research Center
Alborz
Iran
Email: m.sirati@merc.ac.ir
And
Department of Material Science and Engineering
School of Engineering
shiraz university
Shiraz, Fars
Iran
Email: siratigohari9830152@shirazu.ac.ir

Seyed Ali Rezaei
Research Department of Ceramic Materials and Energy Research Center
Alborz
Iran
Email: sa.rezaei@merc.ac.ir

Sourav Kr. Saha
Department of Materials Science and Engineering
Pusan National University
Busan 46241
Republic of Korea
Email: sksaha@pusan.ac.kr

Namhyun Kang
Department of Materials Science and Engineering
Pusan National University
Busan 46241
Republic of Korea
Email: nhkang@pusan.ac.kr

Gokul Ram Nishad
Department of Chemistry
Govt. Digvijay Autonomous Postgraduate College
Rajnandgaon
Chhattisgarh
India
Email: nishadgokul505@gmail.com

Ashwani Kumar Sharma
Department of Chemistry
Govt. Digvijay Autonomous Postgraduate College
Rajnandgaon
Chhattisgarh
India

Dakeshwar Kumar Verma
Department of Chemistry
Govt. Digvijay Autonomous Postgraduate College
Rajnandgaon
Chhattisgarh
India

https://doi.org/10.1515/9783110782820-016

Omar Dagdag
Institute of Nanotechnology and Water Sustainability
College of Science
Engineering and Technology
University of South Africa
Johannesburg 1710
South Africa
Email: dagdao@unisa.ac.za

Rajesh Haldhar
School of Chemical Engineering
Yeungnam University
Gyeongsan 38541
Republic of Korea

Seong-Cheol Kim
School of Chemical Engineering
Yeungnam University
Gyeongsan 38541
Republic of Korea

Elyor Berdimurodov
Faculty of Chemistry
National University of Uzbekistan
Tashkent 100034
Uzbekistan
Email: elyor170690@gmail.com

Chandrabhan Verma
Center of Research Excellence in Corrosion
Research Institute
King Fahd University of Petroleum and Minerals
Dhahran 31261
Saudi Arabia

Ekemini D. Akpan
Institute of Nanotechnology and Water Sustainability
College of Science
Engineering and Technology
University of South Africa
Johannesburg 1710
South Africa

Eno E. Ebenso
Institute of Nanotechnology and Water Sustainability
College of Science
Engineering and Technology
University of South Africa
Johannesburg 1710
South Africa
Email: ebensee@unisa.ac.za

Sanjukta Zamindar
Surface Engineering & Tribology Group
CSIR-Central Mechanical Engineering Research Institute
Mahatma Gandhi Avenue
Durgapur 713209
West Bengal
India
And
Academy of Scientific and Innovative Research (AcSIR)
CSIR-HRDC Campus
Sector-19
Kamla Nehru Nagar
Ghaziabad 201002
India

Manilal Murmu
Surface Engineering & Tribology Group
CSIR-Central Mechanical Engineering Research Institute
Mahatma Gandhi Avenue
Durgapur 713209
West Bengal
India
And
Academy of Scientific and Innovative Research (AcSIR)
CSIR-HRDC Campus
Sector-19
Kamla Nehru Nagar
Ghaziabad 201002
India

Naresh Chandra Murmu
Surface Engineering & Tribology Group
CSIR-Central Mechanical Engineering
Research Institute
Mahatma Gandhi Avenue
Durgapur 713209
West Bengal
India
And
Academy of Scientific and Innovative
Research (AcSIR)
CSIR-HRDC Campus
Sector-19
Kamla Nehru Nagar
Ghaziabad 201002
India

Priyabrata Banerjee
Surface Engineering & Tribology Group
CSIR-Central Mechanical Engineering
Research Institute
Mahatma Gandhi Avenue
Durgapur 713209
West Bengal
India
And
Academy of Scientific and Innovative
Research (AcSIR)
CSIR-HRDC Campus
Sector-19
Kamla Nehru Nagar
Ghaziabad 201002
India
E-mail: pr_banerjee@cmeri.res.in

Avni Berisha
Department of Chemistry
Faculty of Natural and Mathematics Science
University of Prishtina
10000 Prishtina
Kosovo
E-mail. avni.berisha@uni-pr.edu

Roli Jain
Department of chemistry
Dr. Hari Singh Gour University sagar
Madhya Pradesh
India

Daniel Amoako Darko
Institute for Environment and Sanitation
Studies
University of Ghana
Legon

Bhawana Jain
Department of Chemistry
Govt. V.Y.T. PG. Autonomous College
Durg (C.G.) India

Ruchi Sharma
Department of Chemistry
GGDSD College
Palwal
Haryana 121102
India

Reena Rawat
Department of Chemistry
Echelon Institute of Technology
Faridabad 121101
Haryana
India
Email: renunegi2007@gmail.com

Seyyed Arash Haddadi
School of Engineering
University of British Columbia
Kelowna, BC
V1V 1V7
Canada

Saeed Ghaderi
School of Engineering
University of British Columbia
Kelowna, BC
V1V 1V7
Canada

Mohammad Ebrahim Haji Naghi Tehrani
Department of Surface Coatings and
Corrosion
Institute for Color Science and Technology
P.O. Box 16, 765654
Tehran
Iran

Bahram Ramezanzadeh
Department of Surface Coatings and Corrosion
Institute for Color Science and Technology
P.O. Box 16, 765654
Tehran
Iran
Email: ramezanzadeh-bh@icrc.ac.ir

Taiwo W. Quadri
Department of Chemistry
School of Chemical and Physical Sciences and Material Science Innovation & Modelling (MaSIM) Research Focus Area
Faculty of Natural and Agricultural Sciences
North-West University
Private Bag X2046
Mmabatho 2735
South Africa
Email: taiwoquadri27@gmail.com

Lukman O. Olasunkanmi
Department of Chemistry
Faculty of Science
Obafemi Awolowo University
Ile Ife 220005
Nigeria
And
Department of Chemical Sciences
University of Johannesburg
P.O. Box 17, 011
Doornfontein Campus
Johannesburg 2028
South Africa

Omolola E. Fayemi
Department of Chemistry
School of Chemical and Physical Sciences and Material Science Innovation & Modelling (MaSIM) Research Focus Area
Faculty of Natural and Agricultural Sciences
North-West University
Private Bag X2046
Mmabatho 2735
South Africa

Eno E. Ebenso
Institute for Nanotechnology and Water Sustainability
College of Science
Engineering and Technology
University of South Africa
Johannesburg 1710
South Africa

Navid Hosseinabadi
Department of Materials Engineering and Metallurgy
Faculty of Engineering
Shiraz Branch
Islamic Azad University
P.o. Box 74,731-71987
Shiraz
Iran
Email: hosseinabadi@iaushiraz.ac.ir

Abhinay Thakur
Department of Chemistry
Faculty of Technology and Science
Lovely Professional University
Phagwara
Punjab
India

Praveen Kumar Sharma
Department of Chemistry
Faculty of Technology and Science
Lovely Professional University
Phagwara
Punjab
India

Ashish Kumar
NCE
Department of Science and Technology
Government of Bihar
India
Email: drashishchemlpu@gmail.com

Index

https://doi.org/10.1515/9783110782820-017